O-GLCNACYLATION: EXPANDING THE FRONTIERS

EDITED BY: Tarik Issad and Tony Lefebvre
PUBLISHED IN: Frontiers in Endocrinology

frontiers Research Topics

frontiers

ISSN 1664-8714
ISBN 978-2-88963-425-5
DOI 10.3389/978-2-88963-425-5

About Frontiers

Frontiers is more than just an open-access publisher of scholarly articles: it is a pioneering approach to the world of academia, radically improving the way scholarly research is managed. The grand vision of Frontiers is a world where all people have an equal opportunity to seek, share and generate knowledge. Frontiers provides immediate and permanent online open access to all its publications, but this alone is not enough to realize our grand goals.

Frontiers Journal Series

The Frontiers Journal Series is a multi-tier and interdisciplinary set of open-access, online journals, promising a paradigm shift from the current review, selection and dissemination processes in academic publishing. All Frontiers journals are driven by researchers for researchers; therefore, they constitute a service to the scholarly community. At the same time, the Frontiers Journal Series operates on a revolutionary invention, the tiered publishing system, initially addressing specific communities of scholars, and gradually climbing up to broader public understanding, thus serving the interests of the lay society, too.

Dedication to Quality

Each Frontiers article is a landmark of the highest quality, thanks to genuinely collaborative interactions between authors and review editors, who include some of the world's best academicians. Research must be certified by peers before entering a stream of knowledge that may eventually reach the public - and shape society; therefore, Frontiers only applies the most rigorous and unbiased reviews.
Frontiers revolutionizes research publishing by freely delivering the most outstanding research, evaluated with no bias from both the academic and social point of view. By applying the most advanced information technologies, Frontiers is catapulting scholarly publishing into a new generation.

What are Frontiers Research Topics?

Frontiers Research Topics are very popular trademarks of the Frontiers Journals Series: they are collections of at least ten articles, all centered on a particular subject. With their unique mix of varied contributions from Original Research to Review Articles, Frontiers Research Topics unify the most influential researchers, the latest key findings and historical advances in a hot research area! Find out more on how to host your own Frontiers Research Topic or contribute to one as an author by contacting the Frontiers Editorial Office: researchtopics@frontiersin.org

O-GLCNACYLATION: EXPANDING THE FRONTIERS

Topic Editors:
Tarik Issad, Centre National de la Recherche Scientifique (CNRS), France
Tony Lefebvre, Lille University of Science and Technology, France

Citation: Issad, T., Lefebvre, T., eds. (2020). O-GlcNAcylation: Expanding the Frontiers. Lausanne: Frontiers Media SA. doi: 10.3389/978-2-88963-425-5

Table of Contents

05 ***Editorial: O-GlcNAcylation: Expanding the Frontiers***
Tarik Issad and Tony Lefebvre

08 ***O-GlcNAc: A Sweetheart of the Cell Cycle and DNA Damage Response***
Caifei Liu and Jing Li

19 ***Apart From Rhoptries, Identification of* Toxoplasma gondii*'s O-GlcNAcylated Proteins Reinforces the Universality of the O-GlcNAcome***
Moyira Osny Aquino-Gil, Mattis Kupferschmid, Hosam Shams-Eldin, Jörg Schmidt, Nao Yamakawa, Marlène Mortuaire, Frédéric Krzewinski, Stéphan Hardivillé, Edgar Zenteno, Christian Rolando, Fabrice Bray, Eduardo Pérez Campos, Jean-François Dubremetz, Yobana Perez-Cervera, Ralph T. Schwarz and Tony Lefebvre

30 ***Real Talk: The Inter-play Between the mTOR, AMPK, and Hexosamine Biosynthetic Pathways in Cell Signaling***
Gentry K. Cork, Jeffrey Thompson and Chad Slawson

39 ***Nutrient-Driven O-GlcNAcylation at Promoters Impacts Genome-Wide RNA Pol II Distribution***
Michael W. Krause, Dona C. Love, Salil K. Ghosh, Peng Wang, Sijung Yun, Tetsunari Fukushige and John A. Hanover

55 ***AMP-Activated Protein Kinase and O-GlcNAcylation, Two Partners Tightly Connected to Regulate Key Cellular Processes***
Roselle Gélinas, Justine Dontaine, Sandrine Horman, Christophe Beauloye, Laurent Bultot and Luc Bertrand

62 ***Interplay Between Phosphorylation and O-GlcNAcylation of Sarcomeric Proteins in Ischemic Heart Failure***
Thomas Mercier, Marion Bouvet, Emilie Dubois-Deruy, Arthur Dechaumes, Olivia Beseme, Vincent Richard, Paul Mulder and Florence Pinet

72 ***Cross-Dysregulation of O-GlcNAcylation and PI3K/AKT/mTOR Axis in Human Chronic Diseases***
Ninon Very, Anne-Sophie Vercoutter-Edouart, Tony Lefebvre, Stéphan Hardivillé and Ikram El Yazidi-Belkoura

82 ***A Novel Glycoproteomics Workflow Reveals Dynamic O-GlcNAcylation of COPγ1 as a Candidate Regulator of Protein Trafficking***
Nathan J. Cox, Peter M. Luo, Timothy J. Smith, Brittany J. Bisnett, Erik J. Soderblom and Michael Boyce

98 ***Involvement of O-GlcNAcylation in the Skeletal Muscle Physiology and Physiopathology: Focus on Muscle Metabolism***
Matthias Lambert, Bruno Bastide and Caroline Cieniewski-Bernard

110 ***O-GlcNAc as an Integrator of Signaling Pathways***
Qunxiang Ong, Weiping Han and Xiaoyong Yang

119 ***Direct Crosstalk Between O-GlcNAcylation and Phosphorylation of Tau Protein Investigated by NMR Spectroscopy***
Gwendoline Bourré, François-Xavier Cantrelle, Amina Kamah, Béatrice Chambraud, Isabelle Landrieu and Caroline Smet-Nocca

132 ***Chronic O-GlcNAcylation and Diabetic Cardiomyopathy: The Bitterness of Glucose***
Simon Ducheix, Jocelyne Magré, Bertrand Cariou and Xavier Prieur

143 ***FGF23 Induction of O-Linked N-Acetylglucosamine Regulates IL-6 Secretion in Human Bronchial Epithelial Cells***
Stefanie Krick, Eric Scott Helton, Samuel B. Hutcheson, Scott Blumhof, Jaleesa M. Garth, Rebecca S. Denson, Rennan S. Zaharias, Hannah Wickham and Jarrod W. Barnes

153 ***Protein O-GlcNAcylation in Cardiac Pathologies: Past, Present, Future***
Marine Ferron, Manon Denis, Antoine Persello, Raahulan Rathagirishnan and Benjamin Lauzier

165 ***Binding Specificity of Native Odorant-Binding Protein Isoforms is Driven by Phosphorylation and O-N-Acetylglucosaminylation in the Pig* Sus scrofa**
Patricia Nagnan-Le Meillour, Alexandre Joly, Chrystelle Le Danvic, Arul Marie, Séverine Zirah and Jean-Paul Cornard

179 ***Cyclin D1 Stability is Partly Controlled by O-GlcNAcylation***
Louis Masclef, Vanessa Dehennaut, Marlène Mortuaire, Céline Schulz, Maïté Leturcq, Tony Lefebvre and Anne-Sophie Vercoutter-Edouart

191 ***Regulation of Polycomb Repression by O-GlcNAcylation: Linking Nutrition to Epigenetic Reprogramming in Embryonic Development and Cancer***
Amélie Decourcelle, Dominique Leprince and Vanessa Dehennaut

200 ***Identification of O-Glcnacylated Proteins in* Trypanosoma cruzi**
Elia Torres-Gutiérrez, Yobana Pérez-Cervera, Luc Camoin, Edgar Zenteno, Moyira Osny Aquino-Gil, Tony Lefebvre, Margarita Cabrera-Bravo, Olivia Reynoso-Ducoing, Martha Irene Bucio-Torres and Paz María Salazar-Schettino

213 ***O-GlcNAcylation is Involved in the Regulation of Stem Cell Markers Expression in Colon Cancer Cells***
Gabriela Fuentes-García, M. Cristina Castañeda-Patlán, Anne-Sophie Vercoutter-Edouart, Tony Lefebvre and Martha Robles-Flores

226 ***O-GlcNacylation Links TxNIP to Inflammasome Activation in Pancreatic β Cells***
Gaelle Filhoulaud, Fadila Benhamed, Patrick Pagesy, Caroline Bonner, Yann Fardini, Anissa Ilias, Jamileh Movassat, Anne-Françoise Burnol, Sandra Guilmeau, Julie Kerr-Conte, François Pattou, Tarik Issad and Catherine Postic

frontiers in Endocrinology

EDITORIAL
published: 13 December 2019
doi: 10.3389/fendo.2019.00867

Editorial: *O*-GlcNAcylation: Expanding the Frontiers

Tarik Issad[1*†] *and Tony Lefebvre*[2*†]

[1] *Université de Paris, CNRS UMR8104, INSERM U1016, Institut Cochin, Paris, France,* [2] *Université de Lille, CNRS, UMR 8576, UGSF, Lille, France*

Keywords: *O*-linked N-acetylglucosaminylation, post-translational modification, epigenetics, inflammation, cardiovascular diseases, cancer, *O*-GlcNAcomics

Editorial on the Research Topic

O-GlcNAcylation: Expanding the Frontiers

O-linked N-acetylglucosaminylation (*O*-GlcNAcylation) is a fascinating post-translational modification (PTM) that controls numerous biological processes, including epigenetic regulations, gene expression, proteostasis, energy metabolism, cell signaling, growth and proliferation (1). Whereas it essentially remained confidential during the first decades following its discovery, the importance of this protein modification in life sciences is now undisputed. In 2014, we celebrated the 30 years anniversary of its discovery by editing a Research Topic in Frontiers in Endocrinology (2). As everyone can notice, time is speeding up and this is particularly true in Science. Almost 5 years now after launching the publication of this Research Topic, it seems to us that significant progresses and new discoveries have been made in the field that justify another issue on this subject.

Alike phosphorylation, *O*-GlcNAcylation is a reversible PTM that occurs on serine and threonine residues of cytosolic, nuclear and mitochondrial proteins. Only two enzymes, OGT (*O*-GlcNAc transferase) and OGA (*O*-GlcNAcase), control the *O*-GlcNAc dynamics on proteins. OGT utilizes UDP-GlcNAc, provided by the hexosamine biosynthesis pathway (HBP), to add GlcNAc on proteins, whereas OGA removes it. UDP-GlcNAc, which is at the cross-road of several metabolic pathways, is considered as a sensor of the nutritional state of the cell. Thus, *O*-GlcNAcylation regulates cellular homeostasis according to metabolic environment, but also in response to signaling molecules (e.g., hormones and cytokines). Widespread in most living organisms studied so far, *O*-GlcNAcylation is highly susceptible to stress and injuries, and is involved in many human pathologies including diabetes, cancer and neurodegenerative diseases (3–5).

This E-book, which comprises reviews and original articles, provides up-to date examples of the implication of *O*-GlcNAcylation in diverse organisms and of its role in various physiological and pathological processes.

A remarkable feature of *O*-GlcNAcylation is its capacity to modulate other PTMs, which confers it the capability to interfere with various signaling and nutrient sensing pathways. AMP-activated protein kinase and mTOR pathways, regulated by AMP/ATP ratio and amino-acid levels, respectively, are major players in nutrient sensing. Reviews by Gélinas et al., Cork et al., and Very et al. extensively discuss different aspects of the dialogues between HBP, OGT, AMPK, and mTOR signaling at the cellular and molecular levels, as well as their dysregulation in pathophysiological situations. In the same vein, Ong et al. speculate on *O*-GlcNAc as an integrator of signaling pathways, emphasizing the necessity of maintaining what these authors called the "*O*-GlcNAc meter" at an optimal level, between a lower limit necessary for maintenance of cell structural integrity and critical functions, and a higher limit above which persistent *O*-GlcNAcylation leads to aberrant signaling.

OPEN ACCESS

Edited and reviewed by:
Pierre De Meyts,
Université Catholique de Louvain, Belgium

***Correspondence:**
Tarik Issad
tarik.issad@inserm.fr
Tony Lefebvre
tony.lefebvre@univ-lille.fr

† These authors have contributed equally to this work

Specialty section:
This article was submitted to Molecular and Structural Endocrinology, a section of the journal Frontiers in Endocrinology

Received: *25 November 2019*
Accepted: *26 November 2019*
Published: *13 December 2019*

Citation:
Issad T and Lefebvre T (2019) Editorial: O-GlcNAcylation: Expanding the Frontiers. Front. Endocrinol. 10:867. doi: 10.3389/fendo.2019.00867

Also, *O*-GlcNAcylation now appears as a major player in the immune system, and its role in inflammation constitutes an important area of investigation (6). In this Research Topic, two original articles deal with these aspects. Krick et al. provided data indicating that in human bronchial epithelial cells, FGF23, an important endocrine pro-inflammatory mediator, induces IL6 production. This effect is mediated by a FGFR4/Phospholipase Cγ/Nuclear factor activated T-cells (NFAT) signaling pathway and involves increased protein *O*-GlcNAcylation upon FGF23 stimulation. This work points out the potential role for *O*-GlcNAcylation in pathogenesis of chronic inflammatory airways diseases.

Chronic inflammation is also a hallmark of metabolic diseases such as diabetes and obesity. Hyperglycaemia is considered to be an important player in the initiation and persistence of inflammation associated with these pathologies (7). In pancreatic β-cells, high glucose concentrations stimulate the interaction of thioredoxin interacting protein (TxNIP) with the inflammasome protein NLRP3 (NLR family, pyrin domain containing 3), thereby promoting interleukin-1β (IL1β) maturation and secretion. Filhoulaud et al. demonstrated that TxNIP protein is modified by *O*-GlcNAcylation in rodent and human pancreatic β-cells, resulting in increased association with NLRP3, inflammasome activation, and production of mature IL1β. These data provide a new link between *O*-GlcNAcylation, inflammation, and glucotoxicity in pancreatic β-cells.

O-GlcNAcylation has largely been involved in diabetic complications associated with glucotoxicity, including cardiovascular dysfunctions (4). In the article by Mercier et al., a potential interplay between phosphorylation and *O*-GlcNAcylation of sarcomeric proteins in ischemic heart failure was examined, and the authors paid a particular attention to the intermediate filament structure essential component desmin. In addition, whereas the review by Ducheix et al. focused on the cellular and molecular mechanisms by which chronic *O*-GlcNAcylation affects cardiac function in diabetic cardiomyopathy, Ferron et al. evaluated the potential impact of modulating *O*-GlcNAc levels in acute cardiovascular pathologies, including haemorrhagic shock and myocardial ischemia-reperfusion injury.

The beneficial effects of physical exercise for prevention and treatment of human chronic diseases, including diabetes, cancer, and neurodegenerative diseases, are now largely documented. Skeletal muscle is quantitatively the most important glucose consumer tissue of the organism, and as such a crucial determinant of whole-body insulin sensitivity. It is also a major site of lipid oxidation and protein turn-over. In this Research Topic, Lambert et al. reviewed the involvement of *O*-GlcNAcylation in skeletal muscle chronic and acute exercise, as well as in pathophysiological situations, such as muscular atrophy or insulin resistance.

O-GlcNAcylation has also been involved in the control of cell cycle (8). One of the functions of the cell cycle is to replicate the DNA so that each daughter cell resulting from the division can inherit a copy conforming to the mother cell. But when the cell cycle is upset, errors in DNA replication can arise. *O*-GlcNAcylation intervenes both in the fine-tune control of cell cycle and in the maintenance of genome integrity by controlling DDR (DNA damage response). This field of particular interest is the topic of the review by Liu and Li who gave a comprehensive overview of the issue.

Cyclins are master regulators of the cell cycle. Cyclin D1 interacts with CDK4/6 to control cell cycle entry and progression in G1 phase. Masclef et al. showed that the fate of cyclin D1 depends upon *O*-GlcNAc status. Mechanistically, these authors demonstrated that cyclin D1 interacts with OGT; this leads to its *O*-GlcNAcylation which thwarts its ubiquitination and its subsequent targeting to the proteasome.

In this special issue, the role of *O*-GlcNAcylation in stemness was also investigated. Fuentes-García et al. showed that inhibition of OGT in colon cell lines interferes with the expression of the two stem cell markers CD44 and CD133, and coincides with an increased clonogenicity and spheroid formation capabilities. Of particular interest, the authors suggest that *O*-GlcNAc serves as a sensor giving the cancer cells the ability to face nutrient stressful conditions.

Dysregulation of *O*-GlcNAcylation is also associated with neurodegenerative disorders including Alzheimer's disease as previously documented (9). While a reciprocal relationship between *O*-GlcNAcylation and phosphorylation on Tau protein has been reported (10, 11), molecular details of this interaction remain largely unknown. Bourré et al. used NMR spectroscopy approach to map *O*-GlcNAc sites on the longest isoform of Tau and to gain insight into the crosstalk between *O*-GlcNAcylation and phosphorylation. They propose that both PTMs can affect Tau in a more intricate relationship than a single direct reciprocal manner. This interesting paper reinforces a little more the complexity of protein regulation by PTMs.

O-GlcNAcylation is now recognized as an important player in epigenetic regulations (12). In a mini-review, Decourcelle et al. compared the structure of the human and drosophila Polycomb Repressor Complexes and discuss their regulation by *O*-GlcNAcylation in drosophila embryonic development and in human cancer cells. Moreover, original work by Krause et al. evaluated the link between *O*-GlcNAcylation, nutritional status and epigenetic regulation of gene expression by studying genome wide RNA Polymerase II binding in response to starvation and feeding, in *C. elegans* mutants lacking either OGT or OGA. Interestingly, they observed that in wild-type animals, *O*-GlcNAc marks on promoters were surprisingly very similar in fed and starved conditions, but responded aberrantly to nutrient flux when *O*-GlcNAc cycling was blocked by OGA knock out. They suggested that in wild-type animals, the dynamic cycling of *O*-GlcNAc is required to maintain buffered levels of *O*-GlcNAcylation at gene promoters, reminiscent of the optimal intracellular *O*-GlcNAcylation level proposed by Ong et al..

O-GlcNAcylation is nearly universal in the living kingdom. This was further demonstrated in parasites by two original studies, in which *O*-GlcNAcylated proteins were identified in *Toxoplasma gondii* (Aquino-Gil et al.) and *Trypanosoma cruzi* (Torres-Gutiérrez et al.). Identification of *O*-GlcNAc on proteins involved in invasion, such as rhoptries in *T. gondii*, or in microtubules formation in *T. cruzi*, may suggest new therapeutic strategies against infections by these parasites.

A little on the fringes of what could be considered today as the classical *O*-GlcNAcylation pathway, that is modification of nucleocytoplasmic proteins, Nagnan-Le Meillour et al. focused on odorant-binding proteins (OBP) secreted in the nasal mucus. By a set of different approaches including mass spectrometry, they managed to identify several sites of *O*-GlcNAcylation and phosphorylation on OBP. Interestingly, they showed that phosphorylated isoforms of OBP only slightly modify interaction with lipid ligands, whereas O-GlcNAcylation of OBP favors binding. These data reveal a new regulatory mechanism by which PTMs and specifically extracellular *O*-GlcNAcylation, managed by EOGT (the *endoplasmic reticulum*-resident form of OGT), can modulate recognition of odorant molecules by OBP, enlarging the panel of odors discrimination.

Finally, an interesting technical contribution to this Research Topic is dedicated to the development of a novel *O*-GlcNAcomics workflow based on GalNAz labeling of cells and quantitative proteomics analysis Cox et al. As a proof of concept Cox et al. identified *O*-GlcNAcylation of COP1γ (a component of COPI). They pinpointed several *O*-GlcNAc sites on COP1γ and proposed that *O*-GlcNAc is a regulator of mammalian vesicle trafficking within the Golgi apparatus and from the Golgi to the *endoplasmic reticulum*.

Looking back through the series of reviews and original articles gathered here, we feel that this Research Topic has been an opportunity for several young researchers to present their first work on this particularly exciting modification. As such, it may reflects the beginning of a new era of investigation on *O*-GlcNAcylation. Because of its wide distribution in the living world and the numerous biological processes it controls, there is no doubt that in the near future other new teams will get on board for the study of *O*-GlcNAc.

AUTHOR CONTRIBUTIONS

All authors listed have made a substantial, direct and intellectual contribution to the work, and approved it for publication.

REFERENCES

1. Hart GW. Nutrient regulation of signaling and transcription. *J Biol Chem.* (2019) 294:2211–31. doi: 10.1074/jbc.AW119.003226
2. Lefebvre T, Issad T. 30 Years Old: O-GlcNAc reaches the age of reason - Regulation of cell signaling and metabolism by O-GlcNAcylation. *Front Endocrinol.* (2015) 6:17. doi: 10.3389/fendo.2015.00017
3. Lefebvre T, Dehennaut V, Guinez C, Olivier S, Drougat L, Mir AM, et al. Dysregulation of the nutrient/stress sensor O-GlcNAcylation is involved in the etiology of cardiovascular disorders, type-2 diabetes and Alzheimer's disease. *Biochim Biophys Acta*. (2009) 1800:67–79. doi: 10.1016/j.bbagen.2009.08.008
4. Issad T, Masson E, Pagesy P. O-GlcNAc modification, insulin signaling and diabetic complications. *Diabetes Metab.* (2010) 36:423–35. doi: 10.1016/j.diabet.2010.09.001
5. Fardini Y, Dehennaut V, Lefebvre T, Issad T. O-GlcNAcylation: a new cancer hallmark? *Front Endocrinol.* (2013) 4:99. doi: 10.3389/fendo.2013.00099
6. Baudoin L, Issad T. O-GlcNAcylation and inflammation: a vast territory to explore. *Front Endocrinol.* (2015) 5:235. doi: 10.3389/fendo.2014.00235
7. Kempf K, Rose B, Herder C, Kleophas U, Martin S, Kolb H. Inflammation in metabolic syndrome and type 2 diabetes: impact of dietary glucose. *Ann N Y Acad Sci.* (2006) 1084:30–48. doi: 10.1196/annals.1372.012
8. Slawson C, Zachara NE, Vosseller K, Cheung WD, Lane MD, Hart GW. Perturbations in O-linked beta-N-acetylglucosamine protein modification cause severe defects in mitotic progression and cytokinesis. *J Biol Chem.* (2005) 280:32944–56. doi: 10.1074/jbc.M503396200
9. Zhu Y, Shan X, Yuzwa SA, Vocadlo DJ. The emerging link between O-GlcNAc and Alzheimer disease. *J Biol Chem.* (2014) 289:34472–81. doi: 10.1074/jbc.R114.601351
10. Gatta E, Lefebvre T, Gaetani S, dos Santos M, Marrocco J, Mir AM, et al. Evidence for an imbalance between tau O-GlcNAcylation and phosphorylation in the hippocampus of a mouse model of Alzheimer's disease. *Pharmacol Res.* (2016) 105:186–97. doi: 10.1016/j.phrs.2016.01.006
11. Yu Y, Zhang L, Li X, Run X, Liang Z, Li Y, et al. Differential effects of an O-GlcNAcase inhibitor on tau phosphorylation. *PLoS ONE.* (2012) 7:e35277. doi: 10.1371/journal.pone.0035277
12. Leturcq M, Lefebvre T, Vercoutter-Edouart AS. O-GlcNAcylation and chromatin remodeling in mammals: an up-to-date overview. *Biochem Soc Trans.* (2017) 45:323–38. doi: 10.1042/BST20160388

Conflict of Interest: The authors declare that the research was conducted in the absence of any commercial or financial relationships that could be construed as a potential conflict of interest.

frontiers in Endocrinology

REVIEW
published: 30 July 2018
doi: 10.3389/fendo.2018.00415

O-GlcNAc: A Sweetheart of the Cell Cycle and DNA Damage Response

*Caifei Liu and Jing Li**

Beijing Key Laboratory of DNA Damage Response and College of Life Sciences, Capital Normal University, Beijing, China

The addition and removal of O-linked N-acetylglucosamine (O-GlcNAc) to and from the Ser and Thr residues of proteins is an emerging post-translational modification. Unlike phosphorylation, which requires a legion of kinases and phosphatases, O-GlcNAc is catalyzed by the sole enzyme in mammals, O-GlcNAc transferase (OGT), and reversed by the sole enzyme, O-GlcNAcase (OGA). With the advent of new technologies, identification of O-GlcNAcylated proteins, followed by pinpointing the modified residues and understanding the underlying molecular function of the modification has become the very heart of the O-GlcNAc biology. O-GlcNAc plays a multifaceted role during the unperturbed cell cycle, including regulating DNA replication, mitosis, and cytokinesis. When the cell cycle is challenged by DNA damage stresses, O-GlcNAc also protects genome integrity via modifying an array of histones, kinases as well as scaffold proteins. Here we will focus on both cell cycle progression and the DNA damage response, summarize what we have learned about the role of O-GlcNAc in these processes and envision a sweeter research future.

Keywords: O-GlcNAc, mitosis, replication, cytokinesis, DNA damage response

OPEN ACCESS

Edited by:
Tony Lefebvre,
Lille University of Science and Technology, France

Reviewed by:
Anne-Sophie Edouart,
Centre National de la Recherche Scientifique (CNRS), France
Hai-Bin Ruan,
University of Minnesota Twin Cities, United States
Chad Slawson,
Kansas University of Medical Center Research Institute, United States

***Correspondence:**
Jing Li
jing_li@mail.cnu.edu.cn

Specialty section:
This article was submitted to Molecular and Structural Endocrinology, a section of the journal Frontiers in Endocrinology

Received: *20 April 2018*
Accepted: *02 July 2018*
Published: *30 July 2018*

Citation:
Liu C and Li J (2018) O-GlcNAc: A Sweetheart of the Cell Cycle and DNA Damage Response. Front. Endocrinol. 9:415. doi: 10.3389/fendo.2018.00415

INTRODUCTION

The study of O-linked N-acetylglucosamine (O-GlcNAc), O-GlcNAc transferase (OGT), and O-GlcNAcase (OGA) was pioneer by Dr. Hart in 1984 (1). OGT modifies the substrate protein at Ser/Thr residues with the O-GlcNAc group, while OGA reverses it. Since then, both biologists and chemists have been working hand in hand to solve the sweet mystery. In this review, we will first cover the laboratory routine to study protein O-GlcNAcylation, and then venture onto the recently identified function of O-GlcNAc in regulating cell cycle and the DNA damage response (DDR). For the versatile role of O-GlcNAc in other biological processes, please refer to other comprehensive and exhaustive reviews (2–5).

AN OVERVIEW OF O-GLCNAC

Of all the glucose that we consume every day, ∼2−5% enters the hexosamine biosynthetic pathway (HBP), which provides UDP-N-acetyl-D-glucosamine (UDP-GlcNAc) (6), the donor substrate for OGT. UDP-GlcNAc is highly responsive to cellular nutrient variations, as its synthesis relies heavily on the metabolism of glucose, amino acids, fatty acids, and nucleotides (7). Hence, O-GlcNAc may serve as a reporter for the functional status of multiple pathways and is considered an ideal metabolic sensor (8), and defunct O-GlcNAc signaling underscores many metabolic diseases (3, 5).

O-GlcNAc Is Implicated in Various Human Diseases

O-GlcNAcylation is most abundant in the pancreas, followed by the brain (3). Thus it has been intimately linked with a plethora of human diseases, especially diabetes, and Alzheimer's disease (AD).

In diabetes, hyperglycemia leads to chronic hyper-O-GlcNAcylation, which brings mayhem to cellular signaling networks. And inhibiting O-GlcNAc was found to blockade arrhythmias in diabetic animals (9). Recent investigations show that OGT in pancreatic β cells regulates the β cell mass. And OGT disruption results in diabetes via the endoplasmic reticulum (ER) stress and the Akt pathway (10). The vital player in AD, Tau, is O-GlcNAcylated in normal brains, but hyperphosphorylated in AD brains (3). Interestingly, increasing O-GlcNAc in mice decreases neuronal losses (11).

O-GlcNAc in Cancer Metabolism

One characteristic of cancer cells is the Warburg effect, namely, elevated glycolytic flux, including glycolysis, the pentose phosphate pathway (PPP), and the HBP. Moreover, enhanced O-GlcNAcylation levels have been pinpointed as a common cancer feature (12). Many studies have impinged O-GlcNAc as a sweet accomplice of cancer.

Upon entering the cell, glucose is phosphorylated by hexokinase to become glucose-6-phosphate (G6P). G6P then either undergoes glycolysis and the tricarboxylic acid (TCA) cycle to generate ATP, NADPH, and pyruvate, or produce ribose-5-phosphate and NADPH through PPP (13). PPP maintains redox homoeostasis in rapidly dividing cells, especially in cancer cells. In the glycolytic pathway, phosphofructokinase 1 (PFK1) is O-GlcNAcylated at S529 upon hypoxia, inhibiting PFK1 activity and directing the glucose metabolism to the PPP (14). Concomitantly, the rate-limiting enzyme of the PPP, G6P dehydrogenase (G6PD), is also O-GlcNAcylated during hypoxia, thus being activated to increase glucose flux via PPP (15). Taken together, O-GlcNAc activates the PPP to promote cancer proliferation.

In the TCA cycle, fumarase both reversibly catalyzes fumarate to malate in the mitochondria, and regulates amino acid and fumarate metabolism in the cytoplasm. Fumarase is O-GlcNAcylated at S75, which antagonizes phosphorylation by AMPK at the exact same residue when glucose is scarce (16). pS75 mediates fumarase-ATF2 interaction, blocks KDM2A activity, stabilizes H3K36me2 and thus redirecting the cell proliferation to growth arrest (16). Hence in cancer cells, where OGT activity is particularly high, pS75 levels are relatively low, conferring growth advantage to cancer cells.

Equally important, OGT also regulates lipid metabolism in cancer. To sustain growth, cancer cells usually utilize *de novo* lipogenesis, which encompass activation of key enzymes, such as fatty acid synthase (FAS), and master transcription factors, such as the sterol regulatory element binding protein (SREBP-1). OGT suppression leads to lipogenic defects, which could be rescued by SREBP-1 overproduction (17). OGT regulates SREBP-1 protein abundance, probably via AMPK (17). On the other hand, FAS binds with OGA, and the interaction increases during oxidative stress (18). FAS inhibits OGA activity, so the O-GlcNAc levels elevate under oxidative stress in mammalian cells (18).

In conclusion, O-GlcNAc integrates various nutrient signaling with growth signaling and may provide new venues for therapeutic purposes.

Crosstalks Between O-GlcNAc and Other Post-translational Modifications (PTMs)

Then how does O-GlcNAc weave its magic wand? The answer lies largely in crosstalk with other PTMs. Due to the large size of the O-GlcNAc moiety, steric hindrance is imposed upon the O-GlcNAcylated protein, thus impeding other PTMs at the same or adjoining sites. For instance, when a mixture of two OGA inhibitors, PUGNAc and NAG-thiazoline, was utilized to analyze the ∼700 phosphopeptides, phosphorylation levels of 131 peptides (18.4%) escalated and 234 (32.9%) peptides dampened (19). In a quantitative phosphoproteomics study using OGT wild-type and null cells, 232 phosphosites increased and 133 decreased out of the 5,529 sites in the null cells (20). Thus, a yin-yang relationship has been proposed between O-GlcNAcylation and phosphorylation (3).

Discordant results against the "yin-yang" model have also been recorded. In a 2008 study, researchers closely monitored phosphorylation sites when O-GlcNAcylation was elevated (19). As a result, 280 phosphorylation sites decreased, while 148 sites increased (19). In a recent quantitative phosphoproteomics study, a great many DDR proteins were identified to be O-GlcNAcylated, among which was checkpoint kinase 1 (Chk1) (20). When OGT is deleted, pT113 of Chk1 increases, consistent with the "yin-yang" model, but pS151 decreases, against the model (20). Another case in hand is the intermediate filament protein, vimentin. Vimentin filament severing is a key step for completion of cytokinesis, and many phosphorylation events intricately mediate this process. In particular, cyclin-dependent kinase 1 (CDK1) phosphorylates vimentin at S55 (21) to prime vimentin for subsequent phosphorylation by polo-like kinase 1 (Plk1) at S82 (22), thus inhibiting vimentin filament assembly. Other kinases, such as Aurora B and the Rho kinase, also phosphorylate vimentin at S72 and S71, respectively, thus localizing vimentin to the cleavage furrow (23–25). When cells were depleted of OGT by siRNA, pS71 levels were hampered; vimentin filament thus could not be severed during cytokinesis, leading to cytokinesis failure (26). In sum, the relationship between phosphorylation and O-GlcNAcylation needs to be analyzed case by case, and there might not be a clear-cut rule.

The relationship between O-GlcNAcylation and ubiquitination and hence protein stability was tested recently. Using a newly developed quantitative time-resolved O-linked GlcNAc proteomics (qTOP), 533 O-GlcNAcylated proteins were examined for stability, and 14% were identified to be hyper-stably O-GlcNAcylated (27). Of this pool of ∼75 proteins, O-GlcNAcylation has a significant impact on the protein stability, and O-GlcNAcylation mainly promotes protein stability (27).

Abbreviations: (O-GlcNAc), O-linked N-acetylglucosamine; (OGT), O-GlcNAc transferase; OGA, O-GlcNAcase; DDR, DNA damage response; TLS, DNA translesion synthesis; ETD, electron transfer dissociation; MS, mass spectrometry; HCD, higher energy collisional dissociation; PTM, post-translational modification; IP, immunoprecipitate; IB, immunoblot; UV, ultraviolet; MEF, mouse embryonic fibroblast; DSB, double-strand break; ATM, ataxia telangiectasia mutated; ATR, ATM and Rad3 related; DNA-PK, and DNA-dependent protein kinase; MDC1, mediator of DNA damage checkpoint protein 1.

Congruent with this study, O-GlcNAcylation has been identified to augment protein abundance in an array of studies. O-GlcNAcylation of the circadian clock proteins, BMAL1 and CLOCK, inhibits their ubiquitination and stabilizes protein levels (28). During gluconeogenesis, the master regulator PGC-1α is O-GlcNAcylated to bind the deubiquitinase BAP1, thus dampening ubiquitination, and enhancing protein abundance (29). The mixed lineage leukemia 5 (MLL5) protein forms a stable complex with OGT and ubiquitin specific protease 7 (USP7), and OGT suppresses MLL5 ubiquitination and increases its stability (30). The histone methyltransferase enhancer of zeste homolog 2 (EZH2) is O-GlcNAcylated at S75, which maintains its protein stability (31). Besides proteasome-mediated degradation, ubiquitination also plays other roles in signal transduction. And crosstalks have also been identified in these scenarios. For instance, O-GlcNAcylation of DNA polymerase Polη promotes its polyubiquitination and subsequent removal from replication forks (32).

With more people joining in the O-GlcNAc venture, communication among O-GlcNAc and more PTMs, such as methylation, SUMOylation, acetylation, ADP-ribosylation is bound to be unveiled.

THE TOOLBOX OF O-GLCNAC RESEARCH

As the Chinese saying goes, "Nice craftsmanship entails utilization of nice tools." The toolbox of O-GlcNAc has been limited, compared to other PTMs, e. g., phosphorylation and ubiquitination. The common practice to identify O-GlcNAcylated proteins is by immunoprecipitating (IP) proteins of interest, then immunoblotting (IB) with O-GlcNAc antibodies. Below we will briefly delineate the lab routine to identify and study protein O-GlcNAcylation.

Antibodies

O-GlcNAc antibodies encompass RL2 and CTD110.6, among others (33). CTD110.6, an IgM, recognizes YSPTS(O-GlcNAc)PSK and also non-specifically binds terminal β-linked-GlcNAc (β-GlcNAc) and other N-glycan cores (34). RL2, on the contrary, is an IgG, and its antigen is pore complex-lamina fraction purified from rat liver nuclear envelopes (34). The RL2 and CTD110.6 are considered pan-O-GlcNAc antibodies, and might be promiscuous. They have overlapping, yet somewhat distinct ranges of protein targets. Hence it has been recommended to adopt both antibodies to conclude the O-GlcNAc modification. Alternatively, GlcNAc could be added during antibody blotting to compete against antibody binding, so that signals from O-GlcNAcylated proteins could be validated (35).

Another method is to perform *in vitro* O-GlcNAcylation assays. Using tritiated UDP-Galactose (UDP-[^{3}H]-Galactose) as a donor, the addition of "hot" O-GlcNAc onto proteins can be traced. However, this is not a trivial experiment. First, the OGT enzyme is sensitive to salt and reducing agents, thus the purified proteins need to be desalted (36). Second, tritium has a long half-life of 12.3 years, so the storage of residue materials is a valid concern. Third, tritium is not as sensitive as ^{32}P, hence autoradiography might take an extended period of time to be detected. Alternatively, RL2 and CTD110.6 could be used in IB experiments on the *in vitro* reaction products (37), thus avoiding the tritium issue.

Inhibitors

The aforementioned identification of O-GlcNAcylated proteins could be facilitated by using OGA inhibitors, thus enhancing O-GlcNAc signals (36). Two most commonly utilized OGA inhibitors are O-(2-acetamido-2-deoxy-D-glucopyranosylidene) amino N-phenylcarbamate (PUGNAc) and Thiamet-G (TMG). PUGNAc is a 1,5-hydroximolactone. It is a non-selective inhibitor of OGA and inhibits glycosyl hydrolases in general, in particular lysosomal hexosaminidases (38). Treating 3T3-L1 adipocytes with PUGNAc increased globular O-GlcNAc levels and resulted in insulin resistance, the hallmark of diabetes (39), consistent with the current view that elevated O-GlcNAcylation correlates with diabetes. However, such effects could not be repeated by treating cells or animals with TMG (40). Since TMG is more specific for OGA compared to PUGNAc, the results above suggest that the effect of PUGNAc was non-specific. It is more promising in treating AD, as treating AD mice with TMG increased Tau O-GlcNAcylation, attenuated Tau phosphorylation and hence aggregation, thus opening new venues for AD therapy (11).

Unlike OGA inhibitors, OGT inhibitors have been difficult to come along (38). Alloxan is the first reported inhibitor for OGT (41). As a uracil analog, it inhibits OGT, but its toxicity affects many cellular processes (41). Other inhibitors have been used anecdotally. 6-diazo-5-oxo-L-norleucine (DON), which is an inhibitor of glutamine-utilizing enzymes, such as the CTP synthase (CTPS) and NAD synthase, has been shown to inhibit O-GlcNAcylation (35). Two OGT inhibitors have been reported recently. One is a naturally produced OGT inhibitor, L01 (42), whose effects are yet to be tested. The other is uridine diphospho-5-thio-N-acetylglucosamine (UDP-5SGlcNAc), a substrate analog of O-GlcNAc that might be a competitive inhibitor of OGT (43). When the inhibitor per-O-acetylated 2-acetamido-2-deoxy-5-thioglucopyranose (Ac-5SGlcNAc) is added into cells, it is coverted to UDP-5S-GlcNAc, which is the most frequently used OGT inhibitor today (44–46).

Mass Spectrometry (MS)

Last three decades have witnessed significant strides in developing MS instruments, especially electron transfer dissociation (ETD) MS (47, 48) and higher energy collisional dissociation (HCD) MS (49). These two apparatuses differ greatly from each other: HCD cannot specify the amino acid that is modified, while ETD is only efficient toward peptides. For more details about identification of O-GlcNAc sites by MS, please refer to a more in-depth review (33).

Mutagenesis Studies

Following MS, the potential sites will be mutagenized to confirm whether they are indeed the modification sites. O-GlcNAc-deficient mutations are normally Ser/Thr to Ala, but O-GlcNAc-mimicking mutations are not well defined. Wang et al. (50)

mutated the O-GlcNAc sites of the Ser/Thr kinase AKT1, T305, and T312, to Tyr, to mimic the bulky steric hindrance imposed by the O-GlcNAc moiety. But it has not been commonly adopted.

The mutant proteins will subsequently be IBed against the O-GlcNAc antibodies, RL2 and CTD110.6. Site-specific O-GlcNAc antibodies are yet to be developed, unlike site-specific phospho-antibodies, which have been a standard practice to study protein phosphorylation.

Most of the time, MS identifies more than one O-GlcNAc site (32, 51, 52). It has been noted that in this scenario, single mutants will sometimes display elevated O-GlcNAcylation, while the double/triple/quadruple mutants will down-regulate O-GlcNAcylation (32, 51, 52). The single residue might be a preferred modification site, the abolishing of which might result in prolonged interaction between OGT and the target protein. But the exact molecular details are lacking.

O-GLCNAC REGULATES CELL CYCLE PROGRESSION

The cell cycle, comprising G1, S, G2, and M phases, has entranced biologists from the earliest times. How is the genomic DNA faithfully replicated? How is the chromosome segregation process synchronized? How do the two daughter cells part from each other? These are just a few questions that have baffled biologists and the answers are still much sought after.

As has long been appreciated, the faithful execution and success completion of cell cycle is governed by a multitude of master kinases, phosphatases, ubiquitin E3 ligases and a network of protein machineries. Recent years have witnessed a surge of reports on the role of OGT in the cell cycle. Henthforth, we will first have a bird's eye view on the role of OGT, and then delve into the substrates of O-GlcNAc in cell cycle (**Tables 1**, **2**). Of note, these tables are by no means comprehensive. **Table 2** only contains proteins whose molecular mechanism is well studied. Many other proteins have been identified in many proteomic screens, but their functional significance is not well understood.

An Overall Role of OGT/OGA in the Cell Cycle

Although a late comer to the cell cycle arena, there has been mounting evidence that OGT underscores cellular proliferation (67).O-GlcNAc levels fluctuate during distinct phases of the cell cycle. Upon entering the S phase, the OGA activity increases and the global O-GlcNAc levels decrease (53). During G2/M, reports have been incongruous. In *X. laevis* oocytes, global increase of O-GlcNAc is discernable during G2/M transition (55). In cultured mammalian cells, however, increased O-GlcNAc delays G2/M transition (54), and OGA disruption hinders G2/M transition (56). The discrepancy could be partly due to different species.

During mitosis, O-GlcNAc levels decrease (54, 57). OGA disruption results in lagging chromosomes and micronuclei (60), and stable OGA knockdown HeLa cell lines manifest aberrant spindles and mitotic exit effects (61). Meanwhile, OGT overproduction leads to chromosome bridges and delays mitosis (50). The mitotic spindle is an important apparatus to ensure accurate chromosome segregation (68), and its integrity impinges on the appropriate level of O-GlcNAcylation, as either OGT or OGA overproduction leads to aberrant mitotic spindles (69).

During cytokinesis, both OGA disruption and OGT overexpression lead to polyploidy and cytokinesis failure (26, 54, 60). Studies from our lab show that Chk1 phosphorylates OGT at S20 specifically during cytokinesis (26). This modification stabilizes OGT abundance and ensures a sufficient level of pS71 of vimentin (26). Thus OGT knockdown leads to vimentin bridges (26). In sum it is suffice to say that an appropriate O-GlcNAc level is pivotal for all phases. If chemical interrogation or genetic ablation renders O-GlcNAc above or below that level, cellular reproduction will be seriously affected.

Cytologically, OGT localizes to the spindle during M phase (54, 58). And it localizes to the midbody during cytokinesis (26, 54, 57). The localization pattern of OGA is quite different. At mitosis, OGA is ubiquitous, but absent from the newly formed nuclear membranes of the two daughter cells (54). During cytokinesis, OGA is diffused, without a distinct midbody localization (57).

O-GlcNAc and the Mitotic Master Kinases Are Intertwined

A link between O-GlcNAc and the mitotic master kinases have also been identified. The cell cycle is regulated by a concerted choreography of cyclins and CDKs (70). Investigations show that O-GlcNAc modulates cyclin stability. To begin with, cyclin D abundance increases during G1 and declines in S and M phases. OGA overproduction delays the increase of cyclin D (54), while OGT overproduction constitutively decreases cyclin D levels, partly due to delayed mitosis (54). Another example is cyclins A and B. Cyclin B peaks during prophase and decreases during metaphase, and cyclin A peaks in G2. In cells that overproduce OGT or OGA, protein abundance of cyclins A and B fails to decline, probably due to mitotic exit defects (54).

O-GlcNAc regulates two key mitotic kinases, CDK1 and Plk1 (**Figure 1**). CDK1 regulates Plk1 through Myosin phosphatase targeting protein 1 (MYPT1), which is a targeting subunit of protein phosphatase 1cβ(PP1cβ) (72). During mitosis, Cdk1 phosphorylates MYPT1 at S473, creating a binding pocket between MYPT1 and Plk1. Thus MYPT1 recruits PP1cβ to dephosphorylate Plk1 at pT210, the activation phosphorylation site (71). Intriguingly, MYPT1 is also a targeting subunit of OGT in neuroblastoma cells (73), raising the tantalizing possibilty that MYPT1 targets both PP1β and OGT to the same substrate, so that the substrate protein could be dephosphorylated and O-GlcNAcylated simultaneously. Indeed, Plk1 is identified to be O-GlcNAcylated in an *in vitro* OGT assay (74), but whether this occurs *in vivo,* or O-GlcNAcylation interplays with pT210 of Plk1 is elusive. To add yet another layer of complexity, MYPT1 itself is O-GlcNAcylated (73). We are yet to find out the exact function of this PTM.

Overproduction of OGT decreases mRNA levels of Plk1 and therefore Plk1 protein levels, which further decreases the abundance of Membrane Associated Tyrosine and Threonine cdc2 inhibitory Kinase (MYT1) and increases

TABLE 1 | Effects of OGT and OGA on cell cycle progression.

Cell cycle phase	O-GlcNAcylation levels	OGT localization patterns, overproduction/deletion studies	OGA localization patterns, overproduction/deletion studies
S phase	O-GlcNAc decreases (53)		OGA activity increases (53)
G2/M	Increased O-GlcNAc delays G2/M in cultured cells (54). Increased O-GlcNAc is observed in G2/M entry in *X. laevis* (55).		OGA inhibition hampered G2/M transition (56)
M phase	O-GlcNAc levels decrease (54, 57)	OGT localizes to the spindle (58).	OGA is ubiquitous, but absent from the newly formed nuclear membranes of the two daughter cells (54).
		OGT protein amounts decrease (58). OGT mRNA levels decrease (59) OGT overproduction leads to chromosome bridges, inhibits CDK1 activity (50), reduces both mRNA and protein levels of Polo-like kinase 1 (PLK1) (50).	OGA disruption results in lagging chromosomes and micronuclei (60); OGA knockdown HeLa cell lines manifested spindle defects and mitotic exit effects (61)
Cytokinesis		OGT localizes to the midbody (26, 57). OGT deletion results in vimentin bridges (26). OGT overexpression results in polypoidy (26, 54).	OGA is diffuse, not at the midbody (57). OGA disruption leads to cytokinesis failure (60)

TABLE 2 | O-GlcNAcylated proteins during the unperturbed cell cycle*.

Cell cycle phase	Protein name	Molecular details	References
G1 phase	Retinoblastoma (Rb)	Rb is O-GlcNAcylated *in vitro* and *in vivo*. And this modification increases in G1.	(62)
	Minichromosome maintenance protein (MCM)	Mcm3,6,7 are O-GlcNAcylated.	(53)
M phase	Histone 3 (H3)	H3 is O-GlcNAcylated at T32, and antagonizes phosphorylation at S10 of H3.	(56)
		Increasing UDP-GlcNAc suppresses phosphorylation at S10 of H3.	(63)
	Cdh1	Cdh1 is O-GlcNAcylated in both cultured cells and mouse brain extracts. O-GlcNAc antagonizes its phosphorylation, promotes its interaction with Anaphase Promoting Complex/Cyclosome (APC/C) and enhances the activity of APC/C.	(51)
	NuMA1	O-GlcNAcylated NuMA1 interacts with Galectin-3, localizes to the spindle pole, essential for mitotic spindle cohesion	(64)
	Ewing Sarcoma Breakpoint Region 1 (EWS)	EWS is O-GlcNAcyated to promote its nuclear localization. O-GlcNAc of EWS increases in OGA KO cells, resulting in uneven distribution of the spindle mizdone	(65) (61)
Cytokinesis	Vimentin	Vimentin is O-GlcNAcylated. During cytokinesis, O-GlcNAcylation promotes phosphorylation of S71 of vimentin, results in vimentin filament disassembly and ensures a complete cytokinesis.	(57) (26, 66)

**This table only contains proteins whose molecular mechanism is well studied. Many other proteins have been identified in many proteomic screens, but their functional significance is not well understood.*

the activity of MYT1. As MYT1 phosphorylates CDK1 in an inhibitory manner, thus OGT overexpression increases the inhibitory phosphorylation of CDK1 (50). Another branch of the network concerns Cdc25, the activating phosphatase of CDK1. On one hand, Plk1 phosphorylates Cdc25, which in turn dephosphorylates and activates CDK1. On the other hand, OGT overproduction curbs mRNA levels of Cdc25 and subsequent protein levels, thus inactivating CDK1 (50). In sum, O-GlcNAc exerts its role through protein abundance at the transcriptional level. OGT overproduction increases the inhibitory phosphorylation of CDK1, and decreases phosphorylation levels of its substrates (50).

A third key kinase, Aurora B, is also extensively studied (75). Aurora B is a component of the chromosomal passenger complex (CPC) that also comprises INCENP, Survivin, and Borealin. CPC is an essential driver of the late mitotic events, including assembly and disassembly of the mitotic spindle, activation of the spindle assembly checkpoint and cytokinesis (75). Both OGT and OGA are in a complex with Aurora B and protein phosphatase 1 (PP1) during M phase by coIP studies (57). Moreover, chemical inhibition of Aurora B enhances OGT protein abundance and therefore cellular O-GlcNAcylation levels during M phase (57). Importantly, the spindle localization of OGT is derailed by Aurora B inhibition (57). It will be of particular interest to investigate whether Aurora B phosphorylates OGT or OGA in due course.

O-GlcNAcylated Proteins in the S Phase

The retinoblastoma protein (RB) is a classical tumor suppressor that is key for the replication process (76). In the G1 phase,

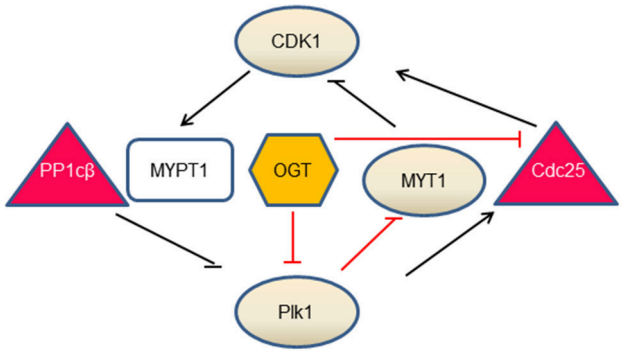

FIGURE 1 | The interlinked network between O-GlcNAc and mitotic kinases. Our current understandings comprise three branches. During mitosis, CDK1 phosphorylates MYPT1 to promote its interaction with Plk1. MYPT1 recruits PP1cβ to dephosphorylate and inactivate Plk1 (71). In the second branch, OGT decreases Plk1 protein levels, which further increases MYT1 levels and decreases MYT1 phosphorylation. As MYT1 inhibits CDK1 by phosphorylation, OGT thus promotes inhibitory phosphorylation of CDK1. In the third branch, OGT inactivates CDK1, via down-regulating the mRNA levels of Cdc25-the activating phosphatase of CDK1 (50). Whether OGT is enmeshed in the MYPT1 branch is not understood. Kinases are in circles, phosphatases are in triangles, MYPT1 is in a square and OGT is in a hexagon. Lines in black denote direct effects (phosphorylation or dephosphorylation), and lines in red demarcate indirect effects (mRNA or protein levels).

Rb is hypophosphorylated and binds the transcription factor E2F-1, an essential transcription factor for many S phase genes. In the late G1 phase, Rb is hyperphosphorylated by CDKs, thus releasing E2F-1 to transcribe downstream S phase genes (76). Consequently, cells will enter S phase. Both *in vitro* and *in vivo* experiments show that Rb is O-GlcNAcylated, with the highest O-GlcNAc levels in the G1 phase, suggesting that O-GlcNAcylation of Rb antagonizes CDK-dependent phosphorylation and inactivates the transcriptional activities of E2F1 (62). It will be of further interest to pinpoint the modification residues and study its effects on cell cycle.

Conversely, the transcription levels of *OGT* and *OGA* are also regulated by Rb/E2F1 (77). *OGT* and *OGA* expression is reduced by overproduction of E2F1 in HEK293 cells and is increased in $E2F1^{-/-}$ mouse fibroblasts and $Rb^{-/-}$mouse embryonic fibroblasts (MEFs). E2F1 overproduction does not change *OGT* or *OGA* expression levels in $Rb^{-/-}$MEFs, suggesting that E2F1 negatively regulates *OGT* and *OGA* expression in an Rb-dependent manner (77). Mechanistically, consensus E2F binding sequences were identified on *OGT* and *OGA* and confirmed by reporter-based assays and *in silico* modeling (77). Therefore, expression of *OGT* or *OGA* is not constant, but subject to multiple layers of regulations.

The minichromosome maintenance (MCM) replicative helicase, comprising Mcm2-7, is loaded onto the DNA in the G1 phase, thus restricting one round of DNA replication per cell cycle (78). The Mcm2-7 is activated in S phase to unwind DNA. Investigations have shown that loading and activation never occur concomitantly, and not all MCMs loaded are activated in one cell cycle (79). Based on the recent cryoelectron microscopy (cryo-EM) data, an elaborate Acrobat Model has been proposed to elucidate how the MCMs are loaded to form a double hexamer (80). Phosphorylation (79), SUMOylation (81), and ubiquitination (82, 83) have been identified to distinct subunits of MCMs to regulate their recruitment, activation and disassembly. Interestingly, MCM3, 6, 7 are O-GlcNAcylated, with the alteration pattern of Mcm7 different from Mcm3 and 6 (53). The significance of this modification is still up in the air.

O-GlcNAcylated Proteins in Mitosis

All four core histones, H2A, H2B, H3, and H4 are found to be O-GlcNAcylated (63). By centrifugal elutriation, histone O-GlcNAcylation is found to be high in the G1 phase, decreases during the S phase and elevates during S/G2 transition (63). Glycosylated H3, specifically, is higher in interphase than mitosis (56). Histone H3 Ser10 phosphorylation (H3pS10), a landmark of mitosis, is interconnected with O-GlcNAcylation. Mechanistically, H3 is O-GlcNAcylated at T32, and O-GlcNAcylated H3 reduces H3pS10 (56). In general, overproduction of OGT increases H3K9Ac and H3K27me3 levels in mitosis, decreases H3pS10 levels in mitosis and decreases H3R17me2 levels in both asynchronous and mitotic cells (58).

Besides histones, our study about Fizzy-related protein homolog (Cdh1) provides another example of the yin-yang paradigm of O-GlcNAc. Cdh1 is the coactivator of the E3 ligase, anaphase promoting complex (APC), and is phosphorylated at multiple sites (84), with four significant phosphorylation residues at S40, T121, S151, and S163 suppressing the activity of APC (85). O-GlcNAc of Cdh1 has been identified *in vitro* (86). Our assays reveal that O-GlcNAcylation occurs at a peptide harboring S40, and O-GlcNAcylation antagonizes phosphorylation, thus activating APC (51).

The proto-oncoprotein Ewing Sarcoma Breakpoint Region 1 (EWS) binds with both RNA and DNA and localizes to the nucleus, cytosol and cell membranes. Upon adipogenic stimuli EWS is O-GlcNAcylated, which partly promotes its nuclear localization (65). In mitosis, EWS recruits Aurora B and CPC to the spindle midzone (87). In OGA-knockdown cells, O-GlcNAcylation of EWS elevates significantly, resulting in uneven distribution of the spindle mizdone (61).

In an extensive glycoproteomic and phosphoproteomics screen, 141 new O-GlcNAc sites were pinpointed on proteins involved in the spindle apparatus and cytokinesis (50). Many proteins involved in mitosis have also been identified to be O-GlcNAcylated, including the nuclear mitotic apparatus protein 1 (NuMA1), nuclear pore protein 153 (Nup153) and BRCA2-interacting transcriptional repressor EMSY (50). Follow-up investigations reveal that NuMA1 interacts with Galectin-3 in an O-GlcNAcylation-dependent manner (64). Galectin-3 is a small soluble lectin of the Galectin family that localizes to the centrosomes. The newly identified Galectin-3-O-GlcNAc-NuMA1 complex not only localizes NuMA1 to spindle poles, but also is essential for mitotic spindle cohesion (64).

Paradoxically, OGT itself is subject to O-GlcNAcylation (58, 88), which is completely abolished during mitosis, and reappears in G1 (58). It will be an intriguing possibility that O-GlcNAcylation of OGT itself promotes its own stability, so that its abundance declines when the modification drops. Further studies

will surely provide more mechanistic insights of O-GlcNAc in mitosis.

O-GlcNAclated Proteins in Cytokinesis

Vimentin is an intermediate filament protein, and there have been a few reports on its O-GlcNAcylation. Vimentin is O-GlcNAcylated during M phase, and is also subject to phosphorylation by Cdk1, Plk1, Aurora B, and Rho kinase (21–25, 57). *In vitro* studies suggest that vimentin interacts with GlcNAc-bearing polymers, which promotes phosphorylation of vimentin S71 (66). Cellular assays suggest that vimentin pS71 levels increase when either OGT or OGA is overexpressed (57). Our studies show that when cells are synchronized in cytokinesis, O-GlcNAcylation of vimentin promotes pS71 (26). *OGT* knockdown by siRNA significantly attenuates vimentin pS71, thus forming elongated vimentin bridges during cytokinesis, and impeding daughter cell separation (26). Moreover, Chk1, a kinase pivotal for both DDR and cytokinesis, phosphorylates OGT at S20 specifically during cytokinesis. This phosphorylation is vital for OGT to localize to midbodies and maintain cellular O-GlcNAcylation levels (26). Thus, OGT-S20A mutant cells display vimentin bridge defects due to compromised O-GlcNAcylation levels and consequently quench pS71 of vimentin (26). It will be of keen interest to explore more O-GlcNAcylated proteins in cytokinesis.

O-GLCNAC IN THE DDR: A GUARDIAN OF THE GENOME

Our discussion on cell cycle events will not be complete without DDR. The genomic DNA is subject to many intrinsic or extrinsic lesions, such as double-strand breaks (DSBs), DNA crosslinking damage or DNA alkylation damage. Failure to repair these damages will lead to not only chromosomal abnormalities on the cellular level, but also fatal diseases such as cancer (89). Facing these genomic insults, organisms develop elaborate surveillance mechanisms-DNA damage checkpoints-to ensure genome integrity (90). The term "checkpoint" was coined by the Nobel Laureate, Dr. Leland Hartwell, almost three decades ago to describe the series of concerted responses to deleterious signals, including cell cycle arrest, transcription activation or suppression, and DNA repair. If the damage is beyond repair, then cells might undergo senescence or apoptosis (91).

In-depth investigations have identified an extensive network of proteins as guardians of our genomes to sense, mediate, and repair the damages (92). And these proteins are subject to phosphorylation, mono- or polyubiquitination, or SUMOylation. The very first step in the DDR pathway is the phosphorylation of H2AX (γH2AX) by a group of phosphatidylinositide-3 (PI-3)-like kinases, including ataxia telangiectasia mutated (ATM), ATM, and Rad3 related (ATR) and DNA-dependent protein kinase (DNA-PK) (92). Then γH2AX is recognized by checkpoint mediator proteins, such as mediator of DNA damage checkpoint protein 1 (MDC1). MDC1, along with other mediators, is phosphorylated by ATM, and the DDR signal is propagated downstream to transducer kinases, such as Chk1 and checkpoint kinase 2 (Chk2) (92), to execute homologous recombination (HR) or non-homologous end joining (93) and other repair pathways (92) (**Figure 2**).

As O-GlcNAcylation is deemed as a stress signal, its effects on DNA damage have been of intense interest. As early as 2004, global O-GlcNAcylation levels were investigated after cells were irradiated by the ultraviolet (UV)-B light for 90 s, then recovered for 8 h. It was discovered that O-GlcNAc increased dose-dependently on the UV radiation durations (95). Then in 2015, a comprehensive proteomic study using OGT-null MEFs demonstrated that 232 phosphosites were upregulated compared with OGT wild-type cells (20), among which were ATM pS1987 and Chk1 pS317. Recently, O-GlcNAc was caught at the scene of crime. DNA damages increase O-GlcNAc levels at the damage sites, where both OGT and OGA are recruited (96). OGT abrogation reduces cell viability during DDR (96).

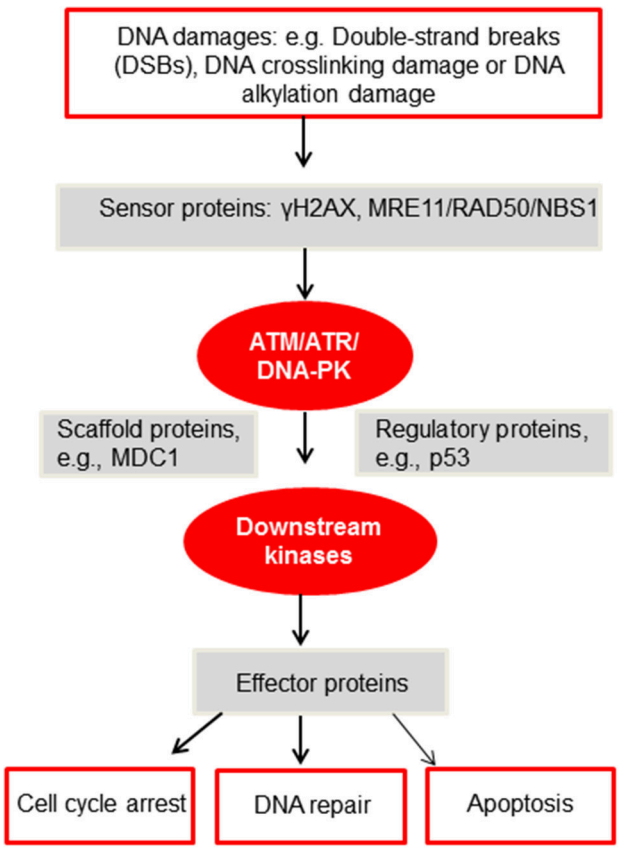

FIGURE 2 | A simplified diagram of the DDR network adapted from Furgason and Bahassi (94). When genomic DNA is faced with various DNA damages, such as but not limited to DSBs, DNA crosslinking damage or alkylation damage, sensor proteins such as γH2AX and the MRE11/RAD50/NBS1 (MRN) complex will then recruit and activate the PIKK kinases, including ATM, ATR and DNA-PK. These PIKK kinases will then phosphorylate downstream targets, including scaffold proteins, regulatory proteins and downstream kinases. Upon activation, these proteins will subsequently phosphorylate effector proteins to undergo cell cycle arrest, DNA repair or apoptosis. For a detailed mechanistic analysis of the DDR, please refer to Ciccia and Elledge (92).

TABLE 3 | O-GlcNAcylated proteins during the DNA damage response.

Protein name	Molecular mechanisms	References
Histone H2AX (H2AX)	H2A is O-GlcNAcylated at T101 at basal levels, and at S139 upon DDR.	(96)
Histone 2B (H2B)	DSBs induce O-GlcNAcylation at S112 of H2B, leading to its binding with Nijmegen breakage syndrome 1 (NBS1), mediating focus formation of NBS1 and subsequent homologous recombination (HR) and nonhomologous end-joining (NHEJ)	(97)
Histone 2A (H2A)	Camptothecin (CPT) or Etoposide (ETP) induces O-GlcNAcylation at S40 of H2A, which coIPs with acetylated H2AZ and γH2AX. O-GlcNAcylated H2AS40 localizes to DNA damage sites. Its aberration prevents recruitment of DNA-PKcs and Rad51.	(98, 99)
Ataxia-telangiectasia mutated (ATM)	In HeLa and primary neuron cells, ATM interacts with OGT and is O-GlcNAcylated. O-GlcNAcylation enhances X-ray induced ATM activation at S1981.	(100)
	In mouse embryonic fibroblasts (MEFs), OGT deletion upregulates ATM activation at S1987.	(20)
DNA-dependent protein kinase (DNA-PK)	DNA-PK is O-GlcNAcylated, and this modification increases upon ER stress, but not upon oxidative stress, osmotic stress, or double-strand breaks (DSBs).	(101)
Mediator of DNA damage checkpoint protein 1 (MDC1),	O-GlcNAcylation of H2AX suppresses its expansion on chromatin during DDR. MDC1 is O-GlcNAcylated upon DDR, which antagonizes its phosphorylation.	(96)
Polη	O-GlcNAcylation at T457 of Polη promotes $CRL4^{CDT2}$-dependent Polη polyubiquitination at K462 and subsequent p97-dependent removal from replication forks, ensuring translesion DNA synthesis (TLS)	(32)

In spite of the significance of DDR, a search of "O-GlcNAc, DNA damage response" in the PubMed only yielded 12 publications. The 2015 quantitative phosphoproteomics study (20) thus provides us a timely route map to explore this uncharted territory. Herein we will review the O-GlcNAcylated DDR proteins, and more importantly, its underlying molecular underpinnings (**Table 3**).

O-GlcNAcylation of Histones

Histone modification is integral to epigenetics, and OGT has been central to epigenetics (102). Here we will only cover histones involved in DDR, including H2AX, H2AS40, and H2B.

Histone H2A has many variants (103) and γH2AX is vital to DDR. H2AX is O-GlcNAcylated at T101 at basal levels and at S139 upon DDR, which restricts the expansion of damage signals, thus limiting DDR (96).

Viviparous animals have either Ser40 (S40) or Ala40 (A40) types of H2A, while non-mammals only have A40 (98, 99). Specific to viviparous organisms, Camptothecin (CPT) or Etoposide (ETP) (both inhibitors for Topoisomerase) induce O-GlcNAcylation at S40 of H2A (98, 99). This modification interacts with γH2AX, recruits DNA-PK and the recombinase Rad51 to the damage sites, and facilitates DDR (98, 99).

Besides H2AX and H2AS40, H2B is O-GlcNAcylated at S112 upon DSBs (97). Then the O-GlcNAcylated H2B binds with the Nijmegen breakage syndrome 1 (NBS1) protein, promoting its recruitment to DSBs and the following repairing events.

O-GlcNAc of Kinases and Scaffolds

Among the DDR proteins, the ATM, DNA-PK kinases, and the scaffold protein MDC1 have been reported to be O-GlcNAcylated. O-GlcNAc of DNA-PK is elevated upon ER stress, but not during oxidative, osmotic or DSB stresses (101). The mediator MDC1 is also O-GlcNAcylated, which counteracts ATM-dependent phosphorylation (96).

Reports about ATM have been controversial. Miura et al. (100) reported that in HeLa cells and primary cultured neurons ATM is O-GlcNAcylated (with CTD110.6) and endogenous ATM coIPs with OGT. O-GlcNAc of ATM enhances ATM activation at S1981 upon X-ray (100), thus O-GlcNAc plays a positive role. Meanwhile, Zhong et al. (20) failed to detect O-GlcNAc of ATM in MEFs. OGT deletion upregulates the activation phosphorylation of ATM at S1987 (the mouse equivalent of human S1981) (20), thus OGT plays a negative role. The discrepancy might lie in different species. Phosphorylation of S1981 has been a hallmark of ATM activation in humans, but mutation of S1987 to Ala does not impede ATM function in mice (104, 105). More in-depth studies are needed to solve the mystery.

The exact modification sites of these proteins were not investigated, probably because ATM, DNA-PK, and MDC1 are all large proteins. Fragmentation studies and precise site mapping will be needed in the future. And whether there are other distinctions between mice and humans, as far as O-GlcNAc is concerned, is at anyone's wild guess.

OGT in DNA Translesion Synthesis (TLS)

TLS utilizes a flurry of distinct and specialized DNA polymerases to replicate damaged regions of DNA (106). Polη is specifically involved in replicative bypass of cyclobutane pyrimidine dimers (CPDs) induced by UV, as well as damages induced by cisplatin (107). It is error prone, with an error rate of 10^{-2}-10^{-3}, thus it is vital to timely remove Polη after DDR.

A peptide of Polη was O-GlcNAcylated *in vitro* (86) and T457 was identified to be O-GlcNAcylated upon DDR in cultured cells (32). This modification promotes polyubiquitination at K462 and subsequent removal of Polη from replication forks. Moreover, O-GlcNAcylated Polη is essential for cisplatin-induced DDR. The deficient T457A mutant enhances UV-induced mutagenesis and also increases cellular sensitivity to cisplatin (32).

Collectively, the reports of OGT in DDR are emerging. From the current few investigations, O-GlcNAc seems to play an overall

positive role: OGT is recruited to damaged sites, where it helps recruit NBS1; it antagonizes phosphorylated H2AX and MDC1 to restrict damage signal expansion; it promotes error-prone Polη to dissociate from chromatin after TLS to bypass UV-induced CPDs. Considering that DDR utilizes distinct pathways in response to each and every DNA damage type, we need more time and energy to elucidate how O-GlcNAc fine-tunes the DDR process.

CONCLUSIONS

In less than two score years, great strides have been made in the field of O-GlcNAcylation. We have witnessed really exciting things in glycobiology, and its utilization in medicine and clinical practice. As we have realized, most bedside applications will depend on our understandings of underlying molecular mechanisms to the ultimate level of resolution. Achieving that will not only enable us to comprehend various biological events, but also bestow upon us rich information as well as rich opportunities to be exploited. As we begin to elucidate the molecular basis of O-GlcNAc and its interaction, we are going to be able to leap profoundly forward into our future.

AUTHOR CONTRIBUTIONS

All authors listed have made a substantial, direct and intellectual contribution to the work, and approved it for publication.

ACKNOWLEDGMENTS

This work was supported by the Capacity Building for Sci-Tech Innovation - Fundamental Scientific Research Funds (025185305000) to JL. We apologize to other colleagues whose work we cannot cite due to space limitations.

REFERENCES

1. Torres CR, Hart GW. Topography and polypeptide distribution of terminal N-acetylglucosamine residues on the surfaces of intact lymphocytes. Evidence for O-linked GlcNAc. *J Biol Chem.* (1984) 259:3308–17.
2. Slawson C, Hart GW. O-GlcNAc signalling: implications for cancer cell biology. *Nat Rev Cancer* (2011) 11:678–84. doi: 10.1038/nrc3114
3. Hart GW, Slawson C, Ramirez-Correa G, Lagerlof O. Cross talk between O-GlcNAcylation and phosphorylation: roles in signaling, transcription, and chronic disease. *Annu Rev Biochem.* (2011) 80:825–58. doi: 10.1146/annurev-biochem-060608-102511
4. Levine ZG, Walker S. The Biochemistry of O-GlcNAc transferase: which functions make it essential in mammalian cells? *Annu Rev Biochem.* (2016) 85:631–57. doi: 10.1146/annurev-biochem-060713-035344
5. Yang X, Qian K. Protein O-GlcNAcylation: emerging mechanisms and functions. *Nat Rev Mol Cell Biol.* (2017) 18:452–65. doi: 10.1038/nrm.2017.22
6. Marshall S, Bacote V, Traxinger RR. Discovery of a metabolic pathway mediating glucose-induced desensitization of the glucose transport system. Role of hexosamine biosynthesis in the induction of insulin resistance. *J Biol Chem.* (1991) 266:4706–12.
7. Lucena MC, Carvalho-Cruz P, Donadio JL, Oliveira IA, De Queiroz RM, Marinho-Carvalho MM, et al. Epithelial mesenchymal transition induces aberrant glycosylation through hexosamine biosynthetic pathway activation. *J Biol Chem.* (2016) 291:12917–29. doi: 10.1074/jbc.M116.729236
8. Vasconcelos-Dos-Santos A, Oliveira IA, Lucena MC, Mantuano NR, Whelan SA, Dias WB, et al. Biosynthetic machinery involved in aberrant glycosylation: promising targets for developing of drugs against cancer. *Front Oncol.* (2015) 5:138. doi: 10.3389/fonc.2015.00138
9. Erickson JR, Pereira L, Wang L, Han G, Ferguson A, Dao K, et al. Diabetic hyperglycaemia activates CaMKII and arrhythmias by O-linked glycosylation. *Nature* (2013) 502:372–6. doi: 10.1038/nature12537
10. Alejandro EU, Bozadjieva N, Kumusoglu D, Abdulhamid S, Levine H, Haataja L, et al. Disruption of O-linked N-acetylglucosamine signaling induces ER stress and beta cell failure. *Cell Rep.* (2015) 13:2527–38. doi: 10.1016/j.celrep.2015.11.020
11. Yuzwa SA, Shan X, Macauley MS, Clark T, Skorobogatko Y, Vosseller K, et al. Increasing O-GlcNAc slows neurodegeneration and stabilizes tau against aggregation. *Nat Chem Biol.* (2012) 8:393–9. doi: 10.1038/nchembio.797
12. Ma Z, Vosseller K. Cancer metabolism and elevated O-GlcNAc in oncogenic signaling. *J Biol Chem.* (2014) 289:34457–65. doi: 10.1074/jbc.R114.577718
13. Buchakjian MR, Kornbluth S. The engine driving the ship: metabolic steering of cell proliferation and death. *Nat Rev Mol Cell Biol.* (2010) 11:715–27. doi: 10.1038/nrm2972
14. Yi W, Clark PM, Mason DE, Keenan MC, Hill C, Goddard WA, et al. Phosphofructokinase 1 glycosylation regulates cell growth and metabolism. *Science* (2012) 337:975–80. doi: 10.1126/science.1222278
15. Rao X, Duan X, Mao W, Li X, Li Z, Li Q, et al. O-GlcNAcylation of G6PD promotes the pentose phosphate pathway and tumor growth. *Nat Commun.* (2015) 6:8468. doi: 10.1038/ncomms9468
16. Wang T, Yu Q, Li J, Hu B, Zhao Q, Ma C, et al. O-GlcNAcylation of fumarase maintains tumour growth under glucose deficiency. *Nat Cell Biol.* (2017) 19:833–43. doi: 10.1038/ncb3562
17. Sodi VL, Bacigalupa ZA, Ferrer CM, Lee JV, Gocal WA, Mukhopadhyay D, et al. Nutrient sensor O-GlcNAc transferase controls cancer lipid metabolism via SREBP-1 regulation. *Oncogene* (2018) 37:924–34. doi: 10.1038/onc.2017.395
18. Groves JA, Maduka AO, O'meally RN, Cole RN, Zachara NE. Fatty acid synthase inhibits the O-GlcNAcase during oxidative stress. *J Biol Chem.* (2017). 292:6493–511. doi: 10.1074/jbc.M116.760785
19. Wang Z, Gucek M, Hart GW. Cross-talk between GlcNAcylation and phosphorylation: site-specific phosphorylation dynamics in response to globally elevated O-GlcNAc. *Proc Natl Acad Sci USA.* (2008) 105:13793–8. doi: 10.1073/pnas.0806216105
20. Zhong J, Martinez M, Sengupta S, Lee A, Wu X, Chaerkady R, et al. Quantitative phosphoproteomics reveals crosstalk between phosphorylation and O-GlcNAc in the DNA damage response pathway. *Proteomics* (2015) 15:591–607. doi: 10.1002/pmic.201400339
21. Tsujimura K, Ogawara M, Takeuchi Y, Imajoh-Ohmi S, Ha MH, Inagaki M. Visualization and function of vimentin phosphorylation by cdc2 kinase during mitosis. *J Biol Chem.* (1994) 269:31097–106.
22. Yamaguchi T, Goto H, Yokoyama T, Sillje H, Hanisch A, Uldschmid A, et al. Phosphorylation by Cdk1 induces Plk1-mediated vimentin phosphorylation during mitosis. *J Cell Biol.* (2005) 171:431–6. doi: 10.1083/jcb.200504091
23. Goto H, Yasui Y, Kawajiri A, Nigg EA, Terada Y, Tatsuka M, et al. Aurora-B regulates the cleavage furrow-specific vimentin phosphorylation in the cytokinetic process. *J Biol Chem.* (2003) 278:8526–30. doi: 10.1074/jbc.M210892200
24. Goto H, Kosako H, Tanabe K, Yanagida M, Sakurai M, Amano M, et al. Phosphorylation of vimentin by Rho-associated kinase at a unique amino-terminal site that is specifically phosphorylated during cytokinesis. *J Biol Chem.* (1998) 273:11728–36. doi: 10.1074/jbc.273.19.11728
25. Yasui Y, Goto H, Matsui S, Manser E, Lim L, Nagata K, et al. Protein kinases required for segregation of vimentin filaments in mitotic process. *Oncogene* (2001) 20:2868–76. doi: 10.1038/sj.onc.1204407
26. Li Z, Li X, Nai S, Geng Q, Liao J, Xu X, et al. Checkpoint kinase 1-induced phosphorylation of O-linked beta-N-acetylglucosamine transferase regulates

the intermediate filament network during cytokinesis. *J Biol Chem.* (2017) 292:19548–55. doi: 10.1074/jbc.M117.811646
27. Qin W, Lv P, Fan X, Quan B, Zhu Y, Qin K, et al. Quantitative time-resolved chemoproteomics reveals that stable O-GlcNAc regulates box C/D snoRNP biogenesis. *Proc Natl Acad Sci USA.* (2017) 114:E6749–58. doi: 10.1073/pnas.1702688114
28. Li MD, Ruan HB, Hughes ME, Lee JS, Singh JP, Jones SP, et al. O-GlcNAc signaling entrains the circadian clock by inhibiting BMAL1/CLOCK ubiquitination. *Cell Metab.* (2013) 17:303–10. doi: 10.1016/j.cmet.2012.12.015
29. Ruan HB, Han X, Li MD, Singh JP, Qian K, Azarhoush S, et al. O-GlcNAc transferase/host cell factor C1 complex regulates gluconeogenesis by modulating PGC-1alpha stability. *Cell Metab.* (2012) 16:226–37. doi: 10.1016/j.cmet.2012.07.006
30. Ding X, Jiang W, Zhou P, Liu L, Wan X, Yuan X, et al. Mixed Lineage Leukemia 5 (MLL5) Protein Stability Is Cooperatively Regulated by O-GlcNac Transferase (OGT) and Ubiquitin Specific Protease 7 (USP7). *PLoS ONE* (2015) 10:e0145023. doi: 10.1371/journal.pone.0145023
31. Chu CS, Lo PW, Yeh YH, Hsu PH, Peng SH, Teng YC, et al. O-GlcNAcylation regulates EZH2 protein stability and function. *Proc Natl Acad Sci USA.* (2014) 111:1355–60. doi: 10.1073/pnas.1323226111
32. Ma X, Liu H, Li J, Wang Y, Ding YH, Shen H, et al. Poleta O-GlcNAcylation governs genome integrity during translesion DNA synthesis. *Nat Commun.* (2017) 8:1941. doi: 10.1038/s41467-017-02164-1
33. Ma J, Hart GW. O-GlcNAc profiling: from proteins to proteomes. *Clin Proteomics* (2014) 11:8. doi: 10.1186/1559-0275-11-8
34. Tashima Y, Stanley P. Antibodies that detect O-linked beta-D-N-acetylglucosamine on the extracellular domain of cell surface glycoproteins. *J Biol Chem.* (2014) 289:11132–42. doi: 10.1074/jbc.M113.492512
35. Ramakrishnan P, Clark PM, Mason DE, Peters EC, Hsieh-Wilson LC, Baltimore D. Activation of the transcriptional function of the NF-kappaB protein c-Rel by O-GlcNAc glycosylation. *Sci Signal.* (2013) 6:ra75. doi: 10.1126/scisignal.2004097
36. Zachara NE, Vosseller K, Hart GW. Detection and analysis of proteins modified by O-linked N-acetylglucosamine. *Curr Protoc Mol Biol.* (2011). Chapter 17:Unit 17.6 doi: 10.1002/0471142727.mb1706s95
37. Xu Q, Yang C, Du Y, Chen Y, Liu H, Deng M, et al. AMPK regulates histone H2B O-GlcNAcylation. *Nucleic Acids Res.* (2014) 42:5594–604. doi: 10.1093/nar/gku236
38. Banerjee PS, Hart GW, Cho JW. Chemical approaches to study O-GlcNAcylation. *Chem Soc Rev.* (2013) 42:4345–57. doi: 10.1039/C2CS35412H
39. Vosseller K, Wells L, Lane MD, Hart GW. Elevated nucleocytoplasmic glycosylation by O-GlcNAc results in insulin resistance associated with defects in Akt activation in 3T3-L1 adipocytes. *Proc Natl Acad Sci USA.* (2002) 99:5313–8. doi: 10.1073/pnas.072072399
40. Macauley MS, Shan X, Yuzwa SA, Gloster TM, Vocadlo DJ. Elevation of Global O-GlcNAc in rodents using a selective O-GlcNAcase inhibitor does not cause insulin resistance or perturb glucohomeostasis. *Chem Biol* (2010) 17:949–58. doi: 10.1016/j.chembiol.2010.07.005
41. Trapannone R, Rafie K, Van Aalten DM. O-GlcNAc transferase inhibitors: current tools and future challenges. *Biochem Soc Trans.* (2016) 44:88–93. doi: 10.1042/BST20150189
42. Liu Y, Ren Y, Cao Y, Huang H, Wu Q, Li W, et al. Discovery of a low toxicity O-GlcNAc transferase (OGT) inhibitor by structure-based virtual screening of natural products. *Sci Rep.* (2017) 7:12334. doi: 10.1038/s41598-017-12522-0
43. Gloster TM, Zandberg WF, Heinonen JE, Shen DL, Deng L, Vocadlo DJ. Hijacking a biosynthetic pathway yields a glycosyltransferase inhibitor within cells. *Nat Chem Biol.* (2011) 7:174–81. doi: 10.1038/nchembio.520
44. Sodi VL, Khaku S, Krutilina R, Schwab LP, Vocadlo DJ, Seagroves TN, et al. mTOR/MYC Axis Regulates O-GlcNAc Transferase Expression and O-GlcNAcylation in Breast Cancer. *Mol Cancer Res.* (2015) 13:923–33. doi: 10.1158/1541-7786.MCR-14-0536
45. Ma Z, Vocadlo DJ, Vosseller K. Hyper-O-GlcNAcylation is anti-apoptotic and maintains constitutive NF-kappaB activity in pancreatic cancer cells. *J Biol Chem.* (2013) 288:15121–30. doi: 10.1074/jbc.M113.470047
46. Perez-Cervera Y, Dehennaut V, Aquino Gil M, Guedri K, Solorzano Mata CJ, Olivier-Van Stichelen S, et al. Insulin signaling controls the expression of O-GlcNAc transferase and its interaction with lipid microdomains. *FASEB J.* (2013) 27:3478–86. doi: 10.1096/fj.12-217984
47. Syka JE, Coon JJ, Schroeder MJ, Shabanowitz J, Hunt DF. Peptide and protein sequence analysis by electron transfer dissociation mass spectrometry. *Proc Natl Acad Sci USA.* (2004) 101:9528–33. doi: 10.1073/pnas.0402700101
48. Schroeder MJ, Webb DJ, Shabanowitz J, Horwitz AF, Hunt DF. Methods for the detection of paxillin post-translational modifications and interacting proteins by mass spectrometry. *J Proteome Res.* (2005) 4:1832–41. doi: 10.1021/pr0502020
49. Chalkley RJ, Burlingame AL. Identification of GlcNAcylation sites of peptides and alpha-crystallin using Q-TOF mass spectrometry. *J Am Soc Mass Spectrom.* (2001) 12:1106–13. doi: 10.1016/S1044-0305(01)00295-1
50. Wang Z, Udeshi ND, Slawson C, Compton PD, Sakabe K, Cheung WD, et al. Extensive crosstalk between O-GlcNAcylation and phosphorylation regulates cytokinesis. *Sci Signal.* (2010) 3:ra2. doi: 10.1126/scisignal.2000526
51. Tian J, Geng Q, Ding Y, Liao J, Dong MQ, Xu X, et al. O-GlcNAcylation Antagonizes Phosphorylation of CDH1 (CDC20 Homologue 1). *J Biol Chem.* (2016) 291:12136–44. doi: 10.1074/jbc.M116.717850
52. Fardini Y, Perez-Cervera Y, Camoin L, Pagesy P, Lefebvre T, Issad T. Regulatory O-GlcNAcylation sites on FoxO1 are yet to be identified. *Biochem Biophys Res Commun.* (2015) 462:151–8. doi: 10.1016/j.bbrc.2015.04.114
53. Drougat L, Olivier-Van Stichelen S, Mortuaire M, Foulquier F, Lacoste AS, Michalski JC, et al. Characterization of O-GlcNAc cycling and proteomic identification of differentially O-GlcNAcylated proteins during G1/S transition. *Biochim Biophys Acta* (2012) 1820:1839–48. doi: 10.1016/j.bbagen.2012.08.024
54. Slawson C, Zachara NE, Vosseller K, Cheung WD, Lane MD, Hart GW. Perturbations in O-linked beta-N-acetylglucosamine protein modification cause severe defects in mitotic progression and cytokinesis. *J Biol Chem.* (2005) 280:32944–56. doi: 10.1074/jbc.M503396200
55. Lefebvre T, Baert F, Bodart JF, Flament S, Michalski JC, Vilain JP. Modulation of O-GlcNAc glycosylation during Xenopus oocyte maturation. *J Cell Biochem.* (2004) 93:999–1010. doi: 10.1002/jcb.20242
56. Fong JJ, Nguyen BL, Bridger R, Medrano EE, Wells L, Pan S, et al. beta-N-Acetylglucosamine (O-GlcNAc) is a novel regulator of mitosis-specific phosphorylations on histone H3. *J Biol Chem.* (2012) 287:12195–203. doi: 10.1074/jbc.M111.315804
57. Slawson C, Lakshmanan T, Knapp S, Hart GW. A mitotic GlcNAcylation/phosphorylation signaling complex alters the posttranslational state of the cytoskeletal protein vimentin. *Mol Biol Cell* (2008) 19:4130–40. doi: 10.1091/mbc.e07-11-1146
58. Sakabe K, Hart GW. O-GlcNAc transferase regulates mitotic chromatin dynamics. *J Biol Chem.* (2010) 285:34460–8. doi: 10.1074/jbc.M110.158170
59. Whitfield ML, Sherlock G, Saldanha AJ, Murray JI, Ball CA, Alexander KE, et al. Identification of genes periodically expressed in the human cell cycle and their expression in tumors. *Mol Biol Cell* (2002) 13:1977–2000. doi: 10.1091/mbc.02-02-0030
60. Yang YR, Song M, Lee H, Jeon Y, Choi EJ, Jang HJ, et al. O-GlcNAcase is essential for embryonic development and maintenance of genomic stability. *Aging Cell* (2012) 11:439–48. doi: 10.1111/j.1474-9726.2012.00801.x
61. Lanza C, Tan EP, Zhang Z, Machacek M, Brinker AE, Azuma M, et al. Reduced O-GlcNAcase expression promotes mitotic errors and spindle defects. *Cell Cycle* (2016) 15:1363–75. doi: 10.1080/15384101.2016.1167297
62. Wells L, Slawson C, Hart GW. The E2F-1 associated retinoblastoma-susceptibility gene product is modified by O-GlcNAc. *Amino Acids* (2011) 40:877–83. doi: 10.1007/s00726-010-0709-x
63. Zhang S, Roche K, Nasheuer HP, Lowndes NF. Modification of histones by sugar beta-N-acetylglucosamine (GlcNAc) occurs on multiple residues, including histone H3 serine 10, and is cell cycle-regulated. *J Biol Chem.* (2011) 286:37483–95. doi: 10.1074/jbc.M111.284885
64. Magescas J, Sengmanivong L, Viau A, Mayeux A, Dang T, Burtin M, et al. Spindle pole cohesion requires glycosylation-mediated localization of NuMA. *Sci Rep.* (2017) 7:1474. doi: 10.1038/s41598-017-01614-6
65. Li Q, Kamemura K. Adipogenesis stimulates the nuclear localization of EWS with an increase in its O-GlcNAc glycosylation in 3T3-L1 cells. *Biochem Biophys Res Commun.* (2014) 450:588–92. doi: 10.1016/j.bbrc.2014.06.013

66. Komura K, Ise H, Akaike T. Dynamic behaviors of vimentin induced by interaction with GlcNAc molecules. *Glycobiology* (2012) 22:1741–59. doi: 10.1093/glycob/cws118
67. Tan EP, Duncan FE, Slawson C. The sweet side of the cell cycle. *Biochem Soc Trans* (2017) 45:313–22. doi: 10.1042/BST20160145
68. Prosser SL, Pelletier L. Mitotic spindle assembly in animal cells: a fine balancing act. *Nat Rev Mol Cell Biol.* (2017) 18:187–201. doi: 10.1038/nrm.2016.162
69. Tan EP, Caro S, Potnis A, Lanza C, Slawson C. O-linked N-acetylglucosamine cycling regulates mitotic spindle organization. *J Biol Chem.* (2013) 288:27085–99. doi: 10.1074/jbc.M113.470187
70. Guardavaccaro D, Pagano M. Stabilizers and destabilizers controlling cell cycle oscillators. *Mol Cell* (2006) 22:1–4. doi: 10.1016/j.molcel.2006.03.017
71. Yamashiro S, Yamakita Y, Totsukawa G, Goto H, Kaibuchi K, Ito M, et al. Myosin phosphatase-targeting subunit 1 regulates mitosis by antagonizing polo-like kinase 1. *Dev Cell* (2008) 14:787–97. doi: 10.1016/j.devcel.2008.02.013
72. Ito M, Nakano T, Erdodi F, Hartshorne DJ. Myosin phosphatase: structure, regulation and function. *Mol Cell Biochem.* (2004) 259:197–209. doi: 10.1023/B:MCBI.0000021373.14288.00
73. Cheung WD, Sakabe K, Housley MP, Dias WB, Hart GW. O-linked beta-N-acetylglucosaminyltransferase substrate specificity is regulated by myosin phosphatase targeting and other interacting proteins. *J Biol Chem.* (2008) 283:33935–41. doi: 10.1074/jbc.M806199200
74. Dias WB, Cheung WD, Hart GW. O-GlcNAcylation of kinases. *Biochem Biophys Res Commun.* (2012) 422:224–8. doi: 10.1016/j.bbrc.2012.04.124
75. Carmena M, Wheelock M, Funabiki H, Earnshaw WC. The chromosomal passenger complex (CPC): from easy rider to the godfather of mitosis. *Nat Rev Mol Cell Biol.* (2013) 13:789–803. doi: 10.1038/nrm3474
76. Fischer M, Muller GA. Cell cycle transcription control: DREAM/MuvB and RB-E2F complexes. *Crit Rev Biochem Mol Biol.* (2017) 52:638–62. doi: 10.1080/10409238.2017.1360836
77. Muthusamy S, Hong KU, Dassanayaka S, Hamid T, Jones SP. E2F1 Transcription Factor Regulates O-linked N-acetylglucosamine (O-GlcNAc) Transferase and O-GlcNAcase Expression. *J Biol Chem.* (2015) 290:31013–24. doi: 10.1074/jbc.M115.677534
78. Bochman ML, Schwacha A. The Mcm complex: unwinding the mechanism of a replicative helicase. *Microbiol Mol Biol Rev.* (2009) 73:652–83. doi: 10.1128/MMBR.00019-09
79. Deegan TD, Diffley JF. MCM: one ring to rule them all. *Curr Opin Struct Biol.* (2016) 37:145–51. doi: 10.1016/j.sbi.2016.01.014
80. Zhai Y, Li N, Jiang H, Huang X, Gao N, Tye BK. Unique Roles of the Non-identical MCM Subunits in DNA replication licensing. *Mol Cell* (2017) 67:168–79. doi: 10.1016/j.molcel.2017.06.016
81. Wei L, Zhao X. A new MCM modification cycle regulates DNA replication initiation. *Nat Struct Mol Biol.* (2016) 23:209–16. doi: 10.1038/nsmb.3173
82. Moreno SP, Bailey R, Campion N, Herron S, Gambus A. Polyubiquitylation drives replisome disassembly at the termination of DNA replication. *Science* (2014) 346:477–81. doi: 10.1126/science.1253585
83. Maric M, Maculins T, De Piccoli G, Labib K. Cdc48 and a ubiquitin ligase drive disassembly of the CMG helicase at the end of DNA replication. *Science* (2014) 346:1253596. doi: 10.1126/science.1253596
84. Kramer ER, Scheuringer N, Podtelejnikov AV, Mann M, Peters JM. Mitotic regulation of the APC activator proteins CDC20 and CDH1. *Mol Biol Cell* (2000) 11:1555–69. doi: 10.1091/mbc.11.5.1555
85. Lukas C, Sorensen CS, Kramer E, Santoni-Rugiu E, Lindeneg C, Peters JM, et al. Accumulation of cyclin B1 requires E2F and cyclin-A-dependent rearrangement of the anaphase-promoting complex. *Nature* (1999) 401:815–8. doi: 10.1038/44611
86. Pathak S, Alonso J, Schimpl M, Rafie K, Blair DE, Borodkin VS, et al. The active site of O-GlcNAc transferase imposes constraints on substrate sequence. *Nat Struct Mol Biol.* (2015) 22:744–50. doi: 10.1038/nsmb.3063
87. Park H, Turkalo TK, Nelson K, Folmsbee SS, Robb C, Roper B, et al. Ewing sarcoma EWS protein regulates midzone formation by recruiting Aurora B kinase to the midzone. *Cell Cycle* (2014) 13:2391–9. doi: 10.4161/cc.29337
88. Kreppel LK, Blomberg MA, Hart GW. Dynamic glycosylation of nuclear and cytosolic proteins. Cloning and characterization of a unique O-GlcNAc transferase with multiple tetratricopeptide repeats. *J Biol Chem.* (1997) 272:9308–15. doi: 10.1074/jbc.272.14.9308
89. Finn K, Lowndes NF, Grenon M. Eukaryotic DNA damage checkpoint activation in response to double-strand breaks. *Cell Mol Life Sci.* (2012) 69:1447–73. doi: 10.1007/s00018-011-0875-3
90. Hartwell LH, Weinert TA. Checkpoints: controls that ensure the order of cell cycle events. *Science* (1989) 246:629–34. doi: 10.1126/science.2683079
91. Harper JW, Elledge SJ. The DNA damage response: ten years after. *Mol Cell* (2007) 28:739–45. doi: 10.1016/j.molcel.2007.11.015
92. Ciccia A, Elledge SJ. The DNA damage response: making it safe to play with knives. *Mol Cell* (2010) 40:179–204. doi: 10.1016/j.molcel.2010.09.019
93. Li J, Xu X. DNA double-strand break repair: a tale of pathway choices. *Acta Biochim Biophys Sin.* (2016) 48:641–6. doi: 10.1093/abbs/gmw045
94. Furgason JM, Bahassi El M. Targeting DNA repair mechanisms in cancer. *Pharmacol Ther.* (2013) 137:298–308. doi: 10.1016/j.pharmthera.2012.10.009
95. Zachara NE, O'donnell N, Cheung WD, Mercer JJ, Marth JD, Hart GW. Dynamic O-GlcNAc modification of nucleocytoplasmic proteins in response to stress. A survival response of mammalian cells. *J Biol Chem.* (2004) 279:30133–42. doi: 10.1074/jbc.M403773200
96. Chen Q, Yu X. OGT restrains the expansion of DNA damage signaling. *Nucleic Acids Res.* (2016) 44:9266–78. doi: 10.1093/nar/gkw663
97. Wang P, Peng C, Liu X, Liu H, Chen Y, Zheng L, et al. OGT mediated histone H2B S112 GlcNAcylation regulates DNA damage response. *J Genet Genomics* (2015) 42:467–75. doi: 10.1016/j.jgg.2015.07.002
98. Hayakawa K, Hirosawa M, Tani R, Yoneda C, Tanaka S, Shiota K. H2A O-GlcNAcylation at serine 40 functions genomic protection in association with acetylated H2AZ or gammaH2AX. *Epigenetics Chromatin* (2017) 10:51. doi: 10.1186/s13072-017-0157-x
99. Hirosawa M, Hayakawa K, Yoneda C, Arai D, Shiota H, Suzuki T, et al. Novel O-GlcNAcylation on Ser(40) of canonical H2A isoforms specific to viviparity. *Sci Rep.* (2016) 6:31785. doi: 10.1038/srep31785
100. Miura Y, Sakurai Y, Endo T. O-GlcNAc modification affects the ATM-mediated DNA damage response. *Biochim Biophys Acta* (2012) 1820:1678–85. doi: 10.1016/j.bbagen.2012.06.013
101. Zachara NE, Molina H, Wong KY, Pandey A, Hart GW. The dynamic stress-induced "O-GlcNAc-ome" highlights functions for O-GlcNAc in regulating DNA damage/repair and other cellular pathways. *Amino Acids* (2011) 40:793–808. doi: 10.1007/s00726-010-0695-z
102. Lewis BA, Hanover JA. O-GlcNAc and the epigenetic regulation of gene expression. *J Biol Chem.* (2014) 289:34440–8. doi: 10.1074/jbc.R114.595439
103. Vardabasso C, Hasson D, Ratnakumar K, Chung CY, Duarte LF, Bernstein E. Histone variants: emerging players in cancer biology. *Cell Mol Life Sci.* (2014) 71:379–404. doi: 10.1007/s00018-013-1343-z
104. Pellegrini M, Celeste A, Difilippantonio S, Guo R, Wang W, Feigenbaum L, et al. Autophosphorylation at serine 1987 is dispensable for murine Atm activation *in vivo*. *Nature* (2006) 443:222–5. doi: 10.1038/nature05112
105. Shiloh Y, Ziv Y. The ATM protein kinase: regulating the cellular response to genotoxic stress, and more. *Nat Rev Mol Cell Biol.* (2013) 14:197–210. doi: 10.1038/nrm3546
106. Sale JE. Translesion DNA synthesis and mutagenesis in eukaryotes. *Cold Spring Harb Perspect Biol.* (2013) 5:a012708. doi: 10.1101/cshperspect.a012708
107. Prakash S, Johnson RE, Prakash L. Eukaryotic translesion synthesis DNA polymerases: specificity of structure and function. *Annu Rev Biochem.* (2005) 74:317–53. doi: 10.1146/annurev.biochem.74.082803.133250

Conflict of Interest Statement: The authors declare that the research was conducted in the absence of any commercial or financial relationships that could be construed as a potential conflict of interest.

frontiers in Endocrinology

ORIGINAL RESEARCH
published: 20 August 2018
doi: 10.3389/fendo.2018.00450

Apart From Rhoptries, Identification of *Toxoplasma gondii's* *O*-GlcNAcylated Proteins Reinforces the Universality of the *O*-GlcNAcome

Moyira Osny Aquino-Gil[1,2,3], Mattis Kupferschmid[4], Hosam Shams-Eldin[4], Jörg Schmidt[4], Nao Yamakawa[1], Marlène Mortuaire[1], Frédéric Krzewinski[1], Stéphan Hardivillé[1], Edgar Zenteno[5], Christian Rolando[6], Fabrice Bray[6], Eduardo Pérez Campos[2,3], Jean-François Dubremetz[7], Yobana Perez-Cervera[2,3], Ralph T. Schwarz[1,4†] and Tony Lefebvre[1†]*

[1] Univ. Lille, CNRS, UMR 8576, UGSF, Unité de Glycobiologie Structurale et Fonctionnelle, Lille, France, [2] Instituto Tecnológico de Oaxaca, Tecnológico Nacional de México, Oaxaca, Mexico, [3] Centro de Investigación Facultad de Medicina UNAM-UABJO, Facultad de Odontología, Universidad Autónoma Benito Juárez de Oaxaca, Oaxaca, Mexico, [4] Laboratory of Parasitology, Institute for Virology, Philipps-University, Marburg, Germany, [5] Facultad de Medicina de la Universidad Nacional Autónoma de México, Mexico City, Mexico, [6] CNRS, MSAP USR 3290, FR 3688 FRABIO, FR 2638 Institut Eugène-Michel Chevreul, Université de Lille, Lille, France, [7] Unité Mixte de Recherche 5235, Dynamique des Interactions Membranaires Normales et Pathologiques, Université Montpellier, Montpellier, France

O-linked β-N-acetylglucosaminylation or *O*-GlcNAcylation is a widespread post-translational modification that belongs to the large and heterogeneous group of glycosylations. The functions managed by *O*-GlcNAcylation are diverse and include regulation of transcription, replication, protein's fate, trafficking, and signaling. More and more evidences tend to show that deregulations in the homeostasis of *O*-GlcNAcylation are involved in the etiology of metabolic diseases, cancers and neuropathologies. *O*-GlcNAc transferase or OGT is the enzyme that transfers the N-acetylglucosamine residue onto target proteins confined within the cytosolic and nuclear compartments. A form of OGT was predicted for *Toxoplasma* and recently we were the first to show evidence of *O*-GlcNAcylation in the apicomplexans *Toxoplasma gondii* and *Plasmodium falciparum*. Numerous studies have explored the *O*-GlcNAcome in a wide variety of biological models but very few focus on protists. In the present work, we used enrichment on sWGA-beads and immunopurification to identify putative *O*-GlcNAcylated proteins in *Toxoplasma gondii*. Many of the proteins found to be *O*-GlcNAcylated were originally described in higher eukaryotes and participate in cell shape organization, response to stress, protein synthesis and metabolism. In a more original way, our proteomic analyses, confirmed by sWGA-enrichment and click-chemistry, revealed that rhoptries, proteins necessary for invasion, are glycosylated. Together, these data show that regardless of proteins strictly specific to organisms, *O*-GlcNAcylated proteins are rather similar among living beings.

Keywords: *T. gondii*, *O*-GlcNAcome, *O*-GlcNAcylation, proteomics, toxoplasmosis, rhoptries

OPEN ACCESS

Edited by:
Xiaoyong Yang,
Yale School of Medicine, Yale University, United States

Reviewed by:
Chad Slawson,
Kansas University of Medical Center Research Institute, United States
Michelle R. Bond,
National Institutes of Health (NIH), United States

****Correspondence:***
Tony Lefebvre
tony.lefebvre@univ-lille.fr

† These authors have contributed equally to this work

Specialty section:
This article was submitted to Molecular and Structural Endocrinology, a section of the journal Frontiers in Endocrinology

Received: *14 May 2018*
Accepted: *20 July 2018*
Published: *20 August 2018*

Citation:
Aquino-Gil MO, Kupferschmid M, Shams-Eldin H, Schmidt J, Yamakawa N, Mortuaire M, Krzewinski F, Hardivillé S, Zenteno E, Rolando C, Bray F, Pérez Campos E, Dubremetz J-F, Perez-Cervera Y, Schwarz RT and Lefebvre T (2018) Apart From Rhoptries, Identification of Toxoplasma gondii's O-GlcNAcylated Proteins Reinforces the Universality of the O-GlcNAcome. Front. Endocrinol. 9:450. doi: 10.3389/fendo.2018.00450

INTRODUCTION

Most of the proteins are subjected to covalent chemical modifications that occur co- or post-translationally. Post-translational modifications (PTMs) are very diverse and consist in the addition—usually enzymatically—of simple or complex (e.g., peptides, proteins, glycosylphosphatidylinositol) groups, or in the proteolytic cleavage to enlarge the complexity of the proteome (1). To date, many hundreds of PTMs have been described among which are found a wide variety of glycosylations including the *O*-linked β-N-acetylglucosaminylation (*O*-GlcNAcylation). *O*-GlcNAcylation is a modification of cytosolic, nuclear and mitochondrial proteins by a single residue of N-acetylglucosamine transferred from UDP-GlcNAc which is provided by the hexosamine biosynthetic pathway (HBP). *O*-GlcNAcylation cycles on and off targeted proteins, and the addition and hydrolysis of the GlcNAc moiety is respectively controlled by OGT (*O*-GlcNAc transferase) and OGA (*O*-GlcNAcase) (2, 3). The functions managed by *O*-GlcNAcylation abound as testified by the non-exhaustive list of processes in which the PTM is involved: cell signaling, adaptation to stress, epigenetics, gene expression, protein synthesis and degradation, glycolysis, glucose sensing, enzymatic activity, circadian clock, immune response [for recent reviews see (3–6)]. Regulation of protein-to-protein interactions by *O*-GlcNAcylation (1, 7) directly or in close cooperation with other PTMs (1) seems to be at the nexus of such diversity of functions. Surprisingly, it was found that beyond protein *O*-GlcNAcylation, OGT also proteolytically processes the cell cycle regulator HCF-1 (Host cell factor-1) into a mature form through a glutamate glycosylation dependent manner (8, 9). Deregulations in *O*-GlcNAcylation cycling were reported in different human pathologies: cancers, type-2 diabetes, cardiovascular and neuronal disorders (10).

While extensively studied in cultured cell lines and animal models, few investigations have been reported regarding *O*-GlcNAcylation in intracellular parasites. In the early nineties, Dieckman-Schuppert and collaborators documented, for the very first time, *O*-GlcNAcylation in apicomplexans (11). Analyses of erythrocytes infected with *Plasmodium falciparum* indicated that parasite's *O*-glycans exhibiting terminal GlcNAc were *O*-GlcNAc.

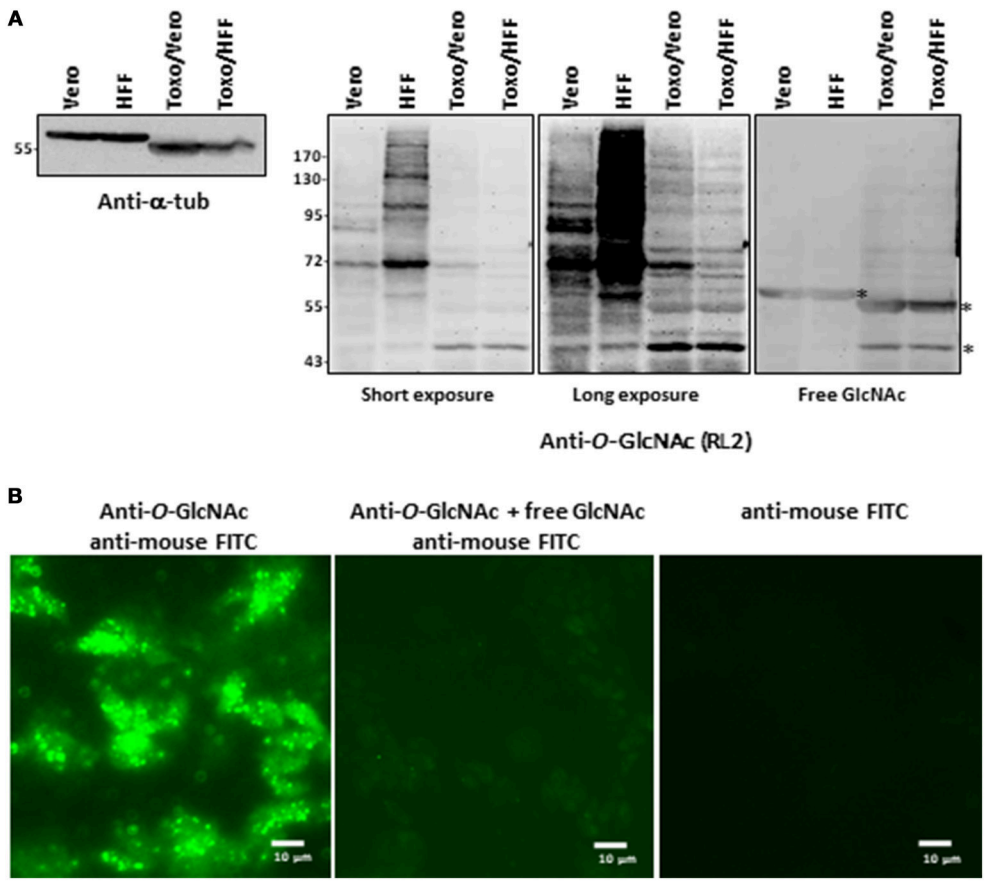

FIGURE 1 | (A) Parasites were produced either in Vero cells or HFF. After homogenization, proteins were resolved by SDS-PAGE and electroblotted onto nitrocellulose and probed with anti-alpha-tubulin antibody or with RL2 anti-*O*-GlcNAc antibody alone or in conjunction with free GlcNAc to analyse their purity and their *O*-GlcNAcylation content respectively. **(B)** Parasites were stained with anti-*O*-GlcNAc antibody as primary antibody and FITC-labeled anti-mouse as secondary antibody and imaged by fluorescent microscopy. Controls were done by co-incubation of anti-*O*-GlcNAc antibody with free GlcNAc and by staining with secondary antibodies alone.*, unspecific bands. HFF, human foreskin fibroblast; T.g., *Toxoplasma gondii*; FITC, Fluorescein isothiocyanate.

Ten years were necessary to identify MSP1 (Merozoite Surface Protein-1) expressed and GPI-anchored at the cell surface of *P. falciparum* to bear *O*-GlcNAc moieties (12). Nevertheless, due to its extracellular localization, MSP1 *O*-glycosylation is likely related to the extracellular glycosylation and not to the nucleocytoplasmic *O*-GlcNAcylation. But, in the late 2000's, OGTs expressed by *Cryptosporidium parvum*, that is phylogenetically close to *Plasmodium* and *Toxoplasma gondii*, and by the minimalist protist *Giardia lamblia* were characterized (13). Later, our team revealed that *T. gondii* unambiguously expresses the nuclear and cytoplasmic modification and strongly suggested its occurrence in *P. falciparum* (14). Very recently, we identified 13 *O*-GlcNAcylated proteins expressed in *P. falciparum* among which Hsp70, alpha-tubulin, actin and glycolytic enzymes (15). In the present report, we used similar approaches and revealed part of *Toxoplasma gondii*'s *O*-GlcNAcome which, except rhoptry proteins, is very close to those found not only in *Plasmodium falciparum* but also in higher eukaryotes. Together, these findings tend to demonstrate that a large part of the *O*-GlcNAcome is universal, that is conserved through species.

MATERIALS AND METHODS

Culture and Preparation of the Parasites

T. gondii grown in African green monkey kidney cells (Vero cells, ATCC CCL-81) or in human foreskin fibroblast (HFF, ATCC SCRC-1041), were cultured in DMEM (Dulbecco's Modified Eagle Medium, Gibco BRL), and supplemented with 10% (v/v) fetal calf serum (FCS, Gibco), 2 mM glutamine, 100 units/mL penicillin, and 0.1 mg/mL streptomycin. Parasites (5×10^7) were added to confluent monolayer of cells (175 cm^2), harvested after being cultivated for 72 h, and liberated from their host cells using a Mixer Mill homogenizer (Retsch). The suspension was run through a 20 mL glass-wool column to remove cellular debris. The purity of the tachyzoite suspension was monitored microscopically. Cell lines and parasites were routinely tested for *Mycoplasma* contamination. To control the efficiency of parasite purification, *T. gondii* cells liberated from their host cells were mixed with homogenized Vero cells, and the mixture was purified using glass-wool columns as described previously (16).

Protein Extraction

The parasites were lysed on ice in the following buffer: 10 mM Tris/HCl, 150 mM NaCl, 1 mM EDTA, 1% (v/v) Triton X-100, 0.5% (w/v) sodium desoxycholate, 0.1% (w/v) SDS, pH 7,4. After vigorous mixing, the lysate was centrifuged at 20,000 g for 10 min at 4°C. The pellet was discarded and the supernatant saved for further analyses. For sWGA (succinylated-Wheat Germ Agglutinin)-beads enrichment, parasites were lysed in homogenization buffer containing 10 mM Tris/HCl, 1 mM EDTA, 1 mM EGTA, 0.5% (v/v) Triton X-100, pH 7.5. A cocktail of proteases inhibitors was added freshly to buffers before use.

SDS-PAGE and Western Blot

Proteins were resolved on 8 or 10% SDS-PAGE and either silver stained or electroblotted onto nitrocellulose membrane. Equal loading and transfer efficiency were checked using Ponceau red staining. Membranes were saturated in 5% (w/v) non-fatty milk in Tris buffered Saline (TBS)-Tween (15 mM Tris,

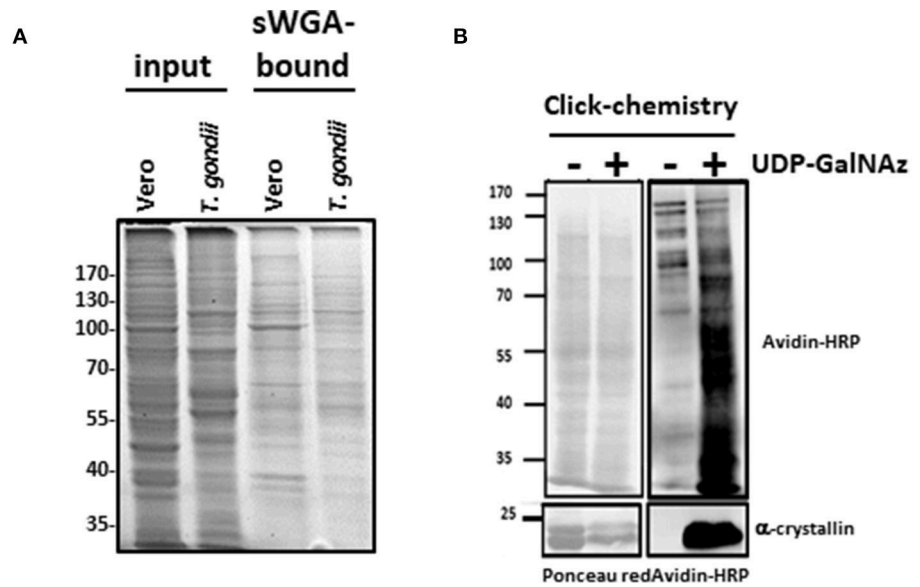

FIGURE 2 | (A) *O*-GlcNAc-bearing proteins from Vero cells (host cells) and *T. gondii* were enriched by sWGA-beads. Gels were brilliant blue stained. **(B)** *T. gondii* proteins were analyzed after labeling of the *O*-GlcNAc-bearing proteins by GalNAz and biotin alkyne using the Click-it™ *O*-GlcNAc enzymatic labeling system and the Click-it™ Glycoprotein detection kit as described in the Material and methods section. After labeling, *T. gondii* samples were separated by SDS-PAGE and Western blot was performed using HRP-labeled avidin to assess presence of the labeled *O*-GlcNAc-proteins. Equal loading was controlled by staining proteins with Ponceau red. Alpha-crystallin was used to control labeling efficiency.

140 mM NaCl, 0.05% (v/v) Tween) for 1 h or in 5% (w/v) bovine serum albumin (BSA) in TBS-Tween overnight. The primary antibodies anti-*O*-GlcNAc, anti-tubulin and anti-rhoptries were incubated overnight at 4°C. Then nitrocellulose membranes were washed three times for 10 min each in TBS-Tween and incubated with horseradish peroxidase-labeled secondary antibodies for 1 h or with avidin-HRP for 45 min. HRP-rPVL was used as previously described (17). Finally, three washes of 10 min each were performed with TBS-Tween and detection was carried out with enhanced chemiluminescence (GE Healthcare).

Succinylated-WGA Protein Enrichment

Prior to sWGA-beads enrichment, 500 μg of proteins were incubated with sWGA beads overnight in a buffer containing 10 mM Tris/HCl, 100 mM NaCl, 0.4% (w/v) sodium deoxycholate, 0.3% (w/v) SDS and 0.2% (w/v) Nonidet P-40. Beads were washed four times using the same buffer without and then with free GlcNAc. After boiling in Laemmli buffer, proteins were resolved by SDS-PAGE.

Labelling of *O*-GlcNAcylated Proteins by Click-Chemistry

Labelling of *O*-GlcNAc-bearing proteins by GalNAz and biotin alkyne was done using the Click-it *O*-GlcNAc enzymatic labeling system and the Click-it Glycoprotein detection kit (Biotin alkyne) according to the manufacturer's instructions (Fischer Scientific) (18). Bovine α-crystallin was used as a positive control. After labeling, proteins were precipitated using the methanol/chloroform protocol and resuspended in 50 μL of Tris/HCl pH 8.0 containing 0.1% (w/v) SDS. 700 μL of

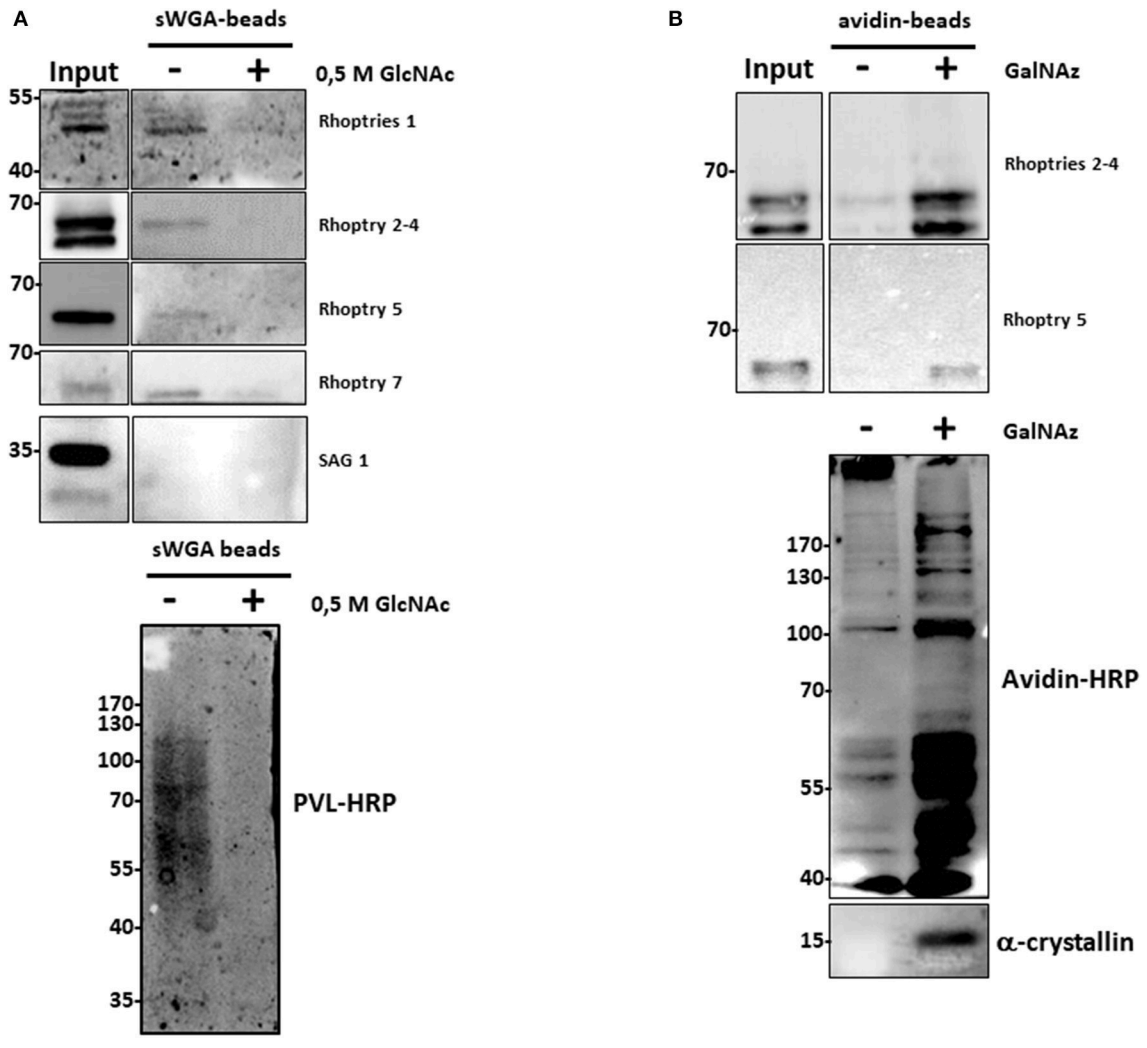

FIGURE 3 | (A) After enrichment on sWGA-beads as described in the materials and methods section, bound proteins were submitted to SDS-PAGE and Western blot. Membranes were probed with different anti-rhoptries antibodies, anti-SAG 1 antibody or with the lectin PVL-HRP. Specificity of PVL-HRP was confirmed by incubation in presence of free GlcNAc. **(B)** *T. gondii* proteins were enzymatically labeled with GalNAz and then chemically with avidin. Proteins were enriched by avidin-beads and samples were resolved by SDS-PAGE and western blotted. Membranes were probed with indicated anti-rhoptries antibodies. Control was performed by staining clicked-proteins with avidin-HRP. Alpha-crystallin was used as a control of labeling.

enrichment buffer (1% (v/v) Triton X-100 and 0.1% (w/v) SDS in PBS) was added to the sample before incubating with 50 µL of avidin-coupled beads (1 h, 4°C). Avidin-bound proteins were collected, washed three times with enrichment buffer, resuspended in Laemmli buffer and boiled. Controls of labeling and enrichment followed the same procedure except that the chemical labeling with UDP-GalNAz was omitted.

Mass Spectrometry

Proteins from *T. gondii* were enriched using either sWGA as specifed above or using the anti-*O*-GlcNAc antibody RL2 as described in Dehennaut et al. (18). Bound-proteins were resolved by SDS-PAGE and silver stained or Coomassie blue stained. Specific bands were excised from the gels. The pieces of gel were dehydrated using a 50:50 dilution of 50 mM Ammonium Bicarbonate (Bic) (HPLC Grade, Prolabo) and Acetonitrile (ACN) (Sigma A) followed by 100% ACN. They were then reduced in 20 mM DTT (Sigma) in 50 mM Bic and alkylated in 100 mM iodoacetamide (Bio-Rad) in 50 mM Bic. After washes with ACN/Bic, the bands were digested with 100–200 ng Trypsin Gold (Promega) in 25 mM Bic. Extraction was done using 45% (v/v) ACN and 10% (v/v) formic acid (Sigma). Extracted peptides were purified using C_{18}-Zip-Tip cones using 0.1% (v/v) Formic Acid for washes and 50:50 ACN/0.1% (v/v) Formic Acid for elution. The nano-LC MS/MS analysis was performed on a HPLC system with two LC-20AD nano-flow LC pumps, an SIL-20 AC auto-sampler and an LC-20AB micro-flow LC pump (Shimadzu, Kyoto, Japan) connected to an ion-trap mass spectrometer (amaZon ETD, Bruker Daltonics, Bremen, Germany) equipped with a Captive Spray ion source. Hystar (Version 3.2, Bruker Daltonics, Bremen,

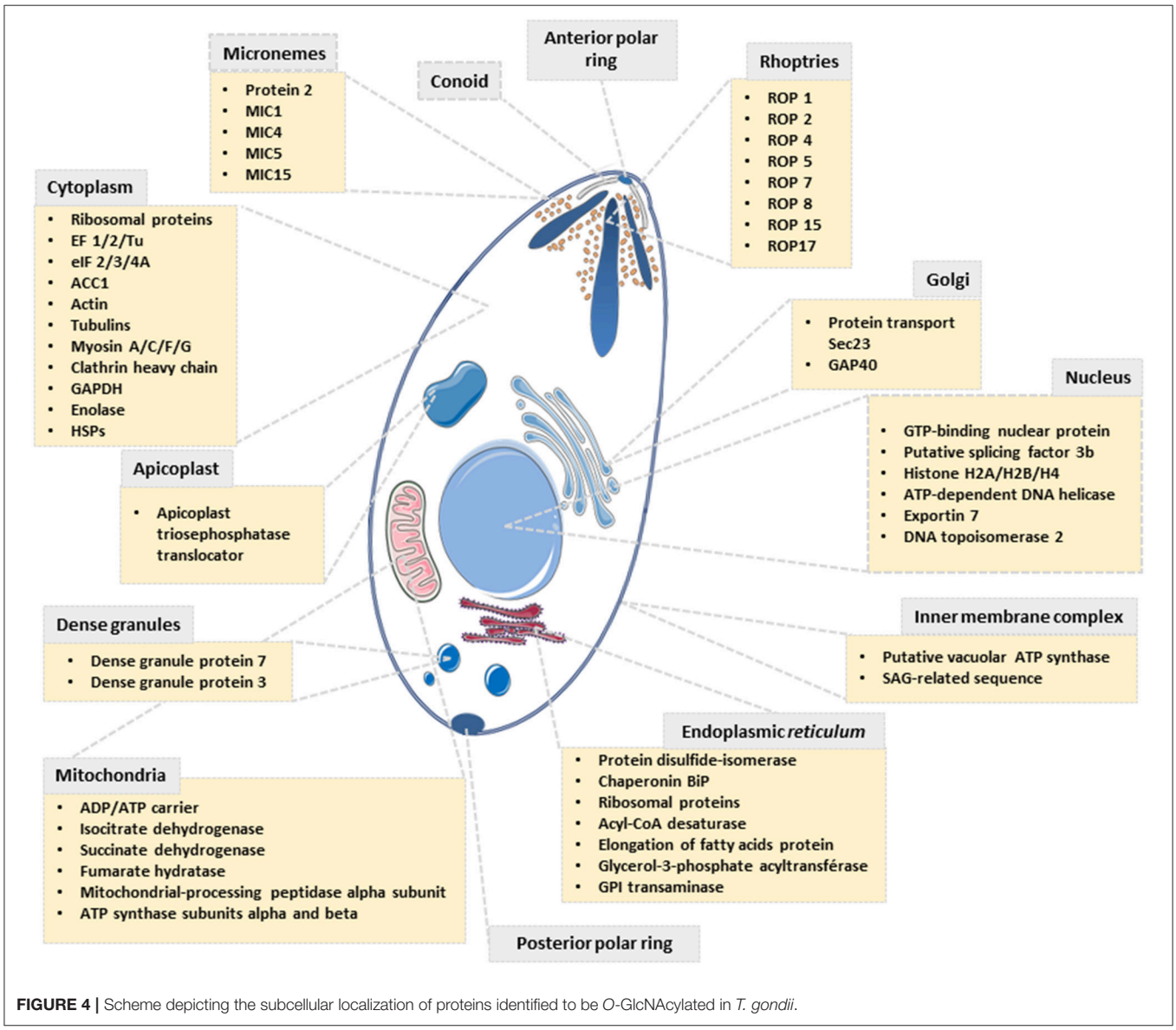

FIGURE 4 | Scheme depicting the subcellular localization of proteins identified to be *O*-GlcNAcylated in *T. gondii*.

Germany) was used to couple and control Shimadzu CBM-20A module (Shimadzu, Kyoto, Japan) for MS acquisition for all experiments.

Trapping and desalting of the peptides was carried out on nano trapping column (Zorbax 300SB-C18, 5 µm, 0.3 × 5 mm, Agilent) using 0.05% (v/v) trifluoroacetic acid solution for 10 min at a flow rate of 10 µL/min. After back-flushing from the trapping column, peptides were separated on a reversed-phase column, ACQUITY UPLC® M-Class Peptide BEH C18 Column (1.7 µm, 130 Å, 100 × 0.75 mm i.d., Waters) using an acetonitrile/0.1% (v/v) formic acid gradient from 15 to 50% (v/v) acetonitrile within 30 min. Fine tuning was achieved using the smart parameter setting (SPS) option for m/z 800, compound stability and trap drive level were set at 100%. Optimization of the Captive Spray source resulted in dry gas temperature, 150°C, dry gas, 3.0 L/min, capillary voltage, −1,200 V, end plate offset, 0 V. The MS1 and MS2 ion detection windows were set at m/z 100–1,700. The five highest no singly charged peaks in each MS1 spectrum were automatically fragmented through collision-induced dissociation (CID).

Data Processing

The LC-MS/MS data was analyzed using DataAnalysis 4.1 software (Bruker Daltonics) and the function Compound–sAutoMS(n) was used to generate 1,200 compound spectra. Generated data were exported as a mascot generic file. Protein identification through primary sequence database searching was performed using the MASCOT search algorithm (MASCOT free version; Matrix Science, London, UK). The following MASCOT settings were used: taxonomy: *Toxoplasma gondii*; database: SwissProt; enzyme: trypsin; fixed modifications: carbamidomethyl (C); variable modifications: oxidation (M, HW), deamidation (NQ), phosphorylation (ST), pyro-Glu (N-term E), and HexNAc (ST); maximum missed cleavages: 1; MS1 peptide tolerance: 0.6 Da; MS/MS tolerance: 0.6 Da.

Immunofluorescence Microscopy

Immuno-labeling of parasites was done in tube (solution) and then were observed on glass slides. Purified *T. gondii* were fixed in 3% (m/v) of paraformaldehyde in cold PBS for 15 min and subsequently washed with PBS. Unreacted aldehyde groups were

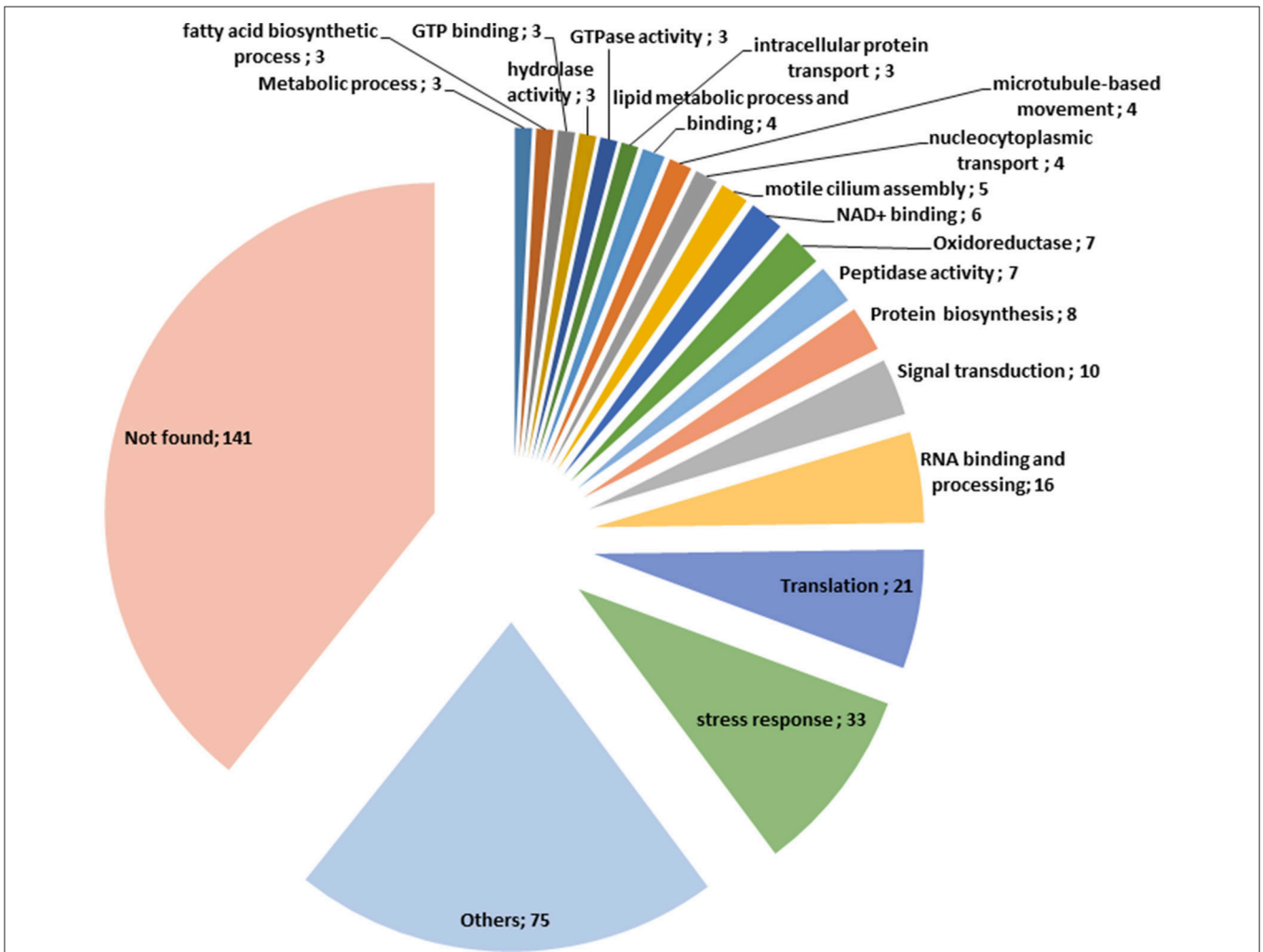

FIGURE 5 | Classification of the *O*-GlcNAcylated proteins found in this study according to their function.

quenched with a solution of 50 mM ammonium chloride for 10 min. After several washes with PBS, cells were permeabilized with 0.1% (v/v) Triton-X100 for 5 min. Nonspecific sites were blocked with goat serum. *T. gondii* were then incubated for 30 min with a dilution of 1:100 in a 10% (v/v) goat serum solution (in PBS) of anti-*O*-GlcNAc antibodies (RL2), complemented or not with free GlcNAc. After 3 washes with PBS, parasites were incubated with fluorescein isothiocyanate (FITC) antibodies (dilution 1:50). *T. gondii* were visualized using an Axioplan 2 imaging microscope (Zeiss, Jena, Germany) and an Axio Cam HRc camera (AxioVision; Zeiss).

RESULTS

Visualization of the *Toxoplasma gondii O*-GlcNAcome

T. gondii used in this study were prepared by infecting either Vero cells or HFF (human foreskin fibroblasts). The absence of contamination of parasite preparations by host cells was unequivocally attested by microscopy examination and anti-α-tubulin staining (**Figure 1A**). α-tubulin is expressed in Vero cells, HFF and *T. gondii* but the difference of molecular weight observed between the two cell types and the parasite asserts that there was no contamination during *T. gondii* purification. Host cells and *T. gondii* proteins were also Coomassie brilliant blue stained and the different protein profiles compared (data not shown).

Distinct approaches based on antibodies, click-chemistry and lectin-beads enrichment were used to visualize the occurrence of *O*-GlcNAcylation in *T. gondii*. First, protein extracts prepared from parasites grown either in Vero or in HFF cells and resolved by SDS-PAGE and electrotransferred onto nitrocellulose membranes were stained with the anti-*O*-GlcNAc antibody RL2—originally raised against nuclear pore proteins (19) (**Figure 1A**). We found that the parasites display distinct *O*-GlcNAcylated proteins profiles, which differ from those of Vero or HFF cells indicating further absence of any cross-contamination by host cells. Incubation of the anti-*O*-GlcNAc antibody with 0.5 M of free N-acetylglucosamine abolished most of the signal, asserting the specificity of the reaction. *O*-GlcNAcylation was also detected by immunofluorescent microscopy by incubating the purified parasites with the RL2 antibodies alone or in conjunction with free GlcNAc, or with the secondary antibodies alone (**Figure 1B**).

Parasite protein extracts were enriched on sWGA-coupled beads (**Figure 2A**) or processed through a Click-chemistry procedure (**Figure 2B**). sWGA is the plant lectin WGA chemically modified with a succinyl group to prevent the lectin to bind to sialic acids. Therefore, when compared to unmodified WGA, sWGA interacts only with GlcNAc residues (20). sWGA was immobilized on beads and incubated with *T. gondii* extracts. After intensive washes (not shown), bound fractions were eluted, resolved by SDS-PAGE and brilliant blue stained as described in Kupferschmid et al. (15). Vero cells were processed according to

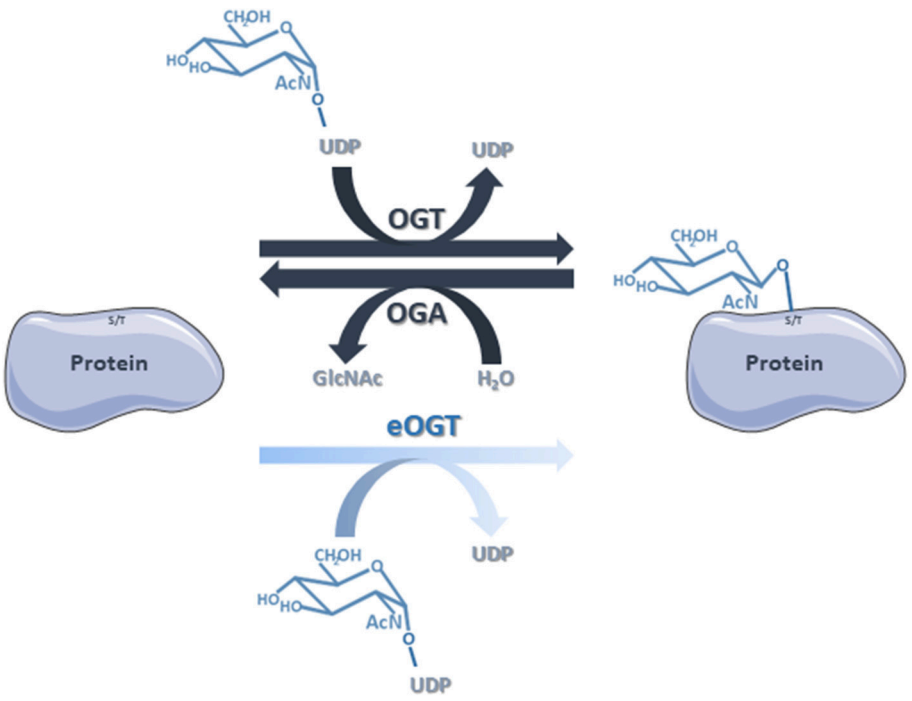

FIGURE 6 | The classical *O*-GlcNAcylation cycling is managed by OGT that transfers the GlcNAc group from the donor UDP-GlcNAc to the target proteins, and OGA that removes the residue by hydrolysis. Nevertheless, we do not rule out that some of the proteins identified in this study are substrates of eOGT. eOGT is located in the endoplasmic *reticulum* where it glycosylates secreted and membrane proteins, and is suggested to modify proteins confined within intracellular compartments. In contrast to *O*-GlcNAcylation driven by OGT/OGA, it is unlikely that eOGT-catalyzed *O*-GlcNAcylation is versatile.

the same procedure and compared to parasites: distinct profiles of sWGA-bound proteins can be observed (**Figure 2A**). Regarding the Click-chemistry approach, we used the Click-iT TM system to biotin-label *O*-GlcNAcylated proteins. Clicked proteins were detected with avidin-labeled HRP (**Figure 2B**). This technique is highly sensitive as attested by the strong signal observed after staining the clicked-proteins with peroxidase-labeled avidin. A negative control, in which UDP-GalNAz has been omitted, was used to differentiate endogenous biotinylation from biotin-labeling. Nevertheless, GalNAz can be grafted to any terminal GlcNAc, therefore this approach alone is not sufficient to discriminate strictly *O*-GlcNAcylation. It is why it was necessary to combine distinct tools (anti-*O*-GlcNAc antibody, sWGA and click-chemistry) to confirm that *T. gondii*'s proteome is largely *O*-GlcNAcylated, and thus, like many other species, possesses its own *O*-GlcNAcome (**Figures 1**, **2**) in accordance with previous reports (14, 21) RL2.

Exploration of *T. gondii*'s *O*-GlcNAcome by Two Independent Approaches

To increase the chance to identify *O*-GlcNAcylated proteins expressed in *T. gondii*, we conducted experiments through two distinct approaches. First, the anti-*O*-GlcNAc antibody RL2 was used to enrich *O*-GlcNAcylated proteins, control experiment was done with non-immune immunoglobulin. The chemically modified plant lectin sWGA was used as a second approach. Bands of the proteins enriched using either the anti-*O*-GlcNAc antibody or sWGA were excised from the gels. Proteins were digested with trypsin and analyzed by tandem mass spectrometry as detailed in the materials and methods section. The protein identification was performed using the Mascot search engine against the SwissProt database restricted to *T. gondii* taxonomy. This allowed the identification of numerous proteins (**Supplementary Data Table 1**): 65.5% using sWGA and 34.5% using the anti-*O*-GlcNAc antibody, fifty proteins being identified by both approaches. Identified proteins can be classified according to their functions and take part in ribosome biogenesis, RNA binding and processing, intracellular transport, signal transduction, lipids metabolism, glycolysis, tricarboxylic acids cycle, organization of cytoskeleton, as well as many other cellular functions.

Surprisingly, several proteins involved in the infection process of *T. gondii,* called rhoptries, were identified by both approaches (sWGA and anti-*O*-GlcNAc antibodies). To confirm that rhoptries are indeed *O*-GlcNAcylated proteins, we tested antibodies specifically directed against this group of proteins

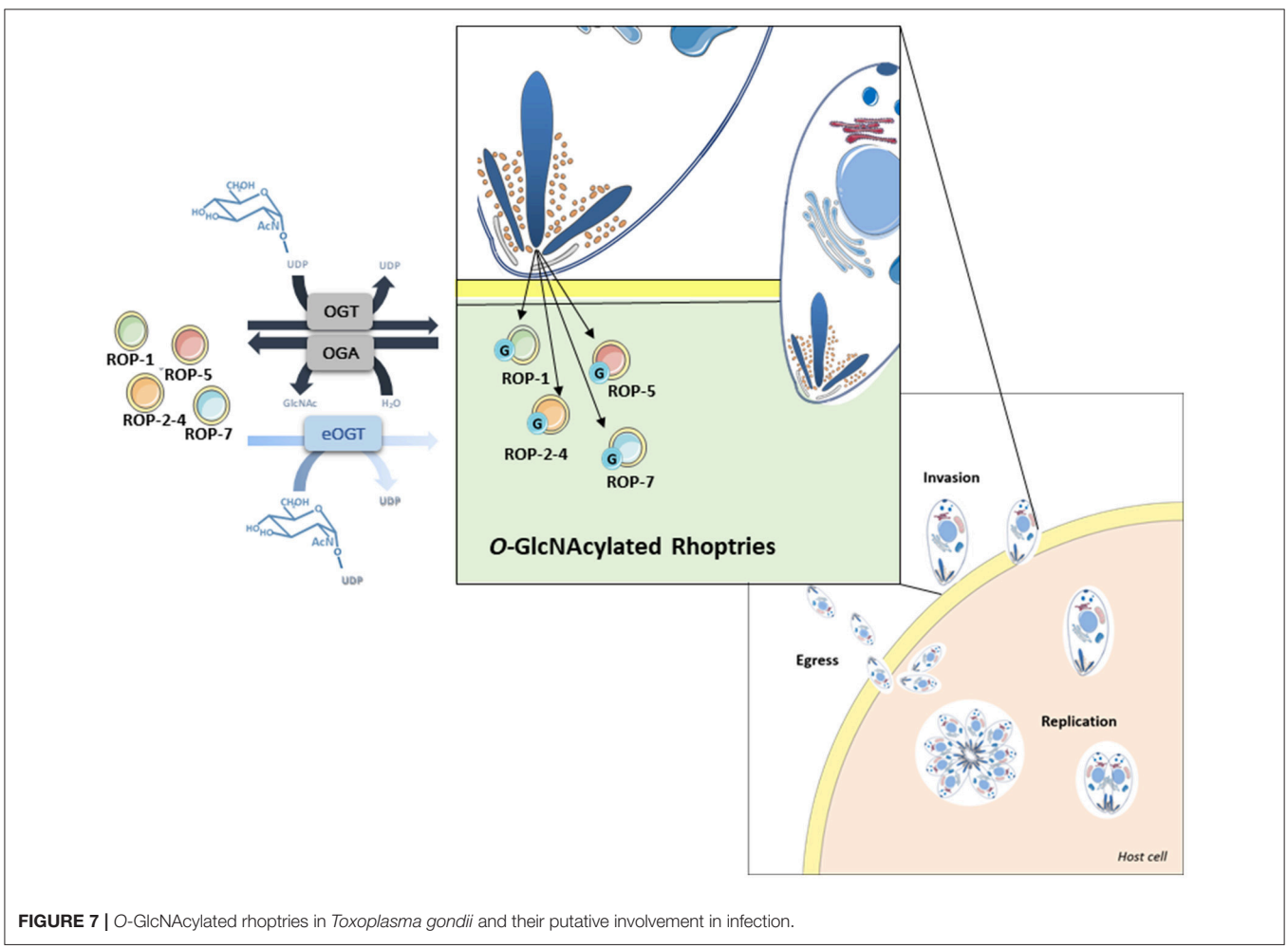

FIGURE 7 | *O*-GlcNAcylated rhoptries in *Toxoplasma gondii* and their putative involvement in infection.

(**Figure 3**). Lysates from *T. gondii* were either enriched using sWGA-beads or processed through the click-chemistry approach followed by enrichment on avidin-beads, resolved by SDS-PAGE and analyzed by Western blot. Rhoptries 1, 2, 5, and 7, and rhoptries 2, 4, and 5 were recovered by sWGA (**Figure 3A**) or click-chemistry (**Figure 3B**) enrichment respectively. SAG 1 was used as a negative control since it is known that its glycans exhibit terminal mannose (22). These two methods associated to our proteomic analyses revealed the *O*-GlcNAcylation of rhoptries.

DISCUSSION

Since its discovery in the eighties (23, 24), *O*-GlcNAcylation has not ceased to arouse the interest of the scientific community. First due to its ubiquitous feature since it is widespread in a large panel of living beings, and secondly because it affects countless proteins, confined within the cytosolic, nuclear and mitochondrial compartments, involved in the regulation of many fundamental biological processes (3, 25). In a recent review, we came back on the different living organisms expressing their own OGT or hijacking the *O*-GlcNAcylation machinery of host cells (2), and stated that OGT emerged as a master regulator of cell homeostasis.

During the last years, *O*-GlcNAcomes of diverse biological models (cell lines, tissues, whole organisms) were explored (1, 15, 18, 25–29). However, very few studies have described *T. gondii*'s glycome and virtually none have investigated its *O*-GlcNAcome. *T. gondii* is an obligate intracellular parasite identified in 1908 in the North African rodent gundi (*Ctenodactylus gundi*) by Nicolle and Manceaux (30). Like other apicomplexans (*Plasmodium* and *Theileria*), *T. gondii* is responsible for debilitating diseases in humans and warm-blooded animals. The worldwide zoonosis toxoplasmosis is one of these major infectious diseases. In France, its seroprevalence in pregnant women is near 54% (31) and it is estimated that a third of human population is infected worldwide. In the majority of the cases, the infection has no serious consequences for immunocompetent patients; nevertheless, a reactivation of the latent parasite in immune compromised individuals may cause encephalitis. It is also noteworthy that cerebral toxoplasmosis is a major cause of morbidity and mortality among AIDS patients. Therefore, fighting the infection by *T. gondii* remains a major challenge to public health, and anything that can contribute to increase the current knowledge on the biology of the parasite can be considered as breakthroughs and opportunities to open novel therapeutic solutions.

Our proteomic analyses revealed the *O*-GlcNAcylation of many proteins involved in a large panel of biological functions (heat shock proteins, glycolytic enzymes, ribosomal proteins, actors of protein synthesis and lipid metabolism) (**Figures 4**, **5**). Most of the *O*-GlcNAcylated proteins identified in this study were previously reported to be *O*-GlcNAc proteins in other models reinforcing the ubiquitous role of *O*-GlcNAcomes found in diverse species. More originally, we highlighted proteins involved in the infection process: rhoptries, microneme proteins and dense granules, all part of secretory organelles and characteristic of the motility of apicomplexans (**Figure 4**). The two former are part of a specific apical complex that also includes a conoid that consists of tubulin fibers (32). Microneme proteins are synthesized by micronemes, specialized organelles involved in secretion, which support several key cellular processes such as invasion, motility and migration through host cells (33). Microneme proteins are first released during infection followed, thereafter, by a second wave of secretion that involves rhoptry proteins. Rhoptry proteins are trafficked from the endoplasmic *reticulum* to the Golgi apparatus, and then are addressed to secretory organelles. Therefore, it cannot be rule out that *O*-GlcNAcylation of rhoptries is performed by EOGT–for EGF (Epidermal Growth Factor) domain-specific OGT (34)–that controls a second form of *O*-GlcNAcylation affecting proteins of the secretory pathway (extracellular matrix proteins, extracellular region of transmembrane proteins) such as Notch receptors (**Figure 6**). A default in the activity of EOGT is responsible for the rare congenital disorder Adams-Oliver syndrome (35). Previously, two independent studies have reported glycosylation of rhoptries (21, 36) by conducting different strategies. Luo and collaborators used a combination of lectins (ConA, WGA and Jacalin) to identify 132 glycoproteins among which rhoptries and microneme proteins (36). Later, *T. gondii*'s glycoproteome has been investigated by the use of unnatural sugars through a bioorthogonal chemical reporter strategy (21). The function of the glycosylation of rhoptries (**Figure 7**) and micronemes in the infection remains unknown, but it should be of interest to determine whether interfering with their *O*-GlcNAcylation reduces motility and invasion of *T. gondii*.

O-GlcNAcylation levels correlate with nutrients status of the cell. UDP-GlcNAc, the substrate of OGT, is at the crossroad of many metabolic pathways (2). Diet may then affect the ability of *T. gondii* to infect host cells and further investigation on whether infectious process of the parasite depends on *O*-GlcNAcylation and/or nutrient is of great interest. It remains also to determine in a near future whether *O*-GlcNAcylation cycling regulates the fate of rhoptry proteins at the expression and degradation levels. Also, it is now well recognized that *O*-GlcNAcylation, like other PTMs, controls protein-protein interactions (1, 7) and the impact of *O*-GlcNAcylation dynamics on biogenesis of rhoptry organelle remains to be investigated.

This paper provides a large-scale analysis of putative *T. gondii*'s *O*-GlcNAcome. Understanding the role of the glycosylation of these proteins may help to elucidate mechanisms involved in invasion and cell life cycle (**Figure 7**), which would lead to improve drug therapy as well as to identify glycoproteins that may prove to be useful as therapeutic targets.

AUTHOR CONTRIBUTIONS

MA-G, YP-C, RS, and TL developed the hypotheses. MA-G performed most of the biochemical experiments and interpreted the data. MK and MM performed experiments and gave important technical training to MA-G. SH gave important advices and help experimenting. HS-E and JS contributed to the culture of *T. gondii*. J-FD produced and provided antibodies against rhoptries. NY, FK, FB, and CR performed the mass

spectroscopic analysis and provided the resulting data. TL, RS, EP, and YP-C initiated the project. MA-G, J-FD, YP-C, EZ, RS, and TL analyzed the results. TL drafted the manuscript. All authors contributed to refining the manuscript, read and approved the final version.

ACKNOWLEDGMENTS

MA-G is holding a fellowship of CONACyT from the government of Mexico. MK was holding a fellowship of the German Centre for Infection Research (DZIF) and acknowledges support for his stay at the University of Lille by a fellowship of the ERASMUS Program of the EU. The authors thank the University of Lille and the Centre National de la Recherche Scientifique, for their financial support. The investigations were supported by CNRS, University of Lille, SFR 3688 FRABio and PAGés. RS and MK thank Prof. S. Becker for his interest and support. The authors thank Mrs. Anja Heiner for helping with the culturing of cells.

SUPPLEMENTARY MATERIAL

The Supplementary Material for this article can be found online at: https://www.frontiersin.org/articles/10.3389/fendo.2018.00450/full#supplementary-material

Supplementary Data Table 1 | List of the proteins identified in this study. Proteins identified by enrichment with sWGA are in green, and by enrichment with RL2 are in pink.

REFERENCES

1. Vercoutter-Edouart A-S, Yazidi-belkoura I El, Baldini S, Mir A, Steenackers A, Dehennaut V, et al. Detection and identification of O-GlcNAcylated proteins by proteomic approaches. *Proteomics* (2015) 15:1039–50. doi: 10.1002/pmic.201400326
2. Aquino-Gil M, Pierce A, Perez-Cervera Y, Zenteno E, Lefebvre T. OGT: a short overview of an enzyme standing out from usual glycosyltransferases. *Biochem Soc Trans.* (2017) 45:365–70. doi: 10.1042/BST20160404
3. Yang X, Qian K. Protein O-GlcNAcylation: emerging mechanisms and functions. *Nat Rev Mol Cell Biol.* (2017) 18:452–65. doi: 10.1038/nrm.2017.22
4. Machacek M, Slawson C, Fields PE. O-GlcNAc: a novel regulator of immunometabolism. *J Bioenerg Biomembr.* (2018) 50:223–9. doi: 10.1007/s10863-018-9744-1
5. Bacigalupa ZA, Bhadiadra CH, Reginato MJ. O-GlcNAcylation: key regulator of glycolytic pathways. *J Bioenerg Biomembr.* (2018) 50:189–90. doi: 10.1007/s10863-018-9742-3
6. Leturcq M, Lefebvre T, Vercoutter-Edouart AS. O-GlcNAcylation and chromatin remodeling in mammals: an up-to-date overview. *Biochem Soc Trans.* (2017) 45:323–38. doi: 10.1042/BST20160388
7. Tarbet HJ, Toleman CA, Boyce M. A sweet embrace: control of protein-protein interactions by O-linked β-N-acetylglucosamine. *Biochemistry* (2018) 57:13–21. doi: 10.1021/acs.biochem.7b00871
8. Kötzler MP, Withers SG. Proteolytic cleavage driven by glycosylation. *J Biol Chem.* (2016) 291:429–34.
9. Lazarus MB, Jiang J, Kapuria V, Bhuiyan T, Janetzko J, Zandberg WF, et al. HCF-1 is cleaved in the active site of O-GlcNAc transferase. *Science* (2013) 342:1235–9. doi: 10.1126/science.1243990
10. Lefebvre T, Dehennaut V, Guinez C, Olivier S, Drougat L, Mir AM, et al. Dysregulation of the nutrient/stress sensor O-GlcNAcylation is involved in the etiology of cardiovascular disorders, type-2 diabetes and Alzheimer's disease. *Biochim Biophys Acta* (2010) 1800:67–79. doi: 10.1016/j.bbagen.2009.08.008
11. Dieckmann-Schuppert A, Bause E, Schwarz RT. Studies on O-glycans of *Plasmodium-falciparum*-infected human erythrocytes evidence for O-GlcNAc and O-GlcNAc-transferase in malaria parasites. *Eur J Biochem.* (1993) 216:779–88.
12. Hoessli DC, Poincelet M, Gupta R, Ilangumaran S, Nasir-ud-Din. *Plasmodium falciparum* merozoite surface protein 1: GLYCOSYLATION and localization to low-density, detergent-resistant membranes in the parasitized erythrocyte. *Eur J Biochem.* (2003) 270:366–75. doi: 10.1046/j.1432-1033.2003.03397.x
13. Banerjee S, Robbins PW, Samuelson J. Molecular characterization of nucleocytosolic O-GlcNAc transferases of *Giardia lamblia* and *Cryptosporidium parvum*. *Glycobiology* (2009) 19:331–6. doi: 10.1093/glycob/cwn107
14. Perez-Cervera Y, Harichaux G, Schmidt J, Debierre-Grockiego F, Dehennaut V, Bieker U, et al. Direct evidence of O-GlcNAcylation in the apicomplexan *Toxoplasma gondii*: a biochemical and bioinformatic study. *Amino Acids* (2011) 40:847–56. doi: 10.1007/s00726-010-0702-4
15. Kupferschmid M, Aquino-Gil MO, Shams-Eldin H, Schmidt J, Yamakawa N, Krzewinski F, et al. Identification of O-GlcNAcylated proteins in *Plasmodium falciparum*. *Malar J.* (2017) 16:1–11. doi: 10.1186/s12936-017-2131-2
16. Grimwood BG, Hechemy K, Stevens ROYW. *Toxoplasma gondii*: purification of trophozoites propagated in cell culture. *Exp Parasitol.* (1979) 286:282–6.
17. Machon O, Baldini SF, Ribeiro JP, Steenackers A, Varrot A, Lefebvre T, et al. Recombinant fungal lectin as a new tool to investigate O-GlcNAcylation processes. *Glycobiology* (2017) 27:123–8. doi: 10.1093/glycob/cww105
18. Dehennaut V, Slomianny MC, Page A, Vercoutter-Edouart AS, Jessus C, Michalski JC, et al. Identification of structural and functional O-linked N-acetylglucosamine-bearing proteins in xenopus laevis oocyte. *Mol Cell Proteomics* (2008) 7:2229–45. doi: 10.1074/mcp.M700494-MCP200
19. Snow CM, Senior A, Gerace L. Monoclonal antibodies identify a group of nuclear pore complex glycoproteins. *J Cell Biol.* (1987) 104:1143–56.
20. Monsigny M, Sene C, Obrenovitch A, Roche AC, Delmotte F, Boschetti E. Properties of succinylated wheat germ agglutinin. *Eur J Biochem.* (1979) 98:39–45.
21. Nazarova LA, Ochoa RJ, Jones KA, Morrissette NS, Prescher JA. Extracellular *Toxoplasma gondii* tachyzoites metabolize and incorporate unnatural sugars into cellular proteins. *Microbes Infect.* (2016) 18:199–210. doi: 10.1016/j.micinf.2015.11.004
22. Zinecker CF, Striepen B, Geyer H, Geyer R, Dubremetz JF, Schwarz RT. Two glycoforms are present in the GPI-membrane anchor of the surface antigen 1 (P30) of *Toxoplasma gondii*. *Mol Biochem Parasitol.* (2001) 116:127–35. doi: 10.1016/S0166-6851(01)00313-9
23. Torres CR, Hart GW. Topography and polypeptide distribution of terminal N-acetylglucosamine residues on the surfaces of intact lymphocytes. evidence for O-linked GlcNAc. *J Biol Chem* (1984) 259:3308–17.
24. Hanover JA, Cohen CK, Willingham MC, Park MK. O-linked N-acetylglucosamine is attached to proteins of the nuclear pore. Evidence for cytoplasmic and nucleoplasmic glycoproteins. *J Biol Chem.* (1987) 262:9887–94.
25. Ma J, Hart GW. O-GlcNAc profiling : from proteins to proteomes. *Clin Proteomics* (2014) 11:1–16. doi: 10.1186/1559-0275-11-8
26. Cieniewski-Bernard C, Bastide B, Lefebvre T, Lemoine J, Mounier Y, Michalski J-C. Identification of O-linked N-acetylglucosamine proteins in rat skeletal muscle using two-dimensional gel electrophoresis and mass spectrometry. *Mol Cell Proteomics* (2004) 3:577–85. doi: 10.1074/mcp.M400024-MCP200
27. Gurcel C, Vercoutter-Edouart AS, Fonbonne C, Mortuaire M, Salvador A, Michalski JC, et al. Identification of new O-GlcNAc modified proteins using a click-chemistry-based tagging. *Anal Bioanal Chem.* (2008) 390:2089–97. doi: 10.1007/s00216-008-1950-y
28. Xu SL, Chalkley RJ, Maynard JC, Wang W, Ni W, Jiang X, et al. Proteomic analysis reveals O-GlcNAc modification on proteins with key regulatory functions in *Arabidopsis*. *Proc Natl Acad Sci USA.* (2017) 114:E1536–43. doi: 10.1073/pnas.1610452114

29. Woo CM, Lund PJ, Huang AC, Davis MM, Bertozzi CR, Pitteri S. Mapping and quantification of over 2,000 O-linked glycopeptides in activated human T cells with isotope-targeted glycoproteomics (IsoTaG). *Mol Cell Proteomics* (2018) 17:764–75. doi: 10.1074/mcp.RA117.000261
30. Nicolle C, Manceaux L. Sur une infection à corps de Leishman (ou organisms voisons) du gondii. *Comptes Rendus Acad des Sci*. (1908) 147:763–6.
31. Flegr J, Prandota J, Sovičková M, Israili ZH. Toxoplasmosis - A global threat. Correlation of latent toxoplasmosis with specific disease burden in a set of 88 countries. *PLoS ONE* (2014) 9:e90203. doi: 10.1371/journal.pone.0090203
32. Mueller C, Klages N, Jacot D, Santos JM, Cabrera A, Gilberger TW, et al. The toxoplasma protein ARO mediates the apical positioning of rhoptry organelles, a prerequisite for host cell invasion. *Cell Host Microbe*. (2013) 13:289–301. doi: 10.1016/j.chom.2013.02.001
33. Liu Q, Li FC, Zhou CX, Zhu XQ. Research advances in interactions related to *Toxoplasma gondii* microneme proteins. *Exp Parasitol*. (2017) 176:89–98. doi: 10.1016/j.exppara.2017.03.001
34. Sakaidani Y, Nomura T, Matsuura A, Ito M, Suzuki E, Murakami K, et al. O-linked-N-acetylglucosamine on extracellular protein domains mediates epithelial cell-matrix interactions. *Nat Commun*. (2011) 2:583. doi: 10.1038/ncomms1591
35. Shaheen R, Aglan M, Keppler-Noreuil K, Faqeih E, Ansari S, Horton K, et al. Mutations in EOGT confirm the genetic heterogeneity of autosomal-recessive Adams-Oliver syndrome. *Am J Hum Genet*. (2013) 92:598–604. doi: 10.1016/j.ajhg.2013.02.012
36. Luo Q, Upadhya R, Zhang H, Madrid-Aliste C, Nieves E, Kim K, et al. Analysis of the glycoproteome of *Toxoplasma gondii* using lectin affinity chromatography and tandem mass spectrometry. *Microbes Infect*. (2011) 13:1199–210. doi: 10.1016/j.micinf.2011.08.013

Conflict of Interest Statement: The authors declare that the research was conducted in the absence of any commercial or financial relationships that could be construed as a potential conflict of interest.

frontiers in Endocrinology

REVIEW
published: 06 September 2018
doi: 10.3389/fendo.2018.00522

Real Talk: The Inter-play Between the mTOR, AMPK, and Hexosamine Biosynthetic Pathways in Cell Signaling

Gentry K. Cork[1,2], *Jeffrey Thompson*[3] *and Chad Slawson*[1]*

[1] *Department of Biochemistry and Molecular Biology, University of Kansas Medical Center, Kansas City, KS, United States,* [2] *Department of Pathology, University of Kansas Medical Center, Kansas City, KS, United States,* [3] *Department of Biostatistics, University of Kansas Medical Center, Kansas City, KS, United States*

O-linked N-acetylglucosamine, better known as O-GlcNAc, is a sugar post-translational modification participating in a diverse range of cell functions. Disruptions in the cycling of O-GlcNAc mediated by O-GlcNAc transferase (OGT) and O-GlcNAcase (OGA), respectively, is a driving force for aberrant cell signaling in disease pathologies, such as diabetes, obesity, Alzheimer's disease, and cancer. Production of UDP-GlcNAc, the metabolic substrate for OGT, by the Hexosamine Biosynthetic Pathway (HBP) is controlled by the input of amino acids, fats, and nucleic acids, making O-GlcNAc a key nutrient-sensor for fluctuations in these macromolecules. The mammalian target of rapamycin (mTOR) and AMP-activated protein kinase (AMPK) pathways also participate in nutrient-sensing as a means of controlling cell activity and are significant factors in a variety of pathologies. Research into the individual nutrient-sensitivities of the HBP, AMPK, and mTOR pathways has revealed a complex regulatory dynamic, where their unique responses to macromolecule levels coordinate cell behavior. Importantly, cross-talk between these pathways fine-tunes the cellular response to nutrients. Strong evidence demonstrates that AMPK negatively regulates the mTOR pathway, but O-GlcNAcylation of AMPK lowers enzymatic activity and promotes growth. On the other hand, AMPK can phosphorylate OGT leading to changes in OGT function. Complex sets of interactions between the HBP, AMPK, and mTOR pathways integrate nutritional signals to respond to changes in the environment. In particular, examining these relationships using systems biology approaches might prove a useful method of exploring the complex nature of cell signaling. Overall, understanding the complex interactions of these nutrient pathways will provide novel mechanistic information into how nutrients influence health and disease.

Keywords: O-GlcNAc, OGT, OGA, mTOR (mammalian target of rapamycin), AMPK 5′ AMP-activated protein kinase

OPEN ACCESS

Edited by:
Tarik Issad,
Institut National de la Santé et de la Recherche Médicale (INSERM), France

Reviewed by:
Stéphanie Olivier-Van Stichelen, National Institutes of Health (NIH), United States
Anna Krzeslak, University of Łódz, Poland

***Correspondence:**
Chad Slawson
cslawson@kumc.edu

Specialty section:
This article was submitted to Molecular and Structural Endocrinology, a section of the journal Frontiers in Endocrinology

Received: *22 June 2018*
Accepted: *21 August 2018*
Published: *06 September 2018*

Citation:
Cork GK, Thompson J and Slawson C (2018) Real Talk: The Inter-play Between the mTOR, AMPK, and Hexosamine Biosynthetic Pathways in Cell Signaling. Front. Endocrinol. 9:522. doi: 10.3389/fendo.2018.00522

INTRODUCTION

At its core, pathology is largely a matter of cell signaling gone awry. Think of it as a game of "Rumors," where a group of players are passing a message down the line by whispering it to each other, but when it reaches the last person and they announce it, the message is entirely different from the original. Now, imagine the people as proteins, and when each one receives the message,

they perform some function that will then signal the next protein in the pathway to perform a function until the endgame target is reached. If one of the components in a signaling pathway deviates from typical behavior or conditions, the resulting "message" can be exceedingly different from the original signal, altering cell behavior. Diseases like cancer, diabetes, and Alzheimer's are often rooted in aberrant signal transduction and abnormal pathway regulation. Nutrient-sensitivity is one of several key factors that impact a pathway's activity. Over- or under-nutrition can heighten or inhibit activity through alterations in post-translational modifications (PTM); any miscommunication in these modifications can push a cell toward pathology. A PTM can propagate a signal cascade to change the function of a final target, act as a sensor for regulators of a pathway, or alter the interactions of specific proteins in the pathway. To understand why these changes are occurring, a greater understanding of the complexity and fine-tuning of a pathway by a PTM is needed.

Along with phosphorylation, acetylation, and methylation; glycosylation is one of the most important protein modifications. O-linked N-Acetylglucosamine (O-GlcNAc) is one of the many kinds of glycosidic PTMs found in eukaryotic cells, but what makes it different from other sugar additions is that it exists purely as an intracellular molecule and does form oligomers (1). The addition and removal of O-GlcNAc is facilitated solely by O-GlcNAc transferase (OGT) and O-GlcNAcase (OGA) (2), so the coordinated activity of these two enzymes creates a versatile signaling dynamic that can quickly alter signaling pathways (3). Therefore, a wide scope of cellular processes is controlled and fine-tuned by O-GlcNAc, including apoptosis, mitochondrial function, proliferation, and gene transcription (4–9). Because O-GlcNAc plays such a crucial and diverse role in eukaryotic cells, atypical O-GlcNAcylation can be a driving force in a variety of pathologies. Alzheimer's disease (10), diabetes, and several types of cancers have been linked to abnormal levels or behavior of O-GlcNAc, OGT, and OGA (5, 9–16). Research into the underlying reasons behind these physiological aberrations has yielded a plethora of new insights into cell signaling mechanisms and the role of O-GlcNAc in overall cellular function, particularly nutrient-sensing. As a nutrient-sensor, O-GlcNAc reacts to fluctuations in specific macromolecule levels in order to direct cellular response in an appropriate manner. However, nutrient-sensing is a vital aspect of many different pathways, including the mammalian target of rapamycin (mTOR) and AMP-activated protein kinase pathways (AMPK). By understanding how these pathways react to nutrient levels and how that impacts their interactions between one another, we can begin to ascertain how nutrient sensing impacts overall cell activity (12).

THE HEXOSAMINE BIOSYNTHETIC PATHWAY, mTOR PATHWAY, AND AMPK PATHWAY PARTICIPATE IN NUTRIENT SENSING

The Hexosamine Biosynthetic Pathway

The Hexosamine Biosynthetic Pathway (HBP) utilizes approximately 3-5% of cellular glucose as well as glutamine, acetyl-Coenzyme A (CoA), and uridine, to generate the OGT substrate, UDP-GlcNAc (12, 17). This process begins with the conversion of a single glucose molecule to glucose-6-phosphate, which is then converted to fructose-6-phosphate. Glutamine:fructose-6-phosphate amidotransferase (GFAT), the rate-limiting enzyme in the HBP, utilizes a glutamine amino acid and fructose-6-phosphate to create glucosamine-6-phosphate (14, 17). Acetyltransferase EMEG2 then generates N-acetylglucosamine-6-phosphate using acetyl-Coenzyme A (CoA) before it is finally converted to uridine 5′-diphospho- N-acetylglucosamine (UDP-GlcNAc) using uridine-5′-triphosphate (17). While glucose is the initial input, HBP's sensitivities extend to fats, amino acids, and nucleotides, as well (**Figure 1**).

Fluctuations in the levels of the macromolecules that feed into the HBP alter the output of this pathway, making it a diverse and responsive nutrient sensor (12). For instance, over-expression of the glucose transporter, GLUT1, in the skeletal muscle of transgenic mice resulted in a 2-to-3-fold increase in UDP-GlcNAc concentration (14). However, GLUT1 over-expression did not increase expression of the rate-limiting enzyme in the HBP, glutamine: fructose-6-phosphate amidotransferase (GFAT), suggesting that glucose intake, as opposed to GFAT levels, could account for the rise in UDP-GlcNAc (14).

While nutrient concentrations *in vivo* can alter the output of the HBP, OGT activity also plays a role in nutrient-sensing. Transgenic mice with skeletal muscle overexpression of OGT demonstrated increased levels of serum insulin, indicating hyperinsulinemia, which is characteristic in type II diabetes (16). Furthermore, in glucose-deprived HepG2 cells, OGA transcription was suppressed and OGT expression was up-regulated coinciding with a dramatic amplification in global O-GlcNAcylation (12) and decreased activity for glycogen synthase (GS), the enzyme responsible for constructing glycogen from individual glucose molecules (12). These data suggest that OGT plays an active role in energy conservation during starvation by inhibiting pathways that store glucose (12). However, there is a dark side to this mechanism. Overfeeding of cells with glucose or glucosamine resulted in significant impairment of insulin activation of glycogen synthase (13). In normal cell physiology, insulin signaling results in activation of glycogen synthase via dephosphorylation by phosphatases and inactivation of glycogen synthase kinase-3 (13). However, the heightened nutrient conditions increased overall O-GlcNAc levels, including O-GlcNAcylation of phosphorylation sites on glycogen synthase resulting in reduced glycogen synthase activity. Since the phosphorylation-dephosphorylation dynamic of glycogen synthase renders it sensitive to insulin signaling, O-GlcNAcylation disturbs this process and instigates insulin resistance (13).

HBP flux regulates multiple steps of the insulin signaling pathway (18). Skeletal muscle of mice containing an OGT-KO showed heightened glucose uptake in response to insulin as opposed to wild type counterparts, suggesting a link between insulin sensitivity and O-GlcNAc levels (19). When looking into the molecular mechanism behind this phenomenon, insulin receptor substrate 1 (IRS-1), a protein phosphorylated by the insulin receptor (IR) tyrosine kinase after it binds extracellular

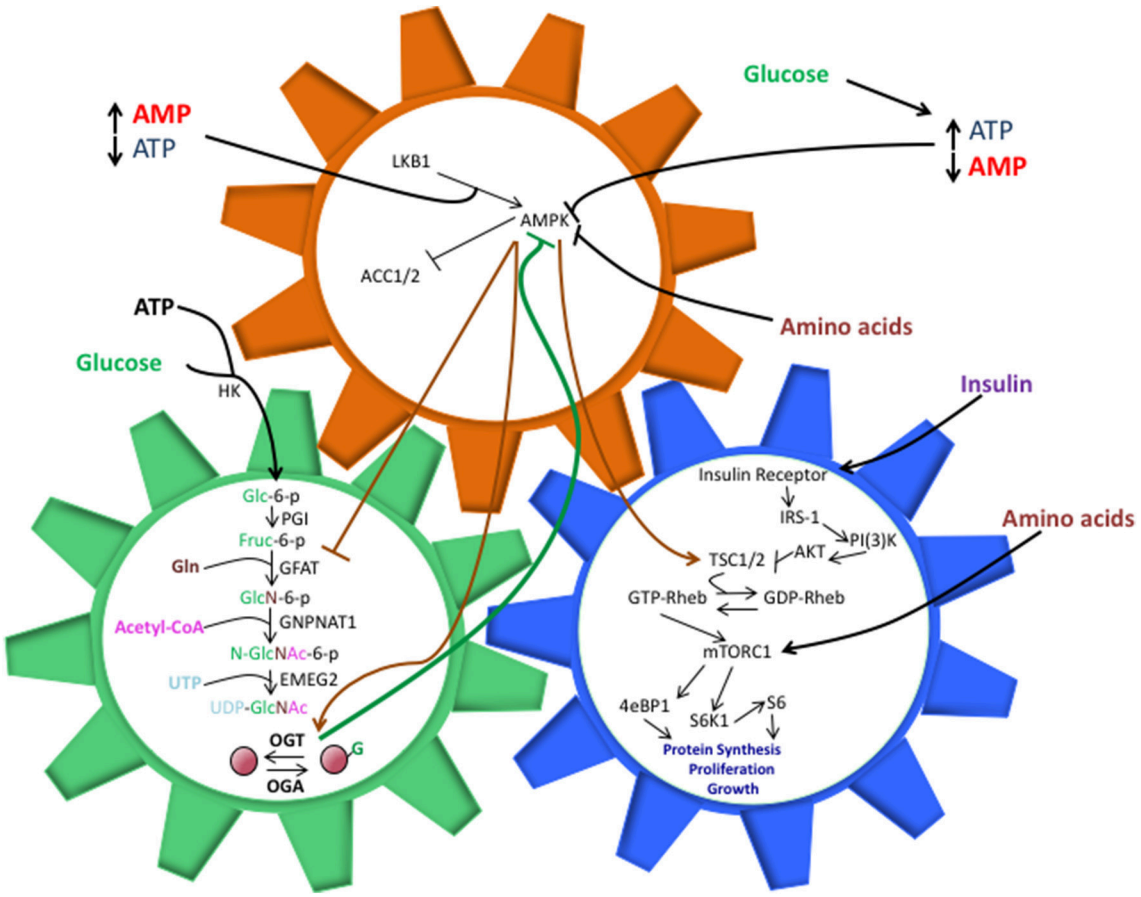

FIGURE 1 | The shared components between the HBP, AMPK, and mTOR pathways allow them to work in a synchronized manner to direct cell activity, but perturbations in these interactions can also drive pathology. O-GlcNAcylation of AMPK inhibits its ability to phosphorylate TSC1/2 and repress mTORC1 activation. This, in turn, can lead to unchecked cell proliferation, a hallmark of cancer and other diseases. The balance of nutrient intake also plays a pivotal role in guiding the interactions between these pathways. Increased glucose levels can bolster ATP production, both of which are necessary components for the HBP. Along with heightened UDP-GlcNAc levels, the ATP:AMP ratio shifts, thus hindering AMPK activation. Increasing amino acid intake contributes to AMPK suppression and direct/indirect mTORC1 activation, though the exact mechanisms behind these phenomenon are not entirely understood.

insulin, has multiple O-GlcNAcylation sites (20). Moreover O-GlcNAcylation of IRS-1 also correlates with a dramatic decrease in phosphorylation of this protein (18), which is a necessary step in activating downstream pathways such as AKT signaling and vesicular trafficking of GLUT4 transporters. Importantly, insulin signaling sees the redistribution of OGT to the plasma membrane within 20–30 min post-insulin induction and suggests that OGT then phosphorylates IRS and IRS2 leading to decreased signaling (21, 22). Overall, increased O-GlcNAc appears to foster insulin insensitivity and hinder cellular glucose uptake making the HBP a novel therapeutic target in type II diabetes research.

The mTOR Pathway

While the HBP is a nutrient-sensor for several major macromolecules (12–14, 16, 17, 23–25), the mTOR pathway also shares several of these sensitivities. The mTOR pathway is a well-characterized signal transduction pathway that is a focal point in studies for diseases like cancer, diabetes, and Alzheimer's. The mTOR protein is a serine/threonine protein kinase that functions as a component in two unique multi-protein complexes, mTORC1 and mTORC2, directing cell activities distinct from one another (26, 27). While mTORC2 regulates cell survival and cytoskeletal organization (26, 27), mTORC1 participates in directing proliferation and biosynthetic pathways (26, 28, 29). Regulation of mTORC2 remains underdeveloped when compared to mTORC1, whose sensitivities to cellular energy levels and amino acids direct its activity (26).

Activation of the mTOR pathway occurs when RAS homolog enriched in brain (Rheb) binds GTP to activate mTORC1 (30–32). Amino acid withdrawal will decrease phosphorylation of the p70S6 kinase, a key mTORC1 target, but overexpression of Rheb rescues p70S6K activation (31), drawing a clear connection between mTORC1 activity and Rheb. However, a protein complex referred to as the Ragulator must first recruit Rheb and mTORC1 to the surface of a lysosome in order for activation of mTORC1 to occur; for cells lacking Ragulator components, mTORC1 activity was undetected, indicating that lysosomal

localization was a necessary step in the mTOR pathway (32). Tuberous sclerosis 1 (TSC1) and TSC2 are upstream inhibitors of mTORC1 that act as GTPase-activating proteins (GAPs) for Rheb (26). Active Rheb (GTP-Rheb) facilitates mTORC1 activation once localized to the surface of a lysosome, while TSC1/2 stimulates Rheb to hydrolyze GTP to GDP, mTORC1 activation becomes repressed (26) (**Figure 1**).

Like the HBP, the mTOR pathway also participates in insulin signaling. Inhibition of TSC1/2 occurs via phosphorylation by AKT (33). First, the IRS proteins gather the components for a class III phosphatidylinositol 3-kinase (PI3K), which converts phosphatidylinositol 2-phosphate (PIP_2) to PIP_3; the increase in PIP_3 signals AKT to localize to the plasma membrane for activation (34). Interestingly, the PI3K protein, Vps34, has demonstrated amino acid-sensitive regulation of mTORC1 activation (34). Cells cultured in high levels of amino acids demonstrated increased Ca^{2+} uptake, which is necessary for calmodulin to bind to Vps34 and facilitate activation (34). In turn, Vps34 generates higher levels of PIP3, which has been speculated to recruit protein domains necessary for the conformational changes in the mTORC1 signalsome that lead to mTORC1 activation (34).

However, amino acids also have the capacity to activate mTORC1 in a TSC1/2 independent manner. For TSC2-null cells that underwent amino acid starvation, phosphorylation of the mTORC1 target, S6K1, was not rescued, indicating the necessity of amino acids for mTORC1 activation (35). Further examination of this phenomenon revealed that amino acid withdrawal prevented mTORC1 localization to the lysosome, a crucial step in mTORC1 activation (32). However, evidence suggests that amino acids alone are not responsible for mTORC1 localization, but are instead mediated by the trimeric Ragulator complex, which localizes to lysosomes in high amino acid conditions (32). For cells lacking Ragulator components, amino acid treatment could not stimulate mTORC1 activation while control cells demonstrated an increase in phosphorylated mTORC1 targets (32). While the exact mechanism is not entirely understood, there has been speculation that amino acids signal Ragulator to bind to the surface of a lysosome and act as a docking scaffold to facilitate mTORC1 activation (32, 36).

Nutrient-sensing in the mTOR pathway also extends to ATP, allowing it to direct cell activity according to energy levels. This sensitivity is evident in mTORC1 regulation of superoxide dismutase 1 (SOD1) (37), which converts reactive oxygen species (ROS) into H_2O_2. Several cell lines treated with a major mTORC1 inhibitor, Rapamycin, demonstrated amplifications in SOD1 activity and decreased phosphorylated SOD1, which was similar to the outcome for glucose starved cells (37). Because glucose starvation halts cytosolic ATP production by glycolysis and mTORC1 is dependent upon these specific ATP reserves (38), mTORC1 inhibition of SOD1 is hinged by ATP availability. This sensitivity even extends to fluctuations in nucleic acids, as demonstrated by mTORC1 suppression in tissue culture cells treated purine synthesis inhibitors, lometrexol (LTX), and methotrexate (MTX). However, when exposed to exogenous nucleosides, only adenosine was able to revive mTORC1 activity, indicating that derivatives of ATP can regulate mTORC1.

The AMPK Pathway

AMP-activated protein kinase (AMPK), another nutrient sensing pathway, senses shifts in the AMP: ATP dynamic and responds inversely to energy levels in relation to mTORC1 (39, 40). While there is not a completed structure for AMPK as of yet, current data suggests that it is a heterotrimeric complex with a catalytic kinase domain and two regulatory regions (40). When energy intake falls and ATP consumption produces large amounts of cytosolic AMP, and in turn, Liver Kinase B1 (LKB1) facilitates the activation of AMPK by utilizing AMP to phosphorylate AMPK (41). For MEFs treated with the AMPK stimulator, 5-aminoimidazole-4-carboxylamine ribonucleotide (AICAR), LKB1-null cells failed to produce AMPK phosphorylated at Thr-172, while wild-type MEFS demonstrated a dramatic surge in phosphorylated AMPK levels when compared with non-treated cells (41) (**Figure 1**).

Once activated, AMPK participates in a wide scope of pathways and cellular processes, including lipid metabolism (42). Acetyl-Coenzyme A carboxylase (ACC), the enzyme responsible for catalyzing the conversion of acetyl-CoA to malonyl-CoA, a precursor in fatty acid synthesis, is a known target of AMPK inhibition (42, 43). While there are three phosphorylation sites on ACC2 and it is a target for three different kinases, AMPK modification of this enzyme most potently decreased the V_{MAX} (43), which is significant when we consider the spectrum of acuteness in regulating enzyme activity. AMPK phosphorylates Ser79 for ACC1 and Ser212 for ACC2, so a double alanine knock-in of both sites in mice revealed a decline in fatty acid oxidation and increased lipogenesis (44), demonstrating that AMPK plays a critical role in fatty acid metabolism. Muscle cells treated with Compound C, an AMPK inhibitor, demonstrated a marked decrease in phosphorylated AMPK in conjunction with heightened triglyceride levels (45). Combining these data, there appears to be a clear role for AMPK in repressing lipid production.

Another AMPK target is the mTORC1 pathway, which accounts for the inverse response of both pathways in respect to AMP:ATP ratios. In poor nutrient conditions, ATP depletion causes the ratio to shift toward AMP bolstering AMPK activation in turn, AMPK phosphorylates TSC1/2 in order to stimulate GAP activity toward Rheb, thus suppressing mTORC1. However, it was also revealed that AMPK inhibits mTORC1 by phosphorylating its scaffold protein, raptor (39). Therefore, AMPK has the capacity to both directly and indirectly regulate mTORC1.

While energy levels drive the dynamic between AMPK and mTORC1, amino acid concentrations also influence this relationship (46). For instance, pancreatic β-cells treated with high doses of glucose, leucine, and glutamine experienced a significant increase in mTORC1 activity, while phosphorylated AMPK diminished (46), indicating a contrasting reaction for AMPK and mTORC1 in terms of amino acid exposure.

Nutrient-sensing is a complex activity that directs the behavior of individual pathways, so when we consider pathways affected by similar macromolecules, we must explore how fluctuations in nutrient concentrations can impact the way these pathways interact and coordinate in cell signaling. For the HBP, mTOR,

and AMPK pathways, there is a complex inter-play in regards to their responses to nutrient levels (**Figure 1**). However, in order to truly understand how O-GlcNAc impacts cell signaling in specific pathologies, we must further analyze the interactions of the HBP with AMPK and mTORC1, respectively.

THE CROSS-TALK BETWEEN THE HBP AND AMPK PATHWAYS

In cell signaling, cross-talk between pathways is a relationship based on a mutual capacity to regulate one another, so the discovery of a cross-talk relationship between OGT and AMPK opened a whole new avenue for exploring inter-pathway dynamics and their impact on cell function (21). The potential for crosstalk between O-GlcNAc and AMPK was first suggested with studies using glucosamine (GlcN) as a supplement. Mice treated with high concentrations of GlcN quickly increase O-GlcNAc levels since GlcN supplementation by-passes GFAT regulation of the HBP (24, 25, 47), but GlcN treatment negatively impaired insulin signaling quickly leading to elevated blood glucose levels. Compounding with the loss of insulin sensitivity, high levels of GlcN treatment rapidly lowers ATP levels due to the actions of hexokinase phosphorylating GlcN (23). Hence, rapid unregulated flux through the HBP increases AMP levels and could activate AMPK (48). Furthermore, low levels of sustained GlcN treatment transiently activates AMPK activity, lowers oxidative phosphorylation, and increases lifespan in *C. elegans* and mice (49). The effect of the GlcN treatment is mediated by changes in O-GlcNAcylation since sustained treatment with OGA inhibitor Thiamet-G (TMG) in mice and cell lines also reduces oxidative phosphorylation, lowers ATP production, and reprograms the transcriptome (7). Together, these data would argue that changes in HBP flux influence AMPK activation via increased cellular O-GlcNAcylation. Of note, AMPK activity is higher in OGT KO mice skeletal muscle cells suggesting loss of OGT activates AMPK (50).

Finally, studies on glucose deprivation revealed (50, 51) distinct, tissue-dependent relationships between O-GlcNAc and AMPK. HepG2 and Neuro-2a cells treated with AMPK inhibitors and subjected to glucose starvation experienced significantly lower global O-GlcNAcylation when compared to cells that were only glucose starved (51), inferring an AMPK-dependent mechanism for heightened O-GlcNAcylation in glucose starvation. However, A459 carcinoma lung cells responded differently than the previously observation; while glucose starvation did result in dramatic increases in O-GlcNAcylation, it did not coincide with any major changes in AMPK activation (50). Treatment with Compound C, an AMPK inhibitor, in conjunction with glucose starvation still resulted in an increase in global O-GlcNAcylation, though the effects were somewhat less pronounced than cells only undergoing glucose starvation (50). AMPK inhibition also resulted in a significant decrease in glycogen synthase, a key enzyme in the process of converting glucose molecules into glycogen, but did not impact the expression of glycogen phosphorylase (GP), an enzyme responsible for catalyzing glycogen degradation (50). Further investigation revealed that inhibition of GP in conjunction with glucose starvation dramatically repressed the starvation-induced increase in global O-GlcNAcylation (50), suggesting that AMPK and GP are responsible for coordinating a shift in glycogen metabolism under starvation periods, possibly to generate large pools of glucose for input into the HBP. Overall, while the impact of AMPK activity on starvation-induced O-GlcNAcylation appears to vary between tissue types, the observed evidence indicates a clear niche for AMPK in regulating metabolism in response to nutrient deprivation stress. However, complicating these conclusions is that glucose starvation induced increases in O-GlcNAcylation is dependent on AMPK activity (51). Hence, these data suggest manipulation of O-GlcNAcylation through HBP flux alters cellular energy usage and could influence AMPK activity although these changes could be tissue specific.

Recently, a study demonstrated that AMPK and OGT are substrates for each other and regulate each other's activity (4). In HEK293T kidney cells treated with OGA inhibitors GlcNAc Thiazoline (GT) or TMG, several AMPK subunits were O-GlcNAcylated leading to decreased AMPK activating phosphorylation. These data clearly demonstrate a regulatory role for OGT in AMPK activity (21). On the other hand, AMPK phosphorylation of Thr44 on OGT increases OGT nuclear localization, increases nuclear O-GlcNAcylation, increases histone H3K9 acetylation (4), while O-GlcNAcylation of the H2B histone is lower (22), revealing AMPK as a regulator of O-GlcNAc mediated epigenetic modifications. Furthermore, AMPK regulation of the HBP is not limited to interactions with OGT. GFAT is an AMPK target for phosphorylation at Ser243 (23), and cardiomyocytes treated with the AMPK activator, A769662, have demonstrated a marked decrease in overall O-GlcNAcylation of proteins as well as increased phosphorylation of GFAT (24), hence UDP-GlcNAc production can be directed by AMPK.

OGT appears to be a clear regulator of AMPK activity in cancer development. In several breast cancer cell lines, either knockdown of OGT expression by shRNA or pharmacological inhibition led to increased LKB1 phosphorylation and activation of AMPK (52). In turn, loss of OGT activity and increased AMPK activity reduced cancer cell growth, impaired HIF-1α activation, and increased SIRT1 activity (52, 53). In LoVo colon cancer cells treated with TMG a marked increase in growth and proliferation occurred (5). Interestingly, TMG-treated cells also demonstrated increased levels of O-GlcNAcylated AMPK, as well as a decrease in phosphorylated AMPK (5) coupled with an increase in phosphorylated p70S6K (Ribosomal Protein S6 Kinase), an mTORC1 target. In these experiments, total cellular levels of O-GlcNAc regulated AMPK activity, with high levels of O-GlcNAc reducing activation while low levels increased activation. These data agree with the previous data showing AMPK O-GlcNAcylation inhibits kinase function (4). Overall, sustained O-GlcNAcylation is linked to suppression of AMPK activation, which could increase mTORC1 activity and heightened cell proliferation rates. Hence, O-GlcNAcylation can influence mTORC1 activity indirectly through AMPK, but is there crosstalk between mTOR and OGT that would influence activity of each pathway?

SUSTAINED O-GLCNACYLATION CORRELATES WITH INCREASED PHOSPHORYLATION OF mTOR TARGETS

Interactions between the HBP and AMPK appear to result in inverse responses between the two, not unlike the opposing dynamic between the AMPK and mTOR pathways. The HBP and mTOR pathway share sensitivities for specific macromolecules and similar responses to fluctuations in nutrition, (12–14, 16, 17, 23–25, 32, 36, 37), leaving a wide door for exploring possible interactions. Recent evidence has suggested that mTOR and O-GlcNAc coordinate together to direct autophagy (54, 55). Autophagy is the process of degrading and recycling organelles, as well as other cellular components, which is significant in maintaining cellular function (54). Treatment with mTOR inhibitors Torin1 and PP242 resulted in induced autophagy and a drop in global O-GlcNAcylation, which occurred with increased OGA and decreased OGT protein expression (54). While it appears that mTOR inhibition couples with active autophagy, another study (55) demonstrated that the acuity of mTOR suppression impacts this dynamic; moderate mTOR suppression resulted in a significant increase in autophagy, but was attenuated with severe mTOR inhibition. What's more, an inter-play between phosphorylation and O-GlcNAcylation of the autophagy regulator, Beclin1, demonstrated that moderate mTOR suppression promoted the former modification, while severe inhibition increased the latter (55). While the exact synergy between O-GlcNAc and mTOR has not been detected in autophagy, there appears to be a clear dynamic that is hinged on the spectrum of mTOR repression.

Obesity is another area of research that has revealed a dynamic between mTOR and O-GlcNAc. When analyzing normal mice and Ob/Ob type mice, there were increased levels of OGT expression and mTOR phosphorylation (56). A corresponding *in vitro* experiment using colon cancer cells also demonstrated higher OGT expression and phosphorylated mTOR, as well as higher levels of O-GlcNAcylation. Treatment of these cell lines with an mTOR activator (MHY1485) showed a slight increase in phosphorylated mTOR, OGT, and O-GlcNAcylation and a significant amplification in phosphorylated p70S6K (56). On the other hand, treatment with an mTOR inhibitor, rapamycin, caused distinct decreases in phosphorylated mTOR, OGT, O-GlcNAcylation and complete inhibition of p70S6K phosphorylation (56).

Interestingly, downstream targets in the mTOR pathway also appear to respond to O-GlcNAcylation. Ribosomal protein S6 (RPS6) is a phosphorylation target of p70S6K, but is also one of many ribosomal components that can be O-GlcNAcylated. Of note, the O-GlcNAc modification on S6 does not appear to be influenced by glucose starvation (57). While the purpose of this is not yet known, it was hypothesized (57) that this phenomenon might play a role regulating translation of proteins associated with glucose metabolism. What's more, O-GlcNAc also impacts mRNA selectivity and translation rates in diabetes via another mTORC1 target, 4E-binding protein 1 (4E-BP1). Hypophosphorylated 4E-BP1 binds to eIF4E, a ribosomal component that binds to the 5′ cap of mRNA, which blocks selective translation and alters the normal pattern of mRNA translation. Examination of the liver tissue of diabetic mice revealed that 4E-BP1 binding of eIF4E was not only dramatically increased, but O-GlcNAcylation of 4E-BP1 was elevated almost 2-fold while 4E-BP1 phosphorylation declined significantly (58), suggesting that O-GlcNAc plays a role in cap-independent translation in diabetes signaling.

While there is not a large amount of literature detailing the interactions between mTORC1 and the HBP, current documentation does reveal an intricate, fine-tuned dynamic between the two pathways. With diabetes in particular, this relationship appears to play a substantial role, which makes it a prime focal point for future research into these diseases. However, when considering the web of interactions occurring between the HBP and the mTOR pathway, as well as their relationships with the AMPK pathway, it is important to understand the complexity of cell behavior and sheer amount of variables required for signaling events. Therefore, exploring the dynamics between these pathways using a systems biology approach, alongside conventional laboratory techniques might be the best approach for future investigations.

SYSTEMS BIOLOGY APPROACHES WILL IMPROVE UNDERSTANDING OF SIGNALING CROSS-TALK BY NUTRIENT SENSING

While the evidence discussed provides a possible framework of interactions between the HBP, mTOR, and AMPK pathways, the intrinsic complexity of cellular function must be considered when formulating our understanding of these relationships. Ultimately, the true story of nutrient sensing and cellular response cannot be reduced to simple interactions, such as the repression of mTORC1 by AMPK. The maintenance of cellular homeostasis is a vital process, which must be finely tuned. Therefore, a more accurate picture would be like the mixing board used in a recording studio or a concert, rather than the volume knob on the radio in a car. There are many inputs, which interact in complex and dynamic ways. Nutritional sensing pathways, such as AMPK, mTORC1, and O-GlcNAc are replete with feedback loops (59, 60), which allow them to self-regulate and accomplish a fine degree of control. Unfortunately, this has substantially complicated efforts to understand these pathways, because they exercise a robust control over many perturbations.

An additional challenge in understanding the complexities of nutrient sensing is biological "noise" in a cell. Biological pathways are frequently represented as an orderly set of protein-protein interactions (PPIs), frequently in the form of a directed graph (61). Naturally, this is an oversimplification of reality. In fact, for any given interaction, an individual protein may have a large number of competitors for its receptor. However, these alternate ligands may not induce

the same effect (e.g. conformational change) in the receptor. From one perspective, this "promiscuity" of proteins involved in PPIs is a major contributor of biological noise in a pathway, but it is important to note that noise is a matter of perspective. In some cases, it would be more accurate to consider these proteins as competing signals. Partly, this arrangement is likely the byproduct of evolution, and the mechanism through which new functions can be introduced (i.e., evolution works with what is already there, so new proteins will have similar binding domains to previous domains, especially early on) (62, 63). Thus, a more specific protein may have to compete with a large number of less specific alternatives. This has contributed to a view that signal transduction, such as that involved in nutrient sensing, is sometimes more probabilistic than deterministic (64, 65).

Nevertheless, a cell must have some method for fine-tuning signals to maintain homeostasis in a noisy environment, which is where we see PTMs come into play (64). One such way that O-GlcNAcylation functions to polish these signaling mechanism is to impede protein degradation (66–68), thus increasing the probability of signal transduction, increase or decrease binding affinity for a particular interaction (69–71), or competetion against other PTMs that might change a protein's function in different ways (72). The rapid cycling of O-GlcNAc may allow for much more granular control of nutrient response (73), so taking a probabilistic view of nutrient sensing, O-GlcNAcylation might be understood as one way a cell has of weighting the dice toward a required response.

The complex and dynamic nature of maintaining glucose homeostasis suggests the need for the more holistic view that can be provided by genomic or even multi-omic methods. However, due to the reactive nature of these pathways, this view requires more than a simple "snapshot" of the cell. Rather, approaches that can paint a picture of cellular dynamics are called for. Such studies are not only expensive, but they require new methods to understand the collected data. Nevertheless, early attempts to tackle this problem show promise (73, 74). A recent computational method was developed after collecting transcriptional data over time, while introducing a change in nitrogen sources for *Saccharomyces cerevisiae* (65) in order to study the effect of metabolic signals on transcriptome perturbations mediated by TORC1. A key requirement in unraveling these complexities is to demonstrate a causal relationship between a change in metabolites and transcription, by ensuring that the metabolite change proceeds the transcriptional change temporally, so a quality dataset is required. Using these data, a probabilistic model was built, which provided evidence that glutamine availability is a regulator of TORC1 and through TORC1 is able to drive changes in other metabolites, such as Inosine monophosphate (IMP) and adenosine (the latter of which may suggest another feedback mechanism for TORC1). The accumulation of IMP, downstream of TORC1 activation is interesting, and may point to one mechanism through which the inverse relationship of TORC1 and AMPK is maintained. AMP is deaminated to IMP by *Amd1*, which may be regulated by TORC1. Further work was built on this approach, demonstrating that TORC1 target *Sch9* may be the kinase responsible phosphorylating *Amd1* (75), pointing to yet another regulatory loop that may tie TORC1 and AMPK together. Naturally, these results are in yeast, but *Sch9* functions similarly to S6K1 (76), which is a known target of mTORC1. Such insights would not be possible without a closely linked computational and experimental approach, such as those used in these studies. Future work could extend these concepts to mammalian organisms and incorporate a more robust range of PTMs, such as O-GlcNAc, to construct a more accurate picture of cell signaling and the fine-tuning that regulates these mechanisms.

SUMMARY

The HBP, AMPK, and mTOR pathways all present a unique niche in cellular function, with respect to nutrient-sensing. However, it is the crosstalk between these pathways that fosters a particularly interesting but unexplored spotlight in cell signaling. While reduced energy levels trigger AMPK inhibition of mTORC1, these conditions can also trigger conservation of energy via increased global O-GlcNAcylation. However, increased glucose and glucosamine uptake bolsters cytosolic ATP production and triggers deviations in cellular behavior, such as insulin resistance, while repressing AMPK and allowing the mTOR pathway to encourage proliferation. Amino acid uptake facilitates mTORC1 activation and can up-regulate the HBP in a fine-tuned manner, while diminishing AMPK activity. Cross-talk between OGT and AMPK presents a mutually inhibitory relationship between the two enzymes based on nutrient availability and stimulation, while the mTOR pathway and O-GlcNAc coordinate with one another to direct autophagy.

Overall, there appears to be an intricate dynamic between the three pathways, where deviations in their communication lend to various pathologies. Future research should elucidate more connections between these pathways using both computational methods and traditional bench work, with the hopes that we'll understand this "real talk" and how to counteract it when it leads to disease-related miscommunication.

AUTHOR CONTRIBUTIONS

All authors listed have made a substantial, direct and intellectual contribution to the work, and approved it for publication.

FUNDING

CS was supported by National Institute of Diabetes and Digestive and Kidney Diseases grant R01DK100595 and National Cancer Institute grant R03CA223949. This work was supported by the Molecular Regulation of Cell Development and Differentiation COBRE P30GM122731 CS.

REFERENCES

1. Torres CR, Hart GW. Topography and polypeptide distribution of terminal N-acetylglucosamine residues on the surfaces of intact lymphocytes. Evidence for O-linked GlcNAc. *J Biol Chem.* (1984) 259:3308–17.
2. Dong DL, Hart GW. Purification and characterization of an O-GlcNAc selective N-acetyl-beta-D-glucosaminidase from rat spleen cytosol. *J Biol Chem.* (1994) 269:19321–30.
3. Chou CF, Smith AJ, Omary MB. Characterization and dynamics of O-linked glycosylation of human cytokeratin 8 and 18. *J Biol Chem.* (1992) 267:3901–6.
4. Bullen JW, Balsbaugh JL, Chanda D, Shabanowitz J, Hunt DF, Neumann D, et al. Cross-talk between two essential nutrient-sensitive enzymes: O-GlcNAc transferase (OGT) and AMP-activated protein kinase (AMPK). *J Biol Chem.* (2014) 289:10592–606. doi: 10.1074/jbc.M113.523068
5. Ishimura E, Nakagawa T, Moriwaki K, Hirano S, Matsumori Y, Asahi M. Augmented O-GlcNAcylation of AMP-activated kinase promotes the proliferation of LoVo cells, a colon cancer cell line. *Cancer Sci.* (2017) 108:2373–82. doi: 10.1111/cas.13412
6. Luanpitpong S, Chanthra N, Janan M, Poohadsuan J, Samart P, U-Pratya Y, et al. Inhibition of O-GlcNAcase sensitizes apoptosis and reverses bortezomib resistance in mantle cell lymphoma through modification of truncated bid. *Mol Cancer Ther.* (2018) 17:484–96. doi: 10.1158/1535-7163.MCT-17-0390
7. Tan EP, McGreal SR, Graw S, Tessman R, Koppel SJ, Dhakal P, et al. Sustained O-GlcNAcylation reprograms mitochondrial function to regulate energy metabolism. *J Biol Chem.* (2017) 292:14940–62. doi: 10.1074/jbc.M117.797944
8. Tan EP, Villar MT, E L, Lu J, Selfridge JE, Artigues A, et al. Altering O-linked beta-N-acetylglucosamine cycling disrupts mitochondrial function. *J Biol Chem.* (2014) 289:14719–30. doi: 10.1074/jbc.M113.525790
9. Shin H, Cha HJ, Na K, Lee MJ, Cho JY, Kim CY, et al. O-GlcNAcylation of the tumor suppressor FOXO3 triggers aberrant cancer cell growth. *Cancer Res.* (2018) 78:1214–24. doi: 10.1158/0008-5472.CAN-17-3512
10. Dos Santos JPA, Vizuete A, Hansen F, Biasibetti R, Goncalves CA. Early and persistent O-GlcNAc protein modification in the streptozotocin model of alzheimer's disease. *J Alzheimers Dis.* (2018) 61:237–9. doi: 10.3233/JAD-170211
11. Chun YS, Kwon OH, Chung S. O-GlcNAcylation of amyloid-beta precursor protein at threonine 576 residue regulates trafficking and processing. *Biochem Biophys Res Commun.* (2017) 490:486–91. doi: 10.1016/j.bbrc.2017.06.067
12. Taylor RP, Parker GJ, Hazel MW, Soesanto Y, Fuller W, Yazzie MJ, et al. Glucose deprivation stimulates O-GlcNAc modification of proteins through up-regulation of O-linked N-acetylglucosaminyltransferase. *J Biol Chem.* (2008) 283:6050–7. doi: 10.1074/jbc.M707328200
13. Parker GJ, Lund KC, Taylor RP, McClain DA. Insulin resistance of glycogen synthase mediated by o-linked N-acetylglucosamine. *J Biol Chem.* (2003) 278:10022–27. doi: 10.1074/jbc.M207787200
14. Buse MG, Robinson KA, Marshall BA, Mueckler M. Differential effects of GLUT1 or GLUT4 overexpression on hexosamine biosynthesis by muscles of transgenic mice. *J Biol Chem.* (1996) 271:23197–202. doi: 10.1074/jbc.271.38.23197
15. Slawson C, Hart GW. O-GlcNAc signalling: implications for cancer cell biology. *Nat Rev Cancer* (2011) 11:678–84. doi: 10.1038/nrc3114
16. McClain DA, Lubas WA, Cooksey RC, Hazel M, Parker GJ, Love DC, et al. Altered glycan-dependent signaling induces insulin resistance and hyperleptinemia. *Proc Natl Acad Sci USA.* (2002) 99:10695–99. doi: 10.1073/pnas.152346899
17. Love DC, Hanover JA. The hexosamine signaling pathway: deciphering the "O-GlcNAc code". *Sci STKE* (2005) 2005:re13. doi: 10.1126/stke.3122005re13
18. Whelan SA, Dias WB, Thiruneelakantapillai L, Lane MD, Hart GW. Regulation of insulin receptor substrate 1 (IRS-1)/AKT kinase-mediated insulin signaling by O-Linked beta-N-acetylglucosamine in 3T3-L1 adipocytes. *J Biol Chem.* (2010) 285:5204–11. doi: 10.1074/jbc.M109.077818
19. Shi H, Munk A, Nielsen TS, Daughtry MR, Larsson L, Li S, et al. Skeletal muscle O-GlcNAc transferase is important for muscle energy homeostasis and whole-body insulin sensitivity. *Mol Metab.* (2018) 11:160–77. doi: 10.1016/j.molmet.2018.02.010
20. Ball LE, Berkaw MN, Buse MG. Identification of the major site of O-linked beta-N-acetylglucosamine modification in the C terminus of insulin receptor substrate-1. *Mol Cell Proteomics* (2006) 5:313–23. doi: 10.1074/mcp.M500314-MCP200
21. Yang X, Ongusaha PP, Miles PD, Havstad JC, Zhang F, So WV, et al. Phosphoinositide signalling links O-GlcNAc transferase to insulin resistance. *Nature* (2008) 451:964–9. doi: 10.1038/nature06668
22. Whelan SA, Lane MD, Hart GW. Regulation of the O-linked beta-N-acetylglucosamine transferase by insulin signaling. *J Biol Chem.* (2008) 283:21411–17. doi: 10.1074/jbc.M800677200
23. Marshall S, Nadeau O, Yamasaki K. Dynamic actions of glucose and glucosamine on hexosamine biosynthesis in isolated adipocytes: differential effects on glucosamine 6-phosphate, UDP-N-acetylglucosamine, and ATP levels. *J Biol Chem.* (2004) 279:35313–19. doi: 10.1074/jbc.M404133200
24. Marshall S, Bacote V, Traxinger RR. Complete inhibition of glucose-induced desensitization of the glucose transport system by inhibitors of mRNA synthesis. Evidence for rapid turnover of glutamine:fructose-6-phosphate amidotransferase. *J Biol Chem.* (1991) 266:10155–61.
25. Rumberger JM, Wu T, Hering MA, Marshall S. Role of hexosamine biosynthesis in glucose-mediated up-regulation of lipogenic enzyme mRNA levels: effects of glucose, glutamine, and glucosamine on glycerophosphate dehydrogenase, fatty acid synthase, and acetyl-CoA carboxylase mRNA levels. *J Biol Chem.* (2003) 278:28547–52. doi: 10.1074/jbc.M302793200
26. Foster KG, Fingar DC. Mammalian target of rapamycin (mTOR): conducting the cellular signaling symphony. *J Biol Chem.* (2010) 285:14071–77. doi: 10.1074/jbc.R109.094003
27. Jacinto E, Loewith R, Schmidt A, Lin S, Ruegg MA, Hall A, et al. Mammalian TOR complex 2 controls the actin cytoskeleton and is rapamycin insensitive. *Nat Cell Biol.* (2004) 6:1122–8. doi: 10.1038/ncb1183
28. He L, Gomes AP, Wang X, Yoon SO, Lee G, Nagiec MJ, et al. mTORC1 promotes metabolic reprogramming by the suppression of GSK3-dependent Foxk1 phosphorylation. *Mol Cell* (2018) 70:949.e4–60. doi: 10.1016/j.molcel.2018.04.024
29. Sun J, Mao L, Yang H, Ren D. Critical role for the Tsc1-mTORC1 pathway in beta-cell mass in Pdx1 deficient mice. *J Endocrinol.* (2018) 238:151–63. doi: 10.1530/JOE-18-0015
30. Inoki K, Zhu T, Guan KL. TSC2 mediates cellular energy response to control cell growth and survival. *Cell* (2003) 115:577–90. doi: 10.1016/S0092-8674(03)00929-2
31. Long X, Lin Y, Ortiz-Vega S, Yonezawa K, Avruch J. Rheb binds and regulates the mTOR kinase. *Curr Biol.* (2005) 15:702–13. doi: 10.1016/j.cub.2005.02.053
32. Sancak Y, Bar-Peled L, Zoncu R, Markhard AL, Nada S, Sabatini DM. Ragulator-Rag complex targets mTORC1 to the lysosomal surface and is necessary for its activation by amino acids. *Cell* (2010) 141:290–303. doi: 10.1016/j.cell.2010.02.024
33. Yoon MS. The role of mammalian target of rapamycin (mTOR) in insulin signaling. *Nutrients* (2017) 9:E1176. doi: 10.3390/nu9111176
34. Gulati P, Gaspers LD, Dann SG, Joaquin M, Nobukuni T, Natt F, et al. Amino acids activate mTOR complex 1 via Ca2+/CaM signaling to hVps34. *Cell Metab.* (2008) 7:456–65. doi: 10.1016/j.cmet.2008.03.002
35. Smith EM, Finn SG, Tee AR, Browne GJ, Proud CG. The tuberous sclerosis protein TSC2 is not required for the regulation of the mammalian target of rapamycin by amino acids and certain cellular stresses. *J Biol Chem.* (2005) 280:18717–27. doi: 10.1074/jbc.M414499200
36. Sancak Y, Peterson TR, Shaul YD, Lindquist RA, Thoreen CC, Bar-Peled L, et al. The rag GTPases bind raptor and mediate amino acid signaling to mTORC1. *Science* (2008) 320:1496–501. doi: 10.1126/science.1157535
37. Tsang CK, Chen M, Cheng X, Qi Y, Chen Y, Das I, et al. SOD1 phosphorylation by mTORC1 couples nutrient sensing and redox regulation. *Mol Cell* (2018) 70:502.e8–15. doi: 10.1016/j.molcel.2018.03.029
38. Hoxhaj G, Hughes-Hallett J, Timson RC, Ilagan E, Yuan M, Asara JM, et al. The mTORC1 signaling network senses changes in cellular purine nucleotide levels. *Cell Rep.* (2017) 21:1331–46. doi: 10.1016/j.celrep.2017.10.029
39. Gwinn DM, Shackelford DB, Egan DF, Mihaylova MM, Mery A, Vasquez DS, et al. AMPK phosphorylation of raptor mediates a metabolic checkpoint. *Mol Cell* (2008) 30:214–26 doi: 10.1016/j.molcel.2008.03.003
40. Hardie DG, Ross FA, Hawley SA. AMPK: a nutrient and energy sensor that maintains energy homeostasis. *Nat Rev Mol Cell Biol.* (2012) 13:251–62. doi: 10.1038/nrm3311

41. Shaw RJ, Kosmatka M, Bardeesy N, Hurley RL, Witters LA, DePinho RA, et al. The tumor suppressor LKB1 kinase directly activates AMP-activated kinase and regulates apoptosis in response to energy stress. *Proc Natl Acad Sci USA.* (2004) 101:3329–35. doi: 10.1073/pnas.0308061100
42. Fullerton MD, Galic S, Marcinko K, Sikkema S, Pulinilkunnil T, Chen ZP, et al. Single phosphorylation sites in Acc1 and Acc2 regulate lipid homeostasis and the insulin-sensitizing effects of metformin. *Nat Med.* (2013) 19:1649–54. doi: 10.1038/nm.3372
43. Munday MR, Campbell DG, Carling D, Hardie DG. Identification by amino acid sequencing of three major regulatory phosphorylation sites on rat acetyl-CoA carboxylase. *Eur J Biochem.* (1988) 175:331–38. doi: 10.1111/j.1432-1033.1988.tb14201.x
44. Wakil SJ, Stoops JK, Joshi VC. Fatty acid synthesis and its regulation. *Annu Rev Biochem.* (1983) 52:537–79. doi: 10.1146/annurev.bi.52.070183.002541
45. Wu W, Feng J, Jiang D, Zhou X, Jiang Q, Cai M, et al. AMPK regulates lipid accumulation in skeletal muscle cells through FTO-dependent demethylation of N(6)-methyladenosine. *Sci Rep.* (2017) 7:41606. doi: 10.1038/srep41606
46. Gleason CE, Lu D, Witters LA, Newgard CB, Birnbaum MJ. The role of AMPK and mTOR in nutrient sensing in pancreatic beta-cells. *J Biol Chem.* (2007) 282:10341–51. doi: 10.1074/jbc.M610631200
47. Traxinger RR, Marshall S. Coordinated regulation of glutamine:fructose-6-phosphate amidotransferase activity by insulin, glucose, and glutamine. Role of hexosamine biosynthesis in enzyme regulation. *J Biol Chem.* (1991) 266:10148–54.
48. Luo B, Parker GJ, Cooksey RC, Soesanto Y, Evans M, Jones D, et al. Chronic hexosamine flux stimulates fatty acid oxidation by activating AMP-activated protein kinase in adipocytes. *J Biol Chem.* (2007) 282:7172–80. doi: 10.1074/jbc.M607362200
49. Weimer S, Priebs J, Kuhlow D, Groth M, Priebe S, Mansfeld J, et al. D-Glucosamine supplementation extends life span of nematodes and of ageing mice. *Nat Commun.* (2014) 5:3563 doi: 10.1038/ncomms4563
50. Kang JG, Park SY, Ji S, Jang I, Park S, Kim HS, et al. O-GlcNAc protein modification in cancer cells increases in response to glucose deprivation through glycogen degradation. *J Biol Chem.* (2009) 284:34777–84. doi: 10.1074/jbc.M109.026351
51. Cheung WD, Hart GW. AMP-activated protein kinase and p38 MAPK activate O-GlcNAcylation of neuronal proteins during glucose deprivation. *J Biol Chem.* (2008) 283:13009–20. doi: 10.1074/jbc.M801222200
52. Ferrer CM, Lynch TP, Sodi VL, Falcone JN, Schwab LP, Peacock DL, et al. O-GlcNAcylation regulates cancer metabolism and survival stress signaling via regulation of the HIF-1 pathway. *Mol Cell* (2014) 54:820–31. doi: 10.1016/j.molcel.2014.04.026
53. Ferrer CM, Lu TY, Bacigalupa ZA, Katsetos CD, Sinclair DA, Reginato MJ. O-GlcNAcylation regulates breast cancer metastasis via SIRT1 modulation of FOXM1 pathway. *Oncogene* (2017) 36:559–69. doi: 10.1038/onc.2016.228
54. ark S, Pak J, Jang I, Cho JW. Inhibition of mTOR affects protein stability of OGT. *Biochem Biophys Res Commun.* (2014) 453:208–12. doi: 10.1016/j.bbrc.2014.05.047
55. Zhang Q, Na Q, Song W. Moderate mammalian target of rapamycin inhibition induces autophagy in HTR8/SVneo cells via O-linked beta-N-acetylglucosamine signaling. *J Obstet Gynaecol Res.* (2017) 43:1585–96. doi: 10.1111/jog.13410
56. Very N, Steenackers A, Dubuquoy C, Vermuse J, Dubuquoy L, Lefebvre T, et al. Cross regulation between mTOR signaling and O-GlcNAcylation. *J Bioenerg Biomembr.* (2018) 50:213–22. doi: 10.1007/s10863-018-9747-y
57. Zeidan Q, Wang Z, De Maio A, Hart GW. O-GlcNAc cycling enzymes associate with the translational machinery and modify core ribosomal proteins. *Mol Biol Cell* (2010) 21:1922–36. doi: 10.1091/mbc.e09-11-0941
58. Dennis MD, Schrufer TL, Bronson SK, Kimball SR, Jefferson LS. Hyperglycemia-induced O-GlcNAcylation and truncation of 4E-BP1 protein in liver of a mouse model of type 1 diabetes. *J Biol Chem.* (2011) 286:34286–97. doi: 10.1074/jbc.M111.259457
59. Loffler AS, Alers S, Dieterle AM, Keppeler H, Franz-Wachtel M, Kundu M, et al. Ulk1-mediated phosphorylation of AMPK constitutes a negative regulatory feedback loop. *Autophagy* (2011) 7:696–706. doi: 10.4161/auto.7.7.15451
60. Sathe A, Chalaud G, Oppolzer I, Wong KY, von Busch M, Schmid SC, et al. Parallel PI3K, AKT and mTOR inhibition is required to control feedback loops that limit tumor therapy. *PLoS ONE* (2018) 13:e0190854. doi: 10.1371/journal.pone.0190854
61. Kanehisa M, Furumichi M, Tanabe M, Sato Y, Morishima K. KEGG: new perspectives on genomes, pathways, diseases and drugs. *Nucleic Acids Res.* (2017) 45:D353–61. doi: 10.1093/nar/gkw1092
62. Aakre CD, Herrou J, Phung TN, Perchuk BS, Crosson S, Laub MT. Evolving new protein-protein interaction specificity through promiscuous intermediates. *Cell* (2015) 163:594–606. doi: 10.1016/j.cell.2015.09.055
63. Alhindi T, Zhang Z, Ruelens P, Coenen H, Degroote H, Iraci N, et al. Protein interaction evolution from promiscuity to specificity with reduced flexibility in an increasingly complex network. *Sci Rep.* (2017) 7:44948 doi: 10.1038/srep44948
64. Ladbury JE, Arold ST. Noise in cellular signaling pathways: causes and effects. *Trends Biochem Sci.* (2012) 37:173–78. doi: 10.1016/j.tibs.2012.01.001
65. Symmons O, Raj A. What's luck got to do with it: single cells, multiple fates, and biological nondeterminism. *Mol Cell* (2016) 62:788–802. doi: 10.1016/j.molcel.2016.05.023
66. Zhu Y, Liu TW, Cecioni S, Eskandari R, Zandberg WF, Vocadlo DJ. O-GlcNAc occurs cotranslationally to stabilize nascent polypeptide chains. *Nat Chem Biol.* (2015) 11:319–25. doi: 10.1038/nchembio.1774
67. Guinez C, Mir AM, Dehennaut V, Cacan R, Harduin-Lepers A, Michalski JC, et al. Protein ubiquitination is modulated by O-GlcNAc glycosylation. *FASEB J.* (2008) 22:2901–11. doi: 10.1096/fj.07-102509
68. Han I, Kudlow JE. Reduced O glycosylation of Sp1 is associated with increased proteasome susceptibility. *Mol Cell Biol.* (1997) 17:2550–8. doi: 10.1128/MCB.17.5.2550
69. Yang X, Su K, Roos MD, Chang Q, Paterson AJ, et al. O-linkage of N-acetylglucosamine to Sp1 activation domain inhibits its transcriptional capability. *Proc Natl Acad Sci USA.* (2001) 98:6611–16. doi: 10.1073/pnas.111099998
70. Han C, Gu Y, Shan H, Mi W, Sun J, Shi M, et al. O-GlcNAcylation of SIRT1 enhances its deacetylase activity and promotes cytoprotection under stress. *Nat Commun.* (2017) 8:1491 doi: 10.1038/s41467-017-01654-6
71. Griffith LS, Schmitz B. O-linked N-acetylglucosamine levels in cerebellar neurons respond reciprocally to pertubations of phosphorylation. *Eur J Biochem.* (1999) 262:824–31. doi: 10.1046/j.1432-1327.1999.00439.x
72. Olivier-Van Stichelen S, Wang P, Comly M, Love DC, Hanover JA. Nutrient-driven O-linked N-acetylglucosamine (O-GlcNAc) cycling impacts neurodevelopmental timing and metabolism. *J Biol Chem.* (2017) 292:6076–85. doi: 10.1074/jbc.M116.774042
73. Chechik G, Oh E, Rando O, Weissman J, Regev A, Koller D. Activity motifs reveal principles of timing in transcriptional control of the yeast metabolic network. *Nat Biotechnol.* (2008) 26:1251–9. doi: 10.1038/nbt.1499
74. Oliveira AP, Dimopoulos S, Busetto AG, Christen S, Dechant R, Falter L, et al. Inferring causal metabolic signals that regulate the dynamic TORC1-dependent transcriptome. *Mol Syst Biol.* (2015) 11:802 doi: 10.15252/msb.20145475
75. Oliveira AP, Ludwig C, Zampieri M, Weisser H, Aebersold R, Sauer U. Dynamic phosphoproteomics reveals TORC1-dependent regulation of yeast nucleotide and amino acid biosynthesis. *Sci Signal* (2015) 8:rs4. doi: 10.1126/scisignal.2005768
76. Urban J, Soulard A, Huber A, Lippman S, Mukhopadhyay D, Deloche O, et al. Sch9 is a major target of TORC1 in *Saccharomyces cerevisiae*. *Mol Cell* (2007) 26:663–74. doi: 10.1016/j.molcel.2007.04.020

Conflict of Interest Statement: The authors declare that the research was conducted in the absence of any commercial or financial relationships that could be construed as a potential conflict of interest.

frontiers in Endocrinology

ORIGINAL RESEARCH
published: 10 September 2018
doi: 10.3389/fendo.2018.00521

Nutrient-Driven *O*-GlcNAcylation at Promoters Impacts Genome-Wide RNA Pol II Distribution

Michael W. Krause[1], *Dona C. Love*[2], *Salil K. Ghosh*[2], *Peng Wang*[2], *Sijung Yun*[1], *Tetsunari Fukushige*[1] *and John A. Hanover*[2]*

[1] *Laboratory of Molecular Biology, National Institute of Diabetes and Digestive and Kidney Diseases, National Institutes of Health, Bethesda, MD, United States,* [2] *Laboratory of Cell and Molecular Biology, National Institute of Diabetes and Digestive and Kidney Diseases, National Institutes of Health, Bethesda, MD, United States*

Nutrient-driven *O*-GlcNAcylation has been linked to epigenetic regulation of gene expression in metazoans. In *C. elegans, O*-GlcNAc marks the promoters of over 800 developmental, metabolic, and stress-related genes; these *O*-GlcNAc marked genes show a strong 5′, promoter-proximal bias in the distribution of RNA Polymerase II (Pol II). In response to starvation or feeding, the steady state distribution of *O*-GlcNAc at promoters remain nearly constant presumably due to dynamic cycling mediated by the transferase OGT-1 and the *O*-GlcNAcase OGA-1. However, in viable mutants lacking either of these enzymes of *O*-GlcNAc metabolism, the nutrient-responsive GlcNAcylation of promoters is dramatically altered. Blocked *O*-GlcNAc cycling leads to a striking nutrient-dependent accumulation of *O*-GlcNAc on RNA Pol II. *O*-GlcNAc cycling mutants also show an exaggerated, nutrient-responsive redistribution of promoter-proximal RNA Pol II isoforms and extensive transcriptional deregulation. Our findings suggest a complex interplay between the *O*-GlcNAc modification at promoters, the kinase-dependent "CTD-code," and co-factors regulating RNA Pol II dynamics. Nutrient-responsive *O*-GlcNAc cycling may buffer the transcriptional apparatus from dramatic swings in nutrient availability by modulating promoter activity to meet metabolic and developmental needs.

Keywords: *O*-GlcNAc, RNA-polymerase II, CTD, transcription, genetic, nutrients, polymerase dynamics, glycobiology

OPEN ACCESS

Edited by:
Tarik Issad,
Institut National de la Santé et de la Recherche Médicale (INSERM), France

Reviewed by:
Chad Slawson,
Kansas University of Medical Center Research Institute, United States
Dehennaut-Lefebvre Vanessa, UMR8161 Mécanismes de la Tumorigenèse et Thérapies Ciblées, France

***Correspondence:**
John A. Hanover
jah@helix.nih.gov

Specialty section:
This article was submitted to Molecular and Structural Endocrinology, a section of the journal Frontiers in Endocrinology

Received: *25 June 2018*
Accepted: *21 August 2018*
Published: *10 September 2018*

Citation:
Krause MW, Love DC, Ghosh SK, Wang P, Yun S, Fukushige T and Hanover JA (2018) Nutrient-Driven O-GlcNAcylation at Promoters Impacts Genome-Wide RNA Pol II Distribution. Front. Endocrinol. 9:521. doi: 10.3389/fendo.2018.00521

INTRODUCTION

Animals have evolved under conditions of fluctuating nutrient availability, requiring them to adapt in order to balance growth and survival. Thus, mechanisms exist to sustain essential cellular functions during prolonged starvation conditions while permitting a rapid metabolic response when conditions become replete. Transcriptional regulation is one such mechanism, controlling a subset of genes that are required for the acute catabolic or anabolic response to nutrient flux or changes in environmental stimuli.

Transcriptional regulation can occur at many different levels, including recruitment of RNA Polymerase II (Pol II) to the promoter and the transcription events of initiation, elongation, splicing, and termination. All of these activities are influenced by the differential phosphorylation of the C-terminal domain (CTD) of Pol II (1) and its associated factors. This "CTD-code" is subject to

elaborate regulation by CTD-kinases (2, 3) and, together with other factors that stably or transiently associate with the polymerase complex, regulate gene expression (4–6).

Although recruitment of Pol II to the relevant promoters has long been thought to be the primary molecular control point for transcriptional responses, recent studies demonstrate that many stress and developmental genes have a pool of Pol II engaged at the promoter that is poised for rapid activation. This mode of control, referred to as Pol II promoter-proximal pausing, has emerged as a common means of transcriptional regulation among many, but not all, animals (7–13). From a biological perspective, this pool of promoter-associated polymerase has been suggested to serve a memory function, which may anticipate the need for rapid mobilization in response to environmental or developmental cues (14).

For the nematode *Caenorhabditis elegans*, life in the soil has subjected the animal to constant cycles of feast and famine throughout its evolution. *C. elegans* has adopted a number of developmental strategies to adapt to nutrient flux, including larval stage 1 (L1) arrest, dauer diapause, adult reproductive diapause and life extension in response to starvation (15–18). Many of these developmental decisions are under transcriptional control. In fact, it has been shown that starvation-induced L1 arrest in *C. elegans* is accompanied by enhanced Pol II promoter-proximal pausing, particularly at promoters for metabolic genes important for growth and stress responses (19, 20). However, unlike *Drosophila* and mammals, Pol II pausing does not appear to be a major mechanism of transcriptional regulation in *C. elegans* (21). Moreover, worms lack a NELF homolog (22), which is a major regulator of Pol II pausing found in other animals, raising the possibility that additional inputs might regulate Pol II dynamics in this organism.

Many different nutrient sensing pathways feed into transcriptional control and developmental decisions. We have previously demonstrated in *C. elegans* that dauer formation, the stress response, and adult longevity, are all strongly influenced by the Hexosamine Signaling Pathway (HSP) (23–25). For many key cellular targets, the HSP provides a dynamic, nutrient driven mechanism to influence protein function in response to the metabolic status of the cell (26, 27). The terminal step of the HSP is the transfer of O-linked *N*-acetylglucosamine (*O*-GlcNAc) to Ser and Thr amino acids in target substrates catalyzed by the enzyme *O*-GlcNAc transferase (OGT). The *O*-GlcNAc modification is reversed by the action of an *O*-GlcNAcase (OGA). This dynamic, post-translational, single sugar modification of nuclear and cytoplasmic proteins is reminiscent of phosphorylation and dephosphorylation of Ser/Thr residues by kinases and phosphatases. Thus, nutrient-driven *O*-GlcNAcylation is capable of producing extensive crosstalk with kinase-dependent, and other, signaling pathways influencing numerous aspects of cell physiology (26–29).

O-GlcNAc cycling has been genetically linked directly to the regulation of gene expression. We, and others, have shown that GlcNAcylation of chromatin-associated substrates is an evolutionarily conserved modification that is localized predominantly to the promoter regions of many genes, raising the possibility that promoter-proximal Pol II dynamics could be directly influenced by nutrient flux (30–33). RNA Pol II has been shown to be GlcNAcylated on the CTD (34–36), including on Ser-2 and Ser-5 residues of the CTD heptad repeat (37–39), and the *O*-GlcNAcase (OGA) shown to be part of the Pol II elongation complex interacting with Pol II pausing factors (40). Much of this previous work has been performed *in vitro* using recombinant OGT and OGA and examining the impact of these activities on template-driven transcription of model reporter constructs. The results of these studies suggest a model in which *O*-GlcNAc plays a role in preinitiation complex formation and interplays with the "CTD code" of phosphorylation on RNA Pol II (34–39).

In efforts to determine the function *O*-GlcNAc on transcription in an intact organism, we have analyzed deletion alleles encoding these enzymes in the mouse and in *Drosophila.* In mouse, OGT is essential (41–43), but OGA null alleles survive until the perinatal period, directly demonstrating that *O*-GlcNAcase is not essential for transcription and development (44). Loss of OGA in *Drosophila* is also non-essential, but impacts the epigenetic machinery allowing *O*-GlcNAc accumulation on RNA Polymerase II and numerous chromatin factors including TRX, ASH1, and SET (33). Here, we have extended the analysis to viable knockout alleles in *C. elegans* of the genes encoding OGT and OGA to explore the role of *O*-GlcNAcylation on Pol II distribution and transcription in a whole organism.

Chromatin immunoprecipitation (ChIP) of starved or fed samples with multiple antibodies specific for either the *O*-GlcNAc modification itself or Pol II CTD phosphorylated isoforms revealed a near constant distribution of Pol II across most genes in wild type animals regardless of growth conditions. In contrast, loss of OGT-1 activity resulted in dramatic changes to Pol II distribution in response to nutrient flux, particularly for genes associated with high levels of GlcNAcylated chromatin at their promoters; a similar, but less dramatic effect was seen with loss of OGA-1 activity. We also find that animals lacking OGT, and to a lesser extent OGA, activity have substantially altered gene expression responses in starved and fed conditions compared to wild type animals. Our results demonstrate that dynamic GlcNAcylation of Pol II and other chromatin associated substrates, predominantly localized at promoters, is part of a homeostatic mechanism that ensures a constant steady state Pol II distribution for most genes during fluctuating nutritional conditions. The post-translational modification of chromatin-associated substrates by nutrient responsive GlcNAcylation provides a direct link between the cellular metabolic state and Pol II promoter-proximal dynamics with epigenetic implications for the organism.

RESULTS

Promoter-Associated *O*-GlcNAc Levels Are Maintained by *O*-GlcNAc Cycling in Conditions of Both Starvation and Nutrient Excess

Previously, we showed that *O*-GlcNAcylated substrates reside at the promoter regions of many genes, microRNAs, and non-coding RNAs in *C. elegans* (32). Transcriptional changes

resulting from the disruption of *O*-GlcNAc cycling described previously (32) suggested that GlcNAcylation might directly impact transcription by modifying one or more chromatin-associated substrates in response to nutrient flux. To extend these findings, we have used the viable null alleles of *O*-GlcNAc to determine the impact of loss of *O*-GlcNAc cycling on RNA polymerase behavior in response to changes in nutrient availability.

Antibodies that specifically recognize the *O*-GlcNAc epitope were used in chromatin immunoprecipitation (ChIP) experiments with synchronous, first larval stage (L1) wild type animals under starved and fed conditions [Experimental Procedures; (32)]. Chromatin derived probes were used for whole genome tiling array hybridization (ChIP-chip) and the data normalized to a common input chromatin sample. We have found that our ChIP-chip data provided a less biased, hybridization-based signal across genes compared with new technology, such as ChIP-seq, and allows direct comparisons with previous work, including our own studies in *Drosophila melanogaster* (33) and *C. elegans* (32). To allow visualization of the ChIP-chip data from multiple genes simultaneously, a common gene model (metagene) of uniform length was defined that extended from the translational start to stop codons based on genome version WS195 to match the arrays that were used (Experimental Procedures); our analyses also included 3 kb upstream of the start site corresponding to hightened *O*-GlcNAc signal intensity.

To validate our ChIP-chip data, multiple chromatin preparations and immunoprecipitations with many different antibodies to *O*-GlcNAc and Pol II were used in various combinations to demonstrate consistency and reproducibility of the results (Experimental Procedures). As previously reported, almost all Pol II antibodies gave similar patterns across the genome regardless of their advertised specificity or preference for different Pol II CTD phosphorylated isoforms (19)(**Supplemental Figure 1**). These results are consistent with our own assays of specificity using both peptide dot blots and *in vivo* antibody staining in early embryos (**Supplemental Figures 1**, **2**). Our data sets also replicated and confirmed a previous study that identified a set of genes with a high level of promoter-proximal Pol II compared to the gene bodies (19)(data not shown). Therefore, we had high confidence that this data could be used to examine chromatin distributions among various gene classes and multiple genetic mutants to explore possible correlations that would inform the functions of chromatin *O*-GlcNAcylation, if any.

We first examined the list of 827 genes previously identified as being associated with elevated promoter *O*-GlcNAc marks in *C. elegans* (32); note that one gene model on the original list is no longer valid, resulting in 826 genes, but we have retained the original naming convention for clarity. Comparison of wild type starved vs. fed data for these "marked" genes revealed nearly identical profiles of *O*-GlcNAc signal relative to the common gene model with a strong promoter region bias in distribution (**Figure 1A**); this was true for each of two independent anti-*O*-GlcNAc antibodies (RL2 and HGAC85) assayed by whole genome ChIP (data not shown). The constant distribution of *O*-GlcNAc in response to nutrient flux was surprising since total *O*-GlcNAc on cellular proteins increases in response to nutritional flux in worms (45). An analysis of the genomic sequence associated with the *O*-GlcNAc promoter intervals revealed an enrichment of two repetitive sequence motifs: GAGAGAGA, ACACACAC, and their inverse complements (**Supplemental Figure 3**). These simple repeats have also been noted in promoter regions in other transcription factor ChIP studies (46, 47) suggesting their presence may simply reflect a general property of promoters rather than a binding site preference for GlcNAcylated chromatin-associated proteins *per se*. The constant *O*-GlcNAcylation at promoters in response to nutrient flux suggested that *O*-GlcNAc levels might be actively regulated at these sites in wild type animals.

Promoter GlcNAcylation Responds Aberrantly to Nutrient Flux When *O*-GlcNAc Cycling Is Blocked

To determine if disruption of active *O*-GlcNAc cycling had an effect on the distribution of chromatin GlcNAcylation in starved vs. fed animals, we assayed the same 827 marked genes in mutants in which either OGT-1 or OGA-1 activity had been eliminated by genomic deletions. We have previously shown that the *ogt-1(ok430)* mutants lack *O*-GlcNAc transferase activity (23) and we used this enzymatic null allele to threshold ChIP-chip experiments in starved animals to define the list of 827 *O*-GlcNAc marked genes (32). As expected, the *O*-GlcNAc ChIP signals in fed or starved *ogt-1(ok430)* mutants is quite low and similar to that observed and defined as background [**Figure 1A**; (32)]. The observed over representation of promoter regions in this mutant, which lacks the enzymatic activity needed to generate the epitope being ChIPed, likely reflects the relative open chromatin associated with promoters that is commonly observed in ChIP studies (48–50).

We have also characterized a viable null mutant in the *O*-GlcNAcase gene in *C. elegans* (*oga-1(ok1207)*) (24). ChIP data from *oga-1(ok1207)* mutants that cannot reverse the *O*-GlcNAc modifications on substrates revealed changes in response to the nutrient status of the organism (**Figure 1A**). Promoter regions of the 827 *O*-GlcNAc marked genes showed a large and statistically different ($p = 0.0002$) increase in *O*-GlcNAcylation signals in response to feeding, an effect that could also be easily visualized on representative individual gene promoters (**Figure 1B**). The *oga-1(ok1207)* results demonstrated that chromatin-associated, GlcNAcylated substrates are rendered nutrient-sensitive when *O*-GlcNAc cycling is disrupted. Taken together, these findings suggest that in wild type animals the dynamic cycling of *O*-GlcNAc is required to maintain the near constant, or buffered, levels of *O*-GlcNAcylation observed at gene promoters.

As described above, the constant distribution of promoter-associated *O*-GlcNAc in response to nutrient flux was surprising because total protein *O*-GlcNAcylation increased in *C. elegans* in response to nutritional flux in the form of excessive glucose (45). We re-examined total protein *O*-GlcNAcylation in L1 populations for wild type, *ogt-1(ok430)*, *ogt-1(ok1474)*, *oga-1(ok1207)* mutant animals by Western blots, comparing starved

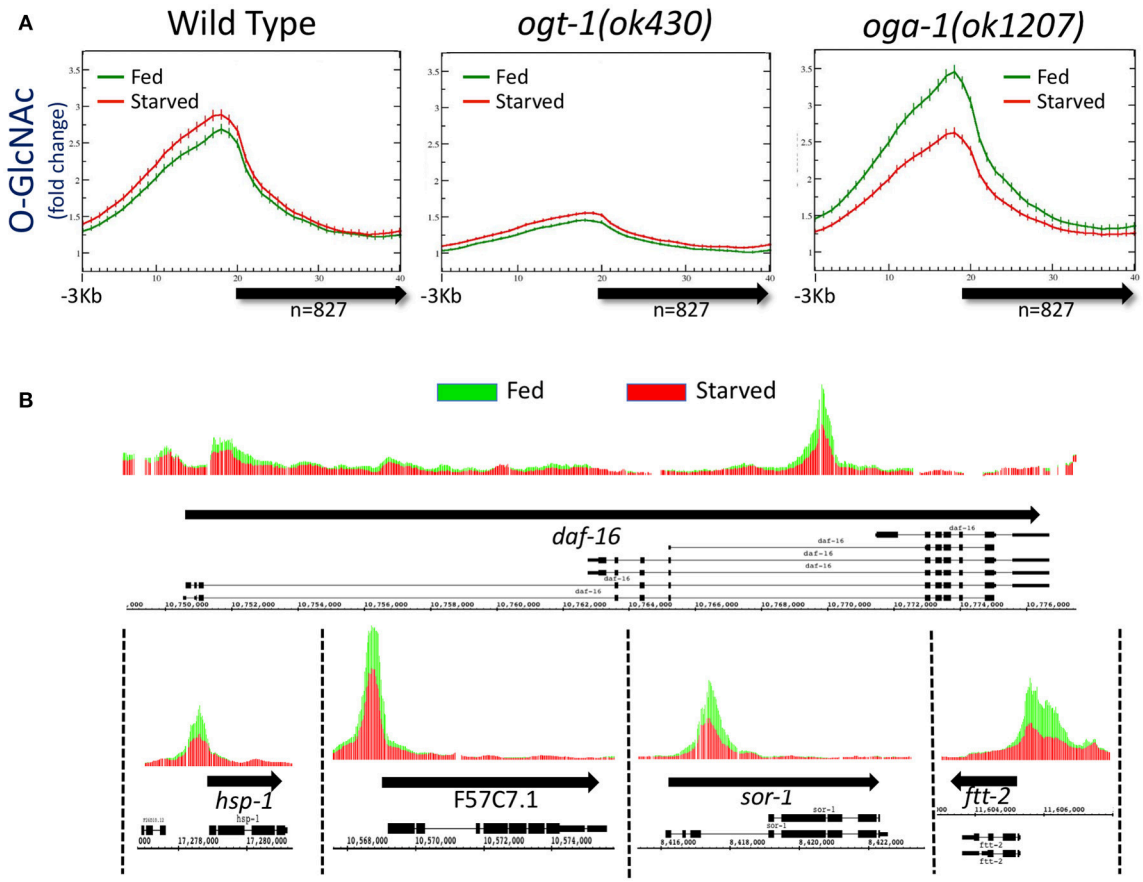

FIGURE 1 | Levels of promoter region *O*-GlcNAcylation are actively regulated in wild type animals. **(A)** Chromatin-associated *O*-GlcNAc signals, as determined by ChIP-chip, are shown relative to a unitary, metagene model (bold arrow) along with 3 kb flanking sequence upstream of the gene model. Fold enrichment over the mean chip value is shown on the y-axis; the x-axis indicates the bin number for consolidated data. Data shown is averaged from 827 previously identified *O*-GlcNAc "marked" genes in wild type or *O*-GlcNAc cycling mutants (*ogt-1(ok430)* and *oga-1(ok1207)*) (32) for both starved (red) and fed (green) conditions; standard error is indicated for each point on the plots. There was little to no change in promoter region *O*-GlcNAcylation in wild type worms in response to changes in nutrient conditions. Comparing the ratio of the promoter region peak to gene body nadir values (Starved = 2.30 ± 0.09; Fed = 2.20 ± 0.08) showed no statistical difference ($p = 0.397$) for wild type animals. The promoter region enrichment observed for *ogt-1* mutant animals represents background as these animals lack the ability to *O*-GlcNAcylate substrates, providing a useful genetic control for ChIP. The dramatic up-regulation of promoter region *O*-GlcNAcylation in response to feeding in *oga-1* mutants reflects disruption of the dynamic cycling of *O*-GlcNAc on chromatin-associated substrates. Comparison of the ratios for promoter region peak to gene body nadir values (Starved = 2.11 ± 0.08; Fed = 2.62 ± 0.11) is significantly different ($p = 0.0002$) in fed vs. starved conditions in *oga-1* mutants. **(B)** The *oga-1(ok1207)* *O*-GlcNAc ChIP-chip profiles for several individual genes, as indicated, in both starved (red) and fed (green) conditions are shown. In each case, the promoter region *O*-GlcNAcylation appears to be nutrient responsive, rising dramatically for fed conditions in the *oga-1* mutant background. Thick black arrows indicate the transcribed region with the exon/intron gene structure for one or more previously defined gene products illustrated below.

vs. fed conditions that mimicked those used for our ChIP studies. Although *O*-GlcNAc signals were either not detected (*ogt-1* mutants) or too low (wild type) to conclude any effect in these experiments, the *oga-1(ok1207)* animals clearly demonstrated dramatically elevated levels of protein *O*-GlcNAcylation that were further increased in fed conditions when compared to starved (**Supplemental Figure 4**). Thus, nutritional status can drive excessive levels of protein *O*-GlcNAcylation with the potential to affect promoter-associated substrates.

RNA Polymerase II Is Dynamically *O*-GlcNAcylated *in vivo*

The C-terminal domain (CTD) of mammalian RNA Polymerase II (Pol II) has been reported to be GlcNAcylated on Ser and Thr residues of the canonical heptad repeat sequences (YSPTSPS) and closely related variants (34, 35, 51). The *C. elegans* large subunit of Pol II, encoded by the *ama-1* gene, has 37 heptad repeats within its CTD of which 10 match the canonical sequence exactly.

We immunoprecipitated Pol II from starved and fed wild type and mutant L1 stage animal extracts using a Pol II antibody (8WG16) that recognizes phosphorylated and non-phosphorylated isoforms (19, 48) (Experimental Procedures). Immunoprecipitation was followed by detection of *O*-GlcNAc by two independent methods. Using antibodies specific for *O*-GlcNAc, we were able to detect Pol II in the *oga-1 (ok1207)* mutant where *O*-GlcNAc removal is blocked; little or no GlcNAcylated Pol II was detected in wild type extracts and none was ever detected in the *ogt-1(ok430)* mutant (**Figure 2A**). We

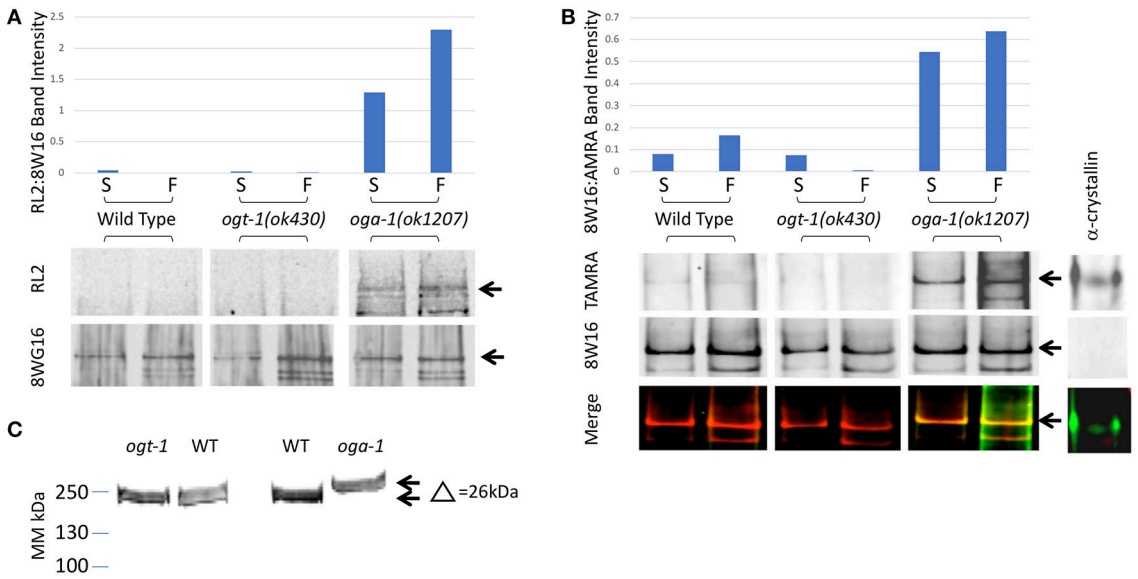

FIGURE 2 | *C. elegans* RNA Polymerase II is *O*-GlcNAcylated. **(A)** RNA Polymerase II (Pol II) was immunopurified from extracts prepared from starved (S) and fed (F) L1 larvae using wild type or *O*-GlcNAc cycling mutant strains. Western blots were probed with an anti-*O*-GlcNAc antibody (RL2) or anti-Pol II antibody that recognizes isoforms independent of CTD phosphoepitopes (8WG16), as indicated. The position of the major Pol II band is indicated by arrows in the blots. This band was quantified in each lane using ImageJ and the relative ratio of RL2 to 8WG16 signal intensity plotted in the graph above. The *oga-1* mutant strain has dramatically increased levels of *O*-GlcNAcylated Pol II that is further increased upon feeding. **(B)** RNA Pol II was immunopurified from extracts prepared from starved (S) and fed (F) animals as in **(A)**. A modified recombinant galactosyltransferase was used to introduce a GalNAz label to *O*-GlcNAc modified proteins (52). The GalNAz label was reacted with an alkyne-TAMRA probe using "Click" chemistry (53). The top row of Western blot images shows the anti-TAMRA antibody detection results. As a positive control, α-crystallin (20 pg) was detected using the same method. The second row of images shows the anti-Pol II signal (8WG16) from an identical blot; note the absence of signal for α-crystallin. The last row of images shows the overlay of signals from the two fluorophores corresponding to *O*-GlcNAc and Pol II. The position of the major Pol II band is indicated by arrows in all three blot images. This band was quantified in each lane using ImageJ and the relative ratio of TAMRA to 8WG16 signal intensity plotted in the graph above. **(C)** Pol II in *oga-1* mutants has a higher molecular mass. The post-nuclear supernatants (see Experimental Procedures) from wild type and mutant strains were run on 10–20% SDS-PAGE gels and transferred for immunoblotting as described in Experimental Procedures. The primary antibody was the RNA Pol II Ser-2-P antibody ab5095 and the secondary IR-labeled anti-mouse IgG. The blot was scanned with an Oddysey IR scanner as described previously (25).

next used a highly sensitive chemoenzymatic detection method (52) based on the selectivity of galactosyltransferase to modify terminal *O*-GlcNAc (54, 55). This method uses 'Click' chemistry to place a fluorescent tag (TAMRA) onto *O*-GlcNAc-modified proteins that can subsequently be identified with an anti-TAMRA antibody on immunoblots. As shown in **Figure 2B**, Pol II GlcNAcylation was readily detected in both the *O*-GlcNAcase mutant strain [*oga-1(ok1207)*] and, to a lesser extent, in wild type; GlcNAcylation of Pol II was undetectable in the *ogt-1(ok430)* strain. When the same blots were probed with an anti-Pol II antibody (8WG16), all stains were shown to have nearly identical levels of Pol II. There was a readily detectable increase in Pol II GlcNAcylation in fed vs. starved samples in the *oga-1(ok1207)* mutant, reminiscent of the fed response observed by *O*-GlcNAc ChIP (**Figure 2A**). In addition, the migration of intact Pol II was detectably different in comparing the three strains [N2, *ogt-1(ok430)* and *oga-1(ok1207)*] using Pol II antibodies, with an upward shift in migration of approximately 26 kDa (**Figure 2C**), suggesting that Pol II is highly modified in the *oga-1(ok1207)* strain that lacks *O*-GlcNAcase. Thus, only a small fraction of total Pol II is likely to be GlcNAcylated at steady state due, in large part, to active cycling by both OGT-1 and OGA-1. When *oga-1* is deleted, the levels of modified Pol II increase greatly. The relatively small fraction of GlcNAcylated Pol II and extensive cross-linking required for ChIP precluded us from doing sequential IP studies to determine if the promoter region *O*-GlcNAc signal is predominantly due to GlcNAcylated Pol II. Therefore, we took advantage of the many tools available to examine Pol II dynamics to determine if altered GlcNAcylation altered Pol II behavior.

Genome-Wide Analysis of RNA Pol II Isoforms in *C. elegans* L1 Larvae

Since Pol II was a confirmed nutrient-driven target of GlcNAcylation in the worm, we have directly examined the genome-wide behavior of Pol II using the genetic and biochemical tools at our disposal. This analysis was carried out at the whole-genome level, allowing a robust metagene analysis that would not be possible by examination of smaller data sets or by examining single genes. Over 36 whole genome arrays were analyzed in this way, with representative data presented for simplicity.

The CTD of Pol II in animals and yeast is regulated by phosphorylation of the heptad repeat (YSPTSPS) on Ser-2,—5,

and−7; Ser-5-P is associated with initiating Pol II, whereas increasing Ser-2-P is linked to elongation [reviewed in (3)]. To determine the genome-wide distribution of Pol II in L1s, we carried out ChIP-chip experiments using anti-Pol II antibodies that had different specificities with respect to CTD post-translational modifications. Antibody 8WG16 is considered phospho-independent, recognizing both phosphorylated and non-phosphorylated forms of the CTD and has been used previously in *C. elegans* for ChIP by multiple groups (19, 20, 48, 56). Antibody 5095 (Abcam) recognizes predominantly Pol II phosphorylated on Ser-2 within the CTD. We also used two non-commercial anti-Pol II antibodies raised against di-heptad CTD repeat peptides phosphorylated on either the Ser-5 or Ser-2 positions (57, 58). We confirmed the specificity of each of these phospho-specific Pol II antibodies using immunoblot dot blots (**Supplemental Figure 1B**) as well as *in vivo* staining of *C. elegans* embryos that have characteristic germline vs. somatic cell nuclear staining patterns for CTD Ser-2-P- or Ser-5-P-specific antibodies (22, 59, 60)(**Supplemental Figure 2**). As others have recently reported (19, 20, 56), we found that the ChIP profiles for all of these Pol II antibodies were very similar (**Supplemental Figures 1A**, **5**). From these extensive genome-wide analyses, we concluded that for *C. elegans* L1 chromatin, Pol II ChIP patterns were very reproducible using a variety of antibodies and multiple, independent chromatin preparations. Moreover, it was not possible to discriminate between initiating or elongating forms of Pol II based on *in vivo* ChIP with these antibodies despite their clear difference for CTD phospho-isoforms *in vitro*.

O-GlcNAc Marked Promoters Show Enhanced Promoter Proximal Pol II With a Distribution That Is Buffered From Nutrient Flux in Wild Type Animals

As noted above, both Pol II and total promoter region *O*-GlcNAc levels are maintained in wild type animals for either starved or fed conditions by dynamic *O*-GlcNAc cycling. To determine if the distribution of Pol II changed in response to nutrient flux, data from ChIP experiments with multiple Pol II antibodies (Experimental Procedures) were analyzed with respect to both starved and fed conditions. Regardless of the Pol II antibody used for ChIP, we found substantial levels of Pol II at the promoter of the set of 827 genes defined as being GlcNAcylated, as represented by the Ser-2-P antibody profile (**Figure 3A**). Like *O*-GlcNAc signals, the Pol II profiles were very similar in both starved and fed conditions, with differences in 5′ promoter peak to gene body nadir ratios not reaching statistical difference ($p = 0.681$). We noted that the Pol II distribution within the 5′ promoter region was very similar to the GlcNAcylated chromatin profile, whereas a very distinct pattern exists within the gene body as modeled by the metagene (**Figure 3A**). Thus, in wild type animals neither the profile nor magnitude of Pol II distribution for the 827 *O*-GlcNAc marked genes was significantly altered in response to nutrient flux.

To determine if the averaged profile of Pol II for most genes remained unchanged during nutrient flux in wild type animals, we analyzed the Pol II ChIP data for gene sets selected for different characteristics. The list of genes used for this analysis are given in **Supplemental Table 1**. For example, data from a set of 100 genes selected for high levels of Pol II at the promoter and in the gene body gave a very different pattern, but similarly showed no change between starved and fed conditions (**Figure 3B**); these gene promoters had relatively low levels of *O*-GlcNAcylation. We also examined the Pol II profiles for 1426 genes transcriptionally upregulated ($\log_2$ fold change of 1.5 or greater) in fed conditions compared to starved and 284 genes upregulated in starved compared to fed (**Figure 3C**). For both of these gene sets, the condition for which they were transcriptionally upregulated corresponded to increased Pol II signals across the gene body, although starved and fed condition profiles overall were not significantly different. We concluded that in wild type animals, (1) nutrient flux does not affect the steady state level of Pol II occupancy for most genes, including those defined as *O*-GlcNAc marked, (2) high levels of promoter region *O*-GlcNAcylation were strongly correlated with a group of genes exhibiting a strong 5′ promoter bias in the Pol II profile, (3) Pol II profiles are different and concordant for sets of genes that show dramatic changes in expression, and (4) Pol II profiles reflect the criteria used to select the gene set.

Enhanced promoter proximal Pol II accumulation, or pausing, has previously been reported in *C. elegans* by multiple groups under starved conditions (19, 47). We compared each of these gene sets with our 827 *O*-GlcNAc marked genes, all of which had high levels of promoter proximal Pol II signals (**Figure 4**); gene lists are available in **Supplemental Table 1**. Although there was some overlap, these defined gene sets were much more different from each other than they were similar. In particular, most of the *O*-GlcNAc marked genes were not among those genes that have more rigorously been defined as having promoter proximal pausing of Pol II, suggesting a more general role for *O*-GlcNAcylation in Pol II dynamics.

O-GlcNAc Cycling Is Required to Buffer Pol II Occupancy and Distribution From Changes in Nutrient Flux

It was possible that there were differences in the genome-wide distribution of Pol II in the *O*-GlcNAc cycling mutants, mirroring difference in the levels of Pol II GlcNAcylation we observed by Western blot analysis. Chromatin from *ogt-1* or *oga-1* mutant populations (starved or fed) were ChIPed with each of the four anti-Pol II antibodies described above. The *ogt-1(ok430)* mutant results were particularly dramatic, with very different starved vs. fed profiles and significant differences ($p = 0.008$) in the 5′ promoter to gene body nadir values (**Figure 5**). In contrast, the *oga-1(ok1207)* mutant profile and peak ratios were very similar to wild type animals and not significantly different ($p = 0.478$). We also examined the behavior of Pol II in the *O*-GlcNAc mutants for several other groups of genes referenced above using the four anti-Pol II antibodies (data not shown). In each case, the results were similar to the effects shown in **Figure 5**, but with a diminished magnitude in deviation from wild type that was correlated with

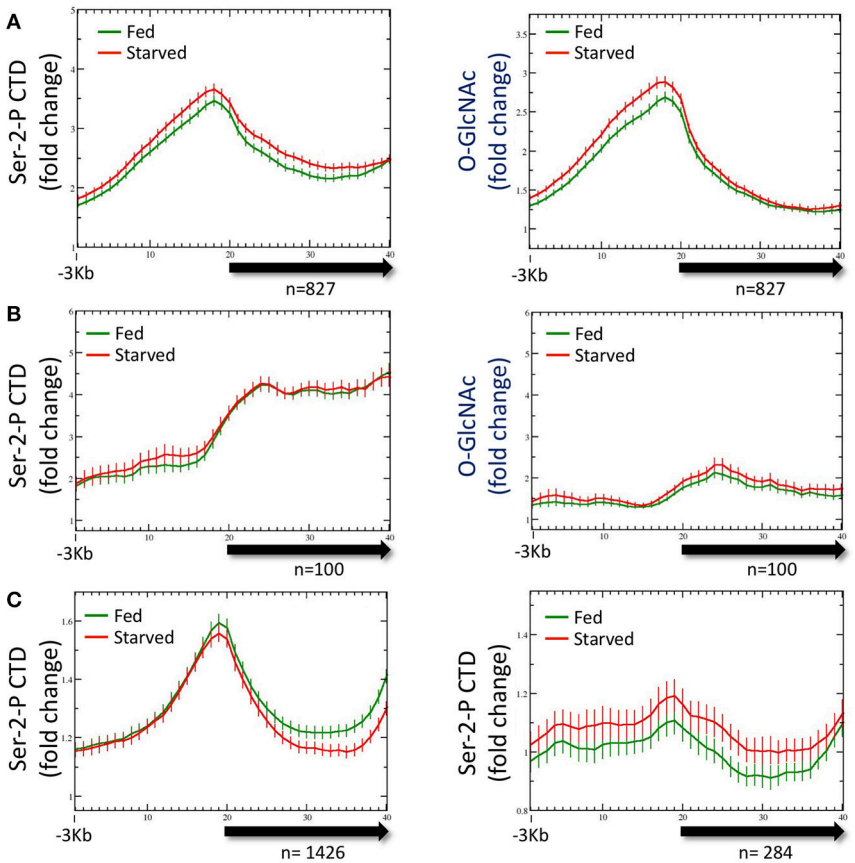

FIGURE 3 | RNA Polymerase II profiles for *O*-GlcNAc marked genes are similar in both starved and fed conditions. **(A)** RNA Pol II Ser-2-P (ab5095), representative of multiple Pol II antibodies used, and *O*-GlcNAc ChIP profiles for the 827 *O*-GlcNAc marked gene set with axis and gene model displays as described in **Figure 1**; the *O*-GlcNAc profile is duplicated from **Figure 1A** (right panel) for side by side comparison to the corresponding Pol II data. Very little difference was observed for the Pol II distribution in comparing fed and starved conditions. Note that while Pol II and *O*-GlcNAc profiles are similar in the promoter regions, the Pol II signal extends into the gene body whereas *O*-GlcNAc does not. **(B)** To determine if the *O*-GlcNAc marked gene set behavior was unusual in being unchanged regardless of feeding condition, we examine several gene sets that were selected using different criteria. Show is a set of 100 genes that had high levels of RNA Pol II within the gene body, but low promoter region *O*-GlcNAc signals. This gene set also shows nearly identical profiles for Pol II (left panel) in either starved or fed conditions, lacks a strong signal for promoter region *O*-GlcNAc (right panel), and has an overall profile that is quite distinct from the 827 *O*-GlcNAc marked genes. **(C)** Genes with nutritionally responsive expression have corresponding changes in Pol II occupancy. As many gene sets showed similar profiles for Pol II in both starved and fed conditions, we identified genes that were nutritionally responsive to these two conditions based only on changes in gene expression ($\log_2$ fold change greater than or equal to 1.5 when comparing starved and fed values). The left panel shows the Pol II profile, represented by the Ser-2-P data, for 1426 genes that are up-regulated in fed conditions compared to starved values. As expected, the fed Pol II profile increases in the gene body of these genes. For genes that are up-regulated in starved conditions ($n = 284$; right panel), the starved Pol II profile is greater than the fed. Thus, the Pol II ChIP profile changes are consistent with the gene expression data for those gene showing the most dynamic response to feeding condition whereas Pol II occupancy profiles for nutritionally unresponsive genes are correspondingly homeostatic.

the relative abundance of *O*-GlcNAc at the promoter region. Taken altogether, the mutant studies demonstrate that disruption of *O*-GlcNAcylation results in deregulation of homeostatic mechanisms that normally function to maintain the steady state Pol II distribution for many genes during periods of nutrient flux.

Promoters With Dynamic Changes in GlcNAcylation Are Dysregulated For Pol II Occupancy in Response to Nutrient Flux

The observation that dramatic changes in the *O*-GlcNAc ChIP signals at promoters in the *O*-GlcNAc cycling mutants were associated with striking deregulation of Pol II occupancy (**Figure 5**) prompted us to examine if these two properties were linked. We reasoned that by looking at promoters that accumulated the highest levels of *O*-GlcNAc upon blocking *O*-GlcNAc cycling, we might enrich for those genes with dramatically altered Pol II distributions. We calculated the difference in *O*-GlcNAc signal between fed and starved samples (delta *O*-GlcNAc) in *oga-1(ok1207)* *O*-GlcNAcase mutants for the 827 marked promoters and plotted those in rank order (**Figure 6A**). One hundred genes from each of three different regions of the distribution representing the highest, middle, and lowest delta *O*-GlcNAc values were chosen and the distribution of Pol II CTD Ser-2-P was examined in either starved or fed

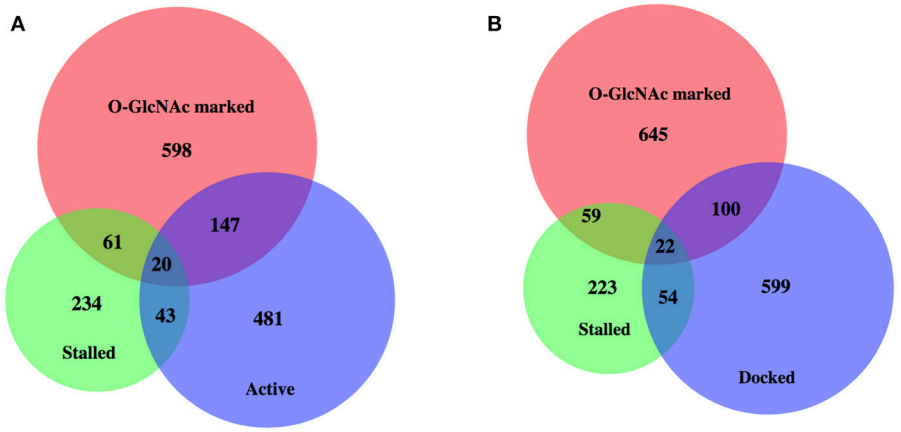

FIGURE 4 | High levels of promoter Pol II for most *O*-GlcNAc marked genes do not indicate polymerase pausing. Proportional area Venn diagrams of gene set overlap among the 827 *O*-GlcNAc marked genes and other gene sets defined as having paused polymerase. Overlaps between the 827 *O*-GlcNAc marked genes (red) and genes identified as having promoter proximal paused Pol II in starved L1s from Zhong et al. (47) ($n = 358$, green) and active [$n = 691$, blue; **(A)**] or docked [$n = 775$, blue; **(B)**] as defined by Maxwell et al. (20). The majority of *O*-GlcNAc marked genes are not included in any of these gene sets previously identified as having promoter proximal Pol II in starved conditions in wild type animals.

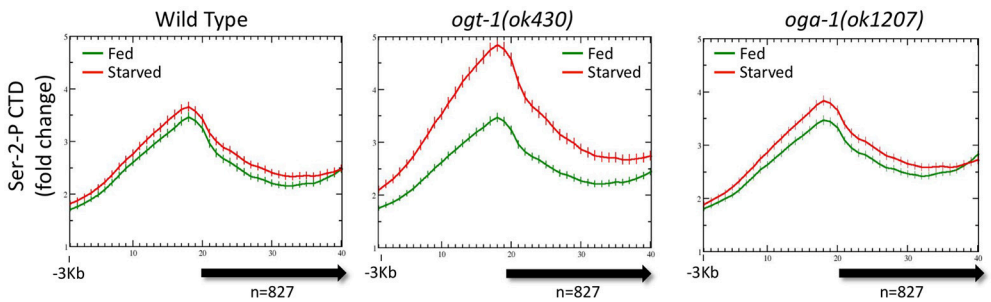

FIGURE 5 | Pol II profiles become deregulated in response to nutrient flux in animals lacking active *O*-GlcNAcylation. The CTD Ser-2-P Pol II profile (ab5095), representative of all PolII II antibodies tested, for the 827 *O*-GlcNAc marked genes are shown relative to the metagene model, as described in **Figure 1**. The ChIP data from wild type (**left**; duplicated for comparison from **Figure 3A**, left) or *O*-GlcNAc cycling mutants *ogt-1(ok430)* (**center**) and *oga-1(ok1207)* (**right**) L1 animals is shown under either starved (red) and fed (green) conditions. Whereas wild type and *oga-1(ok1207)* animals showed no statistically significant change in Pol II profiles for this set of genes in response to nutrient flux, loss of OGT activity resulted in dramatic changes in the 5′ promoter region to gene body nadir signal ratios (Starved = 1.81 ± 0.08; Fed = 1.57 ± 0.05), with starved conditions having significantly ($p = 0.008$) more Pol II occupancy across the promoter and gene body.

conditions for wild type and mutant chromatin. As shown in **Figure 6B**, each gene set had a distinctive Pol II profile, with the highest levels of Pol II observed in the genes with the greatest change in *O*-GlcNAc when comparing starved and fed animal. More importantly, while wild type and *oga-1(ok1207)* mutants showed very similar results for all gene sets, the *ogt-1(ok430)* mutants show dramatic difference in starved vs. fed Pol II profiles. Finally, we noted that when the *O*-GlcNAc accumulation was highest in fed samples (e.g., high delta *O*-GlcNAc value), the 5′ Pol II CTD Ser-2-P occupancy was highest in starved samples in *ogt-1(ok430)* mutants. Therefore, independent of the magnitude of change in promoter region GlcNAcylation during starved or fed conditions, Pol II profiles remained remarkably buffered against nutrient flux in wild type and *oga-1* mutants. In contrast, *ogt-1* mutants have lost that buffering capacity and have dramatically increased levels of Pol II specifically in starved conditions. The dysregulation of Pol II occupancy in *ogt-1*, but not *oga-1*, mutants demonstrates that *O*-GlcNAcylation activity alone has a major role in buffering polymerase occupancy against nutrient flux. Once *O*-GlcNAcylated, the additional levels of this modification resulting from loss of *O*-GlcNAcase activity does little to influence Pol II occupancy.

O-GlcNAc Cycling Mutants Have an Altered Transcriptome and Respond Differentially to Nutritional Status

We previously reported that growth arrested L1 larvae harboring null alleles of *ogt-1* and *oga-1* have dramatically altered gene expression compared to wild type animals (roughly 700 and 500 deregulated genes, respectively) (32). In this report, we

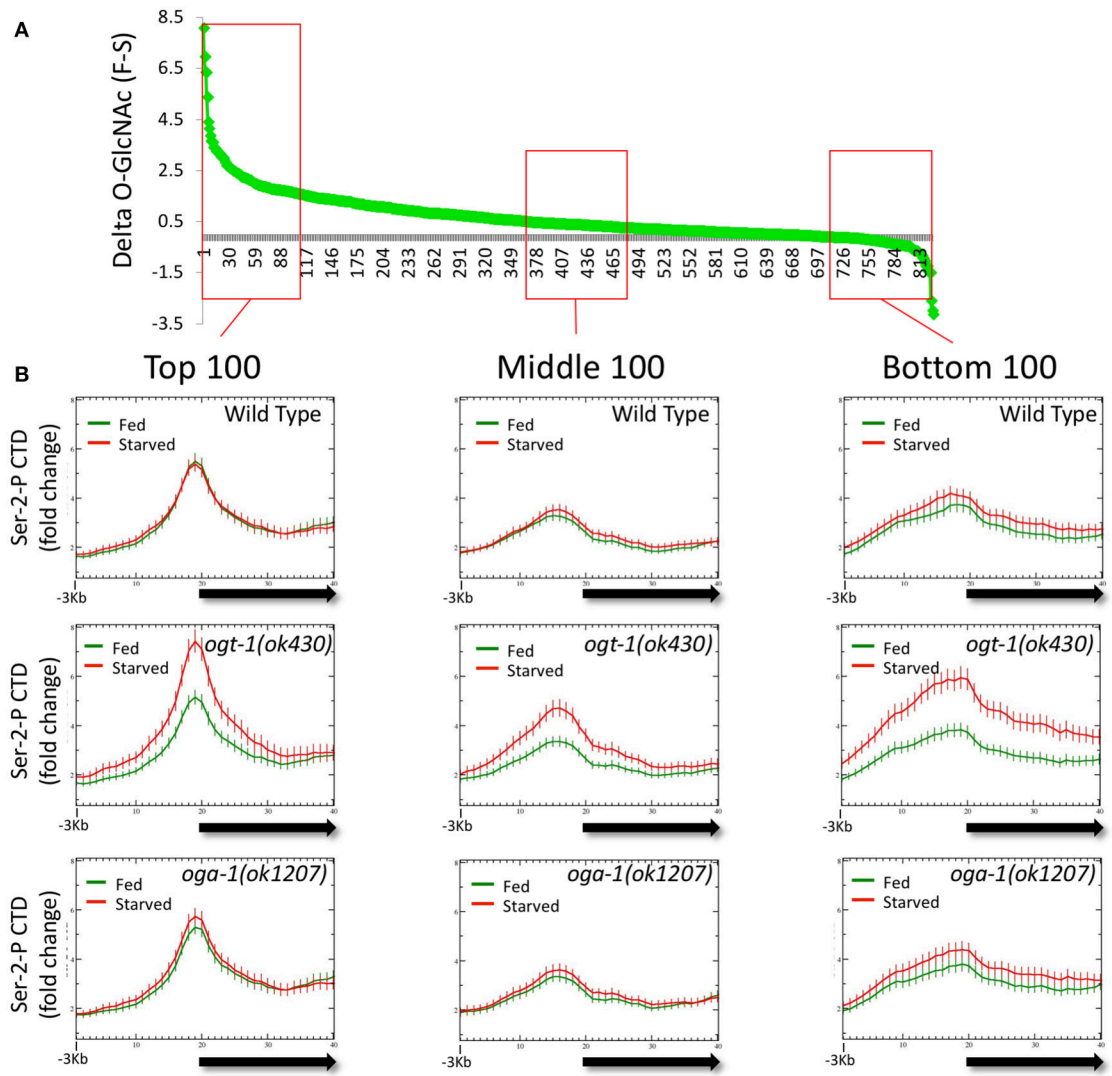

FIGURE 6 | Loss of *O*-GlcNAc activity alone, and not nutrient responsive *O*-GlcNAcylation at promoters, correlates with Pol II dysregulation. The difference in ChIP *O*-GlcNAc signal values for each of the 827 *O*-GlcNAc marked genes in starved vs. fed conditions (delta-*O*-GlcNAc) was calculated from *oga-1(ok1207)* mutant data and plotted in rank order **(A)**. Three bins of 100 genes each were selected from the top, middle, or bottom rankings and the CTD Ser-2-P Pol II ChIP profile (ab5095), representative of all PolII antibodies tested, was plotted (as described in **Figure 1**) for wild type and the *O*-GlcNAc cycling mutants **(B)**. Regardless of ranking based on the nutrient responsiveness of *O*-GlcNAcylation, wild type, and *oga-1* mutants showed very little difference in starved vs. fed Pol II profiles. In contrast, *ogt-1* mutants lacking *O*-GlcNAc activity, show dramatic differences in Pol II profiles in starved vs. fed conditions regardless of nutrient responsive ranking. Gene lists are available in **Supplemental Table 1**.

extended this analysis to fed L1 larvae and compared wild type, *ogt-1(ok430)*, and *oga-1(ok1207)* mutants; the entire dataset is available as GEO accession number GSE18132. We limited our bioinformatic analysis here to those genes substantially deregulated with a 2.8-fold ($\log_2 = 1.5$) or greater change in gene expression. As shown in **Figure 7A**, starved L1s have 63 genes that were differentially deregulated in *ogt-1(ok430)* compared to wild type animals, whereas *oga-1(ok1207)* had 18 differentially deregulated genes. As noted before (32), the genes deregulated in *ogt-1* are associated with innate immunity and the stress response. Of particular interest is the enhanced expression of glutathione transferases (**Supplemental Table 2**). For *oga-1*, the 18 deregulated genes were enriched in serpentine receptors involved in chemosensation, and C-type lectins. We next examined the changes in gene expression for fed L1s (**Figure 7B**). Here, 22 genes were at least 2.8-fold different in *ogt-1(ok430)*; these genes were bioinformatically enriched in membrane receptors involved in chemosensation (**Supplemental Table 2**) and included the piwi-like protein *prg-1* that was highly down-regulated in the fed conditions compared to wild type. The *prg-1* gene encodes an argonaut protein involved in regulating piRNAs, microRNAs and select protein coding mRNAs (61).

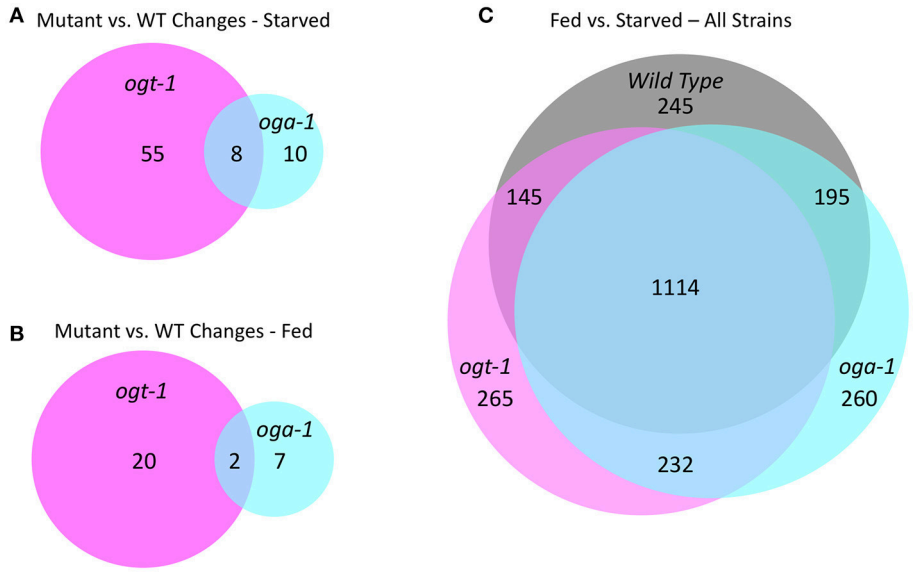

FIGURE 7 | *O*-GlcNAc cycling mutants exhibit transcriptional changes in response to nutritional status. **(A)** An area proportional Venn diagram showing the genes deregulated greater than 2.8-fold ($\log_2 = 1.5$) in starved L1 larvae in *ogt-1 (ok430)* and *oga-1(1207)* mutant strains compared to wild type (WT) animals. **(B)** An area proportional Venn diagram showing the genes deregulated 2.8-fold or greater in fed L1 larvae in *ogt-1 (ok430)* and *oga-1(ok1207)* mutant strains compared to wild type worms. **(C)** An area proportional Venn diagram showing the uniquely deregulated genes comparing starved and fed worms in wild type, *ogt-1 (ok430)* and *oga-1(ok1207)* mutant strains. Gene lists for each condition and genotype can be found in **Supplemental Table 2**. All transcriptional data are available in GEO accession number GSE18132.

Finally, genes deregulated in *oga-1(ok1207)* fed L1 animals were similar to that of starved larvae; serpentine and G-coupled receptors. Thus both in the fed and starved conditions, the *ogt-1* mutants exhibited more striking deregulation of gene expression than the *oga-1* mutants in comparisions to wild type.

To examine the overall nutrient response of the *O*-GlcNAc cycling mutants from a different perspective, we examined the transcriptional responses of three strains in both conditions (**Figure 7C**; **Supplemental Table 1**), again applying a high threshold of 2.8-fold change ($\log_2 = 1.5$) for the analysis. Although there was a core group representing ∼85% of the genes that were commonly deregulated in response to nutrient status, each of the O-GlcNAc cycling mutants showed a substantially altered and strain-specific transcriptional response (**Figure 7C**). Wild type L1s had 245 nutrient responsive genes that were not detected in either *ogt-1(ok430)* or *oga-1(ok1207)* mutants in response to feeding. The *ogt-1(ok430)* strain had 265 genes uniquely deregulated in response to feeding while *oga-1(ok1207)* had 260 deregulated genes. This is consistent with the changes in polymerase occupancy we have observed and the transcriptional alterations seen in *ogt-1* and *oga-1* mutants compared to wildtype. Finally, we examined the relationship between the most nutrient responsive genes in all three strains to our 827 *O*-GlcNAc marked gene set (**Supplemental Figure 6**). In all pair-wise comparisions, the overlap failed to meet statistical significance (Fisher's Exact Test, $p < 0.05$) in exceeding random chance.

DISCUSSION

O-GlcNAc Cycling Is a Nutrient-Responsive Homeostatic Mechanism

Previously, we demonstrated that *O*-GlcNAcylated chromatin-associated protein(s) are preferentially localized to the promoter region of a subset of genes in *C. elegans* (32) and in *Drosophila* (33). Following up on those observations, we now show that Pol II itself is dynamically GlcNAcylated *in vivo*, that the steady state distribution of *O*-GlcNAc and Pol II for most genes in wild type animals is unaffected by nutrient flux, that GlcNAcylated promoters are associated with high promoter proximal Pol II occupancy, and that loss of *O*-GlcNAc cycling results in profound changes in Pol II distribution in response to starvation and feeding. The relatively minor Pol II profile changes in fed vs. starved wild type *C. elegans* L1 larvae may initially seem counterintuitive. However, our results are consistent with those reported by Baugh et al. who assayed various starvation and feeding paradigms by ChIP-seq (19). These studies demonstrated that most genes do not show an acute response to nutrient flux, but instead maintain a steady state level of expression. Our current findings suggest that *O*-GlcNAc cycling underlies, at least in part, the near constant Pol II distribution genome-wide and the relatively minor transcriptional changes associated with dramatic changes in nutrient availability. In the absence of *O*-GlcNAc cycling, this homeostatic mechanism becomes deregulated and Pol II distribution across genes varies greatly in response to nutrient availability. Our results are consistent with a model in which dynamic *O*-GlcNAc cycling directly

impacts Pol II distribution and dynamics for many, if not all, genes.

The "CTD-Code" in *C. elegans*

Although understudied in *C. elegans*, it is generally agreed that there are discrete steps of Pol II action during eukaryotic transcription cycles, including pre-initiation, initiation, pausing, elongation, and termination [reviewed in (3)]. These steps in the transcription process have been linked to specific modifications of the C-terminal domain (CTD) of the large subunit of Pol II that is comprised of numerous identical or variant repeats of the heptad amino acid sequence YSPTSPS. For example, transcriptional initiation and promoter-proximal pausing is associated with hyperphosphorylation of Ser-5 of the heptad repeats. This form of Pol II is converted to an elongating form by the action of PTEF-b, an enzymatic complex that phosphorylates Ser-2 of the heptad repeat and other negative regulatory substrates within the holoenzyme. A second Pol II pause occurs at the 3′ end of genes associated with termination and 3′ end processing. Relatively high levels of Ser-2, and low levels of Ser-5, phosphorylation are associated with this step of transcription. Thus, it is generally agreed that the distribution of CTD heptad repeat phospho-isoforms reflects the various functions of Pol II throughout the transcription cycle.

Profiling the distribution of several Pol II CTD phospho-isoforms with multiple antibodies failed to reveal the canonical pattern of eukaryotic transcription cycle events in *C. elegans* L1 chromatin preparations. Others came to a similar conclusion when examining profiles with several of the same Pol II antibodies we used (19, 20, 56). This suggests that either the mode of regulation for Pol II during the transcription cycle is different in *C. elegans* compared to other organisms or, more likely, that epitope recognition of the phosphorylated CTD *in vivo* is more complex than *in vitro*. We find that the overall pattern of distribution for multiple Pol II CTD phospho-epitopes reflects a shared characteristic of a particular set of selected genes that may reflect a shared mechanism of transcriptional regulation. For the 827 *O*-GlcNAc marked genes, one of the shared characteristics is enhanced promoter proximal Pol II occupancy. The 827 genes marked by *O*-GlcNAc at this developmental stage in *C. elegans* have been bioinformatically linked to longevity, stress and immunity (32). We have previously documented that the *O*-GlcNAc cycling mutants exhibit an altered stress response and have changes in longevity and insulin-dependent phenotypes (23, 24, 45). Moreover, these mutants have wholesale changes in steady state transcript levels suggesting that the observed alterations in Pol II profiles by ChIP are associated with transcriptional consequences.

Transcriptional Deregulation in *O*-GlcNAc Cycling Mutants Is Not Restricted to the "*O*-GlcNAc Marked" Genes

In this study, we document the changes in gene expression in starved and fed worms using wild type (N2), *ogt-1* and *oga-1* mutant strains. The results of these studies suggest that while gene expression changes are widespread, the deregulated genes are not restricted to those 827 genes marked by *O*-GlcNAc at their promoters. We do not find a simple direct correlation between the presence of *O*-GlcNAc promoters and its deregulation of expressed in *O*-GlcNAc cycling mutants; these gene lists show only ∼10% overlap, as reflected in the Venn diagrams shown in **Supplemental Figure 6**. The lack of statistically significant overlap in the gene lists is not surprising given that the magnitude of the profiles differences in the metagene analyses represent at most a ∼40% change in Pol II occupancy and it is unclear that these changes alone would result in differences in steady state RNA levels. Moreover, gene expression in the highly invariant *C. elegans* developmental process is both cell type specific and temporally regulated. Many of O-GlcNAc-occupied promoters may be transcriptionally silent. *O*-GlcNAc marked promoters often reside between protein coding genes complicating assignment to a unique gene. In additional, posttranscriptional mechanisms and the influence of non-coding RNAs are difficult to predict using current tools. However, we can conclude that the presence of *O*-GlcNAc at a promoter of a given developmental stage is not necessarily predictive of transcriptional change upon loss of *O*-GlcNAc cycling.

C. elegans Pol II Is Dynamically *O*-GlcNAcylated *in vivo*

We find that Pol II is a substrate for GlcNAcylation in *C. elegans*, a has been reported previously in many different systems (33–38). Although the mammalian sites of GlcNAcylation include Ser and Thr residues of the CTD, the functional consequences of this modification have not previously been explored in a living organism. The large number of heptad repeats, each having up to four potential *O*-GlcNAcylation sites, suggests Pol II could be a predominant chromatin-associated protein detected by ChIP with antibodies specific for *O*-GlcNAc epitopes. This may explain, at least in part, the coincident profiles we observe for *O*-GlcNAc and Pol II at the 5′ end of many genes. Importantly, GlcNAcylation of the CTD residues that are also targets for phosphorylation would be expected to have profound effects on phosphorylation patterns and Pol II function. A complex interaction between CTD GlcNAcylation, phosphorylation, and transcription cycle progression might explain the many and diverse changes in Pol II patterns observed in *O*-GlcNAc cycling mutants. A complete analysis of this complex interplay will require a detailed analysis of the sites of phosphorylation and GlcNAcylation of the extended CTD domain of RNA Pol II. We note, however, that the redistribution of Pol II observed in *O*-GlcNAc cycling mutants was detectable using both phospho-independent and -dependent antibodies. This finding strongly suggests that *O*-GlcNAc is part of the complex "CTD-code" acting independently of known phosphorylation-dependent mechanisms.

A Model of *O*-GlcNAcylation and the "CTD-Code"

A simple model extending from previous work (34–40), our current observations, and the role of CTD phosphorylation

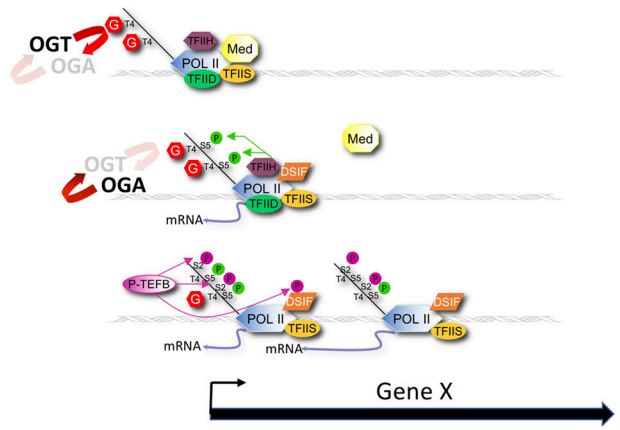

FIGURE 8 | Modeling promoter region *O*-GlcNAcylation and Pol II dynamics. A model for the role of *O*-GlcNAc cycling in promoter proximal Pol II dynamics during nutrient flux based on our results is shown that also draws from earlier studies of Lewis and colleagues (37–40). OGT and OGA enzymatic activity dynamically cycles *O*-GlcNAc on Pol II, and other chromatin substrates, that localize at the promoter of many, if not all, genes. *O*-GlcNAcylation of the Pol II CTD competes with phosphorylation of Ser-2 and Ser-5 residues of the heptad repeats that are required for transcriptional initiation and elongation. Nutrition (e.g., fed condition) drives increased *O*-GlcNAcylation of Pol II that inhibits progression of the Pol II transcription cycle. Conversely, starvation decreases *O*-GlcNAcylation of Pol II, thus promoting transcription events. The consequence of the nutrient-sensitive *O*-GlcNAc cycle is a near constant, or buffered, level of promoter proximal Pol II. In the absence of *O*-GlcNAc activity (*ogt-1* mutant) this buffering system is lost, resulting in Pol II dis-regulation. In the presence of excess *O*-GlcNAcylation (*oga-1* mutant), the inhibitory effects of this modification on Pol II are only slightly greater than in wild type animals, thus minimally affecting Pol II dynamics.

in transcription [reviewed in (3)] is that GlcNAcylation of the CTD (and perhaps other associated substrates) normally serves as a negative regulator of Pol II initiation or elongation by directly competing with phosphorylation events required for transcription cycle progression (**Figure 8**). This O-GlcNAc may serve to stabilize the CTD domain from degradation and serve to limit the action of kinases until the polymerase becomes promoter associated. In wild type animals, the potential increase in Pol II transcription driven by nutrient excess might be balanced by compensatory high levels of negatively acting GlcNAcylation, providing a self-adjusting regulator that would ensure near constant transcription of many genes during times of nutrient flux. In the *O*-GlcNAc cycling mutants, this transcriptional regulator either no longer exists (*ogt-1*) or is hyper-engaged (*oga-1*). The consequences of the deregulated *O*-GlcNAc system is a nutrient-dependent change in Pol II accumulation at the promoter region that could reflect changes in process associated with pre-initiation complex formation, transcriptional initiation, promoter proximal pausing, transcriptional elongation, or any combination thereof.

This model is derived from observations of the 827 most heavily *O*-GlcNAc marked genes, but it appears to be applicable to many genes. That is, promoter region levels of chromatin-associated GlcNAcylation fall on a continuum, which may reflect varying degrees of reliance on this mechanism of homeostatic control. For example, the Pol II profiles of the 827 GlcNAc-marked genes are extremely well buffered during nutrient flux in wild type animals. At the other extreme are those genes with very little promoter region GlcNAcylation and Pol II accumulation; instead, these genes have increasing Pol II signals toward the 3′ end of the gene. These presumably highly transcribed genes are nutrient unresponsive and constitutively on at very high levels. Another set of genes devoid of high levels of promoter GlcNAcylation is the one that responded dramatically to starvation. These genes, which are required for an acute transcriptional response to nutrient flux and/or stress, have high levels of Pol II occupancy at the promoter region but are, by definition, unbuffered.

There may be roles for promoter protein GlcNAcylation beyond the simple nutrient-responsive transcriptional regulation model we present. Animals lacking either one of the *O*-GlcNAc cycling enzymes, or both, are phenotypically wild type with respect to viability, fertility, and morphogenesis. Such observations suggest that there are nutrient regulated transcriptional responses that act in addition to, or that can supersede, *O*-GlcNAc-mediated controls. Moreover, many signaling pathways are integrated into, and impinge upon, transcriptional output, making the simple correlation of one chromatin modification (GlcNAcylation) with transcriptional regulation a difficult task. Like many metabolic regulatory networks, *O*-GlcNAc appears to function to fine-tune cellular responses in concert with many redundant and compensatory pathways. We find that this nutrient responsive, post-translational modification can profoundly influence Pol II occupancy across many genes and is, therefore, a novel player to consider in the context of gene regulation.

O-GlcNAcylation and Higher Order Chromatin Structure

Regardless of the exact role of *O*-GlcNAc in chromatin regulation, this modification is specifically targeted to promoter regions. It is not yet clear how the enzymes of O-GlcNAc cycling are recruited to promoter regions and whether this recruitment is regulated. Targeting could be accomplished by site-specific complexes that recruit GlcNAcylated substrates or the *O*-GlcNAc cycling enzymes themselves. GlcNAcylation of nuclear pores has been extensively studied over the past 25 years (26, 62, 63), suggesting specific chromatin-associate domains within the nucleus could be linked to at least some of the *O*-GlcNAc promoter signals we observe. Another possible recruitment mechanism is suggested by the known mammalian interactions between the transcriptional repressor mSin3a and OGT (64). That is, specific interactions between *O*-GlcNAc cycling enzymes and promoter-specific regulatory, or Pol II-associated, factors might provide a specific docking site. Results from *Drosophila* demonstrate a related recruitment mechanism. Two groups have shown that Polycomb Response Elements (PREs) are prominent sites of *O*-GlcNAc modified chromatin and this mark is completely lost in null alleles of the *Drosophila sxc/ogt* gene (30, 31). PREs are the *cis*-acting elements that regulate transcriptional repression through Polycomb Regulatory Complexes (PRCs),

as first uncovered in the regulation of HOX genes in the fly [reviewed in (65)]. Indeed, *sxc/ogt* genetically interacts with many Polycomb Group members and the PRC complex protein polyhomeiotic has been shown to be GlcNAcylated (30). We have yet to identify any genes that suggest GlcNAcylation of promoter regions for somatically expressed genes in *C. elegans* is involved directly in Polycomb-like repression. It is possible that *O*-GlcNAc-mediated braking of Pol II transcription observed in *C. elegans* has been co-opted to become part of a more robust transcriptional repression system in some species, such as for PRC function in flies and other organisms. It will be interesting to explore the potential for a similar role of GlcNAcylated chromatin in the *C. elegans* germline, where Polycomb-related factors are known to be involved in regulating global aspects of gene expression (66, 67).

Biological Significance of Promoter Region Glcnacylation

The discovery of a dynamic, nutrient responsive mark that is localized to the promoter of many genes provides a direct link between cell metabolism and the transcriptional machinery. Such a link could have profound acute and long-term consequences on the transcriptional output of these genes. Our studies highlight the acute responses seen within 3 h of feeding, demonstrating that changes in nutrient status of cells can be reflected at specific gene promoters. It is not difficult to imagine scenarios in which prolonged exposure to feast or famine would similarly result in persistent epigenetic changes at specific promoters altering transcriptional patterns through many cell divisions somatically or across generations if functioning in the germline. For example, the persistent elevated serum glucose levels of diabetic mothers may reset the transcriptional state of genes within the developing fetus through an *O*-GlcNAc-mediated mechanism. Such a mechanism would provide a molecular explanation for the "vicious cycle" that describes the propensity of children of mothers with diabetes during pregnancy to develop obesity and diabetes at a young age (68). Other studies have linked paternal nutrition metabolic consequences in subsequent generations (69, 70). The challenge ahead is to fully understand the molecular consequences of *O*-GlcNAc cycling, both direct and indirect, on transcription and the relationship of this nutrient responsive epitope on the epigenetic control of gene expression.

EXPERIMENTAL PROCEDURES

Worm Strains

Worm strains were cultured under standard conditions (71), unless otherwise noted. Strain used in this study were: wild type Bristol (N2), *ogt-1(ok430), ogt-1(ok1474),* and *oga-1(ok1207)*.

Starvation and Feeding Paradigm

Gravid adults were bleached, the embryos collected and hatched, and incubated in M9 buffer at 22°C with gentle shaking for 48 h. Half of this starved L1 population for each strain was collected and put on NGM plates with OP50 *E. coli* for 3 h at 22°C to serve as the fed treatment. Three hours was chosen because it was short enough to avoid major developmental changes induced by feeding that occur in the mid- to late-L1 stage and previous work demonstrated that transcriptional changes associated with feeding were near maximal by that time (19). Both starved and fed populations were collected, flash frozen, and stored at −70°C prior to further processing.

Chromatin Immunoprecipitation

Chromatin preparation from frozen samples and immunoprecipitations were carried out as previously described (32). The anti-*O*-GlcNAc antibodies used were RL2 [Abcam (ab2739); (72)] and HGAC85 [Thermo Scientific (MA1-076); (73)]; each gave similar results in all assays, although HGAC85 had better signal to noise for ChIP whereas RL2 was best for *O*-GlcNAc detection by Western blots. The four Pol II antibodies used were 8WG16 (Covance, MMS-126R) that was raised against wheat germ Pol II and recognizes both non-phosphorylated and phosphorylated isoforms of Pol II in *C. elegans* (19), ab5095 (Abcam) that was raised against the Ser-2-phospho (Ser-2-P) isoform of a consensus CTD diheptad repeat, a non-commercial anti-Ser-2-P CTD antibody (58), and anti-Ser-5-P antibody (57).

Immunoblots were performed as described previously (25).

Gene Model and Genome-Wide Analyses

Sample preparation and genome-wide analyses of transcription and ChIP peaks as previously described (32); all array data is publicly available in GEO with accession numbers GSE40371 and GSE18132, respectively. To allow easy visualization of the ChIP-chip data from multiple genes simultaneously, a common gene model (metagene) of uniform length, extending from the translational start to stop codon was defined using genome version WS195 to match the arrays; non-array based gene definitions and analyses used WS235 and ModENCODE gene expression data was retrieved based on WS260. Each gene length was divided into ten equal segments and the signal intensity of all probes within each of these deciles was averaged. Flanking region distances for analysis were empirically determined by taking progressively longer flanks (1 kb increments) for the analysis; 3 kb of upstream sequence was determined to be optimal for data capture and this flank distance was applied to all ChIP data. The 3 Kb upstream flanking sequenced was divided into 20 bins and the probe intensities within each bin averaged and plotted along with the gene data as a moving average with five bins per step. Error bars at each point on the graph represent the standard error (standard deviation divided by the square root of the number of genes). For many plots, we calculated the ratio for the maximum value at the promoter region divided by the minimum value in the gene body region. The error values were calculated from the standard errors considering error propagation of this division. *T*-tests were performed using R, version 3.5.0. Bioinformatic analysis of transcriptional regulation was carried out using GEO2R and enrichment analysis was carried out using DAVID Bioinformatic Resources 6.8 (74, 75).

AUTHOR CONTRIBUTIONS

MK and JH : Design, analysis and interpretation of data, Writing and editing. DL: Design, analysis and preparation of samples; SG

and PW: Analysis and preparation of samples; SY: Biostatistical analysis of data; TF: Analysis, interpretation of data.

ACKNOWLEDGMENTS

Our thanks and appreciation to David Bentley for reagents and discussions throughout this work. We thank the *C. elegans* Gene Knockout Consortium and Japanese National Bioresource Project for deletion alleles and WormBase as a constant resource throughout these studies. This work utilized the computational resources of the NIH HPC Biowulf cluster. (*http://hpc.nih.gov*). This work was funded, in part, by the Intramural Research Program of the National Institute of Diabetes and Digestive and Kidney Diseases, National Institutes of Health.

SUPPLEMENTARY MATERIAL

The Supplementary Material for this article can be found online at: https://www.frontiersin.org/articles/10.3389/fendo.2018.00521/full#supplementary-material

REFERENCES

1. Phatnani HP, Greenleaf AL. Phosphorylation and functions of the RNA polymerase II CTD. *Genes Dev.* (2006) 20:2922–36. doi: 10.1101/gad.1477006
2. Buratowski S. The CTD code. *Nat Struct Biol.* (2003) 10:679–80. doi: 10.1038/nsb0903-679
3. Buratowski S. Progression through the RNA polymerase II CTD cycle. *Mol Cell* (2009) 36:541–6. doi: 10.1016/j.molcel.2009.10.019
4. Hsin JP, Manley JL. The RNA polymerase II CTD coordinates transcription and RNA processing. *Genes Dev.* (2012) 26:2119–37. doi: 10.1101/gad.200303.112
5. Kwak H, Lis JT. Control of transcriptional elongation. *Annu Rev Genet.* (2013) 47:483–508. doi: 10.1146/annurev-genet-110711-155440
6. Ebmeier CC, Erickson B, Allen BL, Allen MA, Kim H, Fong N, et al. Human TFIIH kinase CDK7 regulates transcription-associated chromatin modifications. *Cell Rep.* (2017) 20:1173–86. doi: 10.1016/j.celrep.2017.07.021
7. Guenther MG, Levine SS, Boyer LA, Jaenisch R, Young RA. A chromatin landmark and transcription initiation at most promoters in human cells. *Cell* (2007) 130:77–88. doi: 10.1016/j.cell.2007.05.042
8. Zeitlinger J, Zinzen RP, Stark A, Kellis M, Zhang H, Young RA, et al. Whole-genome ChIP-chip analysis of dorsal, twist, and snail suggests integration of diverse patterning processes in the drosophila embryo. *Genes Dev.* (2007) 21:385–90. doi: 10.1101/gad.1509607
9. Core LJ, Lis JT. Transcription regulation through promoter-proximal pausing of RNA polymerase II. *Science* (2008) 319:1791–2. doi: 10.1126/science.1150843
10. Core LJ, Waterfall JJ, Lis JT. Nascent RNA sequencing reveals widespread pausing and divergent initiation at human promoters. *Science* (2008) 322:1845–8. doi: 10.1126/science.1162228
11. Wu JQ, Snyder M. RNA polymerase II stalling: loading at the start prepares genes for a sprint. *Genome Biol.* (2008) 9:220. doi: 10.1186/gb-2008-9-5-220
12. Jonkers I, Lis JT. Getting up to speed with transcription elongation by RNA polymerase II. *Nat Rev Mol Cell Biol.* (2015) 16:167–77. doi: 10.1038/nrm3953
13. Chen FX, Smith ER, Shilatifard A. Born to run: control of transcription elongation by RNA polymerase II. *Nat Rev Mol Cell Biol.* (2018) 19:464–78. doi: 10.1038/s41580-018-0010-5
14. Levine M. Paused RNA polymerase II as a developmental checkpoint. *Cell* (2011) 145:502–11. doi: 10.1016/j.cell.2011.04.021
15. Kenyon C, Chang J, Gensch E, Rudner A, Tabtiang R. A C. elegans mutant that lives twice as long as wild type. *Nature* (1993) 366:461–4. doi: 10.1038/366461a0
16. Baugh LR, Sternberg PW. DAF-16/FOXO regulates transcription of cki-1/Cip/Kip and repression of lin-4 during *C. elegans* L1 arrest. *Curr Biol.* (2006) 16:780–5. doi: 10.1016/j.cub.2006.03.021
17. Fielenbach N, Antebi A. *C. elegans* dauer formation and the molecular basis of plasticity. *Genes Dev.* (2008) 22:2149–65. doi: 10.1101/gad.1701508
18. Angelo G, Van Gilst MR. Starvation protects germline stem cells and extends reproductive longevity in *C. elegans. Science* (2009) 326:954–8. doi: 10.1126/science.1178343
19. Baugh LR, Demodena J, Sternberg PW. RNA Pol II accumulates at promoters of growth genes during developmental arrest. *Science* (2009) 324:92–4. doi: 10.1126/science.1169628
20. Maxwell CS, Kruesi WS, Core LJ, Kurhanewicz N, Waters CT, Lewarch CL, et al. Pol II docking and pausing at growth and stress genes in *C. elegans*. *Cell Rep.* (2014) 6:455–66. doi: 10.1016/j.celrep.2014.01.008
21. Kruesi WS, Core LJ, Waters CT, Lis JT, Meyer BJ. Condensin controls recruitment of RNA polymerase II to achieve nematode X-chromosome dosage compensation. *Elife* (2013) 2:e00808. doi: 10.7554/eLife.00808
22. Blackwell TK, Walker AK. Transcription mechanisms. In: Wormbook, editor. *The Online Review of C elegans Biology.* (2006). p. 1–16. Available online at: http://www.wormbook.org
23. Hanover JA, Forsythe ME, Hennessey PT, Brodigan TM, Love DC, Ashwell G, et al. A Caenorhabditis elegans model of insulin resistance: altered macronutrient storage and dauer formation in an OGT-1 knockout. *Proc Natl Acad Sci USA.* (2005) 102:11266–71. doi: 10.1073/pnas.0408771102
24. Forsythe ME, Love DC, Lazarus BD, Kim EJ, Prinz WA, Ashwell G, et al. Caenorhabditis elegans ortholog of a diabetes susceptibility locus: oga-1 (*O*-GlcNAcase) knockout impacts *O*-GlcNAc cycling, metabolism, and dauer. *Proc Natl Acad Sci USA.* (2006) 103:11952–7. doi: 10.1073/pnas.0601931103
25. Love DC, Krause MW, Hanover JA. *O*-GlcNAc cycling: emerging roles in development and epigenetics. *Semin Cell Dev Biol.* (2010) 21:646–54. doi: 10.1016/j.semcdb.2010.05.001
26. Hanover JA. The nuclear pore: at the crossroads. *FASEB J.* (1992) 6:2288–95. doi: 10.1096/fasebj.6.6.1312045
27. Butkinaree C, Park K, Hart GW. O-linked beta-N-acetylglucosamine (*O*-GlcNAc): Extensive crosstalk with phosphorylation to regulate signaling and transcription in response to nutrients and stress. *Biochim Biophys Acta* (2010) 1800:96–106. doi: 10.1016/j.bbagen.2009.07.018
28. Love DC, Hanover JA. The hexosamine signaling pathway: deciphering the "*O*-GlcNAc code." *Sci STKE* (2005) 2005:re13. doi: 10.1126/stke.3122005re13
29. Wang Z, Gucek M, Hart GW. Cross-talk between GlcNAcylation and phosphorylation: site-specific phosphorylation dynamics in response to globally elevated *O*-GlcNAc. *Proc Natl Acad Sci USA.* (2008) 105:13793–8. doi: 10.1073/pnas.0806216105
30. Gambetta MC, Oktaba K, Muller J. Essential role of the glycosyltransferase sxc/Ogt in polycomb repression. *Science* (2009) 325:93–6. doi: 10.1126/science.1169727
31. Sinclair DA, Syrzycka M, Macauley MS, Rastgardani T, Komljenovic I, Vocadlo DJ, et al. Drosophila *O*-GlcNAc transferase (OGT) is encoded by the Polycomb group (PcG) gene, super sex combs (sxc). *Proc Natl Acad Sci USA.* (2009) 106:13427–32. doi: 10.1073/pnas.0904638106
32. Love DC, Ghosh S, Mondoux MA, Fukushige T, Wang P, Wilson MA, et al. Dynamic *O*-GlcNAc cycling at promoters of Caenorhabditis elegans genes regulating longevity, stress, and immunity. *Proc Natl Acad Sci USA.* (2010) 107:7413–8. doi: 10.1073/pnas.0911857107
33. Akan I, Love DC, Harwood KR, Bond MR, Hanover JA. Drosophila *O*-GlcNAcase deletion globally perturbs chromatin *O*-GlcNAcylation. *J Biol Chem.* (2016) 291:9906–19. doi: 10.1074/jbc.M115.704783
34. Kelly WG, Dahmus ME, Hart GW. RNA polymerase II is a glycoprotein. Modification of the COOH-terminal domain by *O*-GlcNAc. *J Biol Chem.* (1993) 268:10416–24.

35. Comer FI, Hart GW. Reciprocity between *O*-GlcNAc and O-phosphate on the carboxyl terminal domain of RNA polymerase II. *Biochemistry* (2001) 40:7845–52. doi: 10.1021/bi0027480
36. Lu L, Fan D, Hu CW, Worth M, Ma ZX, Jiang J. Distributive *O*-GlcNAcylation on the highly repetitive C-terminal domain of RNA polymerase II *Biochemistry* (2016) 55:1149–58. doi: 10.1021/acs.biochem.5b01280
37. Ranuncolo SM, Ghosh S, Hanover JA, Hart GW, Lewis BA. Evidence of the involvement of *O*-GlcNAc-modified human RNA polymerase II CTD in transcription *in vitro* and *in vivo*. *J Biol Chem.* (2012) 287:23549–61. doi: 10.1074/jbc.M111.330910
38. Lewis BA, Hanover JA. *O*-GlcNAc and the epigenetic regulation of gene expression. *J Biol Chem.* (2014) 289:34440–8. doi: 10.1074/jbc.R114.595439
39. Lewis BA, Burlingame AL, Myers SA. Human RNA polymerase II promoter recruitment *in vitro* is regulated by O-linked N-acetylglucosaminyltransferase (OGT). *J Biol Chem.* (2016) 291:14056–61. doi: 10.1074/jbc.M115.684365
40. Resto M, Kim BH, Fernandez AG, Abraham BJ, Zhao K, Lewis BA. *O*-GlcNAcase Is an RNA polymerase II elongation factor coupled to pausing factors SPT5 and TIF1beta. *J Biol Chem.* (2016) 291:22703–13. doi: 10.1074/jbc.M116.751420
41. Shafi R, Iyer SP, Ellies LG, O'Donnell N, Marek KW, Chui D, et al. The *O*-GlcNAc transferase gene resides on the X chromosome and is essential for embryonic stem cell viability and mouse ontogeny. *Proc Natl Acad Sci USA.* (2000) 97:5735–9. doi: 10.1073/pnas.100471497
42. Hanover JA, Yu S, Lubas WB, Shin SH, Ragano-Caracciola M, Kochran J, et al. Mitochondrial and nucleocytoplasmic isoforms of O-linked GlcNAc transferase encoded by a single mammalian gene. *Arch Biochem Biophys* (2003) 409:287–97. doi: 10.1016/S0003-9861(02)00578-7
43. O'Donnell N, Zachara NE, Hart GW, Marth JD. Ogt-dependent X-chromosome-linked protein glycosylation is a requisite modification in somatic cell function and embryo viability. *Mol Cell Biol.* (2004) 24:1680–90. doi: 10.1128/MCB.24.4.1680-1690.2004
44. Keembiyehetty C, Love DC, Harwood KR, Gavrilova O, Comly ME, Hanover JA. Conditional knock-out reveals a requirement for O-linked N-Acetylglucosaminase (*O*-GlcNAcase) in metabolic homeostasis. *J Biol Chem.* (2015) 290:7097–113. doi: 10.1074/jbc.M114.617779
45. Mondoux MA, Love DC, Ghosh SK, Fukushige T, Bond M, Weerasinghe GR, et al. O-linked-N-acetylglucosamine cycling and insulin signaling are required for the glucose stress response in Caenorhabditis elegans. *Genetics* (2011) 188:369–82. doi: 10.1534/genetics.111.126490
46. Lei H, Fukushige T, Niu W, Sarov M, Reinke V, Krause M. A widespread distribution of genomic CeMyoD binding sites revealed and cross validated by ChIP-Chip and ChIP-Seq techniques. *PLoS ONE* (2010) 5:e15898. doi: 10.1371/journal.pone.0015898
47. Zhong M, Niu W, Lu ZJ, Sarov M, Murray JI, Janette J, et al. Genome-wide identification of binding sites defines distinct functions for Caenorhabditis elegans PHA-4/FOXA in development and environmental response. *PLoS Genet.* (2010) 6:e1000848. doi: 10.1371/journal.pgen.1000848
48. Whittle CM, McClinic KN, Ercan S, Zhang X, Green RD, Kelly WG, et al. The genomic distribution and function of histone variant HTZ-1 during *C. elegans* embryogenesis. *PLoS Genet.* (2008) 4:e1000187. doi: 10.1371/journal.pgen.1000187
49. Teytelman L, Ozaydin B, Zill O, Lefrancois P, Snyder M, Rine J, et al. Impact of chromatin structures on DNA processing for genomic analyses. *PLoS ONE* (2009) 4:e6700. doi: 10.1371/journal.pone.0006700
50. Whittle CM, Lazakovitch E, Gronostajski RM, Lieb JD. DNA-binding specificity and in vivo targets of Caenorhabditis elegans nuclear factor I. *Proc Natl Acad Sci USA.* (2009) 106:12049–54. doi: 10.1073/pnas.0812894106
51. Comer FI, Hart GW. *O*-GlcNAc and the control of gene expression. *Biochim Biophys Acta* (1999) 1473:161–71. doi: 10.1016/S0304-4165(99)00176-2
52. Khidekel N, Arndt S, Lamarre-Vincent N, Lippert A, Poulin-Kerstien KG, Ramakrishnan B, et al. A chemoenzymatic approach toward the rapid and sensitive detection of *O*-GlcNAc posttranslational modifications. *J Am Chem Soc* (2003) 125:16162–3. doi: 10.1021/ja038545r
53. Kolb HC, Finn MG, Sharpless KB. Click chemistry: diverse chemical function from a few good reactions. *Angew Chem Int Ed Engl.* (2001) 40:2004–21. doi: 10.1002/1521-3773(20010601)40:11<2004::AID-ANIE2004>3.0.CO;2-5
54. Torres CR, Hart GW. Topography and polypeptide distribution of terminal N-acetylglucosamine residues on the surfaces of intact lymphocytes. Evidence for O-linked GlcNAc. *J Biol Chem.* (1984) 259:3308–17.
55. Hanover JA, Cohen CK, Willingham MC, Park MK. O-linked N-acetylglucosamine is attached to proteins of the nuclear pore. Evidence for cytoplasmic and nucleoplasmic glycoproteins. *J Biol Chem.* (1987) 262:9887–94.
56. Pferdehirt RR, Kruesi WS, Meyer BJ. An MLL/COMPASS subunit functions in the *C. elegans* dosage compensation complex to target X chromosomes for transcriptional regulation of gene expression *Genes Dev.* (2011) 25:499–515. doi: 10.1101/gad.2016011
57. Schroeder SC, Schwer B, Shuman S, Bentley D. Dynamic association of capping enzymes with transcribing RNA polymerase II. *Genes Dev.* (2000) 14:2435–40. doi: 10.1101/gad.836300
58. Kim H, Erickson B, Luo W, Seward D, Graber JH, Pollock DD, et al. Gene-specific RNA polymerase II phosphorylation and the CTD code. *Nat Struct Mol Biol.* (2010) 17:1279–86. doi: 10.1038/nsmb.1913
59. Seydoux G, Dunn MA. Transcriptionally repressed germ cells lack a subpopulation of phosphorylated RNA polymerase II in early embryos of *Caenorhabditis elegans* and *Drosophila melanogaster*. *Development* (1997) 124:2191–201.
60. Batchelder C, Dunn MA, Choy B, Suh Y, Cassie C, Shim EY, et al. Transcriptional repression by the *Caenorhabditis elegans* germ-line protein PIE-1. *Genes Dev.* (1999) 13:202–12. doi: 10.1101/gad.13.2.202
61. Wang JJ, Cui DY, Xiao T, Sun X, Zhang P, Chen R, et al. The influences of PRG-1 on the expression of small RNAs and mRNAs. *BMC Genomics* (2014) 15:321. doi: 10.1186/1471-2164-15-321
62. Hart GW. Dynamic O-linked glycosylation of nuclear and cytoskeletal proteins. *Annu Rev Biochem.* (1997) 66:315–35. doi: 10.1146/annurev.biochem.66.1.315
63. Guinez C, Morelle W, Michalski JC, Lefebvre T. *O*-GlcNAc glycosylation: a signal for the nuclear transport of cytosolic proteins? *Int J Biochem Cell Biol.* (2005) 37:765–74. doi: 10.1016/j.biocel.2004.12.001
64. Yang X, Zhang F, Kudlow JE. Recruitment of *O*-GlcNAc transferase to promoters by corepressor mSin3A: coupling protein *O*-GlcNAcylation to transcriptional repression. *Cell* (2002) 110:69–80. doi: 10.1016/S0092-8674(02)00810-3
65. Muller J, Kassis JA. Polycomb response elements and targeting of Polycomb group proteins in Drosophila. *Curr Opin Genet Dev.* (2006) 16:476–84. doi: 10.1016/j.gde.2006.08.005
66. Kelly WG, Fire A. Chromatin silencing and the maintenance of a functional germline in Caenorhabditis elegans. *Development* (1998) 125:2451–6.
67. Bender LB, Cao R, Zhang Y, Strome S. The MES-2/MES-3/MES-6 complex and regulation of histone H3 methylation in *C. elegans. Curr Biol.* (2004) 14:1639–43. doi: 10.1016/j.cub.2004.08.062
68. Pettitt DJ, Jovanovic L. The vicious cycle of diabetes and pregnancy. *Curr Diab Rep.* (2007) 7:295–7. doi: 10.1007/s11892-007-0047-x
69. Anderson LM, Riffle L, Wilson R, Travlos GS, Lubomirski MS, Alvord WG. Preconceptional fasting of fathers alters serum glucose in offspring of mice. *Nutrition* (2006) 22:327–31. doi: 10.1016/j.nut.2005.09.006
70. Pembrey ME, Bygren LO, Kaati G, Edvinsson S, Northstone K, Sjostrom M, et al. Sex-specific, male-line transgenerational responses in humans. *Eur J Hum Genet.* (2006) 14:159–66. doi: 10.1038/sj.ejhg.5201538
71. Brenner S. The genetics of Caenorhabditis elegans. *Genetics* (1974) 77:71–94.

72. Snow CM, Senior A, Gerace L. Monoclonal antibodies identify a group of nuclear pore complex glycoproteins. *J Cell Biol.* (1987) 104:1143–56. doi: 10.1083/jcb.104.5.1143
73. Turner JR, Tartakoff AM. On the relation between distinct components of the cytoskeleton: an epitope shared by intermediate filaments, microfilaments and cytoplasmic foci. *Eur J Cell Biol.* (1990) 51:259–64.
74. Huang da W, Sherman BT, Lempicki RA. Bioinformatics enrichment tools: paths toward the comprehensive functional analysis of large gene lists. *Nucleic Acids Res.* (2009) 37:1–13. doi: 10.1093/nar/gkn923
75. Huang da W, Sherman BT, Lempicki RA. Systematic and integrative analysis of large gene lists using DAVID bioinformatics resources. *Nat Protoc* (2009) 4:44–57. doi: 10.1038/nprot.2008.211

Conflict of Interest Statement: The authors declare that the research was conducted in the absence of any commercial or financial relationships that could be construed as a potential conflict of interest.

frontiers in Endocrinology

MINI REVIEW
published: 13 September 2018
doi: 10.3389/fendo.2018.00519

AMP-Activated Protein Kinase and O-GlcNAcylation, Two Partners Tightly Connected to Regulate Key Cellular Processes

*Roselle Gélinas[1], Justine Dontaine[2], Sandrine Horman[2], Christophe Beauloye[2,3], Laurent Bultot[2] and Luc Bertrand[2]**

[1] Montreal Heart Institute, Université de Montreal, Montreal, QC, Canada, [2] Institut de Recherche Expérimentale et Clinique, Pole of Cardiovascular Research, Université catholique de Louvain, Brussels, Belgium, [3] Division of Cardiology, Cliniques Universitaires Saint-Luc, Brussels, Belgium

OPEN ACCESS

Edited by:
Tarik ISSAD,
Institut National de la Santé et de la Recherche Médicale (INSERM), France

Reviewed by:
Katsutaro Morino,
Shiga University of Medical Science, Japan
Chad Slawson,
Kansas University of Medical Center Research Institute, United States

***Correspondence:**
Luc Bertrand
luc.bertrand@uclouvain.be

Specialty section:
This article was submitted to Molecular and Structural Endocrinology, a section of the journal Frontiers in Endocrinology

Received: 28 June 2018
Accepted: 20 August 2018
Published: 13 September 2018

Citation:
Gélinas R, Dontaine J, Horman S, Beauloye C, Bultot L and Bertrand L (2018) AMP-Activated Protein Kinase and O-GlcNAcylation, Two Partners Tightly Connected to Regulate Key Cellular Processes. Front. Endocrinol. 9:519. doi: 10.3389/fendo.2018.00519

The AMP-activated protein kinase (AMPK) is an important cellular energy sensor. Its activation under energetic stress is known to activate energy-producing pathways and to inactivate energy-consuming pathways, promoting ATP preservation and cell survival. AMPK has been shown to play protective role in many pathophysiological processes including cardiovascular diseases, diabetes, and cancer. Its action is multi-faceted and comprises short-term regulation of enzymes by direct phosphorylation as well as long-term adaptation via control of transcription factors and cellular events such as autophagy. During the last decade, several studies underline the particular importance of the interaction between AMPK and the post-translational modification called O-GlcNAcylation. O-GlcNAcylation means the O-linked attachment of a single N-acetylglucosamine moiety on serine or threonine residues. O-GlcNAcylation plays a role in multiple physiological cellular processes but is also associated with the development of various diseases. The first goal of the present review is to present the tight molecular relationship between AMPK and enzymes regulating O-GlcNAcylation. We then draw the attention of the reader on the putative importance of this interaction in different pathophysiological events.

Keywords: AMPK, O-GlcNAcylation, diabetes, cardiovascular diseases, cancer

INTRODUCTION

The majority of proteins playing essential biological roles undergo post-translational modification (PTM) to regulate their structure, cellular localization, activity and biological function. Accordingly, many metabolic enzymes and regulators, such as acetyl-CoA carboxylase and ULK1, are known to be phosphorylated in conditions of metabolic stress to adapt to energy imbalance (1). Under such circumstances, cells will adjust their metabolism by promoting energy production pathways and shutting down non-essential energy-consuming pathways. An essential actor in the phospho-dependent metabolic reorganization during energy stress is the AMP-activated protein kinase (AMPK) (2). Similar to protein phosphorylation, O-linked β-N-acetylglucosamine (O-GlcNAc) addition on Ser/Thr residues is a dynamic PTM that regulates many cellular processes including stress response (3, 4), transcriptional activity (5, 6), and epigenetic regulation (7). It has

been recently shown that AMPK can interrelate with enzymes regulating protein O-GlcNAcylation. The present review highlights this interplay with an emphasis of how this link could be targeted to prevent and/or treat several diseases.

AMPK, a Key Energy Sensor

AMPK is a heterotrimeric protein composed of one catalytic subunit α (existing in two isoforms, α1, and α2) and two regulatory subunits, β (β1 and β2) and γ (γ1, γ2, and γ3) (8). AMPK is a vital cellular energy sensor that regulates metabolism in order to maintain energy balance (9). During energy stress, the increase in AMP/ATP ratio leads to the binding of AMP to the γ subunit promoting AMPK activation by allosteric regulation and by phosphorylation of the catalytic α subunit on Thr172 (10). Once activated, AMPK phosphorylates downstream targets at Ser/Thr residues within a characteristic sequence motif. Numerous AMPK substrates in various protein networks have been described so far (1, 11, 12). AMPK acts acutely by phosphorylating metabolic enzymes, but also provokes long-term adaptation at a transcriptional level (13). AMPK inhibits anabolic pathways, including protein synthesis (14, 15), and enhances catabolic pathways, such as glycolysis and mitochondrial β-oxidation, to restore energetic balance required for cell survival (16, 17). AMPK activation is considered as a putative future therapeutic target for various pathologies characterized by disorganized cellular metabolism, such as cancer, diabetes, myocardial ischemia and cardiac hypertrophy (18). In order to develop new drugs and treatments, deciphering the mechanisms by which AMPK provides its beneficial action have pushed research in the field. Beside AMPK, a significant proportion of these diseases is also characterized by an atypical O-GlcNAcylation profile. Recent evidences demonstrate interplay between AMPK and O-GlcNAcylation. Interestingly, some of the AMPK beneficial effects seem to be linked to modulation of O-GlcNAcylation.

O-GlcNAcylation, a Particular Post-translational Modification

Protein O-GlcNAcylation is a PTM that promotes the O-linked attachment of a single N-acetylglucosamine moiety on Ser/Thr residues of over 4000 proteins including nuclear, cytosolic, and mitochondrial proteins (5). O-GlcNAcylation depends on the availability of uridine diphosphate-N-acetylglucosamine (UDP-GlcNAc), the end product of hexosamine biosynthesis pathway (HBP), an alternative pathway of glucose metabolism (**Figure 1**). HBP is dependent of glucose, amino acid and nucleotide availability, turning O-GlcNAcylation to a nutrient sensitive PTM that dynamically integrates metabolic signals (19, 20). The increased HBP flux due to chronic metabolic changes gives rise to elevated levels of protein O-GlcNAcylation which are known to play a role in the development of insulin resistance and diabetes (21, 22). Beyond diabetes, aberrant O-GlcNAcylation is associated with several diseases, such as cardiovascular diseases and cancer. Glutamine:fructose-6-phosphate aminotransferase (GFAT), which converts fructose 6-phosphate to glucosamine 6-phosphate, is the rate limiting enzyme of HBP and its deletion causes vital cellular defects (23). GFAT is highly conserved among species and two isoforms from separated genes, GFAT1 and GFAT2, can be found in mammals (24). Their relative expression varies among tissues, GFAT1 being mainly expressed in pancreas, placenta, testis and skeletal muscle whereas GFAT2 can be found in heart and central nervous system (25).

Unlike phosphorylation, which is regulated by numerous protein kinases and phosphatases, O-GlcNAc cycling is regulated by the concerted action of only two enzymes, O-GlcNAc transferase (OGT) that adds *O*-GlcNAc to proteins, and the protein O-GlcNAcase (OGA) that removes it (26) (**Figure 1**). This limited number of actors has suggested that O-GlcNAcylation was an unrefined modification hitting non-specifically a large number of substrates. However, recent evidences show that OGT/OGA localization, their interactions with specific substrates and the competition for Ser/Thr with other PTMs shape the O-GlcNAcylation response in agreement with cellular state. As an example, competition between phosphorylation and O-GlcNAc for the same or proximal site is well documented in the recent review of van der Laarse et al. (27).

Growing evidences indicate that both GFAT and OGT can be substrates of protein kinases including AMPK (28, 29). Conversely, AMPK can be targeted by O-GlcNAcylation (30, 31). The next chapters will present the molecular basis of these molecular interactions and the putative consequences of this interplay in pathologies.

CROSSTALK BETWEEN AMPK AND O-GLCNACYLATION-MEDIATING ENZYMES

Regulation of O-GlcNAcylation by AMPK

GFAT

Regulation of O-GlcNAc by AMPK has been firstly described in 2007 when AMPK was proposed to phosphorylate GFAT1 on Ser243 (32) (**Figure 1**). This phosphorylation was postulated to increase GFAT activity by lowering k_M for fructose-6-phosphate as measured by *in vitro* enzymatic assay. However, more recent studies rather demonstrate that AMPK negatively regulates GFAT activity. Using model of GFAT1 overexpression in mammalian cells, Eguchi and colleagues reported that 2-deoxyglucose-mediated AMPK activation induces GFAT1 phosphorylation on Ser243, concomitantly to its inactivation (28). Similarly, AMPK activation, by 5-aminoimidazole-4-carboxamide riboside (AICAr) or vascular endothelial growth factor (VEGF) in primary human endothelial cells, has been shown to induce a marked increase in endogenous GFAT1 phosphorylation on Ser243, a significant reduction in GFAT activity and a concomitant reduction in O-GlcNAc levels (33, 34). Finally, our research group has shown that AMPK activation by metformin, or by the specific AMPK activator A769662, promotes GFAT phosphorylation on the aforementioned site in both neonatal rat cardiomyocytes (NRVM) and adult mouse heart (35) Once again, this is associated with reduced O-GlcNAc levels (35). Overall,

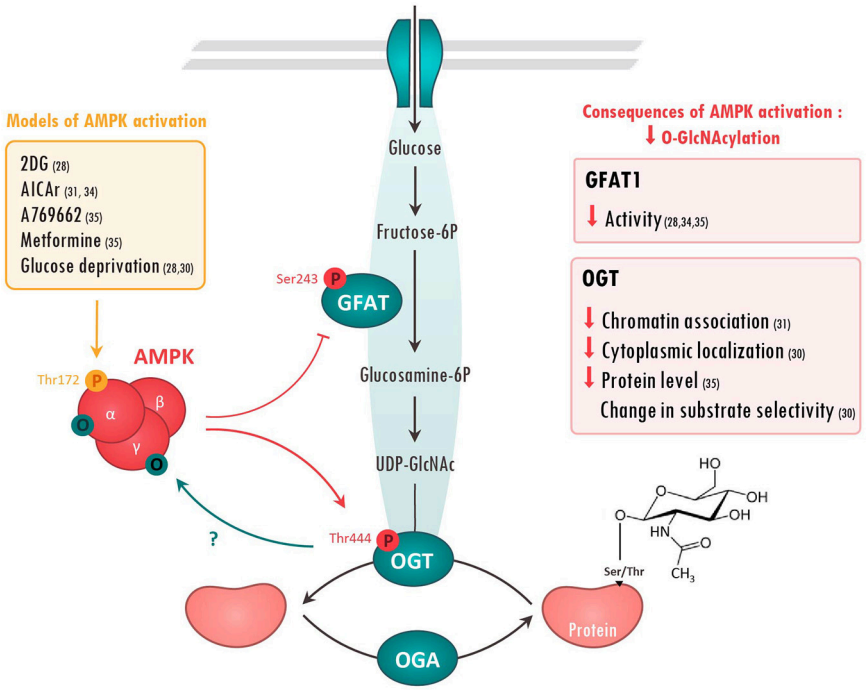

FIGURE 1 | Molecular interactions between AMPK and O-GlcNAcylation-mediating enzymes. Action of AMPK on O-GlcNAcylation-mediating enzymes has been evaluated in the literature using various treatments (left panel). Once activated, AMPK has been shown to phosphorylate Glutamine fructose-6-phosphate aminotransferase (GFAT) on Ser243 and O-GlcNAc transferase (OGT) on Thr444. The consequences of these AMPK-mediated modifications are resumed in the right panels. On the other hand, AMPK can be O-GlcNAcylated on its α and γ subunits, presumably preventing its activation. References are presented in parentheses. 2DG, 2 Deoxyglucose; AICAr, 5 aminoimidazole-4-carboxamide ribonucleoside; O, O-GlcNAcyl; P, phosphoryl group; UDP-Glucose, Uridine diphosphate glucose.

majority of the recent studies demonstrate that AMPK directly phosphorylates and reduces GFAT activity, lowering O-GlcNAc levels (**Figure 1**).

OGT

Besides GFAT, OGT also looks to be regulated by AMPK (Figure 1). It has been shown that AMPK can interact with and phosphorylate OGT on Thr444 *in vitro* (30). Moreover, AMPK activation by A769662 or AICAr triggers OGT phosphorylation on Thr444 in skeletal muscle cells and mouse embryonic fibroblasts (MEF) (30, 31). Interestingly, Thr444 phosphorylation does not affect OGT enzymatic activity, but rather seems to modulate OGT cellular localization and substrate specificity. Xu and colleagues revealed that AMPK phosphorylates nuclear OGT in MEFs, promoting its dissociation from chromatin and the reduction of histone 2B O-GlcNAcylation on Ser112 (31). By contrast, AMPK activation is shown to induce OGT nuclear translocation in C2C12 myotubes, stimulating nuclear protein O-GlcNAcylation and histone acetylation (30). In addition to modulating cellular localization, AMPK seems to alter OGT substrate selectivity by promoting its interaction with particular proteins or by competing with OGT for the same or proximal site(s). As example, AMPK decreases 26S proteasome activity in endothelial cells by promoting its association with OGT and its subsequent O-GlcNAcylation (36). Moreover, competition between O-GlcNAcylation and AMPK phosphorylation for the same or proximal Ser/Thr site is described to have opposite effects on the regulation of several proteins. For example, AMPK phosphorylation and O-GlcNAcylation compete for the same site on chromatin-associated fumarase (FH) and lead to opposite effects (37). Hyaluroran HAS2 activity is also regulated in an opposite manner by AMPK phosphorylation and O-GlcNAcylation on proximal sites, although competition between both is not yet formerly studied (38).

AMPK has also been proposed to regulate OGT expression. In Neuro-2a neuroblastoma cells, glucose deprivation induces an AMPK-dependent increase in OGT mRNA and protein expression, leading to elevated O-GlcNAc levels (39). However, two other studies, performed in other cell types, established that glucose deprivation acts on OGT independently of AMPK (40, 41). In our hands, we showed that metformin-induced AMPK activation leads to a decrease in cardiac OGT expression and O-GlcNAc levels in hypertrophied mouse hearts. In conclusion, the regulation of OGT expression by AMPK seems to highly depend of various parameters such as cell types and physio-pathological status.

OGA

Evidence of direct regulation of OGA by AMPK has not been demonstrated so far. However, mice deficient for the AMPKα2 isoform are characterized by an elevated basal level of cardiac O-GlcNAcylation that is associated with decreased OGA protein

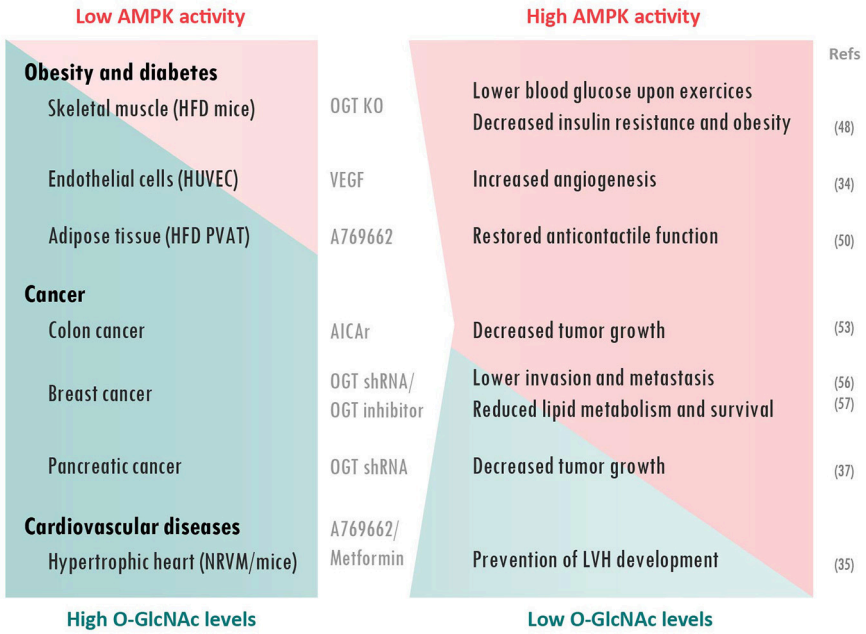

FIGURE 2 | AMPK/O-GlcNAcylation interplay in pathophysiological processes. AMPK activation and O-GlcNAcylation levels are generally inversely correlated in pathologies. Lowering O-GlcNAcylation or increasing AMPK activity prevents adverse effects in diabetes, cancer and cardiac hypertrophy. Treatments and cellular/animal models used are presented between to two columns. AICAr, 5-aminoimidazole-4-carboxamide ribonucleotise; HFD, High-fat diet; HUVEC, Human Umbilical Vein Endothelial Cells; LVH, Left ventricular hypertrophy; NRVM, Neonatal rat ventricular myocytes; OGT KO, O-GlcNAc transferase knock-out; PVAT, Perivascular adipose tissue; shRNA, short hairpin RNA; VEGF, Vascular endothelial growth factor.

levels (35). The molecular mechanism involved remains to be identified.

Regulation of AMPK by O-GlcNAcylation

In a reciprocal way, AMPK can be regulated by O-GlcNAcylation (**Figure 1**). The first evidence dates back to 2007. AMPK was detected in O-GlcNAc precipitates using succinylated wheat germ agglutinin, a lectin that binds O-GlcNAc residues (42). In 2014, two different research groups confirmed that AMPK can be O-GlcNAcylated by OGT. Xu et al. report that AMPKα1 isoform is O-GlcNAcylated *in vitro* in MEFs and that OGT knock-down reduces AMPK phosphorylation on Thr172, suggesting that OGT positively regulates AMPK activity (31). With the same idea, Bullen and collaborators showed that all AMPKα- and γ-subunits are "O-GlcNAcylable" *in vitro* (30). They also demonstrated that O-GlcNAcylation of an over-expressed form of AMPKγ1 subunit occurs in human embryonic kidney (HEK) 293 cells. Interestingly, this O-GlcNAcylation happens when AMPK is activated by glucose deprivation or AICAr treatment and is absent when a kinase dead form of AMPK is over-expressed. This highly suggests that AMPK activation is required for its own O-GlcNAcylation. However, it has to be mentioned that AMPK/O-GlcNAcylation interplay is extremely complex. Indeed, pre-treatment with O-GlcNAc inducers, such as Thiamet G, blunts AMPK activation induced by glucose deprivation, indicating that PTM order plays an important role in AMPK regulation by O-GlcNAcylation (30). Accordingly, EtOH-induced increase in AMPK phosphorylation on Thr172 coincides with a decrease in AMPK O-GlcNAcylation in C2C12 myocytes (43). Other studies report alternatives effects of O-GlcNAcylation on AMPK activity. Laczy and colleagues reported no changes in AMPK activation in isolated rat hearts perfused with glucosamine (44). In the same line, our group established that increasing O-GlcNAc levels using O-GlcNAc inducers or decreasing O-GlcNAcylation with the GFAT inhibitor 6-diazo-5-oxo-L-norleucine (DON), have no impact on AMPK activity in neonatal rat cardiomyocytes and mouse hearts (35).

Besides direct regulation of AMPK by OGT, O-GlcNAcylation may induce AMPK-dependent phosphorylation of specific proteins. As example, ULK1 O-GlcNAcylation promotes AMPK recruitment and AMPK-mediated phosphorylation of ULK1, resulting in increased cellular autophagy (29).

As conclusion of this chapter, molecular crosstalk and/or competition between AMPK and O-GlcNAc pathway is well-documented. This interplay has distinct consequence depending on cell type, chronic/acute stimulation and metabolic status.

PATHOPHYSIOLOGICAL CONSEQUENCES OF AMPK/O-GLCNACYLATION INTERACTION

AMPK signaling and O-GlcNAcylation are associated with various pathologies such as diabetes, cancers and cardiovascular diseases (**Figure 2**). A global rise of O-GlcNAcylation is detected during the developement of these pathologies. Conversely, AMPK activation is generally described to be beneficial on slowing down their development. In this last part, we will

overview how O-GlcNAcylation/AMPK interaction plays a role in these pathological events.

Obesity and Diabetes

During the last 30 years, number of studies provided direct evidences supporting a link between HBP and adverse effects of diabetes [reviewed in (45)]. As nicely reviewed by Copeland and collaborators, elevated protein O-GlcNAcylation is strongly associated with hyperglycemia-induced glucotoxicity and insulin resistance (46). On the other hand, AMPK is described to be beneficial for diabetic patients via a multi-faceted action including an insulin-independent stimulation of glucose transport (47). In addition, interaction between AMPK and O-GlcNAcylation has been highlighted in diabetic conditions. Indeed, it has been recently reported that skeletal muscle-specific OGT knock-out mice show lower blood glucose during exercise and reduced high-fat-mediated obesity and insulin resistance (48). Interestingly, these effects are associated with higher AMPK expression and greater AMPK activation after exercise. It has been proposed by the authors, that the reduction in muscle O-GlcNAcylation has an anti-diabetic effect through an enhancement of the AMPK-dependent glucose utilization during exercise (48).

Vascular complications such as endothelial dysfunction are another important event in type II diabetes. Elevated protein O-GlcNAcylation levels are known to be part of hyperglycaemia-induced inhibition of angiogenesis (49). It has been shown that VEGF promotes angiogenesis in endothelial cells through an AMPK-mediated decrease in protein O-GlcNAcylation (34). AMPK/O-GlcNAcylation was thus proposed as putative future therapeutic target to improve vascular dysfunction in diabetic patients.

Finally, O-GlcNAc and AMPK have also been proposed to be associated with prenatal programming of perivascular adipose tissue (PVAT) associated with obesity-linked hypertension. Indeed, PVAT from male offspring of rodent fed with an obesogenic high-fat diet (HFD) are characterized by reduced anti-contractile effect, elevated O-GlcNAc levels and low AMPK activity (50). Interestingly, incubation of PVAT from male control offspring rat with glucosamine, as O-GlcNAc inducer, reduced AMPK activity and diminished its anti-contractile properties. However, PVAT function was restored by simultaneous AMPK activation, using A769662. Similarly, AMPK activation partially restored anti-contractile effects of PVAT from HFD offspring. Overall, these results support the idea that elevated O-GlcNAcylation levels, seen in obesity are related to reduced AMPK activity and, concomitantly, loss of anti-contractile effect of PVAT.

Cancer

Elevated protein O-GlcNAcylation has been reported in various cancer cells, including prostate, colon, breast and lung cancer as well as chronic myeloid leukemia (51) whereas AMPK has potent anti-tumoral properties (52). Furthermore, increasing O-GlcNAc levels, using Thiamet G or OGT overexpression, leads to an increase in AMPK O-GlcNAcylation and reduced AMPK activity in human colon cancer cells (53). This suppresses the inhibitory action of AMPK on the mammalian target of rapamycin pathway and results in enhanced tumor growth. Consequently, it is suggested that AMPK inactivation, due to elevated O-GlcNAc levels in diabetic patients, could explain the higher risk of colon cancer in this population (54).

Similar data were obtained in breast cancer cell lines by the group of Reginato (55–57). Increasing O-GlcNAcylation using NButGT or overexpression of OGT decreases AMPK activity, while reducing O-GlcNAcylation with OGT knock-down or OGT inhibitor leads to an increase in AMPK phosphorylation. In these studies, AMPK and OGT seem to have opposite effects on various proteins involved in cancer metabolism, such as the transcriptional regulator hypoxia-inducible factor-1α (55) and the deacetylase sirtuin 1 (SIRT1) (56). Among others, they showed that reducing O-GlcNAcylation increases SIRT1 protein levels in an AMPK-dependent manner; promoting degradation of oncogenic transcription factor forkhead box M1 in association with reduced invasion and metastasis of breast cancer. They also demonstrated that O-GlcNAcylation controls lipid metabolism in tumor cells via an AMPK-dependent mechanism. More precisely, inactivation of AMPK by OGT was shown to regulate sterol regulatory element-binding protein-1 phosphorylation and stability, resulting in higher lipid synthesis and, subsequently, in elevated cancer cell growth and survival (57).

Lastly, AMPK and O-GlcNAcylation can compete for a same Ser75 regulatory site of chromatin-associated FH involved in tumorigenesis. This gives rise to opposite effects of FH on the regulation of histone methylation (37). The increase in FH O-GlcNAcylation promotes development of pancreatic tumors (37). Consequently, the decrease of FH phosphorylation correlates with elevated protein O-GlcNAcylation and poor prognosis in pancreatic cancer patients.

Cardiovascular Diseases

An increase in global cardiac protein O-GlcNAcylation is commonly observed in pathological cardiac hypertrophy and heart failure, although the exact mechanism is not fully understood (58–60). AMPK, which is activated during left ventricular hypertrophy, acts as counter-regulatory mechanism and is proved to be largely protective (17). In a recent study, our research group established that the anti-hypertrophic action of AMPK is mainly explained by its inhibitory action on HBP via GFAT phosphorylation (35).

CONCLUSION

Various observations raise evidences that AMPK activation reduces O-GlcNAcylation levels in several pathologies and, consequently, prevents adverse effects. At contrary, O-GlcNAcylation of AMPK observed in different diseases reduces its capacity to play its beneficial role, contributing to the progression of the disease. This highlights AMPK and O-GlcNAcylation crosstalk as novel putative therapeutic target for important diseases such as cancer, diabetes and cardiovascular diseases. However, additional studies are still

required to fully unravel the complexity of the relationship between AMPK and O-GlcNAcylation with respect to these diseases.

AUTHOR CONTRIBUTIONS

RG, JD, LaB, and LuB wrote sections of the first draft of the manuscript. JD realized the figures. RG, SH, CB, LaB, and LuB participated in the fusion of the global version. All authors contributed to manuscript revision, read and approved the submitted version.

ACKNOWLEDGMENTS

Authors are supported by grants from the Fonds National de la Recherche Scientifique et Médicale (FNRS), Belgium, and Action de Recherche Concertée de la Communauté Wallonie-Bruxelles (ARC 16/21-074), Belgium, and by unrestricted grants from Astra Zeneca. LaB is Postdoctoral Researcher, CB is Postdoctorate Clinical Master Specialist, SH is Research Associate whereas LuB is Senior Research Associate of FNRS, Belgium. JD is FRIA (Fund for Research Training in Industry and Agriculture, Belgium) grantee.

REFERENCES

1. Hardie DG, Schaffer BE, Brunet A. AMPK: an energy-sensing pathway with multiple inputs and outputs. *Trends Cell Biol.* (2016) 26:190–201. doi: 10.1016/j.tcb.2015.10.013
2. Herzig S, Shaw RJ. AMPK: guardian of metabolism and mitochondrial homeostasis. *Nat Rev Mol Cell Biol.* (2018) 19:121–35. doi: 10.1038/nrm.2017.95
3. Zachara NE, Hart GW. O-GlcNAc a sensor of cellular state: the role of nucleocytoplasmic glycosylation in modulating cellular function in response to nutrition and stress. *Biochim Biophys Acta* (2004) 1673:13–28. doi: 10.1016/j.bbagen.2004.03.016
4. Chatham JC, Marchase RB. Protein O-GlcNAcylation: a critical regulator of the cellular response to stress. *Curr Signal Transduct Ther.* (2010) 5:49–59. doi: 10.2174/157436210790226492
5. Zachara NE, Hart GW. Cell signaling, the essential role of O-GlcNAc! *Biochim Biophys Acta* (2006) 1761:599–617. doi: 10.1016/j.bbalip.2006.04.007
6. Brimble S, Wollaston-Hayden EE, Teo CF, Morris AC, Wells L. The Role of the O-GlcNAc Modification in Regulating Eukaryotic Gene Expression. *Curr Signal Transduct Ther.* (2010) 5:12–24. doi: 10.2174/157436210790226465
7. Wu D, Cai Y, Jin J. Potential coordination role between O-GlcNAcylation and epigenetics. *Protein Cell* (2017) 8:713–23. doi: 10.1007/s13238-017-0416-4
8. Stapleton D, Woollatt E, Mitchelhill KI, Nicholl JK, Fernandez CS, Michell BJ, et al. AMP-activated protein kinase isoenzyme family: subunit structure and chromosomal location. *FEBS Lett.* (1997) 409:452–6. doi: 10.1016/S0014-5793(97)00569-3
9. Hardie DG, Ross FA, Hawley SA. AMPK: a nutrient and energy sensor that maintains energy homeostasis. *Nat Rev Mol Cell Biol.* (2012) 13:251–62. doi: 10.1038/nrm3311
10. Sanders MJ, Ali ZS, Hegarty BD, Heath R, Snowden MA, Carling D. Defining the mechanism of activation of AMP-activated protein kinase by the small molecule A-769662, a member of the thienopyridone family. *J Biol Chem.* (2007) 282:32539–48. doi: 10.1074/jbc.M706543200
11. Hoffman NJ, Parker BL, Chaudhuri R, Fisher-Wellman KH, Kleinert M, Humphrey SJ, et al. Global phosphoproteomic analysis of human skeletal muscle reveals a network of exercise-regulated kinases and AMPK substrates. *Cell Metab.* (2015) 22:922–35. doi: 10.1016/j.cmet.2015.09.001
12. Schaffer BE, Levin RS, Hertz NT, Maures TJ, Schoof ML, Hollstein PE, et al. Identification of AMPK phosphorylation sites reveals a network of proteins involved in cell invasion and facilitates large-scale substrate prediction. *Cell Metab.* (2015) 22:907–21. doi: 10.1016/j.cmet.2015.09.009
13. Hardie DG, Hawley SA, Scott JW. AMP-activated protein kinase–development of the energy sensor concept. *J Physiol* (2006) 574:7–15. doi: 10.1113/jphysiol.2006.108944
14. Horman S, Browne G, Krause U, Patel J, Vertommen D, Bertrand L, et al. Activation of AMP-activated protein kinase leads to the phosphorylation of elongation factor 2 and an inhibition of protein synthesis. *Curr Biol.* (2002) 12:1419–23. doi: 10.1016/S0960-9822(02)01077-1
15. Krause U, Bertrand L, Hue L. Control of p70 ribosomal protein S6 kinase and acetyl-CoA carboxylase by AMP-activated protein kinase and protein phosphatases in isolated hepatocytes. *Eur J Biochem.* (2002) 269:3751–9. doi: 10.1046/j.1432-1033.2002.03074.x
16. Hardie DG. AMP-activated protein kinase as a drug target. *Annu Rev Pharmacol Toxicol* (2007) 47:185–210. doi: 10.1146/annurev.pharmtox.47.120505.105304
17. Horman S, Beauloye C, Vanoverschelde JL, Bertrand L. AMP-activated protein kinase in the control of cardiac metabolism and remodeling. *Curr Heart Fail Rep.* (2012) 9:164–73. doi: 10.1007/s11897-012-0102-z
18. Hardie DG, Ross FA, Hawley SA. AMP-activated protein kinase: a target for drugs both ancient and modern. *Chem Biol.* (2012) 19:1222–36. doi: 10.1016/j.chembiol.2012.08.019
19. Bond MR, Hanover JA. O-GlcNAc cycling: a link between metabolism and chronic disease. *Annu Rev Nutr.* (2013) 33:205–29. doi: 10.1146/annurev-nutr-071812-161240
20. Hardiville S, Hart GW. Nutrient regulation of signaling, transcription, and cell physiology by O-GlcNAcylation. *Cell Metab.* (2014) 20:208–13. doi: 10.1016/j.cmet.2014.07.014
21. Clark RJ, McDonough PM, Swanson E, Trost SU, Suzuki M, Fukuda M, et al. Diabetes and the accompanying hyperglycemia impairs cardiomyocyte calcium cycling through increased nuclear O-GlcNAcylation. *J Biol Chem.* (2003) 278:44230–7. doi: 10.1074/jbc.M303810200
22. Banerjee PS, Ma J, Hart GW. Diabetes-associated dysregulation of O-GlcNAcylation in rat cardiac mitochondria. *Proc Natl Acad Sci USA.*(2015) 112:6050–5. doi: 10.1073/pnas.1424017112
23. Boehmelt G, Wakeham A, Elia A, Sasaki T, Plyte S, Potter J, et al. Decreased UDP-GlcNAc levels abrogate proliferation control in EMeg32-deficient cells. *EMBO J.* (2000) 19:5092–104. doi: 10.1093/emboj/19.19.5092
24. Oki T, Yamazaki K, Kuromitsu J, Okada M, Tanaka I. cDNA cloning and mapping of a novel subtype of glutamine:fructose-6-phosphate amidotransferase (GFAT2) in human and mouse. *Genomics* (1999) 57:227–34. doi: 10.1006/geno.1999.5785
25. Dassanayaka S, Jones SP. O-GlcNAc and the cardiovascular system. *Pharmacol Ther.* (2014) 142:62–71. doi: 10.1016/j.pharmthera.2013.11.005
26. Gao Y, Wells L, Comer FI, Parker GJ, Hart GW. Dynamic O-glycosylation of nuclear and cytosolic proteins: cloning and characterization of a neutral, cytosolic beta-N-acetylglucosaminidase from human brain. *J Biol Chem.* (2001) 276:9838–45. doi: 10.1074/jbc.M010420200
27. van der Laarse SAM, Leney AC, Heck AJR. Crosstalk between phosphorylation and O-GlcNAcylation: friend or foe. *FEBS J.* (2018). doi: 10.1111/febs.14491. [Epub ahead of print].
28. Eguchi S, Oshiro N, Miyamoto T, Yoshino K, Okamoto S, Ono T, et al. AMP-activated protein kinase phosphorylates glutamine: fructose-6-phosphate amidotransferase 1 at Ser243 to modulate its enzymatic activity. *Genes Cells* (2009) 14:179–89. doi: 10.1111/j.1365-2443.2008.01260.x
29. Ruan HB, Ma Y, Torres S, Zhang B, Feriod C, Heck RM, et al. Calcium-dependent O-GlcNAc signaling drives liver autophagy in adaptation to starvation. *Genes Dev.* (2017) 31:1655–65. doi: 10.1101/gad.305441.117
30. Bullen JW, Balsbaugh JL, Chanda D, Shabanowitz J, Hunt DF, Neumann D, et al. Cross-talk between two essential nutrient-sensitive enzymes: O-GlcNAc transferase (OGT) and AMP-activated protein kinase (AMPK). *J Biol Chem.* (2014) 289:10592–606. doi: 10.1074/jbc.M113.523068
31. Xu Q, Yang C, Du Y, Chen Y, Liu H, Deng M, et al. AMPK regulates histone H2B O-GlcNAcylation. *Nucleic Acids Res.* (2014) 42:5594–604. doi: 10.1093/nar/gku236

32. Li Y, Roux C, Lazereg S, LeCaer JP, Laprevote O, Badet B, et al. Identification of a novel serine phosphorylation site in human glutamine:fructose-6-phosphate amidotransferase isoform 1. *Biochemistry* (2007) 46:13163–9. doi: 10.1021/bi700694c
33. Scott JW, Oakhill JS. The sweet side of AMPK signaling: regulation of GFAT1. *Biochem J.* (2017) 474:1289–92. doi: 10.1042/BCJ20170006
34. Zibrova D, Vandermoere F, Goransson O, Peggie M, Marino KV, Knierim A, et al. GFAT1 phosphorylation by AMPK promotes VEGF-induced angiogenesis. *Biochem J.* (2017) 474:983–1001. doi: 10.1042/BCJ20160980
35. Gelinas R, Mailleux F, Dontaine J, Bultot L, Demeulder B, Ginion A, et al. AMPK activation counteracts cardiac hypertrophy by reducing O-GlcNAcylation. *Nat Commun.* (2018) 9:374. doi: 10.1038/s41467-017-02795-4
36. Xu J, Wang S, Viollet B, Zou MH. Regulation of the proteasome by AMPK in endothelial cells: the role of O-GlcNAc transferase (OGT). *PLoS ONE* (2012) 7:e36717. doi: 10.1371/journal.pone.0036717
37. Wang T, Yu Q, Li J, Hu B, Zhao Q, Ma C, et al. O-GlcNAcylation of fumarase maintains tumour growth under glucose deficiency. *Nat Cell Biol.* (2017) 19:833–43. doi: 10.1038/ncb3562
38. Vigetti D, Viola M, Karousou E, De Luca G, Passi A. Metabolic control of hyaluronan synthases. *Matrix Biol.* (2014) 35:8–13. doi: 10.1016/j.matbio.2013.10.002
39. Cheung WD, Hart GW. AMP-activated protein kinase and p38 MAPK activate O-GlcNAcylation of neuronal proteins during glucose deprivation. *J Biol Chem.* (2008) 283:13009–20. doi: 10.1074/jbc.M801222200
40. Kang JG, Park SY, Ji S, Jang I, Park S, Kim HS, et al. O-GlcNAc protein modification in cancer cells increases in response to glucose deprivation through glycogen degradation. *J Biol Chem.* (2009) 284:34777–84. doi: 10.1074/jbc.M109.026351
41. Taylor RP, Geisler TS, Chambers JH, McClain DA. Up-regulation of O-GlcNAc transferase with glucose deprivation in HepG2 cells is mediated by decreased hexosamine pathway flux. *J Biol Chem.* (2009) 284:3425–32. doi: 10.1074/jbc.M803198200
42. Luo B, Parker GJ, Cooksey RC, Soesanto Y, Evans M, Jones D, et al. Chronic hexosamine flux stimulates fatty acid oxidation by activating AMP-activated protein kinase in adipocytes. *J Biol Chem.* (2007) 282:7172–80. doi: 10.1074/jbc.M607362200
43. Hong-Brown LQ, Brown CR, Navaratnarajah M, Lang CH. Adamts1 mediates ethanol-induced alterations in collagen and elastin via a FoxO1-sestrin3-AMPK signaling cascade in myocytes. *J Cell Biochem.* (2015) 116:91–101. doi: 10.1002/jcb.24945
44. Laczy B, Fulop N, Onay-Besikci A, Des Rosiers C, Chatham JC. Acute regulation of cardiac metabolism by the hexosamine biosynthesis pathway and protein O-GlcNAcylation. *PLoS ONE* (2011) 6:e18417. doi: 10.1371/journal.pone.0018417
45. Dias WB, Hart GW. O-GlcNAc modification in diabetes and Alzheimer's disease. *Mol Biosyst.* (2007) 3:766–72. doi: 10.1039/b704905f
46. Copeland RJ, Bullen JW, Hart GW. Cross-talk between GlcNAcylation and phosphorylation: roles in insulin resistance and glucose toxicity. *Am J Physiol Endocrinol Metab.* (2008) 295:E17–28. doi: 10.1152/ajpendo.90281.2008
47. Hardie DG. Keeping the home fires burning: AMP-activated protein kinase. *J R Soc Interface* (2018) 15:20170774. doi: 10.1098/rsif.2017.0774
48. Murata K, Morino K, Ida S, Ohashi N, Lemecha M, Park SY, et al. Lack of O-GlcNAcylation enhances exercise-dependent glucose utilization potentially through AMP-activated protein kinase activation in skeletal muscle. *Biochem Biophys Res Commun.* (2018) 495:2098–104. doi: 10.1016/j.bbrc.2017.12.081
49. Luo B, Soesanto Y, McClain DA. Protein modification by O-linked GlcNAc reduces angiogenesis by inhibiting Akt activity in endothelial cells. *Arterioscler Thromb Vasc Biol.* (2008) 28:651–7. doi: 10.1161/ATVBAHA.107.159533
50. Zaborska KE, Edwards G, Austin C, Wareing M. The Role of O-GlcNAcylation in perivascular adipose tissue dysfunction of offspring of high-fat diet-fed rats. *J Vasc Res.* (2017) 54:79–91. doi: 10.1159/000458422
51. Lynch TP, Reginato MJ. O-GlcNAc transferase: a sweet new cancer target. *Cell Cycle* (2011) 10:1712–3. doi: 10.4161/cc.10.11.15561
52. Zadra G, Batista JL, Loda M. Dissecting the dual role of AMPK in cancer: from experimental to human studies. *Mol Cancer Res.* (2015) 13:1059–72. doi: 10.1158/1541-7786.MCR-15-0068
53. Ishimura E, Nakagawa T, Moriwaki K, Hirano S, Matsumori Y, Asahi M. Augmented O-GlcNAcylation of AMP-activated kinase promotes the proliferation of LoVo cells, a colon cancer cell line. *Cancer Sci.* (2017) 108:2373–82. doi: 10.1111/cas.13412
54. Coughlin SS, Calle EE, Teras LR, Petrelli J, Thun MJ. Diabetes mellitus as a predictor of cancer mortality in a large cohort of US adults. *Am J Epidemiol.* (2004) 159:1160–7. doi: 10.1093/aje/kwh161
55. Ferrer CM, Lynch TP, Sodi VL, Falcone JN, Schwab LP, Peacock DL, et al. O-GlcNAcylation regulates cancer metabolism and survival stress signaling via regulation of the HIF-1 pathway. *Mol Cell* (2014) 54:820–31. doi: 10.1016/j.molcel.2014.04.026
56. Ferrer CM, Lu TY, Bacigalupa ZA, Katsetos CD, Sinclair DA, Reginato MJ. O-GlcNAcylation regulates breast cancer metastasis via SIRT1 modulation of FOXM1 pathway. *Oncogene* (2017) 36:559–69. doi: 10.1038/onc.2016.228
57. Sodi VL, Bacigalupa ZA, Ferrer CM, Lee JV, Gocal WA, Mukhopadhyay D, et al. Nutrient sensor O-GlcNAc transferase controls cancer lipid metabolism via SREBP-1 regulation. *Oncogene* (2018) 37:924–34. doi: 10.1038/onc.2017.395
58. Lunde IG, Aronsen JM, Kvaloy H, Qvigstad E, Sjaastad I, Tonnessen T, et al. Cardiac O-GlcNAc signaling is increased in hypertrophy and heart failure. *Physiol Genomics* (2012) 44:162–72. doi: 10.1152/physiolgenomics.00016.2011
59. Mailleux F, Gelinas R, Beauloye C, Horman S, Bertrand L. O-GlcNAcylation, enemy or ally during cardiac hypertrophy development? *Biochim Biophys Acta* (2016) 1862:2232–43. doi: 10.1016/j.bbadis.2016.08.012
60. Wright JN, Collins HE, Wende AR, Chatham JC. O-GlcNAcylation and cardiovascular disease. *Biochem Soc Trans.* (2017) 45:545–53. doi: 10.1042/BST20160164

Conflict of Interest Statement: The authors declare that the research was conducted in the absence of any commercial or financial relationships that could be construed as a potential conflict of interest.

frontiers in Endocrinology

ORIGINAL RESEARCH
published: 05 October 2018
doi: 10.3389/fendo.2018.00598

Interplay Between Phosphorylation and O-GlcNAcylation of Sarcomeric Proteins in Ischemic Heart Failure

Thomas Mercier[1], *Marion Bouvet*[1], *Emilie Dubois-Deruy*[1], *Arthur Dechaumes*[1], *Olivia Beseme*[1], *Vincent Richard*[2], *Paul Mulder*[2] *and Florence Pinet*[1]*

[1] INSERM U1167 Unité d'Epidémiologie et de Santé Publique, Lille, France, [2] INSERM UMR1096, Endothélium, Valvulopathies et Insuffisance Cardiaque, Rouen, France

Post-translational modifications (PTMs) of sarcomeric proteins could participate to left ventricular (LV) remodeling and contractile dysfunction leading in advanced heart failure (HF) with altered ejection fraction. Using an experimental rat model of HF (ligation of left coronary artery) and phosphoproteomic analysis, we identified an increase of desmin phosphorylation and a decrease of desmin O-N-acetylglucosaminylation (O-GlcNAcylation). We aim to characterize interplay between phosphorylation and O-GlcNAcylation for desmin in primary cultures of cardiomyocyte by specific O-GlcNAcase (OGA) inhibition with thiamet G and silencing O-GlcNAc transferase (OGT) and, in perfused heart perfused with thiamet G in sham- and HF-rats. In each model, we found an efficiency of O-GlcNAcylation modulation characterized by the levels of O-GlcNAcylated proteins and OGT expression (for silencing experiments in cells). In perfused heart, we found an improvement of cardiac function under OGA inhibition. But none of the treatments either in *in vitro* or *ex vivo* cardiac models, induced a modulation of desmin, phosphorylated and O-GlcNAcylated desmin expression, despite the presence of O-GlcNAc moities in cardiac desmin. Our data suggests no interplay between phosphorylation and O-GlcNAcylation of desmin in HF post-myocardial infarction. The future requires finding the targets in heart involved in cardiac improvement under thiamet G treatment.

Keywords: heart failure, systolic, desmin, interplay, rat models, O-GlcNAcylation, phosphorylation

OPEN ACCESS

Edited by:
Tarik Issad, Institut National de la Santé et de la Recherche Médicale (INSERM), France

Reviewed by:
Caroline Cieniewski-Bernard, Lille University of Science and Technology, France
Yobana Perez-Cervera, Benito Juárez Autonomous University of Oaxaca, Mexico

***Correspondence:**
Florence Pinet
florence.pinet@pasteur-lille.fr

Specialty section:
This article was submitted to Molecular and Structural Endocrinology, a section of the journal Frontiers in Endocrinology

Received: *21 June 2018*
Accepted: *19 September 2018*
Published: *05 October 2018*

Citation:
Mercier T, Bouvet M, Dubois-Deruy E, Dechaumes A, Beseme O, Richard V, Mulder P and Pinet F (2018) Interplay Between Phosphorylation and O-GlcNAcylation of Sarcomeric Proteins in Ischemic Heart Failure. Front. Endocrinol. 9:598. doi: 10.3389/fendo.2018.00598

INTRODUCTION

Heart failure (HF) following myocardial infarction (MI) is characterized by alterations of left ventricle (LV) structure and function, known as LV remodeling (1); this pathophysiological process is a strong predictor of both HF and death as we recently showed in two cohorts of patients REVE and REVE2 dedicated to the analysis of LV remodeling (2, 3). The long-term (>10 years) clinical follow-up of patients included in these two cohorts has shown that LV remodeling remains independently associated with HF and cardiovascular death (4).

Evaluation of post-translational modifications (PTM) of sarcomeric cardiac proteins is a promising new approach to studying the mechanisms of HF. The phosphorylation status of sarcomeric proteins is altered in HF and may thus contribute to the decreased cardiac function (5). Another rapid, dynamic, and reversible PTM is O-N-acetylglucosaminylation (O-GlcNAcylation) (6). Both phosphorylation and O-GlcNAcylation regulate numerous cellular functions by reversibly

adding either phosphate or O-N-acetylglucosamine (O-GlcNAc) to proteins. The crosstalk between these two PTMs may occur by steric competition for occupancy at the either the same or a proximal amino acid site (7). Specific sites of O-GlcNAcylation described in some cardiac myofilament proteins have suggested that O-GlcNAc and O-phosphate modifications of these proteins may interact dynamically (8, 9).

Recently, we have demonstrated interplay between Ser^{208}-phosphorylation and Ser^{190}-O-GlcNAcylation of troponin T in ischaemic HF, linked to decreased activity of both PKCε and O-GlcNAcase (OGA) and increased O-GlcNAc transferase (OGT) activity (10). We also showed recently than another sarcomeric protein, desmin has been identified by differential proteomic analysis to have increased levels of phosphorylation in LV of HF-rats compared to the sham-rats (11). In addition, we found a 2-fold increased serine-desmin phosphorylation in the LV of HF-rats, mainly in the insoluble fraction, suggesting the formation of desmin aggregates, toxic for the cardiomyocyte. Desmin is a 53 kDa protein, particularly localized to the Z-band and is considered as a major integrator of contractile apparatus and a critical factor for maintaining intermediate filament structure. Its increased phosphorylation might lead to the network destabilization and formation of aggregates toxic for the cardiomyocyte (12).

Our objectives were to characterize (1) whether the levels of O-GlcNAcylated desmin are regulated in cardiomyocyte by inhibition or activation of O-GlcNAcylation in *in vitro* and *ex vivo* cardiac models of HF and; (2) whether modulation of O-GlcNAcylation impacts the phosphorylation levels of desmin with the aim to decrease the phosphorylation levels of desmin and the formation of desmin aggregates following HF development.

MATERIALS AND METHODS

Experimental Rat Model of Ischemic Heart Failure

All animal experiments were performed according to the Guide for the Care and Use of Laboratory Animals published by the US National Institutes of Health (NIH publication NO1-OD-4-2-139, revised in 2011). Animals were used and experimental protocols performed under the supervision of a person authorized to perform experiments on live animals (F. Pinet: 59-350126). Approval was granted by the institutional ethics review board (CEEA Nord Pas-de-Calais N°242011, January 2012). Before surgery, rats were anesthetized [sodium methohexital, 50 mg/kg intraperitoneal (IP)], while analgesia was administered before (xylazine 5 mg/kg IP) and 1 h after surgery (xylazine 50 mg/kg subcutaneously) as previously described (13). MI was induced in 10-week-old male Wistar rats (Janvier, Le Genest St isle, France) by ligation of the left anterior descending coronary artery according to the method previously described (1, 13). Haemodynamic and echocardiographic measurements were taken at 2 months after surgery, followed by heart excision as previously described (14). Tissues were kept at −80°C until analysis.

Isolated Heart Perfusion

In vitro LV function was determined in randomly selected control male Wistar rats either untreated (bodyweight: 453 ± 7 g) or treated (bodyweight: 444 ± 14 g) with 100 µL OGA inhibitor, Thiamet G (200 µM diluted in saline buffer, Sigma-Aldrich, Lyon, France) for 2 h. After anesthesia (50 mg/kg of sodium pentobarbital injected intraperitoneally), the heart was rapidly excised and plunged in ice-cold oxygenated KH buffer (5.5 mM glucose, 1.25 mM$CaCl_2$, 120 mM NaCl, 31 mM $NaHCO_3$, 4.7 mM KCl, 1.2 mM $MgSO_4$, 1.2 mM KH2PO4, [pH 7.4]) as previously described (10). The heart was transferred within 30 s to a Langendorf heart perfusion apparatus and perfused at constant hydrostatic pressure (90 mm Hg). A balloon was inserted into the LV and connected to a pressure transducer to record LV (systolic and diastolic) pressure, LV developed pressure and heart rate for 25 min. The balloon was inflated with water, allowing a similar and constant LV distending pressure of 10 mm Hg. At the end of each experiment, the LV was snap-frozen in liquid nitrogen and stored at −80°C until analysis.

Cell Culture

Primary Cultures of Neonatal Rat Cardiomyocytes

Primary cultures of rat neonatal contractile cardiac myocytes (NCM) were prepared from heart ventricles of 1- or 2-day-old rats as previously described (10). Briefly, cardiac cells of newborn rats' ventricles were dissociated by enzymatic digestion with 0.04% collagenase II (Worthington, Lakewood, NJ, USA) and 0.05% pancreatin (Sigma-Aldrich). Non-NCM were removed by 30 min centrifugation at 1,600 g in a discontinuous Percoll gradient (bottom 58.5%, top 40.5% [v/v], Sigma-Aldrich). NCM were then seeded at a density of 4×10^5 cells per well in 6-well plates coated with 0.01% of collagen (Sigma-Aldrich) (8×10^5 cells per well when they are seeded on coverslip) and cultured in a medium containing DMEM/Medium199 (4:1), 10% horse serum (Life Technologies), 5% fetal bovine serum (FBS) (ATCC), 1% penicillin and streptomycin (10,000 U/mL, Life Technologies) for 7 days at 37°C under 5% CO_2 atmosphere.

Small Interfering RNA Transfection

The first two individual pre-designed specific siRNA specifically targeting rat OGT mRNA, rat OGT and non-targeting control were used (ON-TARGETplus siRNA, Dharmacon, GE Healthcare). NCMs were plated (100,000 cells/well) in 6-well plates and were allowed to grow for 24 h without antibiotics. The first 2 individual OGT (OGT1 and OGT2) siRNAs (5 nmol/L) were transfected with the DharmaFECT® reagent (4 µL) according to the manufacturer's recommendations. Total cell extracts were collected 72 h after transfection.

Protein Extraction

Proteins from human hearts and rat LVs were extracted from frozen tissues (after removing the infarcted area) with Dounce-Potter homogenization into ice-cold RIPA buffer (50 mM Tris [pH7.4], 150 mM NaCl, 1% Igepal CA-630, 50 mM deoxycholate, and 0.1% SDS) containing antiproteases (Complete™ EDTA-free, Roche Diagnostics), serine/threonine and tyrosine protein phosphatase inhibitors (Phosphatase inhibitor Cocktail 2 and 3,

Sigma-Aldrich), 1 mM Na_3VO_4 and PUGNAC (50 μM). After 1 h incubation at 4°C, the homogenate was centrifuged at 15,300 g for 15 min at 4°C and the supernatant containing soluble proteins was collected. After treatments, cells were rinsed twice with PBS before being mechanically scraped from the plate in 50 μL of ice-cold RIPA buffer. Soluble and insoluble proteins were extracted as describe above. Protein concentrations for all samples were determined with a Bradford-based method protein assay (Biorad, Marnes-la-Coquette, France).

Immunoprecipitation, Western Blot, Phos-Tag™, and WGA Gels

Immunoprecipitation

Immunoprecipitation was performed with 50 μg of NCM proteins or 100 μg of LV proteins pre-cleared by incubation with protein A/G magnetic beads (88802, Pierce) for 1 h at 4°C with gentle shaking. The pre-cleared proteins were then mixed with 2 μL of anti-desmin antibody (ab3236, Abcam) diluted in 100 μL of RIPA 1X buffer as previously described (11). After overnight incubation at 4°C on a rotating device, immune complexes were precipitated at 4°C for only 2 h on a rotating device with 35 μL of protein A/G magnetic beads. Immunoprecipitated (IP) complexes were then washed four times with 750 μL of RIPA 1X buffer before denaturation in Laemmli buffer at RT for western blot analysis.

Western Blot

Soluble proteins (10–50 μg) were analyzed on 12% SDS-PAGE gels. Proteins were transferred to nitrocellulose membranes and blocked for 1 h in Tris-buffered saline with 0.1% [v/v] Tween-20 (TBS-T) containing 5% [w/v] skim milk or BSA with constant shaking. Membranes were then incubated with primary antibodies diluted in TBS-T with 5% skim milk or BSA overnight at 4°C with constant shaking. The blots were then washed with TBS-T and incubated at RT with horseradish peroxidase labeled secondary antibodies diluted in 5% skim milk or BSA/TBS-T for 1 h. Following the secondary incubation, the membranes were washed with TBS-T before blots imaging. Equal protein loading was confirmed using GAPDH and sarcomeric actin immunoblotting.

For western blots of desmin-IP proteins, membranes were first incubated with RL2 antibody diluted in 5% fresh BSA overnight at 4°C before incubation with other antibodies.

Phos-Tag™ Gels

Soluble proteins were analyzed on 10% gels containing 40 μM of Phos-tag™ (Wako, Osaka, Japan) and 100 μM of Mn^{2+} at 90V for 2.5 h. The excess of metal was removed by washing the gels three times for 10 min in transfer buffer (NuPAGE® Transfer Buffer, Invitrogen) containing 10% methanol and 10 mM EDTA and then three times for 10 min in transfer buffer containing 10% methanol before the proteins were transferred onto 0.2 μm PVDF membrane. To detect desmin and its phosphorylated forms, membranes were blocked 1 h in 5% skim milk/TBS-T before overnight incubation at 4°C with desmin antibody diluted 1/1,000 in blocking solution. The following steps were similar to those described above for western blot. Briefly, the Phos-tag™ molecules incorporated into the SDS-PAGE are able with the cooperation of two Mn^{2+} metal cations to slow down the migration of phosphorylated proteins. Therefore, phosphorylated desmin migrates at higher apparent molecular weight than the non-phosphorylated form. However, at equivalent phosphorylation levels, the position of the phosphate group can also influence the apparent molecular weight of a protein in a Phos-tag™ gel.

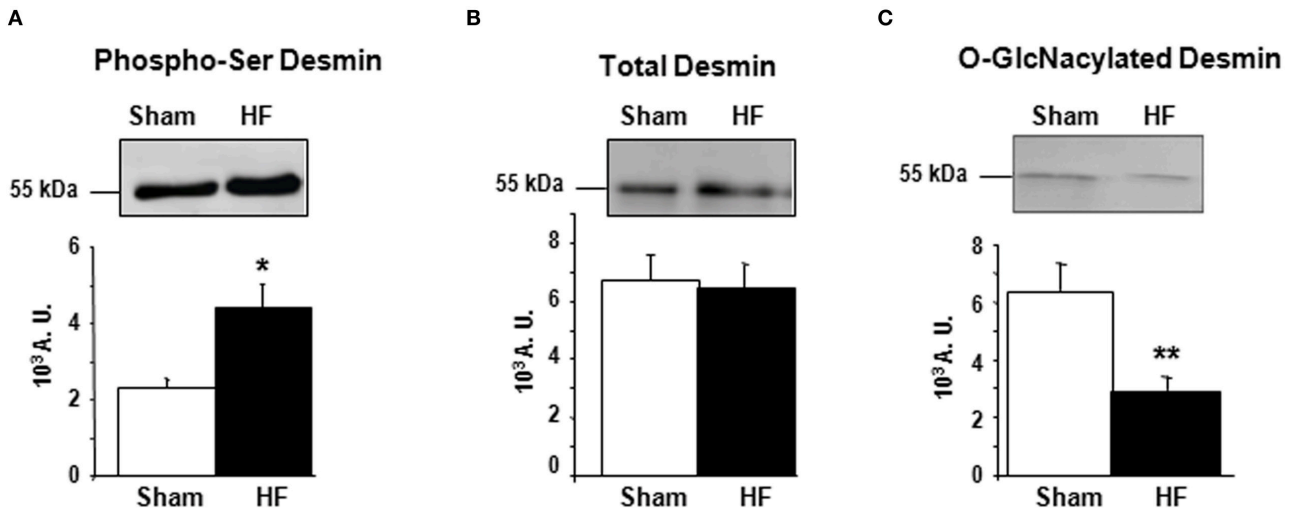

FIGURE 1 | Post-translational modifications of desmin of LV from HF-rats. Quantification of Ser-phosphorylated desmin **(A)**, total desmin levels **(B)**, and O-GlcNAcylated desmin levels **(C)** in LV (50 μg) of sham- ($n = 11$) (white box) and HF- ($n = 11$) (black box) rats at 2 months after MI. The positions of molecular weight are indicated as kilodalton (kDa) on the left. An internal standard was loaded in each gel for the standardization and quantification. Graphs show mean ± SEM values expressed in arbitrary units (A.U.). *$P < 0.05$; **$P < 0.01$.

WGA

Soluble proteins (50 μg) were analyzed on 7% gels containing 3.75 mg/mL of Wheat Germ Agglutinin (WGA) (L9640, Sigma-Aldrich) at 4°C at 20 mA for 2 h as previously described (15). After migration, the same protocol for protein transfer and incubation with primary and secondary antibodies as for classical western blot was applied.

List of Antibodies

Protein	Sample	Reference company	Dilution antibodies
Desmin	Heart	ab32362 Abcam	1/1,000
	NCM		1/5,000
O-GlcNac	Heart/NCM	NB300-524 (RL2) Novus Biological	1/2,000
OGT	NCM	clone DM17, O6264 Sigma-Aldrich	1/1,000
GAPDH	Heart/NCM	sc-36562 Santa Cruz	1/5,000
Phospho-serine	Heart/NCM	P5747, Sigma-Aldrich	1/1,000
Sarcomeric actin	Heart /NCM	MO874 Dako	1/2,000

Blots Imaging

The Chemidoc® XRS+ camera (Biorad) and the Image Lab™ software were used for blots imaging and densitometry analysis. Membranes were incubated for 5 min with Clarity™ Western ECL Substrate (Biorad) before imaging. The signal was quantified from the image obtained just before saturation. The band corresponding to the protein of interest was framed within a defined area to express the signal intensity depending of the area. This value was related to the intensity value of the reference protein (GAPDH or sarcomeric actin). The values were expressed in arbitrary units (U.A.).

Statistical Analysis

Data expressed as means ± SEM were analyzed with GraphPad Prism version 6.01 (GraphPad Software, San Diego, CA) and comparisons were made by Student's *t*-test, Mann-Whitney (two-tailed), one- or two-way analysis of variance (ANOVA) with Tukey's *post-hoc* test, as appropriate. Results were considered statistically significant if the $p < 0.05$.

RESULTS

Post-translational Modification of Desmin Heart Failure Rats

Cardiac remodeling and dysfunction in HF-rats was characterized at 2 months post-MI by significant increases in LV end-diastolic pressure, LV end-diastolic and end-systolic diameters, and LV weight as previously shown (10). We previously investigated cardiac phosphoproteomic changes associated with LV remodeling and dysfunction in this HF-rat model. At 2 months after surgery, proteomic analysis revealed different LV phosphoproteomic patterns between the sham- and HF-rats (16). We previously identified two spots as being desmin (11). We highlighted a significant increase of desmin phospho-species in LV of rats 2 months after MI compared to controls (**Figure 1A**) without any modulation of total desmin protein levels (**Figure 1B**). Then, we looked for interplay between phosphorylation and O-GlcNAcylation of desmin in the same experimental model and found a significant decrease of O-GlcNAcylated desmin in LV of HF rats compared to controls (**Figure 1C**). These data showed that desmin may bear O-GlcNAc residues and that the levels of O-GlcNAcylated desmin were inversely related to the levels of phosphorylated desmin in LV of HF rats. To confirm these data, we tested several modulators of O-GlcNAcylation in several *in vitro* and *ex vivo* models, such as primary culture of cardiomyocyte (NCM) and isolated perfused heart.

Modulation of O-GlcNAcylation *in vitro* in Primary Cultures of Neonate Cardiomycytes

Inhibition of OGA by Thiamet G

First, we studied the impact of OGA inhibition by thiamet G in primary cultures of neonate rat cardiomyocytes (NCM) as designed (**Figure 2A**) and observed a significant increase of O-GlcNAcylated proteins (1.16 ± 0.09 vs. 2.55 ± 0.27, $P < 0.01$) (**Figure 2B**). Thiamet G treatment has no effect on total desmin levels (**Figure 2C**) nor on desmin phosphospecies (**Figure 2D**). To quantify the levels of O-GlcNAcylated desmin, we used immunoprecipitation (IP) of desmin species followed by a western blot with RL2 antibody to detect O-GlcNAcylated proteins (**Figure 2E**). We verified by desmin western blot the efficiency of IP with desmin detected in input, IP (IP Des) and supernatant of IgG IP (S igG) but not in supernatant of desmin IP (S Des). The specificity of this approach was also verified with no O-GlcNAcylated proteins detected in beads. As observed the levels of O-GlcNAcylated desmin was very low in NCM and we did not observe any modulation in NCM treated with thiamet G (**Figure 2E**).

Silencing of OGT

Second, we studied the impact of OGT silencing in primary cultures of neonate rat cardiomyocytes (NCM) as designed (**Figure 3A**) and observed a significant decrease of O-GlcNAcylated proteins [1.08 ± 0.03 vs. 0.54 ± 0.08 (OGT1) and 0.52 ± 0.07 (OGT2), $P < 0.05$] that is due to the significant decrease of OGT validating the efficiency of OGT silencing [0.99 ± 0.13 vs. 0.23 ± 0.02 (OGT1) and 0.20 ± 0.05 (OGT2), $P < 0.01$] (**Figure 3B**). Both OGT siRNA1 and siRNA 2 did not show any effect on total desmin levels (**Figure 3C**) nor in desmin phosphospecies (**Figure 3D**). We then quantified the levels of O-GlcNAcylated desmin as described in **Figure 2E**. Conversely, we observed an unspecific low intensity band for O-GlcNAcylated desmin with beads but we did not observe any

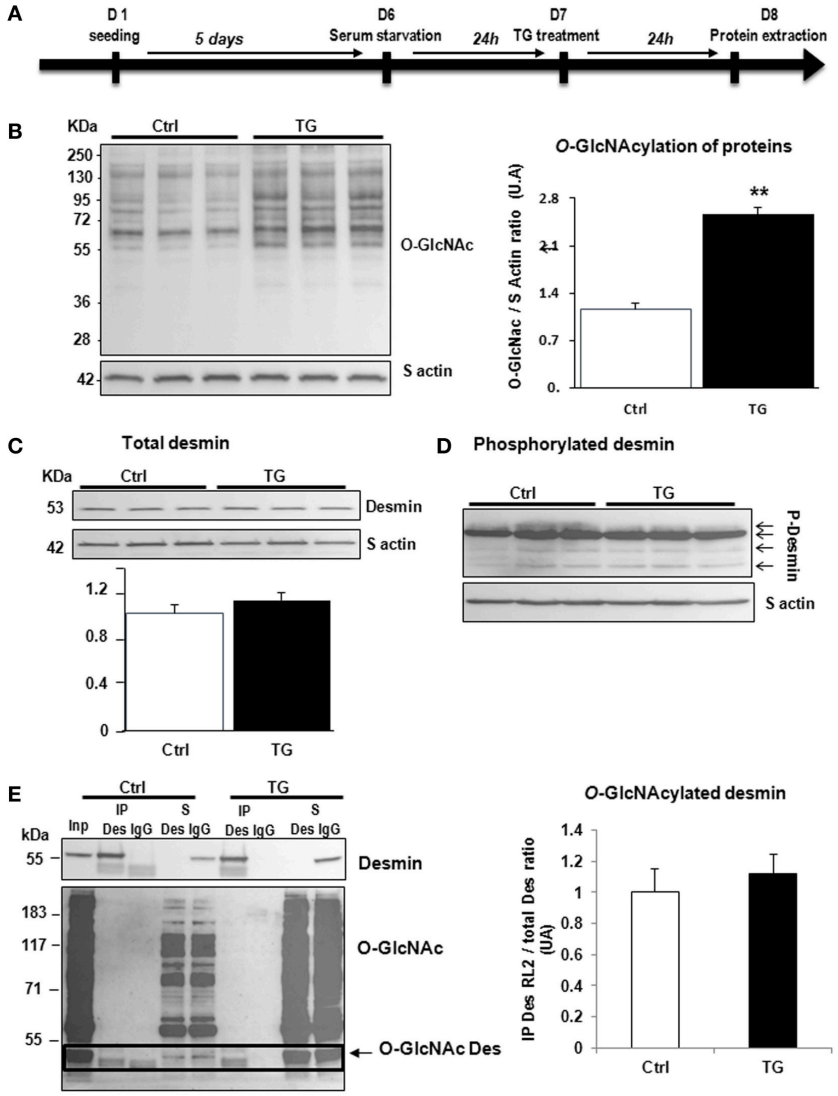

FIGURE 2 | Impact of OGA inhibition by thiamet G in primary cultures of NCM. **(A)** Description of the protocol designed for Thiamet G (TG) treatment of primary culture of neonate cardiomyocytes (NCM). **(B)** Representative western blots (left panel) and quantification (right panel) of O-GlcNAcylated proteins levels in control (Ctrl) and NCM treated with 100 nM of thiamet G (TG) during 24 h ($n = 12$). **(C)** Western blots (upper panel) and quantification (lower panel) of total desmin levels in the same samples. **(D)** Phosphorylation profiles of desmin were analyzed in the same samples by Phos-tag™ gel. **(E)** Representative immunoprecipation (IP) with desmin antibody before western blot with RL2 antibody (left panel) and quantification (right panel) of *O*-GlcNAcylated desmin levels in the same samples. Inp, input; IP, immunoprecipitated proteins; S, IP supernatant; Des, desmin; IgG, Immunoglobulin. The arrow indicates the *O*-GlcNAcylated desmin. Data are expressed as means of an arbitrary unit (A.U.) ± SEM. The positions of molecular weight are indicated as kilodalton (kDa) on the left. $^{**}P < 0.01$.

modulation of O-GlcNAcylated desmin after OGT silencing in NCM (**Figure 3E**).

Modulation of O-GlcNAcylation *ex vivo* in Isolated Perfused Heart

In isolated perfused hearts, we assessed the functional cardiac modification induced by thiamet G, a specific OGA inhibitor, injected 2 h before the perfusion (**Figure 4A**). Thiamet G decreased significantly the coronary flow in only sham-rats. In HF-rats, thiamet G increased significantly LV developed pressure and cardiac output without any effect on heart rate (**Table 1**).

We validated by western blot the inhibitory effect of OGA by thiamet G with significant increase of O-GlcNAcylated LV proteins in sham- and HF-rat heart perfused with the inhibitor (**Figure 4B**). We found a significant decrease of total desmin expression in LV from HF-rat perfused compared to the sham-rats independently of thiamet G perfusion (**Figure 4C**). We visualized desmin phosphospecies by desmin immunoblot of Phos-tag™ gels and we did not find any modulation with different molecular weight desmin species detected in thiamet G-perfused heart (**Figure 4D**).

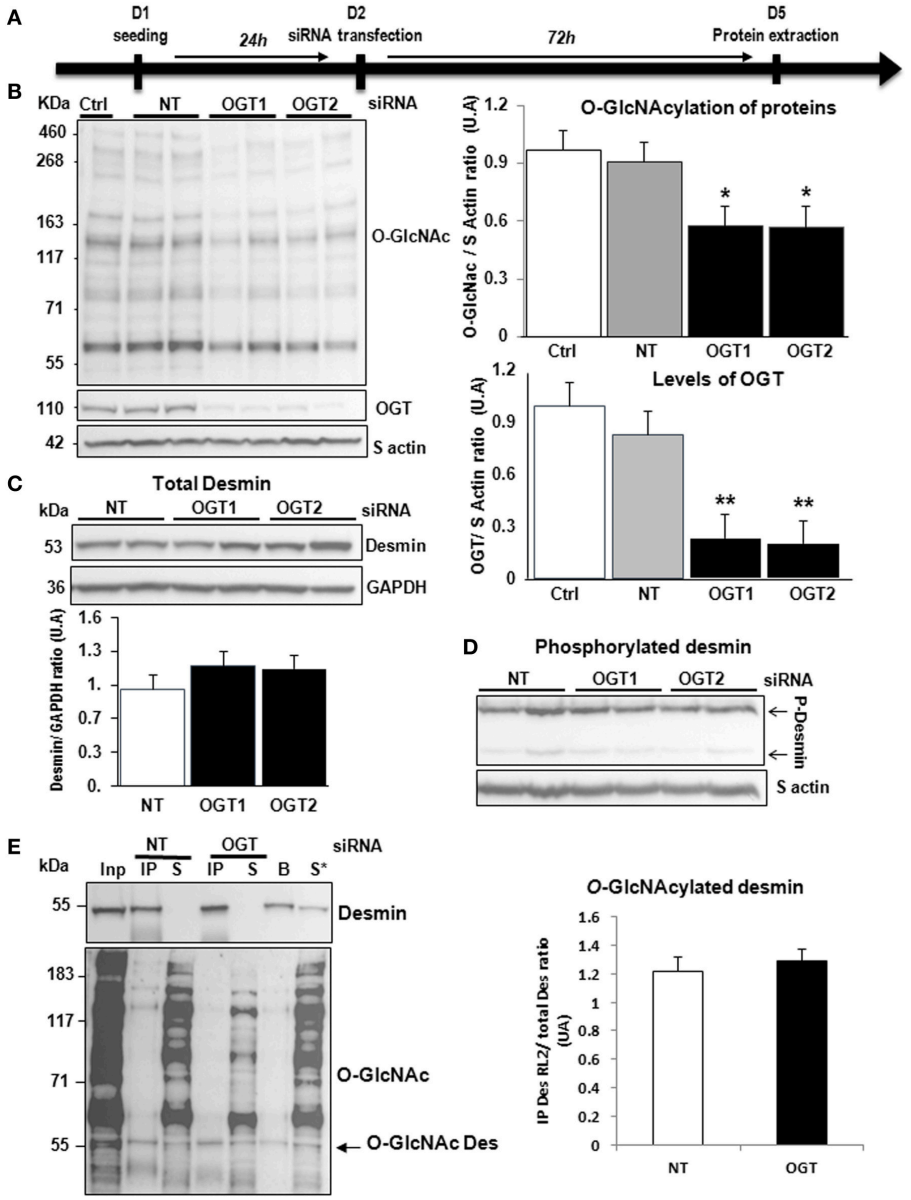

FIGURE 3 | Effect of OGT silencing in primary cultures of NCM. **(A)** Description of the protocol designed for OGT silencing of primary cultures of NCM. **(B)** Western blots (left panel) and quantification of O-GlcNAcylated proteins levels (upper and right panel) and OGT (lower and right panel) in primary cultures of NCM transfected with non-targeting (NT) siRNA control and OGT1 and OGT2 siRNA ($n = 12$). **(C)** Western blots (upper panel) and quantification (lower panel) of total desmin levels in the same samples. **(D)** Phosphorylation profiles of desmin was analyzed in the same samples by Phos-tag^{TM} gel. **(E)** Representative Immunoprecipitation (IP) with desmin antibody before western blot with RL2 antibody (left panel) and quantification (right panel) of O-GlcNAcylated desmin levels in the same samples. Inp, input; IP, immunoprecipitated proteins; S, IP supernatant; B, beads alone; S*, IP supernatant of beads. The arrow indicates the O-GlcNAcylated desmin. Graphs show mean ± SEM values expressed in arbitrary units (A.U.). The positions of molecular weight are indicated as kilodalton (kDa) on the left. *$P < 0.005$; **$P < 0.01$.

New Technology to Detect O-GlcNAcylated Proteins

Due to the difficulties to detect specifically *O*-GlcNAcylated desmin in LV proteins either from cultures of cardiomyocytes or perfused heart, we compare the sensitivity of 2 methods, western blots of O-GlcNAcylated LV proteins separated with classical SDS-PAGE gel (**Figure 5A**) and WGA-SDS-PAGE gel (**Figure 5B**) as recently described (15). First, red ponceau staining of the transferred membranes showed a less sensitivity to detect protein profiles with WGA gel. But conversely, we observed for the detection of *O*-GlcNAcylated LV proteins with RL2 antibody a stronger signal of better quality with WGA gel (**Figure 5B**) by comparison to SDS gel (**Figure 5A**). We then tested the detection of desmin in WGA gel and only found one band with a stronger signal in thiamet G treated samples either in sham- or HF-rats

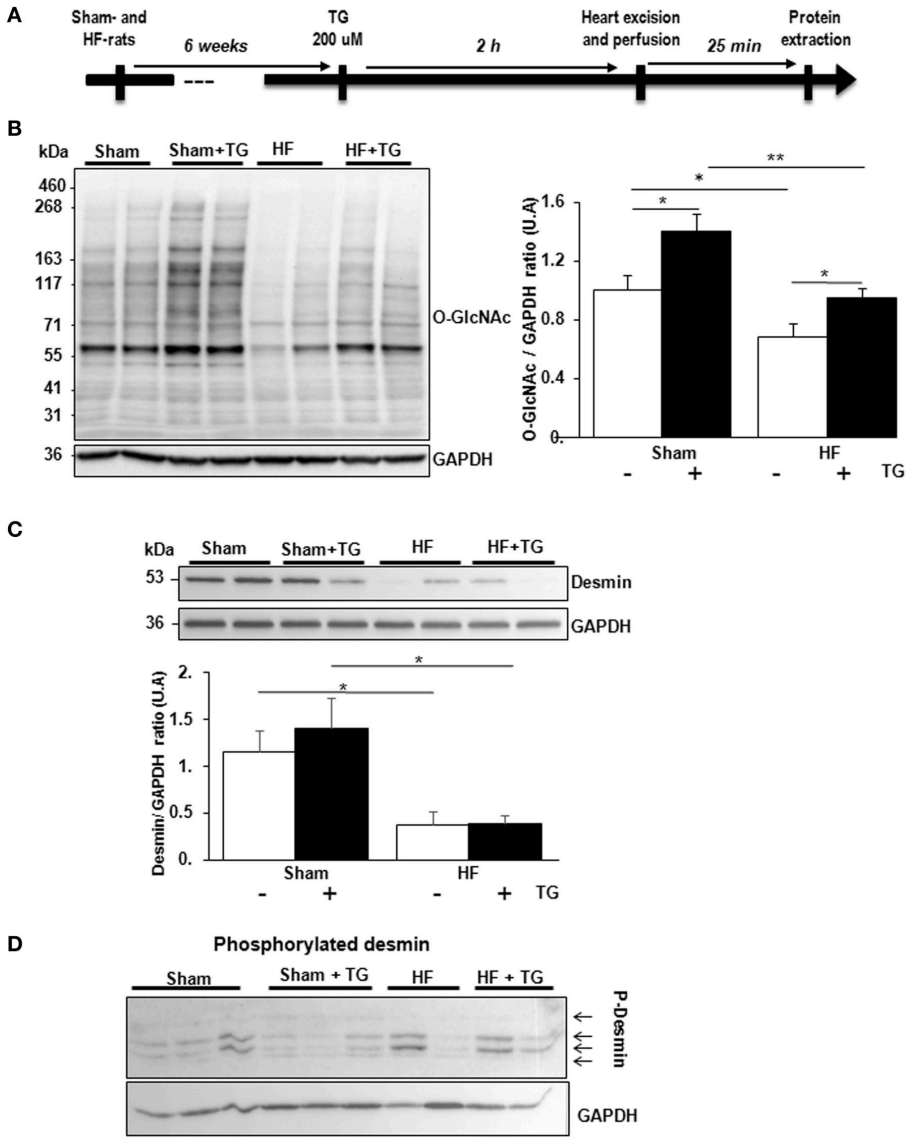

FIGURE 4 | Effect of OGA inhibition by thiamet G in isolated perfused heart. **(A)** Description of the protocol designed for thiamet G (TG) perfusion in sham- ($n = 6$) and HF- ($n = 7$) rats 6 weeks post-MI. **(B)** Western blot (left panel) and quantification (right panel) of *O*-GlcNAcylated proteins levels measured in proteins extracted from LVs of isolated perfused sham- and HF-rat hearts treated or not with 100 μM thiamet G for 2 h ($n = 7$ in each group). **(C)** Western blots (upper panel) and quantification (lower panel) of total desmin levels in the same samples. **(D)** Phosphorylation profiles of desmin were analyzed in the same samples by Phos-tag™ gel. Graphs show mean ± SEM values expressed in arbitrary units (A.U.). The positions of molecular weight are indicated as kilodalton (kDa) on the left. *$P < 0.05$; ** < 0.01.

(**Figure 5B**) that we were unable to quantify due to the strong background.

DISCUSSION

Post-translational modifications of sarcomeric proteins play an important role in HF-induced cardiac dysfunction (17, 18). We previously found a 2-fold increased phosphorylation of desmin levels by phosphoproteomic analysis (11) in a well characterized rat ischemic HF experimental model in which the induction of anterior MI leads to LV remodeling and to HF (19). Nine serine resides conserved between species were identified by mass spectrometry to be phosphorylated (11). In the present study, we found a decrease of O-GlcNAcylation levels of desmin and we hypothesize that a cross-talk between phosphorylation and O-GlcNAcylation of desmin may occur during HF development as we have recently shown for troponin T in in the same rodent model of HF (10). Here, our aim was to determine whether the levels of O-GlcNAcylated desmin are regulated in cardiomyocytes by inhibition or activation of O-GlcNAcylation and whether modulation of O-GlcNAcylation impacts the phosphorylation levels of desmin, in order to identify the serine residues that could be involved in the interplay.

TABLE 1 | Modulation of OGA inhibition by thiamet G in isolated perfused heart.

Parameters	Sham-rats		HF-rats	
	Ctrl ($n = 6$)	TG ($n = 6$)	Ctrl ($n = 6$)	TG ($n = 7$)
LV developed pressure (mmHg)	134 ± 2	135 ± 10	84 ± 11	99 ± 10*
Coronary flow (mL/min)	29 ± 2	21 ± 6*	28 ± 4	34 ± 5
Heart rate (bpm)	248 ± 1	243 ± 12	316 ± 24	283 ± 14
Cardiac output (mmHg)	48 ± 5	47 ± 9	30 ± 2	33 ± 2*

*Ctrl, perfusion without pharmacological agents; TG, thiamet G (200 μM); bpm, beats per minute. *P < 0.05 vs. control in each group.*

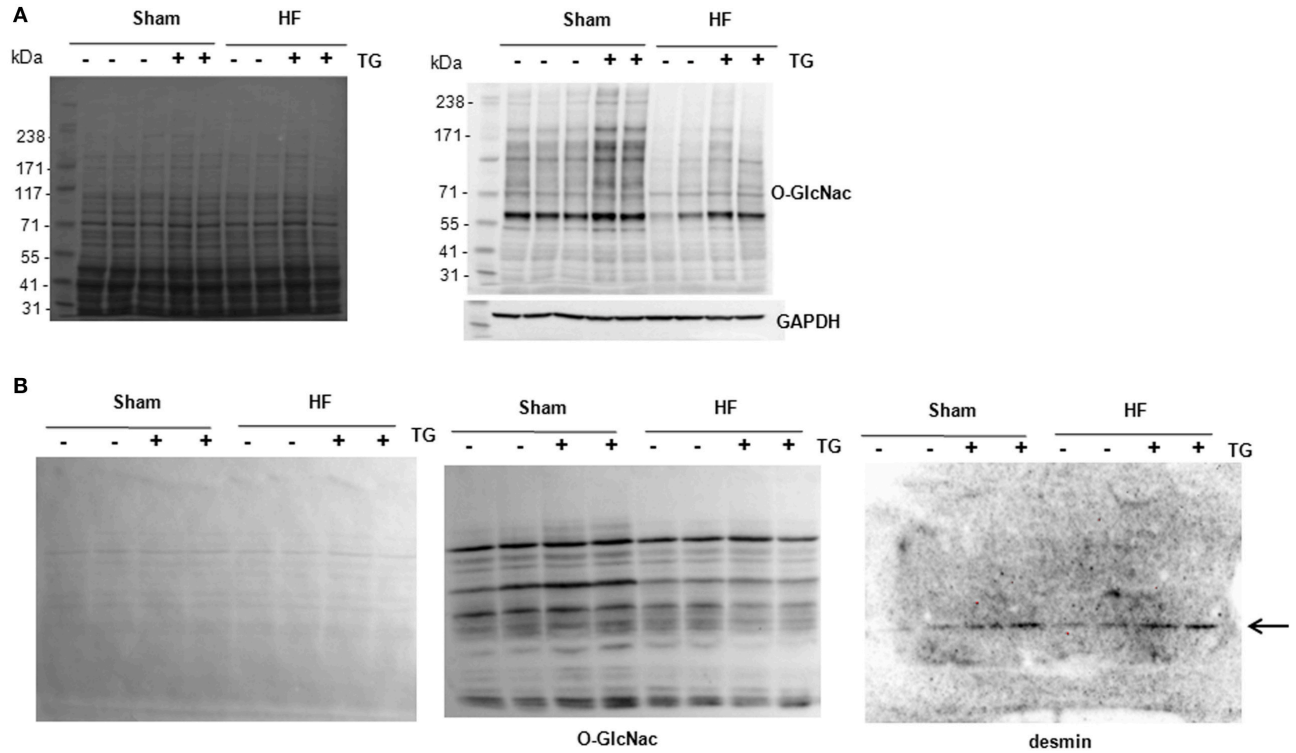

FIGURE 5 | Analysis of O-GlcNAcylated LV proteins by Western blot and WGA-SDS-PAGE gel electrophoresis. **(A)** Red ponceau staining (left panel) and western blot (right panel) of O-GlcNAcylated proteins (50 μg) extracted from sham- and HF-rats treated or not with thiamet G. The positions of molecular weight are indicated as kilodalton (kDa) on the left. **(B)** Red ponceau staining (left panel) and WGA-SDS-PAGE of O-GlcNAcylated proteins levels (middle panel) of O-GlcNAcylated desmin levels (right panel) from the same samples. The arrow in desmin WGA gels indicates the non-O-GlcNAcylated form.

For that purpose, first, we have modulated the levels of O-GlcNAcylated proteins in primary culture of neonate rat cardiomyocytes by either acting on OGA inhibition by treatment of the cardiomyocytes with a specific OGA inhibitor, thiamet G (20), or by OGT silencing. We verified that both treatments were efficient in primary cultures of cardiomyocytes with significant increase of O-GlcNAcylated proteins after OGA inhibition and significant decrease of O-GlcNAcylated proteins after OGT silencing. With both treatments, we did not observe any changes in total desmin protein levels and in the expression of desmin PTMs: phosphorylation and O-GlcNAcylation.

Second, we used an *ex vivo* model of perfused rat heart in order to test the efficiency of thiamet G on cardiac contractility. We found a positive impact of OGA inhibition on several cardiac parameters which were different depending on the sham- (coronary flow) or HF- (LV developed pressure and cardiac output) animals, except for the heart rate which was not modified in both groups of animals after a 2 h perfusion of thiamet G. We verified the efficiency of OGA inhibition by the significant increase of O-GlcNAcylated proteins in perfused heart in both group of animals treated (1.4-fold, $P < 0.05$). And as shown in *in vitro* experiments, we did not observe any modulation of total desmin and its phosphorylated forms, except a significant decrease of desmin expression between sham- and HF- rats after the 2 h perfusion, that can be explained by a degradation during the perfusion, such as calpain (11). We found these negative results by 2 techniques: IP desmin followed by phospho-serine WB (not shown) and Phos-tag™ gels.

Despite these negative results with *in vitro* and *ex vivo* cardiac models of O-GlcNAcylation modulation, we did not want to exclude that the technology used to quantify the levels of O-GlcNAcylated desmin was inappropriate or not enough sensitive. To clarify this hypothesis, we have tested a technique recently published (15). Despite the less sensitivity of the technique to detect the proteins transferred into the membrane (red ponceau staining), we improved the quality of the profile of O-GlcNAcylated proteins by comparison to a classical western blot with the use of the same antibody against the O-GlcNAc moieties. Unfortunately, the quality of the WGA-desmin blot did not allow quantifying the desmin band detected despite the highest intensity of desmin in thiamet G-treated LV samples. Further improvement will be required to use this promising technique to quantify the levels of O-GlcNAcylation of a specific protein.

Our data have shown that despite the presence of O-GlcNAc moieties on desmin from heart, there is no regulation of O-GlcNAcylated desmin by modulators of O-GlcNAcylation and subsequently there is no interplay between phosphorylation and O-GlcNAcylation of desmin.

The future is to find the targets of O-GlcNAcylation in heart that can be involved in cardiac improvement and to find the pharmacological agents able to decrease the levels of phosphorylated desmin which is toxic due to the aggregation of phosphorylated desmin in failing heart.

DATA AVAILABILITY

The data, analytic methods, and study materials presented in this study will be been made available to other researchers for purposes of reproducing the results or replicating the procedure.

AUTHOR CONTRIBUTIONS

MB and ED-D designed the study, make experiments and wrote the paper. TM, AD, and OB make experiments. VR, PM, and FP designed the study and wrote the paper.

FUNDING

This work was granted by the Féderation Hospital-Universitaire FHU REMOD-VHF.

ACKNOWLEDGMENTS

We thank Jean-Paul Henry for the surgical induction of MI in rats.

REFERENCES

1. Pfeffer M, Braunwald E. Ventricular remodeling after myocardial infarction. Experimental observations and clinical implications. *Circulation* (1990) 81:1161–72. doi: 10.1161/01.CIR.81.4.1161
2. Savoye C, Equine O, Tricot O, Nugue O, Segrestin B, Sautière K, et al. Left ventricular remodeling after anterior wall acute myocardial infarction in modern clinical practice (from the REmodelage VEntriculaire [REVE] Study Group). *Am J Cardiol.* (2006) 98:1144–9. doi: 10.1016/j.amjcard.2006.06.011
3. Fertin M, Hennache B, Hamon M, Ennezat PV, Biausque F, Elkohen M, et al. Usefulness of serial assessment of B-type natriuretic peptide, troponin I, and C-reactive protein to predict left ventricular remodeling after acute myocardial infarction (from the REVE-2 Study). *Am J Cardiol.* (2010) 106:1410–6. doi: 10.1016/j.amjcard.2010.06.071
4. Bauters C, Dubois E, Porouchani S, Saloux E, Fertin M, de Groote P, et al. Long-term prognostic impact of left ventricular remodeling after a first myocardial infarction in modern clinical practice. *PLoS ONE* (2017) 12:e0188884. doi: 10.1371/journal.pone.0188884
5. Hamdani N, Kooij V, Van Dijk S, Merkus D, Paulus WJ, Remedios CD, et al. Sarcomeric dysfunction in heart failure. *Cardiovasc Res.* (2008) 77:649–58. doi: 10.1093/cvr/cvm079
6. Zachara NE. The roles of O-linked β-N-acetylglucosamine in cardiovascular physiology and disease. *AJP Hear Circ Physiol.* (2012) 302:H1905–18. doi: 10.1152/ajpheart.00445.2011
7. Wang Z, Gucek M, Hart GW. Cross-talk between GlcNAcylation and phosphorylation: site-specific phosphorylation dynamics in response to globally elevated O-GlcNAc. *Proc Natl Acad Sci USA*. (2008) 105:13793–8. doi: 10.1073/pnas.0806216105
8. Ramirez-Correa GA, Jin W, Wang Z, Zhong X, Gao WD, Dias WB, et al. O-linked GlcNAc modification of cardiac myofilament proteins: a novel regulator of myocardial contractile function. *Circ Res.* (2008) 103:1354–8. doi: 10.1161/CIRCRESAHA.108.184978
9. Hu P, Shimoji S, Hart GW. Site-specific interplay between O-GlcNAcylation and phosphorylation in cellular regulation. *FEBS Lett.* (2010) 584:2526–38. doi: 10.1016/j.febslet.2010.04.044
10. Dubois-Deruy E, Belliard A, Mulder P, Bouvet M, Smet-Nocca C, Janel S, et al. Interplay between troponin T phosphorylation and O-N-acetylglucosaminylation in ischaemic heart failure. *Cardiovasc Res.* (2015) 107:56–65. doi: 10.1093/cvr/cvv136
11. Bouvet M, Dubois-Deruy E, Alayi TD, Mulder P, El Amranii M, Beseme O, et al. Increased level of phosphorylated desmin and its degradation products in heart failure. *Biochem Biophys Rep.* (2016) 6:54–62. doi: 10.1016/j.bbrep.2016.02.014
12. Lowery J, Kuczmarski ER, Herrmann H, Goldman RD. Intermediate filaments play a pivotal role in regulating cell architecture and function. *J Biol Chem.* (2015) 290:17145–53. doi: 10.1074/jbc.R115.640359
13. Mulder P, Devaux B, Richard V, Henry J, Wimart M, Thibout E, et al. Early versus delayed angiotensin-converting enzyme inhibition in experimental chronic heart failure. Effects on survival, hemodynamics, and cardiovascular remodeling. *Circulation* (1997) 95:1314–9. doi: 10.1161/01.cir.95.5.1314
14. Cieniewski-Bernard C, Mulder P, Henry JP, Drobecq H, Dubois E, Pottiez G, et al. Proteomic analysis of left ventricular remodeling in an experimental model of heart failure. *J Proteome Res.* (2008) 7:5004–16. doi: 10.1021/pr800409u
15. Kubota Y, Fujioka K, Takekawa M. WGA-based lectin affinity gel electrophoresis: a novel method for the detection of O-GlcNAc-modified proteins. *PLoS ONE* (2017) 12:1–12. doi: 10.1371/journal.pone.0180714
16. Dubois-Deruy E, Belliard A, Mulder P, Chwastyniak M, Beseme O, Henry J-P, et al. Circulating plasma serine^{208}-phosphorylated troponin T levels are indicator of cardiac dysfunction. *J Cell Mol Med.* (2013) 17:1335–44. doi: 10.1111/jcmm.12112
17. Wu SC, Solaro RJ. Protein kinase C: a novel regulator of both phosphorylation and de-phosphorylation of cardiac sarcomeric proteins. *J Biol Chem.* (2007) 282:30691–8. doi: 10.1074/jbc.M703670200
18. Dubois E, Richard V, Mulder P, Lamblin N, Drobecq H, Henry J-P, et al. Decreased serine207 phosphorylation of troponin T as a biomarker for

left ventricular remodelling after myocardial infarction. *Eur Heart J.* (2011) 32:115–23. doi: 10.1093/eurheartj/ehq108

19. Mulder P, Barbier S, Chagraoui A, Richard V, Henry JP, Lallemand F, et al. Long-term heart rate reduction induced by the selective I(f) current inhibitor ivabradine improves left ventricular function and intrinsic myocardial structure in congestive heart failure. *Circulation* (2004) 109:1674–9. doi: 10.1161/01.CIR.0000118464.48959.1C
20. Vocadlo DJ. O-GlcNAc processing enzymes: catalytic mechanisms, substrate specificity, and enzyme regulation. *Curr Opin Chem Biol.* (2012) 16:488–97. doi: 10.1016/j.cbpa.2012.10.021

Conflict of Interest Statement: The authors declare that the research was conducted in the absence of any commercial or financial relationships that could be construed as a potential conflict of interest.

frontiers in Endocrinology

MINI REVIEW
published: 09 October 2018
doi: 10.3389/fendo.2018.00602

Cross-Dysregulation of *O*-GlcNAcylation and PI3K/AKT/mTOR Axis in Human Chronic Diseases

*Ninon Very, Anne-Sophie Vercoutter-Edouart, Tony Lefebvre, Stéphan Hardivillé and Ikram El Yazidi-Belkoura**

Université Lille, CNRS, UMR 8576—UGSF–Unité de Glycobiologie Structurale et Fonctionnelle, Lille, France

OPEN ACCESS

Edited by:
Peter Blume-Jensen, XTuit Pharmaceuticals, United States

Reviewed by:
Jonas Thue Treebak, University of Copenhagen, Denmark
Edgar Zenteno, Universidad Nacional Autónoma de México, Mexico

****Correspondence:***
Ikram El Yazidi-Belkoura
ikram.el-yazidi@univ-lille.fr

Specialty section:
This article was submitted to Molecular and Structural Endocrinology, a section of the journal Frontiers in Endocrinology

Received: *20 July 2018*
Accepted: *21 September 2018*
Published: *09 October 2018*

Citation:
Very N, Vercoutter-Edouart A-S, Lefebvre T, Hardivillé S and El Yazidi-Belkoura I (2018) Cross-Dysregulation of O-GlcNAcylation and PI3K/AKT/mTOR Axis in Human Chronic Diseases. Front. Endocrinol. 9:602. doi: 10.3389/fendo.2018.00602

The hexosamine biosynthetic pathway (HBP) and the phosphatidylinositol 3-kinase (PI3K)/AKT/mammalian target of rapamycin (mTOR) signaling pathway are considered as nutrient sensors that regulate several essential biological processes. The hexosamine biosynthetic pathway produces uridine diphosphate N-acetylglucosamine (UDP-GlcNAc), the substrate for *O*-GlcNAc transferase (OGT), the enzyme that *O*-GlcNAcylates proteins on serine (Ser) and threonine (Thr) residues. *O*-linked β-N-acetylglucosaminylation (*O*-GlcNAcylation) and phosphorylation are highly dynamic post-translational modifications occurring at the same or adjacent sites that regulate folding, stability, subcellular localization, partner interaction, or activity of target proteins. Here we review recent evidence of a cross-regulation of PI3K/AKT/mTOR signaling pathway and protein *O*-GlcNAcylation. Furthermore, we discuss their co-dysregulation in pathological conditions, e.g., cancer, type-2 diabetes (T2D), and cardiovascular, and neurodegenerative diseases.

Keywords: *O*-GlcNAcylation, PI3K/AKT/mTOR, cancer, diabetes, cardiovascular, neurodegenerative diseases

INTRODUCTION

O-linked β-N-acetylglucosaminylation (*O*-GlcNAcylation) is a dynamic modification of serine (Ser) and threonine (Thr) amino acids of cytoplasmic, nuclear (1), and mitochondrial (2) proteins with a single residue of N-acetylglucosamine (GlcNAc). This post-translational modification is controlled by two single antagonist enzymes: *O*-GlcNAc transferase (OGT) and *O*-GlcNAcase (OGA), which transfer and remove the GlcNAc moiety, respectively. The nucleotide sugar donor, uridine diphosphate N-acetylglucosamine (UDP-GlcNAc), is the final product of the hexosamine biosynthetic pathway that is at the nexus of glucose, amino acid, lipid, and nucleotide metabolisms (**Figure 1**). Consequently, *O*-GlcNAcylation is considered as a cellular nutrient sensor linking nutrient availability to intracellular signaling and biological responses. To date, thousands of *O*-GlcNAcylated proteins endowing a wide range of functions have been identified and most of them are also phosphoproteins (3). In fact, *O*-GlcNAcylation and phosphorylation can modulate each other at the same or adjacent sites (4).

Over the last decade, emerging evidence has indicated that a cross-talk exists between *O*-GlcNAcylation and phosphatidylinositol 3-kinase (PI3K)/AKT/mammalian target of rapamycin (mTOR) signaling pathway (5). The PI3K/AKT/mTOR signaling pathway is a key transducer of metabolic and mitogen signals (such as energy, amino acids, insulin or growth factors) that modulate gene expression, protein translation and cellular metabolism, thus regulating cell growth and proliferation (**Figure 1**). Aberrant activation of this signaling pathway as well as altered protein *O*-GlcNAcylation have both described in several types of cancer, cardiovascular and metabolic diseases, aging, and neurodegeneration in human (6–8). This mini-review summarizes and discusses recent evidence linking cross-regulation and co-dysregulation of *O*-GlcNAcylation and PI3K/AKT/mTOR signaling pathway in physiological conditions and in human chronic diseases, respectively.

THE PI3K/AKT/MTOR SIGNALING PATHWAY AND ITS CROSS-REGULATION WITH PROTEIN *O*-GLCNACYLATION

Binding of insulin or growth factors to their plasma membrane tyrosine kinase receptors (RTK) triggers the phosphorylation of PI3K, either directly by the RTK or indirectly *via* phosphorylation of adapter signaling proteins such as insulin receptor substrate-1 or 2 (IRS-1/2; **Figure 1**). Phospho-PI3K catalyzes the formation of membrane phosphatidylinositol-3,4,5-trisphosphate (PIP3) which drives the activation of the phosphoinositide-dependent protein kinase-1 (PDK-1) and the recruitment of AKT. The latter is partially activated through initial phosphorylation at Thr308 by PDK-1 and fully activated after phosphorylation at Ser473 by the mTOR complex 2 (mTORC2) (9). Once activated, AKT phosphorylates several downstream effectors [e.g., mTOR, forkhead box proteins O (FoxO), glycogen synthase kinase 3 β (GSK3β), BCL-2-associated agonist of cell death (BAD) or endothelial nitric oxide synthase (eNOS)] that in return regulate and coordinate a variety of cellular responses including cell proliferation, survival and growth, glucose metabolism, and angiogenesis (9). Tuberous sclerosis complex 2 (TSC2), inhibited by AKT-dependent phosphorylation, is a critical negative regulator of mTOR complex 1 (mTORC1). mTORC1 induces protein synthesis through phosphorylation of eukaryotic translation initiation factor 4E (eIF4E)-binding protein-1 (4E-BP1) and ribosomal protein S6 kinase (p70S6K) (9). mTORC1 also regulates nucleotide, lipid and glucose metabolisms, angiogenesis and autophagy processes by regulating alpha-activating transcription factor 4 (ATF4), lipin-1, hypoxia-inducible factor-1α (HIF-1α) or Unc-51 like autophagy activating kinase 1 (ULK1) (10, 11). In response to amino acid stimulation, mTORC1 is recruited to the lysosomal surface where it is activated by Ras homolog enriched in brain (Rheb) (9). Upon elevated AMP/ATP ratio, AMP-activated protein kinase (AMPK) phosphorylates, and activates TSC2 leading to inhibition of mTORC1 activity (10, 11).

In parallel, *O*-GlcNAcylation targets proteins involved in transcription, translation, ubiquitin-proteasomal degradation, signal transduction, stress response, cellular trafficking and architecture, cell cycle, apoptosis, and development (12). OGT activity is sensitive to UDP-GlcNAc levels, thus, addition of glucose or glucosamine globally increases levels of *O*-GlcNAcylation (13).

Many studies have established a complex interplay between PI3K/AKT/mTOR signaling pathway and protein *O*-GlcNAcylation (**Figure 1**). After insulin stimulation, the C-terminal PIP-binding domain of OGT (PPO) allows its translocation from the nucleus to the plasma membrane in murine 3T3-L1 adipocytes (14) and African green monkey COS-7 fibroblasts (15), and possibly to lipid rafts as observed in the human hepatic cancer cell line HepG2 (16). This translocation possibly facilitates the tyrosine phosphorylation of OGT by the insulin receptor (IR), which increases its enzymatic activity (17). The cellular energy sensor AMPK also regulates OGT. AMPK phosphorylates OGT at Thr444, which induces its nuclear translocation in differentiated C2C12 skeletal muscle myotubes (18) and promotes its dissociation from chromatin in human embryonic kidney 293T cells (19). In HepG2 cells, it has been further shown that OGT phosphorylation by AMPK inhibits histone H2B *O*-GlcNAcylation and gene transcription (19). In contrast, OGT targets several actors from the PI3K/AKT/mTOR signaling pathway, including IRS-1 (17, 20–24), PI3K (23), PDK1 (17), AKT (21, 25–27), AMPK (18, 19), 4E-BP1 (28), and p70S6K (29). Indeed, these proteins are *O*-GlcNAc-modified in IR and insulin growth factor-1 receptor (IGF-1R) expressing cell types including adipocytes, myocytes, hepatocytes, pancreatic beta (β) cells, endothelial cells, kidney and retina cells (30). However, only few studies have investigated the molecular impacts of *O*-GlcNAcylation on PI3K/AKT/mTOR signaling pathway and the subsequent biological effects under physiological conditions. *O*-GlcNAc modification of IRS-1 and AKT inhibits their activity either by disruption of their interaction with PI3K and PDK1 kinases, respectively, in 3T3-L1 adipocytes and MCF-7 breast cancer cell lines (17, 26), either by a "Yin-Yang" competition mechanism with activating phosphorylation as described in rat primary adipocytes and INS-1 pancreatic β cell lines (25, 27). *O*-GlcNAcylation also enhances 4E-BP1 stability *in vitro* in rat retinal TR-MUL Müller cells an *in vivo* in murine retinal cells, potentially by preventing its phosphorylation-dependent ubiquitin-mediated degradation (28). Protein *O*-GlcNAcylation could hence potentiate cellular nutrient sensing capacity of the PI3K/AKT/mTOR signaling pathway in order to regulate crucial intracellular processes.

Abbreviations: 4E-BP1, eukaryotic translation initiation factor 4E-binding protein-1; AD, Alzheimer's disease; AMPK, adenosine monophosphate-activated protein kinase; BAD, BCL-2-associated agonist of cell death; eNOS, endothelial nitric oxide synthase; FoxO, forkhead box protein O; GlcNAc, N-acetylglucosamine; GLUT, glucose transporter; GSK3β, glycogen synthase kinase 3 β; HBP, hexosamine biosynthetic pathway; HIF-1α, hypoxia-inducible factor-1α; IR, insulin receptor; IRS-1, insulin receptor substrate-1; mTOR, mammalian target of rapamycin; mTORC, mTOR complex; O-GlcNAcylation, O-linked β-N-acetylglucosaminylation; OGA, O-GlcNAcase; OGT, O-GlcNAc transferase; p70S6K, ribosomal protein S6 kinase; PDK-1, phosphoinositide-dependent protein kinase-1; PI3K, phosphatidylinositol 3-kinase; PIP3, phosphatidylinositol-3,4,5-trisphosphate; T2D, type-2 diabetes; Tau, tubulin-associated unit; UDP-GlcNAc, uridine diphosphate N-acetylglucosamine.

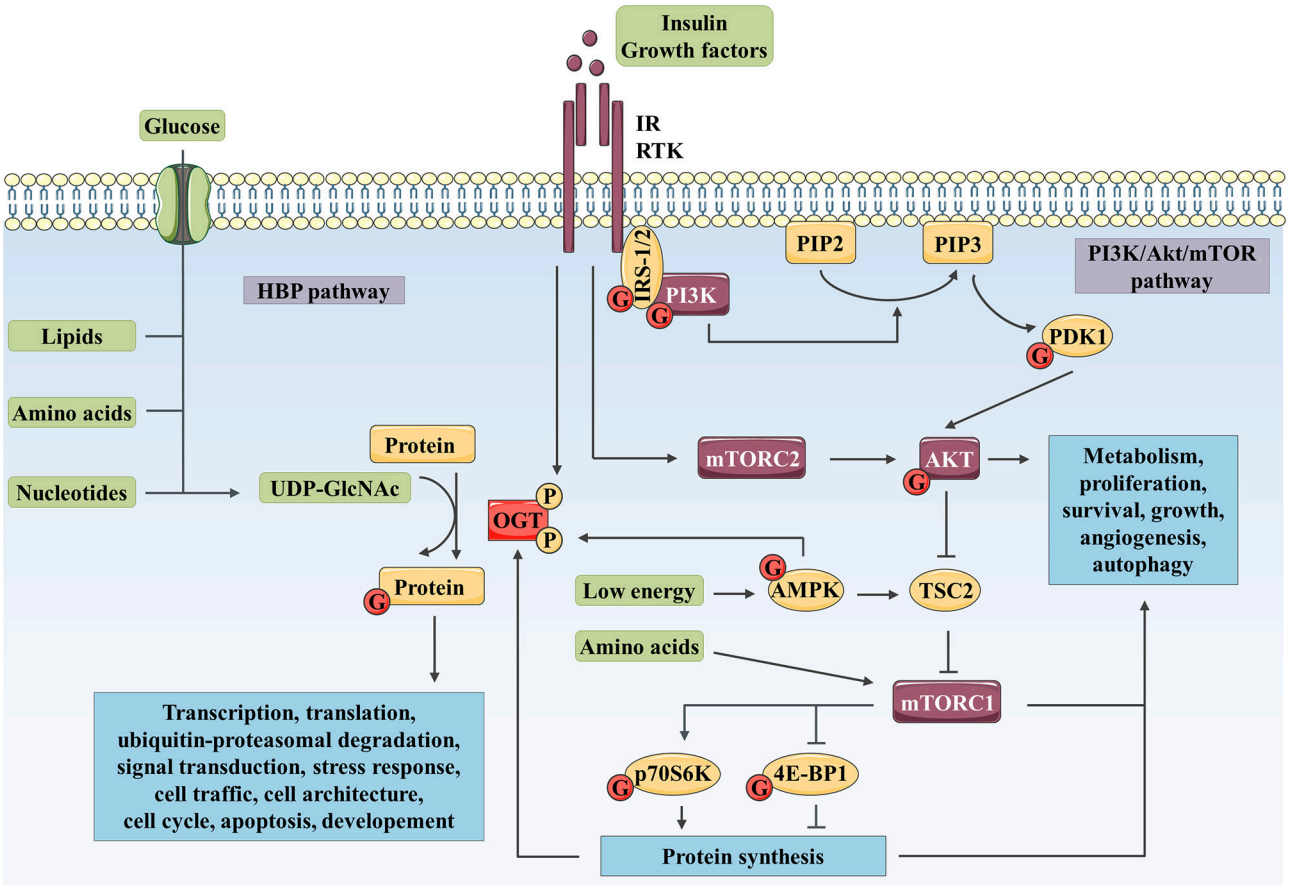

FIGURE 1 | Complex interplay between *O*-GlcNAcylation and PI3K/AKT/mTOR signaling pathway controls numerous biological processes. The HBP integrates a fraction of the glucose entering the cell as well as lipid, nucleotide, and amino acid metabolites to produce UDP-GlcNAc. Then, OGT uses UDP-GlcNAc as a nucleotide sugar donor substrate to add a GlcNAc group on serine and threonine residues of target proteins. Like phosphorylation, *O*-GlcNAcylation is a dynamic and reversible post-translational modification. Its targets are involved in a wide range of biological processes such as transcription, translation, ubiquitin-proteasomal degradation, signal transduction, cell traffic and architecture, cell cycle, apoptosis or development. In parallel, binding of insulin or growth factor to their RTK leads to receptor activation and recruitment of IRS-1/2 and PI3K. PI3K produces PIP3 (from PIP2), which recruits AKT and PDK1 to the plasma membrane. PDK1 and mTOR in mTORC2 activate AKT through phosphorylation. mTORC1 is activated by AKT through TSC2 inhibition and upon amino acid stimulation and, is inhibited in response to low energy by AMPK. mTORC1 promotes protein synthesis via direct phosphorylation of p70S6K and 4E-BP1. By phosphorylating key substrates, AKT and mTORC1 regulate metabolism, cell cycle, proliferation, survival, growth, angiogenesis and autophagy. OGT localization and activity are regulated through phosphorylation by IR and AMPK. OGT stability is indirectly regulated at the protein synthesis level *via* mTORC1. Reciprocally, several actors of the PI3K/AKT/mTOR signaling pathway are modified by *O*-GlcNAcylation such as IRS-1, PI3K, PDK1, AKT, AMPK, p70S6K, and 4E-BP1.

O-GLCNACYLATION AND PI3K/AKT/MTOR SIGNALING PATHWAY CROSS-DYSREGULATION IN HUMAN DISEASES

Cancer

The Warburg effect is a metabolic reprogramming of the cell from oxidative phosphorylation to aerobic glycolysis that allows energy production and *de novo* macromolecule synthesis required to sustain cancer cells proliferation and growth. Enhanced glucose and glutamine uptake observed in the Warburg effect would lead to an increased flux through HBP and the hyper-*O*-GlcNAcylation that has been observed in many cancers (31). Aberrantly activated PI3K/AKT/mTOR signaling pathway is known to play a central role in aerobic glycolytic reprogramming, tumor growth, and survival (32), and a cross-talk between PI3K/AKT/mTOR signaling and *O*-GlcNAcylation has been observed in several cancers.

Insulin or serum growth factors stimulation lead to increased OGT expression in a PI3K-dependent manner in HepG2 and MCF-7 cell lines (16, 33). Although it was not investigated in these studies, it is likely that this effect could be related to mTOR activation. Since it was observed that pharmacological inhibition of mTOR enhances proteasomal and autophagic degradation of OGT in HepG2 cells (34). We have also demonstrated that inhibition of mTOR affects OGT protein level and overall *O*-GlcNAcylation levels in HCT116 colon cancer cell line (35). In breast cancer cell lines the positive regulation of OGT

expression through mTOR is dependent on c-Myc-induced heat shock protein 90A (HSP90A) transcription (36). This chaperone binds to OGT and prevents its proteasomal degradation (36). Additionally, the transcriptional regulator Yes-associated protein (YAP) strongly activates the OGT promoter in hepatic cancer cell lines. In turn, *O*-GlcNAcylation of YAP promotes its stability, and its tumorigenic activity both *in vitro* and *in vivo* in liver cancer mouse models showing that a positive feedback is set up in liver tumorigenesis (37). YAP is activated by PI3K in hepatocellular (38) and mammary carcinoma (39), but has been shown to regulate PI3K/AKT/mTOR signaling in the MCF 10A human immortalized mammary epithelial cell line (40). These recent works highlight once more the tight link that exists in cancer cells between PI3K/AKT/mTOR axis and OGT activity.

O-GlcNAcylation impacts PI3K/AKT and mTOR axis in cancer cells. Pre-B acute lymphocytic leukemia (pre-B-ALL) cells overexpress OGT and exhibit a higher *O*-GlcNAcylation levels and an overactivation of PI3K, AKT and c-Myc compared to normal B cells. This dysregulation is associated with the overexpression of the transcription factor *HIF-1α* and its target glycolytic genes such as *glucose transporter 1* (*GLUT1*), *hexokinase 2* (*HK2*), *phosphofructokinase-1* (*PFK-1*) and *lactate dehydrogenase A* (*LDHA*). *OGT* knockdown, in pre-B-ALL cells, decreases PI3K and AKT activation and glycolysis, resulting in a reduced cell proliferation and apoptosis. These inhibitory effects can be partly rescued by IGF-1 mediated stimulation of PI3K/AKT, indicating that effect of OGT on glycolysis is, in part, PI3K/AKT-dependent (41). Similarly, in 3D cultures of T4-2 breast cancer cells, OGT inhibition or silencing suppresses AKT signaling and glycolytic activity (42) (**Figure 2**).

In addition to glycolysis, regulation of PI3K/AKT signaling by *O*-GlcNAcylation was shown to modulate proliferation, growth and invasion properties of cancer cells (32, 42–47). We have demonstrated that knockdown or pharmacological inhibition of OGT decreases PI3K activation and prevents serum-stimulated cyclin D1 synthesis, leading to a delay in proliferation of MCF-7 cells (33). Since AKT prevents ubiquitin-mediated degradation of cyclin D1 by inhibiting GSK3β activity in the murine NIH/3T3 fibroblast cell line (43), it is likely that the decrease in cyclin D1 level could result from an increase of its proteasomal degradation under low *O*-GlcNAcylation levels. Reciprocally, enhanced *O*-GlcNAcylation level stimulates PIP3 production and AKT phosphorylation in MCF-7 cells (44). Similar results showed that hyper-*O*-GlcNAcylation induced by *OGA* down-regulation in 8305C thyroid anaplastic tumor cell line stimulates proliferation through increased phosphorylation of AKT at Ser473 and cyclin D1 amount (45). Additionally, glucose deprivation in osteosarcoma U2OS cell line attenuates protein *O*-GlcNAcylation, phosphorylation of IRS-1 and AKT, production of PIP3 and suppresses cell growth (46). Importantly, in these cell line, insulin signaling pathway, and tumor growth can be rescued by glucosamine-mediated increased HBP flux and *O*-GlcNAcylation (46). In parallel, increased *O*-GlcNAcylation promotes gastric and thyroid cancer cells invasion in a PI3K/AKT dependent manner, since the pro-invasion effect of *O*-GlcNAcylation is suppressed by PI3K inhibition or *AKT* silencing (47, 48). This may result from the regulation that *O*-GlcNAcylation exerts on AKT-mediated control of a myriad of downstream substrates, such as matrix metalloproteinase-2 (MMP-2) and MMP-9 (49) (**Figure 2**). However, other studies report contradictory results regarding the effect of *O*-GlcNAcylation on the activation of AKT signaling pathway (26, 50). *OGA* overexpression reduces AKT *O*-GlcNAcylation and promotes its activation, albeit in a PI3K-independent manner, both in HepG2 cells and in liver of euglycemic mice (50). Our group also demonstrated that *OGT* silencing prevents AKT Ser473 phosphorylation in HepG2 (16) and MCF-7 (33) cell lines. More recently, this effect has also been described in cholangiocarcinoma cell lines (51). Furthermore, AKT *O*-GlcNAcylation at Thr305 and Thr312 reduces MCF-7 cell proliferation and migration *via* inhibition of AKT phosphorylation at Thr308 and disruption of its interaction with PDK1 (26).

Finally, it was shown that *O*-GlcNAcylation regulates the mitogenic mTOR signaling pathway through targeting the mTOR inhibitor AMPK (35, 52, 53). Increased *O*-GlcNAcylation in colon cancer cells, either by *OGT* overexpression or OGA inhibition, reduces phosphorylation of AMPK at Thr172, activates mTOR and induces cell growth *in vitro* in LoVo cell line and *in vivo* in LoVo cell-derived tumors of BALB/c-nu/nu mice (52). We have confirmed that *O*-GlcNAcylation activates mTOR in HCT116 colon cancer cell line but not in CCD841CoN normal cells (35). Reciprocally, *OGT* silencing or inhibition increases phosphorylation of AMPK, decreases phosphorylation of mTOR downstream effectors 4E-BP1 and p70S6K, decreases *HIF-1a*, *GLUT1,* and *LDHA* expression and impairs glucose uptake and growth in breast cancer cell lines (53) (**Figure 2**).

Together, these studies establish the involvement of *O*-GlcNAcylation in cancer biology (increased glycolysis, proliferation, growth, and invasion) through direct activation of the PI3K/AKT/mTOR axis. One may consider this post-translational modification as a key node between metabolism and cell signaling. However, intricate ties linking metabolism and cancer are not completely elucidated and need further investigations. In parallel, anti-cancer inhibitors targeting mTOR axis are currently in clinical development and must be encouraged (54). Tumor cells resistant to GDC-0941, a PI3K inhibitor, exhibit an increased activation of the PI3K/AKT/mTOR signaling pathway and *OGT* expression in comparison to GDC-0941-sensitive cells. Interestingly, *OGT* silencing sensitizes these cells to GDC-0941 (55). In this sense, targeting OGT in cancer cells and/or adapting patients to low caloric diet could increase the efficiency of anti-PI3K/AKT/mTOR therapeutic strategies and foil drug resistance.

Type 2 Diabetes

Insulin resistance, a hallmark of type 2 diabetes (T2D), refers to impaired insulin sensitivity and glucose uptake of target tissues (liver, skeletal muscle, and adipose tissue). PI3K/AKT signaling pathway plays a key role in the regulation of glucose homeostasis by inhibiting gluconeogenesis and activating glycogenesis *via* the inhibition of FoxO1 and GSK3β respectively

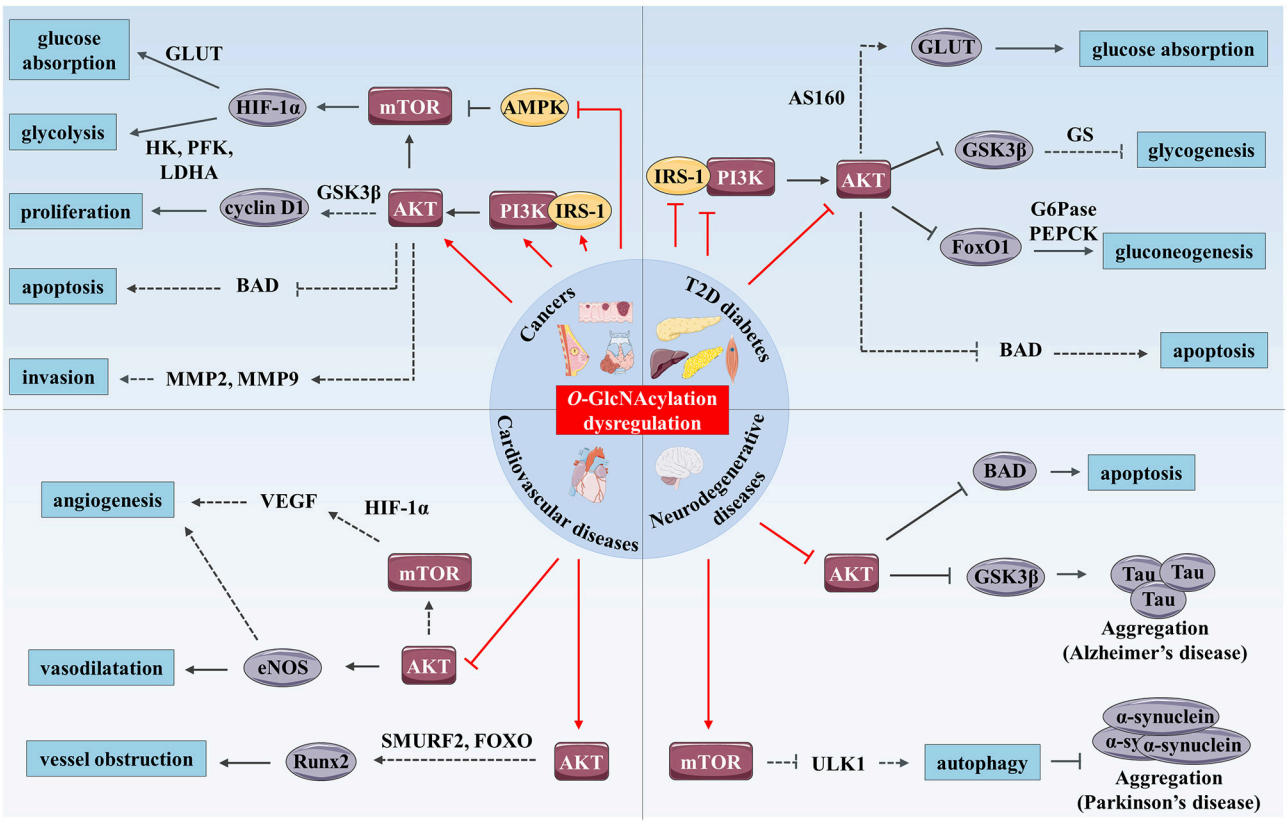

FIGURE 2 | *O*-GlcNAcylation and PI3K/AKT/mTOR signaling pathway cross-dysregulation in human chronic diseases. *O*-GlcNAcylation dysregulation (represented by red arrows) modulates the PI3K/AKT/mTOR signaling pathway and promotes development of human chronic diseases such as cancer, T2D and cardiovascular and neurodegenerative diseases. In cancer, increased *O*-GlcNAcylation stimulates the PI3K/AKT/mTOR signaling pathway by up-regulating expression and activity of IRS-1, PI3K, and AKT and by inhibiting AMPK. mTOR enhances glucose absorption and glycolysis through stimulation of expression of the transcription factor *HIF-1α* and its target genes such as *GLUTs*, *HK*, *PFK,* and *LDHA*. AKT enhances cancer cell proliferation through increased cyclin D1 expression possibly through GSK3β inhibition. Moreover, AKT has anti-apoptotic and pro-invasion activities and these effects may result in the regulation of several targets including BAD, MMP-2, and MMP-9. In T2D, increased *O*-GlcNAcylation associated with hyperglycemia promotes insulin resistance in skeletal muscle, liver and adipose tissue by inhibition of IRS-1/PI3K interaction and down-regulation of IRS-1 and AKT activity. AKT inhibition induces reduced glucose absorption through down-regulation of GLUT4 translocation to the plasma membrane which might be mediated by AS160. Moreover, repression of AKT inhibits glycogenesis and stimulates gluconeogenesis through regulation of GSK3β, FoxO1, and respective targets (GS, G6Pase, and PEPCK). Additionally, *O*-GlcNAc-mediated AKT inhibition induces pancreatic β cell apoptosis. In hyperglycemic or diabetic cardiovascular tissues, *O*-GlcNAcylation reduces vasodilatation vessels and angiogenesis via inhibition of AKT, and probably eNOS and VEGF. Enhanced *O*-GlcNAcylation in these tissues could also promote calcification and therefore vessel obstruction through *Runx2* overexpression possibly mediated by AKT regulation of SMURF2 and/or FoxO. Finally, increased *O*-GlcNAcylation stimulates Tau and α-synuclein aggregations involved in AD and Parkinson's disease respectively. These processes are mediated by AKT inhibition and Tau kinase GSK3β activation in AD, and by mTOR activation and reduced autophagy in Parkinson's disease, which could result from ULK1 inhibition. Furthermore, *O*-GlcNAc-mediated AKT repression promotes neural cell apoptosis in part, by up-regulation of BAD.

(9) (**Figure 2**). Some studies have also established a link between dysregulation of *O*-GlcNAcylation cycling and insulin resistance.

Interestingly, single nucleotide polymorphisms (SNPs) on *OGA* (also called *MGEA5* for *meningioma expressed antigen 5*) gene and *GFPT2* (for *GFAT isomerizing 2*) gene, coding the glutamine fructose-6-phosphate amidotransferase (GFAT) rate-limiting enzyme controlling the production of UDP-GlcNAc, are associated with increased T2D risk in American-Mexican and Caucasian populations, respectively (56, 57). These mutations may lead to reduced *OGA* expression and increased *GFPT2* expression respectively (56, 57), and an up-regulation of cellular *O*-GlcNAcylation levels. *O*-GlcNAcylation levels are significantly increased in skeletal muscle, liver, heart, colon-rectum, erythrocytes, and leukocytes of diabetic animals and humans (35, 58–62). Consistent with these epidemiologic data, *db/db* mice overexpressing *Oga* showed improved hepatic insulin sensitivity (63), whereas *Ogt* overexpression and subsequent elevation of global *O*-GlcNAcylation level inhibits insulin signaling pathway, both *in vitro* in 3T3-L1 adipocyte and Fao hepatic cell lines, and *in vivo* in skeletal muscle and adipose tissue in mice (15, 64, 65). Skeletal muscle-specific *Ogt* knockout mice have increased glucose uptake, insulin signaling and whole-body insulin sensitivity (62). Likewise, inhibition of OGA with *O*-(2-acetamido-2-deoxy-D-glucopyranosylidene) amino-N-phenylcarbamate (PUGNAc) induces insulin resistance in

3T3-L1 and rat primary adipocytes by perturbing both insulin-signaling pathway and glucose absorption (17, 21). Indeed, blockade of OGA increases *O*-GlcNAcylation of IRS-1 and AKT while decreasing their phosphorylation (17, 21). Consequently, a reduction of insulin-stimulated PI3K/IRS-1 interaction, GSK3β phosphorylation (15, 17, 64) and GLUT4 translocation to the plasma membrane is observed (17, 21). This reduced translocation of GLUT4 might be related to the decrease in AKT phosphorylation since phosphorylation of AKT substrate of 160 kDa (AS160) is required for insulin-stimulated translocation of GLUT4 to the plasma membrane (66). Reciprocally, in euglycemic HepG2 and mice hepatic cells, the reduced global *O*-GlcNAcylation levels induced by *OGA* overexpression is associated with an increase of AKT activation but not of PI3K (50). This results in inhibition by phosphorylation of GSK3β (Ser9) and FoxO1 (Ser166), leading to a decrease of gluconeogenic genes transcription, including *glucose-6-phosphatase* (*G6Pase*) and *phosphoenolpyruvate carboxykinase* (*PEPCK*) (50). In addition, glycogen synthase (GS), substrate of GSK3β, is also *O*-GlcNAc-modified in 3T3-L1 cells and this modification blocks its activation, which is associated with insulin resistance (67). These data clearly establish the impact of *O*-GlcNAcylation in the etiology of insulin resistance and, thus, potentially in metabolic related diseases such as diabetes.

However, there are studies showing that OGA inhibition does not cause insulin resistance in 3T3-L1 adipocytes, rat liver and muscle (68, 69), while others show that OGA inhibition induces insulin resistance in rat skeletal muscle in an AKT and GSK3β-independent manner (70). In these studies, authors suggest that conflicting primary results might result from the use of the non-selective OGA inhibitor PUGNAc which has been shown to also inhibit lysosomal hexosaminidases and alter plasma membrane oligosaccharide structures that are critical in signal transduction (71, 72). These contradictory findings could also be due to supraphysiological concentrations of insulin (12 nmol/L) used for stimulation (70). These findings raise the question of whether high *O*-GlcNAcylation levels are responsible for insulin resistance and show to what extent the understanding of the role of *O*-GlcNAcylation in cell signaling regulation in such multifactorial disease needs to be deepened.

In addition to its role in insulin resistance, *O*-GlcNAcylation could also take part in pancreatic islet β cell dysfunction. Pancreatic β cells are the cells in the body in charge of producing, storing and releasing insulin upon increased blood glucose concentration; its dysregulation is a cause of diabetes. OGT and global *O*-GlcNAcylation levels are increased in pancreatic islets of Goto-Kakizaki diabetic rats (73). In murine pancreatic β cells, glucosamine-mediated hyperglycemia increases *O*-GlcNAcylation of AKT and concomitantly reduces its Ser473 phosphorylation (27). Glucosamine induces β cells apoptosis likely through *O*-GlcNAc-mediated inhibition of AKT (27) (**Figure 2**). In contrast, β cell-specific *Ogt* knockout mice develop β cell failure and diabetes. In this model, a reduction of AKT phosphorylation at Ser473 was observed (74). These data suggest that the phospho/*O*-GlcNAc interplay on AKT may play a pivotal role as a regulator of downstream signaling cascades in response to nutrient conditions. The impact of *O*-GlcNAcylation dysregulation may be tissue-specific (75). In conclusion, increased *O*-GlcNAcylation in diabetes toward PI3K/AKT-mediated insulin resistance in target tissues could contribute to the maintenance of the pathology.

Cardiovascular Diseases

Many studies suggest that elevated protein *O*-GlcNAcylation levels contribute to cardiovascular complications (76). Chronic hyperglycemia is a risk factor for cardiovascular diseases and patients with diabetes may develop atherosclerotic carotid plaques with a marked increase of *O*-GlcNAcylation levels (23). Aorta from streptozotocin-induced hyperglycemic mice exhibits high levels of *O*-GlcNAcylation and impaired vascular sprouting (77). Endothelial dysfunction is a feature of cardiovascular diseases that is characterized by reduced bioavailability of nitric oxide (NO) produced by endothelial nitric oxide synthase (eNOS). Endothelial production of NO plays indeed a key role in preventing vascular diseases by preventing thrombosis, inflammation, vascular tone, and remodeling (78). *O*-GlcNAc modification is known to modulate NO production in endothelial cells, promoting macro- and microvascular complications. In response to insulin, AKT induces vasodilatation in primary human aortic endothelial cells (HAEC), and it may exert anti-atherogenic effects by increasing activating phosphorylation of eNOS at Ser615 and Ser1177 (79) (**Figure 2**). Federici and collaborators showed that hyperglycemia or HBP activation decreases eNOS activity through a reduction of AKT and eNOS phosphorylation in human coronary artery endothelial cells (HCAEC) (23). *In vitro*, glucosamine-induced protein *O*-GlcNAcylation also modulates the angiogenic properties of EA.hy926 endothelial cells, most probably by a concomitant increase of AKT *O*-GlcNAcylation that leads to inhibition of its pro-angiogenic activity (77). AKT could directly up-regulate the production of the pro-angiogenic factor NO (80). In addition, PI3K/AKT/mTOR signaling pathway stimulates angiogenesis by increasing expression of *HIF-1α* and its target, the *vascular endothelial growth factor* (*VEGF*) (80) (**Figure 2**). Elevated *O*-GlcNAcylation levels also induce vascular calcification *in vitro* in murine cells, and *in vivo* in aortic arc and descending aorta of diabetic mice. It has been shown, in primary mouse vascular smooth muscle cells (VSMC), that this process results from increased Thr430/Thr479-AKT *O*-GlcNAcylation, which promotes its activation and the expression of *osteogenic runt-related transcription factor 2* (*Runx2*) (81). AKT-mediated Runx2 stabilization by degradation of E3 ubiquitin ligase SMURF2 or by the nuclear exclusion of its transcription regulators FoxO could take part in this mechanism (82) (**Figure 2**). Thus, angiogenesis impairment and vessel obstruction are among the biological effects related to aberrant O-GlcNAcylation of AKT-mediated signaling involved in cardiovascular complications associated with diabetes.

Neurodegenerative Diseases

Dysregulated *O*-GlcNAcylation has been implicated in the pathogenesis of neurodegenerative disorders such as Alzheimer's disease (AD) and Parkinson's disease (83). Neurofibrillary degeneration associated with aggregation of abnormal

hyperphosphorylated tubulin-associated unit (Tau) proteins is one the features of AD. The latter undergoes a "Ying-Yang" competition mechanism between *O*-GlcNAcylation and phosphorylation (83). Using thiamet-G, a blood-brain barrier-permeable OGA inhibitor, several *in vivo* studies evidenced the ability of *O*-GlcNAcylation to protect against Tau aggregation (84–86). Increased levels of *O*-GlcNAcylation in mice brain by intracerebroventricular injection of thiamet-G is associated with Tau site-dependent increased and decreased phosphorylation further confirming the complex relation between modifications on Tau protein (87). Elevated phosphorylation of Tau at Ser199, Ser202, Ser396, and Ser422 is likely to result from the combination of increased Tau *O*-GlcNAcylation, PI3K-independent inhibition of Ser473-AKT phosphorylation and the subsequent over-activation of GSK3β, a key Tau kinase (87) (**Figure 2**). Elevated *O*-GlcNAcylation of proteins is found in Parkinson's disease postmortem brains (88). In rat primary cortical neurons, thiamet-G treatment increases accumulation of α-synuclein, a neuronal protein that aggregates in this pathology, through activation of mTOR and reduction of autophagy (88) (**Figure 2**). Conversely, α-synuclein is *O*-GlcNAcylated at Thr72 and Ser87, leading to reduced aggregation *in vitro* (89, 90). But, these discrepancies could be due to different experimental approaches. Evidence that excessive *O*-GlcNAcylation is detrimental to neurons by increasing α-synuclein accumulation was demonstrated *in vitro* and related to mTOR pathway (88), while *O*-GlcNAc-reduced aggregation of α-synuclein was demonstrated by biochemical approaches (89, 90). Taken together, these results indicate that the mitigation of pathological aggregation of neuronal proteins by direct *O*-GlcNAc modification is a complex mechanism that could be indirectly counterbalanced by AKT/mTOR signaling pathway.

Another common pathological hallmark of neurodegenerative diseases is the loss of neurons as a consequence of neuronal cell death (91). Although not yet studied in such pathological conditions, indirect evidence suggests that *O*-GlcNAcylation could be involved in the regulation of neuronal apoptosis. Elevation of protein *O*-GlcNAcylation after cerebral ischemia is responsible for *O*-GlcNAc-mediated AKT inhibition, BAD activation and neuronal apoptosis in mice (25). An increase of *O*-GlcNAcylation levels is also associated with a default in Thr308-AKT phosphorylation and cellular apoptosis during cortical differentiation of human embryonic stem cells (hESC) (92) (**Figure 2**). These studies strongly support that *O*-GlcNAc-mediated AKT inhibition might be involved in neuronal cell loss of function and apoptosis in neurodegenerative diseases.

CONCLUSION

Highlighted by the studies discussed above *O*-GlcNAcylation and the PI3K/AKT/mTOR signaling pathway appear to be intimately cross-linked. Both are considered as metabolic sensor that regulate folding, stability, subcellular localization, partner interaction, and therefore the activity of a plethora of targets involved in key biological functions. Here, we summarized evidence that *O*-GlcNAcylation can modulate the activation of the PI3K/AKT/mTOR signaling pathway by targeting different signaling actors, and that, reciprocally; expression, localization and activation of OGT are regulated by these signaling pathways (**Figure 1**). Although, further works are required to clarify the roles of *O*-GlcNAcylation on PI3K/AKT/mTOR regulation under normal physiological context, their interplay is highlighted by their associated dysregulation in several types of cancer, T2D, and cardiovascular and neurodegenerative diseases (**Figure 2**). Under pathological glucose conditions, aberrant *O*-GlcNAcylation levels result in activation or inhibition PI3K/AKT/mTOR signaling pathway as found in cancer and diabetes, respectively. Because of the key role of the PI3K/AKT/mTOR signaling pathway in cellular metabolism and physiology, these regulatory mechanisms contribute to pathogenicity by promoting, on one hand, glycolysis, proliferation, growth and invasion of cancer cells, and on the other hand, insulin resistance in insulin target tissues and/or pancreatic β cell dysfunction and death. Moreover, *O*-GlcNAc-mediated disturbance of AKT activity in endothelial cells leads to impairment of angiogenesis and vessel obstruction, supporting cardiovascular diseases associated with T2D. Finally, *O*-GlcNAcylation regulation of the PI3K/AKT/mTOR signaling pathway can indirectly modulate aggregation of neuronal proteins, such as Tau and α-synuclein that are involved in AD and Parkinson's disease, respectively, as well as in neuronal cell death. Taken together, evidence presented here shows that targeting OGT or OGA with selective small molecules to inhibit their activity or their interaction with specific actors of the PI3K/AKT/mTOR signaling pathway, in association with an adapted diet, may be a promising combined therapeutic approach to treat chronic metabolic-related diseases.

AUTHOR CONTRIBUTIONS

NV and IE concepted the plan and wrote the review. A-SV-E, TL, and SH revised it critically for important intellectual content.

FUNDING

SIte de Recherche Intégré sur le Cancer (SIRIC) ONCOLille and FR 3688 FRABio.

ACKNOWLEDGMENTS

The authors thank Mrs. Isabel Gonzales Mariscal (IBIMA—Hospital Regional de Malaga, Spain), a fluent English speaker, for the final reading of our manuscript. This work was supported by the Ligue Contre le Cancer/Comité du Nord, the Fondation ARC (Association pour la Recherche sur le Cancer), the Région Hauts de France (Cancer Regional Program), the University of Lille and the Centre National de la Recherche Scientifique. N.V. is the recipient of a fellowship from the Ministère de l'Enseignement Supérieur et de la Recherche.

REFERENCES

1. Kreppel LK, Blomberg MA, Hart GW. Dynamic glycosylation of nuclear and cytosolic proteins. Cloning and characterization of a unique O-GlcNAc transferase with multiple tetratricopeptide repeats. *J Biol Chem.* (1997) 272:9308–15.
2. Hu Y, Suarez J, Fricovsky E, Wang H, Scott BT, Trauger SA, et al. Increased enzymatic O-GlcNAcylation of mitochondrial proteins impairs mitochondrial function in cardiac myocytes exposed to high glucose. *J Biol Chem.* (2009) 284:547–55. doi: 10.1074/jbc.M808518200
3. Mishra S, Ande SR, Salter NW. O-GlcNAc modification: why so intimately associated with phosphorylation? *Cell Commun Signal* (2011) 9:1. doi: 10.1186/1478-811X-9-1
4. Wang Z, Gucek M, Hart GW. Cross-talk between O-GlcNAcylation and phosphorylation: site-specific phosphorylation dynamics in response to globally elevated O-GlcNAc. *Proc Natl Acad Sci USA.* (2008) 105:13793–8. doi: 10.1073/pnas.0806216105
5. Józwiak P, Forma E, Bryś M, Krześlak A. O-GlcNAcylation and Metabolic reprograming in Cancer. *Front Endocrinol.* (2014) 5:145. doi: 10.3389/fendo.2014.00145
6. Das A, Reis F, Maejima Y, Cai Z, Ren J. mTOR signaling in cardiometabolic disease, cancer, and aging. *Oxid Med Cell Longev.* (2017) 2017:6018675. doi: 10.1155/2017/6018675
7. Saxton RA, Sabatini DM. mTOR signaling in growth, metabolism, and disease. *Cell* (2017) 168:960–76. doi: 10.1016/j.cell.2017.02.004
8. Fruman DA, Chiu H, Hopkins BD, Bagrodia S, Cantley LC, Abraham RT. The PI3K pathway in human disease. *Cell* (2017) 170:605–35. doi: 10.1016/j.cell.2017.07.029
9. Manning BD, Toker A. AKT/PKB signaling: navigating the network. *Cell* (2017) 169:381–405. doi: 10.1016/j.cell.2017.04.001
10. Dibble CC, Manning BD. Signal integration by mTORC1 coordinates nutrient input with biosynthetic output. *Nat Cell Biol.* (2013) 15:555–64. doi: 10.1038/ncb2763
11. Antikainen H, Driscoll M, Haspel G, Dobrowolski R. TOR-mediated regulation of metabolism in aging. *Aging Cell* (2017) 16:1219–33. doi: 10.1111/acel.12689
12. Hart GW, Slawson C, Ramirez-Correa G, Lagerlof O. Cross talk between O-GlcNAcylation and phosphorylation: roles in signaling, transcription, and chronic disease. *Annu Rev Biochem.* (2011) 80:825–58. doi: 10.1146/annurev-biochem-060608-102511
13. Haltiwanger RS, Blomberg MA, Hart GW. Glycosylation of nuclear and cytoplasmic proteins. Purification and characterization of a uridine diphospho-N-acetylglucosamine:polypeptide beta-N-acetylglucosaminyltransferase. *J Biol Chem.* (1992) 267:9005–13.
14. Whelan SA, Lane MD, Hart GW. Regulation of the O-Linked β-N-Acetylglucosamine transferase by insulin signaling. *J Biol Chem.* (2008) 283:21411–7. doi: 10.1074/jbc.M800677200
15. Yang X, Ongusaha PP, Miles PD, Havstad JC, Zhang F, So WV, et al. Phosphoinositide signalling links O-GlcNAc transferase to insulin resistance. *Nature* (2008) 451:964–9. doi: 10.1038/nature06668
16. Perez-Cervera Y, Dehennaut V, Gil MA, Guedri K, Mata CJS, Stichelen SO-V, et al. Insulin signaling controls the expression of O-GlcNAc transferase and its interaction with lipid microdomains. *FASEB J.* (2013) 27:3478–86. doi: 10.1096/fj.12-217984
17. Whelan SA, Dias WB, Thiruneelakantapillai L, Lane MD, Hart GW. Regulation of insulin receptor substrate 1 (IRS-1)/AKT kinase-mediated insulin signaling by O-Linked β-N-acetylglucosamine in 3T3-L1 adipocytes. *J Biol Chem.* (2010) 285:5204–11. doi: 10.1074/jbc.M109.077818
18. Bullen JW, Balsbaugh JL, Chanda D, Shabanowitz J, Hunt DF, Neumann D, et al. Cross-talk between two essential nutrient-sensitive enzymes. *J Biol Chem.* (2014) 289:10592–606. doi: 10.1074/jbc.M113.523068
19. Xu Q, Yang C, Du Y, Chen Y, Liu H, Deng M, et al. AMPK regulates histone H2B O-GlcNAcylation. *Nucleic Acids Res.* (2014) 42:5594–604. doi: 10.1093/nar/gku236
20. Patti ME, Virkamäki A, Landaker EJ, Kahn CR, Yki-Järvinen H. Activation of the hexosamine pathway by glucosamine *in vivo* induces insulin resistance of early postreceptor insulin signaling events in skeletal muscle. *Diabetes* (1999) 48:1562–71.
21. Park SY, Ryu J, Lee W. O-GlcNAc modification on IRS-1 and Akt2 by PUGNAc inhibits their phosphorylation and induces insulin resistance in rat primary adipocytes. *Exp Mol Med.* (2005) 37:220–9. doi: 10.1038/emm.2005.30
22. Klein AL, Berkaw MN, Buse MG, Ball LE. O-linked N-acetylglucosamine modification of insulin receptor substrate-1 occurs in close proximity to multiple SH2 domain binding motifs. *Mol Cell Proteomics* (2009) 8:2733–45. doi: 10.1074/mcp.M900207-MCP200
23. Federici M, Menghini R, Mauriello A, Hribal ML, Ferrelli F, Lauro D, et al. Insulin-dependent activation of endothelial nitric oxide synthase is impaired by O-linked glycosylation modification of signaling proteins in human coronary endothelial cells. *Circulation* (2002) 106:466–72. doi: 10.1161/01.CIR.0000023043.02648.51
24. Ball LE, Berkaw MN, Buse MG. Identification of the major site of O-linked β-N-acetylglucosamine modification in the C terminus of insulin receptor substrate-1. *Mol Cell Proteomics* (2006) 5:313–23. doi: 10.1074/mcp.M500314-MCP200
25. Shi J, Gu J, Dai C, Gu J, Jin X, Sun J, et al. O-GlcNAcylation regulates ischemia-induced neuronal apoptosis through AKT signaling. *Sci Rep.* (2015) 5:14500. doi: 10.1038/srep14500
26. Wang S, Huang X, Sun D, Xin X, Pan Q, Peng S, et al. Extensive Crosstalk between O-GlcNAcylation and Phosphorylation Regulates Akt Signaling. *PLoS ONE* (2012) 7:e0037427 doi: 10.1371/journal.pone.0037427
27. Kang E-S, Han D, Park J, Kwak TK, Oh M-A, Lee S-A, et al. O-GlcNAc modulation at Akt1 Ser473 correlates with apoptosis of murine pancreatic beta cells. *Exp Cell Res.* (2008) 314:2238–48. doi: 10.1016/j.yexcr.2008.04.014
28. Miller WP, Mihailescu ML, Yang C, Barber AJ, Kimball SR, Jefferson LS, et al. The translational repressor 4E-BP1 contributes to diabetes-induced visual dysfunction. *Invest Ophthalmol Vis Sci.* (2016) 57:1327–37. doi: 10.1167/iovs.15-18719
29. Zeidan Q, Wang Z, De Maio A, Hart GW. O-GlcNAc cycling enzymes associate with the translational machinery and modify core ribosomal proteins. *Mol Biol Cell* (2010) 21:1922–36. doi: 10.1091/mbc.E09-11-0941
30. Wilcox G. Insulin and insulin resistance. *Clin Biochem Rev.* (2005) 26:19–39.
31. Ferrer CM, Sodi VL, Reginato MJ. O-GlcNAcylation in cancer biology: linking metabolism and signaling. *J Mol Biol.* (2016) 428:3282–94. doi: 10.1016/j.jmb.2016.05.028
32. Courtnay R, Ngo DC, Malik N, Ververis K, Tortorella SM, Karagiannis TC. Cancer metabolism and the Warburg effect: the role of HIF-1 and PI3K. *Mol Biol Rep.* (2015) 42:841–51. doi: 10.1007/s11033-015-3858-x
33. Olivier-Van Stichelen S, Drougat L, Dehennaut V, El Yazidi-Belkoura I, Guinez C, Mir A-M, et al. Serum-stimulated cell cycle entry promotes ncOGT synthesis required for cyclin D expression. *Oncogenesis* (2012) 1:e36. doi: 10.1038/oncsis.2012.36
34. Park S, Pak J, Jang I, Cho J. Inhibition of mTOR affects protein stability of OGT. *Biochem Biophys Res Commun.* (2014) 453:208–12. doi: 10.1016/j.bbrc.2014.05.047
35. Very N, Steenackers A, Dubuquoy C, Vermuse J, Dubuquoy L, Lefebvre T, et al. Cross regulation between mTOR signaling and O-GlcNAcylation. *J Bioenerg Biomembr.* (2018) 50:213–22. doi: 10.1007/s10863-018-9747-y
36. Sodi VL, Khaku S, Krutilina R, Schwab LP, Vocadlo DJ, Seagroves TN, et al. mTOR/MYC Axis Regulates O-GlcNAc Transferase (OGT) expression and O-GlcNAcylation in breast Cancer. *Mol Cancer Res.* (2015) 13:923–33. doi: 10.1158/1541-7786.MCR-14-0536
37. Zhang X, Qiao Y, Wu Q, Chen Y, Zou S, Liu X, et al. The essential role of YAP O-GlcNAcylation in high-glucose-stimulated liver tumorigenesis. *Nat Commun.* (2017) 8:15280. doi: 10.1038/ncomms15280
38. Xia H, Dai X, Yu H, Zhou S, Fan Z, Wei G, et al. EGFR-PI3K-PDK1 pathway regulates YAP signaling in hepatocellular carcinoma: the mechanism and its implications in targeted therapy. *Cell Death Dis.* (2018) 9:269. doi: 10.1038/s41419-018-0302-x
39. Zhao Y, Montminy T, Azad T, Lightbody E, Hao Y, SenGupta S, et al. PI3K positively regulates YAP and TAZ in mammary tumorigenesis through multiple signaling pathways. *Mol Cancer Res.* (2018) 16:1046–58. doi: 10.1158/1541-7786.MCR-17-0593

40. Tumaneng K, Schlegelmilch K, Russell RC, Yimlamai D, Basnet H, Mahadevan N, et al. YAP mediates crosstalk between the Hippo and PI(3)K–TOR pathways by suppressing PTEN via miR-29. *Nat Cell Biol.* (2012) 14:1322–9. doi: 10.1038/ncb2615
41. Zhang B, Zhou P, Li X, Shi Q, Li D, Ju X. Bitterness in sugar: O-GlcNAcylation aggravates pre-B acute lymphocytic leukemia through glycolysis via the PI3K/Akt/c-Myc pathway. *Am J Cancer Res.* (2017) 7:1337–49.
42. Onodera Y, Nam J-M, Bissell MJ. Increased sugar uptake promotes oncogenesis via EPAC/RAP1 and O-GlcNAc pathways. *J Clin Invest.* (2014) 124:367–84. doi: 10.1172/JCI63146
43. Diehl JA, Cheng M, Roussel MF, Sherr CJ. Glycogen synthase kinase-3β regulates cyclin D1 proteolysis and subcellular localization. *Genes Dev.* (1998) 12:3499–511.
44. Kanwal S, Fardini Y, Pagesy P, N'tumba-Byn T, Pierre-Eugène C, Masson E, et al. O-GlcNAcylation-inducing treatments inhibit estrogen receptor α expression and confer resistance to 4-OH-tamoxifen in human breast cancer-derived MCF-7 cells. *PLoS ONE* (2013) 8:e69150. doi: 10.1371/journal.pone.0069150
45. Krześlak A, Józwiak P, Lipinska A. Down-regulation of β-N-acetyl-D-glucosaminidase increases Akt1 activity in thyroid anaplastic cancer cells. *Oncol Rep.* (2011) 26:743–9. doi: 10.3892/or.2011.1333
46. Jones DR, Keune W-J, Anderson KE, Stephens LR, Hawkins PT, Divecha N. The hexosamine biosynthesis pathway and O-GlcNAcylation maintain insulin-stimulated PI3K-PKB phosphorylation and tumour cell growth after short-term glucose deprivation. *FEBS J.* (2014) 281:3591–608. doi: 10.1111/febs.12879
47. Zhang N, Chen X. Potential role of O-GlcNAcylation and involvement of PI3K/Akt1 pathway in the expression of oncogenic phenotypes of gastric cancer cells *in vitro*. *Biotechnol Appl Biochem.* (2016) 63:841–51. doi: 10.1002/bab.1441
48. Zhang P, Wang C, Ma T, You S. O-GlcNAcylation enhances the invasion of thyroid anaplastic cancer cells partially by PI3K/Akt1 pathway. *Onco Targets Ther.* (2015) 8:3305–13. doi: 10.2147/OTT.S82845
49. Manning BD, Cantley LC. AKT/PKB signaling: navigating downstream. *Cell* (2007) 129:1261–74. doi: 10.1016/j.cell.2007.06.009
50. Soesanto YA, Luo B, Jones D, Taylor R, Gabrielsen JS, Parker et al. Regulation of Akt signaling by O-GlcNAc in euglycemia. *Am J Physiol Endocrinol Metab.* (2008) 295:E974–980. doi: 10.1152/ajpendo.90366.2008
51. Phoomak C, Silsirivanit A, Park D, Sawanyawisuth K, Vaeteewoottacharn K, Wongkham C, et al. O-GlcNAcylation mediates metastasis of cholangiocarcinoma through FOXO3 and MAN1A1. *Oncogene* (2018). doi: 10.1038/s41388-018-0366-1. [Epub ahead of print].
52. Ishimura E, Nakagawa T, Moriwaki K, Hirano S, Matsumori Y, Asahi M. Augmented O-GlcNAcylation of AMP-activated kinase promotes the proliferation of LoVo cells, a colon cancer cell line. *Cancer Sci.* (2017) 108:2373–82. doi: 10.1111/cas.13412
53. Ferrer CM, Lynch TP, Sodi VL, Falcone JN, Schwab LP, Peacock DL, et al. O-GlcNAcylation regulates cancer metabolism and survival stress signaling via regulation of the HIF-1 pathway. *Mol Cell* (2014) 54:820–31. doi: 10.1016/j.molcel.2014.04.026
54. Dienstmann R, Rodon J, Serra V, Tabernero J. Picking the point of inhibition: a comparative review of PI3K/AKT/mTOR pathway inhibitors. *Mol Cancer Ther.* (2014) 13:1021–31. doi: 10.1158/1535-7163.MCT-13-0639
55. Kwei KA, Baker JB, Pelham RJ. Modulators of sensitivity and resistance to inhibition of PI3K identified in a pharmacogenomic screen of the NCI-60 human tumor cell line collection. *PLoS ONE* (2012) 7:e46518. doi: 10.1371/journal.pone.0046518
56. Lehman DM, Fu D-J, Freeman AB, Hunt KJ, Leach RJ, Johnson-Pais T, et al. A single nucleotide polymorphism in MGEA5 encoding O-GlcNAc-selective N-acetyl-beta-D glucosaminidase is associated with type 2 diabetes in Mexican Americans. *Diabetes* (2005) 54:1214–21. doi: 10.2337/diabetes.54.4.1214
57. Zhang H, Jia Y, Cooper JJ, Hale T, Zhang Z, Elbein SC. Common variants in glutamine:fructose-6-phosphate amidotransferase 2 (GFPT2) gene are associated with type 2 diabetes, diabetic nephropathy, and increased GFPT2 mRNA levels. *J Clin Endocrinol Metab.* (2004) 89:748–55. doi: 10.1210/jc.2003-031286
58. Fricovsky ES, Suarez J, Ihm S-H, Scott BT, Suarez-Ramirez JA, Banerjee I, et al. Excess protein O-GlcNAcylation and the progression of diabetic cardiomyopathy. *Am J Physiol Regul Integr Comp Physiol.* (2012) 303:R689–99. doi: 10.1152/ajpregu.00548.2011
59. Springhorn C, Matsha TE, Erasmus RT, Essop MF. Exploring leukocyte O-GlcNAcylation as a novel diagnostic tool for the earlier detection of type 2 diabetes mellitus. *J Clin Endocrinol Metab.* (2012) 97:4640–9. doi: 10.1210/jc.2012-2229
60. Park K, Saudek CD, Hart GW. Increased expression of β-N-acetylglucosaminidase in erythrocytes from individuals with pre-diabetes and diabetes. *Diabetes* (2010) 59:1845–50. doi: 10.2337/db09-1086
61. Ruan H-B, Han X, Li M-D, Singh JP, Qian K, Azarhoush S, et al. O-GlcNAc transferase/host cell factor C1 complex regulates gluconeogenesis by modulating PGC-1α stability. *Cell Metab.* (2012) 16:226–37. doi: 10.1016/j.cmet.2012.07.006
62. Shi H, Munk A, Nielsen TS, Daughtry MR, Larsson L, Li S, et al. Skeletal muscle O-GlcNAc transferase is important for muscle energy homeostasis and whole-body insulin sensitivity. *Mol Metab.* (2018) 11:160–77. doi: 10.1016/j.molmet.2018.02.010
63. Dentin R, Hedrick S, Xie J, Yates J, Montminy M. Hepatic glucose sensing via the CREB coactivator CRTC2. *Science* (2008) 319:1402–5. doi: 10.1126/science.1151363
64. Vosseller K, Wells L, Lane MD, Hart GW. Elevated nucleocytoplasmic glycosylation by O-GlcNAc results in insulin resistance associated with defects in Akt activation in 3T3-L1 adipocytes. *Proc Natl Acad Sci USA*. (2002) 99:5313–8. doi: 10.1073/pnas.072072399
65. McClain DA, Lubas WA, Cooksey RC, Hazel M, Parker GJ, Love DC, et al. Altered glycan-dependent signaling induces insulin resistance and hyperleptinemia. *Proc Natl Acad Sci USA*. (2002) 99:10695–9. doi: 10.1073/pnas.152346899
66. Sano H, Kane S, Sano E, Miinea CP, Asara JM, Lane WS, et al. Insulin-stimulated phosphorylation of a Rab GTPase-activating protein regulates GLUT4 translocation. *J Biol Chem*. (2003) 278:14599–602. doi: 10.1074/jbc.C300063200
67. Parker GJ, Lund KC, Taylor RP, McClain DA. Insulin resistance of glycogen synthase mediated by o-linked N-acetylglucosamine. *J Biol Chem*. (2003) 278:10022–7. doi: 10.1074/jbc.M207787200
68. Macauley MS, Bubb AK, Martinez-Fleites C, Davies GJ, Vocadlo DJ. Elevation of global O-GlcNAc Levels in 3T3-L1 adipocytes by selective inhibition of O-GlcNAcase does not induce insulin resistance. *J Biol Chem.* (2008) 283:34687–95. doi: 10.1074/jbc.M804525200
69. Macauley MS, Shan X, Yuzwa SA, Gloster TM, Vocadlo DJ. Elevation of global O-GlcNAc in rodents using a selective O-GlcNAcase inhibitor does not cause insulin resistance or perturb glucohomeostasis. *Chem Biol.* (2010) 17:949–58. doi: 10.1016/j.chembiol.2010.07.005
70. Arias EB, Kim J, Cartee GD. Prolonged incubation in PUGNAc results in increased protein O-Linked glycosylation and insulin resistance in rat skeletal muscle. *Diabetes* (2004) 53:921–30. doi: 10.2337/diabetes.53.4.921
71. Mehdy A, Morelle W, Rosnoblet C, Legrand D, Lefebvre T, Duvet S, et al. PUGNAc treatment leads to an unusual accumulation of free oligosaccharides in CHO cells. *J Biochem*. (2012) 151:439–46. doi: 10.1093/jb/mvs012
72. Dehennaut V, Lefebvre T. Proteomics and PUGNAcity will overcome questioning of insulin resistance induction by nonselective inhibition of O-GlcNAcase. *Proteomics* (2013) 13:2944–6. doi: 10.1002/pmic.201300363
73. Akimoto Y, Hart GW, Wells L, Vosseller K, Yamamoto K, Munetomo E, et al. Elevation of the post-translational modification of proteins by O-linked N-acetylglucosamine leads to deterioration of the glucose-stimulated insulin secretion in the pancreas of diabetic Goto-Kakizaki rats. *Glycobiology* (2007) 17:127–40. doi: 10.1093/glycob/cwl067
74. Alejandro EU, Bozadjieva N, Kumusoglu D, Abdulhamid S, Levine H, Haataja L, et al. Disruption of O-linked N-acetylglucosamine signaling induces ER stress and β-cell failure. *Cell Rep*. (2015) 13:2527–38. doi: 10.1016/j.celrep.2015.11.020
75. Vaidyanathan K, Wells L. Multiple tissue-specific roles for the O-GlcNAc post-translational modification in the induction of and complications arising from type II diabetes. *J Biol Chem*. (2014) 289:34466–71. doi: 10.1074/jbc.R114.591560
76. Ma J, Hart GW. Protein O-GlcNAcylation in diabetes and diabetic complications. *Expert Rev Proteomics* (2013) 10:365–80. doi: 10.1586/14789450.2013.820536

77. Luo B, Soesanto Y, McClain DA. Protein modification by O-linked GlcNAc reduces angiogenesis by inhibiting Akt activity in endothelial cells. *Arterioscler Thromb Vasc Biol*. (2008) 28:651–7. doi: 10.1161/ATVBAHA.107.159533
78. Zoccali C. Endothelial dysfunction, nitric oxide bioavailability, and asymmetric dimethyl arginine. In: *Cardiorenal Syndrome: Mechanisms, Risk and Treatment*. Berbari AE, Mancia G, editors. Milano: Springer Milan (2010). p. 235–244. doi: 10.1007/978-88-470-1463-3_17
79. Ritchie SA, Kohlhaas CF, Boyd AR, Yalla KC, Walsh K, Connell JMC, et al. Insulin-stimulated phosphorylation of endothelial nitric oxide synthase at serine-615 contributes to nitric oxide synthesis. *Biochem J*. (2010) 426:85–90. doi: 10.1042/BJ20091580
80. Karar J, Maity A. PI3K/AKT/mTOR Pathway in Angiogenesis. *Front Mol Neurosci*. (2011) 4:51 doi: 10.3389/fnmol.2011.00051
81. Heath JM, Sun Y, Yuan K, Bradley WE, Litovsky S, Dell'Italia LJ, et al. Activation of AKT by O-GlcNAcylation induces vascular calcification in diabetes. *Circ Res*. (2014) 114:1094–102. doi: 10.1161/CIRCRESAHA.114.302968
82. Cohen-Solal KA, Boregowda RK, Lasfar A. RUNX2 and the PI3K/AKT axis reciprocal activation as a driving force for tumor progression. *Mol Cancer* (2015) 14:137. doi: 10.1186/s12943-015-0404-3
83. Ma X, Li H, He Y, Hao J. The emerging link between O-GlcNAcylation and neurological disorders. *Cell Mol Life Sci*. (2017) 74:3667–86. doi: 10.1007/s00018-017-2542-9
84. Yuzwa SA, Macauley MS, Heinonen JE, Shan X, Dennis RJ, He Y, et al. A potent mechanism-inspired O-GlcNAcase inhibitor that blocks phosphorylation of tau *in vivo*. *Nat Chem Biol*. (2008) 4:483–90. doi: 10.1038/nchembio.96
85. Yuzwa SA, Shan X, Macauley MS, Clark T, Skorobogatko Y, Vosseller K, et al. Increasing O-GlcNAc slows neurodegeneration and stabilizes tau against aggregation. *Nat Chem Biol*. (2012) 8:393–9. doi: 10.1038/nchembio.797
86. Borghgraef P, Menuet C, Theunis C, Louis JV, Devijver H, Maurin H, et al. Increasing brain protein O-GlcNAcylation mitigates breathing defects and mortality of Tau.P301L mice. *PLoS ONE* (2013) 8:e0084442. doi: 10.1371/journal.pone.0084442
87. Yu Y, Zhang L, Li X, Run X, Liang Z, Li Y, et al. Differential effects of an O-GlcNAcase inhibitor on tau phosphorylation. *PLoS ONE* (2012) 7:e0035277. doi: 10.1371/journal.pone.0035277
88. Wani WY, Ouyang X, Benavides GA, Redmann M, Cofield SS, Shacka JJ, et al. O-GlcNAc regulation of autophagy and α-synuclein homeostasis; implications for Parkinson's disease. *Mol Brain* (2017) 10:32. doi: 10.1186/s13041-017-0311-1
89. Marotta NP, Lin YH, Lewis YE, Ambroso MR, Zaro BW, Roth MT, et al. O-GlcNAc modification blocks the aggregation and toxicity of the Parkinson's disease associated protein α-synuclein. *Nat Chem.* (2015) 7:913–20. doi: 10.1038/nchem.2361
90. Zhang J, Lei H, Chen Y, Ma Y-T, Jiang F, Tan J, et al. Enzymatic O-GlcNAcylation of α-synuclein reduces aggregation and increases SDS-resistant soluble oligomers. *Neurosci Lett.* (2017) 655:90–4. doi: 10.1016/j.neulet.2017.06.034
91. Gorman AM. Neuronal cell death in neurodegenerative diseases: recurring themes around protein handling. *J Cell Mol Med*. (2008) 12:2263–80. doi: 10.1111/j.1582-4934.2008.00402.x
92. Parween S, Varghese DS, Ardah MT, Prabakaran AD, Mensah-Brown E, Emerald BS, et al. Higher O-GlcNAc levels are associated with defects in progenitor proliferation and premature neuronal differentiation during *in-vitro* human embryonic cortical neurogenesis. *Front Cell Neurosci.* (2017) 11:e00415. doi: 10.3389/fncel.2017.00415

Conflict of Interest Statement: The authors declare that the research was conducted in the absence of any commercial or financial relationships that could be construed as a potential conflict of interest.

frontiers in Endocrinology

ORIGINAL RESEARCH
published: 15 October 2018
doi: 10.3389/fendo.2018.00606

A Novel Glycoproteomics Workflow Reveals Dynamic O-GlcNAcylation of COPγ1 as a Candidate Regulator of Protein Trafficking

*Nathan J. Cox[1], Peter M. Luo[1], Timothy J. Smith[1], Brittany J. Bisnett[1], Erik J. Soderblom[2] and Michael Boyce[1]**

[1] Department of Biochemistry, Duke University School of Medicine, Durham, NC, United States, [2] Proteomics and Metabolomics Core Facility, Center for Genomic and Computational Biology, Duke University, Durham, NC, United States

O-linked β-N-acetylglucosamine (O-GlcNAc) is an abundant and essential intracellular form of protein glycosylation in animals and plants. In humans, dysregulation of O-GlcNAcylation occurs in a wide range of diseases, including cancer, diabetes, and neurodegeneration. Since its discovery more than 30 years ago, great strides have been made in understanding central aspects of O-GlcNAc signaling, including identifying thousands of its substrates and characterizing the enzymes that govern it. However, while many O-GlcNAcylated proteins have been reported, only a small subset of these change their glycosylation status in response to a typical stimulus or stress. Identifying the functionally important O-GlcNAcylation changes in any given signaling context remains a significant challenge in the field. To address this need, we leveraged chemical biology and quantitative mass spectrometry methods to create a new glycoproteomics workflow for profiling stimulus-dependent changes in O-GlcNAcylated proteins. In proof-of-principle experiments, we used this new workflow to interrogate changes in O-GlcNAc substrates in mammalian protein trafficking pathways. Interestingly, our results revealed dynamic O-GlcNAcylation of COPγ1, an essential component of the coat protein I (COPI) complex that mediates Golgi protein trafficking. Moreover, we detected 11 O-GlcNAc moieties on COPγ1 and found that this modification is reduced by a model secretory stress that halts COPI trafficking. Our results suggest that O-GlcNAcylation may regulate the mammalian COPI system, analogous to its previously reported roles in other protein trafficking pathways. More broadly, our glycoproteomics workflow is applicable to myriad systems and stimuli, empowering future studies of O-GlcNAc in a host of biological contexts.

Keywords: O-GlcNAc, glycoproteomics, SILAC, click chemistry, COPI vesicle trafficking, protein secretion

OPEN ACCESS

Edited by:
Tony Lefebvre, Lille University of Science and Technology, France

Reviewed by:
Francois Foulquier, Centre National de la Recherche Scientifique (CNRS), France
Ikram Belkoura El Yazidi, Lille University of Science and Technology, France

***Correspondence:**
Michael Boyce
michael.boyce@duke.edu

Specialty section:
This article was submitted to Molecular and Structural Endocrinology, a section of the journal Frontiers in Endocrinology

Received: *21 May 2018*
Accepted: *24 September 2018*
Published: *15 October 2018*

Citation:
Cox NJ, Luo PM, Smith TJ, Bisnett BJ, Soderblom EJ and Boyce M (2018) A Novel Glycoproteomics Workflow Reveals Dynamic O-GlcNAcylation of COPγ1 as a Candidate Regulator of Protein Trafficking. Front. Endocrinol. 9:606. doi: 10.3389/fendo.2018.00606

INTRODUCTION

O-linked β-N-acetylglucosamine (O-GlcNAc) is a major, dynamic post-translational modification (PTM), added by O-GlcNAc transferase (OGT) and removed by O-GlcNAcase (OGA) from serine and threonine residues of intracellular proteins (1–7). O-GlcNAc is broadly conserved among animals, plants and other organisms, and O-GlcNAcylation controls a wide range of cellular

functions, such as nutrient sensing, metabolism and gene expression (1–8). Importantly, aberrant O-GlcNAc cycling is also implicated in numerous human diseases, including cancer (2, 9–12), diabetes (13–16), cardiac dysfunction (17–20), and neurodegeneration (21–24).

Despite this broad pathophysiological significance, major questions about O-GlcNAc signaling remain. For example, O-GlcNAcylation regulates diverse cellular processes and modifies thousands of intracellular proteins, but only a small fraction of substrates change their glycosylation status in response to any given signal or condition (1–4, 25, 26). A central challenge in the field is to identify the most functionally relevant O-GlcNAc changes in response to a stimulus of interest. However, because O-GlcNAc is a transient and sub-stoichiometric PTM, it can be difficult to study with traditional molecular biology or genetics alone.

To address this challenge, we previously reported a two-step chemical biology method to tag and purify O-GlcNAc substrates from live mammalian cells (27–31). Briefly, cells are first metabolically labeled with a peracetylated N-azidoacetylgalactosamine (GalNAz), a synthetic, azide-bearing monosaccharide that is non-toxic and cell-permeable (28, 32). GalNAz is accepted by sugar salvage and epimerase enzymes, resulting in the biosynthesis of a nucleotide-azidosugar, "UDP-GlcNAz," which is used by OGT to install an "O-GlcNAz" moiety onto its native substrates (28). O-GlcNAz can then be tagged via chemical ligation to an alkyne-functionalized probe. Azides and alkynes engage in a copper-catalyzed [3+2] cycloaddition, often called "click chemistry," that proceeds rapidly under biocompatible conditions (33–36). The click reaction between O-GlcNAz moieties and the alkyne probe provides exquisitely specific labeling of OGT substrates with useful handles (e.g., biotin, fluorophores) for downstream analysis (27–31). Because GalNAz treatment labels endogenous OGT substrates, it affords time-resolved tagging of O-GlcNAcylated proteins, without the need for a priori knowledge of their identities. We have previously used this strategy to dissect the functional role of O-GlcNAc in a variety of cell biological contexts (28–31).

We envisioned combining GalNAz labeling with quantitative proteomics to discover changes in O-GlcNAcylated proteins in response to physiological stimuli, stresses, or other cues. As a model cellular process for these proof-of-principle experiments, we selected protein trafficking. More than a third of mammalian proteins transit the secretory system to localize to, and recycle from, specific subcellular locations, including the endoplasmic reticulum (ER), Golgi, plasma membrane, endosomes, lysosomes, and the extracellular space (37–39). In most instances, dedicated protein machinery effects the formation and trafficking of vesicles between discrete locations, as in clathrin-mediated endocytosis from the plasma membrane to endosomes (40), coat protein complex II (COPII)-facilitated transport from the ER to Golgi (41–46), and COPI-mediated trafficking among the Golgi cisternae and from the Golgi to the ER (47–49). Properly regulated protein trafficking is critical for cell and tissue physiology, particularly in professional secretory cell types and organs, including the endocrine system. Indeed, protein trafficking is essential in all eukaryotes and is dysregulated in a wide range of human diseases (44–46).

While the fundamental biochemical steps of vesicle assembly are relatively well understood for some systems (e.g., clathrin, COPII, and COPI), much less is known about how vertebrate cells dynamically adjust trafficking activity in response to developmental cues, fluctuating signals, metabolic demands, or stress (44–46). Interestingly, however, several studies have implicated O-GlcNAc in regulating multiple protein trafficking pathways. For example, key COPII proteins are O-GlcNAcylated (28, 50–53), and we recently demonstrated that specific glycosylation sites on Sec23A, a core COPII protein, are required for its ability to mediate collagen trafficking in both cultured human cells and developing vertebrate embryos (54). Other studies have indicated a role for O-GlcNAc in regulating synaptic vesicle trafficking and clathrin-mediated endocytosis as well (55–63). Taken together, these reports suggest that O-GlcNAc may be a broad regulator of protein trafficking. However, the extent and functional effects of O-GlcNAcylation in mammalian trafficking pathways remain largely uncharacterized.

Here, we leverage GalNAz metabolic labeling and quantitative proteomics to create a novel workflow for identifying stimulus-induced changes in O-GlcNAcylated proteins. In a pilot experiment, we used this glycoproteomics workflow to investigate the role of O-GlcNAc in mammalian protein trafficking. Our results indicate that COPγ1, an essential component of the COPI complex, is dynamically O-GlcNAcylated on up to 11 distinct sites under control conditions but deglycosylated upon perturbation of protein secretion. Our study is the first report of COPI protein O-GlcNAcylation and suggests that O-GlcNAc may regulate mammalian intra-Golgi and/or retrograde Golgi-to-ER protein trafficking. More broadly, we expect that our glycoproteomics strategy will be readily extensible to a wide spectrum of experimental stimuli, conditions and systems beyond protein trafficking, permitting the study of O-GlcNAc function in diverse biological contexts.

MATERIALS AND METHODS

Chemical Synthesis

Thiamet-G and Ac_4GalNAz were synthesized as described (28, 64) by the Duke Small Molecule Synthesis Facility. All other chemicals were purchased from Sigma-Aldrich unless otherwise indicated.

Cell Culture

Ramos cells were cultured in Roswell Park Memorial Institute medium (RPMI) containing 10% fetal bovine serum (FBS), 100 units/ml penicillin, and 100 μg/ml streptomycin in 5% CO_2 at 37°C. FL5.12 (parental N6 and XL4.1 lines) were cultured in RPMI containing 10% FBS, 100 units/ml penicillin, 100 μg/ml streptomycin, 55 μM β-mercaptoethanol, 2 mM L-glutamine, 10 mM HEPES and 500 pg/ml recombinant mouse IL-3 (eBioscience) in 5% CO_2 at 37°C.

Cell Viability Assays

Ten thousand Parental FL5.12 (N6) cells in 100 μl RPMI were seeded into clear-bottom 96-well plates and treated with a dose range of brefeldin A (BFA) for 4 or 24 h. Both MTS (Promega, CellTiter 96 AQueous Proliferation Assay) and ATP (Promega, CellTiter-Glo Luminescent Cell Viability Assay) assays were performed according to the manufacturer's instructions. Independent replicates were evaluated by a 2 × 2 analysis of variance (ANOVA), with BFA dose and treatment time as the independent factors. *Post-hoc* tests for differences between BFA doses and treatment times were conducted with Tukey's honestly significant difference (HSD) test using SAS/JMP software, Version 13.0.0 (SAS Institute Inc.). Significance was defined as $p < 0.05$ (two-tailed).

Alkyne-Biotin Click Reactions and Affinity Purification

Cells were treated with 100 μM GalNAz up to 24 h prior to harvesting. After harvesting, cells were lysed in click buffer (1% Triton X-100, 1% SDS, 150 mM NaCl, 20 mM Tris pH 7.4) supplemented with protease inhibitors, 5 μM PUGNAc and 50 μM UDP to inhibit hexosaminidases and OGT, respectively. Click reactions were assembled on an ice bucket. The following reaction components were added, in order, to the listed final concentration: protein sample, 5 mM sodium ascorbate, 25 μM alkyne-biotin, 100 μM Tris[(1-benzyl-1H-1,2,3-triazol-4-yl)methyl]amine (TBTA), 1 mM $CuSO_4$. Reactions were mixed, rotated gently at room temperature for 1 h and then quenched by addition of 10 mM EDTA (final). For immediate analysis, SDS-PAGE sample buffer was added directly to reactions. For further processing and affinity purification, unreacted alkyne-biotin was removed by methanol-precipitation as follows. Reactions were mixed with ice-cold methanol (10:1 methanol:sample by volume). After mixing, samples were placed on dry ice or incubated at −80°C for 10 min to increase protein precipitation and then centrifuged at 17,000 g to pellet. Supernatants were removed and pellets were resuspended in methanol and placed on ice. This process was repeated a total of four times. After the final precipitation, the protein pellet was dissolved in 4 M guanidine in phosphate-buffered saline (PBS). Biotinylated proteins were captured from the samples by incubating overnight at 4°C with gentle rotation with NeutrAvidin beads (ThermoFisher, Pierce High Capacity NeutrAvidin Agarose). The following day, beads were washed three times with the following buffers, in order: 4 M guanidine in PBS, 5 M NaCl in H_2O, 6 M urea in PBS, and 1% SDS in PBS. Captured proteins were eluted by boiling in 2X SDS-PAGE sample buffer. Reserved input samples in 4 M guanidine were buffer-exchanged into SDS-PAGE buffer via spin column (BioRad, Bio-Spin 6).

Immunoblotting (IB)

IBs were performed via standard methods as previously described (54). The following primary antibodies were used: mouse monoclonal anti-tubulin (T6074, Sigma-Aldrich; 1:100,000), mouse monoclonal anti-biotin (B7653, Sigma-Aldrich, 1:2,000), mouse monoclonal anti-nucleoporin p62 (610498, BD Biosciences, 1:2,000), mouse monoclonal anti-COPγ1 (sc-393977, Santa Cruz Biotechnology, 1:1,000), mouse monoclonal anti-O-GlcNAc antibody 18B10 (MA1-038, ThermoFisher; 1:1,000), mouse monoclonal anti-O-GlcNAc antibody RL2 (SC-59624, Santa Cruz Biotech; 1:500). The following secondary antibody was used: goat anti-mouse IgG (1030-05, horseradish peroxidase (HRP)-conjugated, SouthernBiotech; 1:10,000).

SILAC Labeling

RPMI 1640 medium lacking L-lysine and L-arginine (ThermoFisher) was supplemented with 10% dialyzed and heat-inactivated FBS (Corning), 1% penicillin/streptomycin and amino acids. "Heavy" medium was supplemented with 12.5 mg $^{13}C_6^{15}N_4$-arginine, 12.5 mg $^{13}C_6^{15}N_2$-lysine, and 5 mg proline per 500 ml. "Light" medium was supplemented with 12.5 mg arginine, 12.5 mg lysine, and 5 mg proline per 500 ml. Proline supplementation prevents conversion of arginine to proline (65). XL4.1 cells were passaged for at least 7 doublings in either heavy or light SILAC medium to achieve >99% isotope incorporation. Isotope incorporation was verified via MS at the Duke Proteomics Facility. Full proteomics data are available as Excel files in the **Supplemental Material**.

Subcellular Fractionation

Cells were washed once with cold PBS and resuspended in 5 ml of ice-cold Buffer A (1.5 mM $MgCl_2$, 10 mM KCl, 10 mM HEPES, pH 7.9) supplemented with protease inhibitors, 5 μM PUGNAc and 50 μM UDP. Cells were lysed using a pre-chilled Dounce homogenizer and ∼30 strokes with a tight pestle. Cell integrity was monitored using a hemocytometer. After Douncing, samples were centrifuged at 228 g for 5 min at 4°C, yielding a crude cytoplasmic fraction (supernatant) and a crude nuclear fraction (pellet). Crude nuclear fractions were resuspended in 3 ml of Buffer S1 (0.35 M sucrose, 0.5 mM $MgCl_2$) supplemented with protease inhibitors, PUGNAc and UDP, layered over a cushion of Buffer S3 (0.88 M sucrose, 0.5 mM $MgCl_2$) and centrifuged at 2,800 g for 10 min at 4°C to obtain a pure nuclear pellet. Crude cytoplasmic fractions were centrifuged at >400,000 g for 1 h at 4°C to obtain a pure cytoplasmic fraction (supernatant). Pure nuclear pellets were lysed in click buffer and pure cytoplasmic fractions were supplemented with appropriate concentrations of click buffer ingredients.

Proteomic Analysis of BFA-Induced Changes in O-GlcNacylated Proteins

XL4.1 cells were seeded at 500,000 cells/ml the day before treatment. Cells were treated with 100 μM GalNAz alone for 2 h, then 500 ng/ml BFA or DMSO (vehicle) was added, and cells were harvested 4 h later. Heavy- and light-labeled cells were pooled 1:1, washed twice with cold PBS and fractionated as above. Protein amounts were quantified by BCA Assay (ThermoFisher) and 2 mg of nuclear or cytoplasmic protein was processed further. Alkyne-agarose beads (Click Chemistry Tools) were washed three times in click buffer. Protein samples were precleared with 150 μl bead volume of washed alkyne-agarose beads with gentle rotation for 2 h at room temperature. After

preclearing, supernatants were removed and combined with 50 µl of equilibrated alkyne-agarose beads, 5 mM sodium ascorbate, 100 µM TBTA and 1 mM $CuSO_4$. Reactions were rotated at room temperature for 2 h and then quenched by addition of 10 mM EDTA. Beads were washed sequentially with three 1 ml washes of each of the following: 1% SDS, 20 mM Tris pH 7.4; 1% SDS, 10 mM dithiothreitol (DTT), 20 mM Tris pH 7.4; 1X PBS; 8 M urea; 1X PBS; 6 M guanidine hydrochloride; 1X PBS; 5 M NaCl; 1X PBS; 10X PBS; 1X PBS; 20% isopropanol; 20% acetonitrile; 50 mM ammonium bicarbonate. Washed beads were stored at 4°C in 100 µl 50 mM ammonium bicarbonate until they were submitted for on-bead trypsin digestion, LC-MS/MS analysis and quantification at the Duke Proteomics Facility.

Sample Preparation and Nano-Flow Liquid Chromatography Electrospray Ionization Tandem Mass Spectrometry (LC-MS/MS) Analysis of SILAC Samples

Samples immobilized on alkyne-agarose beads were washed three times with 50 mM ammonium bicarbonate, pH 8.0 and suspended in 30 µl 50 mM ammonium bicarbonate, pH 8.0 supplemented with 0.1% Rapigest SF surfactant (Waters). Samples were reduced with 5 mM DTT for 30 min at 70°C and free sulfhydryls were alkylated with 10 mM iodoacetamide for 45 min at room temperature. Proteolytic digestion was accomplished by the addition of 500 ng sequencing grade trypsin (Promega) directly to the beads with incubation at 37°C for 18 h. Supernatants were collected following a 2-min centrifugation at 1,000 rpm, acidified to pH 2.5 with trifluoroacetic acid and incubated at 60°C for 1 h to hydrolyze the remaining Rapigest. Insoluble hydrolyzed surfactant was cleared by centrifugation at 15,000 rpm for 5 min. Samples were dried using vacuum centrifugation and resuspended in 20 µl of 2% acetonitrile/0.1% formic acid. Two microliters of each sample was subjected to chromatographic separation on a Waters NanoAquity UPLC equipped with a 1.7 µm BEH130 C_{18} 75 µm I.D. X 250 mm reversed-phase column. The mobile phase consisted of (A) 0.1% formic acid in water and (B) 0.1% formic acid in acetonitrile. Following a 5 µl injection, peptides were trapped for 5 min on a 5 µm Symmetry C_{18} 180 µm I.D. X 20 mm column at 20 µl/minute in 99.9% A. The analytical column was held at 5% B for 5 min, then switched in-line and a linear elution gradient of 5% B to 40% B was performed over 90 min at 300 nl/minute. The analytical column was connected to a fused silica PicoTip emitter (New Objective) with a 10 µm tip orifice and coupled to a QExactive Plus mass spectrometer through an electrospray interface. The instrument was set to acquire a precursor MS scan from *m/z* 375–1,600 with $r = 70{,}000$ at *m/z* 400 and a target AGC setting of 1e6 ions. In a data-dependent mode of acquisition, MS/MS spectra of the 10 most abundant precursor ions were acquired at $r = 17{,}500$ at m/z with a target AGC setting of 5e4 ions. Max fill times were set to 60 ms for full MS scans and 60 ms for MS/MS scans with minimum MS/MS triggering thresholds of 5,000 counts. For all experiments, fragmentation occurred with a higher-energy collisional dissociation setting of 27% and a dynamic exclusion of 60 s were employed for previously fragmented precursor ions.

Raw LC-MS/MS data files were processed in Mascot distiller (Matrix Science) and then submitted to independent Mascot database searches (Matrix Science) against SwissProt (*Mus musculus* taxonomy) containing both forward and reverse entries of each protein. Search tolerances were 5 ppm for precursor ions and 0.02 Da for product ions using trypsin specificity with up to two missed cleavages. Carbamidomethylation (+57.0214 Da on Cys) was set as a fixed modification, whereas oxidation (+15.9949 Da on Met) and O-GlcNAcylation (+203 Da on Ser/Thr) were considered variable modifications. All searched spectra were imported into Scaffold (Proteome Software) and protein confidence thresholds were set using a Bayesian statistical algorithm based on the PeptideProphet and ProteinProphet algorithms, which yielded a peptide and protein false discovery rate (FDR) of 1%.

SILAC data were processed using Rosetta Elucidator as previously described (66–68) with the following modifications. Database searching in Mascot used a SwissProt mouse database (downloaded on 4/21/11) with an equal number of reverse entries, 5 ppm precursor and 0.02 Da product ion tolerances and variable modifications on Met (oxidation), Arg (+10), and Lys (+8). Data were annotated at a 1% peptide FDR using the PeptideTeller algorithm. Quantification of labeled pairs required that both members were identified.

Immunoprecipitation (IP)

Cells were washed twice with cold PBS and lysed in IP lysis buffer (1% Triton X-100, 150 mM NaCl, 1 mM EDTA, 20 mM Tris-HCl pH 7.4) supplemented with protease inhibitors, 5 µM PUGNAc and 50 µM UDP. Lysates were probe-sonicated, cleared by centrifugation and quantified by BCA protein assay. IPs were performed on 1–5 mg total protein. Cleared lysates were adjusted to a final total protein concentration of ∼1 mg/ml using IP lysis buffer. For every 1 mg of protein lysate used, 3 µg of mouse monoclonal anti-COPγ1 (sc-393977, Santa Cruz Biotechnology) antibody was added and rotated overnight at 4°C. The following day, 50 µl equilibrated protein A/G UltraLink Resin (ThermoFisher) was added to the lysate and rotated at room temperature for 1 h. Beads were washed three times with 1 ml of IP lysis buffer and then eluted in 2X SDS-PAGE sample buffer with boiling. Eluents were analyzed via IB.

Cloning

The COPγ1-myc-6xHis construct was generated by amplifying the open reading frame of the human COPγ1 cDNA (Harvard PlasmID Repository) by PCR and ligating it into the *Hind*III and *Not*I sites of pcDNA4/myc-6xHis (Invitrogen) using standard methods.

Transfections

293T cells plated at ∼50% confluence were transfected the following day as previously described (54). In brief, 750 µl of prewarmed OPTI-MEM was placed into 1.5 ml tubes with 45 µl of TransIT-293 transfection reagent (Mirus), vortexed briefly, and incubated for 15 min at room temperature. Next, 15 µg of

human COPγ1-myc-6xHis DNA was added to the tube, vortexed briefly, and incubated for 15 min at room temperature. After the final incubation, the mixture was added dropwise to the cells. Cells were harvested 48 h after transfection.

Tandem Purification of COPγ1-myc-6xHis

293T cells transfected with COPγ1-myc-6xHis were treated 8 h prior to harvest with 50 μM Thiamet-G and 4 mM glucosamine to enhance O-GlcNAcylation. Cells were harvested in cold PBS and lysed in IP lysis buffer supplemented with 0.1% SDS, protease inhibitors, 5 μM PUGNAc and 50 μM UDP. Lysates were probe sonicated, cleared by centrifugation, and quantified by BCA protein assay according to the manufacturer's instructions. Myc IPs were performed on ∼100 mg of total protein for MS analysis. Cleared lysates were adjusted to a final protein concentration of 2 mg/ml using IP lysis buffer supplemented with 0.1% SDS, protease inhibitors, 5 μM PUGNAc, and 50 μM UDP. Three micrograms of mouse monoclonal anti-c-myc (9E10, BioLegend) per mg of total protein was added and rotated overnight at 4°C. The following day, 50 μl of washed protein A/G UltraLink Resin (53133, ThermoFisher) was added and the mixture was rotated at room temperature for 1 h. Beads were washed three times with 1 ml of IP lysis buffer with 0.1% SDS and eluted twice in 500 μl using Ni-NTA wash buffer (8 M urea, 300 mM NaCl, 1% Triton X-100, and 5 mM imidazole) with rotation at room temperature. The two 500 μl elutions were pooled, 50 μl of washed 6xHisPur Ni-NTA resin (88223, ThermoFisher) was added to the eluate and the mixture rotated for 2 h at room temperature. The Ni-NTA resin was washed three times with 1 ml of Ni-NTA wash buffer and eluted in 8 M urea plus 250 mM imidazole.

LC-MS/MS Analysis of COPγ1 O-GlcNacylation

Purified COPγ1-myc-6xHis was separated by SDS-PAGE and Coomassie-stained. Stained bands of the correct molecular weight were subjected to standard in-gel trypsin digestion (https://genome.duke.edu/sites/genome.duke.edu/files/InGelDigestionProtocolrevised_0.pdf). Extracted peptides were lyophilized to dryness and resuspended in 12 μl of 0.2% formic acid/2% acetonitrile. Each sample was subjected to chromatographic separation on a Waters NanoAquity UPLC equipped with a 1.7 μm BEH130 C_{18} 75 μm I.D. X 250 mm reversed-phase column. The mobile phase consisted of (A) 0.1% formic acid in water and (B) 0.1% formic acid in acetonitrile. Following a 4 μl injection, peptides were trapped for 3 min on a 5 μm Symmetry C_{18} 180 μm I.D. X 20 mm column at 5 μl/minute in 99.9% A. The analytical column was then switched in-line and a linear elution gradient of 5% B to 40% B was performed over 60 min at 400 nl/minute. The analytical column was connected to a fused silica PicoTip emitter (New Objective, Cambridge, MA) with a 10 μm tip orifice and coupled to a QExactive Plus mass spectrometer (Thermo) through an electrospray interface operating in data-dependent acquisition mode. The instrument was set to acquire a precursor MS scan from m/z 350 to 1,800 every 3 s. In data-dependent mode, MS/MS scans of the most abundant precursors were collected following higher-energy collisional dissociation (HCD) fragmentation at an HCD collision energy of 27%. Within the MS/MS spectra, if any diagnostic O-GlcNAc fragment ions (m/z 204.0867, 138.0545, or 366.1396) were observed, a second MS/MS spectrum of the precursor was acquired with electron transfer dissociation (ETD)/HCD fragmentation using charge-dependent ETD reaction times and either 30 or 15% supplemental collision energy for ≥2+ precursor charge states. For all experiments, a 60-s dynamic exclusion was employed for previously fragmented precursor ions.

Raw LC-MS/MS data files were processed in Proteome Discoverer (Thermo Scientific) and then submitted to independent Mascot searches (Matrix Science) against a SwissProt database (human taxonomy) containing both forward and reverse entries of each protein (20,322 forward entries). Search tolerances were 5 ppm for precursor ions and 0.02 Da for product ions using semi-trypsin specificity with up to two missed cleavages. Both y/b-type HCD and c/z-type ETD fragment ions were allowed for interpreting all spectra. Carbamidomethylation (+57.0214 Da on C) was set as a fixed modification, whereas oxidation (+15.9949 Da on M) and O-GlcNAc (+203.0794 Da on S/T) were considered dynamic mass modifications. All searched spectra were imported into Scaffold (v4.3, Proteome Software) and scoring thresholds were set to achieve a peptide FDR of 1% using the PeptideProphet algorithm. When satisfactory ETD fragmentation was not obtained, HCD fragmentation was used to determine O-GlcNAc residue modification, using the number of HexNAcs identified in combination with the number of serines and threonines in the peptide.

RESULTS

We designed a new quantitative glycoproteomics strategy to discover changes in O-GlcNAcylated proteins in response to physiological stimuli, stress, or other cues. In this workflow (**Figure 1**), cells are first labeled with "light" $^{12}C_6{}^{14}N_2$-lysine and $^{12}C_6^{14}N_4$-arginine or "heavy" $^{13}C_6{}^{15}N_2$-lysine and $^{13}C_6{}^{15}N_4$-arginine, in a standard stable isotope labeling of amino acids in cell culture (SILAC) quantitative proteomics protocol (69, 70). Next, all cells are metabolically labeled with a short pulse of GalNAz to prime the biosynthesis of UDP-GlcNAz. Then, one cell population is treated with the stimulus of interest, leaving the other as a control. All cells are then mixed, nuclear and cytoplasmic extracts are prepared by standard biochemical fractionation (to separate O-GlcNAc from secretory pathway glycans) and labeled O-GlcNAc substrates are covalently ligated to alkyne-functionalized agarose beads via a click reaction, permitting extremely stringent washing. Finally, the captured and washed glycoproteins are trypsinized on-bead, and the resulting peptides are analyzed by SILAC mass spectrometry (MS) proteomics, providing an unbiased quantitation of stimulus-dependent changes in O-GlcNAcylated proteins.

For our pilot glycoproteomics studies, we selected the murine pro-B cell line FL5.12, subclone XL4.1 (71–73), because it is a model system for B lymphocyte activation, a process that vastly expands the protein trafficking burden through cell proliferation

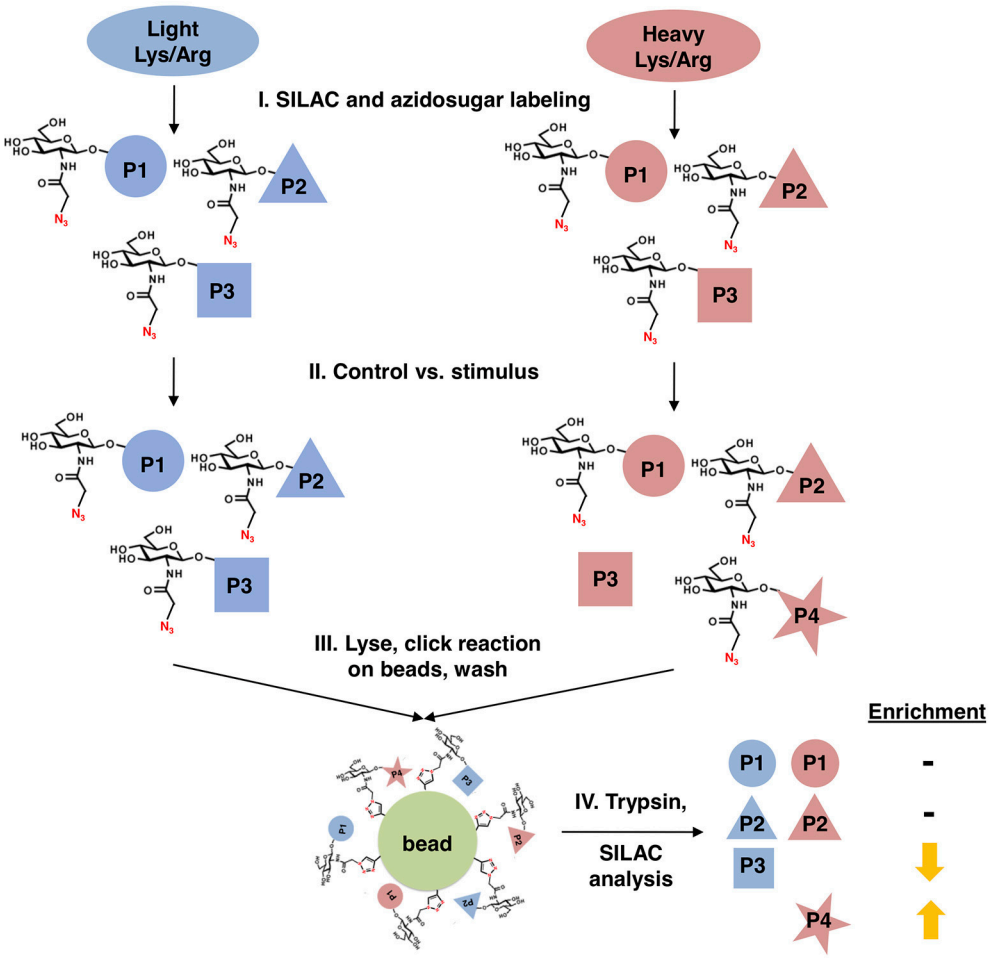

FIGURE 1 | Glycoproteomics workflow. First, cells are stably labeled with either "heavy" (red) or "light" (blue) arginine and lysine to create two distinctly labeled populations, per standard SILAC protocols. Next, cells are treated with GalNAz for a brief period to allow incorporation into endogenous OGT substrates, while limiting the labeling of "housekeeping" proteins. One cell population is treated with a stimulus, inducing changes in O-GlcNAcylation, while the other remains an untreated control. Both cell populations are mixed, fractionated to remove secretory pathway glycans, and covalently ligated to an alkyne-functionalized agarose bead via a click reaction. After extremely stringent washing, the covalently captured glycoproteins are trypsinized on-bead and the resulting peptides are analyzed by quantitative SILAC MS proteomics.

and augmented immunoglobulin secretion (74, 75). Previous work has also indicated that lymphocyte activation induces dramatic changes in global O-GlcNAcylation (76–78). Taken together, these reports suggested that O-GlcNAc might regulate protein trafficking in activated lymphocytes. We incubated XL4.1 cells with GalNAz or vehicle only and captured labeled proteins using our glycoproteomics workflow. Initial MS analysis revealed the strong enrichment of many known O-GlcNAcylated proteins, including numerous nucleoporins (79) and host cell factor 1 (HCF1) (80–82) (**Figure 2**). We concluded that our method specifically captured O-GlcNAcylated proteins, as intended.

Next, we sought to use our glycoproteomics workflow to identify O-GlcNAcylation changes that are functionally important in protein trafficking. We reasoned that a short GalNAz pulse followed by a stimulus would afford the preferential labeling of *de novo*, stimulus-dependent changes in glycoproteins, whereas longer incubations would also label unchanging, background "housekeeping" glycoproteins, as evidenced by the enrichment of nucleoporins after long GalNAz incubation (**Figure 2**). We first verified that we could label endogenous XL4.1 glycoproteins with brief GalNAz incubations. We treated cells with GalNAz for various times and then reacted lysates with alkyne-biotin to label O-GlcNAc substrates. Anti-biotin immunoblot (IB) revealed that endogenous XL4.1 glycoproteins were labeled as early as 2 h after GalNAz treatment (**Figure 3A**). We therefore selected 2 h as a pre-stimulus GalNAz incubation time for our subsequent experiment. Next, as a model stimulus to perturb protein secretion, we selected brefeldin A (BFA), a well-characterized fungal metabolite that inhibits COPI and, secondarily, COPII vesicle trafficking (83–85). We hypothesized that secretory pathway disruption by BFA would trigger changes in O-GlcNAcylation events that

Protein Name	DMSO (total spectral counts)	GalNAz (total spectral counts)
PRRC1	0	48
SF3A1	0	43
CCAR1	0	35
HYOU1	0	32
RBM26	0	31
RBM14	0	31
P66B	0	31
UBQL2	0	29
PRC2C	0	28
MA2B1	0	28
EP400	0	27
NUP54	0	27
RBM27	0	27
MAVS	0	26
HCFC1	1	84
MILK2	1	77
NU214	1	55
UBP2L	1	52
PICAL	1	42
ARI1A	1	40
PO210	1	39
ERO1A	1	36
CATB	1	31
DIDO1	1	27
TFR1	2	50

FIGURE 2 | XL4.1 cells were treated with either DMSO vehicle or 100 μM GalNAz for 24 h and processed via the glycoproteomics workflow. To confirm enrichment, proteins with fewer than 25 spectral counts were excluded, and the remaining proteins were rank-ordered by the ratio of spectral counts from the vehicle and GalNAz samples (low to high). Table displays the top 25 proteins ranked this way. Commonly O-GlcNAcylated substrates (e.g., nucleoporins, HCF1) were identified exclusively in the GalNAz-treated samples, confirming the selective enrichment of endogenous OGT substrates by the workflow. Complete proteomics datasets are available as **Supplemental Material**.

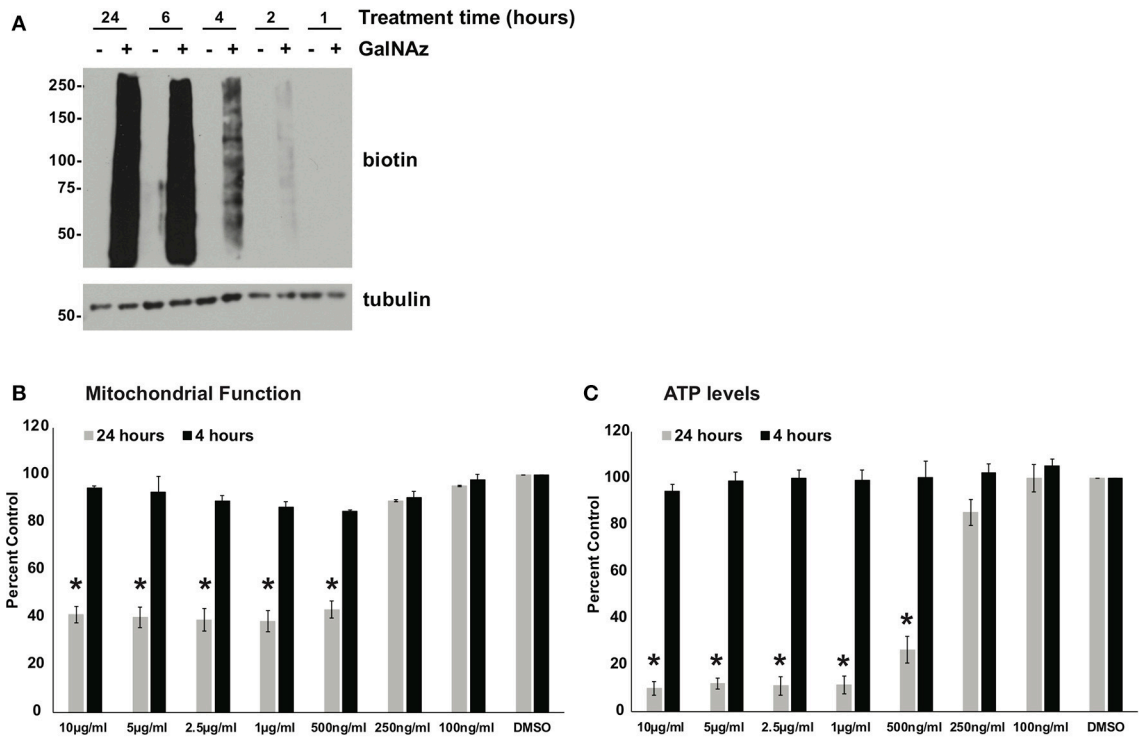

FIGURE 3 | (A) XL4.1 cells were treated with DMSO vehicle or 100 μM GalNAz for the indicated times. Cell lysates were subjected to click reactions with an alkyne-biotin probe and analyzed by IB. GalNAz incorporation is evident as soon as 2 h after treatment. Tubulin is a loading control. **(B,C)** Parental FL5.12 N6 cells were treated with the indicated doses of BFA for 4 or 24 h and mitochondrial function **(B)** ($n = 2$) and ATP levels **(C)** ($n = 3$) were measured. Marked decreases in mitochondrial function and ATP content occurred with ≥500 ng/ml BFA treatment for 24 h, but no changes were observed at those doses after 4 h. In each assay, values were normalized to vehicle-treated control. Error bars are standard error of the mean. *$p < 0.05$ compared to control (DMSO) by Tukey's HSD.

regulate trafficking under homeostatic or stress conditions. To determine the lowest BFA dose that caused strong disruption of the secretory pathway, we treated apoptosis-sensitive parental FL5.12 N6 cells with a range of BFA concentrations for 4 or 24 h and measured cellular ATP and mitochondrial function (**Figures 3B,C**). In these experiments, 500 ng/ml was the lowest BFA dose that caused significant toxicity after 24 h while having little effect on cell viability after only 4 h (**Figures 3B,C**). We therefore selected 4 h of 500 ng/ml BFA as a treatment condition to disrupt protein trafficking without inducing the potentially confounding effects of downstream cell death.

We next performed proof-of-principle experiments with BFA and our glycoproteomic workflow. We treated SILAC-labeled XL4.1 cells with GalNAz for 2 h, followed by 500 ng/ml BFA (heavy-labeled cells) or vehicle control (light-labeled cells) for an additional 4 h. Then, we mixed the intact cells, derived nuclear and cytoplasmic subcellular fractions, captured GalNAz-labeled proteins and analyzed BFA-dependent changes in O-GlcNAc substrates. We calculated the fold-enrichment of every protein in our control (DMSO) vs. BFA-treated SILAC populations (1,253 nuclear and 792 cytoplasmic IDs) (**Figure 4A**). Overall, BFA barely altered the abundance of the vast majority of captured proteins, as expected, with 99% of both nuclear and cytoplasmic IDs changing <4-fold (**Figure 4A**). However, 1 nuclear and 7 cytoplasmic proteins were enriched at least 4-fold in the BFA sample vs. control, and 8 nuclear and 3 cytoplasmic proteins were depleted at least 4-fold in the BFA-treated sample. Similar results were obtained in an independent biological replicate performed with the amino acid and treatment pairings reversed (i.e., heavy/DMSO, light/BFA) (**Figure 4B**).

We next applied stringent filters to the data from both biological replicates to identify candidate BFA-dependent changes in O-GlcNAcylated proteins. First, we compared BFA-induced fold-changes across biological replicates and retained only protein IDs with concordant changes (up or down) across replicates. Then, we retained only nuclear proteins with a fold-change magnitude >2, and only cytoplasmic proteins with a fold-change magnitude >1.5. (A less stringent filter was placed on the cytoplasmic fraction because it exhibited fewer total protein IDs and lower-magnitude fold-changes overall). After applying these filters, we identified 80 nuclear and 17 cytoplasmic proteins displaying consistent, BFA-dependent changes across both experiments (**Figure 4B**). Interestingly, several of these proteins participate directly in protein trafficking, including the COPI protein COPγ1 (depleted 2.27- and 2.078-fold, respectively, from the BFA samples in the two biological replicates) and the retromer component

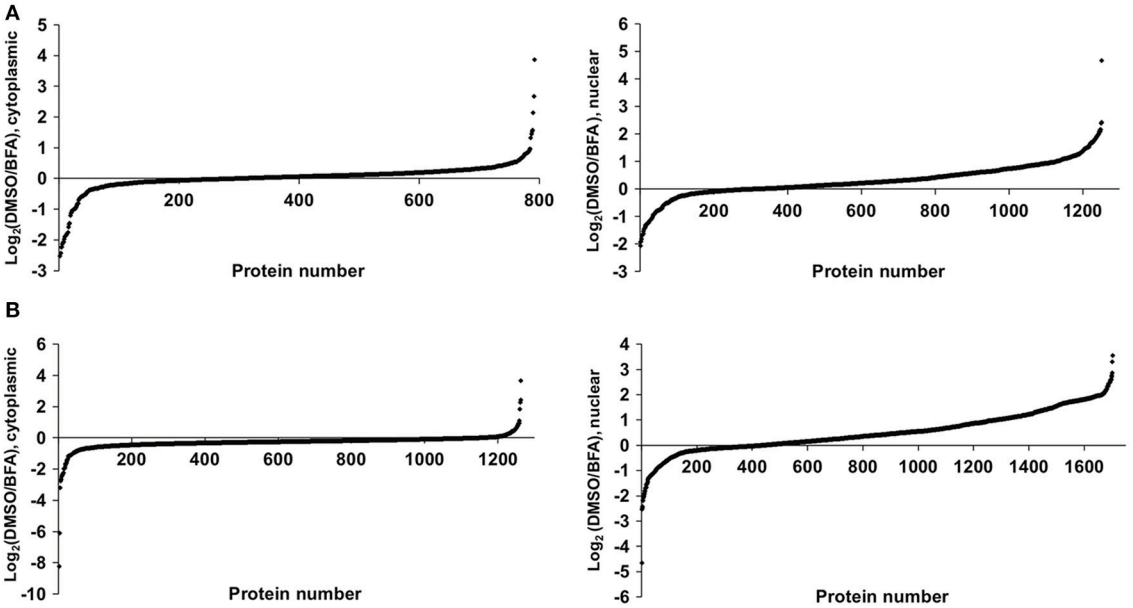

C

Cytoplasmic, biological replicate 1		Cytoplasmic, biological replicate 2		Nuclear, biological replicate 1		Nuclear, biological replicate 2	
Protein name	Fold change	Protein name	Fold Change	Protein name	Fold Change	Protein name	Fold Change
ENTP5	4.707	ERAP1	9.13	FAS	-5.883	FXYD5	4.569
ENPL	4.226	TWSG1	6.259	IMPA1	-5.268	APMAP	4.264
HYOU1	4.016	ENTP5	6.176	TPP2	-4.485	PON3	4.241
HSP13	3.77	HSP13	5.13	PGK1	-4.272	TALDO	-4.011
ERAP1	3.597	TGFB1	4.678	UBA1	-4.076	SAHH	-4.01
TWSG1	3.375	HYOU1	4.39	PON3	4.001	SUN2	3.904
SIL1	2.98	BTD	3.863	NEDD4	-3.838	MINK1	-3.903
OFUT1	2.971	GT251	3.309	YTHD3	-3.726	SERA	-3.886
LYAG	-2.969	OFUT1	3.142	FPPS	-3.687	STIP1	-3.867
TGFB1	2.765	GLU2B	3.126	VPS35	-3.582	HM13	3.803
TXND5	2.172	ENPL	3.094	SAHH	-3.566	RPN2	3.74
BTD	2.049	SIL1	2.847	APMAP	3.557	PROF1	-3.73
CRLF2	-1.787	SAP	2.403	TCPB	-3.484	PGK1	-3.727
GT251	1.759	CALU	2.286	SERA	-3.439	ENOA	-3.679
CALU	1.702	TXND5	2.248	TCPD	-3.421	UBA1	-3.659

D

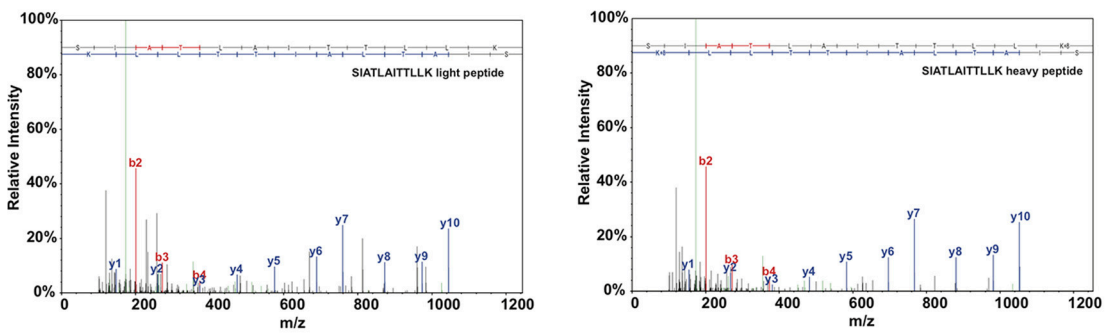

FIGURE 4 | Glycoproteomics workflow detects global BFA-induced changes in O-GlcNAcylated proteins. Data for nuclear and cytoplasmic proteins are displayed as a $\log_2$ transform of the ratio of detected intensities from the DMSO and BFA samples, as described previously (66–68). **(A)** In the first biological replicate, 1,252 nuclear and 792 cytoplasmic proteins were identified. **(B)** In the second biological replicate, 1,703 nuclear and 1,262 cytoplasmic proteins were identified. **(C)** The nuclear and cytoplasmic proteins exhibiting concordant BFA-dependent changes (up or down) across biological replicates were rank-ordered by the magnitude of the fold-change between DMSO and BFA samples, as described previously (66–68). Tables list the top 15 nuclear and cytoplasmic proteins from each biological replicate by this ranking. Some proteins appear in both tables but at different positions, reflecting rank-order in each case. **(D)** Representative MS spectra from one SILAC biological replicate, depicting light and heavy versions of the COPγ1 peptide SIATLAITTLLK. Complete proteomics datasets are available as **Supplemental Material**.

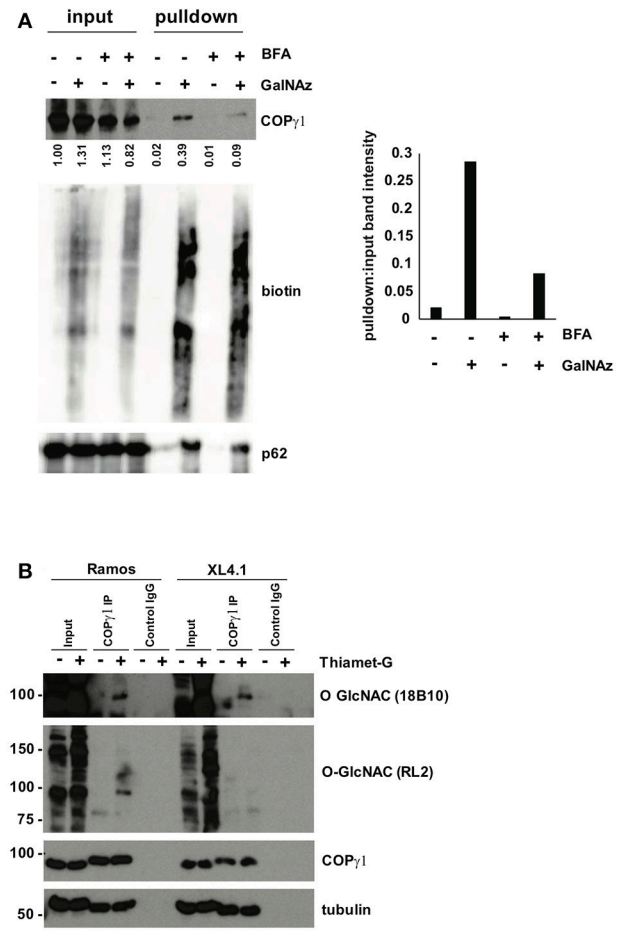

FIGURE 5 | (A) Ramos cells were treated with 100 μM GalNAz or DMSO vehicle for 6 h, followed by 500 ng/ml BFA or DMSO vehicle for an additional 4 h, and then harvested. Nuclear and cytoplasmic fractions were prepared, subjected to click reactions with an alkyne-biotin probe and incubated with streptavidin beads for enrichment. Beads were washed and eluted proteins were analyzed by IB. Nuclear fraction IBs from a representative experiment are shown. Nucleoporin-62, a heavily O-GlcNAcylated protein, is a control for equal loading (input lanes) and biotin enrichment (pulldown lanes). Band intensities in the COPγ1 IB were quantified in ImageJ, normalized to control (DMSO, input lane) and listed below. The ratio of pulldown:input for each treatment was calculated as a measure of COPγ1GalNAz modification and is given in the graph at the right. Consistent with the glycoproteomics results, COPγ1 levels were reduced after BFA treatment, indicating a reduction in O-GlcNAcylation. Similar results were obtained with XL4.1 cells (not shown). (**B**) Ramos (left) and XL4.1 (right) cells were treated with 50 μM Thiamet-G or DMSO vehicle for 8 h and lysates were subjected to anti-COPγ1IP and analyzed via IB.

Vps35 (depleted 3.582- and 2.412-fold from the BFA samples), or are regulators of membrane protein quality control, such as the AAA+ ATPase torsinA (enriched 2.069- and 2.466-fold in the BFA samples) and the ubiquitin E3 ligase NEDD4, which is also a known O-GlcNAc substrate (depleted 3.838- and 3.058-fold from the BFA samples) (**Figures 4C,D** and **Supplemental Material**) (86–101). We concluded that our glycoproteomics workflow identified candidate BFA-dependent changes in O-GlcNAc substrates that may impact on protein trafficking.

From our filtered glycoproteomics data, we selected COPγ1 for further validation experiments because of its well-established role in protein trafficking. COPγ1 is a core component of the heteroheptameric COPI complex, which is recruited to Golgi membranes by the small GTPase ADP ribosylation factor 1 (Arf1) to mediate vesicle formation and trafficking within the Golgi or to the ER (49, 102, 103). COPγ proteins interact with cargo adaptors in the Golgi membrane, with Arf GTPase-activating proteins and with other COPI components in the coat itself (49, 88, 89, 92). COPγ is highly conserved across eukaryotes and is essential for *in vitro* COPI vesicle formation and for viability in budding yeast (49, 104, 105). While phosphorylation, arginine methylation, and ubiquitination of COPγ1 have been observed in several studies (106–116), O-GlcNAcylation of COPγ has never been reported.

To confirm our MS results with COPγ1, we GalNAz-labeled XL4.1 or Ramos cells (a human B cell line) in the presence or absence of BFA treatment, performed click reactions with alkyne-biotin, purified O-GlcNAc substrates by streptavidin affinity chromatography and analyzed the results by IB (**Figure 5A**). Consistent with our glycoproteomics results, anti-COPγ1 IB indicated that BFA treatment reduced the O-GlcNAcylation of COPγ1 without causing dramatic effects on total COPγ1 levels (**Figure 5A**). To extend these results to natural O-GlcNAc, we immunoprecipitated (IP-ed) endogenous COPγ1 from XL4.1 or Ramos cells and observed that it was recognized by anti-O-GlcNAc monoclonal antibodies (**Figure 5B**). This signal was specific, because treatment of cells with Thiamet-G, a small molecule inhibitor of OGA (64), increased both global O-GlcNAc signal and anti-O-GlcNAc immunoreactivity of COPγ1 (**Figure 5B**). We concluded that endogenous COPγ1 is dynamically O-GlcNAcylated in mammalian cells under homeostatic conditions, and deglycosylated upon disruption of protein trafficking by BFA.

As a first step toward characterizing the function of COPγ1 O-GlcNAcylation, we expressed and purified epitope-tagged human COPγ1 to homogeneity from human cells and used MS to map O-GlcNAc-modified residues. We detected 11 O-GlcNAc moieties across six unique peptides and unambiguously assigned five glycosylation sites: T132, S134, T135, T552, and S554 (**Figure 6A** and **Supplemental Material**). COPγ1 is highly conserved between human and mouse (97.3% identical and 99.4% similar), and all candidate O-GlcNAc sites that we identified are identical between the orthologs (**Figures 6A,B**). The candidate O-GlcNAc sites occur in several regions of the COPγ1 protein, with most lying within the last HEAT repeat of the adaptin N-terminal domain or in the appendage domain (**Figure 6B**). The appendage domain interacts with ARFGAP2, which binds the α/β/ε COPI subcomplex and influences vesicle uncoating, suggesting that O-GlcNAcylation in this domain could influence these functions (88). Finally, we modeled the observed O-GlcNAc sites onto crystal structures of COPγ1 in the COPI coat "triad" complex (**Figures 6C,D**) (PDB: 5A1U) (117). Interestingly, the T552 and S554 glycosylation sites of COPγ1 lie close to COPβ1-binding interface and might impact on this

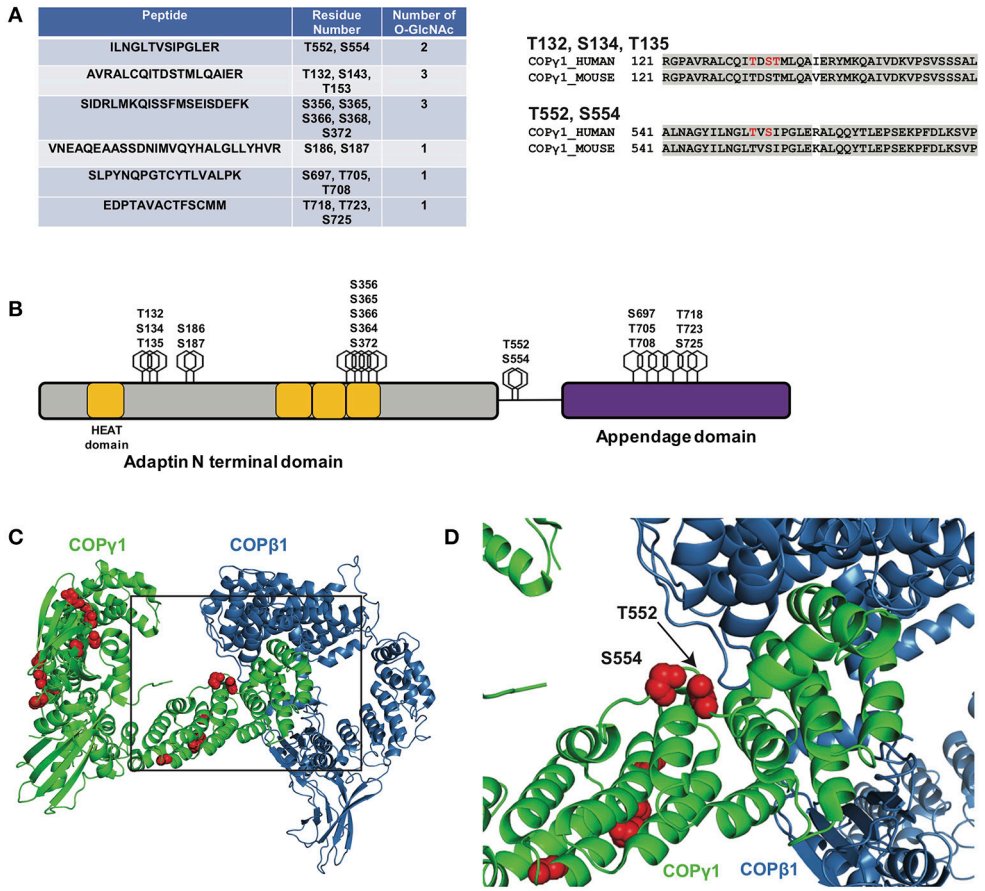

FIGURE 6 | (**A**, left) Myc-6xHis-tagged human COPγ1 was tandem-purified to homogeneity from transfected 293T cells and analyzed via ETD/HCD-MS. Peptide sequence, number of O-GlcNAc moieties detected, and number of serine and threonine residues are displayed for tryptic peptides exhibiting glycosylation. (**A**, right) Alignment of human and mouse COPγ1 regions with unambiguously assigned O-GlcNAc modification sites, denoted in red. Human and mouse COPγ1 are 97.3% identical and are 99.4% similar. All O-GlcNAc sites identified on human COPγ1 are conserved in the mouse ortholog. **(B)** Schematic depicting candidate O-GlcNAc sites on the COPγ1 domain structure. The C-terminal appendage domain contains an ARFGAP2-interacting region and binds the α/β/ε COPI subcomplex. **(C)** Interface of COPγ1 (green) and COPβ1 (blue), with potential O-GlcNAc sites in red, from the previously reported structure of the COPI triad (PDB: 5A1U) (117). **(D)** Zoomed view from **(C)** (black box) of the COPγ1/COPβ1 interface. T552 and S554, two unambiguously assigned O-GlcNAc sites on COPγ1, lie in close proximity to COPβ1. Complete proteomics datasets are available as **Supplemental Material**.

interaction, which is essential for COPI function (117). Taken together, our BFA and MS results suggest that site-specific COPγ1 O-GlcNAcylation may promote or license its activity in the COPI pathway.

DISCUSSION

O-GlcNAc is a highly dynamic PTM that modifies thousands of nuclear, cytoplasmic and mitochondrial proteins. While the number of identified O-GlcNAc substrates continues to rise, the specific functions of O-GlcNAc on most proteins are elusive and assessing stimulus-triggered changes in O-GlcNAcylated proteins remains a significant challenge in the field. Here, we report a novel glycoproteomics workflow enabling the proteome-wide identification and quantification of changes in O-GlcNAc-modified proteins and use it to discover cycling O-GlcNAcylation of mammalian COPγ1 as a candidate regulatory event in Golgi protein trafficking.

Several proteomics-compatible approaches for enriching natural O-GlcNAc exist, including lectin weak-affinity chromatography (LWAC), chemical modification of O-GlcNAc moieties (e.g., β-elimination followed by Michael addition) and chemoenzymatic methods that harness an engineered galactosyltransferase (9, 59, 81, 82, 118–134). Each of these is a well-established and powerful tool for elucidating O-GlcNAc signaling. Our glycoproteomics workflow leverages GalNAz metabolic labeling, which complements these methods in important ways. In our approach, a pulse of GalNAz is added to cultured cells only shortly before the stimulus of interest, permitting the preferential enrichment and characterization of relatively new glycosylation changes. Therefore, our workflow provides time resolution and reduces the labeling of long-lived, unchanging O-GlcNAc moieties (e.g., on the nuclear

pore complex) that could otherwise dominate the proteomics results (**Figure 2**). In addition, our workflow affords the covalent capture of O-GlcNAcylated proteins onto a solid matrix, allowing extremely stringent washing conditions to remove unglycosylated proteins. Although the individual components of our strategy have been reported previously, we have assembled them into a new and optimized workflow in which the proteome-wide profiling of stimulus-dependent O-GlcNAc changes in SILAC-labeled cells can be performed by one worker in as little as 1 week. Moreover, our workflow can be implemented in any cell type or organism that supports azidosugar and SILAC labeling, and can be used to study a wide range of stimuli, stresses or other experimental comparisons. We anticipate that this method will be a useful addition to the quantitative analysis of O-GlcNAc signaling.

In pilot experiments, we used our workflow to address the role of O-GlcNAcylation changes in mammalian protein trafficking, using BFA as an established tool compound. These studies identified the dynamic glycosylation of COPγ1 in mammalian cells (**Figures 4–6** and **Supplemental Material**), and validation experiments demonstrated that endogenous COPγ1 is reversibly modified by natural O-GlcNAc atleast 11 sites, confirming the utility of our approach in characterizing native signaling pathways (**Figures 5**, **6**). (We note that numerous Golgi proteins partitioned to the "nuclear" sample in our fractionation procedure, likely explaining the presence of COPγ1—see full proteomics datasets in the **Supplemental Material**).

COPI trafficking relies on the guanine nucleotide exchange factor GBP1 to exchange GDP for GTP on Arf1 (47–49, 102, 103). Arf1 undergoes a conformational change upon GTP binding, inserting an N-terminal amphipathic α-helix into the Golgi membrane (49, 102, 103). Membrane-bound Arf1 then recruits the stable heteroheptameric COPI coat complex, which includes COPγ1 (49, 102, 103, 135). The assembling COPI heteroheptamers also undergo a major conformational change, promoting oligomerization of the coat complex and eventual vesicle formation and scission (117, 135, 136). BFA perturbs protein trafficking by stabilizing an abortive intermediate of the Arf1 complex, disrupting both the COPI and, subsequently, the COPII pathways (83–85).

Our results suggest that COPγ1 glycosylation may regulate protein trafficking within or from the Golgi. Consistent with this hypothesis, a prior proteomics study identified a putative biochemical interaction between OGT and the COPI component COPε (137). The authors proposed that O-GlcNAc might govern intra-Golgi vesicle transport, although no direct glycosylation of any COPI protein was demonstrated (137). The precise biochemical and functional effects of O-GlcNAcylation on COPγ1 remain to be determined, but our results, combined with prior reports, suggest several possibilities. First, because O-GlcNAc can regulate protein-protein interactions in a variety of contexts (138), glycosylation may affect the interaction of COPγ1 with specific binding partners, such as COPβ1, COPζ, Arf1, or p24 cargo adaptors (49, 105, 139–143). Consistent with this notion, our MS site-mapping revealed O-GlcNAcylation on two sites, T552 and S554, located in close proximity to the interface with COPβ1 in the COPI triad structure (**Figures 6C,D**) (117). Addition of one or more bulky O-GlcNAc moieties in this region of COPγ1 may alter this interaction, which is essential for COPI function. Second, O-GlcNAcylation of COPγ1 may promote or inhibit one of the significant conformational changes that occur during COPI coat assembly (49, 102, 103, 117, 135, 136, 142, 143). Third, O-GlcNAcylation of COPγ1 may regulate the membrane recruitment of the heteroheptameric complex. We have previously demonstrated an analogous role for O-GlcNAc signaling in the COPII pathway, as OGA inhibition impairs the membrane recruitment of the COPII proteins Sec31A and Sec23A (54). Fourth, O-GlcNAc may regulate COPγ1 through cross-talk with other PTMs. Interestingly, five of the candidate O-GlcNAc sites we identified on COPγ1 (S356, S554, T718, T723, and S725) are also reported phosphorylation sites (144). Therefore, COPγ1 function may be regulated by the well-documented, complex interplay between O-GlcNAcylation and O-phosphorylation (2, 145–149). Our site-mapping data have paved the way for future studies to test these hypotheses, and experiments with single and compound glycosylation site mutants are currently underway to determine the impact of COPγ1 O-GlcNAcylation in live-cell trafficking assays.

While many excellent studies have dissected the structures and functions of the core COPI machinery (49, 142, 143), much less is known about how this critical pathway is regulated by mammalian cells in response to rapidly changing physiological and pathological signals. PTMs likely serve as one important mode of COPI regulation. Indeed, several proteomics studies have reported phosphorylation, ubiquitination and arginine methylation of COPγ in particular (107–116), and one study provided functional evidence that phosphorylation of COPβ and COPγ influences coatomer assembly or membrane recruitment (106). Therefore, COPI trafficking may be governed in part by COPγ PTMs. Our results indicate that O-GlcNAc may be a functionally important PTM in the COPI system as well. Moreover, we detected putative BFA-dependent O-GlcNAc changes on proteins operating in distinct parts of the secretory pathway, including Vps35, torsinA, and NEDD4 (**Figure 4**), and previous studies have implicated O-GlcNAcylation in other vesicle transport pathways beyond COPI as well (28, 50–63). Based on these observations, we propose that O-GlcNAcylation may be a widespread mode of dynamic regulation in mammalian protein trafficking.

DATA AVAILABILITY STATEMENT

All datasets generated in this study are included in the manuscript and supplementary files.

AUTHOR CONTRIBUTIONS

NC, ES, and MB contributed conception and design of the study. NC, PL, and TS performed experiments and prepared samples. NC and ES performed and analyzed glycoproteomics

experiments. BB performed statistical analysis of cell viability data and analyses of O-GlcNAc site-mapping data in the context of previously reported COPγ1 structures. NC and MB wrote the manuscript, and all authors contributed to manuscript revision and read and approved the submitted version.

FUNDING

This work was supported by a Scholar Award from the Rita Allen Foundation, a Research Grant from the Mizutani Foundation for Glycoscience and NIH grant R01GM117473 to MB.

ACKNOWLEDGMENTS

We thank Dr. Matthew Foster (Duke University Proteomics and Metabolomics Core Facility) for help with SILAC data analysis and members of the Boyce Lab for helpful discussion and reagents.

SUPPLEMENTARY MATERIAL

The Supplementary Material for this article can be found online at: https://www.frontiersin.org/articles/10.3389/fendo.2018.00606/full#supplementary-material

REFERENCES

1. Hanover JA, Krause MW, Love DC. The hexosamine signaling pathway: O-GlcNAc cycling in feast or famine. *Biochim Biophys Acta* (2010) 1800:80–95. doi: 10.1016/j.bbagen.2009.07.017
2. Hart GW, Slawson C, Ramirez-Correa G, Lagerlof O. Cross talk between O-GlcNAcylation and phosphorylation: roles in signaling, transcription, and chronic disease. *Annu Rev Biochem*. (2011) 80:825–58. doi: 10.1146/annurev-biochem-060608-102511
3. Hart GW. Three decades of research on O-GlcNAcylation - a major nutrient sensor that regulates signaling, transcription and cellular metabolism. *Front Endocrinol.* (2014) 5:183. doi: 10.3389/fendo.2014.00183
4. Bond MR, Hanover JA. A little sugar goes a long way: the cell biology of O-GlcNAc. *J Cell Biol*. (2015) 208:869–80. doi: 10.1083/jcb.201501101
5. Lefebvre T, Issad T. 30 Years Old: O-GlcNAc reaches the age of reason - regulation of cell signaling and metabolism by O-GlcNAcylation. *Front Endocrinol.* (2015) 6:17. doi: 10.3389/fendo.2015.00017
6. Levine ZG, Walker S. The biochemistry of O-GlcNAc transferase: which functions make it essential in mammalian cells? *Annu Rev Biochem*. (2016) 85:631–57. doi: 10.1146/annurev-biochem-060713-035344
7. Yang X, Qian K. Protein O-GlcNAcylation: emerging mechanisms and functions. *Nat Rev Mol Cell Biol*. (2017) 18:452–65. doi: 10.1038/nrm.2017.22
8. Dehennaut V, Leprince D, Lefebvre T. O-GlcNAcylation, an epigenetic mark. focus on the histone code, TET family proteins, and polycomb group proteins. *Front Endocrinol.* (2014) 5:155. doi: 10.3389/fendo.2014.00155
9. Yi W, Clark PM, Mason DE, Keenan MC, Hill C, Goddard, WA III, et al. Phosphofructokinase 1 glycosylation regulates cell growth and metabolism. *Science* (2012) 337:975–80. doi: 10.1126/science.1222278
10. Ma Z, Vosseller K. O-GlcNAc in cancer biology. *Amino Acids* (2013) 45:719–33. doi: 10.1007/s00726-013-1543-8
11. Singh JP, Zhang K, Wu J, Yang X. O-GlcNAc signaling in cancer metabolism and epigenetics. *Cancer Lett*. (2015) 356(2 Pt A):244–50. doi: 10.1016/j.canlet.2014.04.014
12. Ferrer CM, Sodi VL, Reginato MJ. O-GlcNAcylation in cancer biology: linking metabolism and signaling. *J Mol Biol*. (2016) 428:3282–94. doi: 10.1016/j.jmb.2016.05.028
13. Ma J, Hart GW. Protein O-GlcNAcylation in diabetes and diabetic complications. *Expert Rev Proteomics* (2013) 10:365–80. doi: 10.1586/14789450.2013.820536
14. Baudoin L, Issad T. O-GlcNAcylation and inflammation: a vast territory to explore. *Front Endocrinol.* (2014) 5:235. doi: 10.3389/fendo.2014.00235
15. Hardiville S, Hart GW. Nutrient regulation of signaling, transcription, and cell physiology by O-GlcNAcylation. *Cell Metab*. (2014) 20:208–13. doi: 10.1016/j.cmet.2014.07.014
16. Vaidyanathan K, Wells L. Multiple tissue-specific roles for the O-GlcNAc post-translational modification in the induction of and complications arising from type II diabetes. *J Biol Chem*. (2014) 289:34466–71. doi: 10.1074/jbc.R114.591560
17. Darley-Usmar VM, Ball LE, Chatham JC. Protein O-linked beta-N-acetylglucosamine: a novel effector of cardiomyocyte metabolism and function. *J Mol Cell Cardiol*. (2012) 52:538–49. doi: 10.1016/j.yjmcc.2011.08.009
18. Erickson JR, Pereira L, Wang L, Han G, Ferguson A, Dao K, et al. Diabetic hyperglycaemia activates CaMKII and arrhythmias by O-linked glycosylation. *Nature* (2013) 502:372–6. doi: 10.1038/nature12537
19. Dassanayaka S, Jones SP. O-GlcNAc and the cardiovascular system. *Pharmacol Ther*. (2014) 142:62–71. doi: 10.1016/j.pharmthera.2013.11.005
20. Erickson JR. Mechanisms of CaMKII activation in the heart. *Front Pharmacol*. (2014) 5:59. doi: 10.3389/fphar.2014.00059
21. Yuzwa SA, Shan X, Macauley MS, Clark T, Skorobogatko Y, Vosseller K, et al. Increasing O-GlcNAc slows neurodegeneration and stabilizes tau against aggregation. *Nat Chem Biol*. (2012) 8:393–9. doi: 10.1038/nchembio.797
22. Vaidyanathan K, Durning S, Wells L. Functional O-GlcNAc modifications: implications in molecular regulation and pathophysiology. *Crit Rev Biochem Mol Biol*. (2014) 49:140–63. doi: 10.3109/10409238.2014.884535
23. Yuzwa SA, Vocadlo DJ. O-GlcNAc and neurodegeneration: biochemical mechanisms and potential roles in Alzheimer's disease and beyond. *Chem Soc Rev*. (2014) 43:6839–58. doi: 10.1039/C4CS00038B
24. Zhu Y, Shan X, Yuzwa SA, Vocadlo DJ. The emerging link between O-GlcNAc and Alzheimer disease. *J Biol Chem*. (2014) 289:34472–81. doi: 10.1074/jbc.R114.601351
25. Mondoux MA, Love DC, Ghosh SK, Fukushige T, Bond M, Weerasinghe GR, et al. O-linked-N-acetylglucosamine cycling and insulin signaling are required for the glucose stress response in *Caenorhabditis elegans*. *Genetics* (2011) 188:369–82. doi: 10.1534/genetics.111.126490
26. Bond MR, Hanover JA. O-GlcNAc cycling: a link between metabolism and chronic disease. *Annu Rev Nutr*. (2013) 33:205–29. doi: 10.1146/annurev-nutr-071812-161240
27. Boyce M, Bertozzi CR. Bringing chemistry to life. *Nat Methods* (2011) 8:638–42. doi: 10.1038/nmeth.1657
28. Boyce M, Carrico IS, Ganguli AS, Yu SH, Hangauer MJ, Hubbard SC, et al. Metabolic cross-talk allows labeling of O-linked beta-N-acetylglucosamine-modified proteins via the N-acetylgalactosamine salvage pathway. *Proc Natl Acad Sci USA*. (2011) 108:3141–6. doi: 10.1073/pnas.1010045108
29. Palaniappan KK, Hangauer MJ, Smith TJ, Smart BP, Pitcher AA, Cheng EH, et al. A chemical glycoproteomics platform reveals O-GlcNAcylation of mitochondrial voltage-dependent anion channel 2. *Cell Rep*. (2013) 5:546–52. doi: 10.1016/j.celrep.2013.08.048
30. Chen PH, Smith TJ, Wu J, Siesser PF, Bisnett BJ, Khan F, et al. Glycosylation of KEAP1 links nutrient sensing to redox stress signaling. *EMBO J*. (2017) 36:2233–50. doi: 10.15252/embj.201696113
31. Tarbet HJ, Dolat L, Smith TJ, Condon BM, O'Brien ET III, Valdivia RH, et al. Site-specific glycosylation regulates the form and function of the intermediate filament cytoskeleton. *Elife* (2018) 7:e31807. doi: 10.7554/eLife.31807
32. Hang HC, Yu C, Kato DL, Bertozzi CR. A metabolic labeling approach toward proteomic analysis of mucin-type O-linked glycosylation. *Proc Natl Acad Sci USA*. (2003) 100:14846–51. doi: 10.1073/pnas.2335201100
33. Rostovtsev VV, Green LG, Fokin VV, and Sharpless KB. A stepwise huisgen cycloaddition process: copper(I)-catalyzed regioselective "ligation" of azides and terminal alkynes. *Angew Chem Int Ed Engl.* (2002) 41:2596–9. doi: 10.1002/1521-3773(20020715)41:14<2596::AID-ANIE2596>3.0.CO;2-4

34. Tornoe CW, Christensen C, Meldal M. Peptidotriazoles on solid phase: [1,2,3]-triazoles by regiospecific copper(i)-catalyzed 1,3-dipolar cycloadditions of terminal alkynes to azides. *J Org Chem*. (2002) 67:3057–64. doi: 10.1021/jo011148j
35. McKay CS, Finn MG. Click chemistry in complex mixtures: bioorthogonal bioconjugation. *Chem Biol*. (2014) 21:1075–101. doi: 10.1016/j.chembiol.2014.09.002
36. Li L, Zhang Z. Development and applications of the copper-catalyzed Azide-Alkyne Cycloaddition (CuAAC) as a Bioorthogonal Reaction. *Molecules* (2016) 21: E1393. doi: 10.3390/molecules21101393
37. Kaufman RJ. Stress signaling from the lumen of the endoplasmic reticulum: coordination of gene transcriptional and translational controls. *Genes Dev*. (1999) 13:1211–33. doi: 10.1101/gad.13.10.1211
38. Huh WK, Falvo JV, Gerke LC, Carroll AS, Howson RW, Weissman JS, et al. Global analysis of protein localization in budding yeast. *Nature* (2003) 425:686–91. doi: 10.1038/nature02026
39. Barlowe CK, Miller EA. Secretory protein biogenesis and traffic in the early secretory pathway. *Genetics* (2013) 193:383–410. doi: 10.1534/genetics.112.142810
40. Mettlen M, Chen PH, Srinivasan S, Danuser G, Schmid SL. Regulation of clathrin-mediated endocytosis. *Annu Rev Biochem*. (2018) 87:871–96. doi: 10.1146/annurev-biochem-062917-012644
41. Baker D, Hicke L, Rexach M, Schleyer M, Schekman R. Reconstitution of SEC gene product-dependent intercompartmental protein transport. *Cell* (1988) 54:335–44. doi: 10.1016/0092-8674(88)90196-1
42. Ruohola H, Kabcenell AK, Ferro-Novick S. Reconstitution of protein transport from the endoplasmic reticulum to the Golgi complex in yeast: the acceptor Golgi compartment is defective in the sec23 mutant. *J Cell Biol*. (1988) 107:1465–76. doi: 10.1083/jcb.107.4.1465
43. Barlowe C, Orci L, Yeung T, Hosobuchi M, Hamamoto S, Salama N, et al. COPII: a membrane coat formed by Sec proteins that drive vesicle budding from the endoplasmic reticulum. *Cell* (1994) 77:895–907. doi: 10.1016/0092-8674(94)90138-4
44. Routledge KE, Gupta V, Balch WE. Emergent properties of proteostasis-COPII coupled systems in human health and disease. *Mol Membr Biol*. (2010) 27:385–97. doi: 10.3109/09687688.2010.524894
45. Brandizzi F, Barlowe C. Organization of the ER-Golgi interface for membrane traffic control. *Nat Rev Mol Cell Biol*. (2013) 14:382–92. doi: 10.1038/nrm3588
46. Miller EA, Schekman R. COPII - a flexible vesicle formation system. *Curr Opin Cell Biol*. (2013) 25:420–7. doi: 10.1016/j.ceb.2013.04.005
47. Guo Y, Sirkis DW, Schekman R. Protein sorting at the trans-Golgi network. *Annu Rev Cell Dev Biol*. (2014) 30:169–206. doi: 10.1146/annurev-cellbio-100913-013012
48. Rout MP, Field MC. The evolution of organellar coat complexes and organization of the eukaryotic cell. *Annu Rev Biochem*. (2017) 86:637–57. doi: 10.1146/annurev-biochem-061516-044643
49. Bethune J, Wieland FT. Assembly of COPI and COPII vesicular coat proteins on membranes. *Annu Rev Biophys*. (2018) 47:63–83. doi: 10.1146/annurev-biophys-070317-033259
50. Dudognon P, Maeder-Garavaglia C, Carpentier JL, Paccaud JP. Regulation of a COPII component by cytosolic O-glycosylation during mitosis. *FEBS Lett*. (2004) 561:44–50. doi: 10.1016/S0014-5793(04)00109-7
51. Teo CF, Ingale S, Wolfert MA, Elsayed GA, Not LG, Chatham JC, et al. Glycopeptide-specific monoclonal antibodies suggest new roles for O-GlcNAc. *Nat Chem Biol*. (2010) 6:338–43. doi: 10.1038/nchembio.338
52. Zachara NE, Molina H, Wong KY, Pandey A, Hart GW. The dynamic stress-induced "O-GlcNAc-ome" highlights functions for O-GlcNAc in regulating DNA damage/repair and other cellular pathways. *Amino Acids* (2011) 40:793–808. doi: 10.1007/s00726-010-0695-z
53. Lee A, Miller D, Henry R, Paruchuri VD, O'Meally RN, Boronina T, et al. Combined antibody/lectin enrichment identifies extensive changes in the O-GlcNAc Sub-proteome upon oxidative stress. *J Proteome Res*. (2016) 15:4318–36. doi: 10.1021/acs.jproteome.6b00369
54. Cox NJ, Unlu G, Bisnett BJ, Meister TR, Condon BM, Luo PM, et al. Dynamic glycosylation governs the vertebrate COPII protein trafficking pathway. *Biochemistry* (2018) 57:91–107. doi: 10.1021/acs.biochem.7b00870
55. Murphy JE, Hanover JA, Froehlich M, DuBois G, Keen JH. Clathrin assembly protein AP-3 is phosphorylated and glycosylated on the 50-kDa structural domain. *J Biol Chem*. (1994) 269:21346–52.
56. Yao PJ, Coleman PD. Reduced O-glycosylated clathrin assembly protein AP180: implication for synaptic vesicle recycling dysfunction in Alzheimer's disease. *Neurosci Lett*. (1998) 252:33–6. doi: 10.1016/S0304-3940(98)00547-3
57. Yao PJ, Coleman PD. Reduction of O-linked N-acetylglucosamine-modified assembly protein-3 in Alzheimer's disease. *J Neurosci*. (1998) 18:2399–411. doi: 10.1523/JNEUROSCI.18-07-02399.1998
58. Akimoto Y, Comer FI, Cole RN, Kudo A, Kawakami H, Hirano H, et al. Localization of the O-GlcNAc transferase and O-GlcNAc-modified proteins in rat cerebellar cortex. *Brain Res*. (2003) 966:194–205. doi: 10.1016/S0006-8993(02)04158-6
59. Vosseller K, Trinidad JC, Chalkley RJ, Specht CG, Thalhammer A, Lynn AJ, et al. O-Linked N-acetylglucosamine proteomics of postsynaptic density preparations using lectin weak affinity chromatography and mass spectrometry. *Mol Cell Proteomics* (2006) 5:923–34. doi: 10.1074/mcp.T500040-MCP200
60. Tallent MK, Varghis N, Skorobogatko Y, Hernandez-Cuebas L, Whelan K, Vocadlo DJ, et al. *In vivo* modulation of O-GlcNAc levels regulates hippocampal synaptic plasticity through interplay with phosphorylation. *J Biol Chem*. (2009) 284:174–81. doi: 10.1074/jbc.M807431200
61. Graham ME, Thaysen-Andersen M, Bache N, Craft GE, Larsen MR, Packer NH, et al. A novel post-translational modification in nerve terminals: O-linked N-acetylglucosamine phosphorylation. *J Proteome Res*. (2011) 10:2725–33. doi: 10.1021/pr1011153
62. Chun YS, Park Y, Oh HG, Kim TW, Yang HO, Park MK, et al. O-GlcNAcylation promotes non-amyloidogenic processing of amyloid-beta protein precursor via inhibition of endocytosis from the plasma membrane. *J Alzheimers Dis*. (2015) 44:261–75. doi: 10.3233/JAD-140096
63. Chun YS, Kwon OH, Chung S. O-GlcNAcylation of amyloid-beta precursor protein at threonine 576 residue regulates trafficking and processing. *Biochem Biophys Res Commun*. (2017) 490:486–91. doi: 10.1016/j.bbrc.2017.06.067
64. Yuzwa SA, Macauley MS, Heinonen JE, Shan X, Dennis RJ, He Y, et al. A potent mechanism-inspired O-GlcNAcase inhibitor that blocks phosphorylation of tau *in vivo*. *Nat Chem Biol*. (2008) 4:483–90. doi: 10.1038/nchembio.96
65. Lossner C, Warnken U, Pscherer A, Schnolzer M. Preventing arginine-to-proline conversion in a cell-line-independent manner during cell cultivation under stable isotope labeling by amino acids in cell culture (SILAC) conditions. *Anal Biochem*. (2011) 412:123–5. doi: 10.1016/j.ab.2011.01.011
66. Foster MW, Yang Z, Gooden DM, Thompson JW, Ball CH, Turner ME, et al. Proteomic characterization of the cellular response to nitrosative stress mediated by s-nitrosoglutathione reductase inhibition. *J Proteome Res*. (2012) 11:2480–91. doi: 10.1021/pr201180m
67. Yang W, Thompson JW, Wang Z, Wang L, Sheng H, Foster MW, et al. Analysis of oxygen/glucose-deprivation-induced changes in SUMO3 conjugation using SILAC-based quantitative proteomics. *J Proteome Res*. (2012) 11:1108–17. doi: 10.1021/pr200834f
68. Foster MW, Thompson JW, Forrester MT, Sha Y, McMahon TJ, Bowles DE, et al. Proteomic analysis of the NOS2 interactome in human airway epithelial cells. *Nitric Oxide* (2013) 34:37–46. doi: 10.1016/j.niox.2013.02.079
69. Ong SE, Blagoev B, Kratchmarova I, Kristensen DB, Steen H, Pandey A, et al. Stable isotope labeling by amino acids in cell culture, SILAC, as a simple and accurate approach to expression proteomics. *Mol Cell Proteomics* (2002) 1:376–86. doi: 10.1074/mcp.M200025-MCP200
70. Terzi F, Cambridge S. An overview of advanced SILAC-labeling strategies for quantitative proteomics. *Methods Enzymol*. (2017) 585:29–47. doi: 10.1016/bs.mie.2016.09.014
71. Rathmell JC, Vander Heiden MG, Harris MH, Frauwirth KA, Thompson CB. In the absence of extrinsic signals, nutrient utilization by lymphocytes is insufficient to maintain either cell size or viability. *Mol Cell* (2000) 6:683–92. doi: 10.1016/S1097-2765(00)00066-6
72. Wieman HL, Wofford JA, Rathmell JC. Cytokine stimulation promotes glucose uptake via phosphatidylinositol-3 kinase/Akt regulation of Glut1 activity and trafficking. *Mol Biol Cell* (2007) 18:1437–46. doi: 10.1091/mbc.e06-07-0593
73. Caro-Maldonado A, Gerriets VA, Rathmell JC. Matched and mismatched metabolic fuels in lymphocyte function. *Semin Immunol*. (2012) 24:405–13. doi: 10.1016/j.smim.2012.12.002
74. Shaffer AL, Shapiro-Shelef M, Iwakoshi NN, Lee AH, Qian SB, Zhao H, et al. XBP1, downstream of Blimp-1, expands the secretory apparatus and other

organelles, and increases protein synthesis in plasma cell differentiation. *Immunity* (2004) 21:81–93. doi: 10.1016/j.immuni.2004.06.010
75. Ron D, Walter P. Signal integration in the endoplasmic reticulum unfolded protein response. *Nat Rev Mol Cell Biol*. (2007) 8:519–29. doi: 10.1038/nrm2199
76. Kearse KP, Hart GW. Lymphocyte activation induces rapid changes in nuclear and cytoplasmic glycoproteins. *Proc Natl Acad Sci USA*. (1991) 88:1701–5. doi: 10.1073/pnas.88.5.1701
77. Golks A, Tran TT, Goetschy JF, Guerini D. Requirement for O-linked N-acetylglucosaminyltransferase in lymphocytes activation. *EMBO J*. (2007) 26:4368–79. doi: 10.1038/sj.emboj.7601845
78. Woo CM, Lund PJ, Huang AC, Davis MM, Bertozzi CR, Pitteri SJ. Mapping and quantification of over 2000 O-linked glycopeptides in activated human T cells with isotope-targeted glycoproteomics (Isotag). *Mol Cell Proteomics* (2018) 17:764–75. doi: 10.1074/mcp.RA117.000261
79. Li B, Kohler JJ. Glycosylation of the nuclear pore. *Traffic* (2014) 15:347–61. doi: 10.1111/tra.12150
80. Wysocka J, Myers MP, Laherty CD, Eisenman RN, Herr W. Human Sin3 deacetylase and trithorax-related Set1/Ash2 histone H3-K4 methyltransferase are tethered together selectively by the cell-proliferation factor HCF-1. *Genes Dev*. (2003) 17:896–911. doi: 10.1101/gad.252103
81. Wang Z, Pandey A, Hart GW. Dynamic interplay between O-linked N-acetylglucosaminylation and glycogen synthase kinase-3-dependent phosphorylation. *Mol Cell Proteomics* (2007) 6:1365–79. doi: 10.1074/mcp.M600453-MCP200
82. Myers SA, Daou S, Affar el B, Burlingame A. Electron transfer dissociation (ETD): the mass spectrometric breakthrough essential for O-GlcNAc protein site assignments-a study of the O-GlcNAcylated protein host cell factor C1. *Proteomics* (2013) 13:982–91. doi: 10.1002/pmic.201200332
83. Fujiwara T, Oda K, Yokota S, Takatsuki A, Ikehara Y. Brefeldin A causes disassembly of the Golgi complex and accumulation of secretory proteins in the endoplasmic reticulum. *J Biol Chem*. (1988) 263:18545–52.
84. Lippincott-Schwartz J, Yuan LC, Bonifacino JS, Klausner RD. Rapid redistribution of Golgi proteins into the ER in cells treated with brefeldin A: evidence for membrane cycling from Golgi to ER. *Cell* (1989) 56:801–13. doi: 10.1016/0092-8674(89)90685-5
85. Peyroche A, Antonny B, Robineau S, Acker J, Cherfils J, Jackson CL. Brefeldin A Acts to stabilize an abortive ARF–GDP–Sec7 domain protein complex involvement of specific residues of the sec7 domain. *Mol Cell* (1999) 3:275–85. doi: 10.1016/S1097-2765(00)80455-4
86. Staub O, Dho S, Henry P, Correa J, Ishikawa T, McGlade J, et al. WW domains of Nedd4 bind to the proline-rich PY motifs in the epithelial Na+ channel deleted in Liddle's syndrome. *EMBO J*. (1996) 15:2371–80. doi: 10.1002/j.1460-2075.1996.tb00593.x
87. Staub O, Gautschi I, Ishikawa T, Breitschopf K, Ciechanover A, Schild L, et al. Regulation of stability and function of the epithelial Na+ channel (ENaC) by ubiquitination. *EMBO J*. (1997) 16:6325–36. doi: 10.1093/emboj/16.21.6325
88. Watson PJ, Frigerio G, Collins BM, Duden R, Owen DJ. Gamma-COP appendage domain - structure and function. *Traffic* (2004) 5:79–88. doi: 10.1111/j.1600-0854.2004.00158.x
89. Frigerio G, Grimsey N, Dale M, Majoul I, Duden R. Two human ARFGAPs associated with COP-I-coated vesicles. *Traffic* (2007) 8:1644–55. doi: 10.1111/j.1600-0854.2007.00631.x
90. Bonifacino JS, Hurley JH. Retromer. *Curr Opin Cell Biol*. (2008) 20:427–36. doi: 10.1016/j.ceb.2008.03.009
91. Granata A, Schiavo G, Warner TT. TorsinA and dystonia: from nuclear envelope to synapse. *J Neurochem*. (2009) 109:1596–609. doi: 10.1111/j.1471-4159.2009.06095.x
92. Kliouchnikov L, Bigay J, Mesmin B, Parnis A, Rawet M, Goldfeder N, et al. Discrete determinants in ArfGAP2/3 conferring Golgi localization and regulation by the COPI coat. *Mol Biol Cell* (2009) 20:859–69. doi: 10.1091/mbc.e08-10-1010
93. Granata A, Warner TT. The role of torsinA in dystonia. *Eur J Neurol*. (2010) 17(Suppl. 1):81–7. doi: 10.1111/j.1468-1331.2010.03057.x
94. Laney JD, Hochstrasser M. Analysis of protein ubiquitination. *Curr Protoc Protein Sci Chapter* (2011) 14:15. doi: 10.1002/0471140864.ps1405s66
95. Zaro BW, Yang YY, Hang HC, Pratt MR. Chemical reporters for fluorescent detection and identification of O-GlcNAc-modified proteins reveal glycosylation of the ubiquitin ligase NEDD4-1. *Proc Natl Acad Sci USA*. (2011) 108:8146–51. doi: 10.1073/pnas.1102458108
96. Boase NA, Kumar S. NEDD4: The founding member of a family of ubiquitin-protein ligases. *Gene* (2015) 557:113–22. doi: 10.1016/j.gene.2014.12.020
97. Goel P, Manning JA, Kumar S. NEDD4-2 (NEDD4L): The ubiquitin ligase for multiple membrane proteins. *Gene* (2015) 557:1–10. doi: 10.1016/j.gene.2014.11.051
98. Wang S, Bellen HJ. The retromer complex in development and disease. *Development* (2015) 142:2392–6. doi: 10.1242/dev.123737
99. Laudermilch E, Schlieker C. Torsin ATPases: structural insights and functional perspectives. *Curr Opin Cell Biol*. (2016) 40:1–7. doi: 10.1016/j.ceb.2016.01.001
100. Verges M. Retromer in polarized protein transport. *Int Rev Cell Mol Biol*. (2016) 323:129–79. doi: 10.1016/bs.ircmb.2015.12.005
101. Williams ET, Chen X, Moore DJ. VPS35, the retromer complex and Parkinson's Disease. *J Parkinsons Dis*. (2017) 7:219–33. doi: 10.3233/JPD-161020
102. Waters MG, Serafini T, Rothman JE. 'Coatomer': a cytosolic protein complex containing subunits of non-clathrin-coated Golgi transport vesicles. *Nature* (1991) 349:248–51. doi: 10.1038/349248a0
103. Hara-Kuge S, Kuge O, Orci L, Amherdt M, Ravazzola M, Wieland FT, et al. En bloc incorporation of coatomer subunits during the assembly of COP-coated vesicles. *J Cell Biol*. (1994) 124:883–92. doi: 10.1083/jcb.124.6.883
104. Gaynor EC, Graham TR, Emr SD. COPI in ER/Golgi and intra-Golgi transport: do yeast COPI mutants point the way? *Biochim Biophys Acta* (1998) 1404:33–51. doi: 10.1016/S0167-4889(98)00045-7
105. Strating JR, Martens GJ. The p24 family and selective transport processes at the ER-Golgi interface. *Biol Cell* (2009) 101:495–509. doi: 10.1042/BC20080233
106. Sheff D, Lowe M, Kreis TE, Mellman I. Biochemical heterogeneity and phosphorylation of coatomer subunits. *J Biol Chem*. (1996) 271:7230–6. doi: 10.1074/jbc.271.12.7230
107. Christensen GL, Kelstrup CD, Lyngso C, Sarwar U, Bogebo R, Sheikh SP, et al. Quantitative phosphoproteomics dissection of seven-transmembrane receptor signaling using full and biased agonists. *Mol Cell Proteomics* (2010) 9:1540–53. doi: 10.1074/mcp.M900550-MCP200
108. Kim W, Bennett EJ, Huttlin EL, Guo A, Li J, Possemato A, et al. Systematic and quantitative assessment of the ubiquitin-modified proteome. *Mol Cell* (2011) 44:325–40. doi: 10.1016/j.molcel.2011.08.025
109. Imami K, Sugiyama N, Imamura H, Wakabayashi M, Tomita M, Taniguchi M, et al. Temporal profiling of lapatinib-suppressed phosphorylation signals in EGFR/HER2 pathways. *Mol Cell Proteomics* (2012) 11:1741–57. doi: 10.1074/mcp.M112.019919
110. Mertins P, Qiao JW, Patel J, Udeshi ND, Clauser KR, Mani DR, et al. Integrated proteomic analysis of post-translational modifications by serial enrichment. *Nat Methods* (2013) 10:634–7. doi: 10.1038/nmeth.2518
111. Schweppe DK, Rigas JR, Gerber SA. Quantitative phosphoproteomic profiling of human non-small cell lung cancer tumors. *J Proteomics* (2013) 91:286–96. doi: 10.1016/j.jprot.2013.07.023
112. Mertins P, Yang F, Liu T, Mani DR, Petyuk VA, Gillette MA, et al. Ischemia in tumors induces early and sustained phosphorylation changes in stress kinase pathways but does not affect global protein levels. *Mol Cell Proteomics* (2014) 13:1690–704. doi: 10.1074/mcp.M113.036392
113. Sharma K, D'Souza RC, Tyanova S, Schaab C, Wisniewski JR, Cox J, et al. Ultradeep human phosphoproteome reveals a distinct regulatory nature of Tyr and Ser/Thr-based signaling. *Cell Rep*. (2014) 8:1583–94. doi: 10.1016/j.celrep.2014.07.036
114. Stuart SA, Houel S, Lee T, Wang N, Old WM, Ahn NG. A phosphoproteomic comparison of B-RAFV600E and MKK1/2 inhibitors in melanoma cells. *Mol Cell Proteomics* (2015) 14:1599–615. doi: 10.1074/mcp.M114.047233
115. Larsen SC, Sylvestersen KB, Mund A, Lyon D, Mullari M, Madsen MV, et al. Proteome-wide analysis of arginine monomethylation reveals widespread occurrence in human cells. *Sci Signal*. (2016) 9:rs9. doi: 10.1126/scisignal.aaf7329
116. Mertins P, Mani DR, Ruggles KV, Gillette MA, Clauser KR, Wang P, et al. Proteogenomics connects somatic mutations to signalling in breast cancer. *Nature* (2016) 534:55–62. doi: 10.1038/nature18003

117. Dodonova SO, Diestelkoetter-Bachert P, von Appen A, Hagen WJ, Beck R, Beck M, et al. VESICULAR TRANSPORT. A structure of the COPI coat and the role of coat proteins in membrane vesicle assembly. *Science* (2015) 349:195–8. doi: 10.1126/science.aab1121
118. Ramakrishnan B, Qasba PK. Structure-based design of beta 1,4-galactosyltransferase I (beta 4Gal-T1) with equally efficient N-acetylgalactosaminyltransferase activity: point mutation broadens beta 4Gal-T1 donor specificity. *J Biol Chem*. (2002) 277:20833–9. doi: 10.1074/jbc.M111183200
119. Wells L, Vosseller K, Cole RN, Cronshaw JM, Matunis MJ, Hart GW. Mapping sites of O-GlcNAc modification using affinity tags for serine and threonine post-translational modifications. *Mol Cell Proteomics* (2002) 1:791–804. doi: 10.1074/mcp.M200048-MCP200
120. Khidekel N, Arndt S, Lamarre-Vincent N, Lippert A, Poulin-Kerstien KG, Ramakrishnan B, et al. A chemoenzymatic approach toward the rapid and sensitive detection of O-GlcNAc posttranslational modifications. *J Am Chem Soc*. (2003) 125:16162–3. doi: 10.1021/ja038545r
121. Tai HC, Khidekel N, Ficarro SB, Peters EC, Hsieh-Wilson LC. Parallel identification of O-GlcNAc-modified proteins from cell lysates. *J Am Chem Soc*. (2004) 126:10500–1. doi: 10.1021/ja047872b
122. Vosseller K, Hansen KC, Chalkley RJ, Trinidad JC, Wells L, Hart GW, et al. Quantitative analysis of both protein expression and serine / threonine post-translational modifications through stable isotope labeling with dithiothreitol. *Proteomics* (2005) 5:388–98. doi: 10.1002/pmic.200401066
123. Khidekel N, Ficarro SB, Clark PM, Bryan MC, Swaney DL, Rexach JE, et al. Probing the dynamics of O-GlcNAc glycosylation in the brain using quantitative proteomics. *Nat Chem Biol*. (2007) 3:339–48. doi: 10.1038/nchembio881
124. Clark PM, Dweck JF, Mason DE, Hart CR, Buck SB, Peters EC, et al. Direct in-gel fluorescence detection and cellular imaging of O-GlcNAc-modified proteins. *J Am Chem Soc*. (2008) 130:11576–7. doi: 10.1021/ja8030467
125. Chalkley RJ, Thalhammer A, Schoepfer R, Burlingame AL. Identification of protein O-GlcNAcylation sites using electron transfer dissociation mass spectrometry on native peptides. *Proc Natl Acad Sci USA*. (2009) 106:8894–9. doi: 10.1073/pnas.0900288106
126. Rexach JE, Rogers CJ, Yu SH, Tao J, Sun YE, Hsieh-Wilson LC. Quantification of O-glycosylation stoichiometry and dynamics using resolvable mass tags. *Nat Chem Biol*. (2010) 6:645–51. doi: 10.1038/nchembio.412
127. Sakabe K, Wang Z, Hart GW. Beta-N-acetylglucosamine (O-GlcNAc) is part of the histone code. *Proc Natl Acad Sci USA*. (2010) 107:19915–20. doi: 10.1073/pnas.1009023107
128. Wang Z, Udeshi ND, O'Malley M, Shabanowitz J, Hunt DF, Hart GW. Enrichment and site mapping of O-linked N-acetylglucosamine by a combination of chemical/enzymatic tagging, photochemical cleavage, and electron transfer dissociation mass spectrometry. *Mol Cell Proteomics* (2010) 9:153–60. doi: 10.1074/mcp.M900268-MCP200
129. Myers SA, Panning B, Burlingame AL. Polycomb repressive complex 2 is necessary for the normal site-specific O-GlcNAc distribution in mouse embryonic stem cells. *Proc Natl Acad Sci USA*. (2011) 108:9490–5. doi: 10.1073/pnas.1019289108
130. Alfaro JF, Gong CX, Monroe ME, Aldrich JT, Clauss TR, Purvine SO, et al. Tandem mass spectrometry identifies many mouse brain O-GlcNAcylated proteins including EGF domain-specific O-GlcNAc transferase targets. *Proc Natl Acad Sci USA*. (2012) 109:7280–5. doi: 10.1073/pnas.1200425109
131. Rexach JE, Clark PM, Mason DE, Neve RL, Peters EC, Hsieh-Wilson LC. Dynamic O-GlcNAc modification regulates CREB-mediated gene expression and memory formation. *Nat Chem Biol*. (2012) 8:253–61. doi: 10.1038/nchembio.770
132. Ma J, Hart GW. O-GlcNAc profiling: from proteins to proteomes. *Clinical Proteomics* (2014) 11:1–16. doi: 10.1186/1559-0275-11-8
133. Ma J, Liu T, Wei AC, Banerjee P, O'Rourke B, Hart GW. O-GlcNAcomic profiling identifies widespread O-Linked beta-N-Acetylglucosamine modification (O-GlcNAcylation) in oxidative phosphorylation system regulating cardiac mitochondrial function. *J Biol Chem*. (2015) 290:29141–53. doi: 10.1074/jbc.M115.691741
134. Cox NJ, Meister TR, Boyce M. Chemical biology of O-GlcNAc glycosylation. In: Wang L-X, Tan Z, editors. *Chemical Biology of Glycoproteins*. Cambridge: Royal Society of Chemistry (2017). p. 94–149.
135. Langer JD, Roth CM, Béthune J, Stoops EH, Brügger B, Herten DP, et al. A Conformational Change in the α-subunit of Coatomer Induced by Ligand Binding to γ-COP Revealed by Single-pair FRET. *Traffic* (2008) 9:597–607. doi: 10.1111/j.1600-0854.2007.00697.x
136. Reinhard C, Harter C, Bremser M, Brugger B, Sohn K, Helms JB, et al. Receptor-induced polymerization of coatomer. *Proc Natl Acad Sci USA*. (1999) 96:1224–8. doi: 10.1073/pnas.96.4.1224
137. Deng RP, He X, Guo SJ, Liu WF, Tao Y, Tao SC. Global identification of O-GlcNAc transferase (OGT) interactors by a human proteome microarray and the construction of an OGT interactome. *Proteomics* (2014) 14:1020–30. doi: 10.1002/pmic.201300144
138. Tarbet HJ, Toleman CA, Boyce M. A sweet embrace: control of protein-protein interactions by O-linked beta-N-acetylglucosamine. *Biochemistry* (2018) 57:13–21. doi: 10.1021/acs.biochem.7b00871
139. Fiedler K, Veit M, Stamnes MA, Rothman JE. Bimodal interaction of coatomer with the p24 family of putative cargo receptors. *Science* (1996) 273:1396–9. doi: 10.1126/science.273.5280.1396
140. Sohn K, Orci L, Ravazzola M, Amherdt M, Bremser M, Lottspeich F, et al. A major transmembrane protein of Golgi-derived COPI-coated vesicles involved in coatomer binding. *J Cell Biol*. (1996) 135:1239–48. doi: 10.1083/jcb.135.5.1239
141. Bethune J, Kol M, Hoffmann J, Reckmann I, Brugger B, Wieland F. Coatomer, the coat protein of COPI transport vesicles, discriminates endoplasmic reticulum residents from p24 proteins. *Mol Cell Biol*. (2006) 26:8011–21. doi: 10.1128/MCB.01055-06
142. Bykov YS, Schaffer M, Dodonova SO, Albert S, Plitzko JM, Baumeister W, et al. The structure of the COPI coat determined within the cell. *Elife* (2017) 6:e32493. doi: 10.7554/eLife.32493
143. Dodonova SO, Aderhold P, Kopp J, Ganeva I, Rohling S, Hagen WJH, et al. 9A structure of the COPI coat reveals that the Arf1 GTPase occupies two contrasting molecular environments. *Elife* (2017) 6:e266691. doi: 10.7554/eLife.26691
144. Hornbeck PV, Zhang B, Murray B, Kornhauser JM, Latham V, Skrzypek E. PhosphoSitePlus, 2014: mutations, PTMs and recalibrations. *Nucleic Acids Res.* (2015) 43(Database issue):D512–20. doi: 10.1093/nar/gku1267
145. Wang Z, Udeshi ND, Slawson C, Compton PD, Sakabe K, Cheung WD, et al. Extensive crosstalk between O-GlcNAcylation and phosphorylation regulates cytokinesis. *Sci Signal*. (2010) 3:ra2. doi: 10.1126/scisignal.2000526
146. Trinidad JC, Barkan DT, Gulledge BF, Thalhammer A, Sali A, Schoepfer R, et al. Global identification and characterization of both O-GlcNAcylation and phosphorylation at the murine synapse. *Mol Cell Proteomics* (2012) 11:215–29. doi: 10.1074/mcp.O112.018366
147. Wang S, Huang X, Sun D, Xin X, Pan Q, Peng S, et al. Extensive crosstalk between O-GlcNAcylation and phosphorylation regulates Akt signaling. *PLoS ONE* (2012) 7:e37427. doi: 10.1371/journal.pone.0037427
148. Zhong J, Martinez M, Sengupta S, Lee A, Wu X, Chaerkady R, et al. Quantitative phosphoproteomics reveals crosstalk between phosphorylation and O-GlcNAc in the DNA damage response pathway. *Proteomics* (2015) 15:591–607. doi: 10.1002/pmic.201400339
149. Leney AC, El Atmioui D, Wu W, Ovaa H, Heck AJR. Elucidating crosstalk mechanisms between phosphorylation and O-GlcNAcylation. *Proc Natl Acad Sci USA*. (2017) 114:201620529. doi: 10.1073/pnas.1620529114

Conflict of Interest Statement: The authors declare that the research was conducted in the absence of any commercial or financial relationships that could be construed as a potential conflict of interest.

frontiers in Endocrinology

REVIEW
published: 16 October 2018
doi: 10.3389/fendo.2018.00578

Involvement of O-GlcNAcylation in the Skeletal Muscle Physiology and Physiopathology: Focus on Muscle Metabolism

*Matthias Lambert†, Bruno Bastide and Caroline Cieniewski-Bernard**

Equipe Activité Physique, Muscle, Santé, Unité de Recherche Pluridisciplinaire Sport, Santé, Société (EA7369-URePSSS), Faculté des Sciences et Technologies, Université de Lille, Lille, France

OPEN ACCESS

Edited by:
Tony Lefebvre, Lille University of Science and Technology, France

Reviewed by:
Anna Krzeslak, University of Łódz, Poland
Yobana Perez-Cervera, Benito Juárez Autonomous University of Oaxaca, Mexico
Abderrahman Maftah, University of Limoges, France

***Correspondence:**
Caroline Cieniewski-Bernard
caroline.cieniewski-bernard@univ-lille.fr

†Present Address:
Matthias Lambert, Division of Genetics and Genomics, Boston Children's Hospital, Boston, MA, United States; Department of Pediatrics, Harvard Medical School, Boston, MA, United States

Specialty section:
This article was submitted to Molecular and Structural Endocrinology, a section of the journal Frontiers in Endocrinology

Received: *21 June 2018*
Accepted: *11 September 2018*
Published: *16 October 2018*

Citation:
Lambert M, Bastide B and Cieniewski-Bernard C (2018) Involvement of O-GlcNAcylation in the Skeletal Muscle Physiology and Physiopathology: Focus on Muscle Metabolism. Front. Endocrinol. 9:578. doi: 10.3389/fendo.2018.00578

Skeletal muscle represents around 40% of whole body mass. The principal function of skeletal muscle is the conversion of chemical energy toward mechanic energy to ensure the development of force, provide movement and locomotion, and maintain posture. This crucial energy dependence is maintained by the faculty of the skeletal muscle for being a central place as a "reservoir" of amino acids and carbohydrates in the whole body. A fundamental post-translational modification, named O-GlcNAcylation, depends, *inter alia*, on these nutrients; it consists to the transfer or the removal of a unique monosaccharide (N-acetyl-D-glucosamine) to a serine or threonine hydroxyl group of nucleocytoplasmic and mitochondrial proteins in a dynamic process by the O-GlcNAc Transferase (OGT) and the O-GlcNAcase (OGA), respectively. O-GlcNAcylation has been shown to be strongly involved in crucial intracellular mechanisms through the modulation of signaling pathways, gene expression, or cytoskeletal functions in various organs and tissues, such as the brain, liver, kidney or pancreas, and linked to the etiology of associated diseases. In recent years, several studies were also focused on the role of O-GlcNAcylation in the physiology and the physiopathology of skeletal muscle. These studies were mostly interested in O-GlcNAcylation during muscle exercise or muscle-wasting conditions. Major findings pointed out a different "O-GlcNAc signature" depending on muscle type metabolism at resting, wasting and exercise conditions, as well as depending on acute or long-term exhausting exercise protocol. First insights showed some differential OGT/OGA expression and/or activity associated with some differential stress cellular responses through Reactive Oxygen Species and/or Heat-Shock Proteins. Robust data displayed that these O-GlcNAc changes could lead to (i) a differential modulation of the carbohydrates metabolism, since the majority of enzymes are known to be O-GlcNAcylated, and to (ii) a differential modulation of the protein synthesis/degradation balance since O-GlcNAcylation regulates some key signaling pathways such as Akt/GSK3β,

Akt/mTOR, Myogenin/Atrogin-1, Myogenin/Mef2D, Mrf4 and PGC-1α in the skeletal muscle. Finally, such involvement of O-GlcNAcylation in some metabolic processes of the skeletal muscle might be linked to some associated diseases such as type 2 diabetes or neuromuscular diseases showing a critical increase of the global O-GlcNAcylation level.

Keywords: O-GlcNAcylation, slow-twitch muscle, fast-twitch muscle, glucose metabolism, exercise, skeletal muscle atrophy

INTRODUCTION

Just over thirty years ago, the O-linked N-acetyl-β-D-glucosaminylation, termed O-GlcNAcylation, was discovered inside the mouse lymphocyte cells by Torres and Hart (1). From this discovery, about 1,400 studies were focused on this field among hundreds of other known post-translational modifications. Nowadays, scientific community shows a growing interest since half of these previous studies was published in the last 5 years, and provides more and more relevant data to better characterize the impact of O-GlcNAcylation on cellular processes. It is ubiquitous from virus to plantae and metazoan, and to date around 4000 O-GlcNAc-modified proteins have been identified (2). O-GlcNAcylation seems to be an important molecular process in biology, especially since ubiquitous *OGT* and *OGA* knockout mice experiments revealed that O-GlcNAcylation balance is crucial for embryonic stem cell viability and embryonic development (3, 4); recent data also supported the essential role of O-GlcNAcylation in adult life since inducible global knockout of *OGT* dramatically increased mice mortality (5).

O-GlcNAcylation is an atypical, reversible and dynamic glycosylation. Unlike the N- and O- glycans, the O-GlcNAcylation consists of the transfer of a unique monosaccharide which is not elongated, the N-acetyl-D-glucosamine, on a plethora of nucleocytoplasmic (6) and mitochondrial proteins (7). The O-GlcNAc modification is mediated by a couple of antagonist enzymes; the OGT (uridine diphospho-N-acetylglucosamine: peptide beta-N-acetyl-glucosaminyl-transferase) transfers the monosaccharide from the UDP-GlcNAc donor to a serine or threonine hydroxyl group of a protein through a beta linkage (8), while OGA (beta-N-acetylglucosaminidase) hydrolyses the O-GlcNAc moieties from O-GlcNAcylated proteins (9). Very recent data have shown that the moiety can also be added to proteins intended for the extracellular compartment, through a distinct and structurally unrelated OGT (called EGF-OGT) which works in an OGT-independent manner (10–12). Besides its reversibility, O-GlcNAcylation is also highly dynamic. Indeed, the GlcNAc moieties can be added and removed several times along the protein lifetime, and the turn-over is shorter than the protein backbone's one. Moreover, this O-GlcNAc dynamic process could reply to many environmental conditions and physiological signals such as nutriment availability, especially from its UDP-GlcNAc donor, the last product of the Hexosamine Biosynthesis Pathway (13, 14). Finally, O-GlcNAcylation can also interplay with certain other post-translational modifications such as phosphorylation and ubiquitination [for review, see (15–17)].

Nowadays, there is evidence that some fundamental protein functions are modulated through the O-GlcNAcylation, including protein-protein interactions (18, 19), protein stability (20, 21), protein activity (22), or protein localization (23). Akin to phosphorylation, the O-GlcNAcylation is involved in almost all if not all intracellular processes (15, 24, 25) and different data demonstrated that its dysregulation can play a crucial role in the etiology of several diseases including type II diabetes (26, 27), cancer (28, 29), neurodegenerative disorders (30, 31), X-linked intellectual disability (32), neuromuscular (33), or cardiovascular diseases (34, 35), and linked to aging (36).

However, recent data showed that O-GlcNAcylation is also involved in different cellular processes of the skeletal muscle, and its potential role in many disorders related to skeletal muscle defects is still undervalued. This present review discusses the involvement of O-GlcNAcylation in skeletal muscle metabolism (in particular glucose metabolism), the impact of exercise on O-GlcNAcylation, and finally, the potential role of this post-translational modification in skeletal muscle in a context of disease such as type 2 diabetes and neuromuscular disorders.

RELATIONSHIP BETWEEN O-GLCNACYLATION AND METABOLISM IN SKELETAL MUSCLE

In the human body, the skeletal muscle is an essential tissue that converts chemical energy into mechanical energy, i.e., contraction, to generate force and ensure some fundamental functions of the body such as movement production, posture control and thermoregulation (37). The skeletal muscle represents 40% of the total human body weight, contains 50 to 75% of all body proteins and accounts for 30 to 50% of whole-body protein turnover (37). It is a huge reservoir of nutrients (e.g., glycogen and amino acids), a great producer/consumer of energy and accounts for 30% of the resting metabolic rate in adult human. For instance, from basal state to fully state of contraction, the skeletal muscle can 300-fold increase its energy consumption within a few milliseconds (38). Interestingly, O-GlcNAcylation is known to be a cell nutrient sensor and the "O-GlcNAc signature" depends on the biological state of cells (39). Within the unitary contractile apparatus, named sarcomere, and more generally in the overall skeletal muscle cell, diverse proteins have been identified to be O-GlcNAcylated since 2004 (18, 40–43); the nature of these proteins is diversified including contractile,

structural, cytoskeletal, metabolic, chaperones, mitochondrial proteins or proteins involved in signaling pathways. Thus, akin to phosphorylation (37, 44, 45), O-GlcNAcylation could play a significant role, still undervalued, in the skeletal muscle physiology.

Exercise-Mediated O-Glcnacylation Changes in the Skeletal Muscle

Contraction is the main function of the skeletal muscle to provide force generation and ensure movement production and posture control from baseline to exercise conditions. Skeletal muscle is able to develop several adaptations with exercise by changes in contractile protein isoforms, protein turnover, metabolism, mitochondrial functions, intracellular signaling or transcriptional response [for review, see (46–48)]. As described, O-GlcNAcylation highly depends on metabolism through the Hexosamine Biosynthesis Pathway and the UDP-GlcNAc donor. Glucose metabolism has a key role in this process since about 2–5% of the glucose enters the HBP, while the remaining glucose goes to glycogen storage or glycolysis (13, 49). In addition, a study carried out on skeletal muscle, showed that HBP also depends on fatty acids, glutamate or nucleic acids (50). Among other processes, muscle contraction directly impacts glucose homeostasis. For example, exercise increases skeletal muscle glucose uptake through an insulin-dependent/GLUT4 transport pathway (51, 52) or through the activation of CamKII by calcium released upon muscle contraction (53). Thus, we can assume that O-GlcNAcylation could be modulated through muscle-training and induces several effects on muscle functions. However, although many studies reported the importance of exercise in the modulation of cardiac O-GlcNAcylation (54–59), to date there is a very few studies interesting in the skeletal muscle.

It's long recognized that metabolic flexibility concept occurs in skeletal muscle, meaning for example its ability to increase energy supply and provide sufficient and adequate "fuel" for muscle working (48). In this context, it has been recently shown that exercise could also modulate the global O-GlcNAcylation level in rat skeletal muscle (60–62). Two different types of exercise training were applied on rat: a single acute exercise run bout to fatigue and an exhausting 6-weeks interval training program, both on treadmill. Consecutively to the acute exercise, the global level of O-GlcNAcylation was not changed in the slow-twitch oxidative soleus nor in the fast-twitch glycolytic EDL as well (62) (**Table 1**). In contrast, a long-term training program on rat led to an increase of the global O-GlcNAcylation level in the total extract in soleus and EDL as well, whereas its level was not altered in the myofilament fraction (62). In this study, no alteration of the OGT and OGA expression was observed in both exercise protocols, suggesting a potential regulation at the activity level following the long-term exercise. However, in another study, the same authors mentioned a decreased OGA expression in the total extract of the soleus, and not in the myofilament fraction as well as in both extracts in the EDL after a similar long-term training program on rat, suggesting a differential OGA turnover which might explain, partly at least, changes in the O-GlcNAc rate between EDL and soleus (61).

TABLE 1 | Difference of O-GlcNAcylation process and exercise effect on slow-twitch and fast-twitch muscles. The major muscle properties of both muscle types are also indicated.

	Slow-twitch muscle	Fast-twitch muscle
Muscle properties	Red muscle, slow contraction, oxidative metabolism, fatigue resistance *Example:* soleus	White muscle, fast contraction, glycolytic metabolism, fatigue sensitivity *Example:* EDL, white gastrocnemius
O-GlcNAcylation level	O-GlcNAcylation level in soleus > EDL	
Expression of enzymes involved in O-GlcNAcylation process	• Expression of OGT, OGA, GFAT1, GFAT2 in soleus > EDL • OGT activity on soleus > EDL	
VARIATION OF O-GLCNACYLATION LEVEL DURING EXERCISE		
Chronic Exercise	↗	↗
Acute exercise	Ø	Ø
Acute exercise + glutathione depletion	Ø	↗

Otherwise, these O-GlcNAc adaptations following skeletal muscle activity seemed to be fully different according to the exercise protocol as well as the skeletal muscle fiber type. This could be first related to the metabolic flexibility and glucose utilization known to be different and differentially regulated depending on exercise protocols and muscle fiber types (46, 48). Little is known so far how exercise can modulate the glucose flux in the Hexosamine Biosynthesis Pathway. A study demonstrated that hindlimb skeletal muscle UDP-HexNAc concentration increased after a single swimming protocol in *ad libitum*-fed but not in fasted rats. In parallel, muscle glycogen content decreased and the GFAT activity was not altered in these conditions (63). Thus, it would be also interesting to determine how the glucose metabolism could operate a distinct modulation of O-GlcNAcylation in skeletal muscles depending on different exercise protocols since (i) the metabolism is different from fast and slow-twitch muscle, (ii) the O-GlcNAcylation is highly regulated through glucose metabolism and (iii) the glucose uptake through GLUT4 is highly modulated in skeletal muscle during exercise (52). These future directions could bring new insights in the involvement of the O-GlcNAcylation in the modulation of the beneficial effects of exercise in skeletal muscle, as a game changer to develop new strategies that counteract some muscular disorders or metabolic disorders such as obesity or diabetes mellitus.

Moreover, the O-GlcNAc adaptations post-exercise could also be directly linked to a differential modulation of the O-GlcNAc pattern and the O-GlcNAc processing enzymes between both muscle fiber types seen at resting conditions. Indeed, the O-GlcNAcylation level is higher in the slow soleus muscle compared with the fast EDL muscle (62, 64, 65); in parallel, the expression level of OGT, OGA, GFAT1, and GFAT2 is higher in soleus than in EDL (62), as well as the activity of OGT (64) (**Table 1**).

Finally, it is well known that the metabolism and stress response between the fast-twitch glycolytic fibers and the slow-twitch oxidative fibers are different (46). Thus, this concept could support the differential modulation of O-GlcNAcylation inducing variable consequences on cellular functions during basal and exercise conditions. During muscle activity, reactive oxygen species (ROS) are produced in skeletal muscle (66) and the O-GlcNAcylation has been shown to be involved in the modulation of oxidative stress through different signaling pathways including KEAP1/NRF2, FOXO, NFκB, and p53 (67–69). A recent study compared the O-GlcNAc pattern and O-GlcNAc processing enzymes expression between a single Diethyl Maleate (DEM) intraperitoneal injection in order to deplete glutathione, meaning oxidative stress in rat, and a single acute exercise on treadmill (60). Interestingly, in the fast-twitch white gastrocnemius, the global level of O-GlcNAcylation increased after acute exercise as well as glutathione depletion. On the contrary, in the slow-twitch soleus, no significant variation of the global O-GlcNAc level was observed (**Table 1**). These data suggest that the differential oxidant/antioxidant balance between slow and fast-twitch muscle could also be at the origin of the differential modulation of the O-GlcNAcylation level observed in the two muscle types. However, this complex interrelationship between cellular redox state and O-GlcNAcylation seems not to be the only mechanism involved in the O-GlcNAc regulation during exercise since the *OGT* and *GFAT* mRNA expressions were different between acute exercise and glutathione depletion in both muscles (60).

O-GlcNAcylation Could Mediate the Skeletal Muscle Glucose Metabolism

Recent studies demonstrated that energy metabolism, insulin sensitivity and exercise-induced glucose uptake depends on O-GlcNAcylation (65, 70). Indeed, the muscle specific knockout of *OGT* led to the increase of glucose uptake in skeletal muscle in basal conditions (65) as well as consequently to exercise (70). Thus, the specific inhibition of O-GlcNAcylation in skeletal muscle also led to facilitation of glucose utilization in skeletal muscle, leading to greater exercise-induced glucose disposal, involving AMPK (70). Interestingly, the enhancement of glucose uptake was correlated to an increase of glycolytic enzymes activities, suggesting that mice have greater reliance of carbohydrates for energy production (65).

It is worth to note that almost all enzymes of glycolytic pathway such as phosphofructokinase (PFK), fructose bisphosphate aldolase (FBPA), triose phosphate isomerase (TPI), glyceraldehyde-3-phosphate dehydrogenase (GAPDH), beta-enolase (BE), and pyruvate kinase (PK) are O-GlcNAcylated (40, 71–76) [and for review, see (77, 78)] (**Figure 1**). Thus, O-GlcNAcylation may regulate the expression and/or activity of glycolytic enzymes and might consequently be involved in the regulation of glucose metabolism in skeletal muscle. To support this important role of O-GlcNAcylation as nutrient-sensor, it was first demonstrated that O-GlcNAcylation is involved in the regulation of phosphofructokinase 1 and pyruvate kinase M2 activity (71, 73). Indeed, induction of O-GlcNAcylation at serine 529 of PFK1 inhibited PFK1 oligomerization and activity, and reduced glycolytic flux as well (71). Moreover, knockdown of *OGT* led to an increased PKM2 activity (73). In this previous study, the resulting decrease of O-GlcNAc PKM2 level was associated to a decreased PKM2 expression, and to a decrease of PKM2 serine phosphorylation (73). Conversely, the increase of PKM2 O-GlcNAcylation by the use of Thiamet-G, a potent OGA inhibitor, led to upregulation of PKM2 expression and a decreased PKM2 activity (73). More recently, pharmacological inhibition of OGA and knockdown of *OGT* were associated to a respective increase and decrease of GK expression, which is the major regulator of the glucose input into cell and therefore the major regulator of glucose metabolism (79). Thus, O-GlcNAcylation is a key regulator of enzymes of glycolysis; interestingly, two downstream enzymes of PK, lactate dehydrogenase (LD) and pyruvate dehydrogenase (PDH) are also modified by O-GlcNAc moieties (74), suggesting that O-GlcNAcylation may also be an important regulator of the utilization of the glycolysis end-product, i.e., pyruvate, through the anaerobic pathway (lactate dehydrogenase) or the aerobic pathway (TCA cycle; **Figure 1**). Since almost all enzymes of TCA cycle are described to be O-GlcNAc modified [aconitate hydratase (A), isocitrate dehydrogenase (IDH), ketoglutarate dehydrogenase (KGD), succinyl-CoA ligase (SL), succinate dehydrogenase (SDH) and malate dehydrogenase (MDH), so as several subunits of respiratory chain complexes (40, 80, 81)], O-GlcNAcylation might play an important role in the ATP production as well (**Figure 1**). However, to date, neither literature mention a potential O-GlcNAcylation of citrate synthase (CS) and fumarate hydratase (FH). In the same way, the creatine shuttle, permitting the communication between ATP site consumption (i.e., myofibrillar ATPases) and mitochondria (82), could be therefore modulated by O-GlcNAcylation since creatine kinase is itself O-GlcNAcylated (40).

Many data suggest a close association between the myofibrils and the enzymes involved in the metabolism. Indeed, the fructose-bisphosphate aldolase (FBPA), enzyme of glycolysis and neo-glucogenesis, is known to be localized to the Z-line of the sarcomere in association with α-actinin within a multiprotein complex termed metabolon (83, 84). In the same way, the interaction between phosphoglucoisomerase (PGM), phosphofructokinase (PFK), glyceraldehyde-3-phosphate dehydrogenase (GAPDH), pyruvate kinase (PK) and aldolase (FBPA) also occurs with the thin filament (85, 86). These specific interactions between glycolytic enzyme complexes (termed glycolytic metabolon) and the contractile apparatus may ensure a very efficient and dynamic localized production of ATP for myosin ATPase and actomyosin interactions resulting in force development. Indeed, it was recently demonstrated that the global modulation of O-GlcNAcylation level in C2C12 skeletal muscle cells differentiated into myotubes led to the modulation of protein-protein interactions in multiprotein complexes; while this study focused on structural proteins, the proteomic data suggested that the glycolytic metabolon could be modulated by O-GlcNAcylation changes as well (**Figure 1**) (18). Indeed, several glycolytic enzymes (indicated by blue asterisks on **Figure 1**) were identified in protein-protein complexes

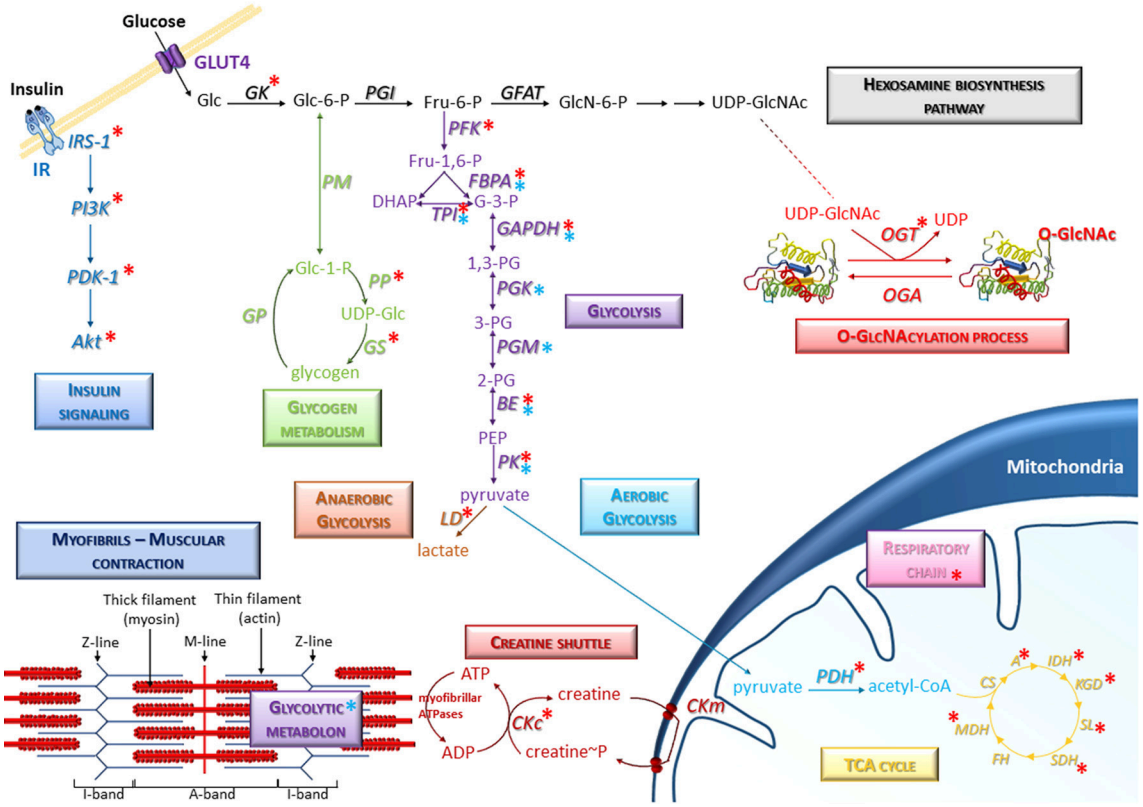

FIGURE 1 | Representative scheme of the presence of O-GlcNAcylation on glucose metabolism in skeletal muscle. Several signaling and metabolic pathways are indicated, in particular the hexosamine biosynthesis pathway, glycolysis (anaerobic and aerobic glycolysis), glycogen metabolism, insulin signaling, and TCA cycle. Specific molecular components of skeletal muscle such as myofibrils and creatine shuttle are also represented. Red asterisks correspond to O-GlcNAcylated proteins; blue asterisks correspond to enzymes including in protein-protein complexes (such as the glycolytic metabolon) which could be potentially modulated consecutively to O-GlcNAcylation changes in skeletal muscle cells. A, Aconitase; BE, Beta-enolase; CKc, Creatine kinase cytoplasmic; CKm, Creatine kinase mitochondrial; CS, Citrate synthase; FBPA, Fructose-bisphosphate aldolase; FH, Fumarate hydratase; GAPDH, Glyceraldehyde-3-phosphate dehydrogenase; GFAT, Glutamine,fructose-6-phosphate aminotransferase; GK, Glucokinase; GP, Glycogen phosphorylase; GS, Glycogen synthase; IDH, Isocitrate dehydrogenase; KGD, Ketoglutarate dehydrogenase; LD, Lactate dehydrogenase; MDH, Malate dehydrogenase; OGA, O-GlcNAcase; OGT, O-GlcNAc transferase; PDH, Pyruvate Dehydrogenase; PFK, Phosphofructokinase; PGI, Phosphoglucose isomerase; PGK, Phosphoglycerate kinase; PGM, Phosphoglycerate mutase; PK, Pyruvate kinase; PM, phosphoglucomutase; PP, UDP-glucose pyrophosphorylase; SDH, Succinate Dehydrogenase; SL, Succinyl-CoA ligase; TPI, Triose-phosphate isomerase.

which were modulated after the global O-GlcNAcylation changes, suggesting that the glycolytic metabolon could be potentially modulated consecutively to O-GlcNAcylation variations.

In addition, O-GlcNAcylation is also involved in the modulation of insulin pathway through the modulation of signaling proteins such as IRS-1, PI3K, PDK1, or Akt. O-GlcNAcylation of these upstream components of insulin signaling pathway occurs after the recruitment of OGT to the membrane, leading to the attenuation of insulin sensitivity (87–89) [for review, see (15, 90)]. Interestingly, the glycogen metabolism could be also modulated by O-GlcNAcylation through the regulation of glycogen synthase, O-GlcNAcylation acting as inhibitory mechanism of this enzyme (15, 91, 92); in addition, the UDP-glucose pyrophosphorylase (PP), which generates UDP-Glc, is also O-GlcNAcylated (75), suggesting that O-GlcNAcylation may be a regulator of glycogen synthesis. Thus, the O-GlcNAcylation, which depends itself of the glucose level through the Hexosamine Biosynthesis Pathway, could act as a nutritional sensor to regulate the glycolytic flow through the modification of glycolytic enzymes, the regulation of protein expression, the modulation of their phosphorylation level and/or the modulation of the metabolon.

Taken together, all these data were gained from different tissues or cell lines, and the precise role of O-GlcNAcylation on the regulation of glucose metabolism in the skeletal muscle remains to be clearly elucidated. In this context, it would also be wise to investigate the exact role of O-GlcNAcylation, not only in the regulation of enzymes expression and/or activities, but also in the modulation of these metabolon since OGT and OGA are also enriched in the Z-line and the I-band of the sarcomere (93). All together, these data strongly argue in favor of a key role of the O-GlcNAcylation process in the regulation of energy metabolism of skeletal muscle, in particular the utilization of glucose as "fuel" to provide energy to ensure muscle contraction.

O-GLCNACYLATION AND SKELETAL MUSCLE DYSFUNCTIONS

O-GlcNAcylation Is Associated to Muscular Atrophy

Muscle atrophy arises from a defect of the balance between protein synthesis and degradation (94, 95). Both intracellular mechanisms maintain protein homeostasis and could be potentially modulated by O-GlcNAcylation (17, 96, 97), but the role of O-GlcNAcylation in the regulation of protein synthesis and degradation is not really investigated in the skeletal muscle. However, this knowledge could be crucial since muscle atrophy is often associated with impairment of contractile and structural functions, metabolism process, and changes of phenotype fiber.

O-GlcNAcylation and skeletal muscle atrophy were firstly associated subsequently to a 14- or 28-days hindlimb unloading (HU) experiments in rat (40, 64, 93). One of the most relevant data was an opposite modulation of the global O-GlcNAc level between the slow-twitch soleus and the fast-twitch EDL (64). A decrease of the global O-GlcNAcylation level was observed in the atrophied rat soleus, while in contrast it was not altered in the non-atrophied rat EDL subsequently to the 14- and 28-days hindlimb unloading. Moreover, OGT activity was also opposite in both muscles by decreasing in soleus and increasing in EDL; however, it has been shown that OGA activity increased in both muscles (64). This first report suggested that O-GlcNAcylation could be related to the muscle atrophy and plasticity processes. Interestingly, the authors demonstrated in parallel that heat-shock proteins expression was also altered. Indeed, in the rat EDL, the HSP70 expression increased, contrary to the atrophied rat soleus after a 14-days HU (64). This heat-shock protein is known to be O-GlcNAcylated, to have lectin properties (98–100), and to have the ability to increase stress tolerance while decreasing protein degradation (101, 102). Thus, in rat EDL, the increase of global O-GlcNAc level, as well as HSP70 expression, could contribute to an improvement of stress tolerance, as suggested in cardiomyocytes (103), and prevent muscle atrophy (64, 104). Interestingly, the expression of another heat-shock protein, the alphaB-crystallin which is also known to be O-GlcNAcylated (105), was decreased in the atrophied soleus and could therefore be involved in the plasticity processes (106).

More recently, different studies focused on the molecular pathways involved in skeletal muscle atrophy, including the relationship between O-GlcNAcylation, signaling pathways and muscular atrophy in skeletal muscle cells model (**Figure 2**). By using Thiamet-G, a potent inhibitor of the O-GlcNAcase, the C2C12 cells showed both a global increase of the O-GlcNAcylation and a modulation of some catabolic and anabolic pathways leading to atrophy (107). First, this study reported a significant decrease of Akt and GSK3β phosphorylation, as well as an increase of myostatin expression, which could lead to an inhibition of some anabolic pathways. Secondly, an increase of Atrogin-1 expression was reported and could lead to an improvement of some catabolic pathways (**Figure 2**). In this way, myostatin is a negative modulator of skeletal muscle growth and inhibits some protein synthesis pathways such as Akt/mTOR; it also promotes degradation of many sarcomeric proteins and seems to be dependent of Atrogin-1 (108). Interestingly, this report of molecular events following OGA deficiency in C2C12 could partly explain muscle wasting induction through glucocorticoid in stress conditions (109). Indeed, in C2C12 cells treated with dexamethasone, the OGA activity was decreased such as its expression (a similar molecular event was described when cells were treated with the Thiamet-G); in parallel, Murf-1 expression, leading to atrophy, increased (107) (**Figure 2**). It was suggested that dexamethasone could repress *OGA* gene *via* binding onto Glucocorticoid Response Element (107, 110); another mechanism could also involve OGT, known to be a cofactor of glucocorticoid receptors promoting transrepression (111). This is a relevant new insight regarding the use of glucocorticoids as the only available therapeutic treatment to maintain essential muscle functions in some muscular dystrophies (112). However, O-GlcNAc-mediated molecular mechanisms could be partly different between glucocorticoid-induced atrophy and disuse atrophy since the O-GlcNAc pattern is different, and the expression of O-GlcNAc processing enzymes is not changed (64).

In parallel, in C2C12 cells, the increase of the global O-GlcNAcylation level by the use of Thiamet-G or another OGA inhibitor such as PUGNAc or another strategy such as *OGA* knockdown, seemed suppress the myogenic differentiation of the muscle cells (113–115). Indeed, the terminal differentiation stage of C2C12 is altered through a decrease of mrf4, myogenin (113), and myoD expression (115) (**Figure 2**). Interestingly, a decreased O-GlcNAcylation of Mef2D, a transcriptional activator of myogenin, suppressed its recruitment to the myogenic factor promoter (114). Moreover, in the case of a global decrease of the O-GlcNAcylation level, the specific O-GlcNAc rate of PGC-1α led to its degradation and suppressed the mitochondrial biogenesis and myogenesis in C2C12 (115) (**Figure 2**). By the way, through OGA manipulation in C2C12 cells, O-GlcNAcylation seemed to be a negative regulator of the myogenesis. This conclusion is reinforced by the overexpression of an inactive OGA variant and the increase of O-GlcNAcylation in a rat model inducing skeletal muscle atrophy (116). In contrast, a skeletal muscle specific *OGT* knockout in mice, leading to a global decrease of O-GlcNAcylation in the tissue, did not induce muscle hypertrophy (65). Indeed, tibialis anterior, EDL and soleus of these mice showed a normal morphology and mass. Interestingly, mice exhibited reduced fat mass (65). Muscle phenotype from global *OGT* or *OGA* knockout in mice is difficult to determine since it has been shown a severe perinatal lethality, and to date there is no available data about an inducible *OGA* knockout or a skeletal muscle specific *OGA* knockout model. Along O-GlcNAcylation, all these recent studies showed complex pathways, but not fully resolved, leading to skeletal muscle atrophy.

Skeletal Muscle O-GlcNAcylation in Physiopathological Context

In various organs or tissues (e.g., heart, brain, pancreas, and kidney), O-GlcNAcylation was previously described to be

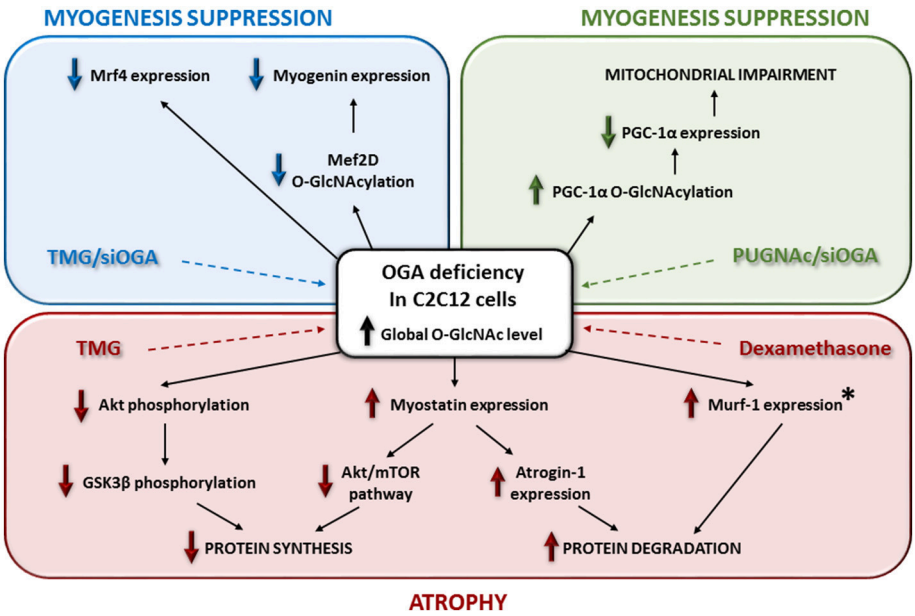

FIGURE 2 | Relationships between O-GlcNAcylation, signaling pathways and muscular atrophy in skeletal muscle cells model. This figure depicts the impact of OGA deficiency on myogenesis and skeletal muscle atrophy. The asterisk means that Murf-1 overexpression occurs with the use of dexamethasone and not with the Thiamet-G in C2C12 cells.

both cell protective from an acute variation and deleterious from chronic and sustained variations especially through the impairment of glucose utilization or the glucose toxicity paradigm that may lead to the progression of several diseases [for review, see (31, 34, 36, 68, 117, 118)]. To date, one of the most defined examples is the involvement of O-GlcNAcylation in the progression of diabetes, characterized by hyperglycemia as the result of body's inability to correctly process blood glucose. Subsequently, all insulin sensitive tissues present hyper-O-GlcNAcylation and many complications. It appeared that a single nucleotide polymorphism in *MGEA5*, encoding OGA, is associated with type 2 diabetes in a mexican american population (119). Moreover, Goto-Kakizaki rats, which develop type 2 diabetes mellitus in early life, express an inactive 90 kDa isoform of OGA (120). Finally, a conditional *OGA* knockout in mice led to a low blood glucose concentration, a decreased insulin sensitivity, and to a perinatal death (121). However, the involvement of O-GlcNAcylation in the onset or in the progression of diabetes is still in debate (118) since a pharmacological inhibition of OGA in adipocytes did not cause insulin resistance or disruption of the glucohomeostasis (122).

Interestingly, among insulin sensitive tissues, the skeletal muscles are responsible for about 75% of insulin-stimulated uptake in the whole human body. In skeletal muscle, a global increase of O-GlcNAcylation induced insulin resistance (123), whereas insulin infusion led to an increase of the HBP flux and the O-GlcNAc content (124). It has been shown that muscular overexpression of GFAT in transgenic mice led to muscle insulin resistance (125, 126). In a same way, upregulation of GFAT expression and activity was described in skeletal muscle of diabetic patients (127). Moreover, overexpression of GFAT in mice is associated to a decrease of GLUT4 translocation to the sarcolemma (128), whereas transgenic mice overexpressing GLUT4 did not show alteration of GFAT expression or activity unlike the overexpression of GLUT1 (129), although both of these mice models showed an increase of glucose uptake and O-GlcNAcylation in muscle (130). Thus, the role of HBP in insulin resistance seems to be complex and still not resolved (131). Recent data provided that TRIB3 may be a novel link between HBP and insulin resistance in skeletal muscle (132).

Experiments with mice overexpressing OGT displayed muscle insulin resistance as well as hyperleptinemia (133). Pharmacological inhibition of OGA (123) or *OGA* knockdown (116) in skeletal muscle cells also induced insulin resistance. In parallel, after induction of insulin in liver, PIP3 recruited OGT from the nucleus to the membrane and caused perturbations of insulin signaling (88). Taken together, these data suggest that O-GlcNAcylation could be a link between insulin resistance and muscle impairment, since O-GlcNAcylation is involved in skeletal muscle contractility, sarcomere structuration, myogenesis, and diabetic patients often display "diabetic myopathy" (134). A significant volume of literature suggested O-GlcNAcylation linking diabetes and cardiovascular complications [for review, see (27, 35)]. In cardiac muscle from mice developing insulin resistance, mitochondrial dysfunction and changes in contractile properties were associated to an increase of O-GlcNAcylation (58). Indeed, it has been shown a correlation between increase of O-GlcNAcylation and decrease

of calcium sensitivity in the cardiac tissue (135), as well as in the skeletal muscle tissue (41, 42). Interestingly, it has been shown that adenoviral transfer of *OGA* (136) or injection of a bacterial homologue of *OGA* (137), reversed the excessive O-GlcNAc content and the cardiac contractile dysfunctions. In this study, many myofibrillar proteins exhibited changes of their O-GlcNAcylation level, but the modulation of contractile properties could be also explained by a modulation of Ca^{2+} handling (138). Indeed, within an insulin resistance context in cardiac tissue, Serca2a expression was changed (58, 136), and an alteration of O-GlcNAc levels significantly affected Ca^{2+} handling, Serca2a (139) and STM1 functions (140). This role of O-GlcNAcylation should be considered also in skeletal muscle since dysfunction of contractibility as well as the Ca^{2+} handling were also measured in skeletal muscle of rat models of diabetes (141), *via* impaired Serca and GLUT4 (142).

Interestingly, OGT and OGA are highly concentrated to the sarcomere (93). Moreover, in cardiac tissue of STZ-diabetic mice, OGA, and OGT mislocalization in the sarcomere was associated to activities alteration as well as changes in the OGA interactions with actin, tropomyosin and MLC1 (137). In parallel, OGT was also mislocalized in mitochondria, the interaction between OGT and complex IV being decreased while the OGA activity decreased (143). O-GlcNAc processing enzymes distribution in the sarcomere of skeletal muscle as well as other compartments, such as mitochondria should be also investigated to better understand the involvement of O-GlcNAcylation in diabetic context. Indeed, different data support a relocalization of O-GlcNAc in atrophy or exercise muscle activity context (61, 62, 93). Recently, in C2C12 cells, an *OGA* knockdown induced insulin resistance and a decrease of the mitochondrial biogenesis with a decreased PGC1α expression (115).

In another context, it has been shown that the global O-GlcNAc level in skeletal muscle is increased in some human neuromuscular diseases (33). Especially, compared to normal muscle fibers, the O-GlcNAc signal seemed to be relocalized from the sarcolemma to the cytoplasm and nuclei in regenerative muscle fibers of muscular dystrophies, myositis and rhabdomyolysis. A strong O-GlcNAc content signal was also displayed in vacuolated fibers in sporadic inclusion body myositis, and distal myopathies with rimmed vacuoles, as well as in neurogenic muscular dystrophy. This O-GlcNAc raise could be associated with the stress response, since HSP70 expression is increased in the cytoplasmic compartment of these neuromuscular diseases. Moreover, a mutation in the *GNE* gene is known to cause distal myopathies with rimmed vacuoles. Interestingly, UDP-GlcNAc is the substrate of the GNE enzyme, and an impairment of GNE expression/activity could altered the UDP-GlcNAc content and so the O-GlcNAcylation mediated by OGT (33).

CONCLUSION AND PERSPECTIVES

In the past ten years, more and more studies concerned O-GlcNAcylation in the skeletal muscle physiology and physiopathology. This glycosylation is mostly related to glucose metabolism, and skeletal muscle is one of the largest consumers of glucose; in addition, numerous studies showed that skeletal muscle is essential for glucose homeostasis and insulin sensitivity. Moreover, muscle plasticity allows skeletal fibers adaptations to physiological conditions in terms of contractile but also metabolism properties. Consequently, the glucose utilization will change depending on resting, wasting or exercise, as well as the fiber type composition. Interestingly, the global O-GlcNAcylation pattern in skeletal muscle changed, depending on these different conditions and fiber types. O-GlcNAcylation may be both a cause or a consequence of the modulation of the glucose utilization, in a virtuous or deleterious cycle, since most of the enzymes from the carbohydrate metabolism are known to be O-GlcNAcylated. This concept clearly raises the O-GlcNAcylation as a potential key regulator of the skeletal muscle glucose metabolism. O-GlcNAcylation has been also shown to regulate some key signaling pathways, as well cellular stress response, involved in the maintenance of the protein synthesis/degradation balance in the skeletal muscle. From these novel insights, a new paradigm is emerging considering the O-GlcNAcylation as a key factor involved in skeletal muscle physiopathology such as atrophy or insulin resistance, and more generally in neuromuscular diseases. However, O-GlcNAc involvements as a cause or consequence of skeletal muscle impairments are currently in debate. After all, it is now clear that O-GlcNAcylation is getting many involvements in the skeletal muscle physiopathology and would be confirmed in the future by larger studies of interest.

Indeed, with the exponential development of mass-spectrometry and innovative enrichment techniques, the identification of O-GlcNAc sites which are modulated subsequently to any stimuli/condition/disease will be clearly the challenge of tomorrow. In fact, O-GlcNAcylation regulates protein activity, protein localization, protein-protein interactions, and can interplay with phosphorylation or ubiquitination. This strategy will lead to a deeper understanding of the precise mechanisms by which O-GlcNAcylation can regulate skeletal muscle metabolism. Secondly, O-GlcNAc processing enzymes behavior should be more precisely investigated, since their localizations and/or interactions, and as consequence, the pattern of O-GlcNAcylation, seemed to be changed through different stimuli in skeletal muscle fibers, especially around the myofilaments. Exercise is one of these stimuli inducing complex O-GlcNAc variations, depending on the muscle phenotype, but also the kind of exercise. Importantly, due to the enhancement of glucose utilization during exercise, the O-GlcNAcylation process in skeletal muscle could be considered as a potential target to alleviate metabolic disorders. Finally, O-GlcNAcylation should be investigated in some precise muscular dystrophies or congenital myopathies, since glucose utilization is often impaired, the sarcomere could be disorganized, the mitochondria biogenesis altered, the nuclei delocalized, or the muscle plasticity changed. It will be worth knowing if O-GlcNAcylation could contribute or alleviate

neuromuscular disorders or being considered as a marker of these diseases.

AUTHOR CONTRIBUTIONS

All authors listed have made a substantial, direct and intellectual contribution to the work, and approved it for publication.

FUNDING

This work was supported by grant from the French National Research Agency (ANR, Agence Nationale de la Recherche, Young Researchers Program, n°11JSV8 006 01). ML is a recipient from the French Ministry for Research and Tertiary Education.

REFERENCES

1. Torres CR, Hart GW. Topography and polypeptide distribution of terminal N-acetylglucosamine residues on the surfaces of intact lymphocytes. Evidence for O-linked GlcNAc. *J Biol Chem.* (1984) 259:3308–17.
2. Ma J, Hart GW. O-GlcNAc profiling: from proteins to proteomes. *Clin Proteomics* (2014) 11:8. doi: 10.1186/1559-0275-11-8
3. Shafi R, Iyer SP, Ellies LG, O'Donnell N, Marek KW, Chui D, et al. The O-GlcNAc transferase gene resides on the X chromosome and is essential for embryonic stem cell viability and mouse ontogeny. *Proc Natl Acad Sci USA* (2000) 97:5735–9. doi: 10.1073/pnas.100471497
4. Yang YR, Song M, Lee H, Jeon Y, Choi E-J, Jang H-J, et al. O-GlcNAcase is essential for embryonic development and maintenance of genomic stability. *Aging Cell* (2012) 11:439–48. doi: 10.1111/j.1474-9726.2012.00801.x
5. Ida S, Morino K, Sekine O, Ohashi N, Kume S, Chano T, et al. Diverse metabolic effects of O-GlcNAcylation in the pancreas but limited effects in insulin-sensitive organs in mice. *Diabetologia* (2017) 60:1761–9. doi: 10.1007/s00125-017-4327-y
6. Hart GW, Housley MP, Slawson C. Cycling of O-linked β-N-acetylglucosamine on nucleocytoplasmic proteins. *Nature* (2007) 446:1017–22. doi: 10.1038/nature05815
7. Gu Y, Ande SR, Mishra S. Altered O-GlcNAc modification and phosphorylation of mitochondrial proteins in myoblast cells exposed to high glucose. *Arch Biochem Biophys*. (2011) 505:98–104. doi: 10.1016/j.abb.2010.09.024
8. Haltiwanger R. S., Holt G. D., Hart G. W. Enzymatic addition of O-GlcNAc to Nuclear and Cytoplasmic Proteins. *J Biol Chem.* (1990) 265:2563–8.
9. Dong DL, Hart GW. Purification and characterization of an O-GlcNAc selective N-acetyl-beta-D-glucosaminidase from rat spleen cytosol. *J Biol Chem.* (1994) 269:19321–30.
10. Nagnan-Le Meillour P, Vercoutter-Edouart A-S, Hilliou F, Le Danvic C, Levy F. Proteomic analysis of Pig (Sus scrofa) olfactory soluble proteome reveals O-Linked-N-acetylglucosaminylation of secreted odorant-binding proteins. *Front Endocrinol.* (2014) 5:202. doi: 10.3389/fendo.2014.00202
11. Ogawa M, Sawaguchi S, Furukawa K, Okajima T. N-acetylglucosamine modification in the lumen of the endoplasmic reticulum. *Biochim Biophys Acta* (2015) 1850:1319–24. doi: 10.1016/j.bbagen.2015.03.003
12. Varshney S, Stanley P. EOGT and O -GlcNAc on secreted and membrane proteins. *Biochem Soc Trans.* (2017) 45:401–8. doi: 10.1042/BST20160165
13. Hanover J a, Krause MW, Love DC. The hexosamine signaling pathway: O-GlcNAc cycling in feast or famine. *Biochim Biophys Acta* (2010) 1800:80–95. doi: 10.1016/j.bbagen.2009.07.017
14. Hart GW, Akimoto Y. The O-GlcNAc Modification. In: Varki A, Cummings RD, Esko JD, Freeze HH, Stanley P, Bertozzi CR, Hart GW, Etzler ME, editors. *Essentials of Glycobiology*, 2nd edition. Cold Spring Harbor, NY: Cold Spring Harbor Laboratory Press (2009). Chapter 18. (2009).
15. Hart GW, Slawson C, Ramirez-Correa G, Lagerlof O. Cross talk between O-GlcNAcylation and phosphorylation: roles in signaling, transcription, and chronic disease. *Annu Rev Biochem.* (2011) 80:825–58. doi: 10.1146/annurev-biochem-060608-102511
16. van der Laarse SAM, Leney AC, Heck AJR. Crosstalk between phosphorylation and O-GlcNAcylation: friend or foe. *FEBS J.* (2018) 285:3152–67. doi: 10.1111/febs.14491
17. Ruan H-B, Nie Y, Yang X. Regulation of protein degradation by O-GlcNAcylation: crosstalk with ubiquitination. *Mol Cell Proteomics* (2013) 12:3489–97. doi: 10.1074/mcp.R113.029751
18. Lambert M, Richard E, Duban-Deweer S, Krzewinski F, Deracinois B, Dupont E, et al. O-GlcNAcylation is a key modulator of skeletal muscle sarcomeric morphometry associated to modulation of protein–protein interactions. *Biochim Biophys Acta Gen Subj.* (2016) 1860:2017–30. doi: 10.1016/j.bbagen.2016.06.011
19. Tarbet HJ, Toleman CA, Boyce M. A sweet embrace: control of protein–protein interactions by O-Linked β- N -Acetylglucosamine. *Biochemistry* (2018) 57:13–21. doi: 10.1021/acs.biochem.7b00871
20. Chu C-S, Lo P-W, Yeh Y-H, Hsu P-H, Peng S-H, Teng Y-C, et al. O-GlcNAcylation regulates EZH2 protein stability and function. *Proc Natl Acad Sci.* (2014) 111:1355–60. doi: 10.1073/pnas.1323226111
21. Li Y, Wang L, Liu J, Zhang P, An M, Han C, et al. O-GlcNAcylation modulates Bmi-1 protein stability and potential oncogenic function in prostate cancer. *Oncogene* (2017) 36:6293–305. doi: 10.1038/onc.2017.223
22. Cividini F, Scott BT, Dai A, Han W, Suarez J, Diaz-Juarez J, et al. O -GlcNAcylation of 8-Oxoguanine DNA Glycosylase (Ogg1) Impairs Oxidative Mitochondrial DNA Lesion Repair in Diabetic Hearts. *J Biol Chem.* (2016) 291:26515–28. doi: 10.1074/jbc.M116.754481
23. Ha JR, Hao L, Venkateswaran G, Huang YH, Garcia E, Persad S. β-Catenin is O-GlcNAc glycosylated at Serine 23: Implications for β-catenin's subcellular localization and transactivator function. *Exp Cell Res.* (2014) 321:153–66. doi: 10.1016/j.yexcr.2013.11.021
24. Hardivillé S, Hart GW. Nutrient regulation of signaling, transcription, and cell physiology by O- GlcNAcylation. *Cell Metab.* (2014) 20:208–13. doi: 10.1016/j.cmet.2014.07.014
25. Bond MR, Hanover J a. A little sugar goes a long way: the cell biology of O-GlcNAc. *J Cell Biol.* (2015) 208:869–80. doi: 10.1083/jcb.201501101
26. Ma J, Hart GW. Protein O-GlcNAcylation in diabetes and diabetic complications. *Expert Rev Proteom.* (2013) 10:365–80. doi: 10.1586/14789450.2013.820536
27. Peterson SB, Hart GW. New insights: A role for O-GlcNAcylation in diabetic complications. *Crit Rev Biochem Mol Biol.* (2016) 9238:1–12. doi: 10.3109/10409238.2015.1135102
28. Fardini Y, Dehennaut V, Lefebvre T, Issad T. O-GlcNAcylation: A new cancer hallmark? *Front Endocrinol.* (2013) 4:99. doi: 10.3389/fendo.2013.00099
29. de Queiroz RM, Carvalho Ã, Dias WB. O-GlcNAcylation: the sweet side of the cancer. *Front Oncol.* (2014) 4:132. doi: 10.3389/fonc.2014.00132
30. Zhu Y, Shan X, Yuzwa SA, Vocadlo DJ. The emerging link between O -GlcNAc and Alzheimer Disease. *J Biol Chem.* (2014) 289:34472–81. doi: 10.1074/jbc.R114.601351
31. Gong C-X, Liu F, Iqbal K. O-GlcNAcylation: a regulator of tau pathology and neurodegeneration. *Alzheimer's Dement* (2016) 12:1078–89. doi: 10.1016/j.jalz.2016.02.011
32. Vaidyanathan K, Niranjan T, Selvan N, Teo CF, May M, Patel S, et al. Identification and characterization of a missense mutation in the O -linked β- N -acetylglucosamine (O -GlcNAc) transferase gene that segregates with X-linked intellectual disability. *J Biol Chem.* (2017) 292:8948–63. doi: 10.1074/jbc.M116.771030
33. Nakamura S, Nakano S, Nishii M, Kaneko S, Kusaka H. Localization of O-GlcNAc-modified proteins in neuromuscular diseases. *Med Mol Morphol.* (2012) 45:86–90. doi: 10.1007/s00795-011-0542-7
34. Dassanayaka S, Jones SP. O-GlcNAc and the cardiovascular system. *Pharmacol Ther.* (2014) 142:62–71. doi: 10.1016/j.pharmthera.2013.11.005
35. Wright JN, Collins HE, Wende AR, Chatham JC. O-GlcNAcylation and cardiovascular disease. *Biochem Soc Trans.* (2017) 45:545–53. doi: 10.1042/BST20160164

36. Banerjee PS, Lagerlöf O, Hart GW. Roles of O-GlcNAc in chronic diseases of aging. *Mol Aspects Med.* (2016) 51:1–15. doi: 10.1016/j.mam.2016.05.005
37. Frontera WR, Ochala J. Skeletal muscle: a brief review of structure and function. *Calcif Tissue Int.* (2015) 96:183–95. doi: 10.1007/s00223-014-9915-y
38. Westerblad H, Bruton JD, Katz A. Skeletal muscle: energy metabolism, fiber types, fatigue and adaptability. *Exp Cell Res.* (2010) 316:3093–9. doi: 10.1016/j.yexcr.2010.05.019
39. Hart GW. *O*-GlcNAcylation: Nutrient Sensor that Regulates Cell Physiology. In: Taniguchi N, Endo T, Hart G, Seeberger P, Wong CH, editors. *Glycoscience: Biology and Medicine*. Springer: Tokyo (2015) p. 1193–9. doi: 10.1007/978-4-431-54841-6_82
40. Cieniewski-Bernard C, Bastide B, Lefebvre T, Lemoine J, Mounier Y, Michalski J-C. Identification of O-linked N-acetylglucosamine proteins in rat skeletal muscle using two-dimensional gel electrophoresis and mass spectrometry. *Mol Cell Proteomics* (2004) 3:577–85. doi: 10.1074/mcp.M400024-MCP200
41. Cieniewski-Bernard C, Montel V, Berthoin S, Bastide B. Increasing O-GlcNAcylation level on organ culture of soleus modulates the calcium activation parameters of muscle fibers. *PLoS ONE* (2012) 7:e48218. doi: 10.1371/journal.pone.0048218
42. Hedou J, Cieniewski-Bernard C, Leroy Y, Michalski JC, Mounier Y, Bastide B. O-linked N-acetylglucosaminylation is involved in the Ca2+ activation properties of rat skeletal muscle. *J Biol Chem.* (2007) 282:10360–9. doi: 10.1074/jbc.M606787200
43. Hédou J, Bastide B, Page A, Michalski JC, Morelle W. Mapping of O-linked beta-N-acetylglucosamine modification sites in key contractile proteins of rat skeletal muscle. *Proteomics* (2009) 9:2139–48. doi: 10.1002/pmic.200800617
44. Kooij V, Stienen GJM, van der Velden J. The role of protein kinase C-mediated phosphorylation of sarcomeric proteins in the heart-detrimental or beneficial? *Biophys Rev.* (2011) 3:107–17. doi: 10.1007/s12551-011-0050-y
45. Mounier R, Théret M, Lantier L, Foretz M, Viollet B. Expanding roles for AMPK in skeletal muscle plasticity. *Trends Endocrinol Metab.* (2015) 26:275–86. doi: 10.1016/j.tem.2015.02.009
46. Egan B, Zierath JR. Exercise metabolism and the molecular regulation of skeletal muscle adaptation. *Cell Metab.* (2013) 17:162–84. doi: 10.1016/j.cmet.2012.12.012
47. Smiles WJ, Hawley JA, Camera DM. Effects of skeletal muscle energy availability on protein turnover responses to exercise. *J Exp Biol.* (2016) 219:214–25. doi: 10.1242/jeb.125104
48. Goodpaster BH, Sparks LM. Metabolic flexibility in health and disease. *Cell Metab.* (2017) 25:1027–36. doi: 10.1016/j.cmet.2017.04.015
49. Marshall S, Bacote V, Traxinger RR. Discovery of a metabolic pathway mediating glucose-induced desensitization of the glucose transport system. Role of hexosamine biosynthesis in the induction of insulin resistance. *J Biol Chem.* (1991) 266:4706–12.
50. Hawkins M, Barzilai N, Liu R, Hu M, Chen W, Rossetti L. Role of the glucosamine pathway in fat-induced insulin resistance. *J Clin Invest.* (1997) 99:2173–82. doi: 10.1172/JCI119390
51. Lee AD, Hansen PA, Holloszy JO. Wortmannin inhibits insulin-stimulated but not contraction-stimulated glucose transport activity in skeletal muscle. *FEBS Lett.* (1995) 361:51–4.
52. Richter EA, Hargreaves M. Exercise, GLUT4, and skeletal muscle glucose uptake. *Physiol Rev.* (2013) 93:993–1017. doi: 10.1152/physrev.00038.2012
53. Ojuka EO, Goyaram V, Smith JAH. The role of CaMKII in regulating GLUT4 expression in skeletal muscle. *Am J Physiol Metab.* (2012) 303:E322–31. doi: 10.1152/ajpendo.00091.2012
54. Myslicki JP, Belke DD, Shearer J. Role of O-GlcNAcylation in nutritional sensing, insulin resistance and in mediating the benefits of exercise. *Appl Physiol Nutr Metab.* (2014) 39:1205–13. doi: 10.1139/apnm-2014-0122
55. Belke DD. Swim-exercised mice show a decreased level of protein O-GlcNAcylation and expression of O-GlcNAc transferase in heart. *J Appl Physiol.* (2011) 111:157–62. doi: 10.1152/japplphysiol.00147.2011
56. Medford HM, Porter K, Marsh SA. Immediate effects of a single exercise bout on protein O-GlcNAcylation and chromatin regulation of cardiac hypertrophy. *Am J Physiol Heart Circ Physiol.* (2013) 305:H114–23. doi: 10.1152/ajpheart.00135.2013
57. Bennett CE, Johnsen VL, Shearer J, Belke DD. Exercise training mitigates aberrant cardiac protein O-GlcNAcylation in streptozotocin-induced diabetic mice. *Life Sci.* (2013) 92:657–63. doi: 10.1016/j.lfs.2012.09.007
58. Johnsen VL, Belke DD, Hughey CC, Hittel DS, Hepple RT, Koch LG, et al. Enhanced cardiac protein glycosylation (O-GlcNAc) of selected mitochondrial proteins in rats artificially selected for low running capacity. *Physiol Genomics* (2013) 45:17–25. doi: 10.1152/physiolgenomics.00111.2012
59. Cox EJ, Marsh SA. Exercise and diabetes have opposite effects on the assembly and O-GlcNAc modification of the mSin3A/HDAC1/2 complex in the heart. *Cardiovasc Diabetol.* (2013) 12:101. doi: 10.1186/1475-2840-12-101
60. Peternelj TT, Marsh SA, Strobel NA, Matsumoto A, Briskey D, Dalbo VJ, et al. Glutathione depletion and acute exercise increase O-GlcNAc protein modification in rat skeletal muscle. *Mol Cell Biochem.* (2014) 400:265–75. doi: 10.1007/s11010-014-2283-0
61. Hortemo KH, Aronsen JM, Lunde IG, Sjaastad I, Lunde PK, Sejersted OM. Exhausting treadmill running causes dephosphorylation of sMLC2 and reduced level of myofilament MLCK2 in slow twitch rat soleus muscle. *Physiol Rep.* (2015) 3:e12285. doi: 10.14814/phy2.12285
62. Halvorsen Hortemo K, Lunde K, Anonsen JH, Kvaløy H, Munkvik M, Rehn TA, et al. Exercise training increases protein O-GlcNAcylation in rat skeletal muscle. *Physiol Rep.* (2016) 4:e12896 doi: 10.14814/phy2.12896
63. Nelson BA, Robinson KA, Koning JS, Buse MG. Effects of exercise and feeding on the hexosamine biosynthetic pathway in rat skeletal muscle. *Am J Physiol.* (1997) 272:E848–55. doi: 10.1152/ajpendo.1997.272.5.E848
64. Cieniewski-Bernard C, Mounier Y, Michalski JC, Bastide B. O-GlcNAc level variations are associated with the development of skeletal muscle atrophy. *J Appl Physiol.* (2006) 100:1499–505. doi: 10.1152/japplphysiol.00865.2005
65. Shi H, Munk A, Nielsen TS, Daughtry MR, Larsson L, Li S, et al. Skeletal muscle O-GlcNAc transferase is important for muscle energy homeostasis and whole-body insulin sensitivity. *Mol Metab.* (2018) 11:160–77. doi: 10.1016/j.molmet.2018.02.010
66. Davies KJ, Quintanilha AT, Brooks GA, Packer L. Free radicals and tissue damage produced by exercise. *Biochem Biophys Res Commun.* (1982) 107:1198–205.
67. Groves JA, Lee A, Yildirir G, Zachara NE. Dynamic O-GlcNAcylation and its roles in the cellular stress response and homeostasis. *Cell Stress Chaperones* (2013) 18:535–58. doi: 10.1007/s12192-013-0426-y
68. Lima VV, Spitler K, Choi H, Webb RC, Tostes RC, Varki A, et al. O-GlcNAcylation and oxidation of proteins: is signalling in the cardiovascular system becoming sweeter? *Clin Sci.* (2012) 123:473–86. doi: 10.1042/CS20110638
69. Chen P-H, Chi J-T, Boyce M. Functional crosstalk among oxidative stress and O-GlcNAc signaling pathways. *Glycobiology* (2018) 28:556–64. doi: 10.1093/glycob/cwy027
70. Murata K, Morino K, Ida S, Ohashi N, Lemecha M, Park S-Y, et al. Lack of O-GlcNAcylation enhances exercise-dependent glucose utilization potentially through AMP-activated protein kinase activation in skeletal muscle. *Biochem Biophys Res Commun.* (2018) 495:2098–104. doi: 10.1016/j.bbrc.2017.12.081
71. Yi W, Clark PM, Mason DE, Keenan MC, Hill C, Goddard WA, et al. Phosphofructokinase 1 glycosylation regulates cell growth and metabolism. *Science* (2012) 337:975–80. doi: 10.1126/science.1222278
72. Champattanachai V, Netsirisawan P, Chaiyawat P, Phueaouan T, Charoenwattanasatien R, Chokchaichamnankit D, et al. Proteomic analysis and abrogated expression of O -GlcNAcylated proteins associated with primary breast cancer. *Proteomics* (2013) 13:2088–99. doi: 10.1002/pmic.201200126
73. Chaiyawat P, Chokchaichamnankit D, Lirdprapamongkol K, Srisomsap C, Svasti J, Champattanachai V. Alteration of O-GlcNAcylation affects serine phosphorylation and regulates gene expression and activity of pyruvate kinase M2 in colorectal cancer cells. *Oncol Rep* (2015) 34:1933–42. doi: 10.3892/or.2015.4178
74. Dehennaut V, Slomianny MC, Page A, Vercoutter-Edouart A-S, Jessus C, Michalski J-C, et al. Identification of Structural and Functional O -Linked N -Acetylglucosamine-bearing Proteins in Xenopus laevis Oocyte. *Mol Cell Proteomics* (2008) 7:2229–45. doi: 10.1074/mcp.M700494-MCP200

75. Wells L, Vosseller K, Cole RN, Cronshaw JM, Matunis MJ, Hart GW. Mapping sites of *O*-GlcNAc modification using affinity tags for serine and threonine post-translational modifications. *Mol Cell Proteomics* (2002) 1:791–804. doi: 10.1074/mcp.M200048-MCP200
76. Clark PM, Dweck JF, Mason DE, Hart CR, Buck SB, Peters EC, et al. Direct in-gel fluorescence detection and cellular imaging of O -GlcNAc-modified proteins. *J Am Chem Soc.* (2008) 130:11576–7. doi: 10.1021/ja8030467
77. Bacigalupa ZA, Bhadiadra CH, Reginato MJ. O-GlcNAcylation: key regulator of glycolytic pathways. *J Bioenerg Biomembr.* (2018) 50:189–98. doi: 10.1007/s10863-018-9742-3
78. Sharma NS, Saluja AK, Banerjee S. "Nutrient-sensing" and self-renewal: O-GlcNAc in a new role. *J Bioenerg Biomembr.* (2018) 50:205–11. doi: 10.1007/s10863-017-9735-7
79. Baldini SF, Steenackers A, Olivier-Van Stichelen S, Mir A-M, Mortuaire M, Lefebvre T, et al. Glucokinase expression is regulated by glucose through O-GlcNAc glycosylation. *Biochem Biophys Res Commun.* (2016) 478:942–8. doi: 10.1016/j.bbrc.2016.08.056
80. Ma J, Banerjee P, Whelan SA, Liu T, Wei A-C, Ramirez-Correa G, et al. Comparative Proteomics Reveals Dysregulated Mitochondrial O-GlcNAcylation in Diabetic Hearts. *J Proteome Res.* (2016) 15:2254–64. doi: 10.1021/acs.jproteome.6b00250
81. Cao W, Cao J, Huang J, Yao J, Yan G, Xu H, Yang P. Discovery and confirmation of O-GlcNAcylated proteins in rat liver mitochondria by combination of mass spectrometry and immunological methods. *PLoS ONE* (2013) 8:e76399. doi: 10.1371/journal.pone.0076399
82. Barclay CJ. Energy demand and supply in human skeletal muscle. *J Muscle Res Cell Motil.* (2017) 38:143–55. doi: 10.1007/s10974-017-9467-7
83. Rakus D, Mamczur P, Gizak A, Dus D, Dzugaj A. Colocalization of muscle FBPase and muscle aldolase on both sides of the Z-line. *Biochem Biophys Res Commun.* (2003) 311:294–9. doi: 10.1016/j.bbrc.2003.09.209
84. Mamczur P, Rakus D, Gizak A, Dus D, Dzugaj A. The effect of calcium ions on subcellular localization of aldolase-FBPase complex in skeletal muscle. *FEBS Lett.* (2005) 579:1607–12. doi: 10.1016/j.febslet.2005.01.071
85. Clarke FM, Masters CJ. Interactions between muscle proteins and glycolytic enzymes. *Int J Biochem.* (1976) 7:359–65. doi: 10.1016/0020-711X(76)90058-6
86. Méjean C, Pons F, Benyamin Y, Roustan C. Antigenic probes locate binding sites for the glycolytic enzymes glyceraldehyde-3-phosphate dehydrogenase, aldolase and phosphofructokinase on the actin monomer in microfilaments. *Biochem J.* (1989) 264:671–7.
87. Klein AL, Berkaw MN, Buse MG, Ball LE. O -Linked N -Acetylglucosamine modification of insulin receptor substrate-1 occurs in close proximity to multiple SH2 domain binding motifs. *Mol Cell Proteomics* (2009) 8:2733–45. doi: 10.1074/mcp.M900207-MCP200
88. Yang X, Ongusaha PP, Miles PD, Havstad JC, Zhang F, So WV, et al. Phosphoinositide signalling links O-GlcNAc transferase to insulin resistance. *Nature* (2008) 451:964–9. doi: 10.1038/nature06668
89. Whelan SA, Lane MD, Hart GW. Regulation of the O-linked beta-N-acetylglucosamine transferase by insulin signaling. *J Biol Chem.* (2008) 283:21411–7. doi: 10.1074/jbc.M800677200
90. Yang X, Qian K. Protein O-GlcNAcylation: emerging mechanisms and functions. *Nat Rev Mol Cell Biol.* (2017) 18:452–65. doi: 10.1038/nrm.2017.22
91. Parker GJ, Lund KC, Taylor RP, McClain DA. Insulin resistance of glycogen synthase mediated by o-linked N-acetylglucosamine. *J Biol Chem.* (2003) 278:10022–7. doi: 10.1074/jbc.M207787200
92. Parker G, Taylor R, Jones D, McClain D. Hyperglycemia and inhibition of glycogen synthase in streptozotocin-treated mice: role of O-linked N-acetylglucosamine. *J Biol Chem.* (2004) 279:20636–42. doi: 10.1074/jbc.M312139200
93. Cieniewski-Bernard C, Dupont E, Richard E, Bastide B. Phospho-GlcNAc modulation of slow MLC2 during soleus atrophy through a multienzymatic and sarcomeric complex. *Pflügers Arch Eur J Physiol.* (2014) 466:2139–51. doi: 10.1007/s00424-014-1453-y
94. Bonaldo P, Sandri M, Allen DL, Unterman TG, Amirouche A, Durieux AC, et al. Cellular and molecular mechanisms of muscle atrophy. *Dis Model Mech.* (2013) 6:25–39. doi: 10.1242/dmm.010389
95. Schiaffino S, Dyar KA, Ciciliot S, Blaauw B, Sandri M. Mechanisms regulating skeletal muscle growth and atrophy. *FEBS J.* (2013) 280:4294–314. doi: 10.1111/febs.12253
96. Zhang F, Su K, Yang X, Bowe DB, Paterson AJ, Kudlow JE. O-GlcNAc modification is an endogenous inhibitor of the proteasome. *Cell* (2003) 115:715–25. doi: 10.1016/S0092-8674(03)00974-7
97. Özcan S, Andrali SS, Cantrell JEL. Modulation of transcription factor function by O-GlcNAc modification. *Biochim Biophys Acta Gene Regul Mech.* (2010) 1799:353–64. doi: 10.1016/j.bbagrm.2010.02.005
98. Walgren JLE, Vincent TS, Schey KL, Buse MG. High glucose and insulin promote O-GlcNAc modification of proteins, including alpha-tubulin. *Am J Physiol Endocrinol Metab.* (2003) 284:E424–34. doi: 10.1152/ajpendo.00382.2002
99. Guinez C, Lemoine J, Michalski J-C, Lefebvre T. 70-kDa-heat shock protein presents an adjustable lectinic activity towards O-linked N-acetylglucosamine. *Biochem Biophys Res Commun.* (2004) 319:21–26. doi: 10.1016/j.bbrc.2004.04.144
100. Guinez C, Losfeld M-E, Cacan R, Michalski J-C, Lefebvre T. Modulation of HSP70 GlcNAc-directed lectin activity by glucose availability and utilization. *Glycobiology* (2006) 16:22–8. doi: 10.1093/glycob/cwj041
101. Zachara NE, O'Donnell N, Cheung WD, Mercer JJ, Marth JD, Hart GW. Dynamic O-GlcNAc modification of nucleocytoplasmic proteins in response to stress. A survival response of mammalian cells. *J Biol Chem.* (2004) 279:30133–42. doi: 10.1074/jbc.M403773200
102. Guinez C, Mir A-M, Leroy Y, Cacan R, Michalski J-C, Lefebvre T. Hsp70-GlcNAc-binding activity is released by stress, proteasome inhibition, and protein misfolding. *Biochem Biophys Res Commun.* (2007) 361:414–20. doi: 10.1016/j.bbrc.2007.07.020
103. Gong J, Jing L. Glutamine induces heat shock protein 70 expression via O-GlcNAc modification and subsequent increased expression and transcriptional activity of heat shock factor-1. *Minerva Anestesiol* (2011) 77:488–95.
104. Naito H, Powers SK, Demirel HA, Sugiura T, Dodd SL, Aoki J. Heat stress attenuates skeletal muscle atrophy in hindlimb-unweighted rats. *J Appl Physiol.* (2000) 88:359–63. doi: 10.1152/jappl.2000.88.1.359
105. Roquemore EP, Chevrier MR, Cotter RJ, Hart GW. Dynamic O-GlcNAcylation of the small heat shock protein alpha B-crystallin. *Biochemistry* (1996) 35:3578–86. doi: 10.1021/bi951918j
106. Atomi Y, Yamada S, Hong YM. Dynamic expression of ALPHA.B-crystallin in skeletal muscle effects of unweighting, passive stretch and denervation. *Proc Japan Acad Ser B Phys Biol Sci.* (1990) 66:203–8. doi: 10.2183/pjab.66.203
107. Massaccesi L, Goi G, Tringali C, Barassi A, Venerando B, Papini N. Dexamethasone-induced skeletal muscle atrophy increases O-GlcNAcylation in C2C12 Cells. *J Cell Biochem.* (2016) 117:1833–42. doi: 10.1002/jcb.25483
108. Lokireddy S, McFarlane C, Ge X, Zhang H, Sze SK, Sharma M, et al. Myostatin induces degradation of sarcomeric proteins through a Smad3 signaling mechanism during skeletal muscle wasting. *Mol Endocrinol.* (2011) 25:1936–49. doi: 10.1210/me.2011-1124
109. Braun TP, Marks DL. The regulation of muscle mass by endogenous glucocorticoids. *Front Physiol.* (2015) 6:12. doi: 10.3389/fphys.2015.00012
110. Ratman D, Vanden Berghe W, Dejager L, Libert C, Tavernier J, Beck IM, et al. How glucocorticoid receptors modulate the activity of other transcription factors: a scope beyond tethering. *Mol Cell Endocrinol.* (2013) 380:41–54. doi: 10.1016/j.mce.2012.12.014
111. Li M-D, Ruan H-B, Singh JP, Zhao L, Zhao T, Azarhoush S, Wu J, Evans RM, Yang X. O-GlcNAc transferase is involved in glucocorticoid receptor-mediated transrepression. *J Biol Chem.* (2012) 287:12904–12. doi: 10.1074/jbc.M111.303792
112. Wong BL, Rybalsky I, Shellenbarger KC, Tian C, McMahon MA, Rutter MM, et al. Long-term outcome of interdisciplinary management of patients with duchenne muscular dystrophy receiving daily glucocorticoid treatment. *J Pediatr.* (2017) 182:296–303.e1. doi: 10.1016/j.jpeds.2016.11.078
113. Ogawa M, Mizofuchi H, Kobayashi Y, Tsuzuki G, Yamamoto M, Wada S, et al. Terminal differentiation program of skeletal myogenesis is negatively regulated by O-GlcNAc glycosylation. *Biochim Biophys Acta - Gen Subj.* (2012) 1820:24–32. doi: 10.1016/j.bbagen.2011.10.011

114. Ogawa M, Sakakibara Y, Kamemura K. Requirement of decreased O-GlcNAc glycosylation of Mef2D for its recruitment to the myogenin promoter. *Biochem Biophys Res Commun.* (2013) 433:558–562. doi: 10.1016/j.bbrc.2013.03.033
115. Wang X, Feng Z, Wang X, Yang L, Han S, Cao K, et al. O-GlcNAcase deficiency suppresses skeletal myogenesis and insulin sensitivity in mice through the modulation of mitochondrial homeostasis. *Diabetologia* (2016) 59:1287–96. doi: 10.1007/s00125-016-3919-2
116. Huang P, Ho SR, Wang K, Roessler BC, Zhang F, Hu Y, et al. Muscle-specific overexpression of NCOATGK, splice variant of O-GlcNAcase, induces skeletal muscle atrophy. *Am J Physiol Cell Physiol.* (2011) 300:C456–65. doi: 10.1152/ajpcell.00124.2010
117. Nagel AK, Ball LE. Intracellular protein O-GlcNAc modification integrates nutrient status with transcriptional and metabolic regulation. *Adv Cancer Res.* 126 : 137–66. doi: 10.1016/bs.acr.2014.12.003
118. Qin CX, Sleaby R, Davidoff AJ, Bell JR, De Blasio MJ, Delbridge LM, et al. Insights into the role of maladaptive hexosamine biosynthesis and O-GlcNAcylation in development of diabetic cardiac complications. *Pharmacol Res.* (2017) 116:45–56. doi: 10.1016/j.phrs.2016.12.016
119. Lehman DM, Fu D-J, Freeman AB, Hunt KJ, Leach RJ, Johnson-Pais T, et al. A single nucleotide polymorphism in MGEA5 encoding O-GlcNAc-selective N-acetyl-beta-D glucosaminidase is associated with type 2 diabetes in Mexican Americans. *Diabetes* (2005) 54:1214–21. doi: 10.2337/diabetes.54.4.1214
120. Toleman C, Paterson AJ, Whisenhunt TR, Kudlow JE. Characterization of the Histone Acetyltransferase (HAT) domain of a bifunctional protein with activable O-GlcNAcase and HAT activities. *J Biol Chem.* (2004) 279:53665–73. doi: 10.1074/jbc.M410406200
121. Keembiyehetty C, Love DC, Harwood KR, Gavrilova O, Comly ME, Hanover JA. Conditional knock-out reveals a requirement for O-linked N-Acetylglucosaminase (O-GlcNAcase) in metabolic homeostasis. *J Biol Chem.* (2015) 290:7097–113. doi: 10.1074/jbc.M114.617779
122. MacAuley MS, He Y, Gloster TM, Stubbs KA, Davies GJ, Vocadlo DJ. Inhibition of O-GlcNAcase using a potent and cell-permeable inhibitor does not induce insulin resistance in 3T3-L1 adipocytes. *Chem Biol.* (2010) 17:937–48. doi: 10.1016/j.chembiol.2010.07.006
123. Arias EB, Kim J, Cartee GD. Prolonged incubation in PUGNAc results in increased protein O-Linked glycosylation and insulin resistance in rat skeletal muscle. *Diabetes* (2004) 53:921–30. doi: 10.2337/diabetes.53.4.921
124. Yki-Järvinen H, Virkamäki A, Daniels MC, McClain D, Gottschalk WK. Insulin and glucosamine infusions increase O-linked N-acetyl-glucosamine in skeletal muscle proteins *in vivo*. *Metabolism* (1998) 47:449–55. doi: 10.1016/S0026-0495(98)90058-0
125. Hebert LF, Daniels MC, Zhou J, Crook ED, Turner RL, Simmons ST, et al. Overexpression of glutamine:fructose-6-phosphate amidotransferase in transgenic mice leads to insulin resistance. *J Clin Invest.* (1996) 98:930–6. doi: 10.1172/JCI118876
126. Hazel M, Cooksey RC, Jones D, Parker G, Neidigh JL, Witherbee B, et al. Activation of the hexosamine signaling pathway in adipose tissue results in decreased serum adiponectin and skeletal muscle insulin resistance. *Endocrinology* (2004) 145:2118–28. doi: 10.1210/en.2003-0812
127. Yki-Järvinen H, Daniels MC, Virkamäki A, Mäkimattila S, DeFronzo RA, McClain D. Increased glutamine:fructose-6-phosphate amidotransferase activity in skeletal muscle of patients with NIDDM. *Diabetes* (1996) 45:302–7.
128. Cooksey RC, Hebert LF, Zhu J-H, Wofford P, Garvey WT, McClain DA. Mechanism of hexosamine-induced insulin resistance in transgenic mice overexpressing glutamine:fructose-6-phosphate amidotransferase: decreased glucose transporter GLUT4 translocation and reversal by treatment with thiazolidinedione. *Endocrinology* (1999) 140:1151–7. doi: 10.1210/endo.140.3.6563
129. Buse MG, Robinson KA, Marshall BA, Mueckler M. Differential effects of GLUT1 or GLUT4 overexpression on hexosamine biosynthesis by muscles of transgenic mice. *J Biol Chem.* (1996) 271:23197–202.
130. Buse MG, Robinson KA, Marshall BA, Hresko RC, Mueckler MM. Enhanced *O* -GlcNAc protein modification is associated with insulin resistance in GLUT1-overexpressing muscles. *Am J Physiol Endocrinol Metab.* (2002) 283:E241–50. doi: 10.1152/ajpendo.00060.2002
131. Buse MG. Hexosamines, insulin resistance, and the complications of diabetes: current status. *Am J Physiol Endocrinol Metab.* (2006) 290:E1–8. doi: 10.1152/ajpendo.00329.2005
132. Zhang W, Liu J, Tian L, Liu Q, Fu Y, Garvey WT. TRIB3 mediates glucose-induced insulin resistance via a mechanism that requires the hexosamine biosynthetic pathway. *Diabetes* (2013) 62:4192–200. doi: 10.2337/db13-0312
133. McClain DA, Lubas WA, Cooksey RC, Hazel M, Parker GJ, Love DC, et al. Altered glycan-dependent signaling induces insulin resistance and hyperleptinemia. *Proc Natl Acad Sci USA* (2002) 99:10695–9. doi: 10.1073/pnas.152346899
134. D'Souza DM, Al-Sajee D, Hawke TJ. Diabetic myopathy: impact of diabetes mellitus on skeletal muscle progenitor cells. *Front Physiol.* (2013) 4:379. doi: 10.3389/fphys.2013.00379
135. Ramirez-Correa GA, Jin W, Wang Z, Zhong X, Gao WD, Dias WB, et al. O-linked GlcNAc modification of cardiac myofilament proteins: a novel regulator of myocardial contractile function. *Circ Res.* (2008) 103:1354–8. doi: 10.1161/CIRCRESAHA.108.184978
136. Hu Y, Belke D, Suarez J, Swanson E, Clark R, Hoshijima M, Dillmann WH. Adenovirus-mediated overexpression of O-GlcNAcase improves contractile function in the diabetic heart. *Circ Res.* (2005) 96:1006–13. doi: 10.1161/01.RES.0000165478.06813.58
137. Ramirez-Correa GA, MA J, Slawson C, Zeidan Q, Lugo-Fagundo NS, Xu M, et al. Removal of abnormal myofilament O-GlcNAcylation restores Ca^{2+} sensitivity in diabetic cardiac muscle. *Diabetes* (2015) 64:3573–87. doi: 10.2337/db14-1107
138. Wende AR. Unsticking the broken diabetic heart: O- GlcNAcylation and calcium sensitivity. *Diabetes* (2015) 64:3339–41. doi: 10.2337/dbi15-0001
139. Suarez J, Hu Y, Makino A, Fricovsky E, Wang H, Dillmann WH. Alterations in mitochondrial function and cytosolic calcium induced by hyperglycemia are restored by mitochondrial transcription factor A in cardiomyocytes. *AJP Cell Physiol.* (2008) 295:C1561–8. doi: 10.1152/ajpcell.00076.2008
140. Zhu-Mauldin X, Marsh SA, Zou L, Marchase RB, Chatham JC. Modification of STIM1 by O-linked N-acetylglucosamine (O-GlcNAc) attenuates store-operated calcium entry in neonatal cardiomyocytes. *J Biol Chem.* (2012) 287:39094–106. doi: 10.1074/jbc.M112.383778
141. Eshima H, Tanaka Y, Sonobe T, Inagaki T, Nakajima T, Poole DC, et al. *In vivo* imaging of intracellular Ca2+ after muscle contractions and direct Ca2+ injection in rat skeletal muscle in diabetes. *AJP Regul Integr Comp Physiol.* (2013) 305:R610–8. doi: 10.1152/ajpregu.00023.2013
142. Safwat Y, Yassin N, Gamal El Din M, Kassem L. Modulation of Skeletal muscle performance and SERCA by exercise and adiponectin gene therapy in insulin-resistant rat. *DNA Cell Biol.* (2013) 32:378–85. doi: 10.1089/dna.2012.1919
143. Banerjee PS, Ma J, Hart GW. Diabetes-associated dysregulation of O-GlcNAcylation in rat cardiac mitochondria. *Proc Natl Acad Sci USA.* (2015) 112:6050–5. doi: 10.1073/pnas.1424017112

Conflict of Interest Statement: The authors declare that the research was conducted in the absence of any commercial or financial relationships that could be construed as a potential conflict of interest.

frontiers in Endocrinology

REVIEW
published: 16 October 2018
doi: 10.3389/fendo.2018.00599

O-GlcNAc as an Integrator of Signaling Pathways

Qunxiang Ong[1,2,3,4], *Weiping Han*[4] *and Xiaoyong Yang*[1,2,3]*

[1] Department of Comparative Medicine, Yale University School of Medicine, New Haven, CT, United States, [2] Program in Integrative Cell Signaling and Neurobiology of Metabolism, Yale University School of Medicine, New Haven, CT, United States, [3] Department of Cellular and Molecular Physiology, Yale University School of Medicine, New Haven, CT, United States, [4] Laboratory of Metabolic Medicine, Singapore Bioimaging Consortium, Agency for Science, Technology and Research (A*STAR), Singapore, Singapore

O-GlcNAcylation is an important posttranslational modification governed by a single pair of enzymes–O-GlcNAc transferase (OGT) and O-GlcNAcase (OGA). These two enzymes mediate the dynamic cycling of O-GlcNAcylation on a wide variety of cytosolic, nuclear and mitochondrial proteins in a nutrient- and stress-responsive fashion. While cellular functions of O-GlcNAcylation have been emerging, little is known regarding the precise mechanisms how the enzyme pair senses the environmental cues to elicit molecular and physiological changes. In this review, we discuss how the OGT/OGA pair acts as a metabolic sensor that integrates signaling pathways, given their capability of receiving signaling inputs from various partners, targeting multiple substrates with spatiotemporal specificity and translocating to different parts of the cell. We also discuss how the pair maintains homeostatic signaling within the cell and its physiological relevance. A better understanding of the mechanisms of OGT/OGA action would enable us to derive therapeutic benefits of resetting cellular O-GlcNAc levels within an optimal range.

Keywords: O-GlcNAc transferase, O-GlcNAcase, signaling integrator, homeostasis, O-GlcNAcylation, spatiotemporal dynamics, metabolic sensor, posttranslational modification

OPEN ACCESS

Edited by:
Tony Lefebvre, Lille University of Science and Technology, France

Reviewed by:
Wagner Barbosa Dias, Universidade Federal do Rio de Janeiro, Brazil
Stéphanie Olivier-Van Stichelen, National Institutes of Health (NIH), United States

***Correspondence:**
Xiaoyong Yang
xiaoyong.yang@yale.edu

Specialty section:
This article was submitted to Molecular and Structural Endocrinology, a section of the journal Frontiers in Endocrinology

Received: *26 June 2018*
Accepted: *20 September 2018*
Published: *16 October 2018*

Citation:
Ong Q, Han W and Yang X (2018) O-GlcNAc as an Integrator of Signaling Pathways. Front. Endocrinol. 9:599. doi: 10.3389/fendo.2018.00599

INTRODUCTION

Proteins are extensively post-translationally modified, with over 450 different types of posttranslational modifications (PTM) that play important roles in cellular signaling, protein-protein interactions or modulation of gene expression (1). The availability of such a PTM code, in addition to spatiotemporal dimensions, provides cells with greater dynamic range to respond to a myriad of stimuli and cellular environment (2). O-GlcNAcylation is a prevalent PTM that is found on serine and threonine residues of proteins in the nucleus, cytoplasm and mitochondria (3, 4). Up to 4,000 and potentially more proteins have been found to be O-GlcNAcylated (5). Remarkably, there is only one enzyme, O-GlcNAc transferase (OGT) (6, 7), that catalyzes the addition of O-GlcNAc to proteins and one that removes the modification, namely O-GlcNAcase (OGA) (8).

O-GlcNAcylation uses the substrate UDP-GlcNAc, the final product of nutrient flux through the hexosamine biosynthetic pathway (HBP) which integrates amino acid, carbohydrate, fatty acid, nucleotide, and energy metabolism (**Figure 1A**). The HBP fluctuates with cellular metabolism and may be dramatically altered under physiological and pathological conditions. The extent of O-GlcNAcylation can reflect metabolic dynamics in the cell. This sets up the OGT/OGA pair to be an "all-in-one" metabolic and nutrient sensor and has been understood to alter diverse cellular processes such as apoptosis, gluconeogenesis, calcium signaling, insulin signaling, and

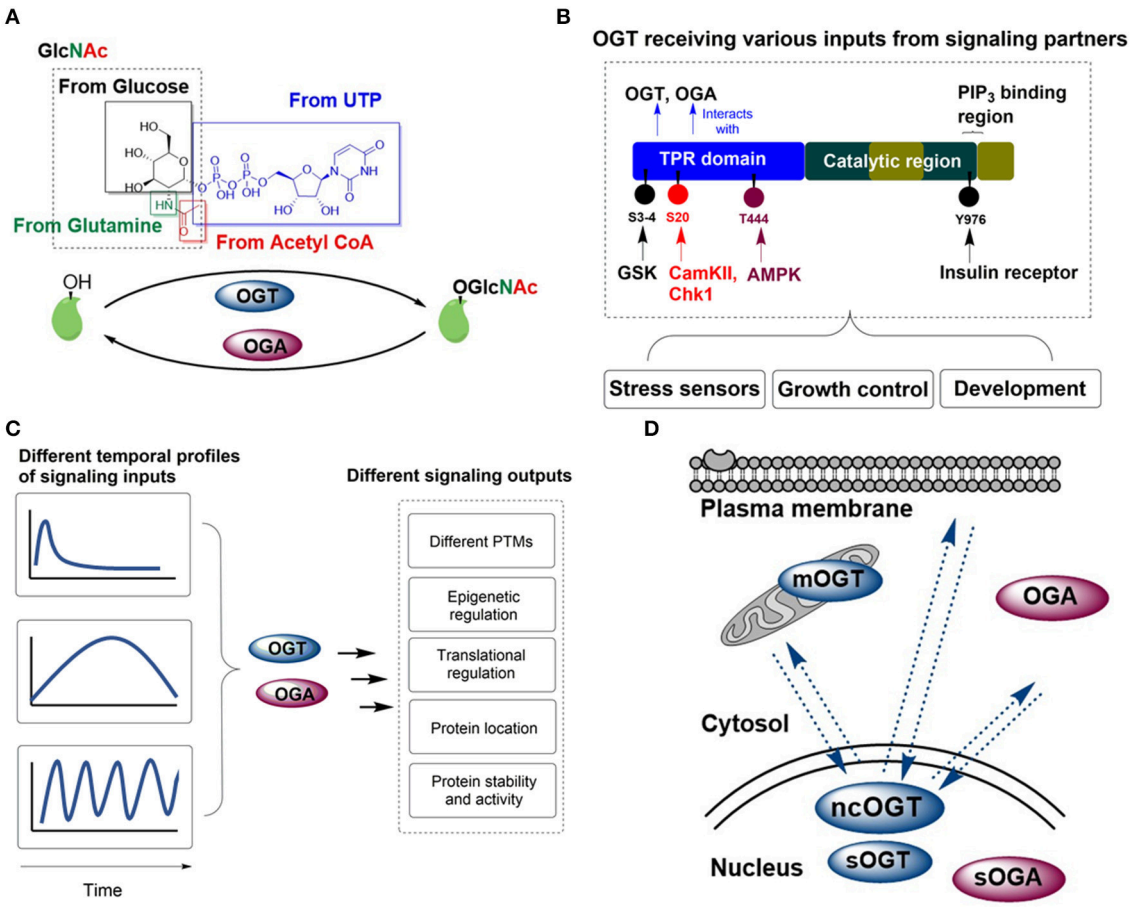

FIGURE 1 | OGT/OGA enzyme pair acts as an integrator for cellular signaling. **(A)** OGT and OGA catalyze the addition and removal of O-GlcNAc on proteins, respectively. The availability of UDP-GlcNAc, the product of amino acid, carbohydrate, fatty acid, nucleotide and energy metabolism, is crucial for OGT function. **(B)** OGT can be phosphorylated by signaling partners (such as AMPK, CamKII, Chk1, GSK, and the insulin receptor), which integrates various inputs and results in O-GlcNAcylation of protein substrates involved in diverse biological responses. **(C)** Temporal control is critical for O-GlcNAcylation of protein subtrates, where OGT/OGA activity is responsive to signaling input changes. **(D)** A unique feature of O-GlcNAcylation is the ability of OGT to shuffle in and out of the nucleus. OGT and OGA isoforms are present in the cytosolic, nuclear and mitochondrial space, whereby the spatial control of signaling can be achieved efficiently.

mitochondrial homeostasis. Physiologically, disruption of OGT and OGA function has been implicated in the pathogenesis of several major health problems, such as diabetes, cancer and neurodegenerative diseases (9). Constitutive deletion knockout of the *ogt* and *oga* gene causes early postnatal lethality in mammals (10, 11).

Remarkable progress in understanding the signaling properties of O-GlcNAcylation has suggested that O-GlcNAcylation and the OGT/OGA enzyme pair may play a key regulatory role in coordinating cellular signaling (3). In this Review, we explore major concepts regarding the role of OGT and O-GlcNAcylation and provide a conceptual understanding of how OGT can potentially act as a metabolic sensor to integrate signaling inputs transduced by other signaling components in the cell.

Traditionally, intracellular signaling has been thought of as linear modules of signaling architecture, from activation of receptors via ligands to information flow through phosphorylation cascades and subsequent activation of transcription and protein synthesis. However, recent advances in mass spectrometry and proteomics have allowed a more holistic assessment of protein and lipid modifications that result from singular events, and the results have indicated that a single stimulus could result in complex responses with multiple pathways being activated simultaneously with feedback loops and cross-talks in place (12, 13). The spatiotemporal dynamics of signaling also contributes to the complexity of the system.

OGT/OGA PAIR AS A SIGNAL INTEGRATOR

A simple way to re-think about signaling proteins and their organization would be to identify key signaling hubs, termed "integrators." A signaling integrator within the cellular environment could be defined as a protein complex which could receive multiple forms of inputs from other signaling molecules, elicit multiple outputs simultaneously with spatiotemporal control and the ability to reset itself in a timely fashion. Its role would be critical in allowing quick coordination of the activity

of several signaling modalities and modulating their signaling dynamics to provide a homeostatic balance or amplification of signaling intensity. While the idea that several signals converge on a specific substrate to elicit defined biological events is a common theme in cellular regulation, the existing ideas prevalent in the field focusses primarily on specific activities of effectors downstream and is limited on the scale of proteome involved. Ideally, the most effective and efficient signal integration would be able to take place almost instantly, allowing the cells to effect quick responses upon gathering external stimuli via global modification and activation of proteins and genetic machinery. The OGT/OGA signaling complex possesses the above-mentioned characteristics that allow them to be an ideal integrator of signaling inputs within cells.

An All-Encompassing Metabolic Sensor

While the substrate of OGT, UDP-GlcNAc, integrates information about nutrient flux within the cell, OGT and OGA are also uniquely positioned to receive information from several key nutrient-sensitive signaling pathways and appropriately transduce this information.

One of the prevailing views in the field is that OGT makes use of its N-terminal tetratricopeptide repeats (TPR) domain, which is an extended superhelical structure of up to 13.5 TPRs, to act as a scaffold for interacting substrates (14). Besides allowing substantial binding plasticity for its downstream signaling substrates, the TPR domain is subject to different posttranslational modifications that regulate its activity, including phosphorylation from adenosine-monophosphate-activated protein kinase (AMPK), calcium/calmodulin-dependent protein kinase II (CaMKII) and insulin-regulated mitotic protein glycogen synthase kinase (GSK3) (**Figure 1B**).

AMPK is an energy sensor that maintains cellular energy level with regard to cellular stress and nutrient availability. Upon its activation, AMPK phosphorylates OGT at threonine 444, resulting in the dissociation of OGT from the chromatin and inhibition of gene expression. Conversely, OGT could mediate O-GlcNAcylation of AMPK, and positively regulate AMPK activity through its phosphorylation at threonine 172 (15, 16). Glucagon signaling is also intricately linked with O-GlcNAcylation activity of OGT, where CaMKII directly activates OGT by phosphorylation at serine 20 (17). On the other hand, in hyperglycemia, CaMKII can be O-GlcNAcylated and activated at serine 279 autonomously, resulting in persistent activation of CaMKII even after the level of calcium declines (18). In the case of AMPK/OGT and CaMKII/OGT signaling, this type of cooperative signaling facilitates feedback mechanisms and allow signaling events to propagate. Checkpoint kinase 1 (Chk1) is also found to induce OGT phosphorylation at serine 20, which stabilizes OGT and is required for cytokinesis (19).

OGT is well known to be involved in insulin-mediated signaling pathways. One of the downstream partners, GSK3β, has been shown to phosphorylate OGT at serine 3 or 4, which leads to increased OGT activity and potential reciprocal regulation (20). Other than the N-terminus, the C-terminal domain of OGT also plays a role in receiving information from protein partners. Insulin stimulation enhances tyrosine 976 phosphorylation of OGT by the insulin receptor and promotes OGT activity (21). Looking further downstream of the insulin receptor, OGT is identified to bind to phosphatidylinositol-3,4,5-trisphosphate (PIP_3) while not possessing the pleckstrin-homology domain like PDK1 and AKT, suggesting different binding affinity toward PIP_3 production (22). This allows OGT to moderate insulin-mediated signaling transduction within 30 min of activation (22). After insulin signaling activation, OGT will be recruited to the plasma membrane where it O-GlcNAcylates and attenuates the multiple components of the insulin signaling pathway (23).

Comparatively, the functions and implications of OGA posttranslational modifications have been less well-studied (as previously reviewed (24, 25). OGA can be O-GlcNAcylated at serine 405 and act as a substrate of OGT (26); however, the implications of O-GlcNAcylation of OGA are unexplored.

Modulation of Major Signaling Pathways in the Cell

O-GlcNAcylation has been well described in previous reviews to regulate and modulate diverse signaling pathways, thus positioning it as an excellent integrator of signals to many effectors within the cell and regulate a wide variety of cellular processes (3, 27–29). O-GlcNAcylation can trigger changes in protein activity, stability and subcellular localization, thereby facilitating signal transduction and propagation. In addition, the dynamic interplay between O-GlcNAc and other posttranslational modifications gives rise to the enormous diversity in signaling modules, which can be mainly classified as reciprocal same-site occupancy and different-site occupancy (29). For the former, phosphorylation and O-GlcNAcylation occur on the same serine and threonine residues and compete with each other. For the latter, the occupancy of one protein region by O-GlcNAc can influence PTMs in another region, and thus affect protein function. The focus in this section is to review and consolidate several exciting new areas in which O-GlcNAcylation plays a key role (**Figure 1B**).

O-GlcNAcylation of Stress Sensors

Global O-GlcNAc levels often show drastic changes in response to cellular stress including heat shock, hypoxia and nutrient deprivation. The targets and functional consequences of stress-mediated O-GlcNAcylation are beginning to be unveiled (3).

Sirtuin 1 (SIRT1) has been established to be a stress sensor (30). Upon genotoxic, oxidative or metabolic stress, SIRT1 is able to deacetylate proteins that regulate stress responses, such as p53 (31) and NF-kB (32). O-GlcNAcylation of SIRT1 at Ser 549 directly increases its deacetylase activity *in vitro* and *in vivo* and protects the cells from apoptosis (33). A recent study showed that an overall increase in O-GlcNAc levels in breast cancer cells reduces SIRT1 levels and activity in an AMPK-dependent

manner. This leads to a decrease in SIRT1-mediated proteosomal degradation of oncogenic transcription factor FOXM1, which promotes cancer cell metastasis (34).

Upon glucose deprivation, chromatin-associated fumarase (FH) is phosphorylated by AMPK at Ser 75, which triggers its association with ATF2 and facilitates gene expression for cell growth arrest (35). In cancer cells, upregulated OGT activity results in O-GlcNAcylation of FH at Ser 75. This impedes FH binding to ATF2 under glucose deficiency and confers survival advantage to these cancer cells (35).

O-GlcNAcylation of Hippo/YAP Pathway in Growth Control

The Hippo/YAP pathway controls organ size in animals and its dysregulation results in cancer (36). Under glucose-rich conditions, O-GlcNAcylation of YAP at Ser 109 by OGT prevents YAP phosphorylation at adjacent Ser 127 and allows YAP translocation into the nucleus. This facilitates expression of genes for proliferation while inhibiting those genes for apoptosis. As a result, glucose-induced YAP O-GlcNAcylation promotes tumorigenesis (37). This study reveals the functional importance of OGT in the Hippo pathway and growth control, further supporting a prevalent role for O-GlcNAcylation in major signaling pathways.

O-GlcNAcylation for Development and Differentiation

O-GlcNAcylation has been known to regulate the activity of proteins involved in embryonic stem cell (ESC) pluripotency and differentiation, such as SOX2 and OCT4 (38). It has also been shown that O-GlcNAcylation is especially important for brain development, where many proteins for neuronal signaling and synaptic plasticity are O-GlcNAcylated (39, 40). OGT inhibition is recently shown to promote human neural cell differentiation (41). In *Oga* knockout models, anatomical defects include delayed brain differentiation and neurogenesis with pronounced changes in expression of pluripotency markers (42). These studies reinforce the importance of OGT and OGA in neural development and function.

Temporal Dynamics of O-GlcNAcylation

For comprehensive integration of signals coming from different signaling partners, timing is an important aspect that is gradually recognized to be extremely important for signal transduction. One important feature of PTMs is that they should enable cells to respond quickly to cues in a reversible fashion, and that these signals could be defined for their intensity and duration (**Figure 1C**). Protein O-GlcNAcylation can be transient, persistent or periodic. These temporal modules can affect different signaling outputs such as protein location, activity, and genetic/epigenetic regulation.

Some studies have indicated the dynamic changes of O-GlcNAcylation during insulin signaling (22, 23), lymphocyte activation (43), calcium stimulus (44) and neuronal depolarization (45). In these scenarios, the fluctuation of O-GlcNAcylation occurs in the order of a few minutes, which indicates that the OGT/OGA signaling integrator is sensitive to intricate regulation of each other. Such dynamic ability of the OGT/OGA complex to influence the O-GlcNAcylation levels in the cell makes it an ideal integrator.

Other than short-term regulation, O-GlcNAcylation can result in long-term changes within the cell, which has been elaborated in many previous reviews (3, 28, 29, 46). O-GlcNAcylation or de-O-GlcNAcylation of proteins may result in their activity and stability to be shifted. O-GlcNAcylation may also regulate transcription and epigenetic programs, engaging in diverse protein complexes in a context-dependent manner to produce longer-term changes within the cell.

Subcellular Distribution and Translocation of OGT/OGA

Signal transduction is profoundly non-uniform in space, and the space in which signaling activities are carried out creates a code for signaling specificity. Alternative splicing results in three variants of OGT, namely nucleocytoplasmic OGT (ncOGT), mitochondrial OGT(mOGT) and short form OGT(sOGT). The longest OGT isoform, ncOGT, is mostly localized in the nucleus but is able to shuttle toward the cytoplasm and plasma membrane in response to signaling cues (7, 47) (**Figure 1D**). One prime example is the recruitment of OGT from the nucleus toward the plasma membrane upon prolonged insulin activation and PIP_3 production (22). OGT is also found to alter its nuclear localization upon acute AMPK activation (15). The mechanism underlying how OGT can be localized in both nucleus and cytosol has recently been elucidated where three amino acids (DFP; residues 451-453) in OGT is able to act as a nuclear localization signal. In addition to the DFP sequence, O-GlcNAcylation of the TPR domain of OGT is required for its direct nuclear translocation (48). The ability to translocate between different cellular locations places OGT at a unique position in coordinating signaling activities within different cellular compartments.

Two isoforms of OGA have been identified and characterized. The long isoform of OGA resides mainly within the cytosol (49), whereas the short isoform (sOGA) localizes at the nucleus and lipid droplets (50). *In vitro* experiments indicate that sOGA exhibits lower enzymatic activity compared to OGA (51, 52). A recent structural study has suggested that these two isoforms may be distinguished by the ability of OGA, but not sOGA, to form dimers (53). The varying location and activity of these OGA isoforms add another layer of complexity in regulation of O-GlcNAc signaling (**Figure 1D**).

LEVELS OF O-GLCNACYLATION SIGNAL PHYSIOLOGICAL NEEDS

As in our proposed integrator model, the OGT/OGA complex integrates many signals to effect modifications on proteins, allowing it to achieve metabolic homeostatic control. Some of these modifications may be transient. Yet in many cases, persistent O-GlcNAcylation is required in several proteins, and chronic disruption in O-GlcNAcylation of these proteins may

have serious consequences for the cell and the organism. One prime example is the hyperphosphorylation of tau, which is involved in the pathogenesis of Alzheimer's Disease (54).

To reconcile the diverse functions and roles of O-GlcNAcylation, it is important to consider the concept of O-GlcNAc homeostasis occurring only at certain cellular O-GlcNAcylation levels within the safe limits (**Figure 2A**). In the "optimal zone" of signaling, O-GlcNAcylation levels are well buffered within a certain range of activity (3, 9). A minimum level of O-GlcNAc levels would be present to ensure O-GlcNAcylation of proteins for their proper functions, while there will be a variable component of O-GlcNAc levels tuned by the OGT/OGA pair for signaling. To further enhance the effectiveness of this pool of O-GlcNAc, the cells could control OGT/OGA activity in the spatiotemporal dimensions to amplify or dampen cellular responses.

Hypo-O-GlcNAcylation usually arises from low UDP-GlcNAc levels or a dramatic imbalance between OGT/OGA expression and activity. Given the observation that some of OGT's protein substrates are constitutively modified at physiological UDP-GlcNAc levels while some vary widely (55), it can be envisioned that the cells would preferentially feed O-GlcNAc moieties toward protein residues that are required for essential structural and functional integrity of the protein (56). At this point, dynamic O-GlcNAc signaling may dampen its amplitude and achieve limited effectiveness. In the event of persistent hypo-O-GlcNAcylation, proteins would then be prone to structural changes without the protective effects from O-GlcNAcylation, thus manifesting states that may have deleterious effects for the cell.

On the other hand, in the hyper-O-GlcNAcylation regime, serine or threonine residues of proteins may shift the equilibrium of phosphorylation toward O-GlcNAcylation. In many types of cancer, tumor cells have altered glucose metabolism, resulting in higher hexosamine flux toward UDP-GlcNAc (57, 58). Oncogenes such as Myc (59, 60) and NF-kB (61) are stabilized with persistent O-GlcNAcylation, thus promoting cancer growth. As such, in an extended duration of hyper-O-GlcNAcylation, O-GlcNAc cycling is not well-buffered and homeostatic signaling by OGT/OGA can be compromised.

It is important to note that O-GlcNAcylation and nutrient availability is not always in a linear relationship. Numerous studies have reported a global increase in cellular O-GlcNAcylation in response to nutrient starvation, a condition in which low UDP-GlcNAc levels are expected (35, 62–64). Furthermore, OGT has preferential selectivity for certain substrates under different UDP-GlcNAc concentrations. For instance, O-GlcNAcylation of PGC-1α peaks at 5 mM glucose and is lower under hypo- and hyperglycemic conditions, indicating that other factors are involved in the nutrient sensitivity of this modification (65). Overall, O-GlcNAc homeostasis is determined by nutrient availability, OGT/OGA expression and activity, protein substrate selectivity, as well as other co-factors (**Figure 2B**).

O-GlcNAcylation of specific proteins can be described as an equilibrium between the forward reaction driven by OGT (denoted as k_1) and the reverse reaction driven by OGA (denoted as k_{-1}) (**Figure 2B**). This equilibrium is dictated by the local microenvironment, including local concentrations of UDP-GlcNAc, protein substrates, and OGT/OGA complexes. Local UDP-GlcNAc levels are affected by the availability of extracellular nutrients, the local activities of metabolic enzymes and the HBP flux rate. In addition to their local concentrations, the conformation and activity of protein substrates, OGT and OGA, and binding partners can have a profound influence on k_1 and k_{-1}. In particular, OGT and OGA can receive various signaling inputs in the form of posttranslational modifications that modulate k_1 and k_{-1} of specific proteins (**Figures 1B**, **2B**).

MACHINERY MAINTAINING O-GLCNAC HOMEOSTASIS

Given that O-GlcNAcylation levels of specific proteins may not be linearly correlated with nutrient availability, the expression and activity of OGT and OGA have to be tightly regulated. The observation that the levels of OGT and OGA transcripts and proteins fluctuate in many processes, such as cell cycle progression, stress response and tissue development, hint at the intricacies of this regulatory machinery at work (24, 66).

Studies have demonstrated that the levels of OGT and OGA would compensate for one another. Upon OGT knockout, inhibition or knockdown, OGA protein levels are reduced (67). This might be a consequence of reducing O-GlcNAc levels within cells, and OGA protein levels are sensitive to such changes at the posttranscriptional level. It has also been suggested that the *Oga* gene is situated within the highly conserved NK homeobox gene cluster. Since this region is targeted by the PcG repressor complex which comprises OGT, it is likely that OGT modulates OGA expression at the transcriptional level (68). Conversely, upon OGA inhibition, OGT levels are downregulated while OGA levels are upregulated (69). Our recent work provides mechanistic insight into mutual regulation of OGT and OGA at the transcriptional level. Specifically, we found that OGA acts as a co-activator that directly promotes OGT transcription through cooperation with C/EBPβ and p300 histone acetyltransferase (70). Another recent work has suggested that there is a conserved OGT intronic splicing silencer that is necessary for OGT intron retention (71). The OGT intron retention is dynamically sensitive to cellular O-GlcNAc levels. At high O-GlcNAc levels, the intron is retained and results in the degradation of OGT transcripts. However, upon low O-GlcNAc levels, the intron is spliced out and OGT proteins are produced, thereby increasing its protein level. These studies highlight the multiple layers of regulation of OGT and OGA expression to ensure O-GlcNAc homeostasis.

While the OGT and OGA levels are well controlled by intricate transcriptional and posttranscriptional mechanisms, it is likely that such regulation can only exist within a well-tolerated "optimal zone" for a limited period of time. Chronic hypo- or hyper-O-GlcNAcylation would potentially undermine the effectiveness of O-GlcNAc signaling, thus contributing to the pathogenesis of human disease.

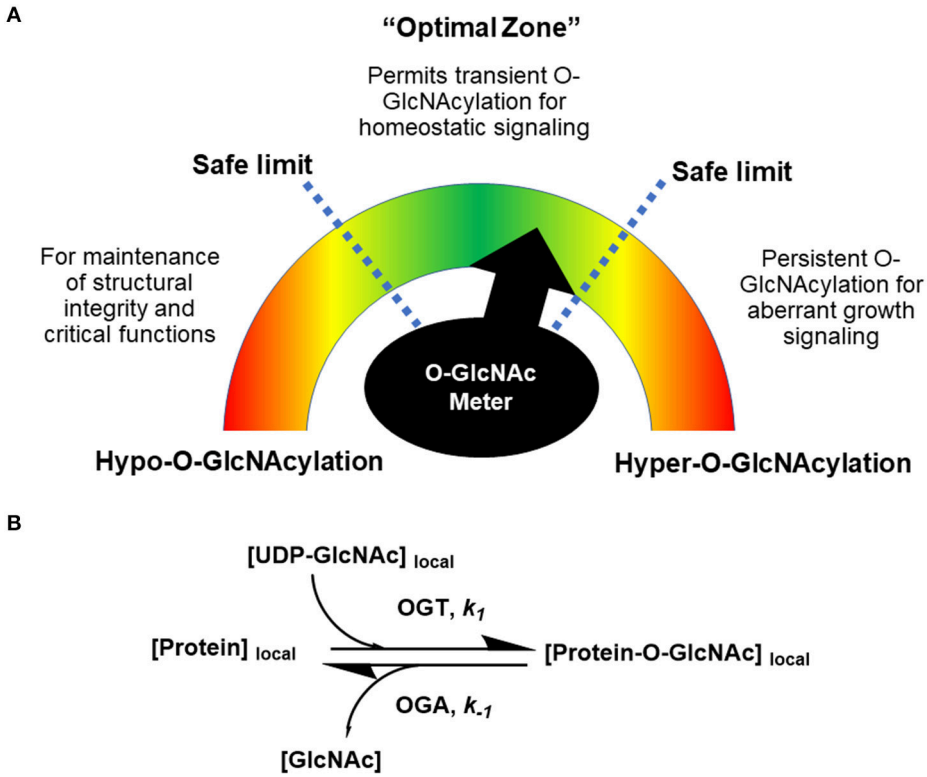

[UDP-GlcNAc] local	[Protein] local	[OGT/OGA] local
• Nutrient availability • Local metabolic enzymes • Local HBP flux	• Expression level • Conformation and activity • Binding partners	• Expression levels • Signaling input • Binding partners

FIGURE 2 | Global and local levels of O-GlcNAcylation gauge signaling responses. **(A)** Global O-GlcNAcylation levels have to be maintained within an optimal range as depicted by an "O-GlcNAc meter" in analogy to a speedometer. Hyper-O-GlcNAcylation, as a result of hyper-OGT activity or high UDP-GlcNAc levels, would result in persistent O-GlcNAcylation of growth signaling proteins, leading to human diseases such as cancer. Hypo-O-GlcNAcylation would impair the structural integrity of protein substrates and their relevant functions. **(B)** The rates of O-GlcNAcylation and de-O-GlcNAcylation of specific proteins, denoted by k_1 and k_{-1}, are tuned by the local microenvironment. The reactions are determined by local concentrations of UDP-GlcNAc, protein substrates, binding partners, and OGT/OGA activity. Signaling inputs converging on posttranslational modifications of OGT and OGA dictate k_1 and k_{-1} of specific proteins.

PERSPECTIVES AND FUTURE DIRECTIONS

While the promiscuity of OGT substrate recognition has made it technically challenging to define the specificity of OGT action, it represents a huge ground of opportunities to be exploited. More tools and technologies have to be developed to understand O-GlcNAc signaling. Due to the diversity of substrates that OGT and OGA can act on to regulate cellular function, and the complex compensatory pathways that could take place, delineating the cause and effect remains a major challenge. Future studies are required to investigate the "O-GlcNAc proteomics" with temporal precision and identify potentially the subsets of proteins that are sensitive to different UDP-GlcNAc levels and in different temporal contexts.

One understudied component of O-GlcNAc signaling is the spatial contexts of O-GlcNAcylation. In various cellular compartments of the cell, such as the nucleus, mitochondria, cytosol and plasma membrane, OGT and OGA have different physiological roles. Within each cellular region, there are different potential binding partners for both OGT and OGA. Local concentrations of UDP-GlcNAc may also contribute to O-GlcNAcylation of specific substrates (**Figure 2B**). Profiling the variability of local UDP-GlcNAc levels and O-GlcNAcylation of proteins in real-time and within individual cells would provide a powerful tool to understand the dynamics of this modification. Developing the tools to visualize the kinetics of OGT/OGA interactions with their signaling partners would also help our understanding of O-GlcNAc regulation in spatial dimensions.

A better understanding of the roles of O-GlcNAylation in diverse signaling pathways would be another major direction to be pursued. Development of site-specific O-GlcNAc antibodies would be essential in accelerating our understanding of the function of specific protein O-GlcNAcylation. As

O-GlcNAcylation is tightly linked with different PTMs in the cellular metabolic network, it would be useful to identify the intricate relationships among various types of PTMs on proteins. Crosstalk between phosphorylation and O-GlcNAcylation has been relatively well studied, where O-GlcNAcylation can occur reciprocally or sequentially with phosphorylation on the same or different residues. Such studies could be extended to explore the link between O-GlcNAcylation and other PTMs, such as acetylation, methylation, and succinylation and ubiquitination.

CONCLUSIONS

The cellular signaling machinery is a complex network of components which is only partially understood. The complexity is not only due to the sheer quantity of participants and its high degree of connectivity, but also to the spatiotemporal dimensions of signaling which confers different functions on the same proteins under various contexts. In this review, we have proposed the OGT/OGA pair as a metabolic sensor and an integrator of cellular signaling processes. This relies on the ability of the OGT/OGA complex to receive metabolic and stress signals from multiple upstream partners, and to drive O-GlcNAc modification on diverse sets of downstream targets with precise spatiotemporal control. The OGT/OGA pair is tightly regulated by multiple layers of transcriptional, posttranscriptional and posttranslational control to maintain cellular O-GlcNAc levels within an optimal zone. This "O-GlcNAc meter" ensures O-GlcNAcylation as an effective toolbox to tune and integrate signaling pathways.

AUTHOR CONTRIBUTIONS

All authors listed have made a substantial, direct and intellectual contribution to the work, and approved it for publication.

ACKNOWLEDGMENTS

We thank members of the Yang laboratory and Lab of Metabolic Medicine for stimulating discussions. This work was supported by the National Institutes of Health (R01DK102648, P01DK057751), American Cancer Society (RSG-14-244-01-TBE) to XY and an intramural funding from A*STAR Biomedical Research Council to WH.

REFERENCES

1. Reorganizing the protein space at the Universal Protein Resource (UniProt). *Nucleic Acids Res.* (2012) 40:D71–5. doi: 10.1093/nar/gkr981
2. Kholodenko BN, Hancock JF, Kolch W. Signalling ballet in space and time. *Nat Rev Mol Cell Biol.* (2010) 11:414–26. doi: 10.1038/nrm2901
3. Yang X, Qian K. Protein O-GlcNAcylation: emerging mechanisms and functions. *Nat Rev Mol Cell Biol.* (2017) 18:452–65. doi: 10.1038/nrm.2017.22
4. Torres CR, Hart GW. Topography and polypeptide distribution of terminal N-acetylglucosamine residues on the surfaces of intact lymphocytes. Evidence for O-linked GlcNAc. *J Biol Chem* (1984) 259:3308–17.
5. Ma J, Hart GW. O-GlcNAc profiling: from proteins to proteomes. *Clin Proteomics* (2014) 11:8. doi: 10.1186/1559-0275-11-8
6. Haltiwanger RS, Holt GD, Hart GW. Enzymatic addition of O-GlcNAc to nuclear and cytoplasmic proteins. Identification of a uridine diphospho-N-acetylglucosamine:peptide beta-N-acetylglucosaminyltransferase. *J Biol Chem* (1990) 265:2563–8.
7. Hanover JA, Yu S, Lubas WB, Shin SH, Ragano-Caracciola M, Kochran J, et al. Mitochondrial and nucleocytoplasmic isoforms of O-linked GlcNAc transferase encoded by a single mammalian gene. *Arch Biochem Biophys.* (2003) 409:287–97. doi: 10.1016/S0003-9861(02)00578-7
8. Dong DL, Hart GW. Purification and characterization of an O-GlcNAc selective N-acetyl-beta-D-glucosaminidase from rat spleen cytosol. *J Biol Chem* (1994) 269:19321–30.
9. Bond MR, Hanover JA. *O*- GlcNAc cycling: a link between metabolism and chronic disease. *Annu Rev Nutr.* (2013) 33:205–29. doi: 10.1146/annurev-nutr-071812-161240
10. Shafi R, Iyer SP, Ellies LG, O'Donnell N, Marek KW, Chui D, et al. The O-GlcNAc transferase gene resides on the X chromosome and is essential for embryonic stem cell viability and mouse ontogeny. *Proc Natl Acad Sci USA.* (2000) 97:5735–9. doi: 10.1073/pnas.100471497
11. Ryoul Yang Y, Song M, Lee H, Jeon Y, Choi EJ, Jang HJ, et al. O-GlcNAcase is essential for embryonic development and maintenance of genomic stability. *Aging Cell* (2012) 11:439–48. doi: 10.1111/j.1474-9726.2012.00801.x
12. Aebersold R, Mann M. Mass spectrometry-based proteomics. *Nature* (2003) 422:198–207. doi: 10.1038/nature01511
13. Kholodenko BN. Cell-signalling dynamics in time and space. *Nat Rev Mol Cell Biol.* (2006) 7:165–76. doi: 10.1038/nrm1838
14. Janetzko J, Walker S. The making of a sweet modification: structure and function of *O* -GlcNAc transferase. *J Biol Chem.* (2014) 289:34424–32. doi: 10.1074/jbc.R114.604405
15. Bullen JW, Balsbaugh JL, Chanda D, Shabanowitz J, Hunt DF, Neumann D, et al. Cross-talk between two essential nutrient-sensitive enzymes: O-GlcNAc transferase (OGT) and AMP-activated protein kinase (AMPK). *J Biol Chem.* (2014) 289:10592–606. doi: 10.1074/jbc.M113.523068
16. Xu Q, Yang C, Du Y, Chen Y, Liu H, Deng M, Zhang H, Zhang L, Liu T, Liu Q, et al. AMPK regulates histone H2B O-GlcNAcylation. *Nucleic Acids Res* (2014) 42:5594–604. doi: 10.1093/nar/gku236
17. Ruan HB, Ma Y, Torres S, Zhang B, Feriod C, Heck RM, et al. Calcium-dependent O-GlcNAc signaling drives liver autophagy in adaptation to starvation. *Genes Dev.* (2017) 31:1655–65. doi: 10.1101/gad.305441.117
18. Erickson JR, Pereira L, Wang L, Han G, Ferguson A, Dao K, et al. Diabetic hyperglycaemia activates CaMKII and arrhythmias by O-linked glycosylation. *Nature* (2013) 502:372–6. doi: 10.1038/nature12537
19. Li Z, Li X, Nai S, Geng Q, Liao J, Xu X, et al. Checkpoint kinase 1-induced phosphorylation of O-linked β-N-acetylglucosamine transferase regulates the intermediate filament network during cytokinesis. *J Biol Chem.* (2017) 292:19548–55. doi: 10.1074/jbc.M117.811646
20. Kaasik K, Kivimäe S, Allen JJ, Chalkley RJ, Huang Y, Baer K, et al. Glucose sensor O-GlcNAcylation coordinates with phosphorylation to regulate circadian clock. *Cell Metab.* (2013) 17:291–302. doi: 10.1016/j.cmet.2012.12.017
21. Whelan SA, Lane MD, Hart GW. Regulation of the *O* -Linked β- *N* -Acetylglucosamine transferase by insulin signaling. *J Biol Chem* (2008) 283:21411–7. doi: 10.1074/jbc.M800677200
22. Yang X, Ongusaha PP, Miles PD, Havstad JC, Zhang F, So WV, et al. Phosphoinositide signalling links O-GlcNAc transferase to insulin resistance. *Nature* (2008) 451:964–9. doi: 10.1038/nature06668
23. Whelan SA, Dias WB, Thiruneelakantapillai L, Lane MD, Hart GW. Regulation of Insulin Receptor Substrate 1 (IRS-1)/AKT Kinase-mediated Insulin Signaling by *O* -Linked β- *N* -Acetylglucosamine in 3T3-L1 Adipocytes. *J Biol Chem.* (2010) 285:5204–11. doi: 10.1074/jbc.M109.077818
24. Nagel AK, Ball LE. O-GlcNAc transferase and O-GlcNAcase: achieving target substrate specificity. *Amino Acids* (2014) 46:2305–16. doi: 10.1007/s00726-014-1827-7

25. Alonso J, Schimpl M, van Aalten DMF. O-GlcNAcase: promiscuous hexosaminidase or key regulator of O-GlcNAc signaling? *J Biol Chem.* (2014) 289:34433–9. doi: 10.1074/jbc.R114.609198
26. Khidekel N, Ficarro SB, Clark PM, Bryan MC, Swaney DL, Rexach JE, et al. Probing the dynamics of O-GlcNAc glycosylation in the brain using quantitative proteomics. *Nat Chem Biol.* (2007) 3:339–48. doi: 10.1038/nchembio881
27. Bond MR, Hanover JA. A little sugar goes a long way: the cell biology of O-GlcNAc. *J Cell Biol.* (2015) 208:869–80. doi: 10.1083/jcb.201501101
28. Zhang K, Yin R, Yang X. O-GlcNAc: a bittersweet switch in liver. *Front Endocrinol.* (2014) 5:221. doi: 10.3389/fendo.2014.00221
29. Hart GW, Housley MP, Slawson C. Cycling of O-linked β-N-acetylglucosamine on nucleocytoplasmic proteins. *Nature* (2007) 446:1017–22. doi: 10.1038/nature05815
30. Chang HC, Guarente L. SIRT1 and other sirtuins in metabolism. *Trends Endocrinol Metab.* (2014) 25:138–45 doi: 10.1016/j.tem.2013.12.001
31. Luo J, Nikolaev AY, Imai S, Chen D, Su F, Shiloh A, et al. Negative control of p53 by Sir2alpha promotes cell survival under stress. *Cell* (2001) 107:137–48. doi: 10.1016/S0092-8674(01)00524-4
32. Yeung F, Hoberg JE, Ramsey CS, Keller MD, Jones DR, Frye RA, et al. Modulation of NF-κB-dependent transcription and cell survival by the SIRT1 deacetylase. *EMBO J.* (2004) 23:2369–80. doi: 10.1038/sj.emboj.7600244
33. Han C, Gu Y, Shan H, Mi W, Sun J, Shi M, et al. O-GlcNAcylation of SIRT1 enhances its deacetylase activity and promotes cytoprotection under stress. *Nat Commun.* (2017) 8:1491. doi: 10.1038/s41467-017-01654-6
34. Ferrer CM, Lu TY, Bacigalupa ZA, Katsetos CD, Sinclair DA, Reginato MJ. O-GlcNAcylation regulates breast cancer metastasis via SIRT1 modulation of FOXM1 pathway. *Oncogene* (2017) 36:559–69. doi: 10.1038/onc.2016.228
35. Wang T, Yu Q, Li J, Hu B, Zhao Q, Ma C, et al. O-GlcNAcylation of fumarase maintains tumour growth under glucose deficiency. *Nat Cell Biol.* (2017) 19:833–43. doi: 10.1038/ncb3562
36. Harvey KF, Zhang X, Thomas DM. The hippo pathway and human cancer. *Nat Rev Cancer* (2013) 13:246–57. doi: 10.1038/nrc3458
37. Peng C, Zhu Y, Zhang W, Liao Q, Chen Y, Zhao X, et al. Regulation of the hippo-YAP pathway by glucose sensor O-GlcNAcylation. *Mol Cell* (2017) 68:591–604.e5. doi: 10.1016/J.MOLCEL.2017.10.010
38. Jang H, Kim TW, Yoon S, Choi SY, Kang TW, Kim SY, et al. O-GlcNAc regulates pluripotency and reprogramming by directly acting on core components of the pluripotency network. *Cell Stem Cell* (2012) 11:62–74. doi: 10.1016/j.stem.2012.03.001
39. Lagerlöf O, Hart GW, Huganir RL. O-GlcNAc transferase regulates excitatory synapse maturity. *Proc Natl Acad Sci USA.* (2017) 114:1684–9. doi: 10.1073/pnas.1621367114
40. Yang YR, Song S, Hwang H, Jung JH, Kim SJ, Yoon S, et al. Memory and synaptic plasticity are impaired by dysregulated hippocampal O-GlcNAcylation. *Sci Rep.* (2017) 7:44921. doi: 10.1038/srep44921
41. Andres LM, Blong IW, Evans AC, Rumachik NG, Yamaguchi T, Pham ND, et al. Chemical modulation of protein O-GlcNAcylation via OGT inhibition promotes human neural cell differentiation. *ACS Chem Biol.* (2017) 12:2030–9. doi: 10.1021/acschembio.7b00232
42. Olivier-Van Stichelen S, Wang P, Comly M, Love DC, Hanover JA. Nutrient-driven O-linked N-acetylglucosamine (O-GlcNAc) cycling impacts neurodevelopmental timing and metabolism. *J Biol Chem.* (2017) 292:6076–85. doi: 10.1074/jbc.M116.774042
43. Golks A, Tran TTT, Goetschy JF, Guerini D. Requirement for O-linked N-acetylglucosaminyltransferase in lymphocytes activation. *EMBO J.* (2007) 26:4368–79. doi: 10.1038/sj.emboj.7601845
44. Dias WB, Cheung WD, Wang Z, Hart GW. Regulation of calcium/calmodulin-dependent kinase IV by O-GlcNAc modification. *J Biol Chem.* (2009) 284:21327–37. doi: 10.1074/jbc.M109.007310
45. Song M, Kim HS, Park JM, Kim SH, Kim IH, Ryu SH, et al. o-GlcNAc transferase is activated by CaMKIV-dependent phosphorylation under potassium chloride-induced depolarization in NG-108-15 cells. *Cell Signal.* (2008) 20:94–104. doi: 10.1016/j.cellsig.2007.09.002
46. Ruan HB, Singh JP, Li MD, Wu J, Yang X. Cracking the O-GlcNAc code in metabolism. *Trends Endocrinol Metab.* (2013) 24:301–9. doi: 10.1016/j.tem.2013.02.002
47. Lubas WA, Frank DW, Krause M, Hanover JA. O-Linked GlcNAc transferase is a conserved nucleocytoplasmic protein containing tetratricopeptide repeats. *J Biol Chem.* (1997) 272:9316–24. doi: 10.1074/JBC.272.14.9316
48. Seo HG, Kim HB, Kang MJ, Ryum JH, Yi EC, Cho JW. Identification of the nuclear localisation signal of O-GlcNAc transferase and its nuclear import regulation. *Sci Rep.* (2016) 6:34614. doi: 10.1038/srep34614
49. Gao Y, Wells L, Comer FI, Parker GJ, Hart GW. Dynamic O-glycosylation of nuclear and cytosolic proteins: cloning and characterization of a neutral, cytosolic beta-N-acetylglucosaminidase from human brain. *J Biol Chem.* (2001) 276:9838–45. doi: 10.1074/jbc.M010420200
50. Comtesse N, Maldener E, Meese E. Identification of a nuclear variant of MGEA5, a cytoplasmic hyaluronidase and a β-N-acetylglucosaminidase. *Biochem Biophys Res Commun.* (2001) 283:634–40. doi: 10.1006/BBRC.2001.4815
51. Kim EJ, Kang DO, Love DC, Hanover JA. Enzymatic characterization of O-GlcNAcase isoforms using a fluorogenic GlcNAc substrate. *Carbohydr Res.* (2006) 341:971–82. doi: 10.1016/J.CARRES.2006.03.004
52. Macauley MS, Vocadlo DJ. Enzymatic characterization and inhibition of the nuclear variant of human O-GlcNAcase. *Carbohydr Res.* (2009) 344:1079–84. doi: 10.1016/J.CARRES.2009.04.017
53. Elsen NL, Patel SB, Ford RE, Hall DL, Hess F, Kandula H, et al. Insights into activity and inhibition from the crystal structure of human O-GlcNAcase. *Nat Chem Biol.* (2017) 13:613–5. doi: 10.1038/nchembio.2357
54. Zhu Y, Shan X, Yuzwa SA, Vocadlo DJ. The emerging link between O-GlcNAc and Alzheimer disease. *J Biol Chem.* (2014) 289:34472–81. doi: 10.1074/jbc.R114.601351
55. Shen DL, Gloster TM, Yuzwa SA, Vocadlo DJ. Insights into *O* -Linked *N* -acetylglucosamine ([0-9] *O* -GlcNAc) processing and dynamics through kinetic analysis of *O* -GlcNAc transferase and *O* -GlcNAcase activity on protein substrates. *J Biol Chem.* (2012) 287:15395–408. doi: 10.1074/jbc.M111.310664
56. Zachara NE, Hart GW. Cell signaling, the essential role of O-GlcNAc! *Biochim Biophys Acta* (2006) 1761:599–617. doi: 10.1016/J.BBALIP.2006.04.007
57. Ma Z, Vosseller K. Cancer metabolism and elevated O-GlcNAc in oncogenic signaling. *J Biol Chem.* (2014) 289:34457–65. doi: 10.1074/jbc.R114.577718
58. de Queiroz RM, Carvalho E, Dias WB. O-GlcNAcylation: the sweet side of the cancer. *Front Oncol.* (2014) 4:132. doi: 10.3389/fonc.2014.00132
59. Chou TY, Dang CV, Hart GW. Glycosylation of the c-Myc transactivation domain. *Proc Natl Acad Sci USA.* (1995) 92:4417–21.
60. Sodi VL, Khaku S, Krutilina R, Schwab LP, Vocadlo DJ, Seagroves TN, et al. Signal transduction mTOR/MYC axis regulates O-GlcNAc transferase expression and O-GlcNAcylation in breast cancer.*Mol Cancer Res.*(2015) 13:923–33. doi: 10.1158/1541-7786.MCR-14-0536
61. Ma Z, Vocadlo DJ, Vosseller K. Hyper- *O* -GlcNAcylation is anti-apoptotic and maintains constitutive NF-κB activity in pancreatic cancer cells. *J Biol Chem.* (2013) 288:15121–30. doi: 10.1074/jbc.M113.470047
62. Trapannone R, Mariappa D, Ferenbach AT, van Aalten DMF. Nucleocytoplasmic human O-GlcNAc transferase is sufficient for O-GlcNAcylation of mitochondrial proteins. *Biochem J.* (2016) 473:1693–702. doi: 10.1042/BCJ20160092
63. Taylor RP, Geisler TS, Chambers JH, McClain DA. Up-regulation of O-GlcNAc transferase with glucose deprivation in HepG2 cells is mediated by decreased hexosamine pathway flux. *J Biol Chem.* (2009) 284:3425–32. doi: 10.1074/jbc.M803198200
64. Taylor RP, Parker GJ, Hazel MW, Soesanto Y, Fuller W, Yazzie MJ, et al. Glucose deprivation stimulates *O* -GlcNAc modification of proteins through up-regulation of *O* -linked *N* -acetylglucosaminyltransferase. *J Biol Chem.* (2008) 283:6050–7. doi: 10.1074/jbc.M707328200
65. Ruan HB, Han X, Li MD, Singh JP, Qian K, Azarhoush S, et al. O-GlcNAc transferase/host cell factor C1 complex regulates gluconeogenesis by modulating PGC-1α stability. *Cell Metab.* (2012) 16:226–37. doi: 10.1016/j.cmet.2012.07.006

66. Olivier-Van Stichelen S, Drougat L, Dehennaut V, El Yazidi-Belkoura I, Guinez C, Mir AM, et al. Serum-stimulated cell cycle entry promotes ncOGT synthesis required for cyclin D expression. *Oncogenesis* (2012) 1:e36. doi: 10.1038/oncsis.2012.36
67. Kazemi Z, Chang H, Haserodt S, McKen C, Zachara NE. O-linked beta-N-acetylglucosamine (O-GlcNAc) regulates stress-induced heat shock protein expression in a GSK-3beta-dependent manner. *J Biol Chem.* (2010) 285:39096–107. doi: 10.1074/jbc.M110.131102
68. Gambetta MC, Oktaba K, Müller J. Essential role of the glycosyltransferase sxc/Ogt in polycomb repression. *Science* (2009) 325:93–6. doi: 10.1126/science.1169727
69. Zhang Z, Tan EP, VandenHull NJ, Peterson KR, Slawson C. O-GlcNAcase Expression is Sensitive to Changes in O-GlcNAc Homeostasis. *Front Endocrinol.* (2014) 5:206. doi: 10.3389/fendo.2014.00206
70. Qian K, Wang S, Fu M, Zhou J, Singh JP, Li MD, et al. Transcriptional regulation of O-GlcNAc homeostasis is disrupted in pancreatic cancer. *J Biol Chem.* 293:13989–14000 (2018). doi: 10.1074/jbc.RA118.004709
71. Park SK, Zhou X, Pendleton KE, Hunter OV, Kohler JJ, O'Donnell KA, et al. A conserved splicing silencer dynamically regulates O-GlcNAc transferase intron retention and O-GlcNAc homeostasis. *Cell Rep.* (2017) 20:1088–99. doi: 10.1016/j.celrep.2017.07.017

Conflict of Interest Statement: The authors declare that the research was conducted in the absence of any commercial or financial relationships that could be construed as a potential conflict of interest.

The reviewer RT and handling editor declared their shared affiliation at the time of review.

frontiers in Endocrinology

ORIGINAL RESEARCH
published: 16 October 2018
doi: 10.3389/fendo.2018.00595

Direct Crosstalk Between *O*-GlcNAcylation and Phosphorylation of Tau Protein Investigated by NMR Spectroscopy

Gwendoline Bourré[1], *François-Xavier Cantrelle*[1], *Amina Kamah*[1], *Béatrice Chambraud*[2], *Isabelle Landrieu*[1] *and Caroline Smet-Nocca*[1]*

[1] Univ. Lille, CNRS UMR8576, Unité de Glycobiologie Structurale et Fonctionnelle, Lille, France, [2] Univ. Paris XI, UMR 1195 Inserm, Le Kremlin Bicêtre, France

OPEN ACCESS

Edited by:
Tarik Issad,
Institut National de la Santé et de la Recherche Médicale (INSERM), France

Reviewed by:
Yobana Perez-Cervera, Benito Juárez Autonomous University of Oaxaca, Mexico
Chad Slawson, Kansas University of Medical Center Research Institute, United States

***Correspondence:**
Caroline Smet-Nocca
caroline.smet-nocca@univ-lille.fr

Specialty section:
This article was submitted to Molecular and Structural Endocrinology, a section of the journal Frontiers in Endocrinology

Received: *20 July 2018*
Accepted: *19 September 2018*
Published: *16 October 2018*

Citation:
Bourré G, Cantrelle F-X, Kamah A, Chambraud B, Landrieu I and Smet-Nocca C (2018) Direct Crosstalk Between O-GlcNAcylation and Phosphorylation of Tau Protein Investigated by NMR Spectroscopy. Front. Endocrinol. 9:595. doi: 10.3389/fendo.2018.00595

The formation of intraneuronal fibrillar inclusions of tau protein is associated with several neurodegenerative diseases referred to as tauopathies including Alzheimer's disease (AD). A common feature of these pathologies is hyperphosphorylation of tau, the main component of fibrillar assemblies such as Paired Helical Filaments (PHFs). *O*-β-linked N-acetylglucosaminylation (*O*-GlcNAcylation) is another important posttranslational modification involved in regulation of tau pathophysiology. Among the benefits of *O*-GlcNAcylation, modulation of tau phosphorylation levels and inhibition of tau aggregation properties have been described while decreased *O*-GlcNAcylation could be involved in the raise of tau phosphorylation associated with AD. However, the molecular mechanisms at the basis of these observations remain to be defined. In this study, we identify by NMR spectroscopy *O*-GlcNAc sites in the longest isoform of tau and investigate the direct role of *O*-GlcNAcylation on tau phosphorylation and conversely, the role of phosphorylation on tau *O*-GlcNAcylation. We show here by a systematic examination of the quantitative modification patterns by NMR spectroscopy that *O*-GlcNAcylation does not modify phosphorylation of tau by the kinase activity of ERK2 or a rat brain extract while phosphorylation slightly increases tau *O*-GlcNAcylation by OGT. Our data suggest that indirect mechanisms act in the reciprocal regulation of tau phosphorylation and *O*-GlcNAcylation *in vivo* involving regulation of the enzymes responsible of phosphate and *O*-GlcNAc dynamics.

Keywords: Tau protein, phosphorylation, *O*-GlcNAcylation, crosstalk, NMR spectroscopy

INTRODUCTION

O-GlcNAcylation is a dynamic posttranslational modification (PTM) based on addition of a single sugar, the β-D-*N*-acetylglucosamine, on serine and threonine residues of nuclear and cytoplasmic proteins (1). The function of *O*-GlcNAcylation is still not fully understood and may act, at least partially, by regulating phosphorylation. The interplay between both PTMs has been observed upon global elevation of *O*-GlcNAcylation at the phospho-proteome level for which decreases have been detected for some site-specific phosphorylation but also increases, although to a lesser extent, at other sites (2). *O*-GlcNAcylation can compete reciprocally with phosphorylation at the

same site or alternatively, both *O*-GlcNAc and phosphate can modify and regulate proximal sites (3). Additionally, the crosstalk between both PTMs may extend to the reciprocal modification of enzymes implicated in phosphorylation and *O*-GlcNAcylation dynamics (2). No consensus sequence has been identified so far for the *O*-GlcNAc modification complicating site mapping. However, frequently occurring motifs exist such as sequences clustering Ser/Thr residues, and bioinformatics tools for *O*-GlcNAc site prediction have been developed that will be of help (4, 5). Recently, a motif frequently occurring in the phosphorylation/*O*-GlcNAcylation crosstalk has been defined involving Ser/Thr proline-directed phosphorylation sites, i.e., sites targeted by proline-directed kinases, that are enriched in the phospho-proteome (6). As a PTM involved in various biological processes, the *O*-GlcNAc modification has been implicated in numerous human diseases including neurodegenerative disorders (7–10).

Variations of *O*-GlcNAc levels in Alzheimer's disease (AD) brain have been detected and are still a matter of debate. It has been shown in some studies that *O*-GlcNAcylation of proteins is lowered in AD brain (9, 11, 12) likely due to decreased glucose uptake/metabolism that is one of the main metabolic changes in aging brain (13). In contrast, overall *O*-GlcNAc levels were also found to be upregulated in AD brain, as associated with a specific increase of *O*-GlcNAc levels of the detergent insoluble protein fraction of cytoskeleton (14) and an imbalance of protein levels involved in the *O*-GlcNAc dynamics as compared to age-matched controls (15). Tau protein, the main component of neurofibrillary tangles (NFTs) (16), one of the two molecular hallmarks of AD with amyloid plaques, is subjected to *O*-GlcNAc modification which was initially estimated to 4 *O*-GlcNAc group per tau molecule on at least 12 Ser/Thr sites (17). It has been shown that tau *O*-GlcNAcylation impairs its phosphorylation and toxicity (11, 18). Furthermore, pharmacological increase of *O*-GlcNAcylation leads to neuroprotective effects and constitutes a potential strategy of treatment of neurodegenerative diseases involving tau pathology.

In AD, tau is hyperphosphorylated (it contains 9–10 moles of phosphate per mol of tau while normal tau contains 2–3 moles of phosphate) (19, 20), undergoes conformational changes (21) and is converted into toxic oligomers and fibrillar aggregates, the straight (SFs) and paired helical filaments (PHFs) (22, 23). Abnormal hyperphosphorylation could be responsible for the conformational changes, oligomerization, fibrillization, and spreading of tau pathology through the brain in specific areas along the course of AD progression (24, 25). Dysregulation of kinase and phosphatase balance is involved in the abnormal phosphorylation of tau but other factors modulate tau phosphorylation. Among them, *O*-GlcNAc has been described in the regulation of tau phosphorylation and reciprocally. *O*-GlcNAc modification is dynamically regulated by only two enzymes, *O*-GlcNAc transferase (OGT) and *O*-GlcNAc hydrolase (OGA), involved in the addition and removal of the GlcNAc moiety, respectively (1, 26–28). Iqbal et al. found that *O*-GlcNAc negatively regulates tau phosphorylation in a site-specific manner in cultured cells, *in vivo* and in metabolically active brain slices (11, 18). In particular, in a mouse model of starvation that mimics impaired glucose metabolism in AD brain, a reduction of tau *O*-GlcNAcylation together with an elevation of tau phosphorylation at specific sites were observed (18). Conversely, inducing hyperphosphorylation of tau with the phosphatase inhibitor okadaic acid leads to a reduction of tau *O*-GlcNAcylation in human neuroblastoma cells together with a reduced transfer into the nucleus (29). Interestingly, hyperphosphorylated tau is less *O*-GlcNAcylated than forms of tau that are less phosphorylated (11, 29). Furthermore, deletion of the *ogt* gene in mice in a neuron-specific manner promotes both an increase of tau amounts and tau hyperphosphorylation, two features that are associated with tau pathology in AD (30). In contrast, stimulating tau *O*-GlcNAcylation by OGT overexpression decreases tau phosphorylation at specific sites (12). Chronic treatment of hemizygous JNPL3 mice carrying the gene for human tau-P301L mutant with Thiamet-G, an OGA inhibitor, leads to a significant reduction of NFTs without altering global tau phosphorylation levels at AD-relevant sites (AT8 and pS422) while *O*-GlcNAc levels were increased significantly, only AT8 immunoreactivity of tangles was reduced (31). The same observation has been made in rTg4510 mice expressing the human tau-P301L protein for which chronic Thiamet-G administration leads to increased tau *O*-GlcNAcylation associated with a decrease of pathological tau aggregates without affecting phosphorylation of non-pathological tau species (32). Hence, OGA inhibition reduces neurofibrillary tangles and neurodegeneration without interfering with tau hyperphosphorylation. Another study has shown that chronic Thiamet-G treatment of tau.P301L transgenic mice although increasing protein *O*-GlcNAcylation has no effect on tau *O*-GlcNAcylation and phosphorylation while improvements of survival and motor deficits have been observed (33). These data suggest that the beneficial effects obtained by elevating *O*-GlcNAc levels may result from enhanced *O*-GlcNAcylation of target proteins other than tau. Furthermore, it was shown that the *O*-GlcNAc modification can directly act on tau aggregation properties by intrinsically decreasing *in vitro* aggregation of recombinant tau induced by heparin without altering its conformation (31, 34).

Recently, however, *O*-GlcNAcylation of endogenous tau has been investigated in mouse models by mass spectrometry identifying a single *O*-GlcNAc modification (at S400) at a low stoichiometry (35) putting into questions the role and mechanism of the *O*-GlcNAc-mediated regulation of tau phosphorylation and pathological aggregation. As *O*-GlcNAcylation could interfere with tau pathology and neurodegeneration, and could be pharmacologically

Abbreviations: Da, Dalton; gS, *O*-GlcNAc serine; HSQC, heteronuclear single quantum correlation; IPTG, isopropyl-β-D-1-thiogalactopyranoside; MALDI-TOF MS, Matrix-Assisted Laser Desorption-Ionization Time-Of-Flight mass spectrometry; M.W., molecular weight; *O*-GlcNAc, *O*-β-linked N-acetylglucosamine; pS, phospho-serine; PTM, posttranslational modification; PUGNAc, *O*-(2-Acetamido-2-deoxy-D-glucopyranosylidene)amino-*N*-phenylcarbamate; RBE, rat brain extract; RP-HPLC, reverse phase high performance liquid chromatography; SDS-PAGE, sodium dodecyl sulfate polyacrylamide gel electrophoresis; TAMRA, tetramethylrhodamine; TFA, trifluoroacetic acid; THP, Tris(hydroxypropyl)phosphine.

targeted to prevent the pathological formation of toxic tau species (31, 36, 37), a detailed examination of *O*-GlcNAcylation-phosphorylation crosstalk of tau protein is required to fully understand the functional role of tau *O*-GlcNAcylation. NMR proved to be a powerful method to investigate PTMs in intrinsically disordered proteins and disordered regions of globular proteins where posttranslational modifications frequently occur (38–40). Based on this strategy, phosphorylation of tau protein was extensively investigated providing phosphorylation patterns of various kinases in a site-specific manner (41–46). *O*-GlcNAc modification of tau was explored in peptides to identify new O-GlcNAc sites (47) and in a fragment of the C-terminal region containing the S400-*O*-GlcNAc modification to probe potential conformational changes (34). Native chemical ligation afforded a site-specific and quantitative S400-*O*-GlcNAc tau using the expressed protein ligation strategy as a useful tool to decipher the molecular role of *O*-GlcNAcylation in tau functions (48, 49). For the first time, we investigate here the *O*-GlcNAc modification in the entire tau protein obtained by enzymatic activity of OGT and its direct crosstalk with phosphorylation by NMR spectroscopy. We found that tau is not extensively *O*-GlcNAcylated since we detected after *O*-GlcNAc enrichment three major *O*-GlcNAc sites in the C-terminal domain and two *O*-GlcNAc sites of lower level in the proline-rich region. We showed that *O*-GlcNAcylation does not modify phosphorylation of tau by the kinase activity of recombinant ERK2 or rat brain extract while phosphorylation leads to a slight increase of tau *O*-GlcNAcylation by OGT. Our findings contrast with previous models in which phosphorylation and *O*-GlcNAcylation of tau were shown to directly compete *in vivo* in a reciprocal manner, supporting the idea of a more intricate relationship between both PTMs than a direct crosstalk.

MATERIALS AND METHODS

Expression and Purification of Tau Protein

BL21 (DE3) *E. coli* strains were transformed with the pET5b plasmid (Novagen, Merck) carrying the longest isoform of *tau* (2N4R isoform) with the S262A mutation for recombinant production. 20 ml of a LB preculture grown at 37°C for 6–8 h were diluted in 2 l of M9 minimal medium. For uniform $^{15}N/^{13}C$-labeling, cells were grown at 37°C in M9 minimal medium containing 2 g/L $^{13}C_6$-glucose, 1 g/L ^{15}N-ammonium chloride, 0.5 g/L $^{15}N/^{13}C$-Isogro® (Sigma), 1 mM $MgSO_4$, MEM vitamin cocktail (Sigma) and 100 mg/L ampicillin. The induction phase was performed by addition of 0.5 mM isopropyl β-D-1-thiogalactopyranoside for 3 h at 37°C. For uniform ^{15}N-labeling, the same growth medium was used except that it contained 4 g/L glucose and 0.5 g/L ^{15}N-Isogro®. Cells were harvested by centrifugation at 5,000 × g for 30 min and the pellet was resuspended in 50 mM NaH_2PO_4/Na_2HPO_4, pH 6.2, 2.5 mM EDTA, 2 mM DTT and 0.5% Triton X-100 supplemented with a Complete™ protease-inhibitor cocktail. The lysate was obtained by homogenizing this suspension using a high-pressure homogenizer followed by centrifugation at 30,000 × g for 30 min at 4°C. The extract was incubated at 75°C for 15 min and centrifuged at 4,000 × g for 20 min at 4°C as a first purification step. The tau protein was then purified by cation-exchange chromatography (HiTrap SP HP 5 ml, GE Healthcare) in 50 mM NaH_2PO_4/Na_2HPO_4, pH 6.4, 2 mM EDTA (buffer A). After loading the extract onto the column and column washing with buffer A, the protein was eluted with a gradient from 0 to 50% buffer B (buffer A supplemented with 2M NaCl) over 20 ml (i.e. 4 column volumes). Fractions were analyzed by SDS-PAGE and fractions containing tau protein with highest purity were pooled together for a next step of purification by RP-HPLC on a Zorbax 300SB-C8 semi-preparative 9.4 × 250 mm column (Agilent) equilibrated in a solution of 0.1% TFA:2% acetonitrile. Proteins were eluted by a 30-min linear gradient from 16% to 40% acetonitrile at 5 ml/min. Fractions containing full-length tau protein are pooled, lyophilized, and buffer-exchanged in 50 mM ammonium bicarbonate (HiPrep 26/10 desalting, GE Healthcare) to avoid acidification of solutions due to residual TFA, and lyophilized again before storage at −20°C until further use (50). Using this procedure, the yield of tau protein was 10 mg per liter of culture.

Expression and Purification of the Nucleocytoplasmic Form of OGT

BL21 (DE3) *E. coli* strains were transformed with the pET24d plasmid (Novagen, Merck) carrying the nucleocytoplasmic isoform of human *ogt* for the recombinant production of ncOGT (51). Freshly plated bacteria were picked up to inoculate a 20 ml culture which was grown at 37°C overnight. The 20 ml culture then inoculated a 2 l culture in LB rich medium that was grown at 37°C for 3 h until O.D. at 600 nm reached 0.6, then the culture was cooled down to 16°C. The protein induction was performed at 16°C for 24 h upon addition of 0.2 mM IPTG. Cells were harvested at 6,000× g for 30 min at 4°C and the pellet was resuspended in 100 ml extraction buffer (50 mM KH_2PO_4/K_2HPO_4 pH 7.60, 250 mM NaCl, 40 mM imidazole, 5% glycerol, 1% Triton X-100 complemented with a 0.3 mg DNase I and EDTA-free protease inhibitor cocktail). Cell lysis was performed with a high-pressure homogenizer at 4°C followed by a brief sonication step. Soluble proteins were isolated from the bacterial extract by centrifugation at 30,000 × g for 30 min at 4°C. An affinity purification step was performed on a 1 ml-HiTrap Chelating column (GE Healthcare) loaded with Ni^{2+} ions. The full-length OGT was eluted with 250 mM imidazole after a truncated form was eluted with 110 mM imidazole. Homogenous fractions containing the full-length recombinant ncOGT as checked on a 10% polyacrylamide-SDS gel were pooled (in a final volume 10 ml) and dialysed at 4°C overnight in 2 l of sample buffer (50 mM KH_2PO_4/K_2HPO_4 pH 7.60, 150 mM NaCl, 1 mM EDTA). After dialysis, the sample was supplemented with 0.5 mM THP and stored at −80°C. Starting from a 2 l-culture, we obtained 5 mg of ncOGT. The *O*-GlcNAc-transferase activity of the recombinant ncOGT was checked on a peptide substrate from casein kinase II (CKII) indicating that the recombinant ncOGT is fully active as it provides an *O*-GlcNAcylated CKII peptide with 95% *O*-GlcNAcylation after 30 min incubation at 37°C (52, 53).

In vitro O-GlcNAc Transferase Reaction of Tau by Recombinant ncOGT

10 mg of $^{15}N/^{13}C$-labeled tau protein (M.W. 48,070 kDa) were solubilized at 0.83 mM in a solution of ncOGT at 10 µM in a final volume of 250 µl of reaction buffer (50 mM KH_2PO_4/K_2HPO_4 pH 7.6, 150 mM NaCl, 1 mM EDTA, 0.5 mM THP, 12.5 mM $MgCl_2$, 10 mM UDP-GlcNAc). As a negative control, a reaction was carried out in the same conditions without UDP-GlcNAc. The *O*-GlcNAcylation reactions were performed at 31°C for 3 days. *O*-GlcNAcylation of tau was checked after incubation periods of 6 and 24 h but higher *O*-GlcNAcylation levels were obtained for longer timescale. After 3 days, the reaction mixtures were heated at 75°C, centrifuged and purified by RP-HPLC on a Zorbax 300SB-C8 semi-preparative column (9.4 × 250 mm, Agilent) equilibrated in buffer A (0.1% TFA: 2% acetonitrile). Proteins were eluted with a linear gradient from 25 to 50% of buffer B (0.1% TFA: 80% acetonitrile) of 25 min. Fractions enriched in *O*-GlcNAc were identified by MALDI-TOF MS and Click-iT^{TM} *O*-GlcNAc labeling and TAMRA detection kits (Molecular Probes) on SDS-PAGE following the manufacturer's instructions (**Figure S1**). Fractions containing protein with low levels of *O*-GlcNAcylation were pooled, lyophilized, desalted in 50 mM ammonium bicarbonate (HiTrap Desalting 5 ml, GE Healthcare) prior to another round of *O*-GlcNAcylation and purification. At the end, the *O*-GlcNAc-enriched fractions corresponding to the two rounds of *O*-GlcNAcylation/purification were lyophilized. This procedure affords about 3-3.5 mg of *O*-GlcNAc enriched tau (hereafter referred to as tau-*O*-GlcNAc) from 10 mg of tau. For an estimation of site-specific *O*-GlcNAc modification by NMR spectroscopy, this procedure was performed twice with two distinct batches of ncOGT.

^{15}N-tau phosphorylated by ERK2, $^{15}N/^{13}C$-tau phosphorylated by a rat brain extract or ^{15}N-tau as a control were subjected to *O*-GlcNAcylation reactions at 0.4 mM in a solution of ncOGT at 10 µM in OGT reaction buffer (50 mM KH_2PO_4/K_2HPO_4 pH 7.6, 150 mM NaCl, 1 mM EDTA, 0.5 mM THP, 12.5 mM $MgCl_2$, 10 mM UDP-GlcNAc) at 31°C for 2 days. As a negative control, reactions were carried out in the same conditions without UDP-GlcNAc. To stop the *O*-GlcNAc reactions, the reaction mixtures were heated at 75°C and centrifuged at 16,000 × g for 15 min at 4°C. Then, the proteins were purified by reverse phase chromatography on a Zorbax 300SB-C8 semi-preparative column (9.4 × 250 mm, Agilent) for NMR analyses. Unlike non-phosphorylated tau, no *O*-GlcNAc enrichment was observed along the elution step of reverse phase chromatography for phosphorylated tau proteins as detected by MALDI-TOF MS. *O*-GlcNAcylation levels of phosphorylated vs. non-phosphorylated tau were quantitatively assessed using the Click-iT^{TM} *O*-GlcNAc labeling and TAMRA detection kits following the manufacturer's instructions. 20 and 5 µg of proteins dissolved at ≈ 2 µg/µl in Laemmli sample buffer 3X were loaded on SDS-PAGE for TAMRA detection and Coomassie staining, respectively. Quantification of TAMRA fluorescence was performed with ImageQuant^{TM} LAS 4000 (GE Healthcare).

For the preparation of NMR samples as well as for the phosphorylation assays, the amount of various protein samples in their *O*-GlcNAcylated and non *O*-GlcNAcylated forms was calculated based on the peak integration at 280 nm assuming that the molar extinction coefficient is the same between *O*-GlcNAc and non *O*-GlcNAc proteins.

MALDI-TOF MS Analyses of Tau Proteins

MALDI-TOF mass spectrometry analyses were performed with sinapinic acid matrix on an Axima Assurance mass spectrometer (Shimadzu) in a linear positive ion mode.

Expression and Purification of ERK2 and MEK3 Kinases and Phosphorylation of Tau

Recombinant mitogen-activated protein kinase ERK2 and a constitutively active mutant of mitogen-activated protein kinase kinase MEK3 (hereafter referred to as MEK3), that phosphorylates and activates ERK2, were produced as described previously (41, 46, 50). Briefly, ERK2 carrying a polyhistidine tag and MEK3 carrying a GST tag were purified by affinity chromatography from 1 l culture in LB after an induction phase at 30°C for 4 h with 0.5 mM IPTG. ERK2 was purified on a 1-ml HisTrap HP column (GE Healthcare) equilibrated in 50 mM NaH_2PO_4/Na_2HPO_4, pH 7.5, 300 mM NaCl, 20 mM imidazole (buffer A) and eluted with a buffer containing 50 mM NaH_2PO_4/Na_2HPO_4, pH 7.5, 300 mM NaCl, 250 mM imidazole (buffer B). MEK3 was purified on glutathione sepharose beads (2 ml) equilibrated in 50 mM Tris.Cl pH 7.5, 300 mM NaCl, 1 mM EDTA (buffer C). After loading of the bacterial extract at 4°C for 3 h and washing beads 5 times with 10 ml of buffer C then 3 times with 10 ml of phosphorylation buffer (50 mM Hepes. KOH, pH 7.8, 12.5 mM $MgCl_2$, 50 mM NaCl, 1 mM EGTA), GST-MEK3 was left on resin beads for phosphorylation reactions.

For the phosphorylation reactions, fractions containing ERK2 eluted from the affinity chromatography step was buffer-exchanged in phosphorylation buffer on a 5 ml Zeba^{TM} Spin desalting column (Thermo Fischer) and mixed with GST-MEK3 beads.

ERK2 activation and tau phosphorylation were performed simultaneously. $^{15}N/^{13}C$-tau-*O*-GlcNAc (3 mg) that was previously *O*-GlcNAcylated by OGT and ^{15}N-tau (10 mg) as a control were dissolved at 100 µM with ERK2 and MEK3 in phosphorylation buffer complemented with 6.25 mM ATP and 1 mM DTT and incubated at 37°C for 5 h. Phosphorylation reactions were stopped by centrifugation of the reaction mixtures at 4,000 × g for 10 min to precipitate the resin beads and incubating the supernatant at 75°C for 15 min followed by centrifugation at 4,000 × g for 15 min. Then, the supernatants were buffer-exchanged in 50 mM ammonium bicarbonate on a 5 ml HiTrap Desalting column (GE Healthcare) and lyophilized. Prior to NMR analyses, phosphorylation was qualitatively checked by a shift in the apparent mobility of the protein band on SDS-PAGE and by MALDI-TOF MS (41, 46). Phosphorylation of tau with activated ERK2 was performed twice with two different batches of ERK2 and MEK3. An average phosphorylation level of 17 ± 2 phosphate per tau molecule was determined by mass spectrometry on intact proteins.

Phosphorylation of Tau by a Rat Brain Extract

A rat brain extract was prepared from adult Sprague-Dawley rats by homogenizing whole brains (∼2 g) in 5 mL of homogenizing buffer, containing 10 mM Tris-HCl, pH 7.4, 5 mM EGTA, 2 mM DTT, 1 μM okadaic acid (OA), 20 μg/mL Leupeptin, and 40 mM Pefabloc®. Insoluble material was precipitated by ultracentrifugation at 100,000 × g and 4°C for 1 h. The supernatant was directly used for its kinase activity. Total protein concentration was estimated at 9 mg/mL by a BCA colorimetric assay. $^{15}N/^{13}C$-tau and $^{15}N/^{13}C$-tau-*O*-GlcNAc were dissolved at 10 μM in 4.5 mL of phosphorylation buffer containing 40 mM Hepes.KOH, pH 7.3, 2 mM $MgCl_2$, 5 mM EGTA, 2 mM DTT, 2 mM ATP, 1 μM OA and supplemented with a Complete™ protease-inhibitor cocktail. PUGNAc (Sigma), an inhibitor of β-hexosaminidases and *O*-GlcNAc hydrolase, was added at 10 μM in the phosphorylation reaction of tau-*O*-GlcNAc to prevent deglycosylation. The proteins were incubated with 500 μL of rat brain extract at 37°C for 24 h. Then, reactions were stopped by heating the mixture at 75°C for 15 min followed by centrifugation at 16,000 × g for 20 min. The supernatants were buffer-exchanged in 50 mM ammonium bicarbonate and the proteins were lyophilized. Evaluation of protein phosphorylation was performed by SDS-PAGE and MALDI-TOF MS, and then the phosphorylation sites were determined by NMR analyses.

NMR Spectroscopy

NMR experiments were performed at 293K on Bruker 900 MHz Avance NEO and 600 MHz Avance III HD spectrometers (Bruker, Karlsruhe, Germany) equipped with a 5-mm TCI and QCI cryogenic probes, respectively. For NMR experiments, tau protein samples were dissolved at a concentration of 200–400 μM in a buffer containing 50 mM NaH_2PO_4/Na_2HPO_4 pH 6.5, 25 mM NaCl, 2.5 mM EDTA, 1 mM DTT, 10% D_2O either in a volume of 200 μl (in 3 mm tubes) or in 300 μl (in Shigemi tubes). ^1H spectra were calibrated with 0.25 mM of sodium 3-(trimethylsilyl) propionate-2,2',3,3'-d_4 as internal standard. ^1H spectra were acquired with 64 scans and 32 dummy scans, and a spectral windows of 14 ppm centered on 4.7 ppm sampled with 32k points. For 2D and 3D experiments, a spectral window of 14 ppm centered on 4.7 ppm was used for the proton dimension.

^1H-^{15}N HSQC spectra were recorded with 64 scans per increment and 16 dummy scans with 3072 and 512 points in the proton and nitrogen dimensions, respectively, and with a window of 25 ppm centered on 118 ppm for the nitrogen dimension. Heteronuclear experiments were recorded with a WATERGATE sequence for water suppression and a double INEPT (INsensitive nuclei Enhanced by Polarization Transfer) for sensitivity improvement. All experiments were acquired with a recycle delay of 1s.

Assignment of modified (phosphorylated or *O*-GlcNAcylated) tau proteins required the acquisition of three-dimensional NMR experiments on $^{15}N/^{13}C$-labeled tau samples at 293K. The HNCACB and HN(CO)CACB experiments were recorded with 32 scans per increment and 16 dummy scans, with 2048, 90, and 120 points in the proton, nitrogen and carbon dimensions, respectively, and with a window of 25 and 60 ppm centered on 118 ppm and 44 ppm for the nitrogen and carbon dimensions, respectively. The HN(CA)NNH experiment was recorded with 24 scans per increment and 16 dummy scans, with 2048, 120, and 180 points in the proton and both nitrogen dimensions, respectively, and with a window of 25 ppm centered on 118 ppm for the nitrogen dimensions.

O-GlcNAc and phosphorylation levels were determined for individual Ser/Thr residues based on intensity of their respective N-H correlations of their modified and non-modified forms from the ^1H-^{15}N HSQC experiment.

RESULTS

Identification of Tau *O*-GlcNAc Sites by NMR Spectroscopy

We first addressed the identification of *O*-GlcNAc sites in full-length tau provided by the enzymatic activity of ncOGT *in vitro* using NMR spectroscopy. The enzymatic *O*-GlcNAcylation of uniformly $^{15}N/^{13}C$-labeled tau protein was performed as described for peptide substrates previously (47, 54). After *O*-GlcNAc enrichment of tau protein by reverse phase chromatography, the MALDI-TOF MS analysis of the tau-*O*-GlcNAc sample indicated an addition of 1.9 GlcNAc per tau molecule taking into account a m/z increment of +203 per GlcNAc.

In the ^1H-^{15}N HSQC experiment, additional signals were observed as compared to non-modified tau spectrum as a control indicating either *O*-GlcNAc sites or residues located in their neighborhood (**Figure S2**). The NMR-based detection of *O*-GlcNAc sites within tau protein further made use of the chemical shift changes of $^{13}C\alpha$ and $^{13}C\beta$ values upon Ser/Thr *O*-GlcNAcylation (38, 47, 54). Acquisition of three-dimensional HNCACB and HNcoCACB experiments afforded ^{13}C chemical shifts of each residue (i) and its preceding residue (i-1) in the protein sequence allowing amino acid identification in the context of an intrinsically disordered protein such as tau. By selecting $^{13}C\alpha$ and $^{13}C\beta$ values of 56.5 ppm and 70.6 ppm, respectively, ^1H-^{15}N planes were extracted from HNCACB corresponding to ^1H-^{15}N HSQC sub-spectra of *O*-GlcNAc Ser residues (**Figure 1**) (54). The same processing of HNcoCACB afforded (i+1) residues of *O*-GlcNAc serines (**Figure 1**). The HNcaNNH experiment that provides ^{15}N values of (i-1) and (i+1) residues confirmed the identification of *O*-GlcNAc sites.

With this strategy, three *O*-GlcNAc Ser residues were identified in the C-terminal region of tau at position S400, S412, and S413 (**Table S1**). No threonine residues were detected with the same strategy taking into account ^{13}C chemical shifts changes of Thr residues upon *O*-GlcNAcylation. Resonance intensities in the two-dimension ^1H-^{15}N HSQC experiment corresponding to *O*-GlcNAc and non-modified forms gave the *O*-GlcNAcylation level for each *O*-GlcNAc site providing a quantitative *O*-GlcNAc pattern of tau protein with a relative distribution of the mono-*O*-GlcNAc species of 63 ± 7% for S400, 27 ± 2% for S412

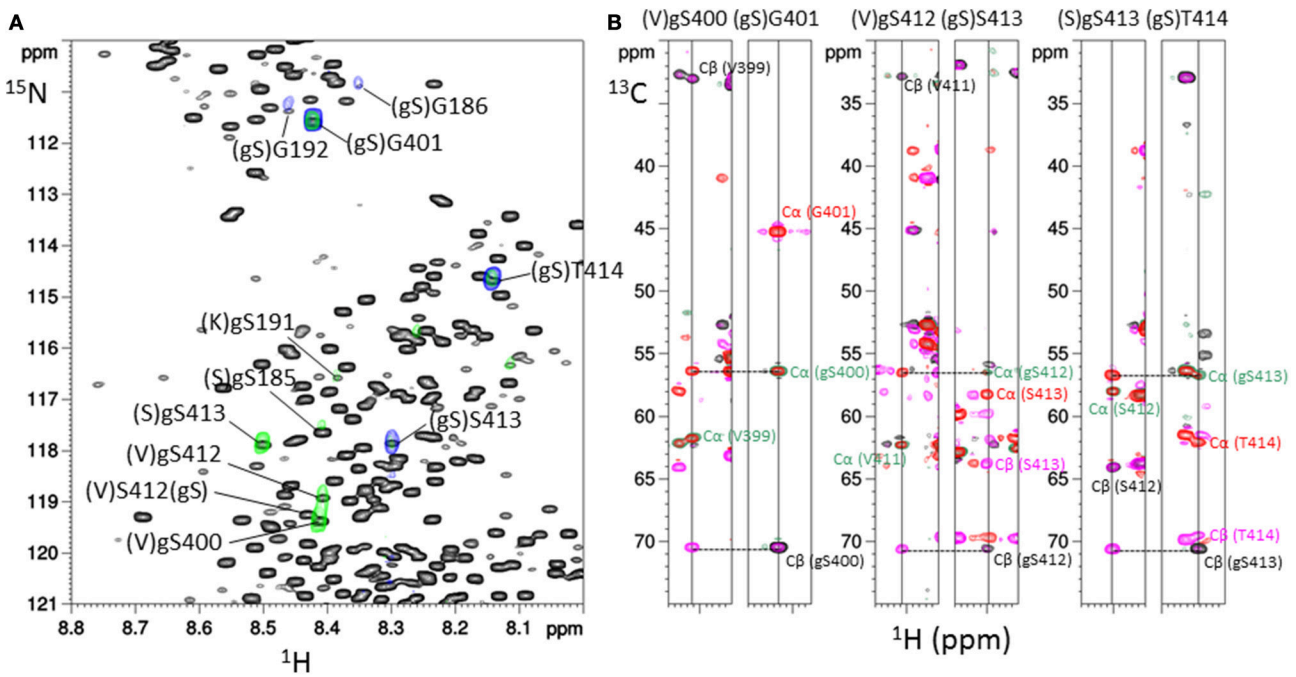

FIGURE 1 | Assignment strategy of *O*-GlcNAc sites in full-length tau protein. **(A)** Superimposition of ^{1}H-^{15}N HSQC spectrum of tau-*O*-GlcNAc (black) and ^{1}H-^{15}N planes extracted from HNCACB (green) and HNcoCACB (blue) three-dimensional experiments at a ^{13}C value of 70.6 ppm corresponding to the Cβ resonance of *O*-GlcNAc serine, highlighting the resonances of the *O*-GlcNAc sites (i residues) and their (i+1) residues, respectively. **(B)** ^{1}H-^{13}C planes from HNCACB (red and pink for the Cα and Cβ resonances, respectively) and HNcoCACB (green and black for the Cα and Cβ resonances, respectively) extracted at ^{15}N values corresponding to resonances of residues indicated above and shown in the ^{1}H-^{15}N HSQC experiment in **(A)**.

and 47 ± 9% for S413 (**Figure 2**). Given the relative abundance of both gS412 and gS413 at vicinal positions, a di-*O*-GlcNAc specie would have a theoretical relative abundance of 13% and should be detected. However, we found neither (gS)gS413 nor another (V)gS412 resonance indicating the presence of a di-*O*-GlcNAc form. This suggests that both *O*-GlcNAc modifications are mutually exclusive. Additionally, two (gS)G motifs were detected in the ^{1}H-^{15}N plane extracted from the HNcoCACB experiment at the ^{13}Cβ chemical shift of Ser-*O*-GlcNAc pointing to two *O*-GlcNAc sites, S185 and S191, in the proline-rich domain that were also detected in the HNCACB experiment (**Table S1**). S191 *O*-GlcNAc level was estimated to 11 ± 1% while the level of S185 *O*-GlcNAc could not be determined based on signals of S185 due to signal overlap of both the *O*-GlcNAc and non-modified forms, but seems to be of the same order of magnitude than S191-*O*-GlcNAc based on the resonances of G186 in the *O*-GlcNAc and non-glycosylated forms. Other resonances were detected in the HSQC indicating the presence of additional *O*-GlcNAc sites but they were not unambiguously assigned due to their low intensity (**Figure 1**) suggesting that they were *O*-GlcNAcylated at a level inferior to 5%.

Phosphorylation Improves Direct Tau *O*-GlcNAcylation by OGT

As both C-terminal and proline-rich domains where *O*-GlcNAc sites were found are enriched in proline-directed Ser/Thr phosphorylation sites, *O*-GlcNAcylation of phosphorylated tau was also evaluated in a similar manner as the non-modified form although *O*-GlcNAc-enrichment of the phosphorylated tau failed, probably due to PTM heterogeneity of the sample. We first address the effect of a phosphorylation pattern obtained by kinase activity of a rat brain extract complemented by ATP in which phosphatase activity was blocked by okadaic acid (41, 55, 56). The kinase activity was moderate (≈4.5 ± 1 mol of phosphate per mol of tau protein) as determined by mass spectrometry (see **Figure 4A**) as compared to patterns previously described. Phosphorylated tau was *O*-GlcNAcylated by OGT as well as non-phosphorylated tau as a control and overall *O*-GlcNAc levels were determined by mass spectrometry (**Figure S3**) and selective enzymatic labeling of tau-*O*-GlcNAc by azide-modified GalNAc and copper-mediated click chemistry with an alkyne derivative of TAMRA for detection of modified tau protein. The *O*-GlcNAc transferase reaction of phosphorylated tau with recombinant OGT resulted in a slightly higher level of *O*-GlcNAcylation than unmodified tau (**Figures 3A,B,E**).

We next investigated the effect of a higher level of phosphorylation on the *O*-GlcNAc transferase activity of OGT. Hyperphosphorylation was obtained with kinase activity of recombinant ERK2 with an overall level of 19 ± 1 phosphate per tau molecule (**Figure S4A**). The phosphorylation pattern determined by NMR spectroscopy was similar to those previously described including all proline-directed Ser/Thr in tau sequence (41, 55). A quantitative phosphorylation was obtained for

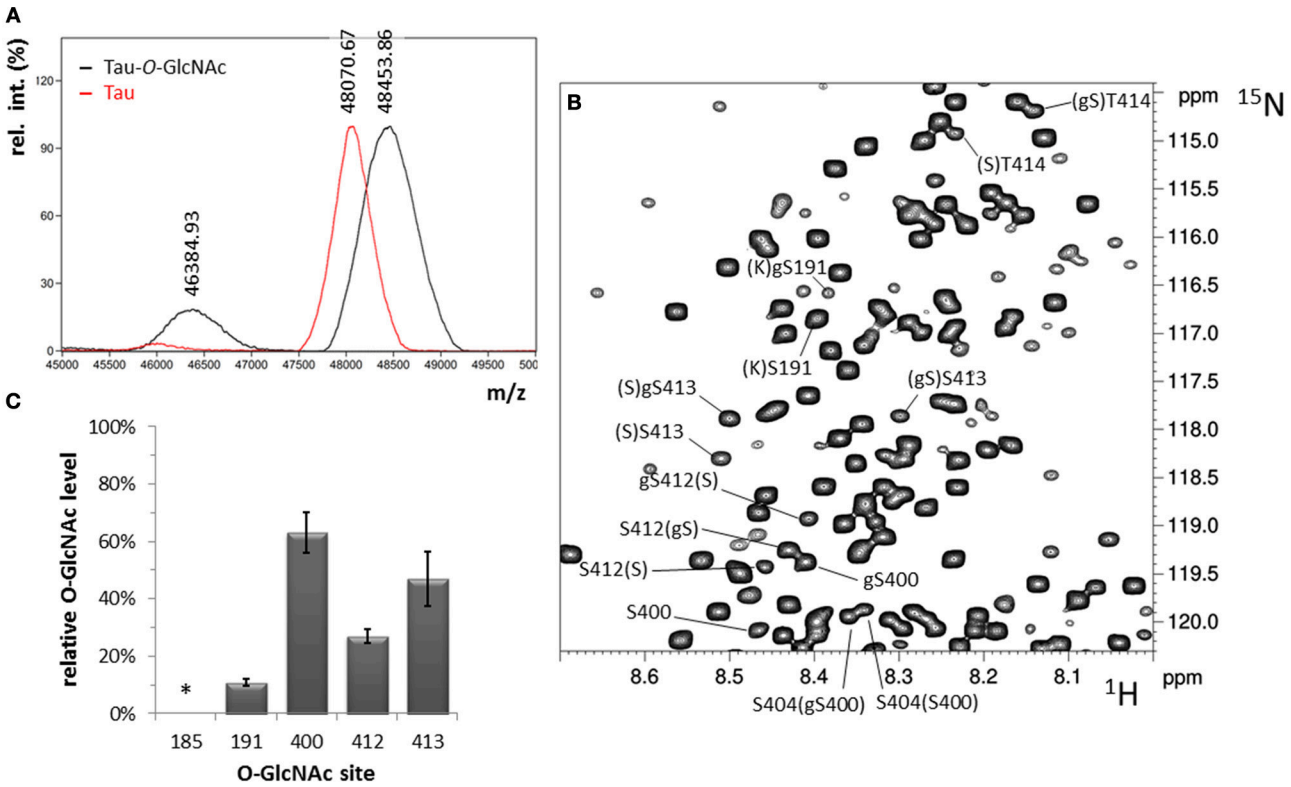

FIGURE 2 | *O*-GlcNAcylation of tau. **(A)** Overall *O*-GlcNAcylation level determined by MALDI-TOF MS. **(B)** ^{1}H-^{15}N HSQC spectrum of tau-*O*-GlcNAc with assignment of *O*-GlcNAc sites. **(C)** Site-specific *O*-GlcNAc levels determined by NMR spectroscopy. The *O*-GlcNAc level indicated by an asterisk cannot be calculated due to signal overlap.

most sites (**Figure S4B**). In particular, S396, S404, and S422 in the C-terminal domain were phosphorylated at high levels of 94, 97, and 85%, respectively, and S191 in the proline-rich domain at 68%. In this hyperphosphorylated tau sample, the *O*-GlcNAc transferase activity of OGT was 1.4-fold higher than in unphosphorylated tau (**Figures 3C-E**) which is a higher activity than those measured with the phosphorylation pattern of the rat brain extract for which phosphorylation level was lower. At the residue level, only a splitting of pS404 resonance was observed among the resonances of phospho-residues in the ^{1}H-^{15}N HSQC spectrum upon *O*-GlcNAcylation on top of tau phosphorylation by ERK2 indicating that pS404 amide resonance is perturbed by proximal *O*-GlcNAcylation, likely S400 *O*-GlcNAcylation. This effect on pS404 in contrast to pS396 resonance revealed a specific interaction with S400 *O*-GlcNAcylation which could be due to local conformational changes induced either by *O*-GlcNAcylation, phosphorylation or both of them. Except resonances corresponding to *O*-GlcNAc sites previously identified in tau, no additional resonance was detected in the spectrum pointing to new *O*-GlcNAc sites. Together our data indicate that phosphorylation leads to an overall moderate improvement of OGT activity on tau protein without additional *O*-GlcNAc sites that can be detected by NMR.

Regulation of Tau Phosphorylation by *O*-GlcNAcylation

We first determined the effect of *O*-GlcNAcylation on kinase activity of a rat brain extract complemented by okadaic acid to inhibit phosphatase activities (41, 55, 56). Additionally, PUGNAc, a β-hexosaminidase and *O*-GlcNAcase inhibitor (57), was added to prevent *O*-GlcNAc hydrolysis during incubation of tau-*O*-GlcNAc protein with the extract. The kinase activity barely increased in tau-*O*-GlcNAc compared to unmodified tau as detected by mass spectrometry with ≈6 ± 0.5 mol of phosphate per mol of tau protein which is slightly higher than the overall level of phosphorylation obtained with non-modified tau (**Figure 4A**). Furthermore, phosphorylation patterns of tau and tau-*O*-GlcNAc were examined using high resolution NMR spectroscopy to evaluate direct modulation of site-specific phosphorylation by *O*-GlcNAcylation (**Figure 4B** and **Figure S5**). We found no major change in the phosphorylation pattern of tau except for S404 and S202. S404 phosphorylation was slightly decreased in tau-*O*-GlcNAc likely due to its proximity with the S400-*O*-GlcNAc site of highest occupancy. As described previously, the resonances of pS404 and S404 were splitted in tau-*O*-GlcNAc/p-RBE ^{1}H-^{15}N HSQC spectrum due to incomplete S400 *O*-GlcNAcylation which induces a modification of the chemical environment of S404 residue

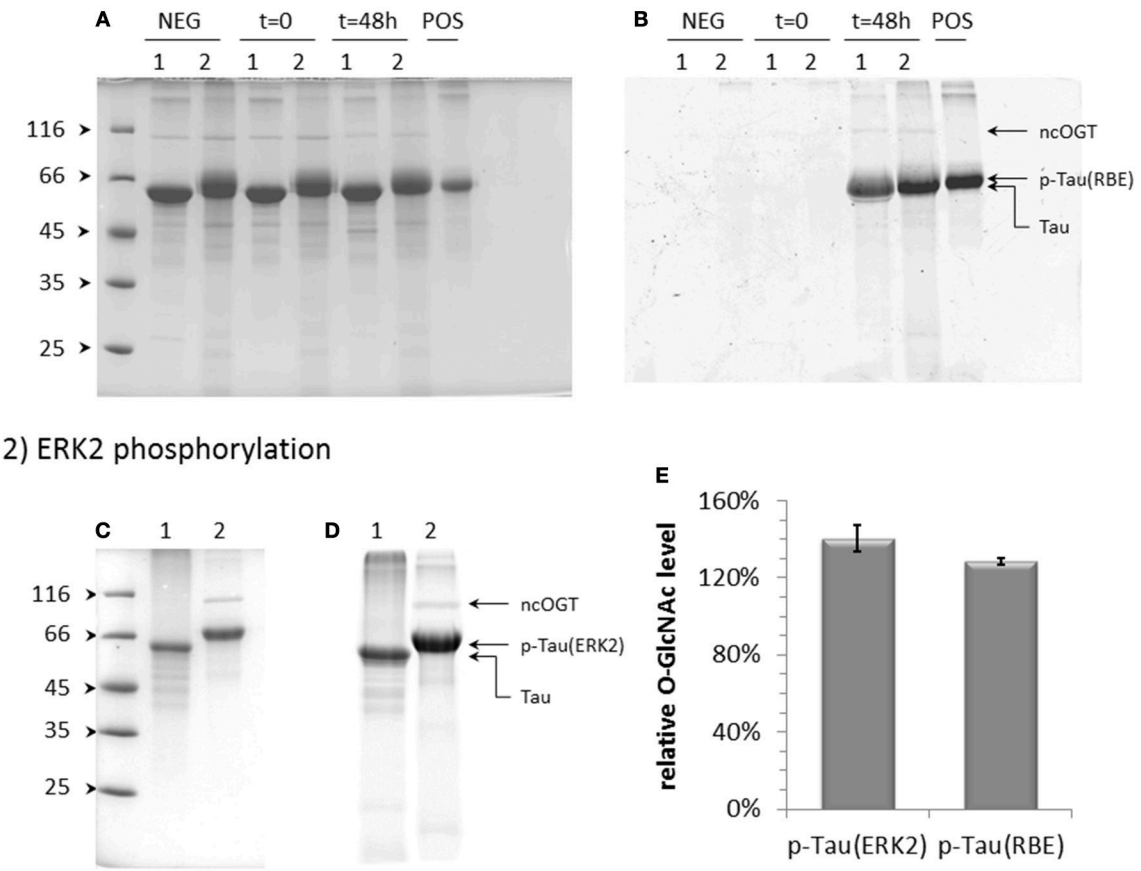

FIGURE 3 | Effect of phosphorylation on tau *O*-GlcNAcylation by OGT. Effect of phosphorylation by kinase activity of a rat brain extract (RBE) **(A,B)** or activated ERK2 **(C,D)** on tau *O*-GlcNAcylation detected by TAMRA fluorescence in polyacrylamide gel **(B,D)** after *O*-GlcNAc labeling. Protein loading on SDS-PAGE was checked by Coomassie staining **(A,C)**. Lanes 1 correspond to unmodified tau and lanes 2 to phosphorylated tau incubated for 48 h at 31°C with OGT and 10 mM UDP-GlcNAc; $t = 0$ is given for starting reaction of RBE phosphorylated tau as a control of protein degradation during the *O*-GlcNAc transferase reaction; NEG indicates *O*-GlcNAc transferase reaction performed in absence of UDP-GlcNAc as a negative control; POS corresponds to tau-*O*-GlcNAc sample as a positive control of *O*-GlcNAc labeling and TAMRA-alkyne click reactions. **(E)** Quantification of *O*-GlcNAc relative levels of tau proteins phosphorylated either by ERK2, p-Tau(ERK2), or by RBE, p-Tau(RBE), normalized on the signal of non-phosphorylated tau.

in both its phosphorylated and non-phosphorylated forms. S404 phosphorylation of 53% in tau-*O*-GlcNAc/p-RBE was distributed into 46 and 65% in the *O*-GlcNAcylated and non-*O*-GlcNAcylated forms, respectively, indicating a preference for S404 phosphorylation in the S400 non-glycosylated form (**Figures 4C,D**). In contrast, phosphorylation of S202 was increased upon prior *O*-GlcNAcylation. However, S202 phosphorylation level was probably underestimated in p-tau(RBE) due to overlap of S202 and S422 resonances in their non-phosphorylated states while both resonances were resolved in tau-*O*-GlcNAc/p-RBE making phosphorylation changes of S202 and S422 less reliable.

Similarly, the impact of tau *O*-GlcNAcylation on ERK2 phosphorylation which provides hyperphosphorylated tau was studied. No change of phosphorylation level was detected by mass spectrometry upon prior *O*-GlcNAcylation as compared to unmodified tau (**Figure 5A** and **Figure S4**). At the site-specific level, almost all phosphorylation sites were quantitatively phosphorylated (**Figure S4**) whether in tau or tau-*O*-GlcNAc sample. In particular, a quantitative phosphorylation of S404 was reached since no resonance of non-phosphorylated S404 can be detected with S400 being *O*-GlcNAcylated or not (**Figure 5B** and **Figure S6**). Furthermore, there is a direct competition for S191 site occupancy which is *O*-GlcNAcylated at 11% in tau-*O*-GlcNAc and phosphorylated at 68% in p-tau(ERK2). Only S400-*O*-GlcNAc resonance was affected by ERK2 phosphorylation indicating that S412 an S413 *O*-GlcNAc sites did not interact with phosphorylation sites. As observed with RBE phosphorylation, a splitting of pS404 resonance upon S400 *O*-GlcNAcylation indicates a local interaction between both PTMs in a site-specific manner (**Figures 4D**, **5B** and **Figures S5**, **S6**). In contrast, an absence of splitting of the pS396 resonance suggests that S400-*O*-GlcNAc did not interact with pS396 (**Figure S6**). Together, these data showed a limited crosstalk between tau

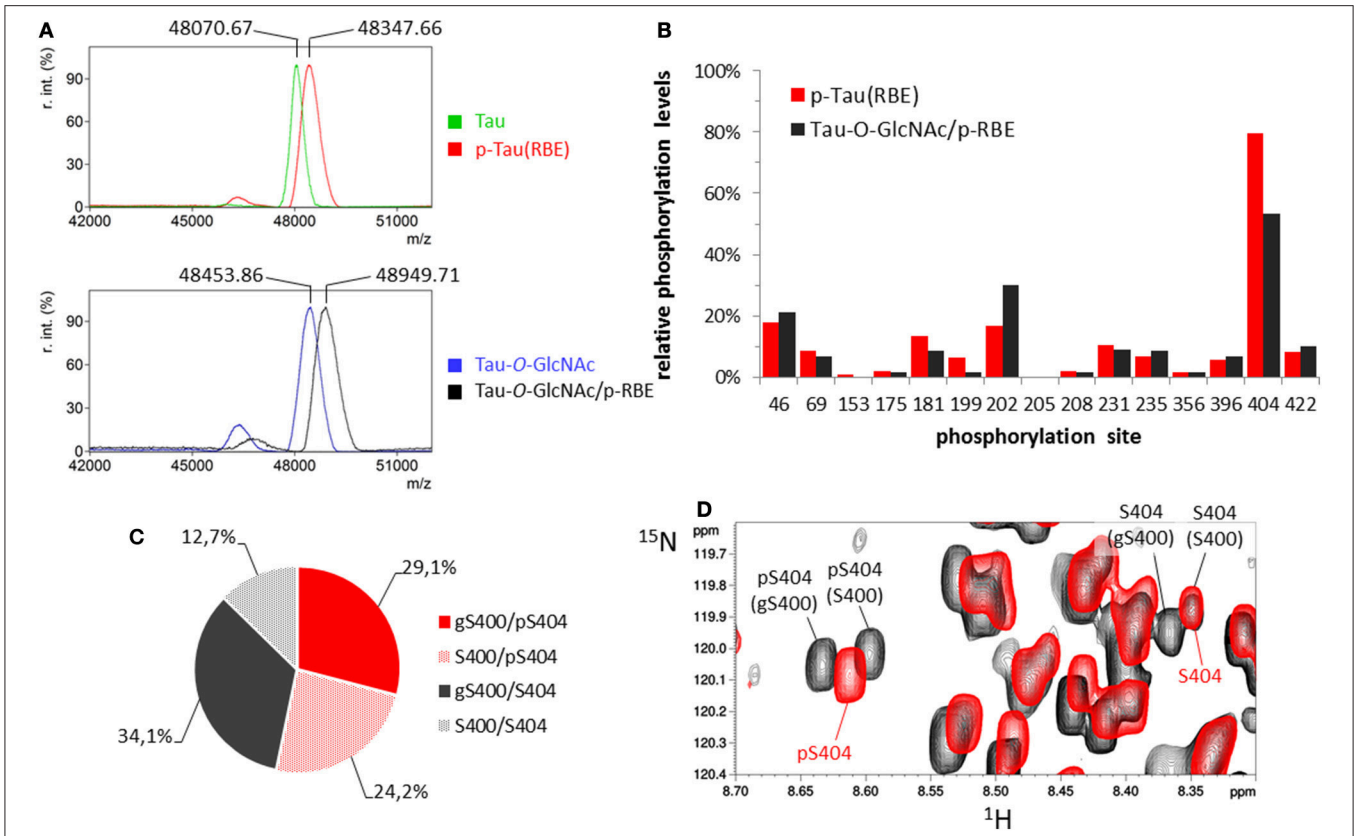

FIGURE 4 | *O*-GlcNAc-mediated regulation of tau phosphorylation. **(A)** MALDI-TOF mass spectra of $^{15}N/^{13}C$-tau before (green) and after phosphorylation by RBE (red), and $^{15}N/^{13}C$-tau-*O*-GlcNAc before (blue) and after phosphorylation by RBE (black). **(B)** Phosphorylation pattern of tau (red) and tau-*O*-GlcNAc (black) phosphorylated by RBE. **(C,D)** Distribution of phosphorylated and *O*-GlcNAcylated species at the C-terminal S400/S404 sites. **(C)** Phosphorylated S404 (pS404) is depicted in the pie chart by red sectors and non-phosphorylated S404 by gray sectors; *O*-GlcNAcylated S400 (gS400) is depicted by plain sectors and non-*O*-GlcNAcylated S400 by dotted sectors. *O*-GlcNAcylation of S400 was estimated to 63% and S404 phosphorylation in tau-*O*-GlcNAc/p-RBE to 53%. **(D)** Superimposition of ^{1}H-^{15}N HSQC spectra of p-tau(RBE) (red) and tau-*O*-GlcNAc/p-RBE (black) showing the resonances of pS404 and S404.

O-GlcNAcylation and phosphorylation, and suggest that in conditions of hyperphosphorylation, *O*-GlcNAcylation is not able to regulate site-specific phosphorylation level, but only modulates it in conditions of moderate phosphorylation which approximates physiological levels.

DISCUSSION

Here, we describe for the first time the *O*-GlcNAc pattern of tau protein in its longest isoform using high resolution NMR spectroscopy. Three *O*-GlcNAc sites were found concentrated over a short region of the C-terminus and two *O*-GlcNAc sites in the proline-rich domain, both regions being targeted by multiple phosphorylations (**Figure 6**). Tau *O*-GlcNAcylation sites (**Table S1**) found in this study were predicted among others by prediction tools (58, 59). The S400 *O*-GlcNAc site has been previously described in several studies (31, 34, 60–62) and was the sole *O*-GlcNAc site detected in endogenous tau protein from normal and transgenic mice expressing human amyloid precursor protein after enrichment of *O*-GlcNAc proteins while, in contrast, as many as 50 phosphorylation sites were detected (35). This *O*-GlcNAc site was also found in a tau-enriched protein fraction isolated from rat brain in which among 8 sites found in 7 proteins only S400 was identified in tau (62). In addition to S400, Vocadlo and collaborators found in recombinant *O*-GlcNAc modified tau an *O*-GlcNAc site at T123 in the N-terminus which has not been detected here and another one at either S409, S412, or S413 (60). We found both S412 and S413 mono-*O*-GlcNAc species but no di-*O*-GlcNAc form suggesting that both *O*-GlcNAc modifications at vicinal positions are mutually exclusive. Furthermore, S185 and S191 were *O*-GlcNAcylated at lower levels in the proline-rich domain. Taken altogether, these findings refute the statement that tau is an extensively *O*-GlcNAcylated protein (17).

When studying the direct crosstalk between *O*-GlcNAcylation and phosphorylation, we found that hyperphosphorylation obtained with ERK2 and normal phosphorylation (i.e. a phosphorylation level that reproduces physiological phosphorylation of tau) provided by the kinase activity of RBE slightly stimulates tau *O*-GlcNAcylation as detected by a chemoenzymatic labeling strategy. Examination of

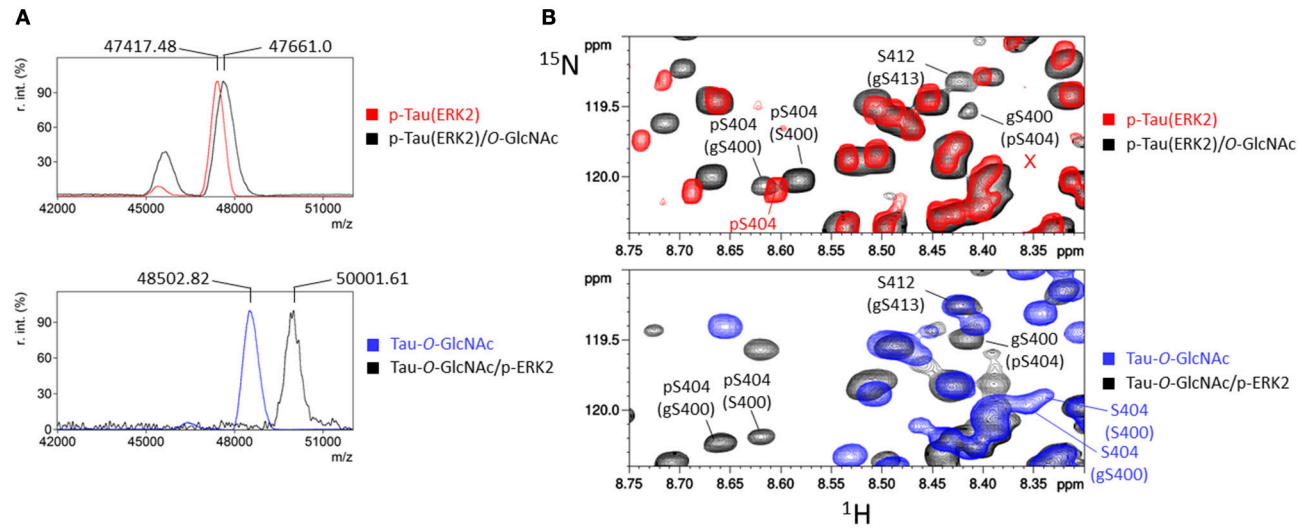

FIGURE 5 | ERK2 phosphorylation of tau and tau-*O*-GlcNAc proteins. **(A)** MALDI-TOF mass spectra of ^{15}N-p-tau(ERK2) before (red) and after *O*-GlcNAcylation by OGT (black), and ^{15}N/^{13}C-tau-*O*-GlcNAc before (blue) and after phosphorylation by ERK2 (black). **(B)** Superimposition of ^{1}H-^{15}N HSQC spectra of p-tau(ERK2) (red), tau-*O*-GlcNAc (blue) and tau-*O*-GlcNAc/p-ERK2 (black, lower panel) or p-tau(ERK2)/*O*-GlcNAc (black, upper panel) showing the resonances of pS404 and gS400. The red cross marks the absence of S404 resonance indicating a quantitative phosphorylation of S404.

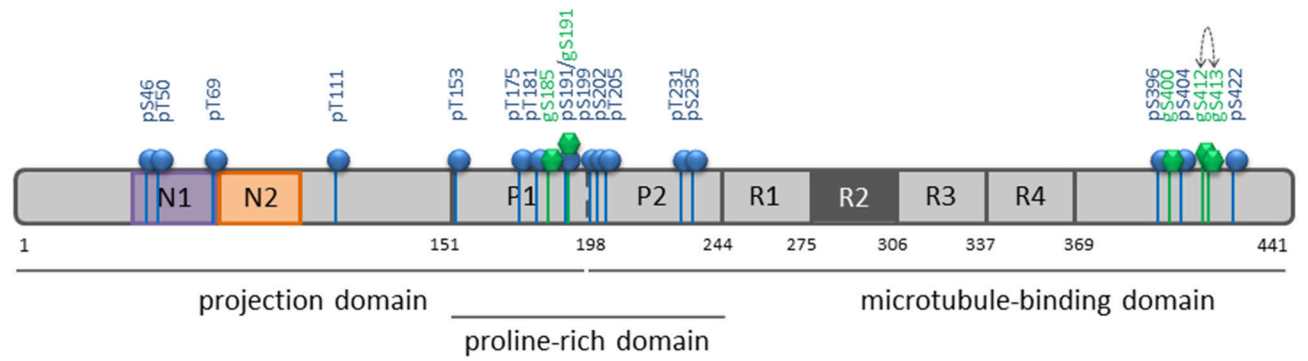

FIGURE 6 | Summary of *O*-GlcNAcylation and phosphorylation sites of tau protein in its longest isoform. ERK2-mediated phosphorylation is depicted by blue bars and balls along the tau primary sequence, and *O*-GlcNAc sites provided by OGT by green bars and hexagons. The dotted arrow indicates mutually exclusive *O*-GlcNAc sites.

a phosphorylated/*O*-GlcNAcylated tau sample in which phosphorylation by ERK2 preceded *O*-GlcNAcylation by OGT did not allow finding additional *O*-GlcNAc sites suggesting that phosphorylation increases levels of existing *O*-GlcNAc sites. This finding is in sharp contrast with what has been established in cellular models and in rat brain in which upon perturbations of phosphorylation dynamics, phosphorylation was found to be antagonistic of the *O*-GlcNAc modification (11, 12, 29). Furthermore, hyperphosphorylated forms of tau were found to be significantly less *O*-GlcNAcylated than the non- or less phosphorylated forms (11, 29). Here, we showed that phosphorylation did not inhibit tau *O*-GlcNAcylation by OGT but, in contrast, increasing phosphorylation level improves *O*-GlcNAcylation. Hence, our data argue in favor of an indirect regulation in *in vivo* or *in vitro* models in which tuning the phosphorylation balance could induce a dysregulation of enzymes involved in the *O*-GlcNAc dynamics which in turn, has an impact on the *O*-GlcNAcylation state of tau. Moreover, it has been shown that pharmacological elevation of tau *O*-GlcNAcylation was a potent mechanism to slow down neurodegeneration, reduce tauopathy, and inhibit tau aggregation (31, 34, 36). Our data suggest that hyperphosphorylation of tau is not antagonistic of glycosylation and may rather directly contribute to an increase of tau *O*-GlcNAcylation which could be a salvage mechanism to protect cells from tau toxicity and fibrillar aggregation, two processes which seems to have their origins in tau hyperphosphorylation. This protective mechanism could be impaired in AD brain where the *O*-GlcNAc dynamics is strongly perturbed due to lower glucose metabolism/uptake.

Then, we have investigated the direct effect of *O*-GlcNAcylation on tau phosphorylation provided either by RBE or ERK2 kinase activity. We found that, within the RBE phosphorylation pattern, *O*-GlcNAcylation weakly decreases phosphorylation at a proximal position, S404, but had no significant effect on the overall phosphorylation pattern at the quantitative level. Interestingly, S400 *O*-GlcNAc site is located within the pathological PHF-1 phospho-epitope (pS396/pS404) and interacts with pS404 as both S400 and S404 resonances are affected by the modification of each other, unlike S396 which has no interaction with S400 glycosylation. On the other hand, S400 is the sole *O*-GlcNAc site involved in a crosstalk with phosphorylation. These data suggest that S400 *O*-GlcNAcylation and/or S404 phosphorylation induce a local conformational change allowing a crosstalk between both specific PTMs. In conditions of physiological phosphorylation level, we have noticed that S404 is preferentially phosphorylated in the S400 non-glycosylated form (65% vs. 46% in the S400-*O*-GlcNAc form) but is not inhibited by proximal glycosylation. Interestingly, similar values were found in a short peptide of tau (residues 392–411) phosphorylated by the CDK2/cyclineA3 complex in which S404 phosphorylation level of 61% was reduced to 41% when S400 was *O*-GlcNAcylated (47). Hence, glycosylation of S400 can down-regulate phosphorylation of S404 which is a priming site of GSK3β (44, 47), one of the potential kinases involved in tau hyperphosphorylation associated to tau pathology, and directly compete with S400 phosphorylation preventing from the formation of the PHF-1 phospho-epitope. In contrast, in conditions of hyperphosphorylation, S404 and S396 are almost quantitatively phosphorylated and S400 *O*-GlcNAcylation does not prevent hyperphosphorylation of both sites. Together our data suggest that *O*-GlcNAcylation could be involved in the control of normal phosphorylation but fails to prevent from hyperphosphorylation.

Several studies have shown a reciprocal negative regulation of tau phosphorylation and *O*-GlcNAcylation in cellular models or transgenic mice. In most cases, site-specific tau phosphorylation was increased upon mouse starvation mimicking low glucose metabolism/uptake of AD brain or OGT knock-down, both decreasing protein *O*-GlcNAcylation (11, 18). Conversely, a negative regulation of tau phosphorylation was detected upon increasing *O*-GlcNAcylation with Thiamet-G, a potent OGA inhibitor (36, 61). However, an activation of GSK3β in mouse brain after Thiamet-G injection was observed through an inhibition of AKT phosphorylation (AKT negatively regulates GSK3β via phosphorylation of S9) leading to an increase of site-specific tau phosphorylation (63). Our data giving a quantitative picture of the direct crosstalk between phosphorylation and *O*-GlcNAcylation are contradictory with the findings that *O*-GlcNAcylation of tau has a large effect on site-specific phosphorylation distributed along the entire protein sequence. Hence, this points to an indirect effect on tau phosphorylation resulting from the perturbation of *O*-GlcNAc dynamics *in vitro* or *in vivo* such as an *O*-GlcNAc-mediated regulation of enzymes involved in the phosphorylation balance, e.g. kinases implicated in tau (hyper)phosphorylation (52, 64–67), or other actors in tau pathology such as chaperones and heat-shock proteins (33).

AUTHOR CONTRIBUTIONS

CS designed research; GB, AK, and FC performed research; GB, AK, BC, and CS contributed new materials, analytic tools; GB and CS analyzed data; IL and CS wrote the paper.

ACKNOWLEDGMENTS

This work was supported by the Mizutani Foundation for Glycoscience (2018 Research Grant number 180122) and by grants from the LabEx (Laboratory of Excellence) DISTALZ (Development of Innovative Strategies for a Transdisciplinary approach to Alzheimer's disease).

The NMR facilities were funded by the Région Nord, CNRS, Pasteur Institute of Lille, European Community (FEDER), French Research Ministry and the University of Sciences and Technologies of Lille. We acknowledge support from the TGE RMN THC (FR-3050, France), FRABio (FR 3688, France), Lille NMR and RPE Health and Biology core facility.

SUPPLEMENTARY MATERIAL

The Supplementary Material for this article can be found online at: https://www.frontiersin.org/articles/10.3389/fendo.2018.00595/full#supplementary-material

REFERENCES

1. Hart GW. Dynamic O-linked glycosylation of nuclear and cytoskeletal proteins. *Annu Rev Biochem.* (1997) 66:315–35. doi: 10.1146/annurev.biochem.66.1.315
2. Wang Z, Gucek M, Hart GW. Cross-talk between GlcNAcylation and phosphorylation: site-specific phosphorylation dynamics in response to globally elevated O-GlcNAc. *Proc Natl Acad Sci USA*. (2008) 105:13793–8. doi: 10.1073/pnas.0806216105
3. Hart GW, Greis KD, Dong LY, Blomberg MA, Chou TY, Jiang MS, et al. O-linked N-acetylglucosamine: the "yin-yang" of Ser/Thr phosphorylation? Nuclear and cytoplasmic glycosylation. *Adv Exp Med Biol.* (1995) 376:115–23.
4. Ma J, Hart GW. O-GlcNAc profiling: from proteins to proteomes. *Clin Proteomics* (2014) 11:8. doi: 10.1186/1559-0275-11-8
5. Chalkley RJ, Thalhammer A, Schoepfer R, Burlingame AL. Identification of protein O-GlcNAcylation sites using electron transfer dissociation mass spectrometry on native peptides. *Proc Natl Acad Sci USA*. (2009) 106:8894–9. doi: 10.1073/pnas.0900288106
6. Leney AC, El Atmioui D, Wu W, Ovaa H, Heck AJR. Elucidating crosstalk mechanisms between phosphorylation and O-GlcNAcylation. *Proc Natl Acad Sci USA*. (2017) 114:E7255–61. doi: 10.1073/pnas.1620529114
7. Wani WY, Chatham JC, Darley-Usmar V, McMahon LL, Zhang J. O-GlcNAcylation and neurodegeneration. *Brain Res Bull.* (2016) 133:80–7. doi: 10.1016/j.brainresbull.2016.08.002
8. Zhu Y, Shan X, Yuzwa SA, Vocadlo DJ. The emerging link between O-GlcNAc and Alzheimer disease. *J Biol Chem.* (2014) 289:34472–81. doi: 10.1074/jbc.R114.601351

9. Gong C-X, Liu F, Iqbal K. O-GlcNAcylation: a regulator of tau pathology and neurodegeneration. *Alzheimers Dement.* (2016) 12:1078–89. doi: 10.1016/j.jalz.2016.02.011
10. Ma X, Li H, He Y, Hao J. The emerging link between O-GlcNAcylation and neurological disorders. *Cell Mol Life Sci.* (2017) 74:3667–86. doi: 10.1007/s00018-017-2542-9
11. Liu F, Shi J, Tanimukai H, Gu J, Gu J, Grundke-Iqbal I, et al. Reduced O-GlcNAcylation links lower brain glucose metabolism and tau pathology in Alzheimer's disease. *Brain* (2009) 132:1820–32. doi: 10.1093/brain/awp099
12. Robertson LA, Moya KL, Breen KC. The potential role of tau protein O-glycosylation in Alzheimer's disease. *J Alzheimers Dis.* (2004) 6:489–95. doi: 10.3233/JAD-2004-6505
13. Heiss W-D, Szelies B, Kessler J, Herholz K. Abnormalities of energy metabolism in Alzheimer's disease studied with PETa. *Ann NY Acad Sci.* (1991) 640:65–71.
14. Griffith LS, Schmitz B. O-linked N-acetylglucosamine is upregulated in Alzheimer Brains. *Biochem Biophys Res Commun.* (1995) 213:424–31. doi: 10.1006/bbrc.1995.2149
15. Förster S, Welleford AS, Triplett JC, Sultana R, Schmitz B, Butterfield DA. Increased O-GlcNAc levels correlate with decreased O-GlcNAcase levels in Alzheimer disease brain. *Biochim Biophys Acta* (2014) 1842:1333–9. doi: 10.1016/j.bbadis.2014.05.014
16. Grundke-Iqbal I, Iqbal K, Quinlan M, Tung YC, Zaidi MS, Wisniewski HM. Microtubule-associated protein tau. A component of Alzheimer paired helical filaments. *J Biol Chem.* (1986) 261:6084–9.
17. Arnold CS, Johnson GV, Cole RN, Dong DL, Lee M, Hart GW. The microtubule-associated protein tau is extensively modified with O-linked N-acetylglucosamine. *J Biol Chem.* (1996) 271:28741–4. doi: 10.1074/jbc.271.46.28741
18. Liu F, Iqbal K, Grundke-Iqbal I, Hart GW, Gong CX. O-GlcNAcylation regulates phosphorylation of tau: a mechanism involved in Alzheimer's disease. *Proc Natl Acad Sci USA.* (2004) 101:10804–9. doi: 10.1073/pnas.0400348101
19. Köpke E, Tung YC, Shaikh S, Alonso AC, Iqbal K, Grundke-Iqbal I. Microtubule-associated protein tau. Abnormal phosphorylation of a non-paired helical filament pool in Alzheimer disease. *J Biol Chem.* (1993) 268:24374–84.
20. Grundke-Iqbal I, Iqbal K, Tung YC, Quinlan M, Wisniewski HM, Binder LI. Abnormal phosphorylation of the microtubule-associated protein tau (tau) in Alzheimer cytoskeletal pathology. *Proc Natl Acad Sci USA.* (1986) 83:4913–7. doi: 10.1073/pnas.83.13.4913
21. Mirbaha H, Chen D, Morazova OA, Ruff KM, Sharma AM, Liu X, et al. Inert and seed-competent tau monomers suggest structural origins of aggregation. *eLife* (2018) 7:e36584. doi: 10.7554/eLife.36584
22. Brion JP, Couck AM, Passareiro E, Flament-Durand J. Neurofibrillary tangles of Alzheimer's disease: an immunohistochemical study. *J Submicrosc Cytol.* (1985) 17:89–96.
23. Fitzpatrick AWP, Falcon B, He S, Murzin AG, Murshudov G, Garringer HJ, et al. Cryo-EM structures of tau filaments from Alzheimer's disease. *Nature* (2017) 547:185–90. doi: 10.1038/nature23002
24. Falcon B, Cavallini A, Angers R, Glover S, Murray TK, Barnham L, et al. Conformation determines the seeding potencies of native and recombinant Tau aggregates. *J Biol Chem.* (2015) 290:1049–65. doi: 10.1074/jbc.M114.589309
25. Clavaguera F, Bolmont T, Crowther RA, Abramowski D, Frank S, Probst A, et al. Transmission and spreading of tauopathy in transgenic mouse brain. *Nat Cell Biol.* (2009) 11:909–13. doi: 10.1038/ncb1901
26. Hart GW. Three decades of research on O-GlcNAcylation - a major nutrient sensor that regulates signaling, transcription and cellular metabolism. *Front Endocrinol.* (2014) 5:183. doi: 10.3389/fendo.2014.00183
27. Hart GW, Housley MP, Slawson C. Cycling of O-linked beta-N-acetylglucosamine on nucleocytoplasmic proteins. *Nature* (2007) 446:1017–22. doi: 10.1038/nature05815
28. Bullen JW, Balsbaugh JL, Chanda D, Shabanowitz J, Hunt DF, Neumann D, et al. Cross-talk between two essential nutrient-sensitive enzymes: O-GlcNAc transferase (OGT) and AMP-activated protein kinase (AMPK). *J Biol Chem.* (2014) 289:10592–606. doi: 10.1074/jbc.M113.523068
29. Lefebvre T, Ferreira S, Dupont-Wallois L, Bussière T, Dupire M-J, Delacourte A, et al. Evidence of a balance between phosphorylation and O-GlcNAc glycosylation of Tau proteins–a role in nuclear localization. *Biochim Biophys Acta* (2003) 1619:167–76. doi: 10.1016/S0304-4165(02)00477-4
30. O'Donnell N, Zachara NE, Hart GW, Marth JD. Ogt-dependent X-chromosome-linked protein glycosylation is a requisite modification in somatic cell function and embryo viability. *Mol Cell Biol.* (2004) 24:1680–90. doi: 10.1128/MCB.24.4.1680-1690.2004
31. Yuzwa SA, Shan X, Macauley MS, Clark T, Skorobogatko Y, Vosseller K, et al. Increasing O-GlcNAc slows neurodegeneration and stabilizes tau against aggregation. *Nat Chem Biol.* (2012) 8:393–9. doi: 10.1038/nchembio.797
32. Graham DL, Gray AJ, Joyce JA, Yu D, O'Moore J, Carlson GA, et al. Increased O-GlcNAcylation reduces pathological tau without affecting its normal phosphorylation in a mouse model of tauopathy. *Neuropharmacology* (2014) 79:307–13. doi: 10.1016/j.neuropharm.2013.11.025
33. Borghgraef P, Menuet C, Theunis C, Louis JV, Devijver H, Maurin H, et al. Increasing brain protein O-GlcNAc-ylation mitigates breathing defects and mortality of Tau.P301L mice. *PLoS ONE* (2013) 8:e84442. doi: 10.1371/journal.pone.0084442
34. Yuzwa SA, Cheung AH, Okon M, McIntosh LP, Vocadlo DJ. O-GlcNAc modification of tau directly inhibits its aggregation without perturbing the conformational properties of tau monomers. *J Mol Biol.* (2014) 426:1736–52. doi: 10.1016/j.jmb.2014.01.004
35. Morris M, Knudsen GM, Maeda S, Trinidad JC, Ioanoviciu A, Burlingame AL, et al. Tau post-translational modifications in wild-type and human amyloid precursor protein transgenic mice. *Nat Neurosci.* (2015) 18:1183–9. doi: 10.1038/nn.4067
36. Hastings NB, Wang X, Song L, Butts BD, Grotz D, Hargreaves R, et al. Inhibition of O-GlcNAcase leads to elevation of O-GlcNAc tau and reduction of tauopathy and cerebrospinal fluid tau in rTg4510 mice. *Mol Neurodegener.* (2017) 12:39. doi: 10.1186/s13024-017-0181-0
37. Yuzwa SA, Shan X, Jones BA, Zhao G, Woodward ML, Li X, et al. Pharmacological inhibition of O-GlcNAcase (OGA) prevents cognitive decline and amyloid plaque formation in bigenic tau/APP mutant mice. *Mol Neurodegener.* (2014) 9:42. doi: 10.1186/1750-1326-9-42
38. Theillet F-X, Smet-Nocca C, Liokatis S, Thongwichian R, Kosten J, Yoon M-K, et al. Cell signaling, post-translational protein modifications and NMR spectroscopy. *J Biomol NMR* (2012) 54:217–36. doi: 10.1007/s10858-012-9674-x
39. Smet-Nocca C, Launay H, Wieruszeski JM, Lippens G, Landrieu I. Unraveling a phosphorylation event in a folded protein by NMR spectroscopy: phosphorylation of the Pin1 WW domain by PKA. *J Biomol NMR* (2013) 55:323–37. doi: 10.1007/s10858-013-9716-z
40. Kamah A, Huvent I, Cantrelle F-X, Qi H, Lippens G, Landrieu I, et al. Nuclear magnetic resonance analysis of the acetylation pattern of the neuronal Tau protein. *Biochemistry* (2014) 53:3020–32. doi: 10.1021/bi500006v
41. Qi H, Prabakaran S, Cantrelle F-X, Chambraud B, Gunawardena J, Lippens G, et al. Characterization of neuronal tau protein as a target of extracellular signal-regulated kinase. *J Biol Chem.* (2016) 291:7742–53. doi: 10.1074/jbc.M115.700914
42. Landrieu I, Lacosse L, Leroy A, Wieruszeski JM, Trivelli X, Sillen A, et al. NMR analysis of a Tau phosphorylation pattern. *J Am Chem Soc.* (2006) 128:3575–83. doi: 10.1021/ja054656+
43. Landrieu I, Leroy A, Smet-Nocca C, Huvent I, Amniai L, Hamdane M, et al. NMR spectroscopy of the neuronal tau protein: normal function and implication in Alzheimer's disease. *Biochem Soc Trans.* (2010) 38:1006–11. doi: 10.1042/BST0381006
44. Leroy A, Landrieu I, Huvent I, Legrand D, Codeville B, Wieruszeski J-M, et al. Spectroscopic studies of GSK3β phosphorylation of the neuronal tau protein and its interaction with the N-terminal domain of apolipoprotein E. *J Biol Chem.* (2010) 285:33435–44. doi: 10.1074/jbc.M110.149419
45. Lippens G, Sillen A, Smet C, Wieruszeski J-M, Leroy A, Buée L, et al. Studying the natively unfolded neuronal Tau protein by solution NMR spectroscopy. *Protein Pept Lett.* (2006) 13:235–46. doi: 10.2174/092986606775338461
46. Danis C, Despres C, Bessa LM, Malki I, Merzougui H, Huvent I, et al. Nuclear magnetic resonance spectroscopy for the identification of multiple phosphorylations of intrinsically disordered proteins. *J Vis Exp.* (2016) 118:e55001. doi: 10.3791/55001

47. Smet-Nocca C, Broncel M, Wieruszeski J-M, Tokarski C, Hanoulle X, Leroy A, et al. Identification of O-GlcNAc sites within peptides of the Tau protein and their impact on phosphorylation. *Mol Biosyst.* (2011) 7:1420–9. doi: 10.1039/c0mb00337a
48. Reimann O, Smet-Nocca C, Hackenberger CPR. Traceless purification and desulfurization of tau protein ligation products. *Angew Chem Int Ed Engl.* (2015) 54:306–10. doi: 10.1002/anie.201408674
49. Schwagerus S, Reimann O, Despres C, Smet-Nocca C, Hackenberger CPR. Semi-synthesis of a tag-free O-GlcNAcylated tau protein by sequential chemoselective ligation. *J Pept Sci.* (2016) 22:327–33. doi: 10.1002/psc.2870
50. Qi H, Despres C, Prabakaran S, Cantrelle F-X, Chambraud B, Gunawardena J, et al. The study of posttranslational modifications of tau protein by nuclear magnetic resonance spectroscopy: phosphorylation of tau protein by ERK2 recombinant kinase and rat brain extract, and acetylation by recombinant creb-binding protein. In: Smet-Nocca, editor. *Tau Protein: Methods and Protocols.* (2017) New York, NY: Springer New York. p. 179–213. Available at: http://dx.doi.org/10.1007/978-1-4939-6598-4_11
51. Gross BJ, Kraybill BC, Walker S. Discovery of O-GlcNAc transferase inhibitors. *J Am Chem Soc.* (2005) 127:14588–9. doi: 10.1021/ja0555217
52. Lubas WA, Hanover JA. Functional expression of O-linked GlcNAc transferase. Domain structure and substrate specificity. *J Biol Chem.* (2000) 275:10983–8. doi: 10.1074/jbc.275.15.10983
53. Dehennaut V, Hanoulle X, Bodart JF, Vilain JP, Michalski JC, Landrieu I, et al. Microinjection of recombinant O-GlcNAc transferase potentiates Xenopus oocytes M-phase entry. *Biochem Biophys Res Commun.* (2008) 369:539–46. doi: 10.1016/j.bbrc.2008.02.063
54. Smet-Nocca C, Page A, Cantrelle F-X, Nikolakaki E, Landrieu I, Giannakouros T. The O-β-linked N-acetylglucosaminylation of the Lamin B receptor and its impact on DNA binding and phosphorylation. *Biochim Biophys Acta* (2018) 1862:825–35. doi: 10.1016/j.bbagen.2018.01.007
55. Despres C, Byrne C, Qi H, Cantrelle F-X, Huvent I, Chambraud B, et al. Identification of the Tau phosphorylation pattern that drives its aggregation. *Proc Natl. Acad Sci USA.* (2017) 114:9080–5. doi: 10.1073/pnas.1708448114
56. Alonso A, Zaidi T, Novak M, Grundke-Iqbal I, Iqbal K. Hyperphosphorylation induces self-assembly of tau into tangles of paired helical filaments/straight filaments. *Proc Natl Acad Sci USA.* (2001) 98:6923–8. doi: 10.1073/pnas.121119298
57. Haltiwanger RS, Grove K, Philipsberg GA. Modulation of *O* -linked *N* -acetylglucosamine levels on nuclear and cytoplasmic proteins *in vivo* using the peptide *O* -GlcNAc-β- *N* -acetylglucosaminidase Inhibitor *O* -(2-Acetamido-2-deoxy-dglucopyranosylidene)amino- *N* -phenylcarbamate. *J Biol. Chem.* (1998) 273:3611–7. doi: 10.1074/jbc.273.6.3611
58. Gupta R, Brunak S. Prediction of glycosylation across the human proteome and the correlation to protein function. *Pac Symp Biocomput.* (2002) 7:310–322. doi: 10.1142/9789812799623_0029
59. Jia C, Zuo Y, Zou Q. O-GlcNAcPRED-II: an integrated classification algorithm for identifying O-GlcNAcylation sites based on fuzzy undersampling and a K-means PCA oversampling technique. *Bioinformatics* (2018) 34:2029–36. doi: 10.1093/bioinformatics/bty039
60. Yuzwa SA, Yadav AK, Skorobogatko Y, Clark T, Vosseller K, Vocadlo DJ. Mapping O-GlcNAc modification sites on tau and generation of a site-specific O-GlcNAc tau antibody. *Amino Acids* (2011) 40:857–68. doi: 10.1007/s00726-010-0705-1
61. Yuzwa SA, Macauley MS, Heinonen JE, Shan X, Dennis RJ, He Y, et al. A potent mechanism-inspired O-GlcNAcase inhibitor that blocks phosphorylation of tau *in vivo*. *Nat Chem Biol.* (2008) 4:483–90. doi: 10.1038/nchembio.96
62. Wang Z, Udeshi ND, O'Malley M, Shabanowitz J, Hunt DF, Hart GW. Enrichment and site mapping of O-linked N-acetylglucosamine by a combination of chemical/enzymatic tagging, photochemical cleavage, and electron transfer dissociation mass spectrometry. *Mol Cell Proteomics* (2010) 9:153–60. doi: 10.1074/mcp.M900268-MCP200
63. Yu Y, Zhang L, Li X, Run X, Liang Z, Li Y, et al. Differential effects of an O-GlcNAcase inhibitor on tau phosphorylation. *PLoS ONE* (2012) 7:e35277. doi: 10.1371/journal.pone.0035277
64. Dias WB, Cheung WD, Hart GW. O-GlcNAcylation of kinases. *Biochem Biophys Res Commun.* (2012) 422:224–8. doi: 10.1016/j.bbrc.2012.04.124
65. Wang S, Huang X, Sun D, Xin X, Pan Q, Peng S, et al. Extensive crosstalk between O-GlcNAcylation and phosphorylation regulates Akt signaling. *PLoS ONE* (2012) 7:e37427. doi: 10.1371/journal.pone.0037427
66. Xie S, Jin N, Gu J, Shi J, Sun J, Chu D, et al. O-GlcNAcylation of protein kinase A catalytic subunits enhances its activity: a mechanism linked to learning and memory deficits in Alzheimer's disease. *Aging Cell* (2016) 15:455–64. doi: 10.1111/acel.12449
67. Shi J, Wu S, Dai C, Li Y, Grundke-Iqbal I, Iqbal K, et al. Diverse regulation of AKT and GSK-3β by O-GlcNAcylation in various types of cells. *FEBS Lett.* (2012) 586:2443–50. doi: 10.1016/j.febslet.2012.05.063

Conflict of Interest Statement: The authors declare that the research was conducted in the absence of any commercial or financial relationships that could be construed as a potential conflict of interest.

frontiers in Endocrinology

REVIEW
published: 29 October 2018
doi: 10.3389/fendo.2018.00642

Chronic O-GlcNAcylation and Diabetic Cardiomyopathy: The Bitterness of Glucose

Simon Ducheix[1], *Jocelyne Magré*[1], *Bertrand Cariou*[2] *and Xavier Prieur*[1]*

[1] *l'institut du thorax, INSERM, CNRS, UNIV Nantes, Nantes, France,* [2] *l'institut du thorax, INSERM, CNRS, UNIV Nantes, CHU Nantes, Nantes, France*

Type 2 diabetes (T2D) is a major risk factor for heart failure. Diabetic cardiomyopathy (DC) is characterized by diastolic dysfunction and left ventricular hypertrophy. Epidemiological data suggest that hyperglycaemia contributes to the development of DC. Several cellular pathways have been implicated in the deleterious effects of high glucose concentrations in the heart: oxidative stress, accumulation of advanced glycation end products (AGE), and chronic hexosamine biosynthetic pathway (HBP) activation. In the present review, we focus on the effect of chronic activation of the HBP on diabetic heart function. The HBP supplies N-acetylglucosamine moiety (O-GlcNAc) that is O-linked by O-GlcNAc transferase (OGT) to proteins on serine or threonine residues. This post-translational protein modification modulates the activity of the targeted proteins. In the heart, acute activation of the HBP in response to ischaemia-reperfusion injury appears to be protective. Conversely, chronic activation of the HBP in the diabetic heart affects Ca^{2+} handling, contractile properties, and mitochondrial function and promotes stress signaling, such as left ventricular hypertrophy and endoplasmic reticulum stress. Many studies have shown that O-GlcNAc impairs the function of key protein targets involved in these pathways, such as phospholamban, calmodulin kinase II, troponin I, and FOXO1. The data show that excessive O-GlcNAcylation is a major trigger of the glucotoxic events that affect heart function under chronic hyperglycaemia. Supporting this finding, pharmacological or genetic inhibition of the HBP in the diabetic heart improves heart function. In addition, the SGLT2 inhibitor dapagliflozin, a glucose lowering agent, has recently been shown to lower cardiac HBP in a lipodystophic T2D mice model and to concomitantly improve the diastolic dysfunction of these mice. Therefore, targeting cardiac-excessive O-GlcNAcylation or specific target proteins represents a potential therapeutic option to treat glucotoxicity in the diabetic heart.

Keywords: glucotoxicity, diabetes, metabolism, cardiomyopathy, O-GlcNAcylation

OPEN ACCESS

Edited by:
Tarik Issad,
Institut National de la Santé et de la Recherche Médicale (INSERM), France

Reviewed by:
Caroline Cieniewski-Bernard, Lille University of Science and Technology, France
Hai-Bin Ruan, University of Minnesota Twin Cities, United States
Emily Johnson, Providence Medical Research Center, United States

***Correspondence:**
Xavier Prieur
xavier.prieur@univ-nantes.fr

Specialty section:
This article was submitted to Molecular and Structural Endocrinology, a section of the journal Frontiers in Endocrinology

Received: *29 June 2018*
Accepted: *09 October 2018*
Published: *29 October 2018*

Citation:
Ducheix S, Magré J, Cariou B and Prieur X (2018) Chronic O-GlcNAcylation and Diabetic Cardiomyopathy: The Bitterness of Glucose. Front. Endocrinol. 9:642. doi: 10.3389/fendo.2018.00642

INTRODUCTION

The incidence of heart failure (HF) is 2.5-fold higher in patients with type 2 diabetes (T2D) than in healthy subjects (1). Although the number of myocardial infarctions has been reduced by 25% in the T2D population over the last 10 years, HF is becoming the chronic diabetic complication of greatest concern (2). Ischaemic heart disease and hypertension are associated with HF in 65

and 75% patients with T2D, respectively (3). However, a fraction of patients with T2D display HF without ischaemic injuries; this observation has led to the identification of specific diabetes-related cardiomyopathy (DC) (4). DC is characterized by diastolic dysfunction and left ventricular hypertrophy (5, 6). In a large cohort study, Iribarren and colleagues demonstrated that for each 1% increase in glycated hemoglobin (HbA1C), the HF-related death or hospitalization rate increased by 8% (7). A recent study confirmed that HF-related hospitalization is more frequent in patients with higher HbA1c levels (8). These clinical observations suggest that hyperglycaemia *per se* contributes to the development of DC.

Indeed, a large body of evidence supports that altered cardiac energetic substrate utilization and metabolic inflexibility contribute to DC physiopathology (5, 6). The diabetic heart is characterized by an insulin resistance that compromises glucose uptake and metabolism (9), resulting in an increased reliance on lipids (10) and leading to increased fatty acid uptake (11) and ectopic lipid accumulation in cardiomyocytes (12). In the diabetic heart, pyruvate dehydrogenase (PDH) activity is inhibited by the accumulation of acetyl-CoA as a result of elevated fatty acid catabolism via the ß-oxidation pathway (5). In addition, insulin resistance directly inhibits the activity of phosphofructokinase-2, which regulates glycolysis rate (9). In heart of *ob/ob* insulin-resistant mice, insulin is unable to stimulate glucose oxidation (13). Overall, the diabetic heart is characterized by a glucose overload (14). Cellular studies have demonstrated that high glucose activates apoptosis in cardiomyocytes (15), thereby leading to the development of the concept of glucotoxicity.

Several cellular pathways are suspected to mediate the deleterious effects of high-glucose concentrations in the heart: oxidative stress, accumulation of advanced glycation end-products (AGEs), and chronic hexosamine biosynthetic pathway (HBP) activation [for a review, see (16)]. Hyperglycaemia can feed the pentose phosphate pathway that produces NADPH from glucose-6-phosphate (17). NADPH is the substrate of the cytosolic NADPH oxidase, an enzymatic complex that generates reactive oxygen species (ROS) (18). Therefore, hyperglycaemia contributes to ROS production and eventually oxidative stress, which can affect cardiac function. In addition, high glucose levels favor the non-enzymatic glycation reaction that produces AGEs (19). In the context of diabetes, AGEs have been shown to impair the function of glycated proteins, modify the properties of extra-cellular matrix, and activate RAGE, the AGE receptor that induces ROS production and thus contributes to oxidative stress (20). Furthermore, chronic activation of the HBP has been extensively studied in the diabetic heart. The HBP supplies UDP-N-acetylglucosamine moiety (UDP-GlcNAc) that is O-linked by O-GlcNAc transferase (OGT) to proteins on serine or threonine residues (21). This post-translational protein modification modulates the activity of the targeted proteins and has been described in different organisms and organs as a cellular stress response (22). UDP-GlcNAc can also be N-linked to asparagine residues and other HBP intermediary products and can display biological activity independently of the O-GlcNAcylation process. However, in this review, we focus on the effects of the general HBP pathway and the O-GlcNAcylation process in the diabetic heart due to the greater knowledge of these phenomena than of UDP-GlcNAc-related processes.

In the heart, HBP is increased in response to ischaemia/reperfusion and appears to be protective by limiting cytosolic calcium entry (23, 24); it is also increased during trauma hemorrhage (25, 26). After ischaemia/reperfusion, OGT over-expression promotes cell survival and attenuates oxidative stress and calcium overload (27, 28). A large body of work suggests that pharmacological or genetic activation of the HBP is beneficial for post-ischaemic function [for reviews, see (22, 29)]. In contrast, cardio-specific and inducible deletion of OGT exacerbates cardiac dysfunction after ischaemic/reperfusion injury (30). However, as with most stress-response pathways, although acute induction is often protective, chronic activation might be deleterious. In this report, we review how chronic HBP activation contributes to the deleterious effects of glucose overload in the diabetic heart. We review the specific actors of the HBP and discuss therapeutic interest in targeting this pathway for developing pharmaceutical approaches to treat DC.

CHRONIC ACTIVATION OF THE HBP IN THE DIABETIC HEART

Early studies demonstrated that chronic activation of the HBP is associated with the development of insulin resistance in adipose tissue (31) and skeletal muscle (32). While the enzymatic activities of the rate-limiting enzyme of the HBP, glutamine: fructose-6-phosphate amino-transferase (GFAT), and of O-GlcNAc transferase (OGT) are present in most insulin-sensitive tissues, OGT activity has been found to be particularly elevated in the heart (33). As hyperglycaemia was suspected to be involved in the cardiac dysfunction associated with diabetes, Ren et al. tested the effects of elevated glucose concentration on cardiomyocyte properties (34). Using neonatal cardiomyocytes, these researchers demonstrated that high-glucose exposure induces excitation-contraction (E-C) coupling impairment and that this induction was mimicked by glucosamine treatment but not by treatment with non-metabolically active glucose analogs. These results suggested that glucose metabolism intervenes in this induction effect and, more precisely, that HBP chronic activation might lead to cardiomyocyte dysfunction. The effects observed with glucosamine treatment suggested that HBP activation not only is correlated with cardiomyocyte dysfunction but is also able to compromise E-C coupling. Further investigating the HBP pathway, Pang et al. confirmed that hyperglycaemia modifies the calcium entry in neonatal cardiomyocytes and that this modification was reversed by treatment with azaserine, an inhibitor of GFAT (35). In accordance with a role of HBP in cardiac function, Clark et al. demonstrated that calcium cycling alteration was associated with an increase in the abundance of total O-GlcNAcylated protein levels in neonatal cardiomyocytes (36). *Ex vivo*, in heart isolated from streptozotocin (STZ)-treated mice, a mouse model of type 1 diabetes (T1D), phenylephrine-induced inotropy was blunted, and this blunting was correlated with UDP-GlcNAc accumulation (37).

Supporting these *in vitro* and *ex vivo* observations, O-GlcNAcylated protein accumulation was first found in STZ-treated mice (38). Similarly, in most common mouse models of T2D, cardiac dysfunction has been associated with increased levels of O-GlcNAcylated protein (39–42). Importantly, O-GlcNAcylated protein levels are increased in cardiac biopsies isolated from human patients with heart failure (43).

Recently, we performed cardiac phenotyping of seipin KO (SKO) mice, a model for generalized lipodystrophy, a rare genetic disease characterized by a near absence of adipose tissue, insulin resistance, and T2D (44). SKO mice display a DC phenotype with diastolic dysfunction and left ventricular hypertrophy (LVH) that correlate with hyperglycaemia. The most hyperglycaemic mice display the more severe cardiac phenotype. The heart of SKO mice displays glucose overload evidenced by strong induction of the HBP. In contrast, we did not identify any lipotoxic hallmark in the heart of SKO, nor did we observe ROS production, AGE accumulation, or fibrosis. To the best of our knowledge, this report describes the first mouse model of DC in which chronic HBP activation is the only glucose-overload hallmark present. It can be hypothesized that excessive O-GlcNAcylation alone can trigger the cardiac abnormalities associated with hyperglycaemia in T2D.

Altogether, *in vitro* and *in vivo* evidence strongly indicates that chronic HBP activation is associated with cardiac dysfunction in diabetes. This observation raises the question of causality: How do elevated O-GlcNAcylated protein levels affect cardiac function?

CHRONIC HBP AND CARDIAC CONTRACTILE PROPERTIES

The diabetic heart is characterized by impairments of the contractile and electrophysiological properties, which might be mainly due to defects in calcium handling and myofilament function. These two parameters are intrinsically linked, as myofilament properties define calcium sensitivity (ECa_{50}^{2+}), an indication of myofilament strength production at the basal calcium level. As previously mentioned, high-glucose exposure was initially associated *in vitro* with HBP activation and E-C impairment (34). This E-C impairment is reversed by OGT inhibition (35). Therefore, several research groups have aimed to understand how chronic HBP activation alters calcium handling and, in turn, E-C in cardiomyocytes. As cardiac-type sarcoplasmic reticulum Ca^{2+} ATPase (SERCA2) is central in calcium handling in the cardiomyocyte, Yokoe et al. tested the ability of O-GlcNAcylation to modulate its activity (45). Following the treatment of cardiomyocytes with an inhibitor of OGA (PUGNAC) to increase the levels of O-GlcNAcylation, they did not observe an increase in the levels of O-GlcNAcylated SERCA2 but did observe an increase in phospholamban O-GlcNAc levels. This finding suggests that *in vitro*, HBP induction itself prevents normal Ca^{2+} pumping after excitation. Phospholamban regulates SERCA2 activity: In its unphosphorylated state, it inhibits SERCA2 activity, whereas it induces SERCA2 activity when phosphorylated on Ser16. In STZ-induced diabetic mice heart, an opposite pattern of regulation of O-GlcNAcylation on the phosphorylation of phospholamban on Ser16 was reported, with elevated O-GlcNAc levels leading to reduced phospholamban phosphorylation. Such increased O-GlcNAcylation of Ser-16 and its reciprocal decrease in phosphorylation leading to depressed SERCA2 activity was also observed in isolated cardiomyocytes. The *in vivo* relevance of the reciprocal post-translational modification of phospholamban has been established in a mouse model of T2D, in which mice display progressive ser16-phosphorylation decrease and O-GlcNAcylation increase concomitant with the appearance of diastolic dysfunction (40).

Another key actor in heart calcium homeostasis that is regulated by O-GlcNAcylation is calmodulin-dependent protein kinase II (CAMKII). Erickson et al. showed that high glucose induced CAMK activity in isolated cardiomyocytes and that this induction was repressed by pharmacological inhibition of OGT (46). These researchers identified an O-GlcNAc site on CAMKII and later demonstrated that CAMKII activation increases the frequency of the Ca^{2+} spark. The levels of O-GlcNAc-CAMKII measured in cardiac biopsies from T2D/HF patients have been found to be markedly elevated relative to the levels of non-diabetic controls. This finding is in agreement with the potential deleterious effect of chronic CAMKII activation in HF. In addition to regulating the ER Ca^{2+} store, the capacitative calcium entry (CCE) pathway controls Ca^{2+} entry in the cell. In neonatal cardiomyocytes, hyperglycaemia exposure inhibits CCE, which is reversed by azaserine, thereby directly involving the HBP (35). O-GlcNAcylation of STIM1, an ER protein involved in CCE, prevents its interaction with the plasma membrane and in turn disturbs CCE (47). However, O-GlcNAc levels of STIM1 have not yet been evaluated in diabetic heart. Altogether, these data indicate that phospholamban, CAMKII and STIM1 activity are modified by chronic HBP activation, thereby altering Ca^{2+} homeostasis in the diabetic heart.

Hypothesizing that calcium handling alone cannot account for the contractile dysfunction observed in the diabetic heart, Ramirez-Correa et al. highlighted the potential role of myofilament proteins (48). In an initial study, they identified O-GlcNAc sites in actin and troponin 1 and showed that O-GlcNAcylation decreased myofilament sensitivity to Ca^{2+} and consistently increased ECa^{2+} 50. The O-GlcNAcylated levels of several contractile proteins, including myosin heavy chain, actin, and tropomyosin, are increased in STZ-treated mice heart (48, 49). These increases in O-GlcNAcylation levels are concomitant with changes in OGT/OGA activity, and, interestingly, diabetes is associated with a sarcomeric re-localization of OGT and OGA. Although in control heart, OGT and OGA are mainly located at the Z-line and the A-band, respectively, this distribution is greatly altered in the diabetic heart, raising the hypothesis that the OGT/OGA activity ratio is partially determined by their sub-cellular localization (49). Interestingly, removing GlcNAc residues by recombinant OGA restores the ECa^{2+} 50 in cardiac skinned fibers isolated from T1D heart. Therefore, chronic HBP activation alters

the activity of proteins involved in Ca^{2+} handling and directly controls the contractile properties of the Ca^{2+}-sensitive myofilament component, thus regulating cardiac contraction and relaxation (49).

In addition to diastolic dysfunction and contractile properties, prolonged QT is associated with increased risk of ventricular arrhythmias in the diabetic heart. In the heart of STZ mice, increased O-GlcNAc-modified NAV1.5 levels have been associated with increased arrhythmia scores, suggesting that HBP chronic activation may directly affect cardiomyocyte electrical activity (50).

HBP CHRONIC ACTIVATION PROMOTES HYPERTROPHY SIGNALING

Left ventricular hypertrophy (LVH) is a common feature in cardiac dysfunction and is found in several pathophysiological contexts. In cardiac conditions such as aortic stenosis, aortic banding and myocardial infection, LVH was found to be positively correlated with elevated levels of O-GlcNAc protein, suggesting that chronic HBP activation may lead to LVH (43). Interestingly, both chronic glucose overload in the heart and aorta banding lead to increased UDP-N-acetylglucosamine, which has been associated with LVH (51). In both metabolic and physical models, LVH results in a similar pressure overload-induced hypertrophy pattern involving increased expression of ßMHC, the fetal isoform of MHC (51). Transcription factors NFAT (52), GATA4, and MEF2C (53) induce a cardiac hypertrophy gene expression program, e.g., inducing atrial (ANP) and B-type (BNP) natriuretic peptide mRNA expression, following their activation by O-GlcNAcylation. Consistent with the direct induction of HBP, pharmacological inhibition of GFAT in isolated cardiomyocytes prevents the mRNA induction of ANP and BNP under phenylephrin hypertrophic signaling. These findings clearly indicate that O-GlcNAcylation can induce hypertrophy through regulating gene expression; however, the direct involvement of this mechanism *in vivo* in the context of diabetes has not yet been described. Ding et al. aimed to identify the mechanism involved in cardiac hypertrophy in the diabetic heart (54) and found that in isolated cardiomyocytes, high-glucose exposure induced increases in cardiomyocyte size and ANP, BNP and ßMHC mRNA levels. This hypertrophic pattern was associated with elevated HBP activity and was reversed by HBP inhibition (55). The authors proposed that the HBP-induced hypertrophy was due to ERK1/2 and Cyclin D2 activation that paralleled the O-GlcNAcylation increase. In diabetic STZ rats, elevated O-GlcNAc levels have similarly been associated with a hypertrophic profile (of cardiomyocyte size and gene expression) and the induction of the ERK1/2 pathway (54). This work further suggests the involvement of O-GlcNAc in diabetic-associated LVH but does not explain how O-GlcNAcylation modulates the ERK1/2 pathway. Cyclin D2 activation by the transcription factor c-MYC has also been found to be involved in cardiac hypertrophy (56). Interestingly, c-MYC has an O-GlcNAcylation site (55), but the effect of its O-GlcNAcylation in the diabetic heart remains unknown.

Although NFAT and ERK1/2 activation have been found to be involved in O-GlcNAcylation-mediated hypertrophy, recent studies indicate that the relationships are complex. Gelinas et al. have shown that AMPK activation counteracts cardiomyocyte hypertrophy both *in vitro* and *in vivo* (57). Unexpectedly, AMPK activation did not prevent NFAT or ERK1/2 hypertrophic-associated induction but was required to lower HBP activity. Furthermore, AMPK activation led to the normalization of troponin T O-GlcNAcylation levels: Troponin T O-GlcNAcylated levels were elevated in the hypertrophic heart and reduced after AMPK activation. Previous work reported that in heart failure, increased troponin T O-GlcNAcylation was concomitant with reduced phosphorylation levels (58). Therefore, troponin T is potentially an important target of the HBP in hypertrophic heart or heart failure; however, to date, no relevant data are available for the diabetic heart. Further work is needed to determine whether troponin T O-GlcNAcylation is elevated in the diabetic heart.

In addition to its effects in cardiomyocytes, high-glucose exposure increases O-GlcNAcylation of the transcription factor Sp1 in rat cardiac fibroblasts. Chromatin immunoprecipitation experiments demonstrated that SP1 O-GlcNAcylation increases its ability to bind collagen 1 promoter and, in turn, to increase its expression, thereby contributing to hypertrophy-associated fibrosis (59).

CHRONIC HBP ACTIVATION IMPAIRS MITOCHONDRIAL FUNCTION

The diabetic heart displays an altered energetic substrate utilization profile, and mitochondrial dysfunction appears central in this feature. Notably, cardiac fibers isolated from patients with T2D but not those from obese patients display a disturbances in the mechanical properties associated with mitochondrial dysfunction (60). In rat neonatal cardiomyocytes, high-glucose exposure induces an increase in mitochondrial protein O-GlcNAc levels, which is reversed by OGA overexpression (61). Both mitochondrial complex I subunit NDUFA9 and the complex IV component COXI display elevated O-GlcNAc levels. Consistently, complex I and complex IV activities, O_2 consumption and ATP production were reduced in high-glucose exposed cardiomyocytes, and these reductions were reversed by OGA overexpression. These findings were confirmed in hearts from insulin-resistant rats, in which O-GlcNAcylation of NDUFA9, COXI, and VDAC, the voltage dependent anion channel, was increased (62). Mitochondrial activity is also regulated by the dynamic balance between fusion and fission. In cardiomyocytes, O-GlcNAcylation has been shown to increase the function of the mitochondrial fission regulator, DRP1 (63). Importantly, increased O-GlcNAcylated DRP1 levels are associated with mitochondrial fragmentation, which leads to reduced mitochondria activity. Such increases in DRP1 O-GlcNAcylated levels have also been observed *in vivo* in diabetic rat hearts.

Excessive mitochondrial O-GlcNAcylation was recently shown to compromise mitochondria integrity. In STZ-treated

mice, 8-oxoguanine DNA glycosylase (OGG1), a key enzyme in the mitochondrial DNA repair machinery, is modulated by O-GlcNAcylation (64). Although *Ogg1* expression is induced in diabetic hearts, its enzymatic activity is blunted. Using *in vitro* and *in vivo* approaches, researchers demonstrated that O-GlcNAcylation of OGG1 decreased its activity. Furthermore, these researchers showed that *in vivo* inhibition of O-GlcNAcylation improved mtDNA repair in the heart of STZ-treated mice (64).

Overall, growing evidence suggests that mitochondria are major sites for O-GlcNAcylation. Banerjee et al. revealed the dynamics of mitochondrial branching and hydrolysis of UDP-GlcNAc as well as its transport through the mitochondrial inner membrane in the T1D rat heart. The authors also showed that diabetes affects the mitochondrial levels of OGA and OGT and their localization and activity. Moreover, they identified that UDP-GlcNAc was actively imported within mitochondrial matrix through Pyrymidine Nucleotide Carrier (Pnc1). Furthermore, they modulated OGA and OGT in neonatal rat cardiomyocytes and showed that OGA but not OGT inhibition reduced ATP production and the oxygen consumption rate (65). In addition, a general proteomic analysis of cardiac mitochondria isolated from STZ-treated rats revealed that numerous proteins involved in many and varied biochemical processes such as pyruvate decarboxylation, fatty acid (CPT1) and Ca^{2+} transport, fatty acid oxidation, electron transport chain processes, and oxidative scavenging undergo the O-GlcNAc process (66). Identifying the precise role of each O-GlcNAcylation (for some proteins at different sites) is of interest to decipher the contribution of mitochondrial O-GlcNAc in diabetes-associated cardiac dysfunction.

ER STRESS, AUTOPHAGY AND THE HBP

Unresolved activation of the unfolded protein response (UPR), i.e., the endoplasmic reticulum (ER) stress response, has been observed in several metabolic complications, such as liver steatosis and insulin resistance (67, 68). Regarding DC, elevated ER stress has been reported (69, 70), but its exact contribution to DC physiopathology is not clear. After ischaemia/reperfusion injury, Wang et al. observed concomitant increases in key players involved in the HBP and UPR, such as spliced X-Box Binding Protein 1 (XBP1), the chaperone BIP and the pro-apoptotic transcription factor CHOP in heart lysates. At the mechanistic level, they demonstrated that XBP1 binds the GFAT1 promoter and activates its expression, but they did not observe an increase in XBP1 O-GlcNAcylation (71). Acute UPR activation appears to be protective during the acute induction of HBP by ischaemia/reperfusion. Further work is required to determine whether a common mechanism is activated in DC. It would be interesting to test whether ER stress induction can, in addition to hyperglycaemia, contribute to the chronic induction of HBP.

Several studies have observed a cross-talk between the UPR and autophagy that involves several key players, such as the elongation factor eIF2A (72–74). Autophagy is a cell process in which unused or defective cellular materials, such as unused/defective macromolecules or organelles, are degraded and recycled. It occurs via a complex pathway, the regulation of which is finely controlled by nutrient availability and hormonal status, that involves a high number of genes. In the heart, autophagy is associated with aging and several cardiac pathologies, such as myocardial infarction and ischaemia/reperfusion injury, cardiac hypertrophy, cardiotoxicity and diabetic cardiomyopathies [for a recent review, see (75)]. Regarding type 1 and type 2 diabetes-associated cardiomyopathies, the role of autophagy remains debated. In T1D animal models, autophagy has been described to be either protective (76–78) or deleterious in the heart (78). Autophagy is repressed in the heart of different T2D mice models (76, 79, 80), where its induction appears beneficial (76). However, other studies have reported unchanged and elevated levels of myocardial autophagy in HFD models (81) and fructose-induced insulin resistance (82), respectively. Autophagy is also upregulated in the heart of patients with T2D (83). Such different levels of autophagy observed in both T1D and T2D might be explained by the variation in the models used; additional studies are needed to decipher whether autophagy is a beneficial or a deleterious process in the diabetic heart. Nevertheless, autophagy was shown to be blunted in cardiomyocytes isolated from *db/db* mice, and this blunting was reversed by HBP inhibition (80). Interestingly, in the hepatocyte cell-line HepG2, autophagy induction by mTOR inhibition resulted in HBP inhibition, further suggesting a link between these two pathways. Taken together, several elements suggest potential cross-talk among ER stress, autophagy and HBP, but their relationships in the context of DC warrant further investigation.

TARGETING EXCESSIVE O-GLCNACYLATION AS A THERAPEUTIC STRATEGY

Data from the literature strongly suggest that excessive O-GlcNAcylation during chronic HBP activation affects Ca^{2+} handling, contractile properties, and mitochondrial function and promotes stress signaling, such as that involved in hypertrophy and ER stress (impacted cardiac physio-pathological processes and proteins are highlighted in **Figure 1** and **Table 1**). Therefore, excessive O-GlcNAcylation might be considered an innovative target to treat cardiac dysfunction associated with diabetes. Interestingly, in most of the above-described experiments with isolated cardiomyocytes, pharmacological inhibition of GFAT or OGT was used to modulate the HBP. Pharmacological modulation of the HBP *in vivo* is more challenging. The first proof of concept that targeting the HBP is beneficial was achieved in STZ mice with cardiac overexpression of OGA: The reduction in O-GlcNAcylated protein levels concomitantly improved the contractile properties (38). At the mechanistic level, the adenoviral vector-mediated OGA overexpression was shown to improve Ca^{2+} handling

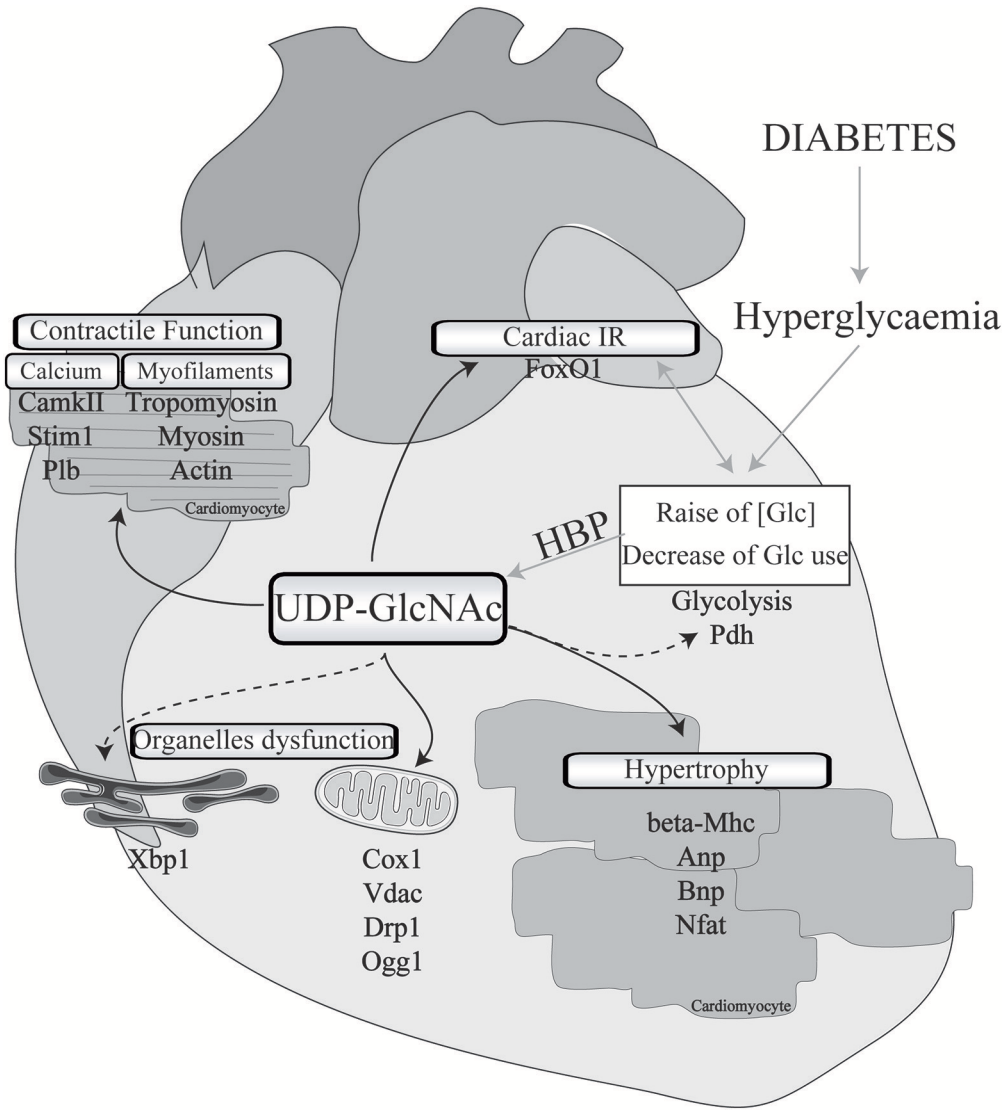

FIGURE 1 | Implication of O-GlcNAcylation in diabetes-associated cardiomyopathies. Cardiac physio-pathological processes that have been shown to be affected by O-GlcNAc during diabetes are highlighted with black arrows. Pathways or proteins that have been shown to be modulated by O-GlcNAc in non-diabetic cardiac injury or in other organs with a diabetic background are indicated with black dotted arrows. IR, insulin resistance; Glc, glucose; HBP, hexosamine biosynthesis pathway; Pdh, pyruvate dehydrogenase; Mhc, myosin, heavy polypeptide; Anp, natriuretic peptide type A; Bnp, natriuretic peptide type B; Nfat, nuclear factor of activated T-cells; Cox1, cytochrome c oxydase subunit I; Vdac, voltage-dependent anion channel; Drp1, dynamin-related protein 1; Ogg1, 8-oxoguanine DNA-glycosylase 1; Xbp1, X-box binding protein 1; CamkII, calcium/calmodulin-dependent protein kinase II; Stim1, stromal interaction molecule 1; Plb, phospholamban; FoxO1, forkhead box O1.

and to restore phospholamban phosphorylation levels. Such a beneficial effect on Ca^{2+} handling was confirmed in T2D mice, where inducible overexpression of OGA led to improvements in the LV properties assessed by normalization of the fractional shortening (40). Another way to modulate OGA expression is to use a microRNA-539 inhibitor (84). In a post-myocardial infarction HF mouse model, OGA mRNA levels were found to be reduced in association with the induction of miRNA-539. In neonatal cardiomyocytes, the overexpression of miRNA-539 suppressed OGA expression and consequently increased general O-GlcNAc levels, whereas an miRNA-539 inhibitor rescued OGA protein expression and restored O-GlcNAcylation (84). It would be very interesting to study anti-miR-539 in a T2D mouse model and its effects on the HBP and cardiac function.

Genetic deletions of OGT have also been used to modulate the HBP. As total KO for OGT is lethal, Watson et al. used constitutive cardio-specific deletion of OGT. They reported only 12% survival and the surviving animals displayed dilated cardiomyopathy and heart failure (reduced ejection fraction and cardiac output) (85). The same research group developed an inducible cardio-specific deletion of OGT (30, 85), but to our

TABLE 1 | O-GlcNAcylated targets in the diabetic heart.

Protein	O-GlcNAcylation	Physiological effect	Effect on activity
Phospholamban	Yes-S16	E-C alteration	Decrease
CAMKII	Yes-S279	Increased Ca2+ spark frequency	Increase
MHC	Yes-S844, S1471, S1472, T1601, S1917	Reduced myofilament calcium sensitivity	Decrease
Actin	Yes-T326	Reduced myofilament calcium sensitivity	Decrease
aTropomyosin	Yes-S87	Reduced myofilament calcium sensitivity	Decrease
Nav1.5	Yes	Arrhythmia	Decrease
NFAT	No	Hypertrophy	Increase
GATA4	Yes	Hypertrophy	Increase
MEF2C	Yes	Hypertrophy	Increase
SP1	Yes	Collagen over-production	Increase
NDUFA9	Yes	Reduced mitochondria activity	Decrease
COXI	Yes	Reduced mitochondria activity	Decrease
VDAC	Yes	Reduced mitochondria activity	Decrease
CPT1B	Yes S180	Reduced mitochondria activity	Decrease
DRP1	Yes T585, T586	Fragmentation/Reduced mitochondria activity	Increase
OGG1	Yes	Alteration of mitochondria integrity	Decrease
FOXO1	Yes	Association with insulin resistance	?

These proteins display elevated O-GlcNAc level in the diabetic heart. The table indicates whether formal demonstration of O-GlcNAcylation (IP/WB of the O-GlcNAc form or spectrometry) has been made, and, when known, the O-GlcNAc sites. The physiological effects of elevated O-GlcNAc levels in DC and the effects on target activity are listed.

knowledge, this model has not been applied in the context of DC. Such an investigation is crucial as a proof-of-concept test evaluating whether OGT alone is a suitable target.

In addition to the effects of direct HBP modulation on cardiac dysfunction, the effects of other therapeutic interventions on cardiac O-GlcNAc levels highlight the potential therapeutic value of modulating the HBP. As mentioned earlier, in a mouse model of angiotensin II-induced cardiac hypertrophy, AMPK activation exerts its beneficial effect on the heart by reducing HBP, especially troponin T-O-GlcNAc levels (57). Importantly, these effects are lost under treatment with NbutGt, an OGA inhibitor, which indicates that the effects are specific and O-GlcNAc dependent. Again, it would be interesting to conduct similar experiments in T2D mouse models.

As mentioned earlier, in our mouse model of congenital generalized lipodytrophy, we hypothesized that glucotoxicity is central to the cardiac phenotype. Treatment of those mice with dapagliflozin, an SGLT2 inhibitor, normalized glycaemia and, concomitantly, O-GlcNAc protein levels and cardiac function (44). These results are encouraging, although a formal demonstration that HBP normalization contributes to the cardiac benefits has yet to be made.

It has been shown that exercise training mitigates chronic activation of the HBP in type 1 diabetic rats. Two months of daily swim training improved rat heart rate and normalized the protein levels of the calcium pump SERCA2. These improvements were associated with a reduction in OGT activity, a decrease in total O-GlcNAcylated protein levels and a reduction in O-GlcNAcylated Sp1 level (86). These findings raise the hypothesis that the beneficial effect of training on cardiac function might be, at least partially, attributable to an effect of exercise on the HBP. These interesting finding have been challenged by another report showing that exercise increased the general levels of O-GlcNAcylation in *db/db* mice (87). Further studies are needed to describe the potential benefits of exercise on cardiac HBP chronic activation in diabetes.

FUTURE DIRECTIONS AND CONCLUSIONS

Fifteen years ago, chronic activation of the HBP was described as a hallmark of glucose overload in the diabetic heart. In the following years, excessive O-GlcNAcylation has been shown to impair calcium handling and contractile properties, promote hypertrophy, and compromise mitochondrial functions. Several direct targets of O-GlcNAcylation, including phospholamban, CAMKII and troponin I, appear to play central roles in the deleterious effect of HBP chronic activation. Interestingly, O-GlcNAc often occurs at the same or nearby Ser/Thr amino acid residues as phosphorylation, and competition may exist between the two phenomena to control the activity of important players in heart activity and metabolism. Such interplay has been extensively reviewed previously (88, 89).

Despite the fact that DC is associated with a state of insulin resistance, few studies have highlighted the effect of the HBP on insulin resistance. Whereas, O-GlcNAcylation of several insulin-signaling key players (such as AKT, PT1B, and PDK1) has been shown to be associated with insulin resistance in the liver (90–93), the effect of the HBP on insulin signaling in the heart has not been adequately addressed. Recently, we reported that FOXO1 was O-GlcNAcylated in the heart of lipodystrophic diabetic mice and that SGLT2i treatment reversed this increase (44). O-GlcNAcylation of FOXO1 increases its activity. FOXO1 is believed to be a key mediator of glucotoxicity in different organs (94). Notably, it has been found to be involved in

metabolically induced cardiac dysfunction, especially insulin resistance. FOXO1 knock-down was shown to be protective in a model of diet-induced cardiomyopathy (95, 96). Our work revealed that FOXO1 O-GlcNAcylation is associated with heart insulin resistance and cardiac dysfunction. In our study, the levels of O-GlcNAcylated AKT2 appeared unchanged. Further studies are needed to explore whether FOXO1 O-GlcNAcylation is a common hallmark in DC, whether it occurs in other heart samples from T2D models, and whether other insulin-signaling players are O-GlcNAcylated in DC. The question that needs to be addressed is whether O-GlcNAcylation is solely a mediator of diabetic associated glucotoxicity in DC or whether it also disturbs insulin sensitivity and thus promotes cardiac insulin resistance?

As chronic HBP activation occurs in DC concomitantly with other metabolic abnormalities such as lipotoxicity, ROS production, AGE accumulation and other cardiac pathological manifestations such as fibrosis, it is difficult to determine its direct effects on cardiac function. *In vitro* studies with glucosamine or PUGNAC (OGA inhibitor) treatment have indicated that the HBP not only is correlated with cardiomyocyte dysfunction under chronic hyperglycaemia but can also induce associated abnormalities (e.g., in E-C coupling and contractile properties). However, *in vivo* evidence that chronic HBP can by itself cause DC remains weak, and to the best of our knowledge, there are no publications showing the effect of OGT overexpression or OGA deletion in the heart *in vivo*. Nonetheless, several attempts to suppress the HBP in DC, either by pharmacological approaches, mainly *in vitro*, or by genetic overexpression *in vivo*, suggest that excessive O-GlcNAcylation alone might trigger DC. In addition, in SKO mice, we reported DC associated only with HBP chronic activation, i.e., with HBP chronic activation in absence of any other DC hallmark. Altogether, these observations raise the question of whether the HBP can be modulated as a therapeutic target to treat DC. Several issues should be addressed. First, the HBP is a very balanced pathway, and the modulation of OGT might induce a feedback loop by OGA and *vice versa*. This possibility suggests moderate modulation be attempted. Second, the HBP is a very broad pathway that operates in all tissues; thus, the question of tissue specificity should be addressed. Finally, although pharmacological interventions have been used *in vitro*, they have not been widely used *in vivo*. Genetic interventions seem to be the most suitable way to modulate the HBP. For these reasons, a targeted approach could be considered. Consideration should be given to the possibility of targeting the O-GlcNAcylation of specific proteins in specific tissues, which would require the identification of HBP targets in the diabetic heart.

AUTHOR CONTRIBUTIONS

XP wrote the manuscript and supervise the work between the authors. SD, JM, and BC wrote the manuscript.

ACKNOWLEDGMENTS

SD is supported by the Fondation pour la Recherche Médicale (FRM). This research was supported by the FRM and the Fondation de France (FDF). Graphical design: The heart background present in **Figure 1** is modified from an artwork downloaded in Servier Medical Art website. http://smart.servier.com/.

REFERENCES

1. Nichols GA, Gullion CM, Koro CE, Ephross SA, Brown JB. The incidence of congestive heart failure in type 2 diabetes: an update. *Diabetes Care* (2004) 27:1879–84. doi: 10.2337/diacare.27.8.1879
2. Norhammar A, Bodegård J, Nyström T, Thuresson M, Eriksson JW, Nathanson D. Incidence, prevalence and mortality of type 2 diabetes requiring glucose-lowering treatment, and associated risks of cardiovascular complications: a nationwide study in Sweden, 2006-2013. *Diabetologia* (2016) 59:1692–701. doi: 10.1007/s00125-016-3971-y
3. Nichols GA, Hillier TA, Erbey JR, Brown JB. Congestive heart failure in type 2 diabetes: prevalence, incidence, and risk factors. *Diabetes Care* (2001) 24:1614–9. doi: 10.2337/diacare.24.9.1614
4. Rubler S, Dlugash J, Yuceoglu YZ, Kumral T, Branwood AW, Grishman A. New type of cardiomyopathy associated with diabetic glomerulosclerosis. *Am J Cardiol.* (1972) 30:595–602. doi: 10.1016/0002-9149(72)90595-4
5. Taegtmeyer H, McNulty P, Young ME. Adaptation and maladaptation of the heart in diabetes: Part I: general concepts. *Circulation* (2002) 105:1727–33. doi: 10.1161/01.CIR.0000012466.50373.E8
6. Young ME, McNulty P, Taegtmeyer H, Adaptation and maladaptation of the heart in diabetes: Part II: potential mechanisms. *Circulation* (2002) 105:1861–70. doi: 10.1161/01.CIR.0000012467.61045.87
7. Iribarren C, Karter AJ, Go AS, Ferrara A, Liu JY, Sidney S, et al. Glycemic control and heart failure among adult patients with diabetes. *Circulation* (2001) 103:2668–73. doi: 10.1161/01.CIR.103.22.2668
8. Elder DH, Singh JS, Levin D, Donnelly LA, Choy AM, George J, et al. Mean HbA1c and mortality in diabetic individuals with heart failure: a population cohort study. *Eur J Heart Fail.* (2016) 18:94–102. doi: 10.1002/ejhf.455
9. Bertrand L, Horman S, Beauloye C, Vanoverschelde JL. Insulin signalling in the heart. *Cardiovasc Res* .(2008) 79:238–48. doi: 10.1093/cvr/cvn093
10. Wende AR, Symons JD, Abel ED. Mechanisms of lipotoxicity in the cardiovascular system. *Curr Hypertens Rep.* (2012) 14:517–31. doi: 10.1007/s11906-012-0307-2
11. Labbé SM, Grenier-Larouche T, Noll C, Phoenix S, Guérin B, Turcotte EE, et al. Increased myocardial uptake of dietary fatty acids linked to cardiac dysfunction in glucose-intolerant humans. *Diabetes* (2012) 61:2701–10. doi: 10.2337/db11-1805
12. Drosatos K, Schulze PC. Cardiac lipotoxicity: molecular pathways and therapeutic implications. *Curr Heart Fail Rep.* (2013) 10:109–21. doi: 10.1007/s11897-013-0133-0
13. Mazumder PK, O'Neill BT, Roberts MW, Buchanan J, Yun UJ, Cooksey RC, et al. Impaired cardiac efficiency and increased fatty acid oxidation in insulin-resistant ob/ob mouse hearts. *Diabetes* (2004) 53:2366–74. doi: 10.2337/diabetes.53.9.2366
14. Taegtmeyer H, Beauloye C, Harmancey R, Hue L. Insulin resistance protects the heart from fuel overload in dysregulated metabolic states. *Am J Physiol Heart Circ Physiol.* (2013) 305:H1693–7. doi: 10.1152/ajpheart.00854.2012
15. Cai L, Li W, Wang G, Guo L, Jiang Y, Kang YJ. Hyperglycemia-induced apoptosis in mouse myocardium: mitochondrial cytochrome C-mediated caspase-3 activation pathway. *Diabetes* (2002) 51:1938–48. doi: 10.2337/diabetes.51.6.1938

16. Brahma MK, Pepin ME, Wende AR. My Sweetheart is broken: role of glucose in diabetic cardiomyopathy. *Diabetes Metab J.* (2017) 41:1–9. doi: 10.4093/dmj.2017.41.1.1
17. Kolwicz SC, Tian R. Glucose metabolism and cardiac hypertrophy. *Cardiovasc Res.* (2011) 90:194–201. doi: 10.1093/cvr/cvr071
18. Bendall JK, Damy T, Ratajczak P, Loyer X, Monceau V, Marty I, et al. Role of myocardial neuronal nitric oxide synthase-derived nitric oxide in beta-adrenergic hyporesponsiveness after myocardial infarction-induced heart failure in rat. *Circulation* (2004) 110:2368–75. doi: 10.1161/01.CIR.0000145160.04084.AC
19. Giacco F, Brownlee M. Oxidative stress and diabetic complications. *Circ Res.* (2010) 107:1058–70. doi: 10.1161/CIRCRESAHA.110.223545
20. Brownlee M. The pathobiology of diabetic complications: a unifying mechanism. *Diabetes* (2005) 54:1615–25. doi: 10.2337/diabetes.54.6.1615
21. Chatham JC, Marchase RB. The role of protein O-linked beta-N-acetylglucosamine in mediating cardiac stress responses. *Biochim Biophys Acta* (2010) 1800:57–66. doi: 10.1016/j.bbagen.2009.07.004
22. Dassanayaka S, Jones SP. O-GlcNAc and the cardiovascular system. *Pharmacol Ther.* (2014) 142:62–71. doi: 10.1016/j.pharmthera.2013.11.005
23. Champattanachai V, Marchase RB, Chatham JC. Glucosamine protects neonatal cardiomyocytes from ischemia-reperfusion injury via increased protein-associated O-GlcNAc. *Am J Physiol Cell Physiol.* (2007) 292:C178–87. doi: 10.1152/ajpcell.00162.2006
24. Fulop N, Zhang Z, Marchase RB, Chatham JC. Glucosamine cardioprotection in perfused rat hearts associated with increased O-linked N-acetylglucosamine protein modification and altered p38 activation. *Am J Physiol Heart Circ Physiol.* (2007) 292:H2227–36. doi: 10.1152/ajpheart.01091.2006
25. Yang S, Zou LY, Bounelis P, Chaudry I, Chatham JC, Marchase RB. Glucosamine administration during resuscitation improves organ function after trauma hemorrhage. *Shock* (2006) 25:600–7. doi: 10.1097/01.shk.0000209563.07693.db
26. Not LG, Marchase RB, Fulop N, Brocks CA, Chatham JC. Glucosamine administration improves survival rate after severe hemorrhagic shock combined with trauma in rats. *Shock* (2007) 28:345–52. doi: 10.1097/shk.0b013e3180487ebb
27. Ngoh GA, Watson LJ, Facundo HT, Jones SP. Augmented O-GlcNAc signaling attenuates oxidative stress and calcium overload in cardiomyocytes. *Amino Acids* (2011) 40:895–911. doi: 10.1007/s00726-010-0728-7
28. Ngoh GA, Watson LJ, Facundo HT, Dillmann W, Jones SP. Non-canonical glycosyltransferase modulates post-hypoxic cardiac myocyte death and mitochondrial permeability transition. *J Mol Cell Cardiol.* (2008) 45:313–25. doi: 10.1016/j.yjmcc.2008.04.009
29. Mailleux F, Gélinas R, Beauloye C, Horman S, Bertrand L. O-GlcNAcylation, enemy or ally during cardiac hypertrophy development? *Biochim Biophys Acta* (2016) 1862:2232–43. doi: 10.1016/j.bbadis.2016.08.012
30. Watson LJ, Facundo HT, Ngoh GA, Ameen M, Brainard RE, Lemma KM, et al. O-linked β-N-acetylglucosamine transferase is indispensable in the failing heart. *Proc Natl Acad Sci USA.* (2010) 107:17797–802. doi: 10.1073/pnas.1001907107
31. Marshall S, Bacote V, Traxinger RR. Discovery of a metabolic pathway mediating glucose-induced desensitization of the glucose transport system. Role of hexosamine biosynthesis in the induction of insulin resistance. *J Biol Chem.* (1991) 266:4706–12.
32. Hawkins M, Barzilai N, Liu R, Hu M, Chen W, Rossetti L. Role of the glucosamine pathway in fat-induced insulin resistance. *J Clin Invest.* (1997) 99:2173–82. doi: 10.1172/JCI119390
33. Yki-Jarvinen H, Vogt C, Iozzo P, Pipek R, Daniels MC, Virkamaki A, et al. UDP-N-acetylglucosamine transferase and glutamine: fructose 6-phosphate amidotransferase activities in insulin-sensitive tissues. *Diabetologia* (1997) 40:76–81. doi: 10.1007/s001250050645
34. Ren J, Gintant GA, Miller RE, Davidoff AJ. High extracellular glucose impairs cardiac E-C coupling in a glycosylation-dependent manner. *Am J Physiol.* (1997) 273:H2876–83. doi: 10.1152/ajpheart.1997.273.6.H2876
35. Pang Y, Hunton DL, Bounelis P, Marchase RB. Hyperglycemia inhibits capacitative calcium entry and hypertrophy in neonatal cardiomyocytes. *Diabetes* (2002) 51:3461–7. doi: 10.2337/diabetes.51.12.3461
36. Clark RJ, McDonough PM, Swanson E, Trost SU, Suzuki M, Fukuda M, et al. Diabetes and the accompanying hyperglycemia impairs cardiomyocyte calcium cycling through increased nuclear O-GlcNAcylation. *J Biol Chem.* (2003) 278:44230–7. doi: 10.1074/jbc.M303810200
37. Pang Y, Bounelis P, Chatham JC, Marchase RB. Hexosamine pathway is responsible for inhibition by diabetes of phenylephrine-induced inotropy. *Diabetes* (2004) 53:1074–81. doi: 10.2337/diabetes.53.4.1074
38. Hu Y, Belke D, Suarez J, Swanson E, Clark R, Hoshijima M, et al. Adenovirus-mediated overexpression of O-GlcNAcase improves contractile function in the diabetic heart. *Circ Res.* (2005) 96:1006–13. doi: 10.1161/01.RES.0000165478.06813.58
39. Fülöp N, Mason MM, Dutta K, Wang P, Davidoff AJ, Marchase RB, et al. Impact of Type 2 diabetes and aging on cardiomyocyte function and O-linked N-acetylglucosamine levels in the heart. *Am J Physiol Cell Physiol.* (2007) 292:C1370–1378. doi: 10.1152/ajpcell.00422.2006
40. Fricovsky ES, Suarez J, Ihm SH, Scott BT, Suarez-Ramirez JA, Banerjee I, et al. Excess protein O-GlcNAcylation and the progression of diabetic cardiomyopathy. *Am J Physiol Regul Integr Comp Physiol.* (2012) 303:R689–99. doi: 10.1152/ajpregu.00548.2011
41. Medford HM, Chatham JC, Marsh SA. Chronic ingestion of a Western diet increases O-linked-beta-N-acetylglucosamine (O-GlcNAc) protein modification in the rat heart. *Life Sci.* (2012) 90:883–8. doi: 10.1016/j.lfs.2012.04.030
42. Marsh SA LJ., Dell'Italia, Chatham JC. Activation of the hexosamine biosynthesis pathway and protein O-GlcNAcylation modulate hypertrophic and cell signaling pathways in cardiomyocytes from diabetic mice. *Amino Acids* (2011) 40:819–28. doi: 10.1007/s00726-010-0699-8
43. Lunde IG, Aronsen JM, Kvaloy H, Qvigstad E, Sjaastad I, Tonnessen T, et al. Cardiac O-GlcNAc signaling is increased in hypertrophy and heart failure. *Physiol Genomics* (2012) 44:162–72. doi: 10.1152/physiolgenomics.00016.2011
44. Joubert M, Jagu B, Montaigne D, Marechal X, Tesse A, Ayer A, et al. The sodium-glucose cotransporter 2 inhibitor dapagliflozin prevents cardiomyopathy in a diabetic lipodystrophic mouse model. *Diabetes* (2017) 66:1030–40. doi: 10.2337/db16-0733
45. Yokoe S, Asahi M, Takeda T, Otsu K, Taniguchi N, Miyoshi E, et al. Inhibition of phospholamban phosphorylation by O-GlcNAcylation: implications for diabetic cardiomyopathy. *Glycobiology* (2010) 20:1217–26. doi: 10.1093/glycob/cwq071
46. Erickson JR, Pereira L, Wang L, Han G, Ferguson A, Dao K, et al. Diabetic hyperglycaemia activates CaMKII and arrhythmias by O-linked glycosylation. *Nature* (2013) 502:372–6. doi: 10.1038/nature12537
47. Zhu-Mauldin X, Marsh SA, Zou L, Marchase RB, Chatham JC. Modification of STIM1 by O-linked N-acetylglucosamine (O-GlcNAc) attenuates store-operated calcium entry in neonatal cardiomyocytes. *J Biol Chem.* (2012) 287:39094–106. doi: 10.1074/jbc.M112.383778
48. Ramirez-Correa GA, Jin W, Wang Z, Zhong X, Gao WD, Dias WB, et al. O-linked GlcNAc modification of cardiac myofilament proteins: a novel regulator of myocardial contractile function. *Circ Res.* (2008) 103:1354–8. doi: 10.1161/CIRCRESAHA.108.184978
49. Ramirez-Correa GA, Ma J, Slawson C, Zeidan Q, Lugo-Fagundo NS, Xu M, et al. Removal of abnormal myofilament O-GlcNAcylation restores Ca2+ sensitivity in diabetic cardiac muscle. *Diabetes* (2015) 64:3573–87. doi: 10.2337/db14-1107
50. Yu P, Hu L, Xie J, Chen S, Huang L, Xu Z, et al. O-GlcNAcylation of cardiac Nav1.5 contributes to the development of arrhythmias in diabetic hearts. *Int J Cardiol.* (2018) 260:74–81. doi: 10.1016/j.ijcard.2018.02.099
51. Young ME, Yan J, Razeghi P, Cooksey RC, Guthrie PH, Stepkowski SM, et al. Proposed regulation of gene expression by glucose in rodent heart. *Gene Regul Syst Bio* (2007) 1:251–62. doi: 10.4137/GRSB.S222
52. Facundo HT, Brainard RE, Watson LJ, Ngoh GA, Hamid T, Prabhu SD, et al. O-GlcNAc signaling is essential for NFAT-mediated transcriptional reprogramming during cardiomyocyte hypertrophy. *Am J Physiol Heart Circ Physiol.* (2012) 302:H2122–30. doi: 10.1152/ajpheart.00775.2011
53. Cannon MVH, Silljé HW, Sijbesma JWA, Vreeswijk-Baudoin I, Ciapaite JB., et al. Cardiac LXRα protects against pathological cardiac hypertrophy and dysfunction by enhancing glucose uptake and utilization. *EMBO Mol Med.* (2015) 7:1229–1243. doi: 10.15252/emmm.201404669

54. Ding F, Yu L, Wang M, Xu S, Xia Q, Fu G. O-GlcNAcylation involvement in high glucose-induced cardiac hypertrophy via ERK1/2 and cyclin D2. *Amino Acids* (2013) 45:339–49. doi: 10.1007/s00726-013-1504-2
55. Chou TY, Dang CV, Hart GW. Glycosylation of the c-Myc transactivation domain. *Proc Natl Acad Sci USA*. (1995) 92:4417–21. doi: 10.1073/pnas.92.10.4417
56. Zhong W, Mao S, Tobis S, Angelis E, Jordan MC, Roos KP, et al. Hypertrophic growth in cardiac myocytes is mediated by Myc through a Cyclin D2-dependent pathway. *EMBO J.* (2006) 25:3869–79. doi: 10.1038/sj.emboj.7601252
57. Gélinas R, Mailleux F, Dontaine J, Bultot L, Demeulder B, Ginion A, et al. AMPK activation counteracts cardiac hypertrophy by reducing O-GlcNAcylation. *Nat Commun*. (2018) 9:374. doi: 10.1038/s41467-017-02795-4
58. Dubois-Deruy E, Belliard A, Mulder P, Bouvet M, Smet-Nocca C, Janel S, et al. Interplay between troponin T phosphorylation and O-N-acetylglucosaminylation in ischaemic heart failure. *Cardiovasc Res.* (2015) 107:56–65. doi: 10.1093/cvr/cvv136
59. Aguilar H, Fricovsky E, Ihm S, Schimke M, Maya-Ramos L, Aroonsakool N, et al. Role for high-glucose-induced protein O-GlcNAcylation in stimulating cardiac fibroblast collagen synthesis. *Am J Physiol Cell Physiol.* (2014) 306:C794–804. doi: 10.1152/ajpcell.00251.2013
60. Montaigne D, Marechal X, Coisne A, Debry N, Modine T, Fayad G, et al. Myocardial contractile dysfunction is associated with impaired mitochondrial function and dynamics in type 2 diabetic but not in obese patients. *Circulation* (2014) 130:554–564. doi: 10.1161/CIRCULATIONAHA.113.008476
61. Hu Y, Suarez J, Fricovsky E, Wang H, Scott BT, Trauger SA, et al. Increased enzymatic O-GlcNAcylation of mitochondrial proteins impairs mitochondrial function in cardiac myocytes exposed to high glucose. *J Biol Chem.* (2009) 284:547–55. doi: 10.1074/jbc.M808518200
62. Johnsen VL, Belke DD, Hughey CC, Hittel DS, Hepple RT, Koch LG, et al. Enhanced cardiac protein glycosylation (O-GlcNAc) of selected mitochondrial proteins in rats artificially selected for low running capacity. *Physiol Genomics* (2013) 45:17–25. doi: 10.1152/physiolgenomics.00111.2012
63. Gawlowski T, Suarez J, Scott B, Torres-Gonzalez M, Wang H, Schwappacher R, et al. Modulation of dynamin-related protein 1 (DRP1) function by increased O-linked-β-N-acetylglucosamine modification (O-GlcNAc) in cardiac myocytes. *J Biol Chem.* (2012) 287:30024–34. doi: 10.1074/jbc.M112.390682
64. Cividini F, Scott BT, Dai A, Han W, Suarez J, Diaz-Juarez J, et al. O-GlcNAcylation of 8-oxoguanine DNA glycosylase (Ogg1) impairs oxidative mitochondrial DNA lesion repair in diabetic hearts. *J Biol Chem.* (2016) 291:26515–28. doi: 10.1074/jbc.M116.754481
65. Banerjee PS, Ma J, Hart GW. Diabetes-associated dysregulation of O-GlcNAcylation in rat cardiac mitochondria. *Proc Natl Acad Sci USA*. (2015) 112:6050–5. doi: 10.1073/pnas.1424017112
66. Ma J, Banerjee P, Whelan SA, Liu T, Wei AC, Ramirez-Correa G, et al. Comparative proteomics reveals dysregulated mitochondrial O-GlcNAcylation in diabetic hearts. *J Proteome Res.* (2016) 15, 2254–2264. doi: 10.1021/acs.jproteome.6b00250
67. Baiceanu A, Mesdom P, Lagouge M, Foufelle F. Endoplasmic reticulum proteostasis in hepatic steatosis. *Nat Rev Endocrinol.* (2016) 12:710–22. doi: 10.1038/nrendo.2016.124
68. Hotamisligil GS. Endoplasmic reticulum stress and the inflammatory basis of metabolic disease. *Cell* (2010) 140:900–917. doi: 10.1016/j.cell.2010.02.034
69. Gray S, Kim JK. New insights into insulin resistance in the diabetic heart. *Trends Endocrinol Metab.* (2011) 22:394–403. doi: 10.1016/j.tem.2011.05.001
70. Miki T, Miura T, Hotta H, Tanno M, Yano T, Sato T, et al. Endoplasmic reticulum stress in diabetic hearts abolishes erythropoietin-induced myocardial protection by impairment of phospho-glycogen synthase kinase-3beta-mediated suppression of mitochondrial permeability transition. *Diabetes* (2009) 58:2863–72. doi: 10.2337/db09-0158
71. Wang ZV, Deng Y, Gao N, Pedrozo Z, Li DL, Morales CR, et al. Spliced X-box binding protein 1 couples the unfolded protein response to hexosamine biosynthetic pathway. *Cell* (2014) 156, 1179–1192. doi: 10.1016/j.cell.2014.01.014
72. Wiersma M, Meijering RAM, Qi XY, Zhang D, Liu T, Hoogstra-Berends F, et al. (2017). Endoplasmic reticulum stress is associated with autophagy and cardiomyocyte remodeling in experimental and human atrial fibrillation. *J Am Heart Assoc.* 6:e006458. doi: 10.1161/JAHA.117.006458
73. Petrovski G, Das S, Juhasz B, Kertesz A, Tosaki A, Das DK. Cardioprotection by endoplasmic reticulum stress-induced autophagy. *Antioxid Redox Signal* (2011) 14:2191–200. doi: 10.1089/ars.2010.3486
74. Jang I, Kim HB, Seo H, Kim JY, Choi H, Yoo JS, et al. O-GlcNAcylation of eIF2alpha regulates the phospho-eIF2alpha-mediated ER stress response. *Biochim Biophys Acta* (2015) 1853:1860–9. doi: 10.1016/j.bbamcr.2015.04.017
75. Lampert MA, Gustafsson AB. Balancing autophagy for a healthy heart. *Curr Opin Physiol.* (2018) 1:21–6. doi: 10.1016/j.cophys.2017.11.001
76. Kanamori H, Takemura G, Goto K, Tsujimoto A, Mikami A, Ogino A, et al. Autophagic adaptations in diabetic cardiomyopathy differ between type 1 and type 2 diabetes. *Autophagy* (2015) 11:1146–60. doi: 10.1080/15548627.2015.1051295
77. Zhang J, Cheng Y, Gu J, Wang S, Zhou S, Wang Y, et al. Fenofibrate increases cardiac autophagy via FGF21/SIRT1 and prevents fibrosis and inflammation in the hearts of Type 1 diabetic mice. *Clin Sci.* (2016) 130:625–41. doi: 10.1042/CS20150623
78. Xu X, Kobayashi S, Chen K, Timm D, Volden P, Huang Y, et al. Diminished autophagy limits cardiac injury in mouse models of type 1 diabetes. *J Biol Chem.* (2013) 288:18077–92. doi: 10.1074/jbc.M113.474650
79. Xu X, Ren J. Macrophage migration inhibitory factor (MIF) knockout preserves cardiac homeostasis through alleviating Akt-mediated myocardial autophagy suppression in high-fat diet-induced obesity. *Int. J. Obesity* (2014) 39:387. doi: 10.1038/ijo.2014.174
80. Marsh SA, Powell PC, Dell'italia LJ, Chatham JC. Cardiac O-GlcNAcylation blunts autophagic signaling in the diabetic heart. *Life Sci.* (2013) 92:648–656. doi: 10.1016/j.lfs.2012.06.011
81. French CJ, Tarikuz Zaman A K. L., McElroy-Yaggy, Neimane DK, Sobel BE. Absence of altered autophagy after myocardial ischemia in diabetic compared with nondiabetic mice. *Coronary Artery Dis.* (2011) 22:479–483. doi: 10.1097/MCA.0b013e32834a3a71
82. Mellor KM, Bell JR, Young MJ, Ritchie RH L, Delbridge MD. Myocardial autophagy activation and suppressed survival signaling is associated with insulin resistance in fructose-fed mice. *J Mol Cell Cardiol.* (2011) 50:1035–1043. doi: 10.1016/j.yjmcc.2011.03.002
83. Munasinghe PE, Riu F, Dixit P, Edamatsu M, Saxena P, Hamer NS, et al. Katare R. Type-2 diabetes increases autophagy in the human heart through promotion of Beclin-1 mediated pathway. *Int J Cardiol.* (2016) 202:13–20. doi: 10.1016/j.ijcard.2015.08.111
84. Muthusamy S, DeMartino AM, Watson LJ, Brittian KR, Zafir A, Dassanayaka S, et al. MicroRNA-539 is up-regulated in failing heart, and suppresses O-GlcNAcase expression. *J Biol Chem.* (2014) 289:29665–76. doi: 10.1074/jbc.M114.578682
85. Watson LJ, Long BW, DeMartino AM, Brittian KR, Readnower RD, Brainard RE, et al. Cardiomyocyte Ogt is essential for postnatal viability. *Am J Physiol Heart Circ Physiol.* (2014) 306:H142–53. doi: 10.1152/ajpheart.00438.2013
86. Bennett CE, Johnsen VL, Shearer J, Belke DD. Exercise training mitigates aberrant cardiac protein O-GlcNAcylation in streptozotocin-induced diabetic mice. *Life Sci.* (2013) 92:657–63. doi: 10.1016/j.lfs.2012.09.007
87. Cox EJ, Marsh SA. Exercise and diabetes have opposite effects on the assembly and O-GlcNAc modification of the mSin3A/HDAC1/2 complex in the heart. *Cardiovasc Diabetol.* (2013) 12:101. doi: 10.1186/1475-2840-12-101
88. Hart GW, Slawson C, Ramirez-Correa G, Lagerlof O. Cross talk between O-GlcNAcylation and phosphorylation: roles in signaling, transcription, and chronic disease. *Annu Rev Biochem.* (2011) 80:825–58. doi: 10.1146/annurev-biochem-060608-102511
89. Qin CX, Sleaby R, Davidoff AJ, Bell JR, De Blasio MJ, Delbridge LM, et al. *Insights into the role of maladaptive hexosamine biosynthesis and O-GlcNAcylation in development of diabetic cardiac complications. Pharmacol Res.* (2017) 116:45–56. doi: 10.1016/j.phrs.2016.12.016
90. Zhao Y, Tang Z, Shen A, Tao T, Wan C, Zhu X, et al. The role of PTP1B O-GlcNAcylation in hepatic insulin resistance. *Int J Mol Sci.* (2015) 16:22856–69. doi: 10.3390/ijms160922856

91. Issad T, Kuo M. O-GlcNAc modification of transcription factors, glucose sensing and glucotoxicity. *Trends Endocrinol Metab.* (2008) 19:380–9. doi: 10.1016/j.tem.2008.09.001
92. Issad T, Masson E, Pagesy P. O-GlcNAc modification, insulin signaling and diabetic complications. *Diabetes Metab.* (2010) 36:423–35. doi: 10.1016/j.diabet.2010.09.001
93. Yang X, Ongusaha PP, Miles PD, Havstad JC, Zhang F, So WV, et al. Phosphoinositide signalling links O-GlcNAc transferase to insulin resistance. *Nature* (2008) 451:964–9. doi: 10.1038/nature06668
94. Kuo M, Zilberfarb V, Gangneux N, Christeff N, Issad T. *O*-GlcNAc modification of FoxO1 increases its transcriptional activity: a role in the glucotoxicity phenomenon? *Biochimie* (2008) 90:679–85. doi: 10.1016/j.biochi.2008.03.005
95. Battiprolu PK, Hojayev B, Jiang N, Wang ZV, Luo X, Iglewski M, et al. Metabolic stress-induced activation of FoxO1 triggers diabetic cardiomyopathy in mice. *J Clin Invest.* (2012) 122:1109–18. doi: 10.1172/JCI60329
96. Qi Y, Zhu Q, Zhang K, Thomas C, Wu Y, Kumar R, et al. Activation of Foxo1 by insulin resistance promotes cardiac dysfunction and β-myosin heavy chain gene expression. *Circ Heart Fail.* (2015) 8:198–208. doi: 10.1161/CIRCHEARTFAILURE.114.001457

Conflict of Interest Statement: The authors declare that the research was conducted in the absence of any commercial or financial relationships that could be construed as a potential conflict of interest.

frontiers in Endocrinology

ORIGINAL RESEARCH
published: 27 November 2018
doi: 10.3389/fendo.2018.00708

FGF23 Induction of O-Linked N-Acetylglucosamine Regulates IL-6 Secretion in Human Bronchial Epithelial Cells

Stefanie Krick[1], *Eric Scott Helton*[1], *Samuel B. Hutcheson*[1], *Scott Blumhof*[1], *Jaleesa M. Garth*[1], *Rebecca S. Denson*[1,2], *Rennan S. Zaharias*[1], *Hannah Wickham*[1,2] *and Jarrod W. Barnes*[1]*

[1] *Division of Pulmonary, Allergy and Critical Care Medicine, School of Medicine, University of Alabama at Birmingham, Birmingham, AL, United States,* [2] *Hillel Connections Program, Bloom Hillel, University of Alabama, Tuscaloosa, AL, United States*

The hexosamine biosynthetic pathway (HBP) generates the substrate for the O-linked β-N-acetylglucosamine (O-GlcNAc) modification of proteins. The HBP also serves as a stress sensor and has been reported to be involved with nuclear factor of activated T-cells (NFAT) activation, which can contribute to multiple cellular processes including cell metabolism, proliferation, and inflammation. In our previously published report, Fibroblast Growth Factor (FGF) 23, an important endocrine pro-inflammatory mediator, was shown to activate the FGFR4/phospholipase Cγ (PLCγ)/nuclear factor of activated T-cells (NFAT) signaling in chronic inflammatory airway diseases such as cystic fibrosis (CF) and chronic obstructive pulmonary disease (COPD). Here, we demonstrate that FGF23 increased the O-GlcNAc modification of proteins in HBECs. Furthermore, the increase in O-GlcNAc levels by FGF23 stimulation resulted in the downstream activation of NFAT and secretion of interleukin-6 (IL-6). Conversely, inhibition of FGF23 signaling and/or O-GlcNAc transferase (OGT)/O-GlcNAc reversed these effects. Collectively, these data suggest that FGF23 induced IL-6 upregulation and secretion is, at least, partially mediated via the activation of the HBP and O-GlcNAc levels in HBECs. These findings identify a novel link whereby FGF23 and the augmentation of O-GlcNAc levels regulate airway inflammation through NFAT activation and IL-6 upregulation in HBECs. The crosstalk between these signaling pathways may contribute to the pathogenesis of chronic inflammatory airway diseases such as COPD and CF as well as metabolic syndromes, including diabetes.

Keywords: O-GlcNAc, FGF23 = fibroblast growth factor 23, NFAT (nuclear factor expression of activated T cell), IL-6 (Interleukin 6), inflammation

OPEN ACCESS

Edited by:
Tony Lefebvre, Lille University of Science and Technology, France

Reviewed by:
Anna Krzeslak, University of Łódz, Poland
Yobana Perez-Cervera, Benito Juárez Autonomous University of Oaxaca, Mexico

***Correspondence:**
Jarrod W. Barnes
barnesj5@uab.edu

Specialty section:
This article was submitted to Molecular and Structural Endocrinology, a section of the journal Frontiers in Endocrinology

Received: *13 September 2018*
Accepted: *09 November 2018*
Published: *27 November 2018*

Citation:
Krick S, Helton ES, Hutcheson SB, Blumhof S, Garth JM, Denson RS, Zaharias RS, Wickham H and Barnes JW (2018) FGF23 Induction of O-Linked N-Acetylglucosamine Regulates IL-6 Secretion in Human Bronchial Epithelial Cells. Front. Endocrinol. 9:708. doi: 10.3389/fendo.2018.00708

INTRODUCTION

Human fibroblast growth factors (FGFs) are classified as intracrine, paracrine, and endocrine FGFs depending on their action process with endocrine FGFs playing key roles in metabolism including bile acid, energy, and phosphate/active vitamin D metabolism (1, 2). FGF23 is a 27-kDa protein that has been shown to be strongly associated with the risk of chronic kidney disease progression, systemic inflammation, and mortality (3, 4). Our recent data characterized FGF23 signaling as an important mediator in inflammatory airway diseases such as cystic fibrosis (CF) and chronic obstructive pulmonary disease (COPD) (5, 6). In the COPD lung, FGF23 activated the

phospholipase Cγ (PLCγ)/nuclear factor of activated T-cells (NFAT) signaling pathway leading to airway inflammation(5).

NFAT signaling has also been linked to inflammatory cytokine production in hepatocytes, angiogenesis, cardiomyocyte hypertrophy, and many other biological processes (7–10). On a molecular level, NFAT is regulated by the phosphatase calcineurin, which dephosphorylates NFAT and triggers cytoplasmic to nuclear translocation. Upon nuclear translocation, NFAT interacts with multiple factors to regulate gene expression of molecules involved in the aforementioned disease processes.

Although the activation of the PLCγ/NFAT signaling pathway by FGF23 has been studied, the downstream molecules that are affected have not been fully characterized. Several reports have shown that the activation of the hexosamine biosynthetic pathway (HBP) (11, 12), a stress sensor, is linked to NFAT activation and may have a definitive role in inflammation (13, 14). It is well-documented that the HBP serves as a precursor for several glycosylation pathways (14–16). Once activated, the HBP generates the sugar nucleotide UDP-N-acetyl-glucosamine (UDP-GlcNAc), which is a substrate for hyaluronan (HA), N-linked glycosylation, and for the O-linked β-N-acetylglucosamine (O-GlcNAc) modification of proteins (17). The O-GlcNAc modification is a single monosaccharide addition to proteins at unoccupied serine and threonine residues and is similar to protein phosphorylation. Addition or removal of O-GlcNAc is a dynamic process that is regulated by the glycosyltransferase OGT (O-GlcNAc transferase) and the glycosyl hydrolase OGA (β-N-acetylglucosaminidase), each of which serves as a stress sensor and flux mediator (16, 18, 19) in response to changes in the cellular microenvironment (i.e., stress stimuli) (20, 21). An imbalance in the OGT/O-GlcNAc axis has been shown to regulate several cellular functions including cell cycle and proliferation, cardiac hypertrophy, cell metabolism, and inflammation (22, 23). We have previously shown that OGT expression/activity was elevated in the pulmonary vascular disease, pulmonary arterial hypertension, regulated pulmonary arterial smooth muscle cell proliferation, and was associated with clinical disease worsening (24). However, its role in chronic inflammatory airway diseases has not been determined. Furthermore, the role the O-GlcNAc modification on PLCγ/NFAT signaling in airway inflammation, specifically upon FGF23 activation, has not been established. Here, we demonstrate that FGF23 stimulates the O-GlcNAc stress response in human bronchial epithelial cells, which is essential for NFAT transcriptional regulation of the inflammatory cytokine, IL-6, and may be involved in chronic inflammatory airway diseases such as COPD and CF.

MATERIALS AND METHODS

Cell Culture, Reagents, and Treatment Conditions

16HBE cells (or HBECs), a SV40-immortalized human bronchial epithelial cell line, were grown on plates, coated with Collagen IV (6.5 μg/cm^2; Sigma; St. Louis, MO), in medium consisting of Eagle's Minimum Essential Medium (EMEM) supplemented with 10% heat-inactivated fetal bovine serum (Atlas Biologicals; Fort Collins, CO) and without antibiotics as shown previously (5). Human recombinant FGF23 was utilized at 20 ng/ml and stocks were prepared in sterile PBS containing 0.1% BSA as recommended by the manufacturer (PeproTech; Rocky Hill, NJ). Where indicated, a 1 h pretreatment for all inhibitors, including the PLCγ inhibitor (U73122; 0.1 mM and 1.0 mM); FGFR4 inhibitor (100 nM R4 final; BLU9931; Selleck Chemicals; Houston, TX); Cyclosporine, a calcineurin inhibitor that down-regulates NFAT activation (CsA; 100 nM final); Thiamet G, an OGA inhibitor (TG; 25 nM final); and OSMI-1, an OGT inhibitor (25 μM final), was performed prior to the addition of FGF23, all incubated for 24 h. Unless indicated otherwise, all inhibitors were purchased from Sigma (St. Louis, MO).

Western Immunoblotting and Antibodies

Cell lysates were prepared in RIPA buffer with 1x protease and phosphatase inhibitor cocktails (RPI; Mount Prospect, IL), PUGNAC (50 μM; Sigma, St. Louis, MO), and Thiamet G (25 μM, Sigma) added to block removal of the O-GlcNAc modification and subjected to immunoblotting as previously described (24). Briefly, nitrocellulose membranes were probed with antisera for the following: (1) anti-mouse O-GlcNAc (1:1,000; clone CTD 110.6 Biolegend, San Diego, CA, USA), anti-rabbit OGT (1:5,000, Sigma), anti-rabbit OGA (1:5,000 Bethyl Laboratories, Montgomery, TX, USA), anti-rabbit phospho-PLCγ (8713S) (Cell Signaling, Danvers, MA, USA), anti-rabbit PLCγ (2822S) (Cell Signaling), anti-rabbit phospho-ERK (9101S) (Cell Signaling), anti-rabbit ERK (4695S) (Cell Signaling), and anti-mouse β-actin (Sigma). Probed blots were developed using enhanced chemiluminescence Supersignal Femto Substrate (Thermo Scientific; Grand Island, NY, USA). All blots were imaged using the GE Imaging System (GE Healthcare, USA) and densitometric analyses was performed using Image J (25).

IL-8 and IL-6 ELISA and mRNA Assessment

IL-8 and IL-6 enzyme-linked immunosorbent assays (ELISA) from Invitrogen (Thermo Scientific) were used according to the manufacturer's protocol. HBECs were stimulated for 24 h with FGF23, TG, or OSMI-1, and 100 μl of the medium (undiluted) was used for measurement.

RNA was extracted using the GeneJET RNA purification kit (Thermo Scientific, Grand Island, NY, USA). For gene expression analysis, qPCR was performed by using Taqman probes (Life technologies/Applied Biosystems, Carlsbad, CA, USA) with the following: Hs00174103_m1 for IL-8, Hs00174131_m1 for IL-6, and Hs02758991_g1 for GAPDH.

Gene Silencing of OGT and NFAT Isoforms Using siRNA

16HBE cells were used for NFAT and OGT siRNA-mediated knockdown (KD) experiments as previously described (5, 25). Briefly, 5×10^4 cells were seeded in coated 24-well plates and transfected for 6 h in 0.5 mL OptiMEM with 5 nmol of either AllStar negative control or OGT siRNAs (Thermo Scientific, Grand Island, NY, USA) or NFATC2 (NFAT2c) or

NFATC3 (NFAT3c) siRNAs (Qiagen; Hilden, Germany) using 1.5 μL/well of Qiagen HiPerFect transfection reagent. Following the transfection, medium was replaced with complete medium and the cells were subjected to an additional 48 h incubation to allow for NFAT or OGT knockdown. After a 24 h treatment with FGF23, wells were washed with 1.0 mL cold phosphate buffered saline (pH 7.4) and RNA was extracted using the GeneJET RNA purification kit (Thermo Scientific, Grand Island, NY, USA). For some experiments, HBECs were transfected with siRNA against OGT or NFAT2c/3c and 100 ul of conditioned medium was collected for ELISA.

NFAT Luciferase Reporter Assay

As described previously (5), 16HBE cells plated at 1.5×10^4 per well in a coated 96-well plate were transfected with 100 ng of DNA mixture containing the constitutively-active Renilla-luciferase construct, as a transfection control, together with a Fire Fly Luciferase reporter construct, and a NFAT reporter construct serving provided with the NFAT Cignal Reporter Assay Kit (Qiagen; Hilden, Germany). Transfection was performed overnight under serum-free conditions in OptiMEM using Lipofectamine 2000 transfection reagent (Thermo Scientific, Grand Island, NY, USA). Cells were collected after an additional 24 h treatment and a Luciferase assay was performed using the Dual-Luciferase Reporter Assay System (Promega; Madison, WI, USA) as directed by the manufacturer (Promega; Madison, WI, USA). Relative light units (RLUs) were measured utilizing a SpectraMax i3x plate reader equipped with dual injectors (Molecular Devices; Sunnyvale, CA, USA).

Statistics

Data were analyzed with Prism5 (GraphPad Software, Inc., La Jolla, CA) and shown as mean ± SEM using Student's *t*-test and analysis of variance or Kruskal–Wallis *H*-test with one-way ANOVA with appropriate post tests for at least three independent experiments. Significance was accepted at $p < 0.05$.

RESULTS

FGF23 Stimulates the HBP/O-GlcNAc Modification of Proteins in Human Bronchial Epithelial Cells

To determine the effect of FGF23 on the O-GlcNAc modification, we assessed the changes in global protein O-GlcNAc levels, and OGT and OGA protein expression in human bronchial epithelial cells (HBECs). FGF23 treatment of HBEC induced global changes in the O-GlcNAc modification of proteins (**Figures 1A,B**; Ctrl: 4.14 ± 0.25; FGF23: 5.23 ± 0.25, $p = 0.0221$), similar to the effects of the OGA inhibitor Thiamet G (Ctrl: 4.14 ± 0.25; TG: 7.22 ± 0.52, $p = 0.0018$), and opposite of the effects of OGT inhibition with OSMI-1 (FGF23: 5.23 ± 0.25; OSMI-1: 3.27 ± 0.43, $p = 0.016$). Consistent with the O-GlcNAc changes, both OGT and OGA levels were also increased following FGF23 stimulation (**Figure 1A**) with more of an increase in OGA than

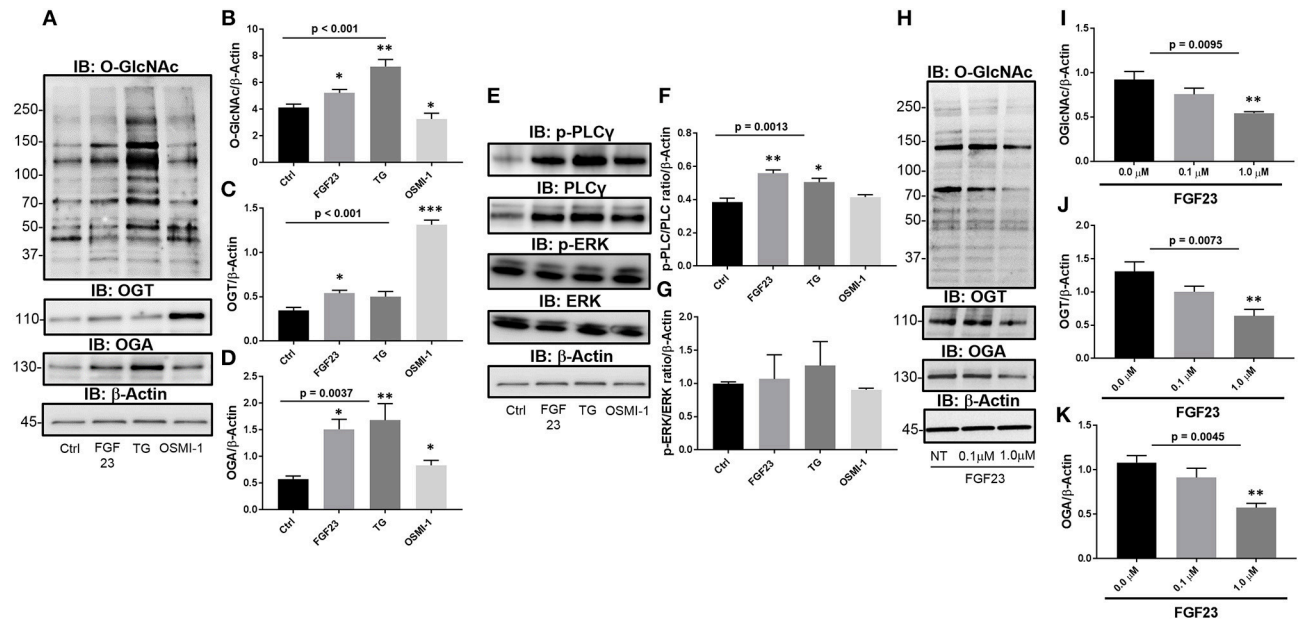

FIGURE 1 | FGF23 stimulates the HBP/O-GlcNAc modification of proteins via the PLCγ signaling pathway in human bronchial epithelial cells. **(A)** Representative Immunoblots showing global O-GlcNAc, OGT, OGA, and β-Actin from HBECs treated as described. **(B–D)** Densitrometric quantitation of O-GlcNAc, OGT, and OGA from **(A)**. **(E)** Representative Immunoblots showing phosphorylation of PLCγ and ERK, total PLCγ and ERK, and β-Actin from HBECs treated as described. **(F,G)** Densitrometric quantitation of Immunoblots from **(A)**. **(H)** Representative Immunoblots of global O-GlcNAc, OGT, OGA, and β-Actin from HBECs treated with a PLCγ inhibitor (U73122 at 0, 0.1, and 1.0 μM) and FGF23 (20 ng/ml) for 24 h. **(I–K)** Densitrometric quantitation of O-GlcNAc, OGT, and OGA from **(H)**. Western blots were performed as triplicates of the same experiment. Statistical analysis was done using ANOVA or Student's *t*-test showing means ± S.E.M. with $^*p < 0.05$, $^{**}p < 0.01$, and $^{***}p < 0.001$. Ctrl, Control; FGF23, fibroblast growth factor 23; TG, thiamet G (OGA inhibitor); OSMI-1, OGT inhibitor.

OGT [**Figures 1C,D**; (OGT: Ctrl: 0.35 ± 0.03; FGF23: 0.54 ± 0.032, $p = 0.0059$) and (OGA: Ctrl: 0.58 ± 0.06; FGF23: 1.5 ± 0.19, $p = 0.003$)], which has been shown in previous reports when O-GlcNAc levels are increased or treated with an OGA inhibitor (26).

Modulation of O-GlcNAc Is Regulated Through the PLCγ Signaling Pathway Upon Stimulation With FGF23

To determine whether FGF23 activates PLCγ (FGFR4-mediated), ERK (FGFR1-mediated), or both FGF23 signaling pathways in HBECs, we immunoblotted for total and phosphorylated PLCγ and ERK proteins Phosphorylation of PLCγ and total PLC was significantly increased without change in ERK phosphorylation following FGF23 administration [**Figures 1E–G**; (p-PLCγ: Ctrl: 0.38 ± 0.02; FGF23: 0.56 ± 0.02, $p = 0.0054$) and (ERK: Ctrl: 1.02 ± 0.02; FGF23: 0.96 ± 0.053, $p = 0.375$)]. Interestingly, OGA inhibition (TG) had a similar effect as FGF23 on the phosphorylation of PLCγ and ERK [**Figures 1E–G**; (p-PLCγ: Ctrl: 0.38 ± 0.02; TG: 0.51 ± 0.023, $p = 0.022$) and (ERK: Ctrl: 1.02 ± 0.02; TG: 0.90 ± 0.068, $p = 0.21$)], whereas OGT inhibition (OSM-I) did not have any affect on the phosphorylation of PLCγ or ERK levels [**Figures 1E–G**; (p-PLCγ: Ctrl: 0.38 ± 0.02; OSMI-1: 0.42 ± 0.01, $p = 0.339$) and (ERK: Ctrl: 1.02 ± 0.02; OSMI-1: 0.77 ± 0.12, $p = 0.102$)].

To determine whether the changes in O-GlcNAc following FGF23 are regulated through the PLCγ signaling pathway, we blocked PLCγ activation using a PLCγ inhibitor (U-73122), which has been shown to block FGF23 signaling through FGFR4 (27, 28). As shown in **Figure 1H**, O-GlcNAc was dose-dependently reduced following PLCγ inhibitor administration (**Figure 1I**: NT: 0.92 ± 0.090; 0.1 μM PLC inhibitor: 0.76 ± 0.07; 1.0 μM PLC inhibitor: 0.54 ± 0.02; $p = 0.0095$). In addition, OGT and OGA protein levels were decreased after PLCγ blockade (**Figures 1H,J,K**: OGT NT: 1.30 ± 0.15; 0.1 μM PLCγ inhibitor: 1.00 ± 0.08; 1.0 μM PLCγ inhibitor: 0.64 ± 0.10; $p = 0.0073$ and OGA NT: 1.08 ± 0.08; 0.1 μM PLCγ inhibitor: 0.91 ± 0.10; 1.0 μM PLCγ inhibitor: 0.57 ± 0.05; $p = 0.0045$) Altogether, these data suggest that FGF23 activates the PLCγ signaling pathway that regulates the O-GlcNAc changes observed in HBECs.

Knockdown of OGT Abrogates the O-GlcNAc Modification of Proteins and the Effects of FGF23 Signaling

Previous reports have shown that there is an extracellular OGT (eOGT), which resides in the ER and transfers the GlcNAc moiety to epidermal growth factor-like domains (29). Interestingly, it has been shown to have high expression in the lung (30). Therefore, we wanted to determine whether the increase O-GlcNAc levels, stimulated by FGF23, is transferred by OGT and not the ER-resident eOGT in HBECs. To confirm that OGT is the sole enzyme responsible for O-GlcNAc transfer in these cells and affected by FGF23 signaling, we used siRNA targeted knockdown of OGT. As shown in **Figure 2**, FGF23 induced O-GlcNAc and

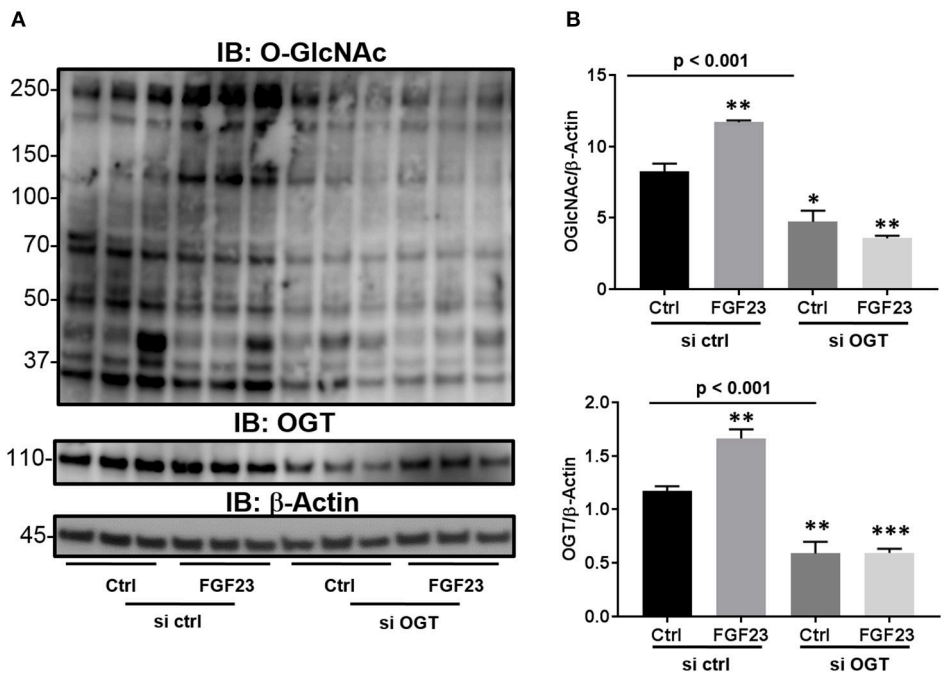

FIGURE 2 | Knockdown of OGT reduces the O-GlcNAc modification of proteins. **(A)** Representative Immunoblots showing global O-GlcNAc, OGT, OGA, and β-Actin from HBECs treated as described or **(B)** HBECs were transfected with siRNA against OGT in the presence and absence of FGF23. Western blots were performed as triplicates of the same experiment. Ctrl, Control; FGF23, fibroblast growth factor 23; si ctrl, small interfering RNA control; and si OGT, small interfering RNA against OGT. Statistical analysis was done using ANOVA or Student's t-test showing means ± S.E.M. with $^*p < 0.05$, $^{**}p < 0.01$, and $^{***}p < 0.001$.

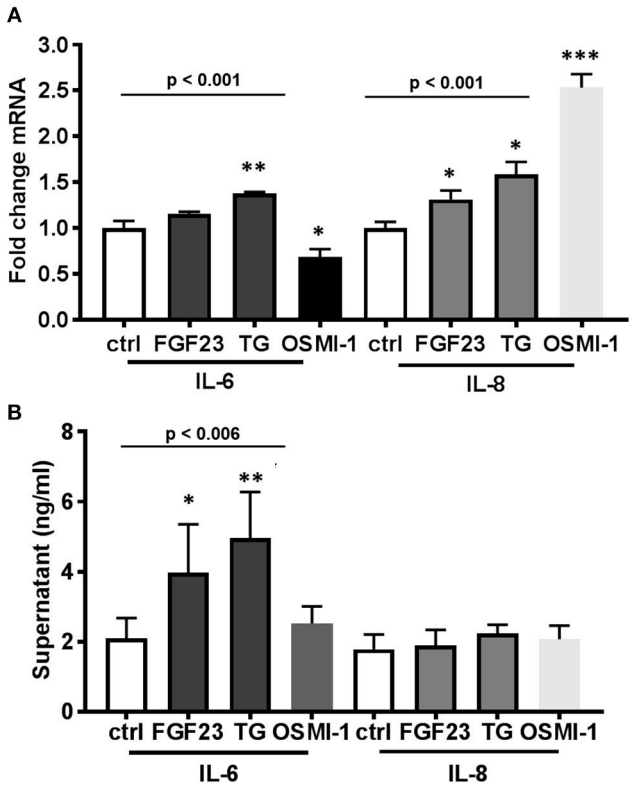

FIGURE 3 | FGF23 and OGA inhibition both increase IL-6 secretion in human bronchial epithelial cells. **(A)** Bar graphs showing transcript analysis and fold change of IL-6 and IL-8 levels in HBECs treated in the presence or absence of FGF23, TG, or OSMI-1 for 24h. **(B)** IL-6 and IL-8 protein amounts determined by ELISA from conditioned media of HBECs. All experiments were done in triplicate and bar graphs shown respresent the mean ± S.E.M.(*$p < 0.05$; **$p < 0.01$, and ***$p < 0.001$). Ctrl, Control; FGF23, fibroblast growth factor 23; TG, thiamet G (OGA inhibitor); OSMI-1, OGT inhibitor.

OGT levels similar to **Figures 1A–C** [(O-GlcNAc: Ctrl: 8.23 ± 0.57; FGF23: 11.7 ± 0.13, $p = 0.004$) and (OGT: 1.18 ± 0.04; FGF23: 1.66 ± 0.09, $p = 0.0068$)]. Knockdown of OGT resulted in decreased O-GlcNAc levels in the presence or absence of FGF23 in HBECs [(O-GlcNAc: Ctrl: 8.23 ± 0.57; KD Ctrl: 4.73 ± 0.77; and KD FGF23: 3.57 ± 0.18, $p < 0.001$) and (OGT: Ctrl 1.18 ± 0.04; KD Ctrl: 0.59 ± 0.11; and KD FGF23: 0.60 ± 0.04, $p < 0.001$)]. Altogether, these results demonstrate that OGT is downstream of FGF23 signaling and solely responsible for the O-GlcNAc transfer. This data, along with **Figure 1**, suggests that FGF23 can modulate O-GlcNAc levels through a PLCγ-dependent signaling pathway, and can be inhibited by knockdown of OGT.

Both FGF23 and OGA Inhibition Regulate IL-6 Secretion in Human Bronchial Epithelial Cells

We previously demonstrated a significant positive correlation between circulating FGF23 and IL-6 levels in plasma of COPD patients (5). However, no studies have investigated the role of FGF23 and O-GlcNAc on inflammatory cytokine production. To determine effects of both FGF23 and O-GlcNAc levels on the inflammatory cytokine production in HBECs, we assessed mRNA and protein levels of IL-6 and IL-8. FGF23 stimulation led to a significant increase in IL-8 transcripts [**Figure 3A**; (IL-8: Ctrl: 1.0 ± 0.07; FGF23: 1.31 ± 0.10, $p = 0.042$)], whereas inhibition of OGA caused a significant increase in both IL-6 and IL-8 mRNA levels [**Figure 3A**; (IL-8: Ctrl: 1.0 ± 0.07; TG: 1.58 ± 0.14, $p = 0.032$) and (IL-6: Ctrl: 1.0 ± 0.08; TG: 1.38 ± 0.01, $p = 0.013$)]. Inhibition of O-GlcNAc transfer by OSMI-1 resulted in a reduction of IL-6 transcripts [**Figure 3A**; (IL-6: Ctrl: 1.0 ± 0.08; OSMI-1: 0.68 ± 0.09, $p = 0.033$)]; however, there was a significant increase in IL-8 mRNA expression upon OGT inhibition [**Figure 3A**; (IL-8: Ctrl: 1.0 ± 0.07; OSMI-1: 2.53 ± 0.15, $p = 0.0006$)]. As shown in **Figure 3B**, assessment of IL-6 protein secretion from conditioned media by ELISA showed a significant ∼2-fold increase in IL-6 levels (IL-6: Ctrl: 2.10 ± 0.24; FGF23: 3.97 ± 0.62, $p = 0.035$) following FGF23 administration that was consistent with OGA inhibition [∼2.5 fold, **Figure 3B** (IL-6: Ctrl: 2.10 ± 0.24; TG: 4.96 ± 0.93, $p = 0.0035$). Inhibition of OGT, though, did not show any effect compared to control. Surprisingly, IL-8 protein secretion, as assessed by ELISA, was not significantly different under any condition (**Figure 3B**, $p = 0.435$). These findings suggest that FGF23 and increased O-GlcNAc can lead to increased secretion of IL-6.

FGF23 Activates NFAT Through O-GlcNAc Augmentation in HBECs

Previously published reports have shown an association between O-GlcNAc signaling and NFAT regulation in cardiomyocyte hypertrophy (13, 31) and in lymphocyte activation (32). In addition, we have recently shown that bronchial epithelial cells express NFAT2c and 3c as main isoforms and are activated by FGF23, which results in airway inflammation (5). To determine the role of FGF23 and O-GlcNAc in NFAT activation, we performed NFAT2c/3c activation assays using a luciferase-conjugated NFAT reporter gene in HBECs. As shown in **Figure 4A**, FGF23 significantly increased NFAT activation (Ctrl: 4.68 ± 0.32; FGF23: 6.68 ± 0.70, $p = 0.035$), $p = 0.012$), which is similar to our previous report (5). Inhibition of O-GlcNAc removal (TG) resulted in a similar increase in NFAT activation (Ctrl: 4.68 ± 0.32; TG: 6.80 ± 0.36, $p = 0.01$). Interestingly, blocking O-GlcNAc transfer significantly reduced NFAT activation (Ctrl: 4.68 ± 0.32; OSMI-1: 0.7 ± 0.16, $p < 0.001$), which was similar to cyclosporine (CsA; Ctrl: 4.68 ± 0.32; CsA: 1.2 ± 0.06, $p = 0.003$) and noticeably different compared to control, FGF23, and TG. Also in **Figure 4A**, FGFR4 blockade (R4) in the presence or absence of FGF23 inhibited NFAT activation consistent with the no treatment results [(R4: Ctrl: 4.68 ± 0.32; R4: 4.42 ± 0.21, $p = 0.49$ and FGF23+R4: Ctrl: 4.68 ± 0.32; FGF23+R4: 4.55 ± 0.39, $p = 0.80$)]. These data suggest that NFAT activation (through FGF23/FGFR4) is regulated by O-GlcNAc modulation in a similar fashion to FGF23 stimulation in HBECs.

To determine whether knockdown of NFAT effects O-GlcNAc modification of proteins, we silenced NFAT2c/3c using siRNA.

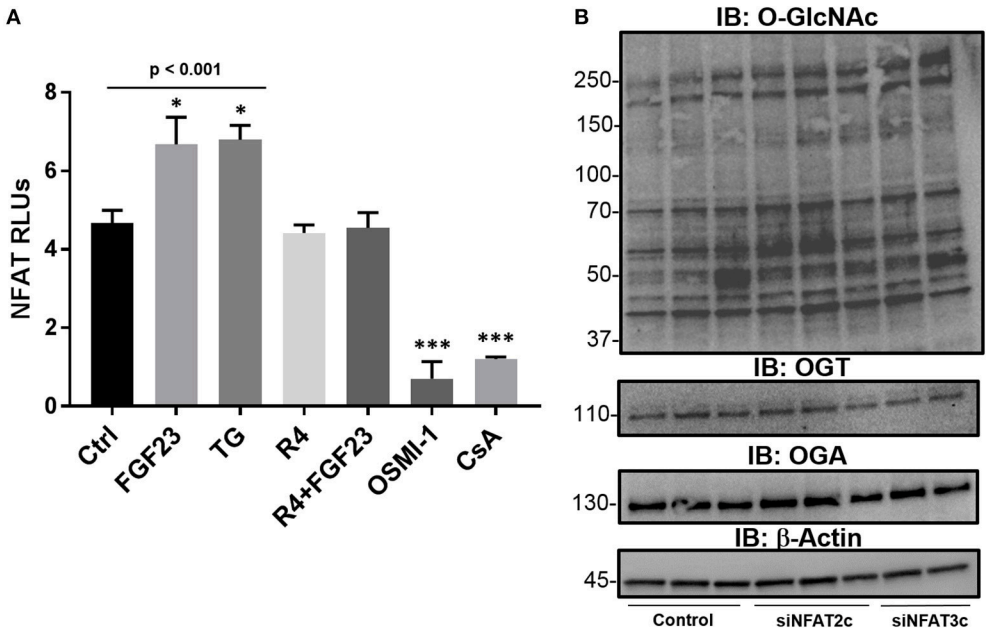

FIGURE 4 | The NFAT activation is regulated by FGF23 and OGA inhibition (TG) and is downstream of O-GlcNAc regulation. **(A)** FGF23 and TG activate NFAT as assessed by a luciferase-based reporter gene assay in HBECs and is reduced to normal levels by an FGFR4 inhibitor (R4) or blocked by OSMI-1 similar to the effects of the NFAT activation inhibitor, cyclosporine (CsA). **(B)** Western blots of O-GlcNAc, OGT, and OGA following knockdown of NFAT2c and NFAT3c. Experiments were performed in triplicate. Statistical analysis was done using ANOVA or Student's *t*-test showing means ± S.E.M. with $*p < 0.05$, and $***p < 0.001$. Ctrl, Control; FGF23, fibroblast growth factor 23; TG, thiamet G (OGA inhibitor); R4, FGFR4 inhibitor; OSMI-1, OGT inhibitor; CsA, cyclosporine; and siNFAT, small interfering RNA against NFAT2c or 3c.

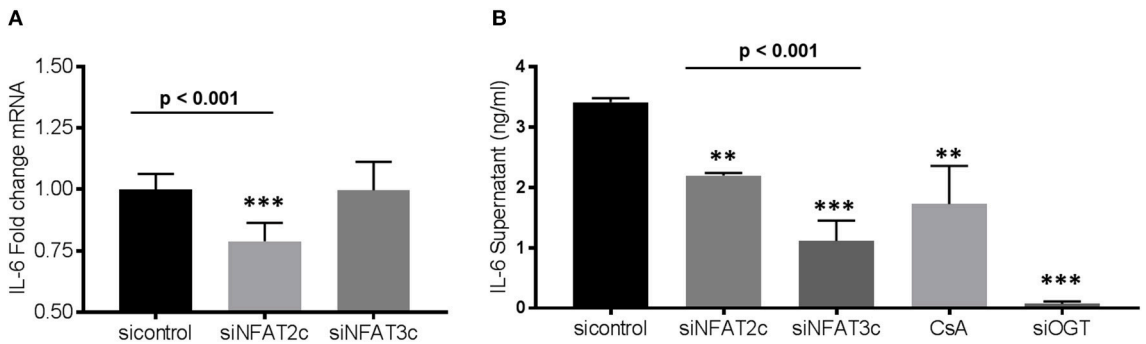

FIGURE 5 | Gene silencing of NFAT2c leads to downregulation of IL-6 expression, while knockdown of both NFAT2c/3c results in reduced IL-6 secretion in HBECs. **(A)** Bar graphs showing transcript analysis and fold change of IL-6 levels following NFAT2/3C knockdown with siRNA in HBECs. **(B)** IL-6 protein level from conditioned media of HBECs as determined by ELISA. All experiments were done in triplicate and statistical analyses was done using ANOVA or Student's *t*-test showing means ± S.E.M. with $**p < 0.01$ and $***p < 0.001$. si control, small interfering RNA control; siNFAT, small interfering RNA against NFAT2c or 3c; small interfering RNA against OGT; and CsA, cyclosporin.

As shown in **Figure 4B**, knockdown of NFAT2c/3c did not affect O-GlcNAc levels, or OGT/OGA protein expression. Altogether, these data combined suggests that NFAT activation is regulated through the FGF23 increase in O-GlcNAc levels, which lies upstream of NFAT in HBECs.

Knockdown of NFAT2c or OGT Leads to Downregulation of IL-6 Expression

As shown above, administration of FGF23 or altering the O-GlcNAc levels in human bronchial epithelial cells resulted in changes in IL-6 expression (**Figure 3**). To determine whether knockdown of NFAT alters IL-6 expression, we silenced NFAT2c/3c and determined IL-6 transcript levels and protein secretion. As shown in **Figure 5A**, IL-6 mRNA was significantly lower in siNFAT2c compared to siNFAT3c and sicontrol (sicontrol: 1.0 ± 0.02; siNFAT2c: 0.79 ± 0.03; and siNFAT3c: 0.99 ± 0.04, $p = 0.0008$). At the protein level, IL-6 secretion was reduced following NFAT2c/3c knockdown and was consistent with CsA treatment (**Figure 5B**: sicontrol: 3.41 ± 0.06; siNFAT2c: 2.20 ± 0.04; siNFAT3c: 1.11 ± 0.33; and CsA: 1.72 ± 0.64,

$p = 0.0014$). These results suggest that silencing NFAT2c/3c, which is downstream of FGF23 and O-GlcNAc, downregulates IL-6 in HBECs similar to blocking O-GlcNAc transfer (shown in **Figure 2**) or silencing OGT (**Figure 5B**: sicontrol: 3.41 ± 0.06; siOGT: 0.07 ± 0.04, $p < 0.001$).

DISCUSSION

In this report, we show that FGF23 can increase O-GlcNAc levels as well as OGT and OGA protein expression in HBECs. This effect seems to be a downstream target via the FGFR4/PLCγ signaling pathway (FGFR1/ERK signaling is not affected) since PLC blockade resulted in decreased O-GlcNAc following FGF23 adminstration (**Figure 1H**). Furthermore, both FGF23 and O-GlcNAc lead to increased secretion of IL-6, but not IL-8 (**Figure 3**). Conversely, reduction of O-GlcNAc levels (by OSMI-1) reduced IL-6 secretion. Upon assessing effects of the NFAT activation in HBECs (**Figure 4**), we found that FGF23 activated NFAT, which is consistent with our previous report (5). In line with this, O-GlcNAc modulation resulted in either an increase in NFAT activation (by blocking O-GlcNAc removal) or a decrease in NFAT upon inhibiting O-GlcNAc transfer (OSMI-1) or FGF23 signaling (through blockade of FGFR4). Interestingly, knockdown of NFAT 2c or 3c did not affect the O-GlcNAc levels or OGA/OGT expression (**Figure 4B**). However, NFAT2c silencing did affect both IL-6 expression and secretion, while NFAT3c knockdown only affected IL-6 secretion (**Figure 5**).

In our results, there were discrepancies in the mRNA expression of IL-6 compared to IL-8 with the different treatments (**Figures 3**, **5**). In addition, there was higher IL-6 protein secretion compared to IL-8, which did not correlate with the respective mRNA levels. This was also similar with the IL-6 results for NFAT3c in **Figure 5**. These discrepancies in the mRNA expression and protein levels of cytokines have been documented in other studies (33). Therefore, caution should be used when interpreting mRNA expression as a proxy to protein levels. In addition, we cannot rule out the fact that the increased levels of IL-6 (or no change in levels of IL-8) in our study may be due to altered cytokine uptake/turnover following treatments. Nevertheless, these data combined suggest that FGF23 stimulation of O-GlcNAc levels is upstream of NFAT signaling in HBECs and regulates the secretion of the pro-inflammatory cytokine IL-6 (**Figure 6**).

FGF23 has been characterized as a hormonal regulator of circulating phosphate and vitamin D levels as well as a prognostic risk factor for cardiovascular mortality in patients with chronic kidney disease (28, 34–36). The role of FGF23 role as an inflammatory facilitator has also been recently studied (5, 37, 38). Interestingly, it may be involved in several metabolic processes, including glucose and fat metabolism. For example, FGF23 was shown to contribute to insulin sensitivity in obese adolescents (39) and was altered in vitamin D deficient patients following an oral glucose load (40). Based on these findings, administration of FGF23 may alter metabolic pathways that are involved in glucose dysregulation and/or inflammation. The O-GlcNAc modification has long been studied and defined as cellular nutrient/stress sensor and the connection between the FGF23 and O-GlcNAc levels is plausible based on these previous reports and our results.

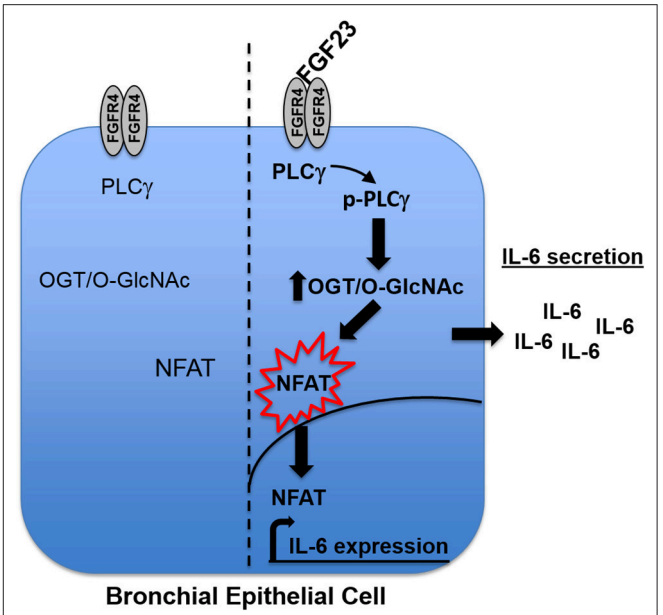

FIGURE 6 | Model. Upon binding to FGFR4 in human bronchial epithelial cells, FGF23 stimulates the phosphorylation of PLCγ, which increases the O-GlcNAc modification of proteins. The increase in O-GlcNAc results in NFAT activation and translocation from the cytoplasm to the nucleus where it drives the expression of IL-6 and subsequent secretion out of the cell.

The O-GlcNAc modification regulates nuclear and cytosolic protein function and cellular signaling. Previous reports have shown a pro- and anti-inflammatory role for O-GlcNAc (23, 41), and this biphasic effect is dependent on different cell types and diseases. Previous reports have also shown that glucosamine activation of the HBP attenuates NFκB activation in chondrocytes (42) or IL-1β mediation chondrocyte activation (43). In addition, inhibition of the NFκB pathway by O-GlcNAc has been shown in acute vascular injury models (44). On the other hand, the O-GlcNAc modification has been shown to activate NFκb under increase glucose concentrations in vascular smooth muscle cells in diabetes and obesity, suggesting a pro-inflammatory phenotype (45). This pro-inflammatory phenotype has been shown in other reports where HBP flux augments the oxidative stress pathways and the expression of other pro-inflammatory markers vascular cell adhesion molecule-1 (VCAM-1), IL6, IL-1β, TNFα, and NFκB (46). To our knowledge, we are the first to show the link between FGF23 and O-GlcNAc regulating IL-6 expression (**Figure 3**).

Several reports have shown that "outside-in" signaling can be modulated by O-GlcNAc. In T cell activation, antigen peptide binding to the T cell receptor have been shown to increase the O-GlcNAc modification of proteins that were associated with inflammatory cytokine production and cellular proliferation (47). In bone morphogenic protein (BMP) signaling on osteoblast differentiation, hyperglycemic conditions or activators of the HBP were shown to alter the O-GlcNAc levels and affect

osteogenic differentiation (48) suggesting a role for glucose dysregulation on normal BMP function and signaling. In another report, FGF signaling was also shown to be altered by loss of function of a gene that encodes an enzyme in the HBP, which resulted in defective O-GlcNAc modification of the FGFR (49, 50). This was shown to impair FGF mediated migration of mesodermal and tracheal cells during fly development. In addition, Miura, T. and colleagues demonstrated that O-GlcNAc modification of PKCζ blocks the signaling effects of FGF4, which resulted in the maintenance of an ESC undifferentiated state (51). A role for the O-GlcNAc modification was also shown for PLC inactivation and subsequent reduction of IP3 and Ca2+ mobilization in myoblast even in response to bradykinin (52). Similar to these findings, we show that FGF23 signaling, through PLCγ, increases the O-GlcNAc modification of proteins that may be involved in inflammatory cytokine production in HBECs (**Figures 1**–**3**). Interestingly, we also observed an increase in total PLCγ protein expression (**Figure 1**). The increase in total PLCγ expression has been shown in other inflammatory associated complications, including cancer and skin conditions (53) that may be associated with altered FGF23 levels (54–56) and is consistent with our findings. Collectively, we show that FGF23 signaling, through PLCγ, increases the O-GlcNAc modification of proteins that may be involved in inflammatory cytokine production in HBECs (**Figures 1**–**3**).

As stated above, NFAT signaling has also been linked to inflammatory cytokine production in hepatocytes, angiogenesis, cardiomyocyte hypertrophy, and many other biological processes (27, 28, 37, 57). In addition, T- and B-lymphocytes activation, which has been documented to be regulated by NFAT (32), can be regulated by the O-GlcNAc modification, which may be required for its nuclear translocation. A similar phenomenon was shown in cardiomyocyte hypertrophy where the activation of NFAT has been linked to increased O-GlcNAc modification (13, 58). Our previous report suggested a role for FGF23 activation of NFAT in the airway (5). However, no experiments have been done to determine the role of O-GlcNAc on NFAT activation through FGF23. Based on our results, combined with our previously published data, we put forth a model (**Figure 6**), whereby FGF23 regulates NFAT activation through the modulation of O-GlcNAc (**Figures 4**, **5**), and stimulates IL-6 expression and secretion in HBECs (**Figures 1**–**3**).

Our findings in this report are the first to describe a role for FGF23 in the augmentation of O-GlcNAc levels. In addition, the role for FGF23 in the activation of NFAT through O-GlcNAc stimulation increases our knowledge of the molecules that may be involved in the process. The impact of O-GlcNAc by way of FGF23 will open new avenues for research in lung diseases associated with chronic airway inflammation such as COPD, cystic fibrosis, and asthma as well as metabolic disorders including diabetes and heart failure.

AUTHOR CONTRIBUTIONS

SK and JB conceived, designed, and analyzed all experiments and wrote the manuscript. EH, SH, SB, JG, RD, RZ, and HW performed experiments that were conceptualized and guided by JB and SK.

ACKNOWLEDGMENTS

This work was supported by the Flight Attendant Medical Research Institute (YFAC152003 to SK), the Cystic Fibrosis Foundation (CFF KRICK1610 to SK) and the NIH (K99HL131866/R00HL131866 to JB).

REFERENCES

1. Richter B, Faul C. FGF23 actions on target tissues-with and without klotho. *Front Endocrinol.* (2018) 9:189. doi: 10.3389/fendo.2018.00189
2. Itoh N, Ohta H, Konishi M. Endocrine FGFs: evolution, physiology, pathophysiology, and pharmacotherapy. *Front Endocrinol.* (2015) 6:154. doi: 10.3389/fendo.2015.00154
3. Gutierrez OM, Mannstadt M, Isakova T, Rauh-Hain JA, Tamez H, Shah A, et al. Fibroblast growth factor 23 and mortality among patients undergoing hemodialysis. *N Engl J Med.* (2008) 359:584–92. doi: 10.1056/NEJMoa0706130
4. Shimada T, Urakawa I, Isakova T, Yamazaki Y, Epstein M, Wesseling-Perry K, et al. Circulating fibroblast growth factor 23 in patients with end-stage renal disease treated by peritoneal dialysis is intact and biologically active. *J Clin Endocrinol Metab.* (2010) 95:578–85. doi: 10.1210/jc.2009-1603
5. Krick S, Grabner A, Baumlin N, Yanucil C, Helton S, Grosche A, et al. Fibroblast growth factor 23 and Klotho contribute to airway inflammation. *Eur Respir J.* (2018) 52:1800236. doi: 10.1183/13993003.00236-2018
6. Krick S, Baumlin N, Aller SP, Aguiar C, Grabner A, Sailland J, et al. Klotho inhibits interleukin-8 secretion from cystic fibrosis airway epithelia. *Sci Rep.* (2017) 7:14388. doi: 10.1038/s41598-017-14811-0
7. Yang TT, Suk HY, Yang X, Olabisi O, Yu RY, Durand J, et al. Role of transcription factor NFAT in glucose and insulin homeostasis. *Mol Cell Biol.* (2006) 26:7372–87. doi: 10.1128/MCB.00580-06
8. Liu Q, Chen Y, Auger-Messier M, Molkentin JD. Interaction between NFkappaB and NFAT coordinates cardiac hypertrophy and pathological remodeling. *Circ Res.* (2012) 110:1077–86. doi: 10.1161/CIRCRESAHA.111.260729
9. Siamakpour-Reihani S, Caster J, Bandhu Nepal D, Courtwright A, Hilliard E, Usary J, et al. The role of calcineurin/NFAT in SFRP2 induced angiogenesis–a rationale for breast cancer treatment with the calcineurin inhibitor tacrolimus. *PLoS ONE* (2011) 6:e20412. doi: 10.1371/journal.pone.0020412
10. Noren DP, Chou WH, Lee SH, Qutub AA, Warmflash A, Wagner DS, et al. Endothelial cells decode VEGF-mediated Ca2+ signaling patterns to produce distinct functional responses. *Sci Signal.* (2016) 9:ra20. doi: 10.1126/scisignal.aad3188
11. Buse MG. Hexosamines, insulin resistance, and the complications of diabetes: current status. *Am J Physiol Endocrinol Metab.* (2006) 290:E1–8. doi: 10.1152/ajpendo.00329.2005
12. Sage AT, Walter LA, Shi Y, Khan MI, Kaneto H, Capretta A, et al. Hexosamine biosynthesis pathway flux promotes endoplasmic reticulum stress, lipid accumulation, and inflammatory gene expression in hepatic cells. *Am J Physiol Endocrinol Metab.* (2010) 298:E499–511. doi: 10.1152/ajpendo.00507.2009
13. Facundo HT, Brainard RE, Watson LJ, Ngoh GA, Hamid T, Prabhu SD, et al. O-GlcNAc signaling is essential for NFAT-mediated transcriptional reprogramming during cardiomyocyte hypertrophy. *Am J Physiol Heart Circ Physiol.* (2012) 302:H2122–30. doi: 10.1152/ajpheart.00775.2011
14. Love DC, Hanover JA, The hexosamine signaling pathway: deciphering the "O-GlcNAc code". *Sci STKE* (2005) 2005:re13. doi: 10.1126/stke.3122005re13
15. Marshall S, Bacote V, Traxinger RR. Discovery of a metabolic pathway mediating glucose-induced desensitization of the glucose transport system.

Role of hexosamine biosynthesis in the induction of insulin resistance. *J Biol Chem.* (1991) 266:4706–12.
16. Wells L, Vosseller K, Hart GW. A role for N-acetylglucosamine as a nutrient sensor and mediator of insulin resistance. *Cell Mol Life Sci.* (2003) 60:222–8. doi: 10.1007/s000180300017
17. Varki A, Cummings RD, Esko JD, Freeze HH, Stanley P, Bertozzi CR, et al. *Essentials In Glycobiology*. Cold Spring Harbor, NY: Cold Spring Harbor Laboratory Press (2009).
18. Myslicki JP, Belke DD, Shearer J. Role of O-GlcNAcylation in nutritional sensing, insulin resistance and in mediating the benefits of exercise. *Appl Physiol Nutri Metab.* (2014) 39:1205–13. doi: 10.1139/apnm-2014-0122
19. Sodi VL, Bacigalupa ZA, Ferrer CM, Lee JV, Gocal WA, et al. Nutrient sensor O-GlcNAc transferase controls cancer lipid metabolism via SREBP-1 regulation. *Oncogene* (2017) 37:924–34. doi: 10.1038/onc.2017.395
20. Slawson C, Housley MP, Hart GW. O-GlcNAc cycling: how a single sugar post-translational modification is changing the way we think about signaling networks. *J Cell Biochem.* (2006) 97:71–83. doi: 10.1002/jcb.20676
21. Hart GW. Three decades of research on O-GlcNAcylation - a major nutrient sensor that regulates signaling, transcription and cellular metabolism. *Front Endocrinol.* (2014) 5:183. doi: 10.3389/fendo.2014.00183
22. Vaidyanathan K, Durning S, Wells L. Functional O-GlcNAc modifications: implications in molecular regulation and pathophysiology. *Crit Rev Biochem Mol Biol.* (2014) 49:140–63. doi: 10.3109/10409238.2014.884535
23. Banerjee PS, Lagerlof O, Hart GW. Roles of O-GlcNAc in chronic diseases of aging. *Mol Aspects Med.* (2016) 51:1–15. doi: 10.1016/j.mam.2016.05.005
24. Barnes JW, Tian L, Heresi GA, Farver CF, Asosingh K, Comhair SA, et al. O-linked beta-N-acetylglucosamine transferase directs cell proliferation in idiopathic pulmonary arterial hypertension. *Circulation* (2015) 131:1260–8. doi: 10.1161/CIRCULATIONAHA.114.013878
25. Schneider CA, Rasband WS, Eliceiri KW. NIH Image to ImageJ: 25 years of image analysis. *Nat Methods* (2012) 9:671–5. doi: 10.1038/nmeth.2089
26. Zhang Z, Tan EP, VandenHull NJ, Peterson KR, Slawson C. O-GlcNAcase expression is sensitive to changes in O-GlcNAc homeostasis. *Front Endocrinol.* (2014) 5:206. doi: 10.3389/fendo.2014.00206
27. Grabner A, Amaral AP, Schramm K, Singh S, Sloan A, Yanucil C, et al. Activation of cardiac fibroblast growth factor receptor 4 causes left ventricular hypertrophy. *Cell Metab.* (2015) 22:1020–32. doi: 10.1016/j.cmet.2015.09.002
28. Faul C, Amaral AP, Oskouei B, Hu MC, Sloan A, Isakova T, et al. FGF23 induces left ventricular hypertrophy. *J Clin Invest.* (2011) 121:4393–408. doi: 10.1172/JCI46122
29. Sakaidani Y, Nomura T, Matsuura A, Ito M, Suzuki E, Murakami K, et al. O-Linked-N-acetylglucosamine on extracellular protein domains mediates epithelial cell–matrix interactions. *Nat Commun.* (2011) 2:583. doi: 10.1038/ncomms1591
30. Sakaidani Y, Ichiyanagi N, Saito C, Nomura T, Ito M, Nishio Y, et al. O-linked-N-acetylglucosamine modification of mammalian Notch receptors by an atypical O-GlcNAc transferase Eogt1. *Biochem Biophys Res Commun.* (2012) 419:14–19. doi: 10.1016/j.bbrc.2012.01.098
31. McLarty JL, Marsh SA, Chatham JC. Post-translational protein modification by O-linked N-acetyl-glucosamine: its role in mediating the adverse effects of diabetes on the heart. *Life Sci.* (2013) 92:621–7. doi: 10.1016/j.lfs.2012.08.006
32. Golks A, Tran TT, Goetschy JF, and Guerini D, Requirement for O-linked N-acetylglucosaminyltransferase in lymphocytes activation. *EMBO J.* (2007) 26:4368–79. doi: 10.1038/sj.emboj.7601845
33. Shebl FM, Pinto LA, García-Piñeres A, Lempicki R, Williams M, Harro C, et al. Comparison of mRNA and protein measures of cytokines following vaccination with human papillomavirus-16 L1 virus-like particles. *Cancer Epidemiol Biomark Prev.* (2010) 19:978–81. doi: 10.1158/1055-9965.EPI-10-0064
34. Quarles LD. Role of FGF23 in vitamin D and phosphate metabolism: implications in chronic kidney disease. *Exp Cell Res.* (2012) 318:1040–8. doi: 10.1016/j.yexcr.2012.02.027
35. Wolf M. Update on fibroblast growth factor 23 in chronic kidney disease. *Kidney Int.* (2012) 82:737–47. doi: 10.1038/ki.2012.176
36. Gutierrez OM, Wolf M, Taylor EN. Fibroblast growth factor 23, cardiovascular disease risk factors, and phosphorus intake in the health professionals follow-up study. *Clin J Am Soc Nephrol.* (2011) 6:2871–8. doi: 10.2215/CJN.02740311
37. Singh S, Grabner A, Yanucil C, Schramm K, Czaya B, Krick S, et al. Fibroblast growth factor 23 directly targets hepatocytes to promote inflammation in chronic kidney disease. *Kidney Int.* (2016) 90:985–96. doi: 10.1016/j.kint.2016.05.019
38. Grabner A, Mazzaferro S, Cianciolo G, Krick S, Capelli I, Rotondi S, et al. Fibroblast growth factor 23: mineral metabolism and beyond. *Contrib Nephrol.* (2017) 190:83–95. doi: 10.1159/000468952
39. Wojcik M, Dolezal-Oltarzewska K, Janus D, Drozdz D, Sztefko K, Starzyk JB. FGF23 contributes to insulin sensitivity in obese adolescents - preliminary results. *Clin Endocrinol.* (2012) 77:537–40. doi: 10.1111/j.1365-2265.2011.04299.x
40. Ursem SR, Vervloet MG, Buttler RM, Ackermans MT, Oosterwerff MM, Eekhoff MV, et al. The interrelation between FGF23 and glucose metabolism in humans. *J Diabetes Complications* (2018) 32:845–50. doi: 10.1016/j.jdiacomp.2018.06.013
41. Hirata Y, Nakagawa T, Moriwaki K, Koubayashi E, Kakimoto K, Takeuchi T, et al. Augmented O-GlcNAcylation alleviates inflammation-mediated colon carcinogenesis via suppression of acute inflammation. *J Clin Biochem Nutr.* (2018) 62:221–9. doi: 10.3164/jcbn.17-106
42. Imagawa K, de Andres MC, Hashimoto K, Pitt D, Itoi E, Goldring MB, et al. The epigenetic effect of glucosamine and a nuclear factor-kappa B (NF-kB) inhibitor on primary human chondrocytes–implications for osteoarthritis. *Biochem Biophys Res Commun.* (2011) 405:362–7. doi: 10.1016/j.bbrc.2011.01.007
43. Shikhman AR, Kuhn K, Alaaeddine N, Lotz M. N-acetylglucosamine prevents IL-1 beta-mediated activation of human chondrocytes. *J Immunol.* (2001) 166:5155–60. doi: 10.4049/jimmunol.166.8.5155
44. Yao D, Xu L, Xu O, Li R, Chen M, Shen H, et al. O-Linked beta-N-acetylglucosamine modification of A20 enhances the inhibition of NF-kappaB (Nuclear Factor-kappaB) activation and elicits vascular protection after acute endoluminal arterial injury. *Arterioscler Thromb Vasc Biol.* (2018) 38:1309–20. doi: 10.1161/ATVBAHA.117.310468
45. Yang WH, Park SY, Nam HW, Kim DH, Kang JG, Kang ES, et al. NFkappaB activation is associated with its O-GlcNAcylation state under hyperglycemic conditions. *Proc Natl. Acad Sci USA.* (2008) 105:17345–50. doi: 10.1073/pnas.0806198105
46. James LR, Tang D, Ingram A, Ly H, Thai K, Cai L, et al. Flux through the hexosamine pathway is a determinant of nuclear factor kappaB- dependent promoter activation. *Diabetes* (2002) 51:1146–56. doi: 10.2337/diabetes.51.4.1146
47. Lund PJ, Elias JE, Davis MM. Global analysis of O-GlcNAc glycoproteins in activated human T cells. *J Immunol.* (2016) 197:3086–98. doi: 10.4049/jimmunol.1502031
48. Sun C, Shang J, Yao Y, Yin X, Liu M, Liu H, et al. O-GlcNAcylation: a bridge between glucose and cell differentiation. *J Cell Mol Med.* (2016) 20:769–81. doi: 10.1111/jcmm.12807
49. Ghabrial AS. A sweet spot in the FGFR signal transduction pathway. *Sci Signal.* (2012) 5:pe1. doi: 10.1126/scisignal.2002789
50. Mariappa D, Sauert K, Marino K, Turnock D, Webster R, van Aalten DM, et al. Protein O-GlcNAcylation is required for fibroblast growth factor signaling in Drosophila. *Sci Signal.* (2011) 4:ra89. doi: 10.1126/scisignal.2002335
51. Miura T, Kume M, Kawamura T, Yamamoto K, Hamakubo T, Nishihara S. O-GlcNAc on PKCzeta Inhibits the FGF4-PKCzeta-MEK-ERK1/2 pathway via inhibition of PKCzeta phosphorylation in mouse embryonic stem cells. *Stem Cell Rep.* (2018) 10:272–86. doi: 10.1016/j.stemcr.2017.11.007
52. Kim YH, Song M, Oh YS, Heo K, Choi JW, Park JM, et al. Inhibition of phospholipase C-beta1-mediated signaling by O-GlcNAc modification. *J Cell Physiol.* (2006) 207:689–96. doi: 10.1002/jcp.20609
53. Kim MJ, Kim E, Ryu SH, Suh PG. The mechanism of phospholipase C-gamma1 regulation. *Exp Mol Med.* (2000) 32:101–9. doi: 10.1038/emm.2000.18
54. Saito T, Fukumoto S. Fibroblast growth factor 23 (FGF23) and disorders of phosphate metabolism. *Int J Pediatr Endocrinol.* (2009) 2009:496514. doi: 10.1186/1687-9856-2009-496514
55. Aukes K, Forsman C, Brady NJ, Astleford K, Blixt N, Sachdev D, et al. Breast cancer cell-derived fibroblast growth factors enhance osteoclast activity and contribute to the formation of metastatic lesions. *PLoS ONE* (2017) 12:e0185736. doi: 10.1371/journal.pone.0185736

56. Kim HJ, Kim KH, Lee J, Oh JJ, Cheong HS, Wong EL, et al. Single nucleotide polymorphisms in fibroblast growth factor 23 gene, FGF23, are associated with prostate cancer risk. *BJU Int.* (2014) 114:303–10. doi: 10.1111/bju.12396
57. Suehiro J, Kanki Y, Makihara C, Schadler K, Miura M, Manabe Y, et al. Genome-wide approaches reveal functional vascular endothelial growth factor (VEGF)-inducible nuclear factor of activated T cells (NFAT) c1 binding to angiogenesis-related genes in the endothelium. *J Biol Chem.* (2014) 289:29044–59. doi: 10.1074/jbc.M114.555235
58. Gelinas R, Mailleux F, Dontaine J, Bultot L, Demeulder B, Ginion A, et al. AMPK activation counteracts cardiac hypertrophy by reducing O-GlcNAcylation. *Nat Commun.* (2018) 9:374. doi: 10.1038/s41467-017-02795-4

Conflict of Interest Statement: The authors declare that the research was conducted in the absence of any commercial or financial relationships that could be construed as a potential conflict of interest.

frontiers in Endocrinology

REVIEW
published: 15 January 2019
doi: 10.3389/fendo.2018.00819

Protein *O*-GlcNAcylation in Cardiac Pathologies: Past, Present, Future

Marine Ferron[1,2]*, *Manon Denis*[2], *Antoine Persello*[2], *Raahulan Rathagirishnan*[3] and *Benjamin Lauzier*[2]

[1] Montreal Heart Institute, Montreal, QC, Canada, [2] l'institut du thorax, INSERM, CNRS, UNIV Nantes, Nantes, France, [3] Faculty of Health Sciences, University of Ottawa, Ottawa, ON, Canada

O-GlcNAcylation is a ubiquitous and reversible post-translational protein modification that has recently gained renewed interest due to the rapid development of analytical tools and new molecules designed to specifically increase the level of protein *O*-GlcNAcylation. The level of *O*-GlcNAc modification appears to have either deleterious or beneficial effects, depending on the context (exposure time, pathophysiological context). While high *O*-GlcNAcylation levels are mostly reported in chronic diseases, the increase in *O*-GlcNAc level in acute stresses such as during ischemia reperfusion or hemorrhagic shock is reported to be beneficial *in vitro*, *ex vivo,* or *in vivo*. In this context, an increase in *O*-GlcNAc levels could be a potential new cardioprotective therapy, but the ambivalent effects of protein *O*-GlcNAcylation augmentation remains as a key problem to be solved prior to their transfer to the clinic. The emergence of new analytical tools has opened new avenues to decipher the mechanisms underlying the beneficial effects associated with an *O*-GlcNAc level increase. A better understanding of the exact roles of *O*-GlcNAc on protein function, targeting or stability will help to develop more targeted approaches. The aim of this review is to discuss the mechanisms and potential beneficial impact of *O*-GlcNAc modulation, and its potential as a new clinical target in cardiology.

Keywords: *O*-GlcNAc, cardiovascular, ischemia-reperfusion, pharmacology, therapy

OPEN ACCESS

Edited by:
Tarik Issad,
Institut National de la Santé et de la Recherche Médicale (INSERM), France

Reviewed by:
Miles J. De Blasio,
Baker Heart and Diabetes Institute, Australia
Adam R. Wende,
University of Alabama at Birmingham, United States

***Correspondence:**
Marine Ferron
ferronmarine@gmail.com

Specialty section:
This article was submitted to Molecular and Structural Endocrinology, a section of the journal Frontiers in Endocrinology

Received: *16 July 2018*
Accepted: *31 December 2018*
Published: *15 January 2019*

Citation:
Ferron M, Denis M, Persello A, Rathagirishnan R and Lauzier B (2019) Protein O-GlcNAcylation in Cardiac Pathologies: Past, Present, Future. Front. Endocrinol. 9:819. doi: 10.3389/fendo.2018.00819

INTRODUCTION

Definition, Pathway, and Regulation

The *O*-N-acetyl glucosaminylation, commonly known as *O*-GlcNAcylation, is a reversible post-translational modification (PTM) that involves the addition of the monosaccharide β-D-N-acetylglucosamine to serine and threonine residues of proteins. It was first described by Torres and Hart on the internal surface of plasma membranes of lymphocytes (1). More recently, it has also been identified on cytosolic, nuclear, mitochondrial and membrane proteins (2–4). Over 3,000 proteins have been identified so far to be *O*-GlcNAcylated (5), and this number will probably increase with the development of new analytical techniques of *O*-GlcNAcylation detection such as the copper-catalyzed azide-alkyne cycloaddition "click" reaction described recently (6). From 1984 to 2004, <200 publications mentioning the MeSH terms "*O*-GlcNAc" or "*O*-GlcNAcylation" are referenced in Pubmed, while in 2017 alone almost 200 references can be found. Initially, little attention was paid to this minor sugar moiety, probably because the tools available to study this PTM were limited. In fact, detecting it is particularly difficult as it cannot be studied with classic techniques such as electrophoresis or high pressure liquid chromatography (HPLC) as the

O-GlcNAc moiety has no impact on molecular weight or isoelectric point, and it is very labile (7). More recently, with the development of more specific pharmacological compounds, protein *O*-GlcNAcylation has regained attention. Whilst it is now evident that protein *O*-GlcNAcylation is involved in many pathologies (from cancer to neurological disorders and cardiac function), the overall impact of protein *O*-GlcNAcylation remains unclear as in some situations it is reported to be beneficial (e.g., ischemia/reperfusion) or deleterious (e.g., diabetes). This suggests a potential role of this PTM in adapting to stress response and its importance in pathophysiological situations.

Protein *O*-GlcNAcylation is regulated by the concerted actions of only three enzymes. When glucose enters a cell it can be metabolized in a number of different metabolic pathways including glycogen synthesis, the pentose phosphate pathway, the glycolysis, or the hexosamine biosynthetic pathway (HBP, **Figure 1**). The first enzyme, glutamine fructose-6P amidotransferase (GFAT) uses glutamine and 2 to 5% of glycolytic fructose-6-P to perform the first step of the HBP. As the rate-limiting enzyme, GFAT controls HBP flow and consequently the *O*-GlcNAcylation level (8, 9). Mammals express two GFAT isoforms, GFAT1 and GFAT2, which are coded by separate genes. Both isoforms are expressed in heart. GFAT1 is ubiquitous, and mainly expressed in placenta, pancreas, testis and skeletal muscle. GFAT2 shares 75% homology with GFAT1, and this isoform is mostly expressed in heart and the central nervous system. Once the UDP-GlcNAc group is formed, it can be added or removed from proteins by two enzymes: the *O*-GlcNAc transferase (OGT) and the β-*N*-acetylglucosaminidase (OGA), respectively (**Figure 1**). As for GFAT, different splice variants of OGT and OGA exist. Alternative splicing of *ogt* results in the generation of three isoforms, a nucleocytoplasmic (116 kDa-ncOGT), a smaller isoform (70 kDa) named short form (sOGT) and a mitochondrial (103 kDa-mOGT) isoform of OGT. It is unclear if this last isoform is active. The first two isoforms are expressed mainly in the cytoplasm and nucleus as heterotrimers consisting of 2 ncOGT and 1 sOGT subunits (8). Two isoforms of OGA have been formerly described, a long one (lOGA) of 102 kDa found in the nucleocytoplasm, and a shorter one (sOGA) of 76 kDa resulting from alternative splicing. The smaller isoform is found in the sarcoplasmic reticulum and lipid droplets and is less active (4). The existence of a functional mitochondrial OGA isoform is debatable and represents an important area of ongoing research.

Pharmacological Regulation

The development of pharmacological tools to modulate protein *O*-GlcNAcylation has been very challenging. As discussed below, potent OGA inhibitors are now available for clinical use, but OGT inhibitors still need further development to be used properly *in vivo*. Altogether, these new molecules have allowed extensive characterization of this PTM.

Decrease in *O*-GlcNAc Levels

GFAT inhibitors

In the 1950's, when *O*-GlcNAc moiety was not yet discovered, *O*-diazoacetyl-L-serine (azaserine) and 6-diaz*O*-5-ox*O*-L-norleucine (DON) were developed to reduce tumor growth (10, 11). These molecules are structural analogs of glutamine and act as competing agonists or antagonists, respectively. They react with the catalytic region of most amidO-transferases, among them GFAT. They have a very low selectivity for GFAT. Whilst these compounds were used to efficiently induce antineoplastic effects, they presented a number of side effects including nausea and vomiting or loss of enthusiasm (12), and DON also causes hepatotoxicity in children (13). Moreover, through amid*O*-transferase inhibition, these compounds had pleiotropic effects in cells (**Table 1**). Developing new GFAT inhibitors represents a challenge because UDP-GlcNAc is also used for other cellular process, and its inhibition could have many side effects. As a result more attention has been paid to the development of OGT and OGA inhibitors.

OGT inhibitors

Different types of OGT inhibitors exist (**Figure 1**, **Table 1**). In this review, we will only focus on the four most described and used molecules. (1) Alloxan is a uracil analog developed at the beginning of the Twentieth Century (34). It was shown to be an OGT inhibitor on isolated pancreatic islets *in vitro* (35), and is absorbed via the glucose transporter GLUT2 in pancreatic β-cells. However, alloxan is highly unstable at physiological pH (half-life 1.5 min), it drives cell toxicity due to ROS production, and is not OGT specific as it also inhibits OGA (14–16). (2) At the end of the 1960's, benzoxazolinones (4-methoxyphenyl 6-acetyl-2-ox*O*-2,3-dihydr*O*-1,3-benzoxazole-3-carboxylate, or BZX) and their derived-compounds were proposed as potential new therapeutics due to their anti-cancer and anti-viral properties (17–19). However, as BZX irreversibly inactivates OGT, it cannot be used clinically due to its potential harmful effects on other cellular process (20). (3) BADGP (benzyl-2-acetymid*O*-2-deoxy-α-D-galactopyranoside), a N-acetylgalactosamine derivative, was also used as an OGT inhibitor (36, 37). Permanent exposure to BADGP induced abnormal *O*-glycosylation of mucins in HT-29 cells with potential negative effects on host defenses against pathogens (21–23). (4) Finally, a last inhibitor: Ac-5SGlcNAc, was proposed in 2011. This compound produced 5S-UDP-GlcNAc that binds to OGT and inhibits its activity. Authors demonstrated dose and time-dependent effects of this inhibitor (from 0.1 to 1,000 μM) and an EC50 at 5 μM in COS7 cells. These results were confirmed in fibroblasts, hepatocytes and neuronal cells, and by others in different cell types especially in an oncologic context. Contrary to the three first OGT inhibitors, Ac-5SGlcNAc does not perturb lectin glycosylation even at the highest dose. Thus, this compound is more frequently used in basic research, however, there is, today, no evaluation of its *in vivo* efficiency and safety (24).

In summary, whilst OGT inhibitors currently lack specificity and selectivity, improvements in OGT inhibitors is necessary

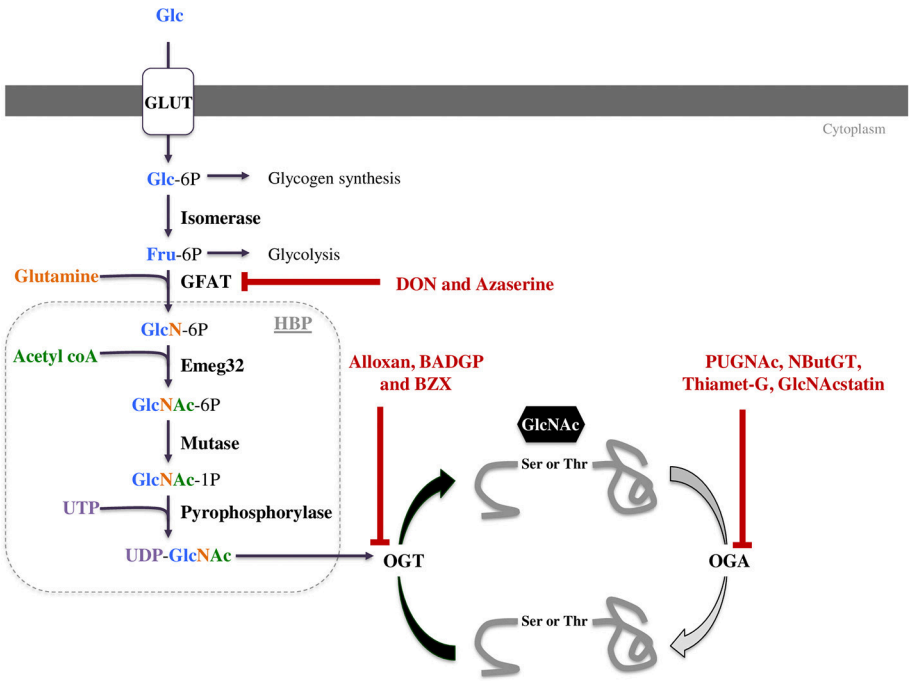

FIGURE 1 | The hexosamine biosynthetic pathway (HBP) leads to UDP-GlcNAc formation and regulates *O*-GlcNAcylation. This pathway is regulated by only three enzymes: GFAT (glutamine fructose-6P aminotransferase), OGT (*O*-GlcNAc transferase) and OGA (*O*-GlcNAcase). These three enzymes can be targeted by pharmacological compounds to modulate *O*-GlcNAc levels. Some of them decrease *O*-GlcNAc levels such as DON and azaserine inhibiting GFAT or Alloxan, BZX and BADGP inhibiting OGT. OGA inhibitors like PUGNAc, NButGT, Thiamet-G and GlcNAcstatin increase protein *O*-GlcNAcylation.

to be able to reduce protein *O*-GlcNAc levels and represents a potentially huge opportunity to reduce cancer or diabetes burden.

Increase in *O*-GlcNAc Levels

The development of strategies to increase *O*-GlcNAc levels has been more successful and can be used in human. Two different approaches are available to increase protein *O*-GlcNAc levels: increase in total UDP-GlcNAc through an increase in HBP flux or pharmacological inhibition of OGA.

Increase in UDP-GlcNAc concentration

Glucosamine (GlcN) bypass the rate limiting enzyme of the HBP, GFAT (38) resulting in higher UDP-GlcNAc levels, consequently it increases protein *O*-GlcNAcylation. Yet, if GlcN increases protein *O*-GlcNAc levels by 2 or 3-fold, this compound also has side effects such as: decrease in ATP production or increase in proteoglycans production (39, 40).

OGA inhibitors

Another way to increase protein *O*-GlcNAcylation is to inhibit OGA, and different molecules have been developed over the last 20 years. (1) The first described in the literature is the *O*-(2-acetamid*O*-2-deoxy-D-glucopyranosyliden)-amin*O*-N-phenylcarbamate commonly known as PUGNAc. It has been the most widely used compound to inhibit OGA for about a decade. However, PUGNAc also reacts with other hexosaminidases (HEX) such as lysosomal β-hexosaminidases with an inhibition ratio OGA/HEX of 1 (29). Recent OGA crystallography studies lead to the development of specific OGA inhibitors (31). These molecules interact directly with the active site of OGA, and include NButGT, Thiamet-G, and GlcNAcstatins. (2) NButGT (1,2- dideoxy-2'-propyl-α-D-glucopyranos*O*-(2,1-d)-Δ2'-thiazoline) is a competitive inhibitor of OGA and has good efficiency and specificity (**Table 1**). However, according to a study by Macauley et al. NButGT has a half-clearance of only 30 min *in vivo*, and lacks stability in solution (few days to weeks) (30). (3) Thiamet-G [(3aR,5R,6S,7R,7aR)-2-ethylamin*O*-3a,6,7,7a-tetrahydr*O*-5-(hydroxymethyl)-5H-pyrano(3,2-d)thiazole-6,7-diol] was developed several years later, and is more stable (31). (4) More recently, GlcNAcstatin has been described. It presents a molecular architecture noticeably similar to PUGNAc (**Table 1**) (32, 33), with a high selectivity and efficiency. Unfortunately, synthesis of GlcNAcstatin remains complex and very expensive (41).

Over the last decade, pharmacological modulators of *O*-GlcNAc levels have been developed for (i) improved knowledge of physiological conditions, as well as (ii) potential utilization as therapeutic strategies in different pathologies.

POTENTIAL IMPACT OF MODULATING *O*-GLCNAC LEVELS IN PATHOLOGIES

The consequence of an increase in protein *O*-GlcNAcylation has mainly been evaluated in diabetes or cancers. In these pathologies, patients with high *O*-GlcNAc levels present with the poorest outcome. In this context, a reduction in *O*-GlcNAc levels

TABLE 1 | Summary of molecules currently available for *O*-GlcNAc level modulation: their actions, specificity, known limits and strengths.

Effects	Action	Molecule	IC50	Strengths	Weaknesses	References
O-GlcNAc decrease	GFAT inhibition	DON		Uses in oncologic research for its anti-neoplastic properties	Low selectivity for GFAT, toxic effects, pleiotropic effect	(10–14)
		Azaserine				
	OGT inhibition	Alloxan	18 μM	Cell permeant through glucose transporter (GLUT2 in pancreatic beta cells)	Off target effects, toxicity, induced ROS production, instable at physiologic pH (half-life 1,5 min)	(14–16)
		BZX	10 μM	Cell permeant, anti-cancer and anti-viral properties	Harmfull effects on cellular process	(17–20)
		BADGP			Abnormal *O*-glycosylation	(21–23)
		Ac-5SGlcNAc	5 μM	No modification of lectin glycosylation, uses in oncologic research	No use in *in vivo* conditions	(24, 25)
O-GlcNAc increase	UDP-GlcNAc increase	Glutamine		Used in hospital	Poor efficiency, pleiotropic effects	(9, 26–28)
		Glucosamine				
	OGA inhibition	PUGNAc		First OGA inhibitors synthetized	Poorly specific(OGA/HEX=1), desensitizes cell to insulin, doesn't cross blood brain barrier	(14, 29)
		NButGT	8 μM	High specificity(OGA/HEX=1,500)	Lack of stability *in vivo* (half clearance 30 min), limited chemical stability in solution	(30, 31)
		Thiamet G	30 nM	High specificity(OGA/HEX=35,000)	Expensive	(31)
		GlcNAcstatin G	4 nM	High specificity(OGA/HEX=900,000)	Expensive, lack of study	(32, 33)

OGA, O-GlcNAcase; OGT, O-GlcNAc transferase; GFAT, glutamine fructose-6P amidotransferase; DON, 6-diazO-5-oxO-L-norleucine; BADGP, benzyl-2-acetymidO-2-deoxy-α-D-galactopyranoside; BZX, benzoxazolinones; IC 50, concentration of inhibitor required for achieving 50% inhibition; GLUT 2, Glucose Transporter Type 2.

appears to be an interesting therapeutic strategy. Alternatively, in acute pathologies, *O*-GlcNAc stimulation using different approaches to increase *O*-GlcNAc levels could be a promising therapeutic approach.

Increasing *O*-GlcNAc Levels in Acute Pathology, a Potent Therapeutic Approach?

Several studies have demonstrated the importance of *O*-GlcNAc response to a stress, and especially an increase in *O*-GlcNAc levels following this stress. This augmentation is reported to improve cell survival through a decrease in pro-apoptotic pathway molecules (p53, FOXO3, caspase 8 or GPAT1) and activation of sirtuin deacetylase (SIRT1) (42–45). Similarly, the beneficial effects of protein *O*-GlcNAcylation stimulation, with GlcN or siOGA, are associated with a decrease in apoptosis (46–48). These *in vitro* results were confirmed *in vivo* for different types of stress (e.g., hypoxia, inflammation, oxidative stress), and in different tissues and/or different pathologies.

In kidney, damage caused by hypoxia or an acute injury using a rabbit model are attenuated by GlcN administration (49). Hu et al. also reported an improvement in renal function and a decrease in apoptosis and oxidative stress markers, and these effects were abolished with alloxan (45). In a brain model, using a middle cerebral artery occlusion (MCAO), it was shown that an increase in *O*-GlcNAc levels, by GlcN or Thiamet G, resulted in reduced infarct volume and an improvement in cognitive function. These effects could be explained by a reduction in apoptosis and inflammation (suglia and NF-κB activation, reduction of cytokine production and leukocyte infiltration) (50–52). In hemorrhagic shock, hypovolemia is associated with an alteration in glucose utilization. Using *in vitro* (neonatal rat ventricular cardiomyocytes) and *in vivo* (rat) models of hemorrhagic shock Chatham's group demonstrated that augmentation of *O*-GlcNAc levels improved global outcomes. Specifically, GlcN improved organ perfusion, cardiac function, the inflammatory state and finally, increased survival (53, 54). Several years later, these results were confirmed with a specific inhibitor of OGA, PUGNAc, validating the potential therapeutic role of protein *O*-GlcNAcylation in this pathology (53, 55). In all these studies, cardiovascular function was significantly improved.

Ischemia-Reperfusion From *ex vivo* to *in vivo*

Myocardial infarction results from an obstruction of a coronary artery creating an ischemia leading to tissue necrosis. Reperfusion, by thrombolysis or invasive procedures, is the only way to preserve cardiac function and to save patient life and must be performed as early as possible and within the first 12 h. Unfortunately, reperfusion exacerbates cardiac injury through

an excessive oxidative stress and inflammatory response. In this context, the introduction of an infarct-limiting therapy in clinical practice might have a clinical and socioeconomic impact (56).

The first evidence of the potential beneficial effects of *O*-GlcNAc was shown *in vitro*. Champattanachai and collaborators reported that an increase in *O*-GlcNAcylated proteins through GlcN infusion in rat neonatal cardiomyocytes improved cell viability following IR. Moreover, with the use of different pharmacological compounds (glucosamine, PUGNAc, azaserine, alloxan), they demonstrated a positive correlation between *O*-GlcNAc levels and cell viability in IR. According to the authors, the beneficial effects of GlcN are associated with a decrease in calcium overload and apoptosis through a reduction in mitochondrial permeability, transitional pores, or mPTP opening (57, 58). A second team confirmed these results by specifically targeting OGA. They modulated *O*-GlcNAc levels by PUGNAc, adenoviral overexpression of OGA or siRNA's against OGA, and demonstrated that an increase in *O*-GlcNAc levels increased cell viability and decreased apoptosis and oxidative stress in responses to IR (59, 60).

To confirm these initial *in vitro* findings, *ex vivo* studies have also been performed. A first study using a Langendorff model of IR demonstrated that glutamine improved cardiac function through an improvement of left cardiac function (ventricular pressures and heart rate) and a decrease in infarct size (cardiac troponin I release). According to these authors, this could be explained by a restoration in cellular ATP concentration (61). Once again, these beneficial effects were confirmed using an OGA inhibitor, NAG thiazolines, and this compound also reduced infarct size and mechanical arrhythmic activity (62).

Intriguingly, the number of *in vivo* studies is quite limited and only focuses on murine models. Considering the potential clinical impact of *O*-GlcNAc stimulation on cardiac function, it remains as an important step to continue toward clinical validation. The only direct *in vivo* evidence confirming *in vitro* results is from mice treated with PUGNAc at the reperfusion stage. This treatment efficiently reduced infarct size, apoptosis and mPTP opening (63). However, many *in vivo* studies indirectly suggest that *O*-GlcNAc stimulation could improve patient outcomes. For example, hearts submitted to preconditioning (two periods of 5 min ischemia and 5 min reperfusion) presented a higher myocardial glucose uptake and a higher protein *O*-GlcNAcylation, and a better recovery. In this context, the authors explained that the *O*-GlcNAc level increase was responsible for the cardioprotective preconditioning effect (64).

TOWARD A POTENTIAL CLINICAL APPLICATION

From Bench to Bedside, a Complicated Step

Several studies in cellular and animal models have demonstrated the potential beneficial effects of *O*-GlcNAc level augmentation in acute pathologies, and especially in cardiac IR. However, several limitations still exist and these need to be studied before a potential clinical application. Whilst acute *O*-GlcNAc level augmentation is cardioprotective in murine models, the adverse effects of a long-term exposure to high *O*-GlcNAc levels should also be considered. For instance, hearts isolated 1 month after myocardial infarction induced by coronary ligation presented high levels of protein *O*-GlcNAcylation, and especially higher *O*-GlcNAcylation of troponin T, and this observation was linked to higher cardiac dysfunction (65). Similarly, in rats subjected to hypoxic conditions (alternating 2 min 21% O_2 and 2 min 6–8% O_2 8 h per day) *O*-GlcNAc levels started to rise 2 weeks after the first stress. This observation was associated with higher apoptosis and inflammatory markers (66). Myocardial infarction and the resulting reperfusion injury is associated with cardiac remodeling, hypertrophy and heart failure, a situation aggravated by high *O*-GlcNAc levels, even if there is still no consensus regarding the link between *O*-GlcNAcylation of proteins and cardiac hypertrophy (67, 68). However, several studies have demonstrated an increase in cardiac protein *O*-GlcNAcylation in *in vitro* and *in vivo* models of hypertrophy (69–73). *O*-GlcNAc levels in the left ventricular myocardium were increased in patients with heart failure (73). Furthermore, increases in *O*-GlcNAc levels were associated with heart failure development (65, 74). In parallel, augmentation of protein *O*-GlcNAcylation turns out to be an adverse therapy for diabetic patients. In diabetic IR conditions, hyperglycemia and high *O*-GlcNAc levels are also associated with an aggravation of cardiac dysfunction and infarct size (75, 76).

In summary, before clinical trials can be conducted, more studies are necessary to characterize the potential long-term impact of *O*-GlcNAc stimulation and to evaluate the best dose, time-point and duration of treatment to avoid adverse effects.

To Future Potential Clinical Trial in Cardiology

Glutamine and glucosamine are metabolites used in the HBP pathway and could be a way to increase *O*-GlcNAc levels via an increase in HBP flux. These two molecules are already used clinically to treat inflammatory disease or improve cardiac function, and could provide proof of potential utilization in cardiac acute pathologies like IR. Despite this, their impact on *O*-GlcNAc level has never been tested in humans.

Glutamine supplementation is now recommended for parenteral or enteral supplementation in neonatal, pediatric and adult intensive care units and seems to be safe (26, 27). Moreover, in pediatric or adult intensive care units, patients with low plasma glutamine (<420 μmol/l) at admission are at higher risk of mortality and increased incidence of multiple organ failure (77, 78). Whilst this observation suggests a potential benefit from increasing glutamine concentration the consequence on protein *O*-GlcNAcylation has never been studied. Enteral glutamine supplementation has been shown to reduce the incidence of serious neonatal infections in preterm and/or very low birth weight children (79) and enterocolitis (80, 81). In critical conditions, glutamine enteral supplementation decreases the incidence of sepsis, pneumonia, and bacteremia in trauma (82) and burn patients (83). Moreover, glutamine may have a

perioperative cardioprotective role. Glutamine use in patients with ischemic heart disease operated under conditions of extracorporeal blood circulation or cardiopulmonary bypass reduces troponin release at day 1, the systemic vascular resistance index and improves cardiac and stroke index (84, 85). As well, perioperative glutamine supplementation during aortic surgery can compensate renal arginine synthesis loss induced by aortic clamping and could also improve post-operative renal function (86). A recent clinical trial showed that patients who receive oral glutamine have less complications, myocardial damage, morbidity and mortality after coronary revascularization under cardiopulmonary bypass (87). A similar protocol in chronic angina patients, delayed the time to onset of more than 1.0 mm of ST segment depression on the electrocardiogram (ECG) by 38 s, but did not improve hemodynamic response to exercise, the time of onset of angina symptoms, maximum workload or total exercise time (88).

GlcN is largely used for osteoarthritis at an average dose of 1,500 mg per day but its usefulness in other pathologies has not been explored in clinical trials. Whereas, long term treatment seems to delay the progression of knee arthritis (28), multiple studies have shown no superiority of glucosamine vs. placebo (89), no improvement of cartilage damage (90) and no role in prevention of osteoarthritis in overweight women (91). Moreover, at the usual doses, GlcN may induce an increase in intraocular pressure (92). This possible deleterious effect of high dose GlcN is supported by a recent review that showed this molecule is not beneficial for all population subgroups (93). Clinical use of GlcN has been associated with potential side effects *in vivo*, among them vomiting and diarrhea (94) and has also been associated with intracellular ATP depletion (95). Overall, GlcN utilization for joint pain appears to be safe.

Glutamine or GlcN supplementation has demonstrated its benefits for a few pathologies but these molecules are not specific to the HBP, and the link between the benefits and an increase in protein *O*-GlcNAcylation has not been demonstrated. Recently, new molecules targeting OGA have been studying for the treatment of tauopathy. MK-8719, a selective and potent small molecule inhibitor of OGA has shown promising results in the treatment of tauopathy such as Progressive Supranuclear Palsy (PSP). It has been evaluated in a recent phase I study in healthy volunteers. Interestingly, MK-8719 administration elicited PBMC *O*-GlcNAcylated protein increases in a dose dependent-manner, consistent with preclinical observations. Moreover, ASN120290, a brain-permeable small-molecule OGA inhibitor, has been also studied in a randomized, double-blind, placebo-controlled phase I study. These molecules seem to be safe and well tolerated (96).

These molecules represent a huge opportunity for progression to future clinical trials. Despite the beneficial impact of an increase in total *O*-GlcNAc level in IR, the treatment remains non-selective and can have potential side effects that have not been clearly evaluated in most studies. In future studies, more attention should be paid to doses and administration time to avoid any drawback.

What Should be Confirmed Prior to Performing Clinical Trials?

Understanding Metabolism and *O*-GlcNAc Level Variation Through Aging

O-GlcNAc levels are linked to GFAT activity and cellular metabolism, particularly that of glucose. This observation is particularly important in cardiac tissue as cardiac metabolism constantly adapts to conditions and evolves throughout the first stage of life, especially the substrate selection for energy production. The predominant substrates for energy production in fetal hearts are carbohydrates (mainly glucose, lactate and pyruvate) and cardiac metabolism is mainly anaerobic. After birth, the ability of hearts to oxidize fatty acids increases within the first week (97), and in the adult heart, energy is mainly supplied by fatty acid oxidation (60–80%), carbohydrates (20–30%) and ketone bodies (10%). These proportions are constantly modulated to fit requirements and substrate availability. During fetal life, cardiac glucose uptake is controlled by a low affinity insulin-independent glucose membrane transporter, Glucose transporter type I (GLUT1). Shortly after birth, cardiac glucose transporters switch from the GLUT1 isoform to the GLUT4 isoform. GLUT4 is an insulin-sensitive glucose transporter, which is the predominant transporter in the adult heart (97). This observation is of particular importance as changes in glucose transporter expression, such as GLUT1 and GLUT4, have been shown to influence UDP-GlcNAc levels in mice. Interestingly, GFAT activity and glucose flux via the HBP are increased in muscles of GLUT1-overexpressing mice but not GLUT4-overexpressing mice (98). Consequently, during the first days of life, cardiac metabolism is subjected to dramatic changes with a major increase in fatty acid oxidation and a reduction in carbohydrate metabolism, whilst the impact on protein *O*-GlcNAcylation remains unknown. Altogether, the metabolic modification associated with the first days of life could impact *O*-GlcNAc levels and be of great importance in cardiac development and maturation. They could also be responsible for the higher capacity of the heart to withstand stress during the first days of life (99–101). Furthermore, in situations of stress or specific pathological conditions, the proportion of carbohydrates metabolized will increase to sustain cardiac needs. In the long run, this modification will affect HBP flux and modulate *O*-GlcNAc levels resulting in a potential impact on cardiac function. Interestingly, no study has evaluated if these modifications actually have an impact on cardiac *O*-GlcNAcylation.

While metabolism is subject to modifications throughout aging, and while protein *O*-GlcNAcylation has been described as a metabolic sensor, the exact link between metabolism's age-associated variations and *O*-GlcNAc levels has never been explored. In fact, many authors have only focused on senescence, and demonstrated that *O*-GlcNAc levels have an impact on the development and the progression of chronic diseases (102, 103).

The variation of *O*-GlcNAc levels during aging has not reached a consensus yet. Fülöp et al. showed a decrease in *O*-GlcNAc levels in rat hearts which was associated with a reduction in OGT expression between adolescence (6 weeks)

and adulthood (22 weeks) (104). However, in another study, the authors showed an increase in *O*-GlcNAc levels in rat hearts between 5 and 24 months, which surprisingly, was associated with a decrease in OGT expression (105). In the brain, which is the most studied organ for this question, age-associated variation of protein *O*-GlcNAcylation is not clear. *O*-GlcNAc levels rapidly decrease between the 1st and the 24th month (106) or increase between 5 and 24th month (105), whereas Rex-Mathes et al. showed no change in protein *O*-GlcNAcylation between the 3rd and 13th month (107) (**Figure 2**).

The lack of consensus on *O*-GlcNAc level variation throughout aging and in organ function underlines the need for new standardized studies to improve the understanding of *O*-GlcNAc levels on cellular development, survival and potential impacts on pathology or treatment responses.

Doses and Timing of Treatment

The ambiguous effects of *O*-GlcNAc is not restricted to the differences in basal *O*-GlcNAc levels, as it is now evident that there are dose-dependent effects of protein *O*-GlcNAcylation. The beneficial effects associated with increase in *O*-GlcNAc are lost for high increase in *O*-GlcNAc level. Gu et al. showed for brain IR that a high increase in *O*-GlcNAc levels (∼7 fold) compared to a moderate increase in *O*-GlcNAc level (∼3 fold) leads to a detrimental effect with an increase in infarct size. Strikingly, most of the beneficial effects described in the literature are associated with a 2–5 fold increase in protein O-GlcNAcylation levels in the heart (45, 57, 61), and in the brain (51, 108–110). Champattanachai et al. showed similar results, and highlighted a close link between O-GlcNAc levels and cell viability in their model (57). Unfortunately, few studies have focused on O-GlcNAc level modulation in physiological or pathophysiological conditions. In addition, the same authors showed that GlcN increases the level of protein *O*-GlcNAcylation by 1.5 fold in normoxia, and by 3 fold in hypoxia (57). The stimulation of this PTM could induce different responses in pathophysiological conditions. Interestingly, a recent clinical study showed that delayed sepsis treatment using 0.35 g/kg of glutamine per day *i.v.* and 30 g per day glutamine given via enteral administration to patients with two or more failing organs, had no effect on the outcome of organ failure and infections. It even increased mortality in hospital and at 6 months (111). These results might be explained by the high dose of glutamine (dose-dependent effect) and/or the late initiation of the protocol (time-dependent effect).

The lack of data on dose and time of treatment remains the key safety issue that needs to be satisfied in order to progress toward a clinical trial. Only one study has focused on establishing an optimal glutamine supplementation dose in pediatric cancer patients, however they did not evaluate the impact on *O*-GlcNAc levels (112).

IMPROVEMENT OF TOOLS

In order to improve the understanding of the impact of *O*-GlcNAc on proteins and cell survival considerable progress has been made in developing new tools. Three main themes are of particular importance and have gained momentum over the last couple of years: (i) identifying *O*-GlcNAcylation sites on protein using mass spectrometry, (ii) improving pharmacological tools to improve specificity and biocompatibility, and (iii) understanding the impact of *O*-GlcNAcylation on specific proteins.

Emerging Analytical Tools

As discussed above, there is a significant conundrum for protein *O*-GlcNAcylation, with on one-hand, potential short-term

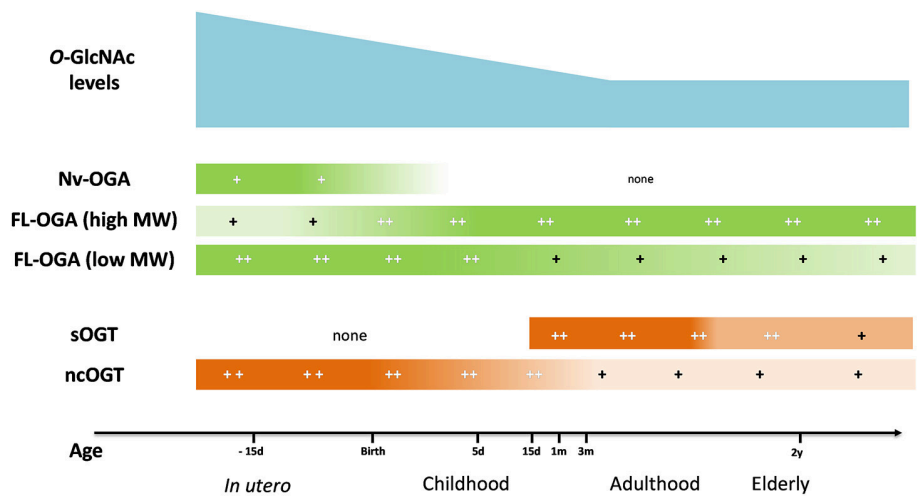

FIGURE 2 | Evolution of *O*-GlcNAc levels, OGA and OGT expression in brain tissue throughout lifespan. OGA, *O*-GlcNAcase; OGT, *O*-GlcNAc transferase; FL-OGA, full-length OGA; high MW, high molecular weight, low MW, low molecular weight; Nv-OGA, Nuclear variant OGA; ncOGT, nucleo-cytoplasmic OGT; sOGT, short OGT;−15 d, 15 days before birth; 5 d, 5 days post-natal; 15 d, 15 days; 1 m, 1 month; 3 m, 3 months; 2 y, 2 years (105–107).

beneficial effects and on the other hand long-term deleterious effects. It is important to decipher which *O*-GlcNAc sites are of interest and potentially beneficial or potentially detrimental. Hopefully, in the near future, specifically targeting these sites will potentiate the beneficial effects and limit adverse effects associated with untargeted increases in *O*-GlcNAc level. Global mapping of *O*-GlcNAcylated proteins and peptides has recently been possible using mass spectrometry approaches. Recent advances in analytical techniques have also allowed to determine *O*-GlcNAcylation sites. For example, Thompson et al. highlighted "emerging technologies for quantitative, site-specific MS-based *O*-GlcNAc proteomics (*O*-GlcNAcomics), which allow proteome-wide tracking of *O*-GlcNAcylation dynamics at individual sites." In this article, the authors listed the current technique for *O*-GlcNAc identification using mass spectrometry (6). Many papers have described the successful use of a combination of fractionation and click chemistry to label and identify *O*-GlcNAc sites on proteins. For example, Griffin et al. extensively studied the *O*-GlcNAcylation site on OGT with a chemically cleavable tag and suggested a potential implication of *O*-GlcNAc on the regulation of protein function (113). More recently, Deracinois et al. used this approach on skeletal muscle proteins and reported that some *O*-GlcNAcylation sites were located in interaction sites that open new area of research for this PTM (114). Thanks to the development and thorough validation of these new tools, consensus sequences have recently been proposed (115). Recent advances in technologies represent a huge opportunity and will definitely help to improve the understanding of the role of this PTM.

Toward Specific Pharmacological Tools

Pharmacology has long been used to study different pathways and targets, and OGA, GFAT and OGT inhibitors have been known about since the early 90's. At present however, the main drawback of these compounds are their lack of specificity and affinity and their toxicity.

OGA inhibitors have been most beneficial and are now available for clinical trials. In fact, they have been the prime targets to develop a therapeutic strategy (29). The remaining challenge is in the potential directed system administration, in order to limit the potential off target effects. While the use of enzymatically triggered prodrugs is well known in the field of cancer, this strategy is poorly developed for treatment of other pathologies. In parallel, a second strategy could be to design new OGA inhibitors targeting specific organelles (e.g., mitochondria) or organs. Such tools would present two major advantages as they would help to: (i) decipher the role of this PTM on different organelles and (ii) improve treatment specificity. On the other hand, while OGT inhibitors potentially represent an interesting therapeutic strategy for cancer, they still lack specificity, are not cell permeant or are toxic.

Recent advances in crystallography opens potentially new avenues to study the impact of *O*-GlcNAc levels on cellular function. The next step will be to specifically target cellular compartments and/or specific proteins to be able to maximize potential beneficial impacts on selected pathways or cellular processes (61, 115–118).

Site Specific Evaluation

Recent advances in *O*-GlcNAc proteomics has produced a very large quantity of potential sites to explore. It is now important to develop screening tools to be able to further advance our understanding of protein *O*-GlcNAcylation. Because only two enzymes are involved in *O*-GlcNAcylation, a solution may rely on biochemistry, and more specifically on site-specific mutagenesis through the incorporation of non-natural amino acids (NAA) such as selenocysteine derivatives. NAA are useful tools to add new properties to proteins at specific positions. They can be incorporated into a protein sequence during translation through genetic code expansion by an orthogonal (i.e., not interfering with the natural amino acids system) aminoacyl-tRNA synthetase (aaRS). This TAG codon is positioned in an appropriate position into the recombinant proteins gene (119, 120). Protein function could then be evaluated through enzymatic assays for example.

CONCLUSION

Over the last 30 years, knowledge on protein *O*-GlcNAcylation has increased considerably in many areas, yet, the cardiovascular field remains largely underexplored. A pubmed search using the "cardiovascular" and "*O*-GlcNAc" MeSH term retrieved only 187 papers in October 2018. More effort has been expended on chronic pathologies such as diabetes, cancer, and Alzheimers disease, leading to potential new approaches for the patient. On the acute side, augmentation of *O*-GlcNAc levels may represent a new therapeutic solution for cardiovascular dysfunction or ischemia/reperfusion, yet its potential harmful effects at higher doses, or the impact of long term stimulation remain to be determined. Furthermore, deciphering which protein or pathway is involved in *O*-GlcNAc effects represents the key element to be able to specifically target them. The future may be hidden in organelle specific *O*-GlcNAc modulation or in new proteomic approaches with powerful tools to study *O*-GlcNAcylation. Increasing the understanding of this very specific PTM will open complete new area of research for protein-targeted mutation.

AUTHOR CONTRIBUTIONS

MF, MD, AP, and RR wrote the review. BL corrected the final manuscript.

ACKNOWLEDGMENTS

We would like to thank Dr. Bryce Van Denderen for English revision. We would also thank Fédération Française de Cardiologie, Fondation d'entreprises Génavie for their financial support and the IBISA core facility Therassay for its assistance and their technical support.

REFERENCES

1. Torres CR, Hart GW. Topography and polypeptide distribution of terminal N-acetylglucosamine residues on the surfaces of intact lymphocytes. Evidence for O-linked GlcNAc. *J Biol Chem.* (1984) 259:3308–17.
2. Holt GD, Hart GW. The subcellular distribution of terminal N-acetylglucosamine moieties. Localization of a novel protein-saccharide linkage, O-linked GlcNAc. *J Biol Chem.* (1986) 261:8049–57.
3. Schindler M, Hogan M, Miller R, DeGaetano D. A nuclear specific glycoprotein representative of a unique pattern of glycosylation. *J Biol Chem.* (1987) 262:1254–60.
4. Yang X, Qian K. Protein O-GlcNAcylation: emerging mechanisms and functions. *Nat Rev Mol Cell Biol.* (2017) 18:452–65. doi: 10.1038/nrm.2017.22
5. Ma J, Hart GW. O-GlcNAc profiling: from proteins to proteomes. *Clin Proteomics* (2014) 11:8. doi: 10.1186/1559-0275-11-8
6. Thompson JW, Griffin ME, Hsieh-Wilson LC. Methods for the detection, study, and dynamic profiling of O-GlcNAc glycosylation. *Methods Enzymol.* (2018) 598:101–35. doi: 10.1016/bs.mie.2017.06.009
7. Hart GW, Slawson C, Ramirez-Correa G, Lagerlof O. Cross talk between O-GlcNAcylation and phosphorylation: roles in signaling, transcription, and chronic disease. *Annu Rev Biochem.* (2011) 80:825–58. doi: 10.1146/annurev-biochem-060608-102511
8. Love DC, Hanover JA. The hexosamine signaling pathway: deciphering the "O-GlcNAc code." *Sci. STKE* (2005) 2005:re13. doi: 10.1126/stke.3122005re13
9. Marshall S, Bacote V, Traxinger RR. Discovery of a metabolic pathway mediating glucose-induced desensitization of the glucose transport system. Role of hexosamine biosynthesis in the induction of insulin resistance. *J Biol Chem.* (1991) 266:4706–12.
10. Coffey GL, Ehrlich J, Fisher MW, Hillegas AB, Kohberger DL, Machamer HE, et al. 6-Diazo-5-oxo-L-norleucine, a new tumor-inhibitory substance. I Biologic studies. *Antibiot Chemother.* (1956) 6:487–97.
11. Stock CC, Reilly HC, Buckley SM, Clarke DA, Rhoads CP. Azaserine, a new tumour-inhibitory substance; studies with Crocker mouse sarcoma 180. *Nature* (1954) 173:71–2. doi: 10.1038/173071a0
12. Milewski S. Glucosamine-6-phosphate synthase–the multi-facets enzyme. *Biochim Biophys Acta* (2002) 1597:173–92. doi: 10.1016/S0167-4838(02)00318-7
13. Cervantes-Madrid D, Romero Y, Dueñas-González A. Reviving lonidamine and 6-diazo-5-oxo-L-norleucine to be used in combination for metabolic cancer therapy. *BioMed Res Int.* (2015) 2015:690492. doi: 10.1155/2015/690492
14. Ostrowski A, van Aalten DMF. Chemical tools to probe cellular O-GlcNAc signalling. *Biochem J.* (2013) 456:1–12. doi: 10.1042/BJ20131081
15. Lee TN, Alborn WE, Knierman MD, Konrad RJ. Alloxan is an inhibitor of O-GlcNAc-selective N-acetyl-beta-D-glucosaminidase. *Biochem Biophys Res Commun.* (2006) 350:1038–43. doi: 10.1016/j.bbrc.2006.09.155
16. Trapannone R, Rafie K, van Aalten DMF. O-GlcNAc transferase inhibitors: current tools and future challenges. *Biochem Soc Trans.* (2016) 44:88–93. doi: 10.1042/BST20150189
17. Advani Shyam B, Sam J. Potential anticancer and antiviral agents. Substituted 3-[1′(2′,3′,4′-tri-O-benzoyl-β-d-ribopyranosyl)]-2-benzoxazolinones. *J Heterocycl Chem.* (1968) 5:119–22. doi: 10.1002/jhet.5570050123
18. Caldwell SA, Jackson SR, Shahriari KS, Lynch TP, Sethi G, Walker S, et al. Nutrient sensor O-GlcNAc transferase regulates breast cancer tumorigenesis through targeting of the oncogenic transcription factor FoxM1. *Oncogene* (2010) 29:2831–42. doi: 10.1038/onc.2010.41
19. Itkonen HM, Minner S, Guldvik IJ, Sandmann MJ, Tsourlakis MC, Berge V, et al. O-GlcNAc transferase integrates metabolic pathways to regulate the stability of c-MYC in human prostate cancer cells. *Cancer Res.* (2013) 73:5277–87. doi: 10.1158/0008-5472.CAN-13-0549
20. Jiang J, Lazarus MB, Pasquina L, Sliz P, Walker S. A neutral diphosphate mimic crosslinks the active site of human O-GlcNAc transferase. *Nat Chem Biol.* (2011) 8:72–7. doi: 10.1038/nchembio.711
21. Celiberto LS, Chan JY, Law HT, Bhullar K, Xia L, Cavallini DC, et al. A10 core-1 derived o-glycosylation of the mucin muc2 plays a key role in host defense against enteric citrobacter rodentium infection. *J Can Assoc Gastroenterol.* (2018) 1:15–6. doi: 10.1093/jcag/gwy009.010
22. Hennebicq-Reig S, Lesuffleur T, Capon C, De Bolos C, Kim I, Moreau O, et al. Permanent exposure of mucin-secreting HT-29 cells to benzyl-N-acetyl-alpha-D-galactosaminide induces abnormal O-glycosylation of mucins and inhibits constitutive and stimulated MUC5AC secretion. *Biochem J.* (1998) 334:283–95.
23. Olvera A, Martinez JP, Casadell,à M, Llano A, Rosás M, Mothe B, et al. Benzyl-2-acetamido-2-deoxy-α-d-galactopyranoside increases human immunodeficiency virus replication and viral outgrowth efficacy in vitro. *Front Immunol.* (2018) 8:2010. doi: 10.3389/fimmu.2017.02010
24. Gloster TM, Zandberg WF, Heinonen JE, Shen DL, Deng L, Vocadlo DJ. Hijacking a biosynthetic pathway yields a glycosyltransferase inhibitor within cells. *Nat Chem Biol.* (2011) 7:174–81. doi: 10.1038/nchembio.520
25. Ma Z, Vosseller K. Cancer metabolism and elevated O-GlcNAc in oncogenic signaling. *J. Biol. Chem.* (2014) 289:34457–65. doi: 10.1074/jbc.R114.577718
26. Thompson SW, McClure BG, Tubman TRJ. A randomized, controlled trial of parenteral glutamine in ill, very low birth-weight neonates. *J Pediatr Gastroenterol Nutr.* (2003) 37:550–3. doi: 10.1097/00005176-200311000-00008
27. van den Berg A, van Elburg RM, Teerlink T, Lafeber HN, Twisk JWR, Fetter WPF. A randomized controlled trial of enteral glutamine supplementation in very low birth weight infants: plasma amino acid concentrations. *J Pediatr Gastroenterol Nutr.* (2005) 41:66–71. doi: 10.1097/01.mpg.0000167497.55321.65
28. Pavelká K, Gatterová J, Olejarová M, Machacek S, Giacovelli G, Rovati LC. Glucosamine sulfate use and delay of progression of knee osteoarthritis: a 3-year, randomized, placebo-controlled, double-blind study. *Arch Intern Med.* (2002) 162:2113–23. doi: 10.1001/archinte.162.18.2113
29. Macauley MS, Vocadlo DJ. Enzymatic characterization and inhibition of the nuclear variant of human O-GlcNAcase. *Carbohydr Res.* (2009) 344:1079–84. doi: 10.1016/j.carres.2009.04.017
30. Macauley MS, Whitworth GE, Debowski AW, Chin D, Vocadlo DJ. O-GlcNAcase uses substrate-assisted catalysis: kinetic analysis and development of highly selective mechanism-inspired inhibitors. *J Biol Chem.* (2005) 280:25313–22. doi: 10.1074/jbc.M413819200
31. Yuzwa SA, Macauley MS, Heinonen JE, Shan X, Dennis RJ, He Y, et al. A potent mechanism-inspired O-GlcNAcase inhibitor that blocks phosphorylation of tau in vivo. *Nat Chem Biol.* (2008) 4:483–90. doi: 10.1038/nchembio.96
32. Dorfmueller HC, Borodkin VS, Schimpl M, van Aalten DMF. GlcNAcstatins are nanomolar inhibitors of human O-GlcNAcase inducing cellular hyper-O-GlcNAcylation. *Biochem J.* (2009) 420:221–7. doi: 10.1042/BJ20090110
33. Dorfmueller HC, Borodkin VS, Schimpl M, Shepherd SM, Shpiro NA, van Aalten DMF. GlcNAcstatin: a picomolar, selective O-GlcNAcase inhibitor that modulates intracellular O-glcNAcylation levels. *J Am Chem Soc.* (2006) 128:16484–5. doi: 10.1021/ja066743n
34. Lenzen S, Panten U. Alloxan: history and mechanism of action. *Diabetologia* (1988) 31:337–42. doi: 10.1007/BF02341500
35. Konrad RJ, Zhang F, Hale JE, Knierman MD, Becker GW, Kudlow JE. Alloxan is an inhibitor of the enzyme O-linked N-acetylglucosamine transferase. *Biochem Biophys Res Commun.* (2002) 293:207–12. doi: 10.1016/S0006-291X(02)00200-0
36. Kang E-S, Han D, Park J, Kwak TK, Oh M-A, Lee S-A, et al. O-GlcNAc modulation at Akt1 Ser473 correlates with apoptosis of murine pancreatic β cells. *Exp Cell Res.* (2008) 314:2238–48. doi: 10.1016/j.yexcr.2008.04.014
37. Pantaleon M, Tan HY, Kafer GR, Kaye PL. Toxic effects of hyperglycemia are mediated by the hexosamine signaling pathway and O-linked glycosylation in early mouse embryos. *Biol Reprod.* (2010) 82:751–8. doi: 10.1095/biolreprod.109.076661
38. Marshall S, Nadeau O, Yamasaki K. Dynamic actions of glucose and glucosamine on hexosamine biosynthesis in isolated adipocytes: differential effects on glucosamine 6-phosphate, UDP-N-acetylglucosamine, and ATP levels. *J Biol Chem.* (2004) 279:35313–9. doi: 10.1074/jbc.M404133200
39. Duan W, Paka L, Pillarisetti S. Distinct effects of glucose and glucosamine on vascular endothelial and smooth muscle cells: evidence for a protective role for glucosamine in atherosclerosis. *Cardiovasc Diabetol.* (2005) 4:16. doi: 10.1186/1475-2840-4-16

40. Little PJ, Drennon KD, Tannock LR. Glucosamine inhibits the synthesis of glycosaminoglycan chains on vascular smooth muscle cell proteoglycans by depletion of ATP. *Arch Physiol Biochem.* (2008) 114:120–6. doi: 10.1080/13813450802033909
41. Borodkin VS, van Aalten DMF. An efficient and versatile synthesis of GlcNAcstatins-potent and selective O-GlcNAcase inhibitors built on the tetrahydroimidazo[1,2-a]pyridine scaffold. *Tetrahedron* (2010) 66:7838–49. doi: 10.1016/j.tet.2010.07.037
42. Chuh KN, Batt AR, Zaro BW, Darabedian N, Marotta NP, Brennan CK, et al. The new chemical reporter 6-alkynyl-6-deoxy-GlcNAc reveals O-GlcNAc modification of the apoptotic caspases that can block the cleavage/activation of caspase-8. *J Am Chem Soc.* (2017) 139:7872–85. doi: 10.1021/jacs.7b02213
43. Groves JA, Maduka AO, O'Meally RN, Cole RN, Zachara NE. Fatty acid synthase inhibits theO-GlcNAcase during oxidative stress. *J Biol Chem.* (2017) 292:6493–511. doi: 10.1074/jbc.M116.760785
44. Han C, Gu Y, Shan H, Mi W, Sun J, Shi M, et al. O-GlcNAcylation of SIRT1 enhances its deacetylase activity and promotes cytoprotection under stress. *Nat Commun.* (2017) 8:1491. doi: 10.1038/s41467-017-01654-6
45. Hu J, Chen R, Jia P, Fang Y, Liu T, Song N, et al. Augmented O-GlcNAc signaling via glucosamine attenuates oxidative stress and apoptosis following contrast-induced acute kidney injury in rats. *Free Radic Biol Med.* (2017) 103:121–32. doi: 10.1016/j.freeradbiomed.2016.12.032
46. Chen Y-J, Huang Y-S, Chen J-T, Chen Y-H, Tai M-C, Chen C-L, et al. Protective effects of glucosamine on oxidative-stress and ischemia/reperfusion-induced retinal injury. *Invest Ophthalmol Vis Sci.* (2015) 56:1506–16. doi: 10.1167/iovs.14-15726
47. Lee HJ, Ryu JM, Jung YH, Lee KH, Kim DI, Han HJ. Glycerol-3-phosphate acyltransferase-1 upregulation by O-GlcNAcylation of Sp1 protects against hypoxia-induced mouse embryonic stem cell apoptosis via mTOR activation. *Cell Death Dis.* (2016) 7:e2158. doi: 10.1038/cddis.2015.410
48. Luanpitpong S, Chanthra N, Janan M, Poohadsuan J, Samart P, U-Pratya Y, et al. Inhibition ofO-GlcNAcase sensitizes apoptosis and reverses bortezomib resistance in mantle cell lymphoma through modification of truncated bid. *Mol. Cancer Ther.* (2018) 17:484–96. doi: 10.1158/1535-7163.MCT-17-0390
49. Suh HN, Lee YJ, Kim MO, Ryu JM, Han HJ. Glucosamine-induced Sp1 O-GlcNAcylation ameliorates hypoxia-induced SGLT dysfunction in primary cultured renal proximal tubule cells. *J Cell Physiol.* (2014) 229:1557–68. doi: 10.1002/jcp.24599
50. He Y, Ma X, Li D, Hao J. Thiamet G mediates neuroprotection in experimental stroke by modulating microglia/macrophage polarization and inhibiting NF-κB p65 signaling. *J Cereb Blood Flow Metab Off J Int Soc Cereb Blood Flow Metab.* (2017) 37:2938–51. doi: 10.1177/0271678X16679671
51. Hwang S-Y, Shin J-H, Hwang J-S, Kim S-Y, Shin J-A, Oh E-S, et al. Glucosamine exerts a neuroprotective effect via suppression of inflammation in rat brain ischemia/reperfusion injury. *Glia* (2010) 58:1881–92. doi: 10.1002/glia.21058
52. Shi J, Gu J, Dai C, Gu J, Jin X, Sun J, et al. O-GlcNAcylation regulates ischemia-induced neuronal apoptosis through AKT signaling. *Sci Rep.* (2015) 5:14500. doi: 10.1038/srep14500
53. Nöt LG, Marchase RB, Fülöp N, Brocks CA, Chatham JC. Glucosamine administration improves survival rate after severe hemorrhagic shock combined with trauma in rats. *Shock Augusta Ga* (2007) 28:345–52. doi: 10.1097/shk.0b013e3180487ebb
54. Yang S, Zou L-Y, Bounelis P, Chaudry I, Chatham JC, Marchase RB. Glucosamine administration during resuscitation improves organ function after trauma hemorrhage. *Shock Augusta Ga* (2006) 25:600–7. doi: 10.1097/01.shk.0000209563.07693.db
55. Zou L, Yang S, Hu S, Chaudry IH, Marchase RB, Chatham JC. The protective effects of PUGNAc on cardiac function after trauma-hemorrhage are mediated via increased protein O-GlcNAc levels. *Shock Augusta Ga* (2007) 27:402–8. doi: 10.1097/01.shk.0000245031.31859.29
56. Ibanez B, James S, Agewall S, Antunes MJ, Bucciarelli-Ducci C, Bueno H, et al. 2017 ESC Guidelines for the management of acute myocardial infarction in patients presenting with ST-segment elevation: the task force for the management of acute myocardial infarction in patients presenting with ST-segment elevation of the European Society of Cardiology (ESC). *Eur Heart J.* (2018) 39:119–77. doi: 10.1093/eurheartj/ehx393
57. Champattanachai V, Marchase RB, Chatham JC. Glucosamine protects neonatal cardiomyocytes from ischemia-reperfusion injury via increased protein-associated *O* -GlcNAc. *Am J Physiol-Cell Physiol.* (2007) 292:C178–87. doi: 10.1152/ajpcell.00162.2006
58. Champattanachai V, Marchase RB, Chatham JC. Glucosamine protects neonatal cardiomyocytes from ischemia-reperfusion injury via increased protein O-GlcNAc and increased mitochondrial Bcl-2. *Am J Physiol Cell Physiol.* (2008) 294:C1509–20. doi: 10.1152/ajpcell.00456.2007
59. Ngoh GA, Hamid T, Prabhu SD, Jones SP. O-GlcNAc signaling attenuates ER stress-induced cardiomyocyte death. *Am J Physiol Heart Circ Physiol.* (2009) 297:H1711–9. doi: 10.1152/ajpheart.00553.2009
60. Ngoh GA, Watson LJ, Facundo HT, Jones SP. Augmented O-GlcNAc signaling attenuates oxidative stress and calcium overload in cardiomyocytes. *Amino Acids* (2011) 40:895–911. doi: 10.1007/s00726-010-0728-7
61. Liu J, Marchase RB, Chatham JC. Glutamine-induced protection of isolated rat heart from ischemia/reperfusion injury is mediated via the hexosamine biosynthesis pathway and increased protein O-GlcNAc levels. *J Mol Cell Cardiol.* (2007) 42:177–85. doi: 10.1016/j.yjmcc.2006.09.015
62. Laczy B, Marsh SA, Brocks CA, Wittmann I, Chatham JC. Inhibition of O-GlcNAcase in perfused rat hearts by NAG-thiazolines at the time of reperfusion is cardioprotective in an O-GlcNAc-dependent manner. *Am J Physiol Heart Circ Physiol.* (2010) 299:H1715–27. doi: 10.1152/ajpheart.00337.2010
63. Jones SP, Zachara NE, Ngoh GA, Hill BG, Teshima Y, Bhatnagar A, et al. Cardioprotection by N-Acetylglucosamine Linkage to Cellular Proteins. *Circulation* (2008) 117:1172–82. doi: 10.1161/CIRCULATIONAHA.107.730515
64. Pælestik KB, Jespersen NR, Jensen RV, Johnsen J, Bøtker HE, Kristiansen SB. Effects of hypoglycemia on myocardial susceptibility to ischemia–reperfusion injury and preconditioning in hearts from rats with and without type 2 diabetes. *Cardiovasc Diabetol.* (2017) 16:148. doi: 10.1186/s12933-017-0628-1
65. Dubois-Deruy E, Belliard A, Mulder P, Bouvet M, Smet-Nocca C, Janel S, et al. Interplay between troponin T phosphorylation and O-N-acetylglucosaminylation in ischaemic heart failure. *Cardiovasc Res.* (2015) 107:56–65. doi: 10.1093/cvr/cvv136
66. Guo X, Shang J, Deng Y, Yuan X, Zhu D, Liu H. Alterations in left ventricular function during intermittent hypoxia: possible involvement of O-GlcNAc protein and MAPK signaling. *Int J Mol Med.* (2015) 36:150–8. doi: 10.3892/ijmm.2015.2198
67. Dassanayaka S, Brainard RE, Watson LJ, Long BW, Brittian KR, DeMartino AM, et al. Cardiomyocyte Ogt limits ventricular dysfunction in mice following pressure overload without affecting hypertrophy. *Basic Res Cardiol.* (2017) 112:23. doi: 10.1007/s00395-017-0612-7
68. Mailleux F, Gélinas R, Beauloye C, Horman S, Bertrand L. O-GlcNAcylation, enemy or ally during cardiac hypertrophy development? *Biochim Biophys Acta* (2016) 1862:2232–43. doi: 10.1016/j.bbadis.2016.08.012
69. Cannon MV, Silljé HHW, Sijbesma JWA, Vreeswijk-Baudoin I, Ciapaite J, van der Sluis B, et al. Cardiac LXRα protects against pathological cardiac hypertrophy and dysfunction by enhancing glucose uptake and utilization. *EMBO Mol. Med.* (2015) 7:1229–43. doi: 10.15252/emmm.201404669
70. Facundo HT, Brainard RE, Watson LJ, Ngoh GA, Hamid T, Prabhu SD, et al. O-GlcNAc signaling is essential for NFAT-mediated transcriptional reprogramming during cardiomyocyte hypertrophy. *Am J Physiol Heart Circ Physiol.* (2012) 302:H2122–30. doi: 10.1152/ajpheart.00775.2011
71. Gélinas R, Mailleux F, Dontaine J, Bultot L, Demeulder B, Ginion A, et al. AMPK activation counteracts cardiac hypertrophy by reducing O-GlcNAcylation. *Nat Commun.* (2018) 9:374. doi: 10.1038/s41467-017-02795-4
72. Ledee D, Smith L, Bruce M, Kajimoto M, Isern N, Portman MA, et al. c-Myc alters substrate utilization and O-GlcNAc protein posttranslational modifications without altering cardiac function during early aortic constriction. *PLoS ONE* (2015) 10:e0135262. doi: 10.1371/journal.pone.0135262
73. Lunde IG, Aronsen JM, Kvaløy H, Qvigstad E, Sjaastad I, Tønnessen T, et al. Cardiac O-GlcNAc signaling is increased in hypertrophy and heart failure. *Physiol Genomics* (2012) 44:162–72. doi: 10.1152/physiolgenomics.00016.2011

74. Muthusamy S, DeMartino AM, Watson LJ, Brittian KR, Zafir A, Dassanayaka S, et al. MicroRNA-539 is up-regulated in failing heart, and suppresses O-GlcNAcase expression. *J Biol Chem.* (2014) 289:29665–76. doi: 10.1074/jbc.M114.578682
75. Liu B, Wang J, Li M, Yuan Q, Xue M, Xu F, et al. Inhibition of ALDH2 by O-GlcNAcylation contributes to the hyperglycemic exacerbation of myocardial ischemia/reperfusion injury. *Oncotarget* (2017) 8:19413–26. doi: 10.18632/oncotarget.14297
76. Wang D, Hu X, Lee SH, Chen F, Jiang K, Tu Z, et al. Diabetes exacerbates myocardial ischemia/reperfusion injury by down-regulation of microRNA and up-regulation of O-GlcNAcylation. *JACC Basic Transl Sci.* (2018) 3:350–62. doi: 10.1016/j.jacbts.2018.01.005
77. Ekmark L, Rooyackers O, Wernerman J, Fläring U. Plasma glutamine deficiency is associated with multiple organ failure in critically ill children. *Amino Acids* (2015) 47:535–42. doi: 10.1007/s00726-014-1885-x
78. Oudemans-van Straaten HM, Bosman RJ, Treskes M, van der Spoel HJ, Zandstra DF. Plasma glutamine depletion and patient outcome in acute ICU admissions. *Intensive Care Med.* (2001) 27:84–90. doi: 10.1007/s001340000703
79. Neu J, Roig JC, Meetze WH, Veerman M, Carter C, Millsaps M, et al. Enteral glutamine supplementation for very low birth weight infants decreases morbidity. *J Pediatr.* (1997) 131:691–9. doi: 10.1016/S0022-3476(97)70095-7
80. Bober-Olesinska K, Kornacka MK. [Effects of glutamine supplemented parenteral nutrition on the incidence of necrotizing enterocolitis, nosocomial sepsis and length of hospital stay in very low birth weight infants]. *Med Wieku Rozwoj.* (2005) 9:325–33.
81. Sevastiadou S, Malamitsi-Puchner A, Costalos C, Skouroliakou M, Briana DD, Antsaklis A, et al. The impact of oral glutamine supplementation on the intestinal permeability and incidence of necrotizing enterocolitis/septicemia in premature neonates. *J Matern-Fetal Neonatal Med.* (2011) 24:1294–300. doi: 10.3109/14767058.2011.564240
82. Houdijk AP, Rijnsburger ER, Jansen J, Wesdorp RI, Weiss JK, McCamish MA, et al. Randomised trial of glutamine-enriched enteral nutrition on infectious morbidity in patients with multiple trauma. *Lancet* (1998) 352:772–6.
83. Wischmeyer PE, Lynch J, Liedel J, Wolfson R, Riehm J, Gottlieb L, et al. Glutamine administration reduces Gram-negative bacteremia in severely burned patients: a prospective, randomized, double-blind trial versus isonitrogenous control. *Crit Care Med.* (2001) 29:2075–80. doi: 10.1097/00003246-200111000-00006
84. Lomivorotov VV, Efremov SM, Shmirev VA, Ponomarev DN, Lomivorotov VN, Karaskov AM. Glutamine is cardioprotective in patients with ischemic heart disease following cardiopulmonary bypass. *Heart Surg Forum* (2011) 14:E384–8. doi: 10.1532/HSF98.20111074
85. Lomivorotov VV, Efremov SM, Shmirev VA, Ponomarev DN, Svyatchenko AV, Deryagin MN, et al. Does glutamine promote benefits for patients with diabetes mellitus scheduled for cardiac surgery? *Heart Lung Circ.* (2013) 22:360–5. doi: 10.1016/j.hlc.2012.11.011
86. Brinkmann SJH, Buijs N, Vermeulen MAR, Oosterink E, Schierbeek H, Beishuizen A, et al. Perioperative glutamine supplementation restores disturbed renal arginine synthesis after open aortic surgery: a randomized controlled clinical trial. *Am J Physiol Renal Physiol.* (2016) 311:F567–75. doi: 10.1152/ajprenal.00340.2015
87. Chávez-Tostado M, Carrillo-Llamas F, Martínez-Gutiérrez PE, Alvarado-Ramírez A, López-Taylor JG, Vásquez-Jiménez JC, et al. Oral glutamine reduces myocardial damage after coronary revascularization under cardiopulmonary bypass. *A randomized clinical trial Nutr Hosp.* (2017) 34:277–83. doi: 10.20960/nh.519
88. Khogali SEO, Pringle SD, Weryk BV, Rennie MJ. Is glutamine beneficial in ischemic heart disease? *Nutr Burbank Los Angel Cty Calif* (2002) 18:123–6. doi: 10.1016/S0899-9007(01)00768-7
89. Roman-Blas JA, Castañeda S, Sánchez-Pernaute O, Largo R, Herrero-Beaumont G, CS/GS Combined Therapy Study Group. Combined treatment with chondroitin sulfate and glucosamine sulfate shows no superiority over placebo for reduction of joint pain and functional impairment in patients with knee osteoarthritis: a six-month multicenter, randomized, double-blind, placebo-controlled clinical trial. *Arthritis Rheumatol.* (2017) 69:77–85. doi: 10.1002/art.39819
90. Kwoh CK, Roemer FW, Hannon MJ, Moore CE, Jakicic JM, Guermazi A, et al. Effect of oral glucosamine on joint structure in individuals with chronic knee pain: a randomized, placebo-controlled clinical trial. *Arthritis Rheumatol.* (2014) 66:930–9. doi: 10.1002/art.38314
91. de Vos BC, Landsmeer MLA, van Middelkoop M, Oei EHG, Krul M, Bierma-Zeinstra SMA, et al. Long-term effects of a lifestyle intervention and oral glucosamine sulphate in primary care on incident knee OA in overweight women. *Rheumatol Oxf Engl.* (2017) 56:1326–34. doi: 10.1093/rheumatology/kex145
92. Esfandiari H, Pakravan M, Zakeri Z, Ziaie S, Pakravan P, Ownagh V. Effect of glucosamine on intraocular pressure: a randomized clinical trial. *Eye Lond Engl.* (2017) 31:389–94. doi: 10.1038/eye.2016.221
93. Runhaar J, Rozendaal RM, van Middelkoop M, Bijlsma HJW, Doherty M, Dziedzic KS, et al. Subgroup analyses of the effectiveness of oral glucosamine for knee and hip osteoarthritis: a systematic review and individual patient data meta-analysis from the OA trial bank. *Ann Rheum Dis.* (2017) 76:1862–9. doi: 10.1136/annrheumdis-2017-211149
94. Kongtharvonskul J, Anothaisintawee T, McEvoy M, Attia J, Woratanarat P, Thakkinstian A. Efficacy and safety of glucosamine, diacerein, and NSAIDs in osteoarthritis knee: a systematic review and network meta-analysis. *Eur J Med Res.* (2015) 20:24. doi: 10.1186/s40001-015-0115-7
95. Hresko RC, Heimberg H, Chi MM, Mueckler M. Glucosamine-induced insulin resistance in 3T3-L1 adipocytes is caused by depletion of intracellular ATP. *J Biol Chem.* (1998) 273:20658–68. doi: 10.1074/jbc.273.32.20658
96. Medina M. An overview on the clinical development of Tau-based therapeutics. *Int J Mol Sci.* (2018) 19:1160. doi: 10.3390/ijms19041160
97. Onay-Besikci A. Regulation of cardiac energy metabolism in newborn. *Mol Cell Biochem.* (2006) 287:1–11. doi: 10.1007/s11010-006-9123-9
98. Buse MG, Robinson KA, Marshall BA, Mueckler M. Differential effects of GLUT1 or GLUT4 overexpression on hexosamine biosynthesis by muscles of transgenic mice. *J Biol Chem.* (1996) 271:23197–202. doi: 10.1074/jbc.271.38.23197
99. Haubner BJ, Adamowicz-Brice M, Khadayate S, Tiefenthaler V, Metzler B, Aitman T, et al. Complete cardiac regeneration in a mouse model of myocardial infarction. *Aging* (2012) 4:966–77. doi: 10.18632/aging.100526
100. Porrello ER, Mahmoud AI, Simpson E, Hill JA, Richardson JA, Olson EN, et al. Transient regenerative potential of the neonatal mouse heart. *Science* (2011) 331:1078–80. doi: 10.1126/science.1200708
101. Uygur A, Lee RT. Mechanisms of cardiac regeneration. *Dev Cell* (2016) 36:362–74. doi: 10.1016/j.devcel.2016.01.018
102. Banerjee PS, Lagerlöf O, Hart GW. Roles of O-GlcNAc in chronic diseases of aging. *Mol Aspects Med.* (2016) 51:1–15. doi: 10.1016/j.mam.2016.05.005
103. Lefebvre T, Guinez C, Dehennaut V, Beseme-Dekeyser O, Morelle W, Michalski J-C. Does O-GlcNAc play a role in neurodegenerative diseases? *Expert Rev Proteomics* (2005) 2:265–75. doi: 10.1586/14789450.2.2.265
104. Fülöp N, Mason MM, Dutta K, Wang P, Davidoff AJ, Marchase RB, et al. Impact of Type 2 diabetes and aging on cardiomyocyte function and O-linked N-acetylglucosamine levels in the heart. *Am J Physiol Cell Physiol.* (2007) 292:C1370–8. doi: 10.1152/ajpcell.00422.2006
105. Fülöp N, Feng W, Xing D, He K, Not LG, Brocks CA, et al. Aging leads to increased levels of protein O-linked N-acetylglucosamine in heart, aorta, brain and skeletal muscle in Brown-Norway rats. *Biogerontology* (2008) 9:139. doi: 10.1007/s10522-007-9123-5
106. Liu Y, Li X, Yu Y, Shi J, Liang Z, Run X, et al. Developmental regulation of protein O-GlcNAcylation, O-GlcNAc transferase, and O-GlcNAcase in mammalian brain. *PLoS ONE* (2012) 7:e43724. doi: 10.1371/journal.pone.0043724
107. Rex-Mathes M, Werner S, Strutas D, Griffith LS, Viebahn C, Thelen K, et al. O-GlcNAc expression in developing and ageing mouse brain. *Biochimie* (2001) 83:583–90. doi: 10.1016/S0300-9084(01)01305-0
108. Gu J, Shi J, Dai C, Ge J, Zhao Y, Chen Y, et al. O-GlcNAcylation Reduces Ischemia-Reperfusion–Induced Brain Injury. *Sci Rep.* (2017) 7. doi: 10.1038/s41598-017-10635-0
109. Liu S, Sheng H, Yu Z, Paschen W, Yang W. O-linked β-N-acetylglucosamine modification of proteins is activated in post-ischemic brains of young but not aged mice: implications for impaired functional recovery

from ischemic stress. *J Cereb Blood Flow Metab.* (2016) 36:393–8. doi: 10.1177/0271678X15608393
110. Wang AC, Jensen EH, Rexach JE, Vinters HV, Hsieh-Wilson LC. Loss of O-GlcNAc glycosylation in forebrain excitatory neurons induces neurodegeneration. *Proc Natl Acad Sci USA.* (2016) 113:15120–5. doi: 10.1073/pnas.1606899113
111. Heyland D, Muscedere J, Wischmeyer PE, Cook D, Jones G, Albert M, et al. A randomized trial of glutamine and antioxidants in critically ill patients. *N Engl J Med.* (2013) 368:1489–97. doi: 10.1056/NEJMoa1212722
112. Ward E, Picton S, Reid U, Thomas D, Gardener C, Smith M, et al. Oral glutamine in paediatric oncology patients: a dose finding study. *Eur J Clin Nutr.* (2003) 57:31–6. doi: 10.1038/sj.ejcn.1601517
113. Griffin ME, Jensen EH, Mason DE, Jenkins CL, Stone SE, Peters EC, et al. Comprehensive mapping of O-GlcNAc modification sites using a chemically cleavable tag. *Mol Biosyst.* (2016) 12:1756–9. doi: 10.1039/C6MB00138F
114. Deracinois B, Camoin L, Lambert M, Boyer J-B, Dupont E, Bastide B, et al. O-GlcNAcylation site mapping by (azide-alkyne) click chemistry and mass spectrometry following intensive fractionation of skeletal muscle cells proteins. *J Proteomics* (2018) 186:83–97. doi: 10.1016/j.jprot.2018.07.005
115. Wang Y, Zhu J, Zhang L. Discovery of cell-permeable O-GlcNAc transferase inhibitors via tethering in situ click chemistry. *J Med Chem.* (2017) 60:263–72. doi: 10.1021/acs.jmedchem.6b01237
116. Gross BJ, Kraybill BC, Walker S. Discovery of O-GlcNAc transferase inhibitors. *J Am Chem Soc.* (2005) 127:14588–9. doi: 10.1021/ja0555217
117. Lazarus MB, Nam Y, Jiang J, Sliz P, Walker S. Structure of human *O*-GlcNAc transferase and its complex with a peptide substrate. *Nature* (2011) 469:564–7. doi: 10.1038/nature09638
118. Ortiz-Meoz RF, Jiang J, Lazarus MB, Orman M, Janetzko J, Fan C, et al. A small molecule that inhibits OGT activity in cells. *ACS Chem Biol.* (2015) 10:1392–7. doi: 10.1021/acschembio.5b00004
119. Wang Z, Pandey A, Hart GW. Dynamic interplay between O-linked N-acetylglucosaminylation and glycogen synthase kinase-3-dependent phosphorylation. *Mol Cell Proteomics* (2007) 6:1365–79. doi: 10.1074/mcp.M600453-MCP200
120. Wang P, Lazarus BD, Forsythe ME, Love DC, Krause MW, Hanover JA. O-GlcNAc cycling mutants modulate proteotoxicity in Caenorhabditis elegans models of human neurodegenerative diseases. *Proc Natl Acad Sci USA.* (2012) 109:17669–74. doi: 10.1073/pnas.1205748109

Conflict of Interest Statement: The authors declare that the research was conducted in the absence of any commercial or financial relationships that could be construed as a potential conflict of interest.

frontiers in Endocrinology

ORIGINAL RESEARCH
published: 25 January 2019
doi: 10.3389/fendo.2018.00816

Binding Specificity of Native Odorant-Binding Protein Isoforms Is Driven by Phosphorylation and *O*-N-Acetylglucosaminylation in the Pig *Sus scrofa*

Patricia Nagnan-Le Meillour[1]*, *Alexandre Joly*[1], *Chrystelle Le Danvic*[1,2], *Arul Marie*[3], *Séverine Zirah*[3] and *Jean-Paul Cornard*[4]

[1] Unité de Glycobiologie Structurale et Fonctionnelle, UMR8576, USC-UGSF INRA 1409, CNRS-Université de Lille, Lille, France, [2] ALLICE R&D, Paris, France, [3] Unité Molécules de Communication et Adaptation des Microorganismes, Muséum National d'Histoire Naturelle, UMR 7245 CNRS/MNHN, Paris, France, [4] Laboratoire de Spectroscopie Infrarouge et Raman, UMR8516 CNRS-Université de Lille, Lille, France

OPEN ACCESS

Edited by:
Tarik Issad,
Institut National de la Santé et de la Recherche Médicale (INSERM), France

Reviewed by:
Caroline Cieniewski-Bernard, Lille University of Science and Technology, France
Chad Slawson, University of Kansas Medical Center Research Institute, United States

***Correspondence:**
Patricia Nagnan-Le Meillour
patricia.nagnan@univ-lille.fr

Specialty section:
This article was submitted to Molecular and Structural Endocrinology, a section of the journal Frontiers in Endocrinology

Received: 10 October 2018
Accepted: 27 December 2018
Published: 25 January 2019

Citation:
Nagnan-Le Meillour P, Joly A, Le Danvic C, Marie A, Zirah S and Cornard J-P (2019) Binding Specificity of Native Odorant-Binding Protein Isoforms Is Driven by Phosphorylation and O-N-Acetylglucosaminylation in the Pig Sus scrofa. Front. Endocrinol. 9:816. doi: 10.3389/fendo.2018.00816

Odorant-binding proteins (OBP) are secreted in the nasal mucus at the vicinity of olfactory receptors (ORs). They act, at least, as an interface between hydrophobic and volatile odorant molecules and the hydrophilic medium bathing the ORs. They have also been hypothesized to be part of the molecular coding of odors and pheromones, by forming specific complexes with odorant molecules that could ultimately stimulate ORs to trigger the olfactory transduction cascade. In a previous study, we have evidenced that pig olfactory secretome was composed of numerous olfactory binding protein isoforms, generated by *O*-GlcNAcylation and phosphorylation. In addition, we have shown that recombinant OBP (*stricto sensu*) produced in yeast is made up of a mixture of isoforms that differ in their phosphorylation pattern, which in turn determines binding specificity. Taking advantage of the high amount of OBP secreted by a single animal, we performed a similar study, under exactly the same experimental conditions, on native isoforms isolated from pig, *Sus scrofa*, nasal tissue. Four fractions were obtained by using strong anion exchange HPLC. Mapping of phosphorylation and *O*-GlcNAcylation sites by CID-nanoLC-MS/MS allowed unambiguous localization of phosphosites at S13 and T122 and HexNAc sites at S13 and S19. T112 or T115 could also be phosphorylated. BEMAD analysis suggested extra phosphosites located at S23, S24, S41, S49, S57, S67, and T71. Due to the very low stoichiometry of GlcNAc-peptides and phosphopeptides, these sites were identified on total mixture of OBP isoforms instead of HPLC-purified OBP isoforms. Nevertheless, binding properties of native OBP isoforms to specific ligands in *S. scrofa* were monitored by fluorescence spectroscopy. Recombinant phosphorylated OBP-Pichia isoforms bind steroids and fatty acids with slight differences. Native isoforms, that are phosphorylated but also *O*-GlcNAcylated show radically different binding affinities for the same compounds,

which strongly suggests that *O*-GlcNAcylation increases the binding specificity of OBP isoforms. These findings extend the role of *O*-GlcNAc in regulating the function of proteins involved in many mechanisms of metabolic homeostasis, including extracellular signaling in olfaction. Data is available via ProteomeXChange with identifier PXD011371.

Keywords: *O*-GlcNAc, odorant-binding protein, phosphorylation, CID-nano-LC-MS/MS, fluorescence spectroscopy, pheromone

INTRODUCTION

In olfaction, one major challenge is to understand how odors are encoded in the nasal cavity by molecular players, olfactory receptors (OR) and odorant-binding proteins (OBP). Indeed, since their identification 30 years ago [(1); Nobel Price 2004], most of the OR are still orphan, as their ligands have not been identified. OBPs are secreted by the cells of Bowman's gland in the nasal mucus where dendrites of olfactory receptor neurons containing ORs are bathing (2, 3). OBPs are supposed to at least, act as an interface between airborne odorants and aqueous medium containing ORs. While OBPs binding to odors is well-documented at the biochemical level, very few investigations into OR binding have been reported. Activation of ORs with odorant molecules alone, with OBP bound or unbound to odorants, have been measured by electrophysiology [e.g., (4)] or other indirect techniques [e.g., (5, 6)]. This lack of direct evidence explains why the nature of ORs ligands is still uncertain. In mammals, OBPs have been suggested to form a specific complex with a given odorant that could specifically interact with an OR, leading to the initiation of the olfactory transduction cascade. Such a molecular coding mechanism requests an equal diversity in odorant molecules, OBPs and ORs. In each mammalian species, only a few genes (2–8) encode OBPs, whilst the OR family comprises around 1,000 genes (1), and the number of odorants is theoretically unlimited.

In previous work (7–9), we have evidenced the diversity of OBPs from pig olfactory secretome, which is generated by phosphorylation and/or *O*-GlcNAcylation of the three gene products, OBP (*stricto sensu,* referred as OBP in the text below), Von Ebner's Gland Protein (VEG), and Salivary lipocalin (SAL). These two post-translational modifications (PTM) were unexpected for secreted proteins, as they usually occur in nucleus and cytosol of the cell to regulate the function of many proteins involved in most physiological processes [For review, see (10–12)]. Phosphorylation of secreted proteins is now largely documented. Some candidate kinases may modify the OBP sequence, such as the Golgi kinase FAM20C (13) or ectokinases (14). *O*-GlcNAc modification of proteins passing through the secretion pathway was only shown a decade ago (15), and since then the associated glycosyltransferase (EOGT) has been identified in Drosophila by (16). This enzyme is conserved throughout Evolution, including in the pig genome (9), but it is genetically unrelated to its cytosolic functional counterpart, the *O*-GlcNAc transferase OGT. To date, there is no evidence of a secreted enzyme that could act like the cytosolic *O*-GlcNAcase (OGA) to remove GlcNAc moieties.

In pig, phosphorylation drives binding specificity of recombinant OBP isoforms (17) that are not *O*-GlcNAcylated, at the contrary of native OBP, purified from nasal tissue (9). In order to precisely identify the role of both PTM in OBP binding abilities to pheromone components in pig, we purified OBP isoforms by HPLC and performed a structure-function relationship study. We identified phosphorylation and *O*-GlcNAcylation on 4 OBP isoforms by immunodetection with specific antibodies, along with careful controls. The binding properties of these 4 isoforms were monitored by fluorescence spectroscopy in the exact same conditions previously used for recombinant OBP isoforms (17). The PTM sites were mapped by CID-nano-LC-MS/MS and BEMAD (for phosphorylation) to link observed binding affinities to phosphorylation and *O*-GlcNAcylation patterns of native OBP isoforms. Comparison of binding affinities between recombinant (only phosphorylated) and native (also *O*-GlcNAcylated) isoforms indicates that *O*-GlcNAcylation increases their binding specificity to pheromone components. This is the first work that identifies such PTM sites in OBP using high-resolution-mass spectrometry, and demonstrates their involvement in the discrimination of odorant molecules by OBP isoforms.

MATERIALS AND METHODS

Animals and Tissues

Animals (Large White *Sus scrofa*) were maintained at the Experimental Farm of INRA (UEPAO, Nouzilly, France). Nasal tissue was collected in a slaughterhouse, included in a surgical platform ISO9001-certified, which received European approval (N° E37-175-2) for the slaughter of domestic species like pigs. Respiratory mucosa (RM) was dissected from anesthetized animals (pentobarbital) immediately after death and stored in tubes at −80°C until protein extraction.

Protein Purification and Characterization

Proteins were gently extracted from RM of pre-pubertal males of *S. scrofa* as described previously (7), in order to avoid intracellular protein release. Purification of OBP isoforms was achieved by high-resolution anion exchange chromatography on a ÄKTA purifier HPLC device (GE Healthcare). Proteins were separated on a PROPAC SAX10 column (Dionex, 4 mm × 250 mm), in 50 mM Tris/HCl, pH 7.5 (buffer A), by using an optimized gradient of 0–1 M NaCl (buffer B: 50 mM Tris/HCl, pH 7.5, 1 M NaCl): after 5 min in 100% buffer A, 50% of buffer B was reached in 30 min and maintained for 5 min, then 100% of buffer A was reached in 5 min, and then maintained for 10 min. Samples of 100 µl in buffer A were injected, and resulting

fractions were collected, desalted with PD-10 desalting columns (GE Healthcare), and dried in a Speed-Vac (Eppendorf). Each fraction was re-purified on the same column but with a different NaCl gradient. Dried fractions were re-suspended into 100 µl buffer A, injected and purified with the following gradient: 7 min of 100% buffer A, 25% buffer B in 2 min, 35% buffer B in 10 min, 100% buffer B in 3 min, 7 min of 100% buffer B, then 100% A in 5 min. Resulting fractions were desalted with PD-10 desalting columns. Identical fractions coming from several injections were pooled to obtain homogenous aliquots (5 µg), dried in Speed-Vac and stored at −20°C until subsequent analyses. OBP isoforms were identified in HPLC fractions by western-blotting with anti-OBP antibodies (7). Their identity was confirmed by mass fingerprinting, followed by MALDI-TOF MS as already described (7). Protein concentration was determined by the Bradford method using recombinant porcine OBP (18) as standard (Micro BCA™ Protein Assay Kit, Pierce).

One Dimensional and Two-Dimensional Electrophoresis

All chemicals and reagents were from Sigma-Aldrich, unless specified. For two-dimensional electrophoresis (2D-E), 5 µg of dried proteins were solubilized in 150 µl of the rehydration buffer (8 M Urea, 2 M Thiourea, 2% (w/v) CHAPS, 10 mM dithiothreitol (DTT), 1.2% (v/v) Immobilized pH Gradient (IPG) buffer (pH 4-7) (GE Healthcare) and bromophenol blue). After vigorous shaking, proteins were loaded onto a 7-cm IPG strip (pH 4–7, Bio-Rad) by overnight passive rehydration at room temperature. The first-dimensional isoelectric focusing (IEF) was carried out on a PROTEAN® i12™ IEF system (Bio-Rad) using the following program: 250 V for 30 min (rapid voltage ramping), 1,000 V for 1 h (gradual ramping), 5,000 V for 2 h (gradual ramping) and held at 5,000 V (rapid ramping voltage) until complete IEF (10,000 VH final), with a current limit at 50 µA/gel. Strips were then incubated twice for 15 min in the equilibration buffer (375 mM Tris-HCl pH 8.8, 6 M urea, 2% (w/v) SDS and 30% (v/v) glycerol) complemented with 1.5% (w/v) DTT, followed by 15 min in the equilibration buffer complemented with 2% (w/v) iodoacetamide. The second-dimension separation, as well as mono-dimensional electrophoresis, were performed using 16.8% SDS–PAGE in Mini PROTEAN® Tetra Cell (Bio-Rad) as already described (19).

Staining and Western-Blot

After electrophoresis, gels were either stained with colloidal Coomassie blue R solution (12% trichloroacetic acid, 5% ethanolic solution of 0.035% Serva blue R 250) or transferred onto PVDF (ImmobilonP, Millipore) membranes. For immunodetection, membranes were blocked in 5% (w/v) non-fat dry milk in Tris-Buffered Saline with 0.05% (v/v) Tween 20 (TBS-T) for probing with polyclonal antibodies (home-made anti-OBP) and 3% BSA fraction V in TBS-T for probing with monoclonal anti-*O*-GlcNAc (RL2 and CTD110.6) antibodies or with anti-phosphoserine, -phosphothreonine, and -phosphotyrosine antibodies. Membranes were then incubated with antibodies in TBS-T 1 h at room temperature (RT) (RL2 (Thermofisher) 1:2,000; CTD 110.6 (Thermofisher), 1:5,000; anti-OBP, 1:30,000; anti-phosphoserine (P-Ser, 1:100), anti-phosphotyrosine (P-Tyr, 1:100), and anti-phosphothreonine (P-Thr, 1:500) (Invitrogen). After washes in TBS-T, membranes were incubated with the appropriate horseradish peroxidase-conjugated secondary antibody (anti-mouse IgG-HRP linked, 1:30,000, Thermofisher, for RL2; anti-mouse IgM-HRP linked, 1:30,000, Thermofisher, for CTD 110.6; anti-rabbit IgG-HRP linked, 1:30,000, Thermofisher for other primary antibodies) for 1 h at room temperature. After washes in TBS-T, blots were developed using enhanced chemiluminescence (ECL Plus Reagent, Hyperfilm™ MP, GE Healthcare). For GlcNAc competition assays, proteins were separated by SDS-PAGE, transferred onto PVDF membranes, which were blocked as above. Then, membranes were incubated 1 h (RT) with a pre-incubated mixture (1 h at RT) of CTD110.6 antibodies and 1 M GlcNAc (TCI, ref. A0092) in TBS-T-3% BSA. They were washed and processed as above until ECL detection.

Mapping Post-translational Modification Sites in Native OBP

Mapping of Phosphorylation Sites by BEMAD

Phosphorylation sites of native OBP isoforms were mapped by mild Beta-Elimination, followed by Michael Addition of DTT (BEMAD) and then by MALDI-TOF MS analysis (20). Prior to mild β-elimination and Michael addition of DTT, isoforms were treated with β-*N*-acetylglucosaminidase (Sigma-Aldrich, 1 unit per 5 µg of protein) to remove GlcNAc groups. Proteins were not reduced and alkylated to avoid addition of DTT on cysteines. They were then digested with either trypsin (T) or chymotrypsin (CT) or both (T + CT) (Sigma-Aldrich). After a step of enrichment of DTT-modified peptides by using thiol columns [fully described in Nagnan-Le Meillour et al. (7)], peptides were eluted directly into the matrix (α-cyano-4-hydroxycinnamic acid) with 12.5, 25, and 50% acetonitrile (ACN). Eluates were not pooled in order to obtain higher percentages of peptide recovery in mass spectrometry. The theoretical masses of DTT-modified peptides were calculated from the OBP peptide map (GenBank accession number NP_998961) by using the Peptide Mass software at https://web.expasy.org/peptide_mass/.

Mapping of PTM Sites by CID Mass Spectrometry

Enrichment of O-GlcNAcylated proteins using wheat germ agglutinin columns

Samples were prepared for mass spectrometry by using WGA enrichment of GlcNAc-peptides. The WGA agarose beads (75 µL, Vector Laboratories, in Spin column-Screw caps, Pierce) were washed three times with wash buffer (100 mM Tris/HCl, pH 7.7) and spin down (12,000 rpm, MiniSpin Eppendorf), 5 min at 4°C. Total proteins (200 µg of total RM extract) were resuspended in 300 µL of wash buffer and incubated with WGA beads 2 h, at 4°C and 450 rpm (Thermomixer, Eppendorf). After 2 washes with wash buffer, GlcNAc-enriched proteins were eluted in Laemmli buffer, boiled and resolved on 1-D electrophoresis as described above. Bands were cut out and treated for trypsin digestion as described in Guiraudie et al. (19). Resulting peptides were desalted in reverse-phase C18 Spin columns (Thermofisher) and dried in Speed-Vac until use.

NanoLC-MS/MS analysis

NanoLC-MS/MS experiments were conducted on an Ultimate 3000-RSLC (Thermo Scientific, Massachusetts) using a C_{18} column (RSLC Polar Advantage II Acclaim, 2.2 μm, 120 Å, 2.1 Å∼100 mm, Thermo Scientific, Massachusetts) at a flow rate of 300 μL/min using a mobile phase gradient with A: H_2O + formic acid (FA) 0.1% and B: acetonitrile (ACN) + FA 0.08%. The gradient increased from 2% B to 25% B in 60 min and then to 60% B in 65 min. One microliter of sample was injected and the separated peptides were analyzed by a Q-TOF mass spectrometer (quadrupole-time of flight instrument, Maxis II ETD, Bruker Daltonics, France) interfaced with an ESI (electrospray ionization) source. The Nano spray source was operated at 1,600 V with a nano-booster system and the MS spectra were recorded at 2 Hz between m/z =150 to 2,200. MS/MS spectra were acquired for precursor ions between m/z = 400 to 2,200 with charge states from +2 to +5. Fragmentation rate varied between 1 to 4 Hz depending on the precursor ion intensities. Total cycle time was fixed at 3 sec. Active exclusion time was set to 0.5 min to favor the MS/MS of low intensity ions.

Data analysis

The LC-MS/MS analyses were processed and converted into *.mgf files using Data Analysis software (version 4.3.110, Brüker Daltonics). Database search was carried out using in-house Mascot software (version 2.4.0, MatrixScience.com, London, UK) with following parameters: MS tolerance = 10 ppm, MS/MS tolerance = 0.05 Da, carbamidomethylation of cysteine as fixed modification, oxidation (methionine), pyrrolidone carboxylic acid (Q), phosphorylation (S, T, Y), HexNAcylation (S, T), and Q/N deamidation as variable modifications. Up to two trypsin missed cleavages were allowed. A custom database containing *S. scrofa* OBP isoforms and splicing variants (**Supplementary Data 1**) was used. All the ions in the peak list generated using Data Analysis software were checked manually to construct fragment ion tables and to perform annotation of the spectra with the aid of a Protein Prospector (v 5.22.1 at prospector.ucsf.edu/). The mass spectrometry proteomics data has been deposited to the ProteomeXchange Consortium via the PRIDE (21) partner repository with the dataset identifier PXD011371 and 10.6019/PXD011371.

Fluorescence Binding Assay

Androstenone (3-keto-5α, 16-androstene), androstenol (3α-hydroxy-5α-androst-16-ene), testosterone (17β-hydroxy-3-oxo-4-androstene), palmitic acid (hexadecanoic acid), myristic acid (tetradecanoic acid), and AMA (1-aminoanthracene) were purchased from Sigma-Aldrich. UV-visible spectra were recorded on a Cary-100 double beam spectrometer (Varian) with a cell of 0.5 cm path length. The protein concentration was calculated by UV-visible spectroscopy, by using the molar extinction coefficient of 11,740 $M^{-1}cm^{-1}$ for OBP (calculated by the software "ProtParam tool" at www.expasy.org) at the maximum wavelength of absorption (280 nm). Steady state fluorescence measurements were performed on a Fluoromax-3 (Jobin-Yvon) spectrofluorimeter using a micro quartz cell (0.5 cm light-path) with a reflecting window. 1-Aminoantracene (AMA) was used as a fluorescent probe. The experimental conditions and data treatment have been described previously (17). The dissociation constant (K_d-AMA) of the OBP-AMA complex was calculated from the binding curve by fitting the experimental data with the use of the computer program Origin 7.5 (OriginLab Corporation). The affinities of the five ligands were measured in a competitive binding assay with AMA as the fluorescent probe. AMA was dissolved in 100% ethanol to yield a 1 mM stock solution. For protein titration, aliquots of AMA were successively added to the protein at 1 or 2.5 μM in 50 mM Tris buffer (pH 7.8) and emission spectra were acquired after a 15 min equilibration period. Competitive binding experiments were then carried out with different protein and ligand concentrations. The spectra were recorded 15 min after the ligand addition, and competition was monitored by following the decrease in intensity of fluorescence associated with the band of AMA bound to the protein. The apparent K_d values of the ligand-protein complexes were calculated as described in Brimau et al. (17).

RESULTS

Purification and Identification of Native OBP Isoforms

Since phosphorylation could confer different global charges to isoforms, we used strong anion exchange chromatography with two successive steps of NaCl gradient to purify OBP isoforms from the crude RM extract from pre-pubertal males. The fractions resulting from the first round of purification (**Figure 1A**) were desalted, dried under vacuum (Speed-Vac) and resuspended in sample buffer to be analyzed by 1D SDS-PAGE (**Figure 1C**). Only fractions 1 and 2 were positive after labeling with anti-OBP antibodies (data not shown) and were submitted to the second round of purification, by using an optimized gradient to obtain a better separation of the two peaks containing OBP isoforms (**Figure 1B**). From each peak of the first purification 1 and 2, two fractions were separated (**Figure 1C**), eluted at 0.266 M (fraction 1.1), 0.276 M (fraction 1.2), 0.277 M (fraction 2.1), and 0.280 M (fraction 2.2) of NaCl. The four fractions were immunoreactive to anti-OBP antibodies (**Figure 1D**). Each fraction was individually analyzed by two-dimensional electrophoresis (**Supplementary Figure 1**). For OBP identification, mass fingerprinting was performed on the 2D-E gel spot of each fraction (**Supplementary Table 1**, spectra in **Supplementary Figures 2–5**), giving 75.1% of peptide recovery for fraction 1.1 (referred to as OBP-native-iso1), 61.8% for fraction 1.2 (OBP-native-iso2), 90.4% for fraction 2.1 (OBP-native-iso3), and 100% for fraction 2.2 (OBP-native-iso4). In the theoretical map of trypsin digestion, two peptides allow discrimination between X1 and X2 variants: peptide 73–87 of m/z 1686.7354 specific to the X1 (only found in fraction 2.2), and peptide 73–85 of m/z 1498.6227 specific to X2. Unfortunately, the m/z of the later is closer to the one of peptide 16–28 (1498.7424), which is common to the two variants (in red in **Supplementary Table 1**). The peptide of expected m/z 2439.1820, indicating an additional Lys in C-terminal end (C-term: PAK, 138–158 in X1, and 136–155 in X2), was retrieved

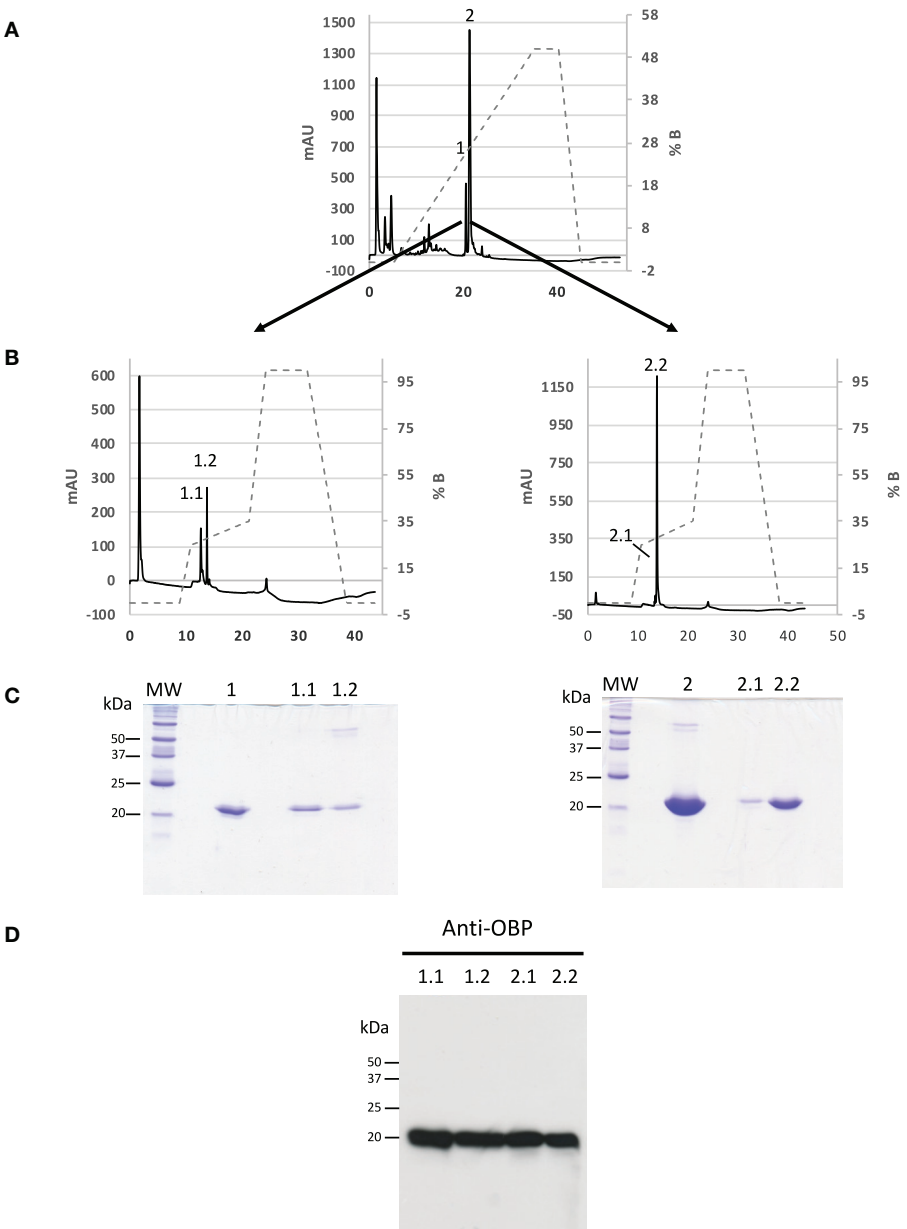

FIGURE 1 | Purification of OBP isoforms from *S. scrofa* by anion-exchange HPLC. Dotted lines represent the gradient of NaCl. **(A)** Chromatogram of the first step of purification from a total RM extract of pre-pubertal male indicating the fractions 1 and 2 containing OBP. **(B)** Proteins of fractions 1 and 2 were separated in a second round of purification leading to two peaks in each fraction. Absorbance was monitored at 215 nm. **(C)** Coomassie blue staining of 16.8% SDS-PAGE of fractions collected in the two successive rounds of purification (molecular weight markers Precision Plus Protein All Blue, BioRad). **(D)** Western-blot with anti-OBP antibodies (5 μg of each fraction, 1:20,000 dilution, ECL Plus detection, 15 s exposure).

only in OBP-native-iso3 (*m/z* 2439.8971), together with the peptide of m/z 2296.6929, typical of PA C-term.

Immunodetection of Post-translational Modifications on Native OBP Isoforms

Aliquots containing the same quantity of each fraction (5 μg) were analyzed by western-blot with specific antibodies raised against the three types of phosphorylation (anti-P-Ser, -P-Tyr, and -P-Thr) and against *O*-GlcNAcylation, RL2 and CTD110.6. The four OBP fractions were immunoreactive to the five antibodies (**Figure 2**). To test the specificity of antibodies, a short-size VEG (9) that is not phosphorylated nor *O*-GlcNAcylated (**Figure 2**) was used as a negative control and was not reactive with any antibodies. The specificity of the RL2 and CTD110.6 antibodies was further confirmed by western-blotting on two samples of RM total extract, one untreated and the other

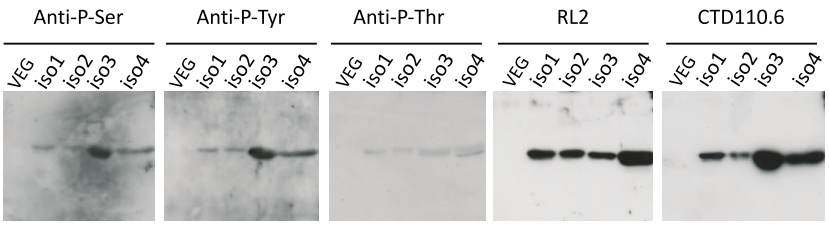

FIGURE 2 | Immunodetection of phosphorylation and *O*-GlcNAcylation of OBP isoforms from *S.scrofa*. Each well contains a normalized quantity (5 μg) of the four HPLC fractions. HPLC-purified short-size VEG was used as negative control. **Anti-P-Ser**: anti-phosphoserine antibodies (1:500 dilution); **Anti-P-Tyr**: anti-phosphotyrosine antibodies (1:2,000); **Anti-P-Thr**: anti-phosphothreonine antibodies (1:500); **RL2** (1:2,000), **CTD110.6** (1:4,000). Secondary antibodies for anti-phosphorylation antibodies at 1:40,000 dilution (rabbit IgG-HRP linked whole antibodies), ECL Plus detection (11 min exposure). Secondary antibodies for *O*-GlcNAc detection: goat anti-mouse IgG-HRP linked (1:30,000) for RL2, and rabbit anti-mouse IgM-HRP linked (1:30,000) for CTD110.6, ECL Plus detection (30 s exposure).

treated with β-*N*-acetylglucosaminidase. RL2 antibodies did not label the treated samples, indicating that the enzyme removed the GlcNAc groups, which assessed the β-linkage of GlcNAc moieties (**Supplementary Figure 6A**). Finally, a competition assay with free GlcNAc was performed to check antibody specificity. In these conditions, no signal was detected (**Supplementary Figure 6B**).

Mapping of Phosphorylation and *O*-GlcNAcylation Sites

Analysis of OBP Phosphorylation by BEMAD

The phosphorylation sites of native OBP isoforms were mapped by using the BEMAD method in the same conditions as previously used for recombinant OBP (17), which is not *O*-GlcNAcylated, unlike native OBP isoforms (**Supplementary Figure 7**). DTT addition confers a tag of defined molecular mass to peptides bearing phosphate groups: 136.2 Da for one DTT, and 272.4 Da for 2 DTT. We used both T and CT enzymes to obtain short peptides allowing a more accurate localization of phosphate groups. The measured masses of peptides obtained after BEMAD treatment were compared to the theoretical list of potential DTT-modified peptides calculated from the OBP protein sequence (GenBank accession number NP_998961). The BEMAD results are given in **Table 1** and the corresponding spectra are provided in **Supplementary Figures 8–11**. This method allowed potential localization of phosphorylation on Ser13, Ser41, Ser49, Ser57, and Thr 122 in OBP-native–iso1, Ser57, and Thr122 in –iso2, Ser23, Ser24, and Ser41 in –iso3, and Ser67 and Thr71 in –iso4. Since the mild beta-elimination does not open the aromatic cycle of tyrosine, PTM that bear this amino acid cannot therefore be detected by this method. However, Tyr residues of OBP isoforms could also be phosphorylated and only localized by high-resolution mass spectrometry. It is widely reported in the literature that the BEMAD method allows localization of phosphorylation with high confidence (22). Indeed, the action of β-*N*-acetylglucosaminidase allows a total elimination of GlcNAc moieties from the primary structure (**Supplementary Figure 6A**). Conversely, we have observed that alkaline phosphatase did not totally remove the phosphate groups, as phosphorylation is still detectable by specific antibodies after action of the enzyme (7). The BEMAD performed with alkaline phosphatase on OBP isoforms did not obtain confident results in *O*-GlcNAc site localization (data not shown). We thus performed mass spectrometry analyses to get more information on OBP isoforms PTM.

Analysis of OBP PTM by High-Resolution Mass Spectrometry

Although we obtained 100% sequence coverage for OBPs from Mascot search, which was expected from HPLC purification and peptide mapping data, only few peptide matches could be identified bearing a PTMs. In fact, <10 out of around 10,000 spectra from total RM OBP and HPLC fractions gave relevant data on PTM presence with 4,987 unassigned peptides. Only ions differing by a $\Delta\ m/z < 0.01$ from theoretical masses given by Protein Prospector were taken into consideration for annotation of spectra and ion tables (**Supplementary Tables 2–4**). Most of the data that confidently allows PTM site localization came from the analysis of the total OBP sample, which was enriched in GlcNAc-proteins on WGA column, at the contrary of the HPLC fractions. In preliminary assays, no result was obtained from an individual HPLC fraction, but peak 1 and peak 2 samples resulting from the first purification round gave information about phosphorylation sites (see below).

Serine 13 was assigned to bear either a phosphate or a GlcNAc group (**Figure 3**) in tryptic peptide 1–40 (QEPQPEQDPFELSGKWITSYIGSSDLEKIGENAPFQVFMR, Mascot scores of 28 and 46, respectively) coming from a total OBP sample. The phosphorylated peptide was detected as $[M+5H]^{5+}$ species at *m/z* 936.8391. Its CID spectrum is shown on **Figure 3A** and the list of fragment ions is provided in **Supplementary Table 2)**. The phosphate group could unambiguously be located at S13 from $y24^{2+}$ and $y17^{2+}$ fragment ions. The HexNAcylated peptide was detected as $[M+5H]^{5+}$ species at *m/z* 960.8576. Its CID spectrum is shown on **Figure 3B** with the list of fragment ions provided as **Supplementary Table 3**. This peptide also carried a methionine oxidation at M39, resulting in - $SOCH_4$ neutral losses on the y-series. The CID spectrum revealed a $b30^{3+}$ ion carrying and HexNAc moiety, while none of the y ions detected (up

TABLE 1 | Beta-elimination followed by Michael addition of dithiothreitol (BEMAD, DTT) performed on OBP isoforms to identify phosphorylation sites.

Calculated mass (Da)			Measured mass $(M + H)^+$	Peptide	Peptide sequence	Modification site
No DTT	1 DTT	2 DTT				
OBP-NATIVE-ISO1						
1711.7809	1847.9808		1847.4896 (T, 50%)	1–15	QEPQPEQDPFELS(*)GK	S13
1140.5354	1276.7354		1276.6440 (T+CT, 50%)	39–47	MRS(*)IEFDDK	S41
1357.6634	1493.8634		1493.7390 (T+CT, 50%)	45–55	DDKES(*)KVLNF	S49
1155.4986	1291.6986		1291.3486 (T, 25%)	57–66	S(*)KENGICEEF	S57
1262.5746	1398.7746		1398.6817 (T, 25%)	121–131	GT(*)DIEDQDLEK	T122
OBP-NATIVE-ISO-2						
1140.5354	1276.7354		1276.5677 (T+CT, 50%)	57–66	S(*)KENGICEEF	S57
1262.5746	1398.7746		1398.8314 (T+CT, 50%)	121–131	GT(*)DIEDQDLEK	T122
OBP-NATIVE-ISO3						
1950.9807		2223.3807	2223.5032 (CT, 50%)	21–38	IGS(*)S(*)DLEKIGENAPFQVF	S23–S24
1140.5354	1276.7354		1276.8341 (T+CT, 25%)	39–47	MRS(*)IEFDDK	S41
OBP-NATIVE-ISO-4						
1539.7359		1812.1359	1812.1110 (T, 25%)	59–72	ENGICEEFS(*)LIGT(*)K	S67–T71

*Peptides derived from MALDI-TOF MS analysis after enrichment by thiol chromatography (Trypsin T, Chymotrypsin CT, both T+CT) and elution at different percentages of acetonitrile (12.5, 25, and 50%). *Denotes mass addition of 136.2 Da at a S or T residue, indicating modification by dithiothreitol (DTT) and potential phosphorylation.*

to y_{25}) showed HexNAcylation. This suggests that the GlcNAc modification is localized at S13, although the lability of GlcNAc moiety upon CID cannot permit to rule out additional modification sites in region 1–40.

Indeed, another site of HexNAcylation was revealed at S19 in peptide 16–40 from total OBP sample (WITSYIGSSDLEKIGENAPFQVFMR, Mascot score 19). The species $[M+4H]^{4+}$ at *m/z* 777.6297 corresponds to a mass shift of 203.0732 Da compared to the unmodified peptide, matching with the theoretical mass of one HexNAc moiety (203.0794 Da). The CID spectrum is shown on **Figure 4** and the list of fragment ions is provided as **Supplementary Table 4**. The fragment ions b_4 and $y_{22}{}^{3+}$ ions permitted to unambiguously localize the HexNAc at S19.

One phosphorylation site has been localized on T122, on the peptide 121–138 (GTDIEDQDLEKFKEVTR) both in total OBP (**Figure 5** and **Supplementary Table 5**) and HPLC fraction (peak 2 of the first round of purification containing OBP-native-iso3 and -iso4, **Supplementary Figure 12**). In total OBP sample data (Mascot score 36), the mass difference between experimental mass of $[M+4H]^{4+} = 526.7421$ and the one calculated for naked peptide is *m/z* 19.9912, giving an addition of *m/z* 79.9648 close to the theoretical mass of the phosphate group (79.9668, mass Δ of 0.002). Ions b3, b4, and b6 indicate that T122 bears the phosphate moiety but not T137. Besides this site localization, other amino acids were identified as potentially modified by phosphorylation. The mass of the peptide 112–133 of sequence TIMTTGLLGKGTDIEDQDLEKFK (HPLC peak 1 containing OBP-native-iso1 and -iso2) indicates the presence of two phosphate groups. Indeed, parent ion $[M+5H]^{5+}$ with $m/z = 523.2381$ corresponds to the mass of the unmodified peptide plus two phosphorylation sites, but we could only confirm the presence of one phosphate by manual analysis of the MS/MS spectrum (**Supplementary Figure 13**). T112 or T115 could be phosphorylated as b5 ion mass corresponds to only one phosphate. In this peptide, T122 is not phosphorylated, which is assessed by ions y2 to $y13^{2+}$, and ions $b12^{2+}$ and $b13^{2+}$, the masses of which correspond to the naked peptide.

Monitoring of Ligand Binding by Fluorescence Spectroscopy

We measured the affinity of the four native OBP isoforms for the five selected ligands under the same experimental conditions that were used previously for recombinant OBP isoforms (17). The four isoforms were first titrated with the fluorescent probe, AMA. OBP-native-iso3 was collected in smaller quantities than the 3 other isoforms and was used at a 1 μM concentration instead of 2.5 μM and saturated with 2 μM AMA, instead of 3.75 μM AMA. The four isoforms displayed a comparable affinity for AMA: the estimated K_{d-AMA} were 0.37 $\pm$ 0.02, 0.23 $\pm$ 0.02, 0.84 $\pm$ 0.08, and 0.50 $\pm$ 0.02 μM for OBP-native-iso1, -iso2, -iso3, and -iso4, respectively. Ligands were then added, displacement curves are reported in **Figure 6** and binding constants calculated are listed in **Table 2**. None of the four native isoforms bound testosterone. Two classes of isoforms, -iso1 and -iso2, bound the two fatty acids and not the steroids. The opposite binding specificity was observed for -iso-3 and –iso-4 (**Table 2**).

DISCUSSION

Competition assays between fluorescent probes and odorant ligands or pheromone components are largely used in olfaction for testing the binding properties and measuring binding affinities of olfactory binding proteins from both insects and mammals. Most of the works were performed on recombinant

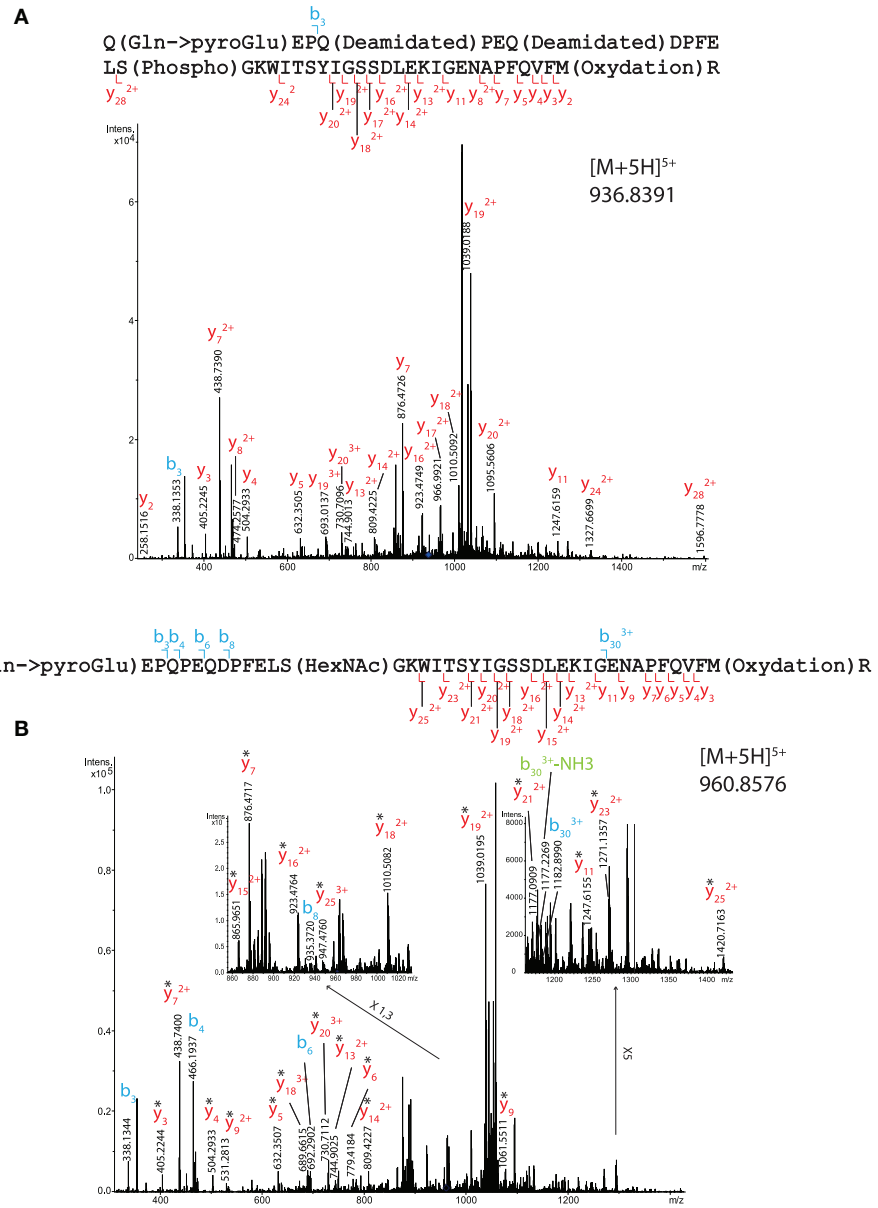

FIGURE 3 | MS/MS CID fragmentation spectra of tryptic peptide 1–40 from total RM extract identifies **(A)** phosphate modification site S13 or **(B)** HexNAc modification site S13. *Denotes loss of $SOCH_4$ (oxidation) on y-series.

OBPs produced in bacteria (*Escherichia coli*) or in yeast (*P. pastoris*), the former being unable to perform mammalian PTMs, and the later lacking of a coding sequence for OGT and EOGT in its genome (Ensembl database search). Since we were the first to evidence the presence of phosphorylation (7) and *O*-GlcNAcylation on a mammalian OBP (8, 9), the purpose of this work was to compare the binding abilities of Pichia-recombinant OBP isoforms with those of native OBP isoforms purified from nasal mucus, and to link their binding affinities to their PTM pattern. Functional assays were performed in the exact same conditions for recombinant (17) and native isoforms, with specific ligands of the pig species chemical communication: the palmitic and myristic fatty acids are part of the maternal appeasing pheromone (19, 23), and androstenol and androstenone compose the sex pheromone of the boar saliva (24).

Native OBP Isoforms Display Different Binding Affinities to Specific Ligands

For direct comparison and clarity purposes, the affinities of OBP isoforms [-native from this work and -Pichia from Brimau et al. (17)] toward each different ligand were expressed in K_a values of the complexes obtained (**Figure 7**). As expected, none of the four isoforms bound testosterone, since testosterone is the

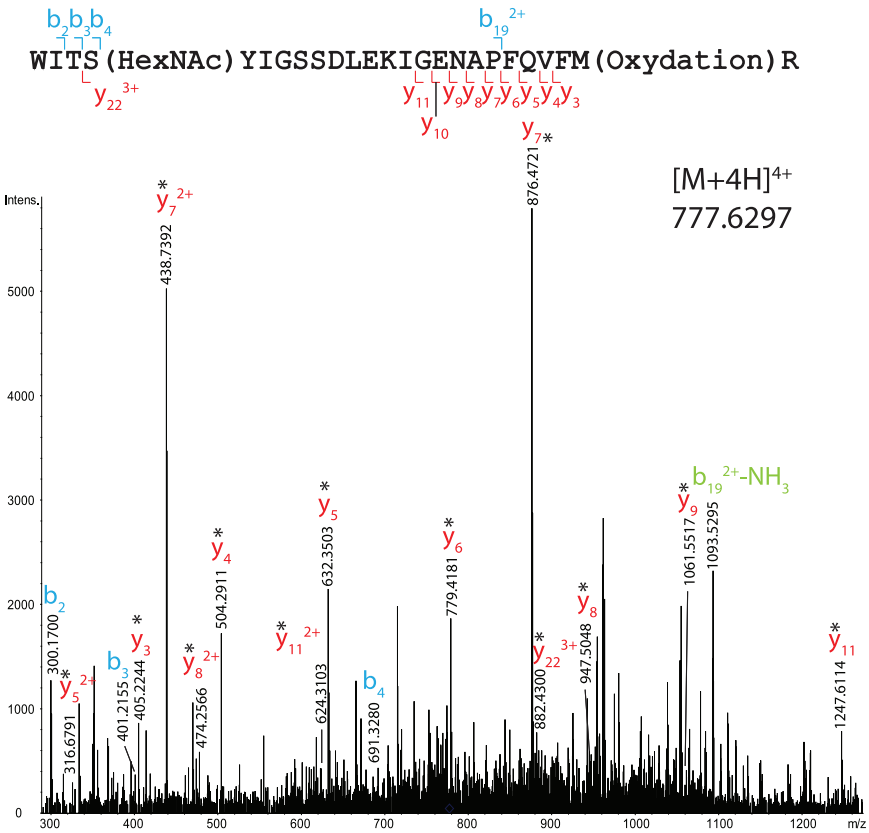

FIGURE 4 | MS/MS CID fragmentation spectrum of tryptic peptide 16–40 from total RM extract identifies HexNAc modification site S19. *Denotes loss of $SOCH_4$ (oxidation) on y-series.

specific ligand of the VEG, another protein of the nasal mucus of *S. scrofa* (8), and was used as negative control. This result demonstrates that differences between binding affinities reflect OBP isoform specificity and do not result from experimental artifacts since the three steroids have similar chemical structures, which are discriminated by OBP isoforms. Indeed, OBP-native-iso1 and -iso2 only bind both fatty acids, with a higher affinity for myristic acid than for palmitic acid. The important binding ability ($K_d = 50$ nM) of OBP-native-iso1 for myristic acid reflects the highest affinity ever reported by fluorescence spectroscopy for an OBP, regardless of its origin (species, native or recombinant) [e. g., (25–28)]. In contrast, OBP-native-iso3 and -iso4 have no affinity for fatty acids, but they bind androstenone and androstenol. Although the affinities of these two isoforms for androstenone are comparable, the K_a value for androstenol is three times greater for OBP-native-iso4 than for OBP-native-iso3. Compared to the OBP-Pichia, the native OBP isoforms appear to have significantly more specific binding power. OBP-Pichia-iso2 more readily bound to fatty acids, but displacement of the fluorescence probe was still observed with the addition of steroids. Conversely, OBP-Pichia-iso3 preferentially bound to the steroids, but also to a lesser extent to myristic acid, but was not able to bind palmitic acid. The lower K_a values and low selectivity of the OBP-Pichia-iso2 and -iso3 compared to the OBP-native isoforms cannot be explained by primary sequence differences or by the crystallographic structure previously published (29–31), but more likely can be explained by different patterns of post-translational modifications.

CID-MS/MS Allowed Identification of Phosphorylation and *O*-GlcNAcylation Sites on OBP Sequence

Although pig secretes a large quantity of OBP, HPLC purification in one side and enrichment in glycoproteins (WGA columns) or phosphopeptides (thiol columns in BEMAD protocol) in the other side resulted in considerable loss of relevant information on PTMs in mass spectrometry analyses. MR extract from a single animal provides just enough material to perform HPLC purification followed by western-blots, BEMAD and mass spectrometry analyses. Given that preliminary assays in glycoprotein enrichment after HPLC purification indicated a near total loss of sample (no PTM signal in western-blot was detected), this enrichment protocol was only performed on total MR extract, so on a mixture of OBP isoforms. In addition, it is known that in MS, the presence of unmodified peptide ions drastically suppresses the ionization of HexNAc-peptides, much more so than for phospho-peptides (32). The WGA

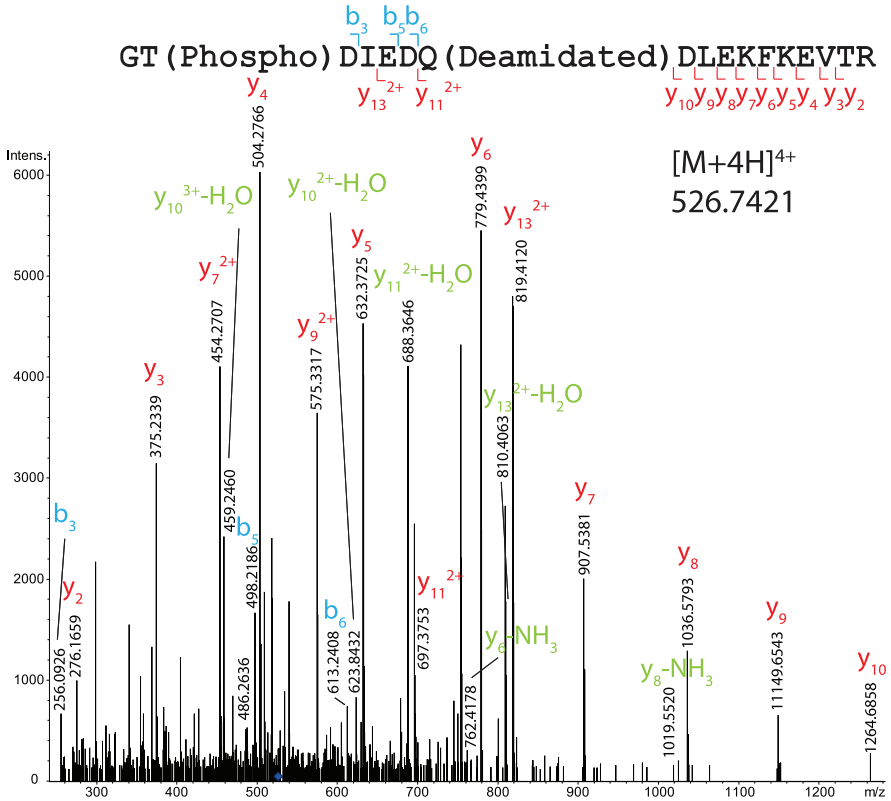

FIGURE 5 | MS/MS CID fragmentation spectrum of tryptic peptide 121–138 from total RM extract identifies phosphate modification site T122.

enrichment protocol was performed on a complex pool of total OBP isoforms containing glycosylated isoforms that were retained on the column. Once eluted, they were digested by trypsin, resulting in a mixture still containing unmodified and modified peptides with a ratio favorable to unmodified peptides, as observed in mass spectrometry. For nuclear and cytoplasmic proteins, *O*-GlcNAcylation has a low stoichiometry at each site, for instance, crystallin, a protein highly *O*-GlcNAcylated, exhibits an *O*-GlcNAc stoichiometry as low as 2% (33). Our analysis suggests that *O*-GlcNAcylation of OBP isoforms would fall within a similar range, leading to a difficult identification of HexNAc-sites, independently of the ionization source. Consequently, CID-MS/MS on HPLC fractions gave scarce information on fractions PTM patterns. Nevertheless, several phospho-sites and HexNAc-sites were confidently identified for the first time on a mammalian OBP. Ascertained and potential modification sites obtained with BEMAD and Mascot analysis of CID MS/MS are summarized in **Figure 8**. Enrichment of GlcNAc peptides could be achieved through using click-chemistry (34, 35) coupled to Electron Transfer Dissociation-MS/MS [ETD-MS/MS, for a review see Ma and Hart (32)] or negative ion CID-MS/MS (36), to improve the coverage of all OBP PTM sites. Nevertheless, glycopeptide enrichment is required to obtain confident data with ETD-MS/MS, which is far less sensitive than the CID mode.

Interestingly, the sites of phosphorylation localized in the total native OBP (7) were all retrieved and dispatched among the 4 isoforms. MS/MS analysis identified two phospho-sites, and confirmed their localization at S13 and T122. Phosphorylation of secreted proteins is nowadays well documented and some candidate kinases could modify the OBP sequence. FAM20C, a Golgi kinase, is responsible for phosphorylating the majority of secreted phosphoproteins at the S-x-E motif and could thus modify OBP at S41 (S-I-E), and S57 (S-K-E). But extensive analysis of secreted phosphoproteins suggests that FAM20C could target substrates lacking this canonical recognition site (13). In this work, no phosphorylation was identified on tyrosine residues by CID-MS, despite the labeling of the four fractions by anti-phosphotyrosine antibodies, particularly strong for OBP-native-iso3 (the less abundant OBP isoform) (**Figure 2**). However, in previous work (37), we have identified phosphosites, which were not all retrieved in this study, particularly at Y78 or Y82. The use of different mass spectrometry conditions (HCD-Orbitrap) and different animals could explain this discrepancy. Phosphorylation on OBP could be done by the vertebrate lonesome kinase (VLK), a secreted kinase that modifies extracellular proteins on Y residues (14). The absence of identified phosphoY-peptides in our MS data is most likely due to their faint quantity compared to phosphoS/T-peptides (22). In vertebrate cells, the phosphoS:phosphoT:phosphoY ratio is

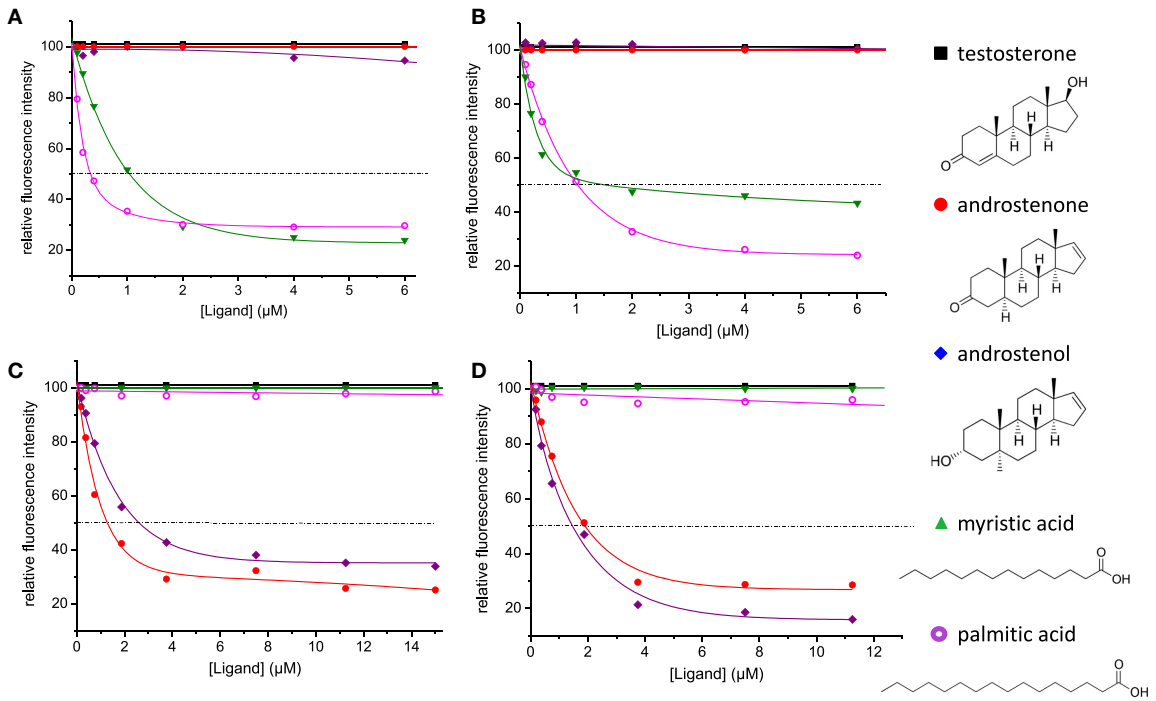

FIGURE 6 | Competitive binding assays of five selected ligands of biological relevance to native OBP isoforms from S. scrofa. **(A)** OBP-native-iso1; **(B)** OBP-native-iso2; **(C)** OBP-native-iso3; and **(D)** OBP-native-iso4. Proteins were used at 2.5 μM **(A,B,D)** or 1 μM **(C)** concentration and were saturated with 3.75 μM **(A,B,D)** or 2 μM **(C)** of the fluorescent probe 1-AMA. Competitors were added at increasing concentration from 0 to 6 μM **(A,B)** or to 15 μM **(C,D)**.

TABLE 2 | Values of [IC50] and calculated dissociation constants (K_d) relative to the binding of ligands to native OBP isoforms.

Ligands	OBP-native-iso1		OBP-native-iso2		OBP-native-iso3		OBP-native-iso4	
	IC_{50}	K_d	IC_{50}	K_d	IC_{50}	K_d	IC_{50}	K_d
Testosterone	–	–	–	–	–	–	–	–
Androstenone	–	–	–	–	1.28	0.23	1.89	0.22
Androstenol	–	–	–	–	2.59	0.49	1.43	0.16
Palmitic acid	1.03	0.16	1.51	0.16	–	–	–	–
Myristic acid	0.33	0.05	1.03	0.11	–	–	–	–

IC_{50} and K_d are expressed in μM.

1800:200:1. Most cytosolic S/T kinases recognize a highly basic consensus sequence, which is the case for five sites predicted by BEMAD and/or CID-MS (R-S41-I, E-S49-K, F-S57-K, G-T71-K, K-T112-I). Despite extensive research that has been reported in the literature and the data that we provide here, the kinase (s) responsible for OBP phosphorylation still remain (s) to be identified.

Two sites of HexNAcylation were unambiguously localized at S13 and S19 of OBP sequence. Due to the novelty of our findings, we were extremely cautious in data acquisition and interpretation. The β-linkage of the HexNAc moiety was demonstrated by both western-blots with specific CTD110.6 and RL2 antibodies and by β-N-acetylglucosaminidase treatment. The competition assay with free GlcNAc confirmed the specificity of CTD110.6 antibodies against *O*-GlcNAc modified OBP. Indeed, it has been reported that CTD110.6 could recognize *O*-GlcNAcylated cell surface proteins, such as Notch1, but also terminal β-GlcNAc of complex N- or O-glycans (38), that could not be the case for OBP. The protein has no consensus site for either N- or O-complex glycosylation, and treatments with appropriate enzymes have confirmed their absence in the past (39). *O*-GlcNAcylation has been thought to be restricted to nuclear and cytoplasmic proteins, and in a lesser extent, mitochondrial ones, until the report of *O*-GlcNAcylation of proteins processed in the secretion pathway (15). The enzyme, named EGF-domain specific *O*-GlcNAc transferase (EOGT) transfers a GlcNAc moiety to proteins with an epidermal growth factor (EGF) repeat on their extracellular domain, such as Notch1

or Dumpy (15, 40). EOGT is ER-resident and so, can theoretically modify any protein that passes through the secretion pathway, not only the membrane attached proteins. Very few proteins secreted in the extracellular medium were reported to be *O*-GlcNAc modified. But findings from Alfaro et al. (41) suggest that EOGT could target additional substrates because some *O*-GlcNAc sites were found on proteins lacking the EGF domain and the consensus motif $C_5XXGXS/TGXXC_6$; porcine OBP also lacks both of them. Among 274 *O*-GlcNAc proteins identified in the *O*-GlcNAcome of rodent brain tissue, only 5 membrane proteins and one secreted cytokine were *O*-GlcNAcylated (41). Therefore, contrary to the assessment that EOGT modifies only secreted and membrane proteins that contain one or more epidermal growth factor-like repeats with a specific consensus sequence, we demonstrated that secreted OBP, without such features in its sequence, is *O*-GlcNAc modified and could be a substrate for the porcine EOGT, already characterized in respiratory mucosa tissues (9).

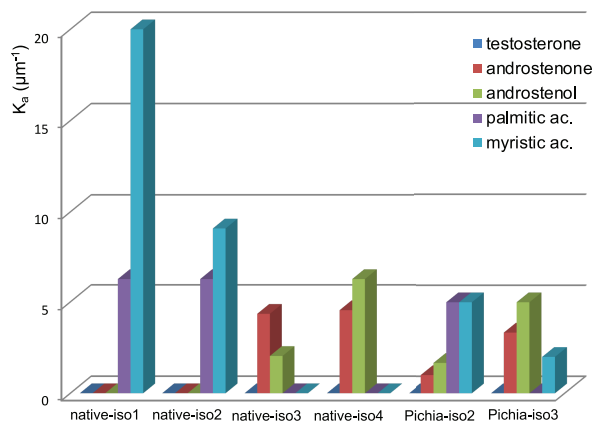

FIGURE 7 | Calculated affinity constants (Ka) for the different isoforms of *S. scrofa* OBP-native (this work) and OBP-Pichia [from Brimau et al. (17)] toward the five tested ligands.

O-GlcNAcylation Increases Both Specificity and Affinity of OBP Isoforms

Recombinant OBP-Pichia isoforms that are phosphorylated bind steroids and fatty acids with slight differences. Conversely, native isoforms, that are phosphorylated but also *O*-GlcNAcylated, show radically different binding affinities for the same compounds, strongly suggesting that *O*-GlcNAcylation increases the binding specificity of OBP isoforms. Moreover, one of the OBP isoforms, OBP-native-iso1, labeled by CTD110.6 antibodies, displayed the highest affinity ever reported for an OBP. Phosphorylation and *O*-GlcNAcylation patterns seem to determine the binding specificity of isoforms, and cause a subset of OBPs to bind specific chemical classes of ligands with affinities in the nanomolar range. The identification of at least two *O*-GlcNAc sites, S13 and S19, interestingly localized on the flexible N-terminus part of the protein (30), will lead to side-directed mutagenesis followed by binding assays to better understand how this little sugar can modify OBP binding properties. Hence, phosphorylation and *O*-GlcNAcylation act together to generate OBP isoforms that are able to perform a first coding of odorant and pheromonal molecules. This suggests that a specific OBP-ligand complex would specifically interact with a given olfactory receptor, highlighting a new olfactory transduction mechanism. As G-protein coupled olfactory receptors (e. g. OR 585; accession number IPI00127945) have been identified to be *O*-GlcNAcylated (35), this exquisite coding might be mediated by sugar-sugar interactions. These findings extend the role of *O*-GlcNAc in regulating the function of many proteins involved in most, if not all, metabolic processes, including extracellular signaling in olfaction.

DATA AVAILABILITY STATEMENT

The mass spectrometry proteomics data have been deposited to the ProteomeXChange consortium via the PRIDE partner repository with the dataset identifier PXD011371 and 10.6019/PXD011371. The raw data (western-blot) supporting the conclusions of this manuscript will be made available by the authors, without undue reservation, to any qualified researcher.

```
                  P
                  G     G       PP
QEPQPEQDPF ELSGKWITSY IGSSDLEKIG ENAPFQVFMR
1          10             20             30             40
P         P          P           P     P
SIEFDDKESK VYLNFFSKEN GICEEFSLIG TKQEGNTYDV
           50             60             70             80
                                        P  P
NYAGNNKFVV SYASETALII SNINVDEEGD KTIMTGLLGK
           90            100            110            120
 P
GTDIEDQDLE KFKEVTRENG IPEENIVNII ERDDCPAK
           130            140            150         158
```

FIGURE 8 | Amino acid sequence of porcine OBP (GI/47523248 - OBP X1j) with PTM sites: P or G above an amino acid symbol indicate a phosphorylation or an HexNAcylation site. PTM sites identified by CID-MS/MS are highlighted in bold and red—phosphorylation: S13, T112 or T115, T122—HexNAcylation: S13, T19. Phosphorylation sites identified by BEMAD are in italic type: S13, S23, S24, S41, S49, S57, S67, T71, T122.

AUTHOR CONTRIBUTIONS

PNLM, CLD, SZ, and JPC contributed to conception and design of the study. CLD performed peptide mapping and MALDI-TOF experiments. PNLM and AJ performed HPLC purification and western-blots. JPC conducted and analyzed fluorescence spectroscopy data. AM and SZ acquired and analyzed nano-LC-MS/MS data. PNLM and AJ analyzed nano-LC-MS/MS data. All authors wrote sections of the manuscript and contributed to manuscript revision, read, and approved the submitted version.

FUNDING

This work was funded by INRA (French Institut National de Recherche Agronomique) and CNRS (French Centre National de Recherche Scientifique).

ACKNOWLEDGMENTS

Authors warmly thank Dr. Fanny Brimau who provided important technical contributions to this work in performing BEMAD and fluorescence spectroscopy assays. PNLM is grateful to the students who helped in OBP isoforms purification, Florent Dubart and Cyrielle Bader, to Anne-Sophie Edouart-Vercoutter for revising the manuscript and to Stephan Hardivillé for improving English grammar. PNLM and AJ are grateful to Louise Le Meillour for her help in Mascot data analyses and in the use of Illustrator software to build figures.

SUPPLEMENTARY MATERIAL

The Supplementary Material for this article can be found online at: https://www.frontiersin.org/articles/10.3389/fendo.2018.00816/full#supplementary-material

REFERENCES

1. Buck L, Axel R. A novel multigene family may encode odorant receptors: a molecular basis for odor recognition. *Cell* (1991) 65:175–87. doi: 10.1016/0092-8674(91)90418-X
2. Bignetti E, Cavaggioni A, Pelosi P, Persaud KC, Sorbi RT, Tirindelli R. Purification and characterisation of an odorant-binding protein from cow nasal tissue. *Eur J Biochem.* (1985) 149:27–31. doi: 10.1111/j.1432-1033.1985.tb08916.x
3. Tegoni M, Pelosi P, Vincent F, Spinelli S, Campanacci V, Grolli S, et al. Mammalian odorant binding proteins. *Biochim Biophys Acta* (2000) 1482:229–40. doi: 10.1016/S0167-4838(00)00167-9
4. Münch J, Billig G, Hübner CA, Leinders-Zufall T, Zufall F, Jentsch TJ. Ca^{2+}-activated Cl- currents in the murine vomeronasal organ enhance neuronal spiking but are dispensable for male-male aggression. *J Biol Chem.* (2018) 293:10392–403. doi: 10.1074/jbc.RA118.003153
5. Harmeier A, Meyer CA, Staempfli A, Casagrande F, Petrinovic MM, Zhang YP, et al. How female mice attract males: a urinary volatile amine activates a trace amine-associated receptor that induces male sexual interest. *Front Pharmacol.* (2018) 9: 924. doi: 10.3389/fphar.2018.00924
6. Trimmer C, Snyder LL, Mainland JD. High-throughput analysis of mammalian olfactory receptors: measurement of receptor activation via luciferase activity. *J Vis Exp.* (2014) e51640. doi: 10.3791/51640
7. Nagnan-Le Meillour P, Le Danvic C, Brimau F, Chemineau P, Michalski JC. Phosphorylation of native porcine olfactory binding proteins. *J Chem Ecol.* (2009) 35:752–60. doi: 10.1007/s10886-009-9663-z
8. Le Danvic C, Guiraudie-Capraz G, Abderrahmani D, Zanetta JP, Nagnan-Le Meillour P. Natural ligands of porcine olfactory binding proteins. *J Chem Ecol.* (2009) 35:741–51. doi: 10.1007/s10886-009-9645-1
9. Nagnan-Le Meillour P, Vercoutter-Edouart AS, Hilliou F, Le Danvic C, Lévy F. Proteomic analysis of pig (*Sus scrofa*) olfactory soluble proteome reveals *O*-linked-N-acetylglucosaminylation of secreted odorant-binding proteins. *Front Endocrinol.* (2014). 5:202. doi: 10.3389/fendo.2014.00202
10. Hart GW. Three decades of research on *O*-GlcNAcylation - A major nutrient sensor that regulates signaling, transcription and cellular metabolism. *Front Endocrinol.* (2014) 5:183. doi: 10.3389/fendo.2014.00183
11. Hardivillé S, Hart GW. Nutrient regulation of signaling, transcription and cell physiology by O-GlcNAcylation. *Cell Metab.* (2014) 20:208–13. doi: 10.1016/j.cmet.2014.07.014
12. Bond MR, Hanover JA. A little sugar goes a long way: the cell biology of *O*-GlcNAc. *J Cell Biol.* (2015) 208:869–80. doi: 10.1083/jcb.201501101
13. Tagliabracci VS, Wiley SE, Guo X, Kinch LN, Durrant E, Wen J, et al. A single kinase generates the majority of the secreted phosphoproteome. *Cell* (2015) 161:1619–32. doi: 10.1016/j.cell.2015.05.028
14. Bordoli MR, Yum J, Breitkopf SB, Thon JN, Italiano JE Jr, Xiao J, et al. A secreted tyrosine kinase acts in the extracellular environment. *Cell* (2014) 158:1033–44. doi: 10.1016/j.cell.2014.06.048
15. Matsuura A, Ito M, Sakaidani Y, Kondo T, Murakami K, Furukawa K, et al. *O*-Linked N-acetylglucosamine is present on the extracellular domain of Notch receptors. *J Biol Chem.* (2008) 283:35486–95. doi: 10.1074/jbc.M806202200
16. Sakaidani, Y., Nomura, T., Matsuura, A., Ito, M., Suzuki, E., Murakami, K., et al. (2011). *O*-Linked-*N*-acetylglucosamine on extracellular protein domains mediates epithelial cell-matrix interactions. *Nat. Commun.* 2:583. doi: 10.1038/ncomms1591
17. Brimau F, Cornard JP, Le Danvic C, Lagant P, Vergoten G, Grebert D, et al. Binding specificity of recombinant odorant-binding protein isoforms is driven by phosphorylation. *J Chem Ecol.* (2010) 36:801–13. doi: 10.1007/s10886-010-9820-4
18. Nagnan-Le Meillour P, Lagant P, Cornard JP, Brimau F, Le Danvic C, Vergoten G, et al. Phenylalanine 35 and tyrosine 82 are involved in the uptake and release of ligand by porcine odorant-binding protein. *Biochim Biophys Acta* (2009) 1794:1142–50. doi: 10.1016/j.bbapap.2009.04.012
19. Guiraudie G, Pageat P, Cain AH, Madec I, Nagnan-Le Meillour P. Functional characterization of olfactory binding proteins for appeasing compounds and molecular cloning in the vomeronasal organ of pre-pubertal pigs. *Chem Senses* (2003) 28:609–19. doi: 10.1093/chemse/bjg052
20. Wells L, Vosseler K, Cole RN, Cronshaw JM, Matunis MJ, Hart GW. Mapping sites of *O*-GlcNac modification using affinity tags for serine and threonine post-translational modifications. *Mol Cell Proteomics* (2002) 1:791–804. doi: 10.1074/mcp.M200048-MCP200
21. Vizcaino JA, Csordas A, del-Toro N, Dianes JA, Griss J, Lavidas I, et al. 2016 update of the PRIDE database and related tools. *Nucleic Acid Res.* (2016) 44:D447–56. doi: 10.1093/nar/gkw880
22. Mann M, Ong SE, Grønborg M, Steen H, Jensen ON, Pandey A. Analysis of protein phosphorylation using mass spectrometry: deciphering the phosphoproteome. *Trends Biotechnol.* (2002) 6:261–8. doi: 10.1016/S0167-7799(02)01944-3
23. Yonezawa T, Koori M, Kikusui T, Mori Y. Appeasing pheromone inhibits cortisol augmentation and agonistic behaviors during social stress in adult miniature pigs. *Zoolog Sci.* (2009) 26:739–44. doi: 10.2108/zsj.26.739
24. Meese GB, Conner DJ, Baldwin BA. Ability of the pig to distinguish between conspecific urine samples using olfaction. *Physiol Behav.* (1975) 15:121–5. doi: 10.1016/0031-9384(75)90289-9
25. Paolini S, Tanfani F, Fini C, Bertoli E, Pelosi P. Porcine odorant-binding protein: structural stability and ligand affinities measured by Fourier-transform infrared spectroscopy and fluorescence spectroscopy. *Biochim Biophys Acta* (1999) 1431:179–88. doi: 10.1016/S0167-4838(99)00037-0

26. Briand L, Nespoulous C, Perez V, Rémy JJ, Huet JC, Pernollet JC. Ligand-binding properties and structural characterisation of a novel rat odorant-binding protein variant. *Eur J Biochem.* (2000) 267:3079–89. doi: 10.1046/j.1432-1033.2000.01340.x
27. Löbel D, Jacob M, Völkner M, Breer H. Odorants of different chemical classes interact with distinct odorant binding protein subtypes. *Chem Senses* (2002) 27:39–44. doi: 10.1093/chemse/27.1.39
28. Zhu J, Arena S, Spinelli S, Liu D, Zhang G, Wei R, et al. Reverse chemical ecology: olfactory proteins from the giant panda and their interactions with putative pheromones and bamboo volatiles. *PNAS* (2017) 114:E9802–10. doi: 10.1073/pnas.1711437114
29. Spinelli S, Ramoni R, Grolli S, Bonicel J, Cambillau C, Tegoni M. The structure of the monomeric porcine odorant binding protein sheds light on the domain swapping mechanism. *Biochemistry* (1998) 37:7913–8. doi: 10.1021/bi980179e
30. Vincent F, Spinelli S, Ramoni R, Grolli S, Pelosi P, Cambillau C, et al. Complexes of porcine odorant-binding protein with odorant molecules belonging to different chemical classes. *J Mol Biol.* (2000) 300:127–39. doi: 10.1006/jmbi.2000.3820
31. Perduca M, Mancia F, Del Giorgio R, Monaco HL. Crystal structure of a truncated form of porcine odorant-binding protein. *Proteins* (2001) 42:201–9. doi: 10.1002/1097-0134(20010201)42:23.3.CO;2-Z
32. Ma J, Hart GW. *O*-GlcNAc profiling: from proteins to proteomes. *Clin Proteomics* (2014) 11:8. doi: 10.1186/1559-0275-11-8
33. Viner RI, Zhang T, Second T, Zabrouskov V. Quantification of post-translationnaly modified peptides of bovine alpha-crystallin using tandem mass tags and electron transfer dissociation. *J Proteomics* (2009) 72:874–85. doi: 10.1016/j.jprot.2009.02.005
34. Parker BL, Gupta P, Cordwell SJ, Larsen MR, Palmisano G. Purification and identification of *O*-GlcNAc-modified peptides using phosphate-based alkyne CLICK chemistry in combination with titanium dioxide chromatography and mass spectrometry. *J Proteome Res.* (2011) 10:1449–58. doi: 10.1021/pr100565j
35. Zaro BW, Yang YY, Hang HC, Pratt MR. Chemical reporters for fluorescent detection and identification of O-GlcNAc-modified proteins reveal glycosylation of the ubiquitin ligase NEDD4-1. *PNAS* (2011) 108:8146–51. doi: 10.1073/pnas.1102458108
36. Wiesner J, Premsler T, Sickmann A. Application of electron transfer dissociation (ETD) for the analysis of posttranslational modifications. *Proteomics* (2008) 8:4466–83. doi: 10.1002/pmic.200800329
37. Bouclon J, Le Danvic C, Guettier E, Bray F, Tokarski C, Rolando C, et al. Identification of post-translational modifications on odorant-binding protein isoforms from pig olfactory secretome by high-resolution mass spectrometry: *O*-β-N-acetylglucosaminylation and phosphorylation. *Front Ecol Evol.* (2017) 5:142. doi: 10.3389/fevo.2017.00142
38. Tashima Y, Stanley P. Antibodies that detect *O*-GlcNAc on the extracellular domain of cell surface glycoproteins. *J Biol Chem.* (2014) 289:11132–42. doi: 10.1074/jbc.M113.492512
39. Paolini S, Scaloni A, Amoresano A, Marchese S, Napolitano E, Pelosi P. Amino acid sequence, post-translational modifications, binding and labelling of porcine odorant-binding protein. *Chem Senses* (1998) 23:689–98. doi: 10.1093/chemse/23.6.689
40. Sakaidani Y, Ichiyanagi N, Saito C, Nomura T, Ito M, Nishio Y, et al. *O*-linked-N-acetylglucosamine modification of mammalian Notch receptors by an atypical *O*-GlcNAc transferase Eogt1. *Biochem Biophys Res Commun.* (2012) 419:14–9. doi: 10.1016/j.bbrc.2012.01.098
41. Alfaro JF, Gong CX, Monroe ME, Aldrich JT, Clauss TRW, Purvine SO, et al. Tandem mass spectrometry identifies many mouse brain *O*-GlcNAcylated proteins including EGF domain-specific *O*-GlcNAc transferase targets. *PNAS* (2012) 109:7280–5. doi: 10.1073/pnas.1200425109

Conflict of Interest Statement: The authors declare that the research was conducted in the absence of any commercial or financial relationships that could be construed as a potential conflict of interest.

frontiers in Endocrinology

ORIGINAL RESEARCH
published: 22 February 2019
doi: 10.3389/fendo.2019.00106

Cyclin D1 Stability Is Partly Controlled by *O*-GlcNAcylation

Louis Masclef[1†], *Vanessa Dehennaut*[2], *Marlène Mortuaire*[1], *Céline Schulz*[1], *Maïté Leturcq*[1], *Tony Lefebvre*[1] *and Anne-Sophie Vercoutter-Edouart*[1*]

[1] Université de Lille, CNRS, UMR 8576, UGSF, Unité de Glycobiologie Structurale et Fonctionnelle, Lille, France, [2] Institut Pasteur de Lille, Université de Lille, CNRS, UMR 8161, M3T: Mechanisms of Tumorigenesis and Targeted Therapies, Lille, France

Cyclin D1 is the regulatory partner of the cyclin-dependent kinases (CDKs) CDK4 or CDK6. Once associated and activated, the cyclin D1/CDK complexes drive the cell cycle entry and G1 phase progression in response to extracellular signals. To ensure their timely and accurate activation during cell cycle progression, cyclin D1 turnover is finely controlled by phosphorylation and ubiquitination. Here we show that the dynamic and reversible *O*-linked β-N-Acetyl-glucosaminylation (*O*-GlcNAcylation) regulates also cyclin D1 half-life. High *O*-GlcNAc levels increase the stability of cyclin D1, while reduction of *O*-GlcNAcylation strongly decreases it. Moreover, elevation of *O*-GlcNAc levels through *O*-GlcNAcase (OGA) inhibition significantly slows down the ubiquitination of cyclin D1. Finally, biochemical and cell imaging experiments in human cancer cells reveal that the *O*-GlcNAc transferase (OGT) binds to and glycosylates cyclin D1. We conclude that *O*-GlcNAcylation promotes the stability of cyclin D1 through modulating its ubiquitination.

Keywords: cyclin D, *O*-GlcNAc, stability, ubiquitination, cell cycle

OPEN ACCESS

Edited by:
Xiaoyong Yang,
School of Medicine, Yale University, United States

Reviewed by:
Michael Boyce,
Duke University, United States
Chad Slawson,
University of Kansas Medical Center Research Institute, United States

***Correspondence:**
Anne-Sophie Vercoutter-Edouart
anne-sophie.vercoutter@univ-lille.fr

†Present Address:
Louis Masclef,
Department of Medicine, Maisonneuve-Rosemont Hospital Research Center, University of Montréal, Montreal, QC, Canada

Specialty section:
This article was submitted to Molecular and Structural Endocrinology, a section of the journal Frontiers in Endocrinology

Received: *05 December 2018*
Accepted: *05 February 2019*
Published: *22 February 2019*

Citation:
Masclef L, Dehennaut V, Mortuaire M, Schulz C, Leturcq M, Lefebvre T and Vercoutter-Edouart A-S (2019) Cyclin D1 Stability Is Partly Controlled by O-GlcNAcylation. Front. Endocrinol. 10:106. doi: 10.3389/fendo.2019.00106

INTRODUCTION

In mammalian cells, progression from G1 to S phase is controlled by the cyclin D-Cyclin-dependent kinase (CDK) 4/6 complexes, in which cyclin D1 is the regulatory subunit and CDK4-6 the catalytic subunit. These complexes initiate the phosphorylation-dependent inactivation of the retinoblastoma protein pRb, promoting the E2F-dependent gene transcription, including cyclin E. Complete inhibition of pRb is then achieved by the cyclin E-CDK2 complex, allowing the expression of target genes necessary for S phase entry. To trigger a timely activation of CDK4/6 in G1 phase, cyclin D1 steady-state level is highly regulated throughout the cell cycle (1, 2). Mitogenic stimulation of quiescent cells induces a dramatic increase of cyclin D1 mRNA and protein expression, mainly through Ras/MAPK and PI3K/Akt signaling pathways which activate many transcription factors including c-Fos/c-Jun, NF-κb and β-catenin/TCF-4 (2–5). Cyclin D1-CDK4/6 complexes are then phosphorylated by CDK-activating kinase (CAK) leading to their activation and translocation to the nucleus (6, 7). Cyclin D1 has a short half-life of around 30 min, its degradation being mediated through the ubiquitin-dependent proteasomal pathway. Once cells progress in S phase, GSK-3β is translocated into the nucleus where it phosphorylates cyclin D1 at Thr286 located in a PEST C-terminal sequence (8, 9). This phosphorylation induces the export of cyclin D1 out of nucleus through a CRM1-dependent mechanism (10, 11). Additionally, phosphorylation at Thr288 by the arginine-directed serine/threonine kinase Mirk/dyrk1B induces a more rapid turnover of cyclin D1 (12). Cyclin D1 is then targeted to the SCF (SKP1 (S-phase-kinase associated protein 1), Cullin-1/Cdc53, F-Box protein) E3 ubiquitin ligase complex that promotes

its polyubiquitination, leading to its subsequent proteasomal degradation (13–16). The ubiquitin-dependent proteolysis of cyclin D1 is antagonized by the deubiquitinating enzyme USP2, thus increasing cyclin D1 half-life (17). More recently, USP22 has also been identified as a deubiquitinase targeting cyclin D1 (18). Pharmacological inhibition of USP2 accelerates cyclin D1 degradation and leads to cell cycle arrest in several cancer cell lines among which the HCT116 colon cancer cell line and MCF7 breast cancer cell line (19). Importantly, deregulation of cyclin D1 stability contributes to its oncogenic potential. The absence of Thr286 in the natural alternative splicing variant cyclin D1b or the mutation T286A induce the nuclear accumulation of the cyclin, due to a defect in the phosphorylation-mediated nuclear export, and increase its oncogenicity in murine fibroblasts (10, 20). Additionally, mutations in Fbxo4 in esophageal tumors affect the E3 ligase activity and lead to overexpression of cyclin D1 (21).

Beside phosphorylation, *O*-linked β-N-acetylglucosaminylation or *O*-GlcNAcylation of proteins takes part in cell cycle regulation (22). The cycling of *O*-GlcNAcylation is controlled solely by two enzymes which are localized in the nucleus and cytoplasm. The *O*-GlcNAc Transferase (OGT) catalyzes the transfer of the GlcNAc moiety from the nucleotide sugar UDP-GlcNAc onto the hydroxyl group of Ser/Thr of resident proteins of the nucleus, cytoplasm and mitochondria, while the *O*-GlcNAc hydrolase (OGA) reverses the reaction. *O*-GlcNAcylation regulates various biological functions, such as protein interactions, protein stability, subcellular localization, and enzyme activity (23–25). Interestingly, a reciprocal relationship between *O*-GlcNAc and phosphorylation has been described for many proteins such as the transcription factors c-Myc and delta-lactoferrin (26, 27), and the signaling kinase Akt (28). Importantly, overexpression of OGT and hyper *O*-GlcNAcylation of proteins have been emerging for the last decade as a landmark of cancer cells (29, 30). Deciphering the molecular mechanisms that are regulated by *O*-GlcNAc cycling is thus crucial to better understand how *O*-GlcNAcylation impacts cancer cells properties. In mammalian cells, *O*-GlcNAc levels are regulated in a cell cycle-dependent manner and dynamics of *O*-GlcNAcylation is important for the correct progression of cell cycle (31–33). Inhibition of OGT catalytic activity or down-regulation of its expression hindered serum-induced cyclin D protein expression and cell cycle entry (34). Serum stimulation of *Ogt*-deficient mouse embryonic fibroblasts failed to enhance the protein levels of c-Fos, c-Jun, and c-Myc, whereas level of the inhibitor $p27^{KIP1}$ was highly increased (35). The stability of $p27^{KIP1}$ was also increased in human cancer cells in which OGT was knockdown, concomitantly to a significant decrease of proliferation (36, 37). Moreover, impairment of *O*-GlcNAc cycling altered the protein levels of cyclins D and E in both OGT- and OGA- overexpressing cells (31), while shOGT decreased cyclin D expression in pancreatic cancer cells (38). Cyclin D expression was also slightly altered in stable OGA knockdown cells (39).

Despite mounting evidence of a link between cyclin D1 steady-state level and *O*-GlcNAc homeostasis, the underlying molecular mechanisms are still unclear. Therefore, we investigated how *O*-GlcNAcylation could regulate cyclin D1 expression and whether cyclin D1 could be *O*-GlcNAcylated. Here, we demonstrate that cyclin D1 stability is positively regulated with *O*-GlcNAcylation levels in human cancer cells. High *O*-GlcNAc conditions perturb the polyubiquitination of cyclin D1, thus slowing down its degradation rate. This study also reveals that OGT binds to cyclin D1, mostly in the nucleus and in a cell cycle-dependent manner. Finally, we describe for the first time the *O*-GlcNAcylation of cyclin D1. Altogether, this work highlights a novel post-translational modification of cyclin D1 that helps its stability. It also provides novel molecular insights into the role of *O*-GlcNAc cycling in cell cycle regulation.

MATERIALS AND METHODS

Cell Culture

HEK293T, MCF7, and HCT116 cells were cultured at 37°C in DMEM supplemented with 10% (v/v) fetal calf serum (Lonza, Ozyme, France), in a humidified atmosphere enriched with 5% (v/v) CO_2.

Plasmids, siRNA, and Inhibitors

pTAT-cyclin D1 expression vector was obtained from Dr. B. Sola (EA4652, Université de Caen Normandie, Caen, France). The FLAG-Cyclin D1 vector was generated by cloning cyclin D1 cDNA into pcDNA3.1 using Kpn1 and EcoRI restriction enzymes. HA-OGT was obtained from Dr. T. Issad (Inserm, U1016, Institut Cochin, Paris, France), pCMV-Myc-Cyclin D was kindly provided by Dr. X. Ye (Institute of Microbiology, Chinese Academy of Sciences, Beijing, China) (40). The Ub-HA expression vector was a gift from Dr. C. Couturier (Institut Pasteur de Lille, U1177, Lille, France). Control siRNA (SIRNA UNIV NEGATIVE CONTROL 1, SIC001) and OGT siRNA (GGAGGCUAUUCGAAUCAGU[dT][dT] and ACUGAUUCGAAUAGCCU-CC[dT][dT]) were purchased from Sigma-Aldrich (La Verpillière, France) and siGENOME Human MGEA5 (10724) siRNA-SMARTpool was purchased from Dharmacon (GE Healthcare Europe GmbH, Velizy-Villacoublay).

The OGT inhibitor Acetyl-5S-GlcNAc (Ac-5S-G, 100 mM stock solution in DMSO) was a kind gift of Dr. G.W. Hart (The Johns Hopkins University School of Medicine, Baltimore, USA). The OGA inhibitor Thiamet G (ThG, 10 mM stock solution in DMSO) and cycloheximide (CHX, 5 mg/ml stock solution in DMSO) were from Sigma-Aldrich. The proteasome inhibitor MG132 (20 mM stock solution in DMSO) was purchased from Cayman Chemical (V.W.R., Fontenay-sous-Bois, France). For controls, vehicle (DMSO) was added at the same final dilution.

Antibodies

Antibodies against cyclin D1 (DCS-6, sc-20044; A12, sc-8396), HA-tag (sc-805), GAPDH (sc-47724), beta-actin (sc-1616) and normal rabbit or mouse IgG were from Santa Cruz (Heidelberg, Germany). Antibodies against FLAG-tag (M2) and OGT (Ti-14 and DM-17) were purchased from Sigma-Aldrich. Rabbit polyclonal anti-MGEA5 antibody (anti-OGA, EPR7154B) was from Abcam (Cambridge, United Kingdom). Anti-*O*-Linked N-Acetylglucosamine monoclonal antibody (RL2) was purchased

from Thermo Scientific (V.W.R.). Secondary rabbit or mouse IgG HRP-linked antibodies were from GE Healthcare (V.W.R.). Anti-rabbit IgG Alexa Fluor 488 and anti-mouse IgG Alexa Fluor 568 (ThermoScientific, Fisher Scientific, France) were used for immunofluorescence.

Transfection

HEK293T (40×10^3 cells per well in 12-wells plate; 8×10^5 cells per 100 mm-Petri dish) and HCT116 (8×10^5 cells per 100 mm-Petri dish) cells were grown for 24 h. Prior to transfection, plasmids were diluted in Ultra-MEM (Lonza, Ozyme) and mixed for 20 min with Lipofectamine 2000 (Life Technologies, Fisher Scientific, Illkirch, France), according to manufacturer's instructions. The DNA-lipid complex (500 ng DNA/well in 12-well plates, 1.25 μg of each vector for co-transfection or 2 μg DNA per 100 mm-dish for HEK293T) was added in fresh medium and transfected cells were analyzed 48 h later. The various treatments with the inhibitors were done as indicated in the text and figure legends. Reverse transfection of siRNA was performed in complete medium (2×10^5 or 3.75×10^5 cells in 6-well plates for HEK 293T and MCF7 cells respectively; 6×10^5 or 1×10^6 in 100-mm dishes for HEK 293T and MCF7 cells, respectively), as previously described (41). Transfected cells were harvested 72 h later.

Quantitative RT-PCR

RNA was isolated using Nucleospin® RNA mini spin kit (Macherey-Nagel) according to the manufacturer's instructions. 1 μg of total RNA was reverse transcribed using random primers and MultiScribe™ reverse transcriptase (Applied Biosystems). Real-time PCR analysis was performed by Power SYBR Green (Applied Biosystems) in a MX3005P fluorescence temperature cycler (Stratagene) according to the manufacturer's instructions. The sequences of the primers used for the RT-qPCR analyses were as follows: OGT forward 5′-TGG CTT CAG GAA GGC TAT TG-3′ and reverse 5′-CAA GTC TTT TGG ATG TTC ATA TG-3′; cyclin D1 forward 5′-CAT CTA CAC CGA CAA CTC CAT CC-3′ and reverse 5′-TGT TCA ATG AAA TCG TGC GG-3′; RPLP0 (ribosomal protein large subunit P0) forward 5′-GTG ATG TGC AGC TGA TCA AGA-3′ and reverse 5′-GAT GAC CAG CCC AAA GGA GA-3′.

Cell Treatment and Synchronization

HCT116 cells (40×10^3) and MCF7 cells (55×10^3) were cultured in 12-well plates for 2 days. Cells were treated overnight with Ac-5S-G (50 or 100 μM) or ThG (1 μM). Then CHX (50 μg/ml) or MG132 (20 μM) were used in time-course experiments. For serum starvation time-course experiments, OGT or OGA inhibitors were added in the complete medium 2 h before starvation and during serum starvation in serum-free medium.

Cell Cycle Analysis

Distribution of cells in G0/G1, S, and G2/M was determined by DNA staining with propidium iodide as previously described (33).

sWGA Lectin Affinity Chromatography

HCT116 cells and cyclin D1-FLAG-transfected HEK293 T cells were treated overnight with vehicle (DMSO) or ThG (1 μM) before lysis in RIPA (50 mM Tris pH 7.5, 150 mM NaCl, 1% NP-40, 0.25% sodium deoxycholate and 0.1% SDS). *O*-GlcNAc-modified proteins were enriched using the non-reducing terminal GlcNAc-specific lectin succinylated wheat germ agglutinin (sWGA) immobilized on agarose beads (Vector Laboratories, Clinisciences, Nanterre, France). Lysates (4 mg, 1 mg/ml) were incubated overnight at 4°C with 200 μl of sWGA-beads. Beads were centrifuged at 1,000 × g for 3 min, and then washed under vigorous stirring twice with 2 ml RIPA-0.1% SDS buffer and then three times with 2 ml RIPA-0.2% SDS buffer. Finally, beads were re-suspended in Laemmli buffer and stirred for 10 min using a vortex mixer before heating at 95°C for 7 min. Negative control was performed by adding 0.5 M free GlcNAc in the cell lysate before incubation with sWGA-beads**.** Eluted proteins were loaded on 10% SDS-PAGE to perform Western-blot analysis.

Enzymatic Labeling and Click Chemistry

Whole cell lysate of cyclin D1-FLAG-transfected HEK293 T cells (200 μg) and α-crystallin (20 μg) as positive control were processed using the click-It™ *O*-GlcNAc enzymatic labeling and click-It™ biotin glycoprotein D kits (Invitrogen, Thermo Fisher scientific), according to manufacturer's instruction. Enrichment of biotinylated proteins was performed as previously described (42).

Immunoprecipitation

Cells were rinsed twice in cold-PBS, then lysed on ice for 20 min in 400 μl RIPA buffer (without SDS for co-immunoprecipitation) supplemented with a protease inhibitor cocktail (Sigma-Aldrich), 10 mM Sodium Fluoride and 1 mM sodium orthovanadate. Cell extracts were centrifuged at 20,000 × g for 15 min at 4°C and supernatants were kept at −20°C. For immunoprecipitation, one mg of total proteins for transfected cells and 2 mg of total proteins for non-transfected cells (volume adjusted for a final concentration of 2 mg/ml) were pre-cleared with protein A/protein G-sepharose beads (20 μl/mg) (GE Healthcare, V.W.R.) for 1 h at 4°C. After centrifugation (1,200 × g, 5 min, 4°C), the supernatant was incubated overnight with the primary antibody (2 μg antibody per mg of protein) under gentle agitation. Protein A/G beads (30 μl/mg) were added for 1 h at 4°C before centrifugation and washes of the beads (three times in 1 ml RIPA and once in modified RIPA containing 450 mM NaCl, 5 min each). Beads were heated at 95°C for 7 min in 25 μl Laemmli buffer before SDS-PAGE.

Western Blot Analysis

Proteins were separated by SDS-PAGE and transferred onto nitrocellulose membrane (Hybond-C Extra, GE Healthcare) at 200 mA for 2 h. Membranes were blocked with 5% (w/v) nonfat dry milk in TBST (15 mM Tris pH 8, 140 mM NaCl, 0.05% (v/v) Tween-20) at room temperature (R.T.) for 45 min, then incubated overnight at 4°C with the primary antibody diluted in the blocking solution [1:1,000 except for anti-OGT and anti-GAPDH (1:2,000), anti-*O*-GlcNAc

(1:4,000) and anti-OGA (1:10,000)]. Membranes were washed with TBST (3 × 7 min) and incubated with secondary HRP-linked antibodies (1:15,000 in TBST) for 1 h at R.T. After three washes in TBST, detection was performed using chemiluminescence (ECL Prime, GE Healthcare; Supersignal West Femto Max., Thermo Scientific) on a CCD camera (Fusion Solo, Vilber Lourmat, France). Membranes were stripped in stripping buffer (ST010, GenBio, Euromedex, Souffelweyersheim, France) for 10 min and extensively washed in TBST before incubation with other antibodies. Quantification of protein expression levels was calculated by densitometry using the ImageJ® software. Student's *t*-test (Excel) was used for statistical analysis; *p*-values were calculated and reported accordingly ($^{*}p < 0.1$, $^{**}p < 0.05$, $^{***}p < 0.005$).

Indirect Immunofluorescence and Proximity Ligation Assay

Cells were grown in 6-well plates on glass coverslips (20×10^4 cells/well) for 2 days. Cells were then starved for 24 h (in DMEM or DMEM-0.5% (v/v) FCS for MCF7 cells) before serum stimulation for the indicated time periods. Immunofluorescence experiments were done as previously described (33). Briefly, after fixation of cells in 4% (w/v) PAF (30 min at R.T.) and permeabilization (0.5% Triton X-100 in PBS, 20 min at R.T.), coverslips were incubated with the blocking buffer containing 2% (v/v) FCS, 2% (w/v) bovine serum albumin, 0.2% (w/v) gelatin in PBS (1 h at R.T.) before incubation with primary antibodies against cyclin D1 (A12) and OGT (Ti-14) (1:100 in blocking buffer, overnight at 4°C) and Alexa Fluor conjugated secondary antibodies (1:600 in blocking buffer, 1 h at R.T). For the Proximity ligation assay (Duolink® *in situ* kit, Sigma-Aldrich), primary antibodies were incubated on fixed cells in the blocking buffer provided in the kit (1:100). Manufacturer's instructions were followed for the incubation with minus and plus probes, the ligation and amplification (120 min, 37°C) steps (Duolink® *in Situ* Detection Reagents Green, Sigma-Aldrich). After mounting coverslips in fluorescence mounting medium (DAKO, Agilent Technologies France, Les Ulis, France), images were acquired using an inverted Zeiss LSM700 confocal microscope with a 40x oil immersion lens at R.T. and data were collected with the ZEN 2010 software (Zeiss, Oberkochen, Germany). Images from PLA were processed with ImageJ® using a home-made plugin developed by TISBio to detect and quantify the nuclear fluorescent dots in labeled cells. Scatter dot plot (median with interquartile range) showing nuclear fluorescence intensity quantified in each cell (two captured images per condition) and statistical analysis were obtained using GraphPad Prism software (one-way ANOVA test, $^{***}p < 0.0001$, $^{**}p < 0.005$, $^{*}p < 0.05$).

RESULTS

Perturbation of *O*-GlcNAc Cycling Modifies the Half-Life of Cyclin D1

To examine the effect of perturbation of *O*-GlcNAc cycling on cyclin D1 expression, MCF7 cells were depleted of their OGT or OGA content by using small interfering RNA (siRNA) strategy. As previously reported, the level of cyclin D1 increased when OGA was silenced and, conversely, decreased when OGT was knocked-down (**Figure 1A**) (34, 38, 39). On the other hand, the mRNA levels of cyclin D1 did not change in OGT depleted condition (siOGT) compared with the control (siCtrl), while the OGT mRNA levels dramatically decreased in siOGT-treated cells (**Figure 1B**). This result demonstrates that the decrease of cyclin D1 protein level in siOGT cells did not result from a diminution of its transcription in MCF7 cells. Similar results were obtained when cyclin D1-FLAG was overexpressed in siOGT- or siOGA-treated HEK293T cells. The knock-down of OGT led to a 40%-decrease of cyclin D1-FLAG steady-state level, whereas elevation of *O*-GlcNAcylation in siOGA-treated cells led to a 30%-increase of the protein (**Figure 1C**). Lastly, when cyclin D1-FLAG was overexpressed in HEK293T cells with increasing amount of the plasmid encoding HA-OGT, we observed a positive correlation between the expression of HA-OGT and cyclin D1 protein levels (**Figure 1D**).

In proliferating cells, the level of cyclin D1 is tightly controlled by the balance between the increase of its expression induced by the activation of mitogenic signaling pathways and its ubiquitin-mediated degradation (2, 5). To monitor the effect of *O*-GlcNAc cycling impairment on cyclin D1 half-life, MCF7 cells were treated overnight with Acetyl-5S-GlcNAc (Ac-5S-G) or Thiamet G (ThG) to inhibit, respectively the OGT and OGA catalytic activities prior to treatment with the protein synthesis inhibitor CHX. Efficiency of OGT or OGA inhibition was confirmed by Western-blot analysis (**Figure 2A**). We observed a significant increase of *O*-GlcNAcylation in ThG-treated cells and conversely a strong decrease of *O*-GlcNAcylation levels in cells treated with Ac-5S-G (**Figure 2B**). We showed by Western blot that the time-dependent decrease of cyclin D1 level was slowed down by ThG treatment compared with control cells (**Figure 2A**): the half-life time of cyclin D1 was 30 min in control cells and reached 50 min in ThG treated cells (**Figure 2C**). In Ac-5S-G treated cells, the initial level of cyclin D1 was decreased by more than a half compared to control cells. However, the time-course degradation of cyclin D1 was slowed down, since 50% of cyclin D1 protein steady-state level was reached after 40 min of CHX treatment (**Figure 2C**).

Downregulation of cyclin D1 upon serum deprivation contributes to cell cycle exit (43). To test whether perturbation of *O*-GlcNAc cycling could affect the decrease of cyclin D1 level induced by serum starvation, HCT116 cells were treated by ThG or Ac-5S-G 2 h prior to serum starvation and cyclin D1 level was monitored by Western-Blot. Efficiency of inhibitors was monitored by Western-blot against *O*-GlcNAcylated proteins (**Figures 2D,E**). Upon mitogen withdrawal, cyclin D1 levels decreased in a time-dependent manner both in control and treated cells (**Figure 2D**). Four hours after serum starvation, we observed a 40% decrease of cyclin D1 level in control cells (**Figure 2F**). This decrease was less pronounced in ThG-treated cells in which a 30% decrease of cyclin D1 was observed 4 h following serum starvation. In contrast, reduction of *O*-GlcNAcylation by inhibiting OGT accelerated the degradation of cyclin D1 since 60% of the protein was lost after 4 h of starvation (**Figure 2F**). These results corroborate our previous

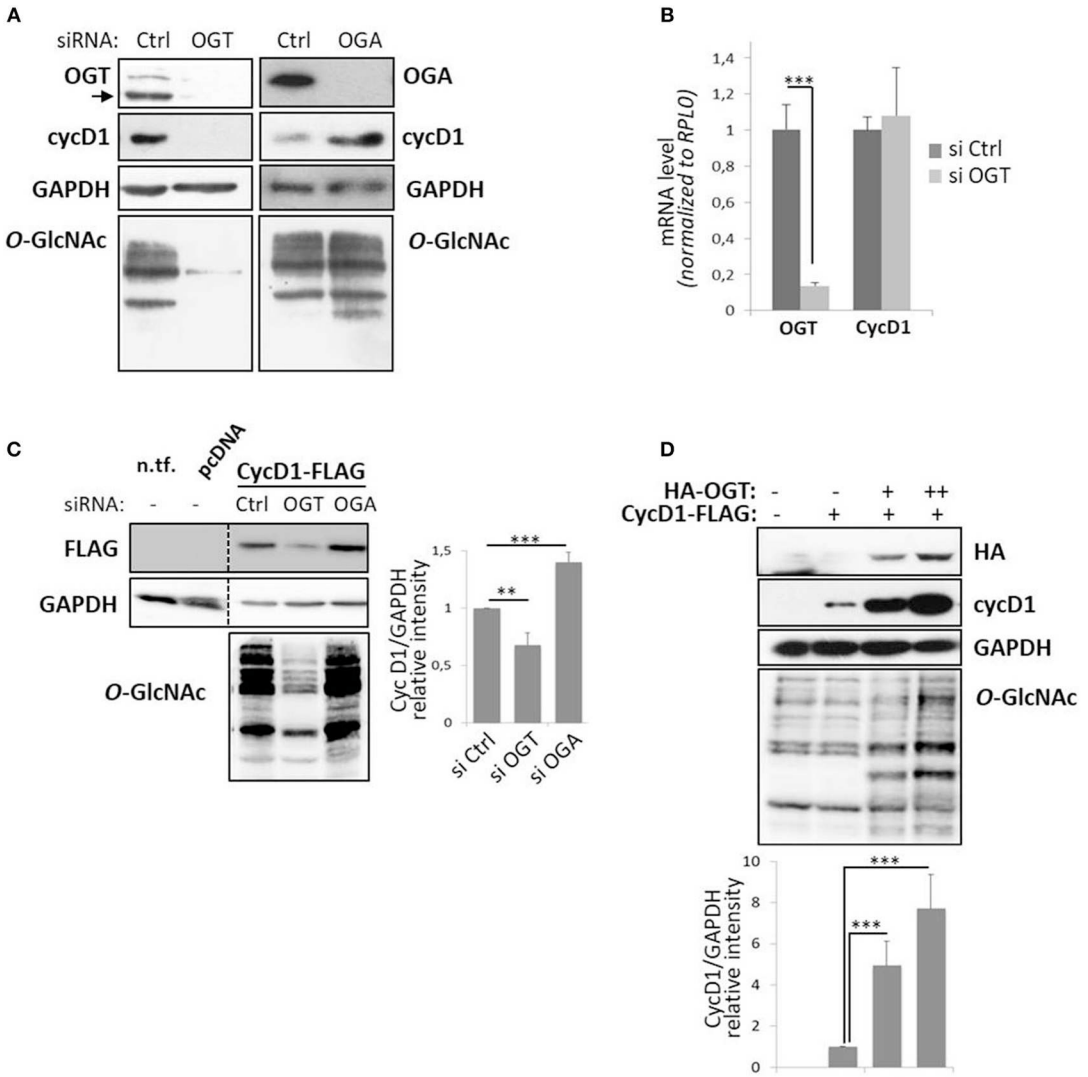

FIGURE 1 | Perturbation of *O*-GlcNAc cycling affects cyclin D1 protein expression level. MCF7 cells were transfected for 72 h with siRNA (Control (Ctrl), OGT, or OGA) and harvested to get protein lysates or mRNA samples. **(A)** Western-blotting analysis following siRNA show depletion of targeted proteins and *O*-GlcNAcylated proteins with concomitant variation in cyclin D1 (cycD1) level. **(B)** OGT and cycD1 mRNA levels were quantified by qPCR using RPLP0 as internal control. Results correspond to the mean value ± s.d. of three independent experiments (***$p < 0.005$). **(C)** HEK293T cells were seeded in 12-well plates with siRNA (Ctrl, OGT, or OGA) for 24 h and then transfected with pcDNA3.1 or CycD1-FLAG (100 ng). Cells were lysed 2 days later (three independent experiments). Lysate from non-transfected HEK293T cells (n.tf.) was also loaded on the same gel. **(D)** HEK293T cells were transfected in 12-well plates for 48 h with CycD1-FLAG (500 ng) and OGT-HA (500 ng or 1 μg) and then lysed in Laemmli buffer (two independent experiments). **(C,D)** The cellular lysates were analyzed by Western blot using specific antibodies. Histograms represent the relative intensity of cyclin D1 expression levels normalized to GAPDH levels. Statistical analyses were performed by Student's *t*-test (***$p < 0.005$, **$p < 0.05$).

observations regarding treatment of cells with CHX, and suggest that *O*-GlcNAc cycling participates in the regulation of cyclin D1 protein level.

OGT Interacts With and Glycosylates Cyclin D1

One of the well-established roles of OGT is to interact with and protect its targets from proteasomal degradation (44–48). To first examine whether OGT binds to cyclin D1, we performed co-immunoprecipitation experiments in HEK293T cells ectopically co-expressing cyclin D1-Myc and HA-OGT. As shown in **Figure 3A**, a band corresponding to OGT was detected in cyclin D1 co-immunoprecipitates when both plasmids were co-transfected in cells (IP cycD1, *lane 3*). Conversely, a small fraction of cyclin D1 was detected when OGT was immunoprecipitated (**Figure 3A**, IP OGT, *lane 1*). Cyclin D1 was undetectable in non-transfected cells although endogenous OGT was successfully immunoprecipitated (**Figure 3A**, IP OGT, *lane 2*). A specific band corresponding to OGA was detected after OGT immunoprecipitation (**Figure 3A**, IP OGT, *lanes 1- 2*) but

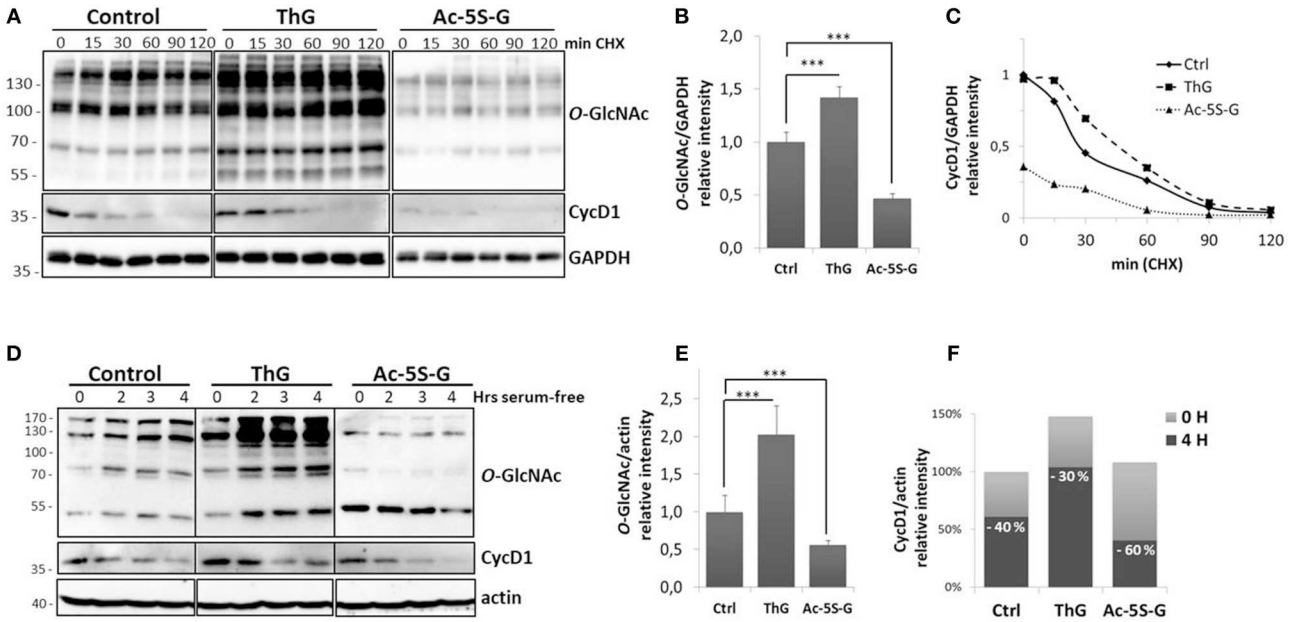

FIGURE 2 | Turnover of cyclin D1 is dependent to *O*-GlcNAc homeostasis. **(A–C)** MCF7 cells were treated overnight with Ac-5S-G (100 μM) or ThG (1 μM). Then CHX (50 μg/ml) was added into the medium before cell lysis at indicated times. **(A)**, Western-blots show the levels of *O*-GlcNAcylated proteins and cyclin D1. GAPDH served as a control for equal loading. **(B)** The histogram represents the relative quantification of *O*-GlcNAc levels in treated cells compared with control cells. **(C)** Graph shows the ratios of cyclin D1 to GAPDH. Representative results of three independent experiments. **(D–F)** HCT116 cells were pretreated 2 h with vehicle (DMSO, Control), ThG (1 μM), or Ac-5S-G (50 μM). Cells were starved in serum-free medium for the indicated times prior to cell lysis. **(D)** Western-blot show the levels of *O*-GlcNAcylated proteins and cyclin D1. Actin served as a control for equal loading. **(E)** The histogram represents the relative quantification of *O*-GlcNAc levels in treated cells compared with control cells. **(F)** The histogram represents the relative intensity of cyclin D1 levels normalized to actin levels (100% is the normalized level of cyclin D1 in the control cells at T0). On each histogram, the percentage of the decrease of cyclin D1 level after 4 h of serum starvation is indicated. Results are representative of two independent experiments. Statistical analysis in (**B**,**E)** was performed by Student's *t*-test (***$p < 0.005$).

not after cyclin D1 immunoprecipitation where we observed the same 130 kDa-band in the IgG negative control (**Figure 3A**, IP cycD1, *lanes 2-4*). This result suggests that cyclin D1 may directly interact with OGT, whereas OGA is present in the complex through its tight interaction with OGT, as previously described (49). We performed the same set of experiments on endogenous OGT and cyclin D1 proteins in HCT116 cells, confirming that both proteins can interact (**Figure 3B**). Treatment of HCT116 cells with ThG did not change the co-immunoprecipitation of cyclin D1 and OGT.

To further characterize cyclin D1/OGT interaction, we performed *in situ* PLA experiments. This approach allows gaining in sensitivity thanks to the ligation and amplification steps. For this purpose, serum-starved quiescent MCF7 cells (T0) were stimulated by addition of serum to re-enter the cell cycle. Cells were fixed in G1 phase (6 h), S phase entry (15 h) and S phase (21 h), as attested by flow cytometry (**Figure 3C**). First, indirect immunofluorescence experiments in synchronized MCF7 cells confirmed that cyclin D1 is translocated to the nucleus upon cell cycle entry, whereas OGT is detected in both the cytoplasm and the nucleus (**Figure 3D**). The PLA signal revealed that cyclin D1/OGT interaction was detectable in quiescent cells, both in the cytoplasm and the nucleus. The intensity of the PLA signal increased in the nucleus as cells progressed through G1 and entered S phase, and then slightly decreased when cells progressed through S phase (**Figure 3E**). Our data indicate that OGT and cyclin D1 are likely to interact in both compartments, but this interaction is mostly detected in the nucleus of G1-cells, concomitantly to the activation and nuclear translocation of cyclin D1 upon serum stimulation.

We next investigated whether cyclin D1 is a direct target or not of OGT by using several experimental approaches. *In situ* PLA is widely used to study protein-protein interaction, but is also used for detecting co-/post-translational modifications such as phosphorylation and glycosylation (50, 51). Here we performed PLA using antibodies against cyclin D1 and *O*-GlcNAcylated proteins (RL2). As shown in **Figure 4A**, fluorescent PLA spots were visible in the cytoplasm and nucleus of asynchronous MCF7 cells, albeit at higher intensity in cytoplasm, suggesting that cyclin D1 was potentially *O*-GlcNAcylated in both compartments. However, since we cannot exclude that our PLA results could reflect the interaction of cyclin D1 with *O*-GlcNAcylated partners, we used biochemical approaches to ascertain the *O*-GlcNAcylation of cyclin D1. We first performed a succinyl-WGA affinity chromatography to enrich *O*-GlcNAcylated proteins from MCF7 cells and cyclin D1-FLAG transfected HEK293T cells (**Figure 4B**). As observed by Western blot analysis, a small part of endogenous cyclin D1 and overexpressed cyclin D1-FLAG

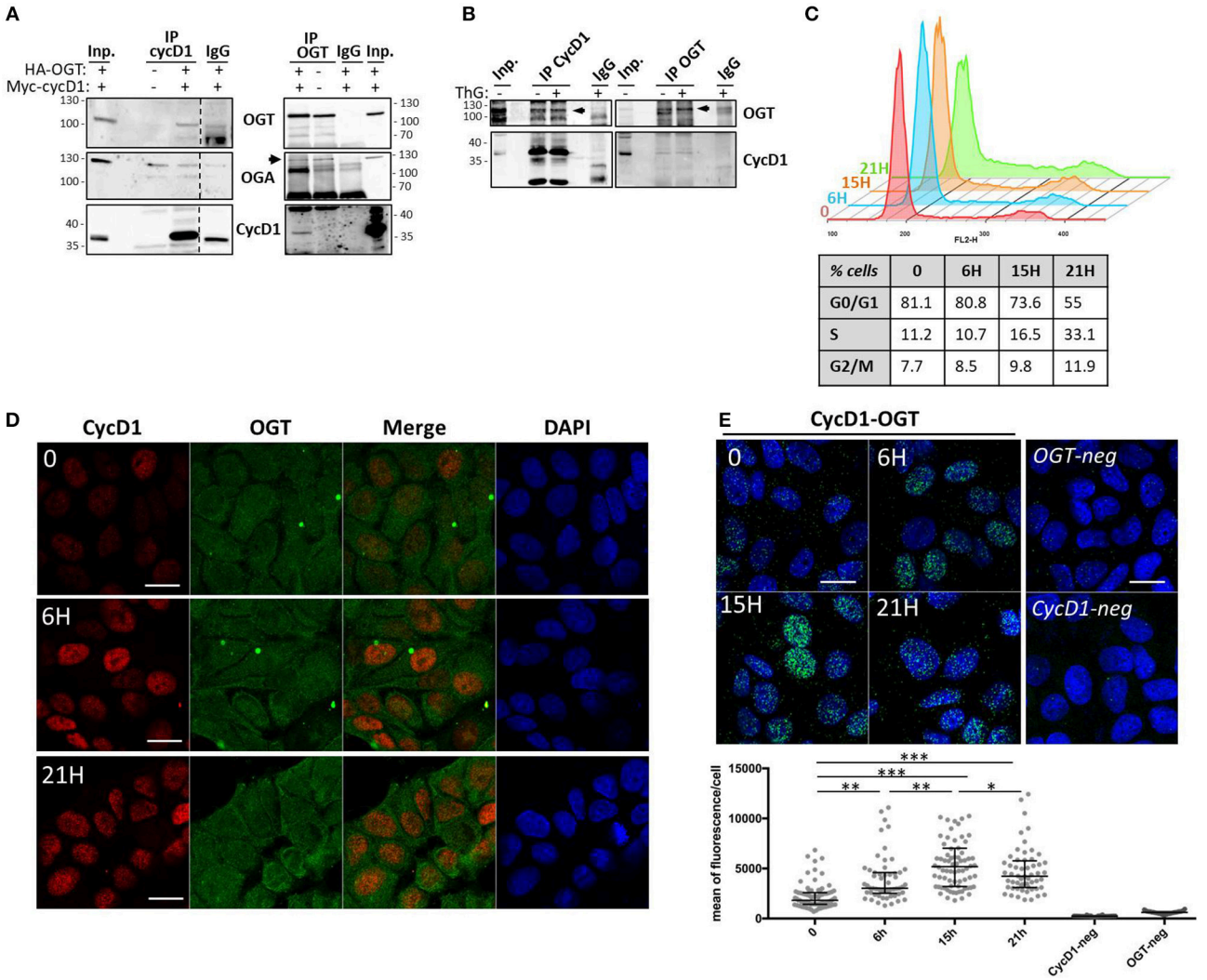

FIGURE 3 | OGT interacts with cyclin D1. **(A)** HEK293T cells were co-transfected with HA-OGT and Myc-cyclin D1 plasmids for 48 h before cell lysis. Cyclin D1 and OGT were immunoprecipitated and Western-blot analysis were performed to detect OGT, OGA and cyclin D1. Negative controls of IP were done using non-relevant IgG (IgG). **(B)** HCT116 cells were treated overnight with DMSO (-) or ThG (1 μM) (+) before cell lysis in RIPA buffer and immunoprecipitation of endogenous cyclin D1 and OGT. Western-blot analysis of immunoprecipitates (IP) and Input (Inp.) using OGT and cycD1 antibodies. **(C–E)** Quiescent MCF7 cells (0) were stimulated with serum for the indicated times. **(C)** Cell cycle profile was monitored by flow cytometry after staining with propidium iodide. The percentage of cells in each phase is reported, according to serum release for each time point. **(D)** Cyclin D1 and OGT were detected in synchronized MCF7 cells by confocal indirect immunofluorescence using specific antibodies. Nuclei were counterstained with DAPI. Scale bar, 20 μM. **(E)** The interaction between OGT and cyclin D1 was detected using *in situ* PLA and immunofluorescent confocal microscopy. Nuclei were stained with DAPI. Pictures are the merge of PLA signal (AlexaFluo488) and DAPI channels. Quantification of PLA is presented as scatter dot plot; each dot represents the mean of PLA fluorescence intensity in the nucleus of a single cell. Bars represents the median with interquartile range for each experience (one-way ANOVA test, $^{***}p < 0.0001$, $^{**}p < 0.005$, $^{*}p < 0.05$). Scale bar, 20 μM.

was detected on sWGA-agarose beads in a specific manner (*lane sWGA*) since signals were abrogated when sWGA-beads were incubated with excess of free GlcNAc (**Figure 4B**). ThG treatment slightly increased the binding of cyclin D1-FLAG on sWGA-agarose beads, which may reflect the moderate increase of cyclin D1-FLAG protein level observed in ThG-treated cells compared with non-treated cells (*Input*, **Figure 4B**). We also performed the enzymatic labeling of *O*-GlcNAc proteins with UDP-GalNAz, followed with the click chemistry reaction using a biotin-alkyne probe as previously described (42). Negative controls were done by omitting either the two compounds, or only the biotin-alkyne probe; α-crystallin served as positive control. Biotinylated proteins were either loaded directly onto the gel (*Input* samples, 5% of the volume,) or enriched on avidin-agarose beads before SDS-PAGE (*Avidin-bound* samples). As shown by Western blot, cyclin D1 was detected in all the inputs although the signal is lower in lane 3 (**Figure 4C**, *Input*). It might be due to a reduction of the ligated biotin epitope accessibility by the cyclin D1 antibody compared to non-modified cyclin D1 in lanes 1 and 2. When biotinylated proteins were eluted from

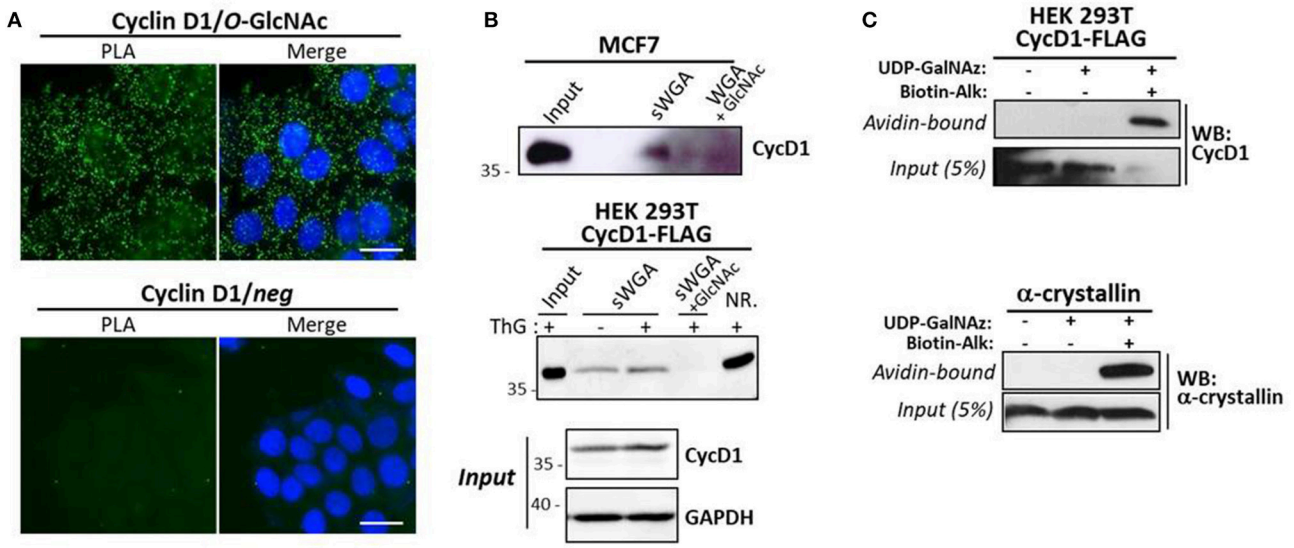

FIGURE 4 | Cyclin D1 is *O*-GlcNAcylated. **(A)** *in situ* PLA experiments by using anti-cyclin D1 and anti-O-GlcNAc (RL2) antibodies on asynchronous MCF7 cells. Nuclei were stained with DAPI. PLA signal was detected by immunofluorescent confocal microscopy. Scale bar, 20 μM. **(B)** MCF7 cells were treated with MG132 (4 μM) for 2 h prior cell lysis. Cyc D1-FLAG transfected HEK293T cells were treated overnight or not with ThG (1 μM) and lysed in RIPA buffer. *O*-GlcNAcylated proteins were enriched on sWGA-agarose beads. Incubation of sWGA beads with 0.5 M GlcNAc was done as a negative control. sWGA-bound Cyclin D1 was detected by Western-blot after lectin affinity chromatography (Input, 30 μg; NR., not retained, 30 μg). **(C)** Enrichment of biotinylated proteins from CycD1-FLAG transfected HEK293T cells or purified α-crystallin after enzymatic labeling with UDP-GalNAz and click chemistry reaction using a biotin-alkyne probe. Cyclin D1 and α-crystallin were revealed by Western-Blot on avidin-bound protein fraction and Input.

avidin beads, cyclin D1 was detected only in the sample in which both UDP-GalNAz and the biotin-alkyne probe were added for the click reaction, as we observed for α-crystallin. This indicates that cyclin D1 bears *O*-GlcNAc residues that could have been modified by click chemistry (**Figure 4C**). Of note, we added the denaturing detergent SDS in the lysis and washing buffers for the sWGA enrichment (0.2% SDS) and click chemistry (up to 1% SDS) experiments; the use of this stringent condition indicates that binding of cyclin D1 on lectin agarose-beads and avidin beads is rather hard suggesting a direct interaction through *O*-GlcNAcylated forms of the cyclin. Altogether our results show that cyclin D1 is *O*-GlcNAcylated in human cells, albeit at a very low extent.

Elevation of *O*-GlcNAcylation Decreases Cyclin D1 Ubiquitination

As the protein level of cyclin D1 in proliferating cells is highly controlled by ubiquitination and since elevation of *O*-GlcNAcylation induced by OGA inhibition (ThG) or knockdown (siOGA) increases the steady-state level of cyclin D1 (**Figures 1**, **2**), we examined the ubiquitination of cyclin D1 in presence of ThG. Cyclin D1-FLAG was ectopically expressed in HEK293T cells which were co-transfected with Ubiquitin-HA. Cyclin D1 was then immunoprecipitated in conditions of proteasome inhibition by using MG132. The ubiquitinated forms of cyclin D1 were detected by Western blot after immunoprecipitation of the cyclin. *O*-GlcNAcylation has been reported to directly modulate the proteasome activity (46, 52). Therefore, we first measured the global pattern of ubiquitinated proteins with or without ThG treatment. As shown in **Figure 5A**, efficiency of MG132 was attested by the increase in the amount of ubiquitinated proteins in a time-dependent manner in both conditions, and ThG treatment slightly increased the ubiquitination of proteins after 30 min of MG132, compared to control condition. However, this subtle difference was not statistically significant after 90 min of MG132 addition (**Figures 5A,B**). We also observed an increase of cyclin D1-FLAG levels in ThG-treated cells (**Figure 5A**), in agreement with our previous results (**Figures 1**, **2**). In contrast, upon MG132 addition, ubiquitination of immunoprecipitated cyclin D1 was reduced by around 30% when cells were treated overnight with ThG, compared with control cells (**Figures 5C,D**). This result suggests that elevation of *O*-GlcNAc levels may protect cyclin D1 from proteasomal degradation, thus stabilizing cyclin D1 in proliferating cells.

DISCUSSION

In quiescent and cycling cells, cyclin D1 levels are regulated both at the transcriptional and post-translational levels in order to finely regulate cell cycle progression (1, 2). We and others have previously shown that cyclin D1 level was impaired in cells in which the dynamics of *O*-GlcNAcylation was disrupted (31, 34, 38, 39). Here, we further investigate the link between *O*-GlcNAc homeostasis and cyclin D1 expression. We show that cyclin D1 levels are positively regulated by *O*-GlcNAcylation (**Figure 1**). Elevation of *O*-GlcNAcylation through silencing of OGA or overexpression of OGT increases cyclin D1 steady-state levels.

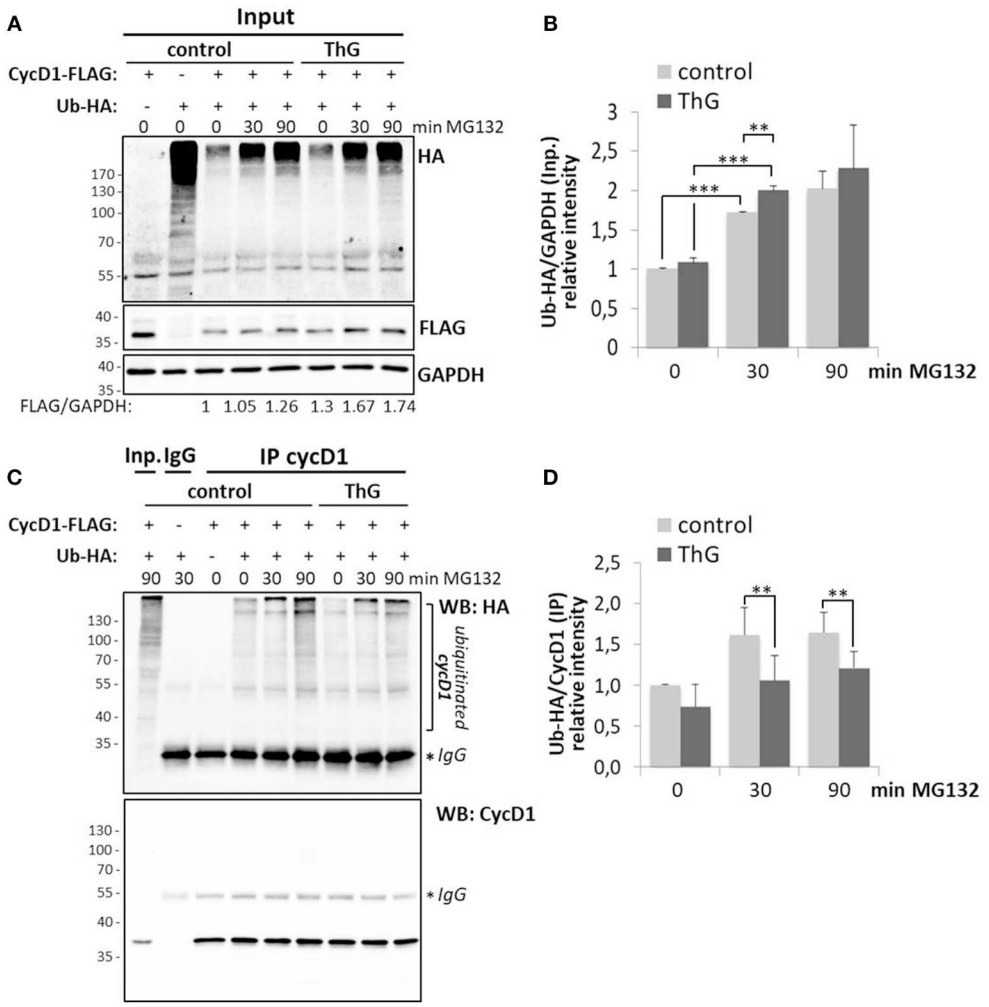

FIGURE 5 | Elevation of *O*-GlcNAc levels decreases ubiquitination of cyclin D1. HEK 293T cells were transfected for 48 h with CycD1-FLAG and Ub-HA plasmids and treated or not with ThG (1 μM) overnight. MG132 (20 μM) was then added into the medium for the indicated times before cell lysis. **(A)** Input (30 μg) were revealed using anti-HA (Ub) and anti-FLAG antibodies. GAPDH was used as a loading control. **(B)** The relative ratios of ubiquitin to GAPDH levels were calculated by densitometry using Image J software (mean ± s.d., two independent experiments). **(C)** CycD1 was immunoprecipitated and Western-blot was revealed using anti-HA (Ub) and anti-CycD1 antibodies. **(D)** The ratios of the ubiquitinated cycD1 levels were calculated by densitometry using Image J® software (mean ± s.d., three independent experiments). Statistical analysis was performed by Student's *t*-test (**$p < 0.05$, ***$p < 0.005$).

Conversely, decrease of *O*-GlcNAcylation by downregulation of OGT strongly reduces cyclin D1 protein level, independently of its mRNA levels (**Figure 1**), indicating that the regulation of cyclin D1 by *O*-GlcNAcylation is unlikely to occur at a transcriptional level. Therefore, we next examined whether dynamics of *O*-GlcNAc could regulate the degradation rate of cyclin D1. Cyclin D1 is a highly labile protein whose degradation is mainly driven by the ubiquitin-dependent proteasomal pathway (2, 8, 9, 15, 17–19). We hypothesized that increase of *O*-GlcNAcylation stabilizes cyclin D1 by interfering with its degradation. We examined the decline of cyclin D1 protein levels either by blocking protein synthesis by CHX or upon serum starvation, in high or low *O*-GlcNAc conditions. We show that increase of *O*-GlcNAc levels by OGA inhibition tends to delay the degradation rate of cyclin D1 in both experiments, while decreasing *O*-GlcNAcylation tends to accelerate it following mitogen deprivation (**Figure 2**). Once exported in the cytoplasm, cyclin D1 is polyubiquitinated prior to proteasomal degradation (9, 13, 14). We then determined if the stabilizing effect of ThG on cyclin D1 protein level was a consequence to a reduction of its ubiquitination. Our results confirmed that increasing *O*-GlcNAc levels reduces the accumulation of polyubiquitinated cyclin D1 (**Figure 5**). All these results taken together indicate that *O*-GlcNAcylation is able to slow down the ubiquitination of cyclin D1, which consequently delays its proteasomal proteolysis and reduces its turnover.

Several proteins harboring a short half-life are protected by *O*-GlcNAcylation, as described for p53, β-catenin and FOXM1 (44–48). Therefore, we investigated whether homeostasis of

O-GlcNAcylation could regulate cyclin D1 turnover through a direct effect of OGT on the cyclin. Our results show for the first time that cyclin D1 binds to and is glycosylated by OGT. Indeed co-immunoprecipitation and PLA experiments highlight that cyclin D1 interacts with OGT in three different human cell lines (MCF7, HCT116, and HEK293T) (**Figure 3**). Our data strengthen the large-scale analysis of cyclin D1 interactome, in which OGT belongs to the top 30 cyclin D1-interacting proteins in MCF7 cells (53). During G1 to S phase progression, OGT is widely detected in the cytoplasm and nucleus, while as expected, cyclin D1 staining is mostly nuclear (**Figure 3D**). Indeed, upon mitogenic stimulation, cyclin D1 is rapidly transported into the nucleus together with its catalytic subunits CDK4/CDK6 (1, 6). PLA results indicate that the interaction between OGT and cyclin D1 can occur in both the cytoplasmic and nuclear compartments but is mainly detected in the nucleus of synchronized cycling cells (**Figure 3E**), suggesting that OGT is a new partner of the cyclin D1-CDK complex. Our study also unveils the potential *O*-GlcNAcylation of cyclin D1. Indeed, cyclin D1 was detected by Western blot following enrichment of *O*-GlcNAcylated proteins using either sWGA lectin-agarose beads or a click chemistry-based strategy (**Figures 4B,C**). *In situ* Duolink experiments using cyclin D1 and *O*-GlcNAc antibodies corroborate our findings (**Figure 4A**). However, it is unlikely that all the fluorescent spots detected by PLA are related to the *O*-GlcNAcylated forms of cyclin D1 since *O*-GlcNAcylation of cyclin D1 appears to occur at a low stoichiometry (**Figures 4B,C**). Given that cyclin D1 is mostly detected in the nucleus (**Figure 3D**), and that cyclin D1 and OGT preferentially interact in this compartment (**Figure 3E**), we hypothesize that OGT glycosylates the cyclin in the nucleus, which corresponds to a few nuclear spots that we observe by PLA (**Figure 4A**). The high PLA signal in the cytoplasm could arise from the binding of cyclin D1 to other potentially *O*-GlcNAcylated proteins with which the cyclin interacts (53). The chaperone Hsc70 could also be a good candidate, since it is highly *O*-GlcNAcylated (54) and promotes the stabilization of newly synthesized cyclin D1 (55). Thus, besides phosphorylation and ubiquitination, *O*-GlcNAcylation appears as an additional mean to finely regulate cyclin D1 turnover.

The effect of *O*-GlcNAcylation on cyclin D1 expression is in agreement with previous works showing that *O*-GlcNAcylation favors the stability of target proteins through the direct inhibition of their proteasomal degradation. *O*-GlcNAc modification can compete with a phosphorylation site that triggers ubiquitination, as previously shown for Ser10 of the transcription factor δ-lactoferrin (27) and Thr41 of β-catenin (47). One of our hypotheses is that OGT might directly impede phosphorylation at Thr286 by occupation of the residue by *O*-GlcNAc. The increase of *O*-GlcNAcylation could help in stabilizing cyclin D1 through a decrease of its GSK-3β-mediated phosphorylation at Thr286 which promotes its ubiquitin-mediated degradation (8, 9). *O*-GlcNAcylation can also compete with an adjacent phosphorylation site which promotes ubiquitination, as demonstrated for the tumor suppressor p53 for which *O*-GlcNAcylation at Ser149 impairs phosphorylation at Thr155 (44). Nine phosphorylation sites have been mapped on human cyclin D1 (Ser90, Ser111, Ser131, Ser197, Ser219, Tyr226, Ser234, Thr286, Thr288; see references in www.phosphosite.org, accession number P24385), but to date only Thr286 and Thr288 residues are known to have a biological effect once phosphorylated, both promoting the proteasomal degradation of cyclin D1 (8, 11, 12). Regarding the ubiquitination sites, over the 10 lysine residues that have been mapped on cyclin D1 (Lys 33, 46, 50, 95, 96, 114, 167, 175, 238, 269; see references in www.phosphosite.org), only Lys269 has been shown to be essential for ubiquitination and subsequent proteolysis of cyclin D1 (15). More experiments for mapping the *O*-GlcNAc site(s) of cyclin D1 are needed to further decipher whether *O*-GlcNAcylation of cyclin D1 competes or not with the phosphorylation or ubiquitination sites of cyclin D1, and thus helps in stabilizing the cyclin.

Other possible mechanism by which OGT may control cyclin D1 turnover is through the *O*-GlcNAcylation of GSK-3β since the kinase is itself *O*-GlcNAcylated (48, 56, 57). The negative regulation of GSK-3β activity by *O*-GlcNAcylation has been shown in HEK293FT cells and MKN45 gastric cancer cells but appears to be cell type-dependent (48, 56). Thiamet G-induced high *O*-GlcNAcylation of GSK3β might contribute to the decrease of cyclin D1 ubiquitination that we report in this study, as a consequence of a decrease in Thr286 phosphorylation. *O*-GlcNAcylation of GSK3β might also impair the activity of Fbxo4, the E3 ubiquitin ligase F-Box subunit which controls the proteasomal degradation of cyclin D1 (21). Indeed, the phosphorylation of Fbxo4 by GSK3β is necessary for its ubiquitin ligase activity (58). To ascertain these hypotheses, further experiments are needed to determine whether sustained *O*-GlcNAcylation of GSK-3β could be involved in the increase of cyclin D1 stability in MCF7 and HCT116 cancer cells, as shown for FoxM1 in gastric cancer cells (48).

On the other hand, OGT could modulate the ubiquitination of cyclin D1 by another ways. *O*-GlcNAc modification has been shown to directly regulate the proteasome activity. Several subunits of the proteasome are indeed *O*-GlcNAcylated (46) and it has been demonstrated that *O*-GlcNAcylation of Rpt2 ATPase in the 19S regulatory particle inhibits the proteolytic activity on some target proteins (52). Therefore, we cannot exclude the possibility that the decrease in cyclin D1 ubiquitination in ThG-treated cells results from a global inhibition of proteasome activity. More recently, fine regulation of the ubiquitin system by OGT has been evidenced. For example, the *O*-GlcNAcylation of the transcriptional cofactor YAP prevents its interaction with the E3 ubiquitin ligase subunit β-TRCP, thus decreasing its degradation (59). Conversely, *O*-GlcNAcylation of the transcriptional regulator PGC1α facilitates the binding of the deubiquitinase BAP1 to PGC1α, leading thus to its stabilization by blocking its ubiquitination (45). The SCF ubiquitin ligase is responsible for the polyubiquitination of cyclin D1. Different F-Box proteins are able to recognize cyclin D1, including Fbxo4, Fbxw8, Fbxo31, and Skp2 (13–16, 60). Cyclin D1 ubiquitination is reversed by the deubiquitinases USP2 and USP22 (17,

18). By using co-immunoprecipitation approaches, we tried to determine whether elevation of *O*-GlcNAcylation favors the binding of USP2 to cyclin D1, as described for BAP1 and PGC1α (45). Unfortunately, we could not conclude because we failed to detect the interaction of both proteins in HCT116 cells (data not shown), although it was previously reported in these cells (17). The potential regulation by OGT of either the ubiquitin ligases or deubiquitinases that control cyclin D1 turnover might also explain how *O*-GlcNAc modification takes part in cyclin D1 homeostasis. Future work would decipher the exact molecular mechanisms underlying the modulation of cyclin D1 ubiquitination by OGT.

To conclude, this study provides new insights into the positive regulation of cyclin D1 stability by *O*-GlcNAcylation and opens new perspectives on the contribution of hyper-*O*-GlcNAcylation to the deregulation of cell proliferation in cancer.

AUTHOR CONTRIBUTIONS

LM, VD, TL, and A-SV-E: designed the experiments; LM, VD, MM, CS, ML, and A-SV-E: performed the experiments; LM, VD, and A-SV-E: analyzed the data; A-SV-E: wrote the manuscript; LM, VD, and TL: edited the manuscript. All the authors approved the manuscript.

ACKNOWLEDGMENTS

We thank B. Sola, T. Issad, X. Ye, and C. Couturier for providing us the plasmids. We are also grateful to G.W. Hart for the pharmacological inhibitor of OGT. Confocal microscopy analysis was performed on the BiCeL (BioImaging Center Lille) core facility (Campus cité scientifique, Univ. Lille). This work was supported by la Ligue Nationale Contre le Cancer (Comités du Nord et de l'Aisne) and the Centre National de la Recherche Scientifique (CNRS).

REFERENCES

1. Massagué J. G1 cell-cycle control and cancer. *Nature* (2004) 432:298–306. doi: 10.1038/nature03094
2. Qie S, Diehl JA. Cyclin D1, cancer progression, and opportunities in cancer treatment. *J Mol Med.* (2016) 94:1313–26. doi: 10.1007/s00109-016-1475-3
3. Lavoie JN, L'Allemain G, Brunet A, Müller R, Pouysségur J. Cyclin D1 expression is regulated positively by the p42/p44MAPK and negatively by the p38/HOGMAPK pathway. *J Biol Chem.* (1996) 271:20608–16.
4. Aktas H, Cai H, and Cooper GM. Ras links growth factor signaling to the cell cycle machinery via regulation of cyclin D1 and the cdk inhibitor p27 Kip1. *Mol Cell Biol.* (1997) 17: 3850–57. doi: 10.1128/MCB.17.7.3850
5. Muise-Helmericks RC, Grimes HL, Bellacosa A, Malstrom SE, Tsichlis PN, Rosen N. Cyclin D expression is controlled post-transcriptionally via a phosphatidylinositol 3-kinase/Akt-dependent pathway. *J Biol Chem.* (1998) 273:29864–72. doi: 10.1074/jbc.273.45.29864
6. Baldin V, Lukas J, Marcote MJ, Pagano M, Draetta G. Cyclin D1 is a nuclear protein required for cell cycle progression in G1. *Genes Dev.* (1993) 7:812–21. doi: 10.1101/gad.7.5.812
7. Chen H, Xu X, Wang G, Zhang B, Wang G, Xin G, et al. CDK4 protein is degraded by anaphase-promoting complex/cyclosome in mitosis and reaccumulates in early G1 phase to initiate a new cell cycle in HeLa cells. *J Biol Chem.* (2017) 292:10131–41. doi: 10.1074/jbc.M116.773226.
8. Diehl JA, Zindy F, Sherr CJ. Inhibition of cyclin D1 phosphorylation on threonine-286 prevents its rapid degradation via the ubiquitin-proteasome pathway. *Genes Dev.* (1997) 11:957–72. doi: 10.1101/gad.11.8.957
9. Guo Y, Yang K, Harwalkar J, Nye JM, Mason DR, Garrett MD, et al. Phosphorylation of cyclin D1 at Thr 286 during S phase leads to its proteasomal degradation and allows efficient DNA synthesis *Oncogene* (2005) 24:2599–612. doi: 10.1038/sj.onc.1208326
10. Alt JR, Cleveland JL, Hannink M, Diehl JA. Phosphorylation-dependent regulation of cyclin D1 nuclear export and cyclin D1-dependent cellular transformation. *Genes Dev.* (2000) 14: 3102–14. doi: 10.1101/gad.854900
11. Benzeno S, Diehl JA. C-terminal sequences direct cyclin D1-CRM1 binding. *J Biol Chem.* (2004) 279:56061–6. doi: 10.1074/jbc.M411910200
12. Zou Y, Ewton DZ, Deng X, Mercer SE, Friedman E. Mirk/dyrk1B kinase destabilizes cyclin D1 by phosphorylation at threonine 288. *J Biol Chem.* (2004) 279:27790–8. doi: 10.1074/jbc.M403042200
13. Lin DI, Barbash O, Kumar KG, Weber JD, Harper JW, Klein-Szanto AJ, et al. Phosphorylation-dependent ubiquitination of cyclin D1 by the SCF(FBX4-alphaB crystallin) complex. *Mol Cell.* (2006) 24:355–66. doi: 10.1016/j.molcel.2006.09.007
14. Okabe H, Lee SH, Phuchareon J, Albertson DG, McCormick F, Tetsu O. A critical role for FBXW8 and MAPK in cyclin D1 degradation and cancer cell proliferation. *PLoS ONE* (2006) 1:e128. doi: 10.1371/journal.pone.0000128
15. Barbash O, Egan E, Pontano LL, Kosak J, Diehl JA. Lysine 269 is essential for cyclin D1 ubiquitylation by the SCF(Fbx4/alphaB-crystallin) ligase and subsequent proteasome-dependent degradation. *Oncogene* (2009) 28:4317–25. doi: 10.1038/onc.2009.287.
16. Kanie T, Onoyama I, Matsumoto A, Yamada M, Nakatsumi H, Tateishi Y, et al. Genetic reevaluation of the role of F-box proteins in cyclin D1 degradation. *Mol Cell Biol.* (2012) 32:590–605. doi: 10.1128/MCB.06570-11.
17. Shan J, Zhao W, Gu W. Suppression of cancer cell growth by promoting cyclin D1 degradation. *Mol Cell.* (2009) 36:469–76. doi: 10.1016/j.molcel.2009.10.018
18. Gennaro VJ, Stanek TJ, Peck AR, Sun Y, Wang F, Qie S, et al. Control of CCND1 ubiquitylation by the catalytic SAGA subunit USP22 is essential for cell cycle progression through G1 in cancer cells. *Proc Natl Acad Sci USA.* (2018) 115:E9298–307. doi: 10.1073/pnas.1807704115
19. Davis MI, Pragani R, Fox JT, Shen M, Parmar K, Gaudiano EF, et al. Small molecule inhibition of the ubiquitin-specific protease USP2 accelerates cyclin D1 degradation and leads to cell cycle arrest in colorectal cancer and mantle cell lymphoma models. *J Biol Chem.* 2016 291:24628–40. doi: 10.1074/jbc.M116.738567
20. Lu F, Gladden AB, Diehl JA. An alternatively spliced cyclin D1 isoform, cyclin D1b, is a nuclear oncogene. *Cancer Res.* (2003) 63: 7056–61.
21. Barbash O, Zamfirova P, Lin DI, Chen X, Yang K, Nakagawa H, et al. Mutations in Fbx4 inhibit dimerization of the SCF(Fbx4) ligase and contribute to cyclin D1 overexpression in human cancer. *Cancer Cell* (2008) 14:68–78. doi: 10.1016/j.ccr.2008.05.017
22. Tan EP, Duncan FE, Slawson C. The sweet side of the cell cycle. *Biochem Soc Trans.* (2017) 45:313–22. doi: 10.1042/BST20160145
23. Bond MR, Hanover JA. *O*-GlcNAc cycling: a link between metabolism and chronic disease. *Annu Rev Nutr.* (2013) 33:205–29. doi: 10.1146/annurev-nutr-071812-161240.
24. Hardivillé S, Hart GW. Nutrient regulation of signaling, transcription, and cell physiology by O-GlcNAcylation. *Cell Metab.* (2014) 20:208–13. doi: 10.1016/j.cmet.2014.07.014
25. Nagel AK, Ball LE. Intracellular protein O-GlcNAc modification integrates nutrient status with transcriptional and metabolic regulation. *Adv Cancer Res.* (2015) 126:137–66. doi: 10.1016/bs.acr.2014.12.003
26. Chou TY, Hart GW, Dang CV. c-Myc is glycosylated at threonine 58, a known phosphorylation site and a mutational hot spot in lymphomas. *J Biol Chem.* (1995) 270:18961–5. doi: 10.1074/jbc.270.32.18961
27. Hardivillé S, Hoedt E, Mariller C, Benaïssa M, Pierce A. O-GlcNAcylation/phosphorylation cycling at Ser10 controls both transcriptional

activity and stability of delta-lactoferrin. *J Biol Chem.* (2010) 285:19205–18. doi: 10.1074/jbc.M109.080572
28. Luo B, Soesanto Y, McClain DA. Protein modification by O-Linked GlcNAc reduces angiogenesis by inhibiting Akt activity in endothelial cells. *Arterioscler Thromb Vasc Biol.* (2008) 28:651–7. doi: 10.1161/ATVBAHA.107.159533
29. Ferrer CM, Sodi VL, Reginato MJ. O-GlcNAcylation in Cancer biology: linking metabolism and signaling. *J Mol Biol.* (2016) 428:3282–94. doi: 10.1016/j.jmb.2016.05.028
30. Chiaradonna F, Ricciardiello F, Palorini R. The nutrient-sensing hexosamine biosynthetic pathway as the hub of cancer metabolic rewiring. *Cells* (2018) 7:E53. doi: 10.3390/cells7060053
31. Slawson C, Zachara NE, Vosseller K, Cheung WD, Lane MD, Hart GW. Perturbations in O-linked beta-N-acetylglucosamine protein modification cause severe defects in mitotic progression and cytokinesis. *J Biol Chem.* (2005) 280:32944–56. doi: 10.1074/jbc.M503396200
32. Sakabe K, Hart GW. O-GlcNAc transferase regulates mitotic chromatin dynamics. *J Biol Chem.* (2010) 285:34460–68. doi: 10.1074/jbc.M110.158170
33. Drougat L, Olivier-Van Stichelen S, Mortuaire M, Foulquier F, Lacoste AS, Michalski JC, et al. Characterization of O-GlcNAc cycling and proteomic identification of differentially O-GlcNAcylated proteins during G1/S transition. *Biochim Biophys Acta* (2012) 1820:1839–48. doi: 10.1016/j.bbagen.2012.08.024
34. Olivier-Van Stichelen S, Drougat L, Dehennaut V, El Yazidi-Belkoura I, Guinez C, Mir AM, et al. Serum-stimulated cell cycle entry promotes ncOGT synthesis required for cyclin D expression. *Oncogenesis* (2012) 1:e36. doi: 10.1038/oncsis.2012.36
35. O'Donnell N, Zachara NE, Hart GW, Marth JD. Ogt-dependent X-chromosome-linked protein glycosylation is a requisite modification in somatic cell function and embryo viability. *Mol Cell Biol.* (2004) 24:1680–90. doi: 10.1128/MCB.24.4.1680-1690.2004
36. Caldwell SA, Jackson SR, Shahriari KS, Lynch TP, Sethi G, Walker S, et al. Nutrient sensor O-GlcNAc transferase regulates breast cancer tumorigenesis through targeting of the oncogenic transcription factor FoxM1. *Oncogene* (2010) 29:2831–42. doi: 10.1038/onc.2010.41
37. Lynch TP, Ferrer CM, Jackson SR, Shahriari KS, Vosseller K, Reginato MJ. Critical role of O-Linked β-N-acetylglucosamine transferase in prostate cancer invasion, angiogenesis, and metastasis. *J Biol Chem.* (2012) 287:11070–81. doi: 10.1074/jbc.M111.302547
38. Ma Z, Vocadlo DJ, Vosseller K. Hyper-O-GlcNAcylation is anti-apoptotic and maintains constitutive NF-κB activity in pancreatic cancer cells. *J Biol Chem.* (2013) 288:15121–30. doi: 10.1074/jbc.M113.470047
39. Lanza C, Tan EP, Zhang Z, Machacek M, Brinker AE, Azuma M, et al. Reduced O-GlcNAcase expression promotes mitotic errors and spindle defects. *Cell Cycle* (2016) 15:1363–75. doi: 10.1080/15384101.2016.1167297
40. Li J, Deng M, Wei Q, Liu T, Tong X, Ye X. Phosphorylation of MCM3 protein by cyclin E/cyclin-dependent kinase 2 (Cdk2) regulates its function in cell cycle. *J Biol Chem.* (2011) 286:39776–85. doi: 10.1074/jbc.M111.226464
41. Leturcq M, Mortuaire M, Hardivillé S, Schulz C, Lefebvre T, Vercoutter-Edouart AS. *O*-GlcNAc transferase associates with the MCM2-7 complex and its silencing destabilizes MCM-MCM interactions. *Cell Mol Life Sci.* (2018) 75:4321–39. doi: 10.1007/s00018-018-2874-0
42. Dehennaut V, Slomianny MC, Page A, Vercoutter-Edouart AS, Jessus C, Michalski JC, et al. Identification of structural and functional O-linked N-acetylglucosamine-bearing proteins in *Xenopus laevis* oocyte. *Mol Cell Proteom.* (2008) 7:2229–45. doi: 10.1074/mcp.M700494-MCP200
43. Guo Y, Harwalkar J, Stacey DW, Hitomi M. Destabilization of cyclin D1 message plays a critical role in cell cycle exit upon mitogen withdrawal. *Oncogene* (2005) 24:1032–42. doi: 10.1038/sj.onc.1208299
44. Yang W, Kim H, Nam JE, Ju HW, Kim JW, Kim HS, et al. Modification of p53 with O-linked N-acetylglucosamine regulates p53 activity and stability. *Nat Cell Biol.* (2006) 8: 1074–83. doi: 10.1038/ncb1470
45. Ruan HB, Han X, Li MD, Singh JP, Qian K, Azarhoush S, et al. O-GlcNAc transferase/host cell factor C1 complex regulates gluconeogenesis by modulating PGC-1α stability. *Cell Metab.* (2012) 16:226–37. doi: 10.1016/j.cmet.2012.07.006
46. Ruan HB, Nie Y, Yang X. Regulation of protein degradation by O-GlcNAcylation: crosstalk with ubiquitination. *Mol Cell Proteom.* (2013) 12:3489–97. doi: 10.1074/mcp.R113.029751
47. Olivier-Van Stichelen S, Dehennaut V, Buzy A, Zachayus JL, Guinez C, Mir AM, et al. O-GlcNAcylation stabilizes β-catenin through direct competition with phosphorylation at threonine 41. *Faseb J.* (2014) 28:3325–38. doi: 10.1096/fj.13-243535
48. Inoue Y, Moriwaki K, Ueda Y, Takeuchi T, Higuchi K, Asahi M. Elevated O-GlcNAcylation stabilizes FOXM1 by its reduced degradation through GSK-3β inactivation in a human gastric carcinoma cell line, MKN45 cells. *Biochem Biophys Res Commun.* (2018) 495:1681–87. doi: 10.1016/j.bbrc.2017.11.179
49. Whisenhunt TR, Yang X, Bowe DB, Paterson AJ, Van Tine BA, Kudlow JE. Disrupting the enzyme complex regulating O-GlcNAcylation blocks signaling and development. *Glycobiology* (2006) 16:551–63. doi: 10.1093/glycob/cwj096
50. Jarvius M, Paulsson J, Weibrecht I, Leuchowius KJ, Andersson AC, Wählby C, et al. *In situ* detection of phosphorylated platelet-derived growth factor receptor b using a generalized proximity ligation method. *Mol Cell Proteom.* (2007) 6: 1500–09. doi: 10.1074/mcp.M700166-MCP200
51. Conze T, Carvalho AS, Landegren U, Almeida R, Reis CA, David L, et al. MUC2 mucin is a major carrier of the cancer-associated sialyl-Tn antigen in intestinal metaplasia and gastric carcinomas. *Glycobiology* (2010) 20:199–206. doi: 10.1093/glycob/cwp161
52. Zhang F, Su K, Yang X, Bowe DB, Paterson AJ, Kudlow JE. O-GlcNAc modification is an endogenous inhibitor of the proteasome. *Cell* (2003) 115:715–25. doi: 10.1016/S0092-8674(03)00974-7
53. Jirawatnotai S, Hu Y, Michowski W, Elias JE, Becks L, Bienvenu F, et al. A function for cyclin D1 in DNA repair uncovered by protein interactome analyses in human cancers. *Nature* (2011) 474:230–4. doi: 10.1038/nature10155
54. Guinez C, Losfeld ME, Cacan R, Michalski JC, Lefebvre T. Modulation of HSP70 GlcNAc-directed lectin activity by glucose availability and utilization. *Glycobiology* (2006) 16:22–8. doi: 10.1093/glycob/cwj041
55. Diehl JA, Yang W, Rimerman RA, Xiao H, Emili A. Hsc70 regulates accumulation of cyclin D1 and cyclin D1-dependent protein kinase. *Mol Cell Biol.* (2003) 23:1764–74. doi: 10.1128/MCB.23.5.1764-1774.2003
56. Shi J, Wu S, Dai CL, Li Y, Grundke-Iqbal I, Iqbal K, et al. Diverse regulation of AKT and GSK-3β by O-GlcNAcylation in various types of cells. *FEBS Lett.* (2012) 586:2443–50. doi: 10.1016/j.febslet.2012.05.063
57. Maury JJ, Ng D, Bi X, Bardor M, Choo AB. Multiple reaction monitoring mass spectrometry for the discovery and quantification of O-GlcNAc-modified proteins. *Anal Chem.* (2014) 86:395–402. doi: 10.1021/ac401821d
58. Barbash, O, Diehl JA. SCF (Fbx4/alphaB-crystallin) E3 ligase: when one is not enough. *Cell Cycle* (2008) 7:2983–86. doi: 10.4161/cc.7.19.6775
59. Zhang X, Qiao Y, Wu Q, Chen Y, Zou S, Liu X, et al. The essential role of YAP O-GlcNAcylation in high-glucose-stimulated liver tumorigenesis. *Nat Commun.* (2017) 8:15280. doi: 10.1038/ncomms15280
60. Li Y, Jin K, Bunker E, Zhang X, Luo X, Liu X, et al. Structural basis of the phosphorylation-independent recognition of cyclin D1 by the SCF^{FBXO31} ubiquitin ligase. *Proc Natl Acad Sci USA.* (2018) 115:319–24. doi: 10.1073/pnas.1708677115

Conflict of Interest Statement: The authors declare that the research was conducted in the absence of any commercial or financial relationships that could be construed as a potential conflict of interest.

frontiers in Endocrinology

MINI REVIEW
published: 27 February 2019
doi: 10.3389/fendo.2019.00117

Regulation of Polycomb Repression by *O*-GlcNAcylation: Linking Nutrition to Epigenetic Reprogramming in Embryonic Development and Cancer

*Amélie Decourcelle, Dominique Leprince and Vanessa Dehennaut**

Université de Lille, CNRS, Institut Pasteur de Lille, UMR8161, M3T: Mechanisms of Tumorigenesis and Targeted Therapies, Lille, France

Epigenetic modifications are major actors of early embryogenesis and carcinogenesis and are sensitive to nutritional environment. In recent years, the nutritional sensor *O*-GlcNAcylation has been recognized as a key regulator of chromatin remodeling. In this review, we summarize and discuss recent clues that OGT and *O*-GlcNAcylation intimately regulate the functions of the Polycomb group proteins at different levels especially during *Drosophila melanogaster* embryonic development and in human cancer cell lines. These observations define an additional connection between nutrition and epigenetic reprogramming associated to embryonic development and cancer.

Keywords: O-GlcNAcylation, Polycomb, epigenetic, drosophila development, cancer

OPEN ACCESS

Edited by:
Tarik Issad, Institut National de la Santé et de la Recherche Médicale (INSERM), France

Reviewed by:
Anna Krzeslak, University of Łódz, Poland
Stéphanie Olivier-Van Stichelen, National Institutes of Health (NIH), United States

****Correspondence:***
Vanessa Dehennaut
vanessa.dehennaut@ibl.cnrs.fr

Specialty section:
This article was submitted to Molecular and Structural Endocrinology, a section of the journal Frontiers in Endocrinology

Received: *10 December 2018*
Accepted: *08 February 2019*
Published: *27 February 2019*

Citation:
Decourcelle A, Leprince D and Dehennaut V (2019) Regulation of Polycomb Repression by O-GlcNAcylation: Linking Nutrition to Epigenetic Reprogramming in Embryonic Development and Cancer. Front. Endocrinol. 10:117. doi: 10.3389/fendo.2019.00117

INTRODUCTION

Epigenetics refer to inherited changes in gene expression that do not involve changes in the underlying DNA sequence (a change in phenotype without a change in genotype). Actually, epigenetic modifications such as DNA methylation and histones post-translational modifications drive reading of the genes through the modulation of chromatin topology that governs DNA accessibility to transcriptional machinery. Epigenetic changes are a natural phenomenon: crucial epigenetic reprogramming events occur during germ cell development and early embryogenesis (1–3). Furthermore, the levels and turnover of epigenetic marks can be influenced directly and indirectly by several factors, including lifestyle and environment, which can lead to a modification of gene expression patterns and, consequently, affect our health for better or worse (4). In that sense, several studies have highlighted the key role of diet and nutritional compounds in the epigenetic regulation of gene expression, especially in the physiopathology of cancers. For instance, it was shown that resveratrol and grape seed proanthocyanidins found in red wine induced a decrease of cell viability and colony forming ability in two human breast cancer cell lines, MDA-MB-231 and MCF-7, with a decrease of histone deacetylase (HDAC) and DNA methyl transferase (DNMT) activities (5). Another study has demonstrated that EGCG (EppiGalloCatechin Gallate), a polyphenolic compound found in green tea, had the ability to inhibit Acute Promyelocytic Leukemia (APL) cells proliferation and to induce apoptosis by downregulating epigenetic modifiers such as DNMT1, HDAC1, HDAC2, the histone methyl transferase (HMT) G9a and some components of the Polycomb Repressive Complex 2 (PRC2) (6). These studies, among others, proved that food consumption can influence epigenetic modifications by directly affecting activities of "writers" and "erasers" of epigenetic modifications and have contributed to the emergence of the

concept of "epigenetic diet" which may have anti-cancer properties (7). On the contrary, many other studies support the hypothesis of a close link between nutritional disorders (obesity, metabolic syndrome, type 2 diabetes …), well-known risk factors for many cancers, and epigenetic reprogramming linked to carcinogenesis (8). For example, hyperglycemia has been shown to increase the chemoresistance of several prostate cancer cell lines to chemotherapy through the increase of histone H3 and H4 acetylation on the promoter region of insulin like growth factor binding protein 2 (IGFB2), a key player of prostate cancer progression (9). Wu et al. recently reported a decrease in DNA cytosine hydroxymethylation (5hmC, the first step of DNA demethylation catalyzed by the ten-eleven translocation (TET) family of dioxygenases) in peripheral blood mononuclear cells (PBMCs) derived from diabetic individuals in comparison with healthy one (10). They demonstrated that this reduction of 5hmC was the result of glucose-regulated phosphorylation of TET2 by the nutrient and energy sensor AMPK (AMP-activated kinase) and that elevated glucose levels interfere with the expression of numerous cancer-associated genes in a TET2-dependent manner. Among the elements that could also connect nutrition to epigenetic reprogramming related to development and cancer, the nutritional sensor *O*-linked-β-N-acetylglucosaminylation (*O*-GlcNAcylation) has emerged, during the last decade as a key epigenetic regulator of gene expression (11, 12).

O-GLCNACYLATION: A NUTRITIONAL SENSOR THAT REGULATES CHROMATIN REMODELING

Discovered in 1984 (13), *O*-GlcNAcylation is a reversible post-translational modification of cytosolic, nuclear, and mitochondrial proteins that consists in the covalent linkage of a unique residue of N-acetylglucosamine (GlcNAc) to serine and threonine moieties of target proteins (**Figure 1**). This post-translational modification is an important actor of cell signaling. *O*-GlcNAcylation targets and regulates thousands of proteins by monitoring their expression, stability, interaction with partners and subcellular localization (14). *O*-GlcNAcylation levels are regulated by a unique couple of enzymes: OGT (*O*-GlcNAc Transferase) catalyzes the transfer of GlcNAc from UDP-GlcNAc onto targeted proteins and OGA (*O*-GlcNAcase) hydrolyzes the residue (15). OGT activity and thus *O*-GlcNAcylation levels are closely dependent upon the concentration of the nucleotide sugar donor UDP-GlcNAc. UDP-GlcNAc is synthetized through the hexosamine biosynthetic pathway (HBP) at the crossroad of carbohydrates, amino-acids, fatty acids, and nucleotides metabolisms (**Figure 1**) and thus concentration of UDP-GlcNAc in cells is highly responsive to nutrients flux. Consistently, cell culture in high concentration of glucose or glucosamine is sufficient to increase *O*-GlcNAcylation levels in numerous cancer cell lines including HT29, HCT116, MCF7 and HepG2 (16–18). *In vivo*, increased *O*-GlcNAcylation has also been evidenced in the colon and the liver of mice refed or force-fed with glucose or glucosamine in comparison with fasting mice (18–20), in mice fed with a high carbohydrate diet and in obese mice (*ob/ob*) compared, respectively, to the normal diet and the wild-type mice (21, 22). Taken together, these studies, amongst others, sustain the hypothesis that UDP-GlcNAc and *O*-GlcNAcylation can be considered as nutritional sensors that can relay the effects of excessive food supply, obesity, and any other metabolic disorders associated to increased risk of cancers. Many studies have also clearly shown that a disruption in *O*-GlcNAcylation homeostasis is found in many cancers; moreover, aberrant *O*-GlcNAcylation contributes to the etiology of cancers at several levels. The role of *O*-GlcNAcylation in cancer emergence and progression has been extensively reviewed (23, 24). In recent years, *O*-GlcNAcylation has emerged as a novel epigenetic modifier affecting chromatin remodeling and gene expression. In that respect, *O*-GlcNAcylation is itself part of the histone code and regulates the occurrence of other PTMs defining this code and more particularly methylation by modulating the function of several methyltransferases like CARM1 and MLL5. OGT interacts in a complex interplay with the DNA demethylase TET family and regulates the activity of several co-repressor complexes among which NuRD and mSin3A. These different aspects of the role of *O*-GlcNAcylation in the epigenetic regulation of gene expression has been reviewed elsewhere (11, 12, 25, 26) and will not be discussed here.

This mini-review will summarize and discuss recent data focusing on how OGT and *O*-GlcNAcylation influence directly and indirectly the function of the Polycomb group (PcG) proteins, master regulators of embryogenesis and actors of human carcinogenesis.

O-GLCNACYLATION REGULATES PCG PROTEINS FUNCTIONS DURING *DROSOPHILA MELANOGASTER* DEVELOPMENT

Organization of the PcG Proteins in *Drosophila Melanogaster*

The polycomb group (PcG) proteins form a diverse and conserved group of epigenetic modifiers and transcriptional

Abbreviations: ASX, Additional Sex Combs; ASXL, Additional Sex Combs Like; BAP1, BRCA1 associated protein-1; BMI1 (PCGF4), B Lymphoma Mo-MLV insertion region-1; CARM1, Coactivator-associated Arginine Methyltransferase 1; CBX2, Chromobox Homolog 2; DNMT, DNA Methyl Transferase; EED, Embryonic Ectoderm Development; ESC, Extra Sex Combs; E(Z), Enhancer of Zeste; EZH2, Enhancer of Zeste Homolog 2; HAT, Histone Acetyl Transferase; HBP, Hexosamine Biosynthetic Pathway; HCF1, Host Cell Factor 1; HDAC, Histone Deacetylase; HIC1, Hypermethylated In Cancer 1; MLL5, Mixed Lineage Leukemia 5; NuRD, Nucleosome Remodeling and Deacetylase; NURF55, Nucleosome Remodeling Factor 55; OGA, *O*-GlcNAcase; *O*-GlcNAcylation, *O*-linked β-N-acetylglucosaminylation; OGT, *O*-GlcNAc Transferase; PC, Polycomb; PcG, Polycomb; PCGF, Polycomb group ring fingers; PER2, Period Circadian Regulator 2; PH, Polyhomeotic; PHO, Pleiohomeotic; PhoRC, Pho-Repressive Complex; PRC1, Polycomb Repressive Complex 1; PRC2, Polycomb Repressive Complex 2; PR-DUB, Pc-Repressive deubiquitinase; PRE, Polycomb Response Element; PSC, Posterior Sex Combs; RbAp46/48, Retinoblastoma Associated protein 46/48; RING1A/B, RING Finger Protein 1A/B; RNF2 (RING1B), Ring Finger Protein 2; Sce, Sex Comb Extra; SU(Z)12, Suppressor of Zeste 12; sxc, Super sex combs; TET, Ten Eleven Translocation; UDP-GlcNAc, Uridine DiPhosphate N-acetylglucosamine; YY1, Yin Yang 1.

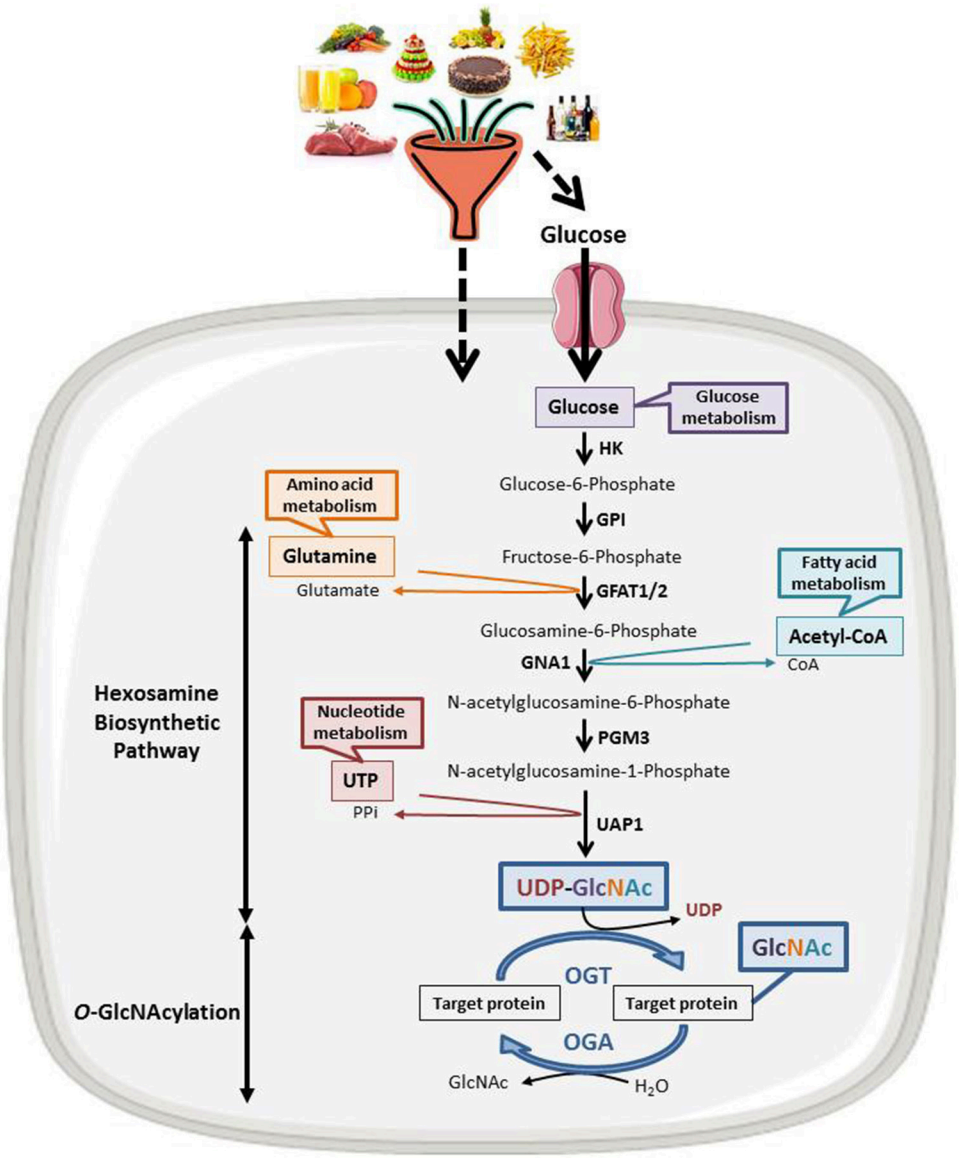

FIGURE 1 | The nutritional sensing *O*-GlcNAcylation. UDP-GlcNAc, OGT's nucleotide sugar donor, is provided by the Hexosamine Biosynthetic Pathway (HBP) at the crossroad of glucose, amino acids, fatty acids and nucleotides metabolisms. UDP-GlcNAc levels are thus tightly correlated to the nutritional status of the organism. *O*-GlcNAcylation levels are regulated by a unique couple of enzymes: OGT that catalyzes the transfer of GlcNAc from UDP-GlcNAc onto the target protein and OGA that hydrolyzes the residue. HK, hexokinase; GPI, glucose-6-phosphate isomerase; GFAT, fructose-6-phosphate amidotransferase; GNA1, Glucosamine 6-phosphate N-acetyltransferase; PGM3, phosphoacetylglucosamine mutase; UAP1, UDP-N-acetylhexosamine pyrophosphorylase.

regulators. PcG proteins were initially discovered in *Drosophila melanogaster* (27). In fly, PcG proteins maintain the repression state of *Hox* genes whose expression patterns define the establishment of the antero-posterior axis of the embryo. PcG proteins form three broad groups of polycomb repressive complexes (PRCs) known as PRC1, PRC2, and Polycomb Repressive DeUBiquitinase (PR-DUB). Each PRC modifies and remodels chromatin by distinct mechanisms tuned by variable compositions of core and accessory subunits (**Figure 2A**). The PRC1 is composed of Sce, PH, PSC and PC. Sce harbors a H2AK119 ubiquitination activity. This H2AK119Ub repressive mark can be removed by the PR-DUB complex which is composed of Calypso and ASX. The association of NURF55, SU(Z)12, ESC and E(Z) leads to the formation of the PRC2. E(Z) has a H3K27 methylation activity. A fourth complex, PhoRC, allows the recruitment of PRC1 and PRC2 to their target genes and includes PHO and dSFMBT (28).

Fruit Fly OGT Is a Polycomb Protein Essential to Early Embryogenesis

Intriguingly, two independent studies published in 2009 showed that the fruit fly *O*-GlcNAc transferase was encoded by the

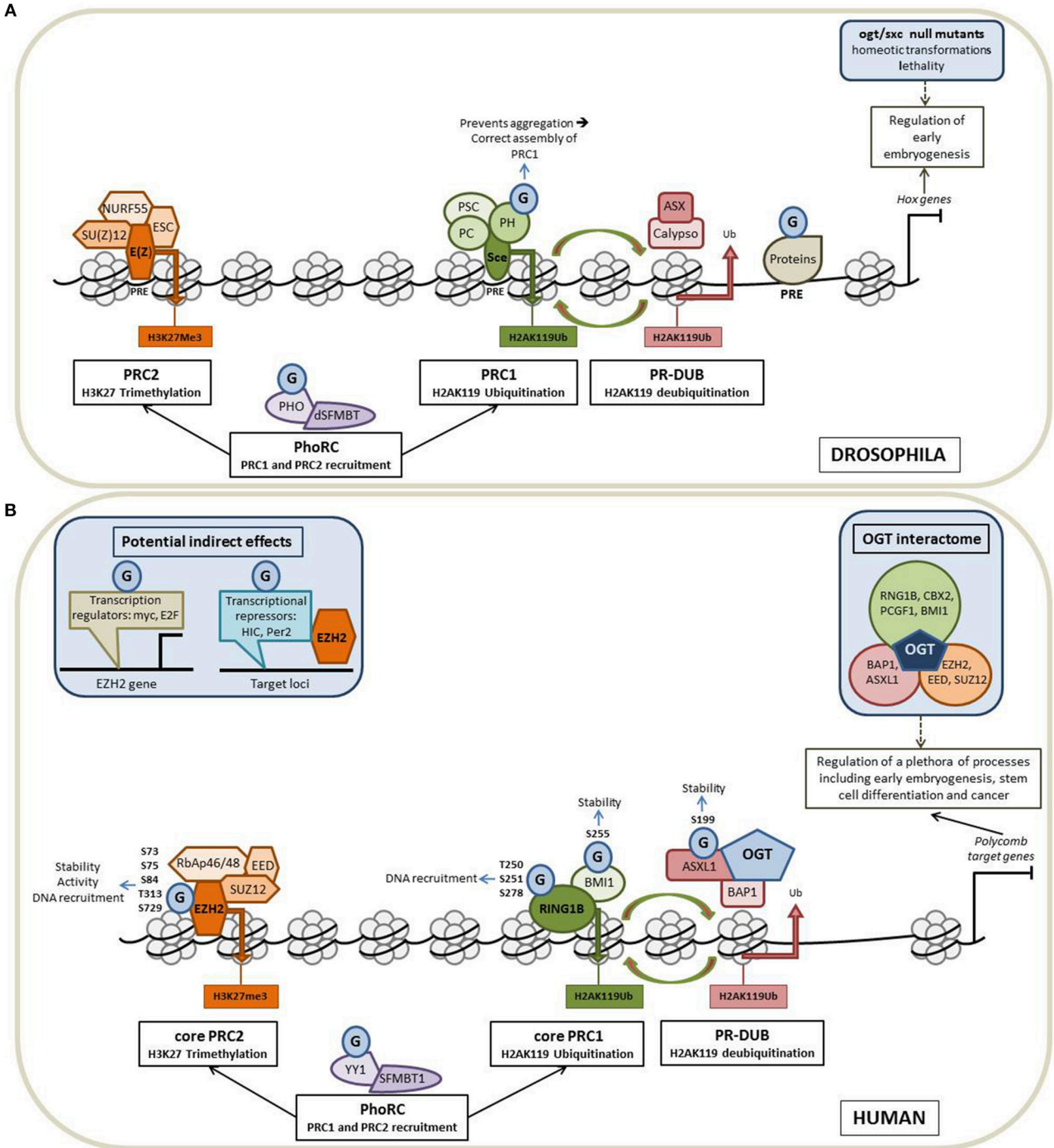

FIGURE 2 | *O*-GlcNAcylation intimately regulates the Polycomb proteins functions. Schematic representation of the organization of the PcG proteins in Drosophila **(A)** and in Human **(B)** and of how *O*-GlcNAcylation processes contribute to the regulation of the Polycomb-mediated gene repression in the two models. **(A)** In fly, PcG proteins maintain the repression state of *Hox* genes whose expression patterns define the establishment of the antero-posterior axis of the embryo. PcG proteins form three broad groups of polycomb repressive complexes (PRCs): PRC1, PRC2 and Polycomb Repressive DeUBiquitinase (PR-DUB). Each PRC modifies and remodels chromatin by distinct mechanisms tuned by variable compositions of core and accessory subunits. The core PRC1 is composed of PH, PSC, PC, and Sce that catalyzes H2AK119 ubiquitination. This repressive mark can be removed by the PR-DUB complex (association of Calypso and ASX). NURF55, SU(Z)12, ESC, and E(Z) forms the PRC2 core complex in which E(Z) has a H3K27 methylation activity. The fourth complex, PhoRC (association of PHO and dSFMBT) helps the recruitment of PRC1 and PRC2 to their target genes. PcG proteins are recruited to their target genes through the recognition of well-characterized regulatory DNA sequences called PREs (Polycomb Responsive Elements). OGT is also a PcG protein encoded by the supersexcomb (*sxc*) gene and *O*-GlcNAcylation regulates the PcG mediated repression at several levels (see the text for more details). G: *O*-GlcNAcylation. **(B)** In Human, PcG proteins repress numerous genes regulating a

(Continued)

FIGURE 2 | plethora of cellular processes, including early embryogenesis, stem cell differentiation and cancer. As in fly, Human Polycomb proteins are organized into four main complexes. The core PRC1 is composed of RING1 proteins (RING1A or RING1B), which display E3 ubiquitin ligase activity and one of the six Polycomb group ring-finger domain proteins (PCGF1–PCGF6). The PR-DUB is composed of BAP1 and ASXL 1 or 2. The association of RbAp46/48, EED, SUZ12, and EZH2 leads to the formation of the PRC2 core complex. PhoRC includes YY1 and SFMBT1. As in fly, OGT interacts and modifies several Human PcG proteins to regulate their functions and *O*-GlcNAcylation could also play a more indirect role through the modification of factors regulating the expression of PcG (see the text for details).

Super sex combs (*sxc*) gene (29, 30) characterized for the first time 25 years earlier as a gene belonging to the Polycomb family (31). Therefore, with rapid generation time and genetic manipulation facilities, *Drosophila* has been a model of choice for understanding the role of *O*-GlcNAcylation in development. Several studies have highlighted homeotic transformations and lethality phenotypes of various null *sxc/ogt* mutants (29–34) and have been ascribed to the glycosyltransferase activity of drosophila OGT (33, 34) thus demonstrating the crucial role of *ogt/sxc* and *O*-GlcNAcylation processes in early development. Consistent with these results, in an elegant approach consisting of probing *O*-GlcNAcylated proteins by harnessing the *O*-GlcNAc binding properties of a catalytic mutant of a bacterial *O*-GlcNAcase (CpOGA^{D298N}), Mariappa et al. demonstrated that the *O*-GlcNAcome was dynamic during the time course of *Drosophila* embryonic development (35). This OGA mutant was then used as a trap to enrich *O*-GlcNAcylated proteins from Drosophila embryo lysates and allowed the identification of the *O*-GlcNAcome associated with Drosophila embryogenesis (36). The authors identified more than 2,000 putative *O*-GlcNAcylated proteins, the majority of which being chromatin-associated proteins that include the HDACs Rpd3 and HDAC3, the putative HAT Enok, the bromodomain containing homeotic protein female sterile [fs(1)h; Brd2 ortholog] and several transcription factors among which Dp, Taf6, Cand1, and fkh. The authors were also able to map several *O*-GlcNAcylation sites on 43 proteins whose half of which are involved in anatomical structure development and morphogenesis according to gene ontology enrichment analysis.

Regulation of PcG Mediated Repression by O-GlcNAcylation

In Drosophila, PcG proteins are recruited to their target genes through the recognition of well-characterized regulatory DNA sequences called PREs (Polycomb Responsive Elements) (37). By ChIP-seq experiments performed in imaginal disc cells from Drosophila larvae, Gambetta and collaborators identified 1,138 sites occupied by *O*-GlcNAcylated proteins among which 490 co-localized with PREs suggesting that *O*-GlcNAcylation regulates the PcG mediated repression of *HOX* genes (29). Such a binding of *O*-GlcNAcylated proteins onto PREs has also been evidenced in two other independent studies (38, 39). This binding of *O*-GlcNAcylated proteins to PREs is in line with the results from Ingham showing that *ogt/sxc* is required for the selective repression of *HOX* genes in different larval segments (31). The Pho repressive complex (PhoRC) is involved in the recruitment of PRC1 and PRC2 (**Figure 2A**), thus the presence of Pho at genomic loci is often considered as a marker for identification of PREs. By ChIP-chip experiments conducted in S2 cells, Akan et al. demonstrated that *O*-GlcNAc and Pho co-occupied many chromatin regions including the *HOX* genes clusters thus reinforcing the hypothesis of the role of *O*-GlcNAcylation in PcG mediated repression (38). Nonetheless, *ogt/sxc* null mutants do not present either any binding modification of PHO and E(Z) to PREs or any difference in H3K27me3 in comparison with wild-type drosophila suggesting that *ogt/sxc* is not essential for PRC2 recruitment to target genes and H3K27me3 activity (29). However, in the same study, the authors demonstrated that PH (Polyhomeotic) is *O*-GlcNAcylated and observed a decrease of its binding on the majority of the PREs in *sxc/ogt* null mutants, underlying the role of *O*-GlcNAcylation in the interaction of PH with DNA. The same team demonstrated that *O*-GlcNAcylation prevents the self-aggregation of PH and is required for the correct assembly of PRC1 (32). Lastly, it was also demonstrated that PHO is *O*-GlcNAcylated but the role of the glycosylation on PHO properties has not been so far investigated (39). However, this post-translational modification does not seem to modify its DNA recruitment according to the results from Gambetta et al. (29).

O-GLCNACYLATION REGULATES THE POLYCOMB PROTEINS FUNCTIONS IN HUMAN CANCER CELL LINES

Organization of the Polycomb Group Proteins in Mammals

Numerous orthologs of Drosophila PcG proteins have been identified in mammals and revealed that the PcG system is much more complex in mammals than in fly (40) (**Figure 2B**). In mammals, PRC1 is subdivided into canonical (cPRC1) and non-canonical complexes (ncPRC1). These two PRC1 complexes share a core complex that is composed of RING1 proteins (RING1A or RING1B), which display E3 ubiquitin ligase activity mediating ubiquitylation of histone H2A on lysine 119 (H2AK119Ub), and one of the six Polycomb group ring-finger domain proteins (PCGF1–PCGF6). The repressive mark H2AK119Ub can be removed by the PR-DUB complex which is composed of BAP1 and ASXL. The association of RbAp46/48, EED, SUZ12 and EZH2 leads to the formation of the mammalian PRC2 core complex. The association of several accessory proteins with the core PRC2 complex defined two subtypes of PRC2: PRC2.1 and PRC2.2. PRC2.1 is defined by its mutually exclusive binding of one of the three Polycomb-like homologs (PCLs) PHF1, PHF19, or MTF2; PRC2.2 is defined by the presence of the zinc-finger proteins AEBP2 and JARID2, which enhance enzymatic activity of the complex and regulate its chromatin binding affinity. Finally, the PhoRC includes YY1 and SFMBT1, and allows the recruitment of PRC1 and PRC2 to their target genes (28, 41).

In mammals, PcG proteins repress *Hox* genes but also control the expression of numerous other genes regulating a plethora of cellular processes, including X chromosome inactivation, genomic imprinting, cell cycle control and stem cell biology (40). Furthermore, misexpression or mutation of many PcG components has been evidenced in several cancers. Many studies have demonstrated that PcG proteins can play an oncogenic role. For example, high levels of EZH2 and the H3K27me3 mark often correlate with a poor prognosis in prostate tumors (42). In colorectal cancer, elevated expression of EZH2, BMI1, and SUZ12 in correlation with advances stages of the disease and poor prognosis has also been evidenced (43). In line of this, the development of PcG-specific inhibitors, particularly compounds targeting EZH2, is an active area of investigation for the treatment of cancers (44) and the in-depth understanding of how PcG functions are regulated, such as by post-translational modifications, is a real challenge to improve the development of such therapeutic tools.

Regulation of PcG Mediated Repression by O-GlcNAcylation

Recent data collected from proteomic analyses aiming at identifying the OGT interactome in Hela cells revealed that the glycosyltransferase interacts with lots of PcG proteins belonging to PRC1, PRC2, PR-DUB, and PhoRC complexes: EZH2, EED, SUZ12, RNF2 (also called RING1B), CBX2, PCGF1, BMI1, BAP1, and ASXL1, thus suggesting that *O*-GlcNAcylation is also a master regulator of PcG functions in mammals (45). Another recent study, dedicated to mapping the human Polycomb complexome, showed that OGT is also an accessory protein of the PR-DUB complex (H2AK119Ub eraser) reinforcing the involvement of *O*-GlcNAcylation in the regulation of PcG (46). In the same way, ChIP Seq experiments performed in the colon cancer cell line HT29 demonstrated that *O*-GlcNAcylated proteins and H3K27 trimethylation were found together at the promoter region of 61 genes among which *MYBL* whose epigenetic regulation by *O*-GlcNAcylation affects the population of cancer stem cells (47). ChIP assays performed in the breast cancer cell line MCF7 indicated that the promoter regions of 16 potential tumor suppressor genes were bound by OGT and were enriched in EZH2 and H3K27me3 in an OGT-dependent manner (48), also arguing for a role of *O*-GlcNAcylation in the regulation of the PRC2-mediated repression in the context of cancer. Interestingly, recent data from Jiang et al. revealed that OGT and EZH2 expression were both post-transcriptionally repressed by microRNA-101 (49). The authors also showed that miRNA-101 was epigenetically silenced by OGT and EZH2 in several colorectal cancer cell lines resulting in the upregulation of the two enzymes in metastatic colorectal cancer in a vicious cycle fashion.

OGT Interacts With and Modifies Several PcG Proteins

To date, among the OGT-interacting PcG proteins, five have been demonstrated to be *O*-GlcNAcylated in Human: EZH2, BMI1 (also called PCGF4), RING1B, ASXL1, and YY1. *O*-GlcNAcylation of EZH2 was first evidenced in breast cancer MCF7 cells (48). In this study, the authors identified the serine 75 of EZH2 as the major *O*-GlcNAc site regulating the stability of the enzyme. Very recently, the same team performed further mass spectrometry analysis of EZH2-FLAG overexpressed in HEK 293T cells and identified four additional *O*-GlcNAcylation sites: S73, S84, T313, and S729 (50). By analyzing *O*-GlcNAcylation site mutants, the authors concluded that *O*-GlcNAcylation in the N-terminal region of EZH2 stabilizes the enzyme whereas the *O*-GlcNAcylation at S279 in the catalytic domain is essential for its methyltransferase activity. However, the role of *O*-GlcNAc modification on EZH2 is not so clear. While some studies confirm the role of *O*-GlcNAcylation in the regulation of EZH2 stability and catalytic activity (49, 51), others propose that the glycosylation regulates rather EZH2 recruitment to some of its target genes such as *FOXC1* (52). BMI1 was found to be *O*-GlcNAcylated at serine 255 in prostate cancer cells (53). *O*-GlcNAcylation of BMI1 prevents its proteasomal degradation and promotes its oncogenic activity. *O*-GlcNAcylation of RING1B was evidenced in human embryonic stem cells and mapped at residues threonine 250, serine 251 and serine 278 (54). By ChiP Seq experiments, the authors demonstrated that the non-GlcNAcylated form of RING1B preferentially binds to genes related to metabolism and cell cycle processes whereas *O*-GlcNAcylated-RING1B was found to the promoter region of genes related to neuronal differentiation. This means that *O*-GlcNAcylation might regulate RING1B DNA recruitment and targeting of the PRC1 complex to specific loci. It has been recently shown that OGT interacts also with ASXL1, a PR-DUB component, and drives its *O*-GlcNAcylation at serine 199 to regulate its stability (51). Finally the *O*-GlcNAcylation of YY1 has been demonstrated in muscle cells but its potential influence on the recruitment of PRC1 and PRC2 has not been yet investigated (55).

Potential Indirect Regulation of PcG Functions by O-GlcNAcylation

Beyond the direct regulation of PcG functions by their own *O*-GlcNAcylation, the glycosylation could play a more distant role through the modification of factors regulating the expression of PcG even if it has not been demonstrated to date. For example, two transcriptional regulators of EZH2: c-myc (56) and E2F (57) are *O*-GlcNAcylated (58, 59). Although the mode of recruitment of the Polycomb proteins to their target genes is well-known in *Drosophila*, this mechanism is not clear in humans and remains to be clarified. Nevertheless, it involves several partners that direct the PcG proteins to specific loci. For example, the tumor suppressor gene HIC1 (60) and the co-repressor PER2 (61) allow the recruitment of PRC2 to some target genes. In the same vein, RING1B and EZH2 have been identified as Snail-interacting proteins (62, 63). Interestingly, these three PRC partners are *O*-GlcNAcylated (64–66); it can be therefore hypothesized, although not yet studied, that *O*-GlcNAcylation influences the interaction of the PRC complexes with these proteins.

CONCLUSION

O-GlcNAcylation processes and epigenetic modifications are both sensitive to nutritional environment and have been evidenced as key regulators of embryogenesis and carcinogenesis. In this review, we summarized evidences that OGT and *O*-GlcNAcylation intimately regulate the functions of the Polycomb group proteins at different levels especially during *Drosophila melanogaster* embryonic development and in human cancer cell lines (**Figure 2**). Although, further works are required to clarify the roles of *O*-GlcNAcylation in PcG mediated repression, especially during cancer emergence and progression, all the data collected here sustain the hypothesis that *O*-GlcNAcylation is a new link between nutrition and epigenetic reprogramming of cancer cells. These observations could explain in part why nutritional disorders like diabetes or metabolic syndromes are often associated with the risk of cancer. Indeed, one can easily hypothesize that nutritional disorders, by increasing cellular levels of UDP-GlcNAc and *O*-GlcNAcylation leads to aberrant activity of PcG proteins misregulating genes driving carcinogenesis. Thus, in the next future, the *O*-GlcNAcylated forms of PcG proteins may be envisaged as diagnostic or prognostic tools in cancer and their targeting may also be studied as new therapeutic approaches.

AUTHOR CONTRIBUTIONS

AD and VD conceived the plan and wrote the review. DL revised it critically for important intellectual content.

ACKNOWLEDGMENTS

We thank the Prof. Tony Lefebvre for the critical reading of our manuscript. Our work is supported by the GEFLUC Flandres/Artois, the Ligue Contre le Cancer/Comité du Nord, the Canceropôle Nord-Ouest and the Centre National de la Recherche Scientifique. AD is the recipient of a fellowship from the Ministère de l'Enseignement Supérieur et de la Recherche.

REFERENCES

1. Shi L, Wu J. Epigenetic regulation in mammalian preimplantation embryo development. *Reprod Biol Endocrinol.* (2009) 7:59. doi: 10.1186/1477-7827-7-59
2. Weaver JR, Susiarjo M, Bartolomei MS. Imprinting and epigenetic changes in the early embryo. *Mamm Genome* (2009) 20:532–43. doi: 10.1007/s00335-009-9225-2
3. Nestorov P, Tardat M, Peters AHFM. H3K9/HP1 and Polycomb: two key epigenetic silencing pathways for gene regulation and embryo development. *Curr Top Dev Biol.* (2013) 104:243–91. doi: 10.1016/B978-0-12-416027-9.00008-5
4. Tiffon C. The impact of nutrition and environmental epigenetics on human health and disease. *Int J Mol Sci.* (2018) 19:3425. doi: 10.3390/ijms19113425
5. Gao Y, Tollefsbol TO. Combinational proanthocyanidins and resveratrol synergistically inhibit human breast cancer cells and impact epigenetic–mediating machinery. *Int J Mol Sci.* (2018) 19:2204. doi: 10.3390/ijms19082204
6. Borutinskaite V, Virkšaite A, Gudelyte G, Navakauskiene R. Green tea polyphenol EGCG causes anti-cancerous epigenetic modulations in acute promyelocytic leukemia cells. *Leuk Lymphoma* (2018) 59:469–78. doi: 10.1080/10428194.2017.1339881
7. Hardy TM, Tollefsbol TO. Epigenetic diet: impact on the epigenome and cancer. *Epigenomics* (2011) 3:503–18. doi: 10.2217/epi.11.71
8. Bishop KS, Ferguson LR. The interaction between epigenetics, nutrition and the development of cancer. *Nutrients* (2015) 7:922–47. doi: 10.3390/nu7020922
9. Biernacka KM, Uzoh CC, Zeng L, Persad RA, Bahl A, Gillatt D, et al. Hyperglycaemia-induced chemoresistance of prostate cancer cells due to IGFBP2. *Endocr Relat Cancer* (2013) 20:741–51. doi: 10.1530/ERC-13-0077
10. Wu D, Hu D, Chen H, Shi G, Fetahu IS, Wu F, et al. Glucose-regulated phosphorylation of TET2 by AMPK reveals a pathway linking diabetes to cancer. *Nature* (2018) 559:637. doi: 10.1038/s41586-018-0350-5
11. Dehennaut V, Leprince D, Lefebvre T. O-GlcNAcylation, an epigenetic mark. focus on the histone code, TET family proteins, and polycomb group proteins. *Front Endocrinol.* (2014) 5:155. doi: 10.3389/fendo.2014.00155
12. Leturcq M, Lefebvre T, Vercoutter-Edouart A-S. O-GlcNAcylation and chromatin remodeling in mammals: an up-to-date overview. *Biochem Soc Trans.* (2017) 45:323–38. doi: 10.1042/BST20160388
13. Torres CR, Hart GW. Topography and polypeptide distribution of terminal N-acetylglucosamine residues on the surfaces of intact lymphocytes. Evidence for O-linked GlcNAc. *J Biol Chem.* (1984) 259:3308–17.
14. Bond MR, Hanover JA. A little sugar goes a long way: the cell biology of O-GlcNAc. *J Cell Biol.* (2015) 208:869–80. doi: 10.1083/jcb.201501101
15. Vocadlo DJ. O-GlcNAc processing enzymes: catalytic mechanisms, substrate specificity, and enzyme regulation. *Curr Opin Chem Biol.* (2012) 16:488–97. doi: 10.1016/j.cbpa.2012.10.021
16. Guinez C, Losfeld M-E, Cacan R, Michalski JC, Lefebvre T. Modulation of HSP70 GlcNAc-directed lectin activity by glucose availability and utilization. *Glycobiology* (2006) 16:22–8. doi: 10.1093/glycob/cwj041
17. Steenackers A, Olivier-Van Stichelen S, Baldini SF, Dehennaut V, Toillon RA, Le Bourhis X, et al. Silencing the nucleocytoplasmic O-GlcNAc transferase reduces proliferation, adhesion, and migration of cancer and fetal human colon cell lines. *Front Endocrinol.* (2016) 7:46. doi: 10.3389/fendo.2016.00046
18. Olivier-Van Stichelen S, Guinez C, Mir A-M, Perez-Cervera Y, Liu C, Michalski J-C, et al. The hexosamine biosynthetic pathway and O-GlcNAcylation drive the expression of β-catenin and cell proliferation. *Am J Physiol Endocrinol Metab.* (2012) 302:E417–24. doi: 10.1152/ajpendo.00390.2011
19. Guinez C, Filhoulaud G, Rayah-Benhamed F, Marmier S, Dubuquoy C, Dentin R, et al. O-GlcNAcylation increases ChREBP protein content and transcriptional activity in the liver. *Diabetes* (2011) 60:1399–413. doi: 10.2337/db10-0452
20. Baldini SF, Steenackers A, Olivier-Van Stichelen S, Mir A-M, Mortuaire M, Lefebvre T, et al. Glucokinase expression is regulated by glucose through O-GlcNAc glycosylation. *Biochem Biophys Res Commun.* (2016) 478:942–8. doi: 10.1016/j.bbrc.2016.08.056
21. Olivier-Van Stichelen S, Dehennaut V, Buzy A, Zachayus JL, Guinez C, Mir A-M, et al. O-GlcNAcylation stabilizes β-catenin through direct competition with phosphorylation at threonine 41. *FASEB J.* (2014) 28:3325–38. doi: 10.1096/fj.13-243535
22. Very N, Steenackers A, Dubuquoy C, Vermuse J, Dubuquoy L, Lefebvre T, et al. Cross regulation between mTOR signaling and O-GlcNAcylation. *J Bioenerg Biomembr.* (2018) 50:213–22. doi: 10.1007/s10863-018-9747-y
23. Fardini Y, Dehennaut V, Lefebvre T, Issad T. O-GlcNAcylation: a new cancer hallmark? *Front Endocrinol.* (2013) 4:99. doi: 10.3389/fendo.2013.00099
24. de Queiroz RM, Carvalho E, Dias WB. O-GlcNAcylation: the sweet side of the cancer. *Front Oncol.* (2014) 4:132. doi: 10.3389/fonc.2014.00132
25. Hardivillé S, Hart GW. Nutrient regulation of signaling, transcription, and cell physiology by O-GlcNAcylation. *Cell Metab.* (2014) 20:208–13. doi: 10.1016/j.cmet.2014.07.014
26. Wu D, Cai Y, Jin J. Potential coordination role between O-GlcNAcylation and epigenetics. *Protein Cell.* (2017) 8:713–23. doi: 10.1007/s13238-017-0416-4

27. Lewis PH. *New Mutants Report*. Drosophila Information Service (1947).
28. Lanzuolo C, Orlando V. Memories from the polycomb group proteins. *Annu Rev Genet.* (2012) 46:561–89. doi: 10.1146/annurev-genet-110711-155603
29. Gambetta MC, Oktaba K, Müller J. Essential role of the glycosyltransferase sxc/Ogt in polycomb repression. *Science* (2009) 325:93–6. doi: 10.1126/science.1169727
30. Sinclair DAR, Syrzycka M, Macauley MS, Rastgardani T, Komljenovic I, Vocadlo DJ, et al. Drosophila O-GlcNAc transferase (OGT) is encoded by the Polycomb group (PcG) gene, super sex combs (sxc). *Proc Natl Acad Sci USA.* (2009) 106:13427–32. doi: 10.1073/pnas.0904638106
31. Ingham PW. A gene that regulates the bithorax complex differentially in larval and adult cells of Drosophila. *Cell* (1984) 37:815–23. doi: 10.1016/0092-8674(84)90416-1
32. Gambetta MC, Müller J. O-GlcNAcylation prevents aggregation of the polycomb group repressor polyhomeotic. *Dev Cell* (2014) 31:629–39. doi: 10.1016/j.devcel.2014.10.020
33. Mariappa D, Zheng X, Schimpl M, Raimi O, Ferenbach AT, Müller HAJ, et al. Dual functionality of O-GlcNAc transferase is required for *Drosophila* development. *Open Biol* (2015) 5:150234. doi: 10.1098/rsob.150234
34. Mariappa D, Ferenbach AT, van Aalten DMF. Effects of hypo-O-GlcNAcylation on Drosophila development. *J Biol Chem.* (2018) 293:7209–21. doi: 10.1074/jbc.RA118.002580
35. Mariappa D, Selvan N, Borodkin V, Alonso J, Ferenbach AT, Shepherd C, et al. A mutant O-GlcNAcase as a probe to reveal global dynamics of the Drosophila O-GlcNAc developmental proteome. *Biochem J.* (2015) 470:255–62. doi: 10.1042/BJ20150610
36. Selvan N, Williamson R, Mariappa D, Campbell DG, Gourlay R, Ferenbach AT, et al. A mutant O-GlcNAcase enriches Drosophila developmental regulators. *Nat Chem Biol.* (2017) 13:882–7. doi: 10.1038/nchembio.2404
37. Kassis JA, Brown JL. Polycomb group response elements in Drosophila and vertebrates. *Adv Genet.* (2013) 81:83–118. doi: 10.1016/B978-0-12-407677-8.00003-8
38. Akan I, Love DC, Harwood KR, Bond MR, Hanover JA. Drosophila O-GlcNAcase deletion globally perturbs chromatin O-GlcNAcylation. *J Biol Chem.* (2016) 291:9906–19. doi: 10.1074/jbc.M115.704783
39. Liu T-W, Myschyshyn M, Sinclair DA, Cecioni S, Beja K, Honda BM, et al. Genome-wide chemical mapping of O-GlcNAcylated proteins in *Drosophila melanogaster*. *Nat Chem Biol.* (2017) 13:161–7. doi: 10.1038/nchembio.2247
40. Schuettengruber B, Bourbon HM, Di Croce L, Cavalli G. Genome regulation by polycomb and trithorax: 70 years and counting. *Cell* (2017) 171:34–57. doi: 10.1016/j.cell.2017.08.002
41. Chittock EC, Latwiel S, Miller TCR, Müller CW. Molecular architecture of polycomb repressive complexes. *Biochem Soc Trans.* (2017) 45:193–205. doi: 10.1042/BST20160173
42. Varambally S, Dhanasekaran SM, Zhou M, Barrette TR, Kumar-Sinha C, Sanda MG, et al. The polycomb group protein EZH2 is involved in progression of prostate cancer. *Nature* (2002) 419:624–9. doi: 10.1038/nature01075
43. Benard A, Goossens-Beumer IJ, van Hoesel AQ, Horati H, Putter H, Zeestraten ECM, et al. Prognostic value of polycomb proteins EZH2, BMI1 and SUZ12 and histone modification H3K27me3 in colorectal cancer. *PLoS ONE* (2014) 9:e108265. doi: 10.1371/journal.pone.0108265
44. Kim KH, Roberts CWM. Targeting EZH2 in cancer. *Nat Med.* (2016) 22:128–34. doi: 10.1038/nm.4036
45. Gao J, Yang Y, Qiu R, Zhang K, Teng X, Liu R, et al. Proteomic analysis of the OGT interactome: novel links to epithelial-mesenchymal transition and metastasis of cervical cancer. *Carcinogenesis* (2018) 39:1222–34. doi: 10.1093/carcin/bgy097
46. Hauri S, Comoglio F, Seimiya M, Gerstung M, Glatter T, Hansen K, et al. A high-density map for navigating the human polycomb complexome. *Cell Rep.* (2016) 17:583–95. doi: 10.1016/j.celrep.2016.08.096
47. Guo H, Zhang B, Nairn AV, Nagy T, Moremen KW, Buckhaults P, et al. O-Linked N-acetylglucosamine (O-GlcNAc) expression levels epigenetically regulate colon cancer tumorigenesis by affecting the cancer stem cell compartment via modulating expression of transcriptional factor MYBL1. *J Biol Chem.* (2017) 292:4123–37. doi: 10.1074/jbc.M116.763201
48. Chu CS, Lo PW, Yeh YH, Hsu PH, Peng SH, Teng YC, et al. O-GlcNAcylation regulates EZH2 protein stability and function. *Proc Natl Acad Sci USA.* (2014) 111:1355–60. doi: 10.1073/pnas.1323226111
49. Jiang M, Xu B, Li X, Shang Y, Chu Y, Wang W, et al. O-GlcNAcylation promotes colorectal cancer metastasis via the miR-101-O-GlcNAc/EZH2 regulatory feedback circuit. *Oncogene* (2019) 38:301–16. doi: 10.1038/s41388-018-0435-5
50. Lo PW, Shie JJ, Chen CH, Wu CY, Hsu TL, Wong CH. O-GlcNAcylation regulates the stability and enzymatic activity of the histone methyltransferase EZH2. *Proc Natl Acad Sci USA.* (2018) 115:7302–7. doi: 10.1073/pnas.1801850115
51. Inoue D, Fujino T, Sheridan P, Zhang Y, Nagase R, Horikawa S, et al. A novel ASXL1–OGT axis plays roles in H3K4 methylation and tumor suppression in myeloid malignancies. *Leukemia* (2018) 32:1327–37. doi: 10.1038/s41375-018-0083-3
52. Forma E, Józwiak P, Ciesielski P, Zaczek A, Starska K, Bryś M, et al. Impact of OGT deregulation on EZH2 target genes FOXA1 and FOXC1 expression in breast cancer cells. *PLoS ONE* (2018) 13:e0198351. doi: 10.1371/journal.pone.0198351
53. Li Y, Wang L, Liu J, Zhang P, An M, Han C, et al. O-GlcNAcylation modulates Bmi-1 protein stability and potential oncogenic function in prostate cancer. *Oncogene* (2017) 36:6293–305. doi: 10.1038/onc.2017.223
54. Maury JJP, El Farran CA, Ng D, Loh YH, Bi X, Bardor M, et al. RING1B O-GlcNAcylation regulates gene targeting of polycomb repressive complex 1 in human embryonic stem cells. *Stem Cell Res.* (2015) 15:182–9. doi: 10.1016/j.scr.2015.06.007
55. Hiromura M, Choi CH, Sabourin NA, Jones H, Bachvarov D, Usheva A. YY1 is regulated by O-linked N-acetylglucosaminylation (O-glcNAcylation). *J Biol Chem.* (2003) 278:14046–52. doi: 10.1074/jbc.M300789200
56. Koh CM, Iwata T, Zheng Q, Bethel C, Yegnasubramanian S, De Marzo AM. Myc enforces overexpression of EZH2 in early prostatic neoplasia via transcriptional and post-transcriptional mechanisms. *Oncotarget* (2011) 2:669–83. doi: 10.18632/oncotarget.327
57. Bracken AP, Pasini D, Capra M, Prosperini E, Colli E, Helin K. EZH2 is downstream of the pRB-E2F pathway, essential for proliferation and amplified in cancer. *EMBO J.* (2003) 22:5323–35. doi: 10.1093/emboj/cdg542
58. Wells L, Slawson C, Hart GW. The E2F-1 associated retinoblastoma-susceptibility gene product is modified by O-GlcNAc. *Amino Acids* (2011) 40:877–83. doi: 10.1007/s00726-010-0709-x
59. Itkonen HM, Minner S, Guldvik IJ, Sandmann MJ, Tsourlakis MC, Berge V, et al. O-GlcNAc transferase integrates metabolic pathways to regulate the stability of c-MYC in human prostate cancer cells. *Cancer Res.* (2013) 73:5277–87. doi: 10.1158/0008-5472.CAN-13-0549
60. Boulay G, Dubuissez M, Van Rechem C, Forget A, Helin K, Ayrault O, et al. Hypermethylated in cancer 1 (HIC1) recruits polycomb repressive complex 2 (PRC2) to a subset of its target genes through interaction with human polycomb-like (hPCL) proteins. *J Biol Chem.* (2012) 287:10509–24. doi: 10.1074/jbc.M111.320234
61. Hwang-Verslues WW, Chang PH, Jeng YM, Kuo WH, Chiang PH, Chang YC, et al. Loss of corepressor PER2 under hypoxia up-regulates OCT1-mediated EMT gene expression and enhances tumor malignancy. *Proc Natl Acad Sci USA.* (2013) 110:12331–6. doi: 10.1073/pnas.1222684110
62. Tong ZT, Cai MY, Wang XG, Kong LL, Mai SJ, Liu YH, et al. EZH2 supports nasopharyngeal carcinoma cell aggressiveness by forming a co-repressor complex with HDAC1/HDAC2 and Snail to inhibit E-cadherin. *Oncogene* (2012) 31:583–94. doi: 10.1038/onc.2011.254
63. Chen J, Xu H, Zou X, Wang J, Zhu Y, Chen H, et al. Snail recruits Ring1B to mediate transcriptional repression and cell migration in pancreatic cancer cells. *Cancer Res.* (2014) 74:4353–63. doi: 10.1158/0008-5472.CAN-14-0181

64. Lefebvre T, Pinte S, Guérardel C, Deltour S, Martin-Soudant N, Slomianny M-C, et al. The tumor suppressor HIC1 (hypermethylated in cancer 1) is O-GlcNAc glycosylated. *Eur J Biochem.* (2004) 271:3843–54. doi: 10.1111/j.1432-1033.2004.04316.x
65. Kaasik K, Kivimäe S, Allen JJ, Chalkley RJ, Huang Y, Baer K, et al. Glucose sensor O-GlcNAcylation coordinates with phosphorylation to regulate circadian clock. *Cell Metab.* (2013) 17:291–302. doi: 10.1016/j.cmet.2012.12.017
66. Park SY, Kim HS, Kim NH, Ji S, Cha SY, Kang JG, et al. Snail1 is stabilized by O-GlcNAc modification in hyperglycaemic condition. *EMBO J.* (2010) 29:3787–96. doi: 10.1038/emboj.2010.254

Conflict of Interest Statement: The authors declare that the research was conducted in the absence of any commercial or financial relationships that could be construed as a potential conflict of interest.

frontiers in Endocrinology

ORIGINAL RESEARCH
published: 29 March 2019
doi: 10.3389/fendo.2019.00199

Identification of *O*-Glcnacylated Proteins in *Trypanosoma cruzi*

Elia Torres-Gutiérrez[1], Yobana Pérez-Cervera[2], Luc Camoin[3], Edgar Zenteno[1], Moyira Osny Aquino-Gil[2,4,5], Tony Lefebvre[5], Margarita Cabrera-Bravo[1], Olivia Reynoso-Ducoing[1], Martha Irene Bucio-Torres[1] and Paz María Salazar-Schettino[1]**

[1] Facultad de Medicina, Universidad Nacional Autónoma de México, Ciudad de México, Mexico, [2] Centro de Investigación Facultad de Medicina-UNAM and Facultad de Odontología, Universidad Autónoma Benito Juárez de Oaxaca, Oaxaca, Mexico, [3] INSERM, Institut Paoli-Calmetes, CRCM, Marseille Protéomique, Aix-Marseille Univ, Marseille, France, [4] Instituto Tecnológico de Oaxaca, Tecnológico Nacional de Mexico, Oaxaca, Mexico, [5] CNRS, UMR 8576, UGSF, Unité de Glycobiologie Structurale et Fonctionnelle,Université de Lille, Lille, France

OPEN ACCESS

Edited by:
Isam Khalaila, Ben-Gurion University of the Negev, Israel

Reviewed by:
Chad Slawson, University of Kansas Medical Center Research Institute, United States
Hai-Bin Ruan, University of Minnesota, United States
Natasha Zachara, Johns Hopkins University, United States

***Correspondence:**
Martha Irene Bucio-Torres
marbu@unam.mx
Paz María Salazar-Schettino
pazmar@unam.mx

Specialty section:
This article was submitted to Molecular and Structural Endocrinology, a section of the journal Frontiers in Endocrinology

Received: *12 October 2018*
Accepted: *11 March 2019*
Published: *29 March 2019*

Citation:
Torres-Gutiérrez E, Pérez-Cervera Y, Camoin L, Zenteno E, Aquino-Gil MO, Lefebvre T, Cabrera-Bravo M, Reynoso-Ducoing O, Bucio-Torres MI and Salazar-Schettino PM (2019) Identification of O-Glcnacylated Proteins in Trypanosoma cruzi. Front. Endocrinol. 10:199. doi: 10.3389/fendo.2019.00199

Originally an anthropozoonosis in the Americas, Chagas disease has spread from its previous borders through migration. It is caused by the protozoan *Trypanosoma cruzi*. Differences in disease severity have been attributed to a natural pleomorphism in *T. cruzi*. Several post-translational modifications (PTMs) have been studied in *T. cruzi*, but to date no work has focused on O-GlcNAcylation, a highly conserved monosaccharide-PTM of serine and threonine residues mainly found in nucleus, cytoplasm, and mitochondrion proteins. O-GlcNAcylation is thought to regulate protein function analogously to protein phosphorylation; indeed, crosstalk between both PTMs allows the cell to regulate its functions in response to nutrient levels and stress. Herein, we demonstrate O-GlcNAcylation in *T. cruzi* epimastigotes by three methods: by using specific antibodies against the modification in lysates and whole parasites, by click chemistry labeling, and by proteomics. In total, 1,271 putative O-GlcNAcylated proteins and six modification sequences were identified by mass spectrometry (data available via ProteomeXchange, ID PXD010285). Most of these proteins have structural and metabolic functions that are essential for parasite survival and evolution. Furthermore, O-GlcNAcylation pattern variations were observed by antibody detection under glucose deprivation and heat stress conditions, supporting their possible role in the adaptive response. Given the numerous biological processes in which O-GlcNAcylated proteins participate, its identification in *T. cruzi* proteins opens a new research field in the biology of Trypanosomatids, improve our understanding of infection processes and may allow us to identify new therapeutic targets.

Keywords: *Trypanosoma cruzi*, O-GlcNAcylated proteins, post translational modification, epimastigote, protist, click chemistry, mass spectrometry

INTRODUCTION

The protozoan *Trypanosoma cruzi* is the causative agent of Chagas disease (CD). Also called American trypanosomiasis, CD is one of the biggest public health problems in Latin America. CD has spread to other continents due to increased population movements to and from Latin America. An estimated 8 million people are infected with the parasite worldwide (1). In 1909, the Brazilian physician Carlos Chagas described the disease in its acute and chronic phases. Most

chronic-phase CD patients are symptom-free, but some may progress to cardiac, digestive, and/or neurological forms of the disease, which can be life-threatening when left untreated. The current treatment of CD is based on nifurtimox and benznidazole; developed in the 1960s and early 1970s. Both drugs have limitations, including a variable efficacy, long treatment courses, and toxicity. With only two drugs available for treatment, it is crucial to search for alternative targets for anti-CD therapies (2, 3). To this end, further information about basic regulatory functions in the parasite life cycle is much needed.

Trypanosoma cruzi is a protozoan parasite with a complex life cycle that requires one mammal and one arthropod host and involves three developmental stages. These changes allow the parasite to face environmental conditions such as variable temperatures and nutrient availability (4–6). The mechanisms that allow parasites to sense environmental changes and trigger a response are vital for their survival and establishment in a host (6, 7). The adaptive response requires modulating protein expression profiles, which are mainly regulated by post-transcriptional and post-translational modifications (PTMs) (8). Several PTMs have been reported in *T. cruzi,* including glycosylation of membrane proteins (9), acetylation of tubulins, and histone (10, 11), ubiquitination (12), SUMOylation (13), and phosphorylation of hundreds of proteins involved in several biological processes (14). Nevertheless, *O*-GlcNAcylation has not been reported yet in *T. cruzi* nor any Kinetoplastid protist.

O-GlcNAcylation is a dynamic PTM of proteins from the nucleus, cytoplasm, and mitochondria; it is involved in many different cell fundamental processes. Addition and removal of *O*-GlcNAc to/from proteins in animals is mediated by the enzymes *O*-GlcNAc transferase (OGT), and *O*-GlcNAcase (OGA) (15). UDP-GlcNAc, the donor substrate of OGT, is the final product of the hexosamine biosynthetic pathway (HBP). *O*-GlcNAcylation is thought to regulate protein functions in an analogous manner to protein phosphorylation. The crosstalk of both PTMs allows the regulation of cellular functions in response to nutrient levels and stress (16).

Protein *O*-GlcNAcylation has been reported in multicellular organisms and in some prokaryotic cells, but their presence in protists is a rather neglected field. Banerjee et al. reported homolog genes for the *O*-GlcNAc cycling enzymes in *Giardia lamblia* and *Cryptosporidium parvum* (17), and Perez Cervera et al. demonstrated the presence of *O*-GlcNAc-modified proteins in *Toxoplasma gondii* and *Plasmodium falciparum* by Western blot with the specific anti- *O*-GlcNAc RL2 and CTD 110.6 antibodies. Some *O*-GlcNAcylated proteins have been identified in these parasites, thirteen from *P. falciparum*, including actin, myosin, and the heat-shock protein HSP70. *O*-GlcNAcylated HSP70 was also identified by immunoprecipitation in *T. gondii*, and recently, proteomic analyses based on s-WGA enrichment and click chemistry revealed 357 *O*-GlcNAcylated proteins with several functions, including rhoptries, that are necessary for invasion (18–20).

This work is aimed to demonstrate the presence and to visualize *O*-GlcNAc-modified proteins in *T. cruzi* epimastigotes, and to evaluate the influence of some environmental conditions on *O*-GlcNAcylation patterns by Western blot, immunofluorescence, and enzymatic labeling. The enrichment of *O*-GlcNAc proteins was improved by a click chemistry-based strategy using an alkyne resin. Then, 1,271 putative *O*-GlcNAcylated proteins and six modification sites were identified by MS/MS.

MATERIALS AND METHODS

Culture of *Trypanosoma cruzi* Epimastigotes

Trypanosoma cruzi epimastigotes were cultured at 28°C in RPMI 1,640 medium supplemented with 10% heat-inactivated fetal bovine serum (FBS). Cultures were maintained in the growth phase.

Heat stress: *T. cruzi* epimastigotes were cultured in 25-cm^2 dishes, in 10 mL of RPMI 1,640 medium either at 28 or 37°C, at a concentration of 10^6 cells/mL. After 4 days of incubation, cultured cells were harvested by centrifugation at 2,500 × *g* for 20 min at 4°C and washed three times with PBS.

Glucose availability: Culture dishes with 10 mL of RPMI 1,640 medium supplemented with various glucose concentrations (17, 11.5, 5.5, and 0 mM) were inoculated with 10^6 parasites/mL and incubated for 5 days. Then, the cells were harvested by centrifugation at 2,500 × g for 20 min at 4°C and washed three times with PBS.

Protein Extraction

Control and experimental parasite cultures were lysed in the following homogenization buffer: 10 mM Tris/HCl, 150 mM NaCl, 1 mM EDTA, 1% (v/v) Triton X-100, 0.5% (w/v) sodium deoxycholate, 0.1% (w/v) SDS, protease inhibitor, pH 7.4. After centrifugation at 20,000 × g for 10 min, supernatants were recovered and frozen until used.

SDS-PAGE and Western Blotting

Proteins were run on 12% SDS-PAGE under reducing conditions. Gels were either stained with Coomassie blue or electroblotted onto a PVDF sheet. Blots were saturated with 5% (w/v) blotting-grade blocker (Bio-Rad) in TBS (Tris-buffered saline)-Tween [15 mM Tris, 140 mM NaCl, 0.5% (v/v) Tween] for 30 min. Primary antibodies were incubated overnight at 4°C. Mouse monoclonal anti-*O*-GlcNAc RL2 (ab2739) was used at a 1:1,000 dilution; mouse polyclonal anti-*O*-GlcNAc CTD 110.6 and anti-alpha tubulin DM1A (Sigma, St Louis Missouri, USA) antibodies were also used. The specificity of the RL2 antibodies was checked by co-incubation with 1 M free *O*-GlcNAc. Then, the membranes were washed three times for 10 min with TBS-Tween and incubated with anti-mouse IgG or IgM, HRP labeled secondary antibodies (Abcam, Cambridge, UK) at a 1:5,000 dilution. The membranes were washed three times for 10 min with TBS-Tween, and spots were detected by enhanced chemiluminescence with Hyperfilms (GE Healthcare, Chicago, USA). Three independent experiments were performed and images were captured using a Bio Rad Gel Doc imaging system and processed with Quantity One software. One representative blot is shown.

Immunoprecipitation

Immunoprecipitation protocol was carried on using magnetic beads (Bio-Rad California, USA). Ten microgram of anti-tubulin DM1A antibody (Sigma) diluted on 200 L of PBS-Tween 0.1% were incubated on Protein C magnetic beads for 10 min at room temperature, then magnetized and supernatant were discarded. After three washes, lysed epimastigotes were added and incubated 1 h. Then three washes were realized and beads transferred to a new tube. Finally, 40 µl of 1x reduced Laemmli Sample Buffer were added and incubated for 10 min at 70°C. SDS PAGE was performed and Wb using anti-*O*-GlcNAc RL2 as primary antibody, HRP conjugated anti-mouse as secondary antibody and revealed using HRP color development reagent (Bio-Rad).

Immunofluorescence Microscopy

For immunolabeling, purified *T. cruzi* epimastigotes were fixed in 4% (m/v) paraformaldehyde in PBS for 1 h at room temperature and washed with PBS. Parasite cells were permeabilized with 0.1% Tween 20 for 90 min. Non-specific sites were blocked with 1% BSA. Anti *O*-GlcNAc antibodies RL2 diluted 1:50 (in PBS) were added and incubated overnight. After three washes with PBS, the parasites were incubated with anti-mouse FITC antibodies (1:100 in PBS) and then fixed on glass slides with Fluoro Shield DAPI (Sigma). A Leica DM2000 microscope with a Leica DFC310 FX camera was used for visualization. The images were processed with the software Image J. One representative figure is shown of three independent experiments.

Enzymatic Labeling of O-GlcNAcylated Proteins

Click-it *O*-GlcNAc Enzymatic Labeling System (Invitrogen C33368) is a method for modification *in vitro* of *O*-GlcNAcylated proteins. Proteins were enzymatically labeled by the permissive mutant B-1,4 galactosyltransferase (Gal T1 Y289L), which transfers azido-modified galactose (GalNAz) from UDP-GalNAz to *O*-GlcNAc residues in the target proteins. A protein extract with no enzymatic treatment was used as a negative control, and α-crystallin, a protein with a low *O*-GlcNAcylation level (2–10%) was used as a positive control. Click-it *O*-GlcNAc enzymatic labeling was performed following the manufacturer's protocols. Labeled proteins were detected by Western blot with the Click-it Biotin Protein Analysis Detection Kit (Invitrogen C33372).

O-GlcNAcylated Proteins Labeling and Enrichment

Click-it *O*-GlcNAc enzymatic labeling was performed on *T. cruzi* protein extracts following the manufacturer's protocols, as described by Hahne et al. (21).

O-GlcNAcylated *T. cruzi* epimastigote proteins with azide tag were then enriched by covalent capture onto an alkyne resin through click chemistry, using the Click-it Protein Enrichment Kit (Invitrogen C10416). This technique uses the Cu(I)-catalyzed Huisgen cycloaddition to promote a cyclic addition reaction between an azide and a terminal alkyne, generating a 1,4-disubstituted 1,2,3-triazole as a covalent linkage. When the click reaction was complete, the beads with *O*-GlcNAcylated proteins were first reduced with 10 mM dithiothreitol (DTT) for 30 min at 55°C and then alkylated with 50 mM iodoacetamide (IAA) for 60 min at room temperature. The resin was subjected to an extensive washing procedure in column as follows: five washes with 1.5 mL of SDS wash buffer (100 mM Tris/HCl, pH 8; 1% SDS; 250 mM NaCl; 5 mM EDTA); five washes with 1.5 mL of urea buffer (8 M urea; 100 mM Tris/HCl, pH 8); 10 washes with 1.5 mL of 20% acetonitrile (ACN); and two washes with 1 mL of digestion buffer (100 mM TEAB, pH 8.2; 10% ACN).

Protein Digestion

Resin-bound proteins were digested overnight in 200 µL of digestion buffer containing 1 µg of trypsin/Lys-C mix. After digestion, the supernatant solution was discarded, and the resin was washed with 500 µL of deionized water. Both solutions, one containing non-retained peptides and the other containing *O*-GlcNAc proteins, were pooled and stored before desalting. The resin was then washed twice with 1.5 mL of MS-grade water, followed by two more washes with 1.5 mL of dephosphorylation buffer (50 mM Tris/HCl, pH 7.6; 100 mM NaCl; 1 mM DTT; 10 mM $MgCl_2$; 1 mM $MnCl_2$). Non-retained peptides were desalted in a C18 reversed-phase column and dried in a centrifugal vacuum system before LC-MS/MS analysis.

Beta-Elimination

To confirm *O*-GlcNAc sites an on-resin dephosphorylation step between the on-resin proteolytic digest and the on-resin β-elimination was added. So ideally all peptides bound to the alkyne resin should be *O*-GlcNAc modified. *O*-GlcNAcylated peptides linked to agarose beads were dephosphorylated at 37°C for 6 h in 400 µL of dephosphorylation buffer using 800 U of λ phosphatase and 20 U of calf intestine phosphatase. After dephosphorylation, the resin was washed twice with 1.5 mL of water and the slurry volume was adjusted to 300 µL with water before treatment with the GlycoProfile β-elimination Kit (Sigma Aldrich). The reaction mixture was incubated in an end-over-end shaker with extensive mixing at 4°C and quenched after 24 h with 1% trifluoroacetic acid (TFA). Agarose beads were discarded, and the solution containing β-eliminated peptides, corresponding to *O*-GlcNAcylated peptides, was desalted in C18 reversed-phase columns and dried in a centrifugal vacuum system before LC-MS/MS analysis.

Mass Spectrometry

The samples were reconstituted with 0.1% TFA in 4% ACN and analyzed by liquid chromatography (LC)-tandem mass spectrometry (MS/MS) using an Orbitrap Fusion Lumos Tribrid Mass Spectrometer (Thermo Electron, Bremen, Germany) online with an Ultimate 3000RSLCnano chromatographic system (Thermo Fisher Scientific, Sunnyvale, CA). The peptides were separated using a Dionex Acclaim PepMap RSLC C18 column. First, the peptides were concentrated and purified with a Dionex pre-column (C18 PepMap100, 2 cm × 100 µm ID, 100 Å pore size, 5 µm particle size) in solvent A (0.1% formic acid, 2% acetonitrile). Then, the peptides were separated on a Dionex reverse-phase LC EASY-Spray C18 column (PepMap RSLC C18, 50 cm × 75 µm ID, 100 Å pore size, 2 µm particle size) at

a 300 nL/min flow rate and 40°C. After column equilibration using 4% of solvent B (20% water-80% ACN-0.1% formic acid), the peptides were eluted from the analytical column by a two-step linear gradient (4–20% ACN/H_2O-0.1% formic acid for 220 min and 20–45% ACN/H_2O-0.1% formic acid for 20 min). For peptide ionization, spray voltage was set at 2.2 kV and the capillary temperature at 275°C. The mass spectrometer was used in data-dependent mode to switch consistently between MS and MS/MS. The time between master scans was set to 3 s. MS spectra were acquired in an *m/z* range of 375–1,500, with a FWHM resolution of 120 000 measured at 200 *m/z*. AGC target was set at 4.0e5 with a maximum injection time of 50 ms. The ion generated from polydimethylcyclosiloxane during the electrospray process the protonated $(Si(CH_3)_2O)_6$) at *m/z* 445.120025 was used as lock mass for internal mass calibration. The most abundant precursor ions were selected, and a higher-energy collisional dissociation fragmentation was performed and analyzed in the Orbitrap analyzer with a resolution of 50,000. The number of precursor ions was automatically defined along run in 3 s windows, using the Inject Ions for All Available Parallelizable Time option with a maximum injection time of 105 ms and an AGC target of 1.0e5. Charge state screening was enabled to include precursors with two and seven charge states. Dynamic exclusion was enabled with a repeat count of one and a duration of 60 s.

Protein Identification and Abundance Quantification

The acquired raw MS data were processed with the software Proteome Discoverer v.1.4.1.14 (Thermo Fisher Scientific). Data were searched via SEQUEST HT against the Uniprot *T. cruzi* reference proteome database (retrieved on February 14, 2018, 44 286 entries). The following parameters were used for searches: (i) trypsin; (ii) two missed cleavages were allowed; (ii) monoisotopic precursor tolerance of 10 ppm, followed by 0.6 Da for fragment ions from MS/MS; and (iii) cysteine carbamidomethylation (+57.0215) and methionine oxidation (+15.995) as variable modifications. False discovery rate (FDR) was processed using Percolator a semi-supervised machine learning to discriminate correct from incorrect peptide-spectrum matches (22), and was set to a *q*-value of 1 and 5% for, respectively, define high and low confident peptides. In addition, only peptide spectrum matches with a delta Cn Sequest HT parameters better than 0.15 were considered and proteins were identified with at least two peptides per protein. Additionally, a threshold was established based on the MS area, which meant that the proteins with the lowest intensities which conformed the summed intensity of 7×10^8 were considered potential background (21). The abundance of the different identified proteins were determined by label-free quantitative proteomics using the TOP 3 method (23, 24). Peptides from β-elimination experiments were identified as described above, except that dehydration of Ser and Thr (−18.011 a.m.u.) and β-elimination of Cys (−33.988 a.m.u.) were added as variable modifications. Mass spectrometry proteomics data were deposited in the ProteomeXchange Consortium via the PRIDE (25) partner repository with the dataset identifier PXD010285.

RESULTS

Trypanosoma cruzi Express O-GlcNAcylated Proteins

After the *O*-GlcNAc modification was first described in 1984, several approaches have been used to detect it. Antibody detection and residue enzymatic elongation by bovine GalT are commonly used. Both assays were performed herein to visualize *T. cruzi O*-GlcNAcome. A wide range of proteins, from 10 to 250 kDa, were recognized when epimastigote proteins were exposed to the broadly used anti *O*-GlcNAc antibodies RL2 (**Figure 1A**) and CTD110.6 (**Figure 1B**). *O*-GlcNAcylation was also detected in whole epimastigotes by immunofluorescence microscopy with the RL2 antibody (**Figure 1D**). To show evidence about the *O*-GlcNAcylation of an specific protein, an immunoprecipitation protocol were performed to isolate alpha tubulin, that were previously described in other protist parasites (19). The *O*-GlcNAcylation was revealed by western blot using RL2 as primary antibody.

To confirm the presence of *O*-GlcNAcylated proteins in *T. cruzi* epimastigotes, a galactose derivative (GalNAz) was bound to GlcNAc moieties by an engineered galactosyltransferase (GalT1 Y289L). This was followed by a selective and specific chemical addition of biotinalkyne to allow the detection of the tagged proteins or peptides by the avidin-peroxidase system (**Figure 2A**). This highly sensitive technique confirmed that the *T. cruzi* proteome is rich in *O*-GlcNAcylated proteins (**Figure 2B**).

These results demonstrate for the first time the presence of *O*-GlcNAc modifications in *T. cruzi*. No previous reports have been published about this PTM in any Kinetoplastid parasite.

Environmental Conditions Influence Protein O-GlcNAcylation Pattern in *T. cruzi* Epimastigotes

Protein *O*-GlcNAcylation exhibits a great dynamism. To assess whether *O*-GlcNAcylation patterns vary under diverse environmental conditions, parasites were grown under different temperatures and glucose availability. While *O*-GlcNAcylation was detected by western blot and immunofluorescence in every condition (**Figure 3C**), *O*-GlcNAcylated protein patterns under low glucose availability (0–5.5 mM) showed a higher reaction in bands of 60, 50, and 45 kDa. The 42 kDa band show higher *O*-GlcNAcylation mainly on 5.5 mM glucose condition (**Figure 3A**). Contrasting, under heat stress (37°C) most components showed reduced *O*-GlcNAcylation, except for 70 kDa band, as shown in **Figure 3B**.

Identification of O-GlcNAcylated Proteins in *T. cruzi*

Once the presence of *O*-GlcNAcylated proteins in *T. cruzi* was established, their identity was studied. Several methods for protein identification have been described, including some based on lectins or antibody enrichment; in the past 10 years, click chemistry-based methods have gained prominence. The highly sensitive labeling of proteins by azide-modified

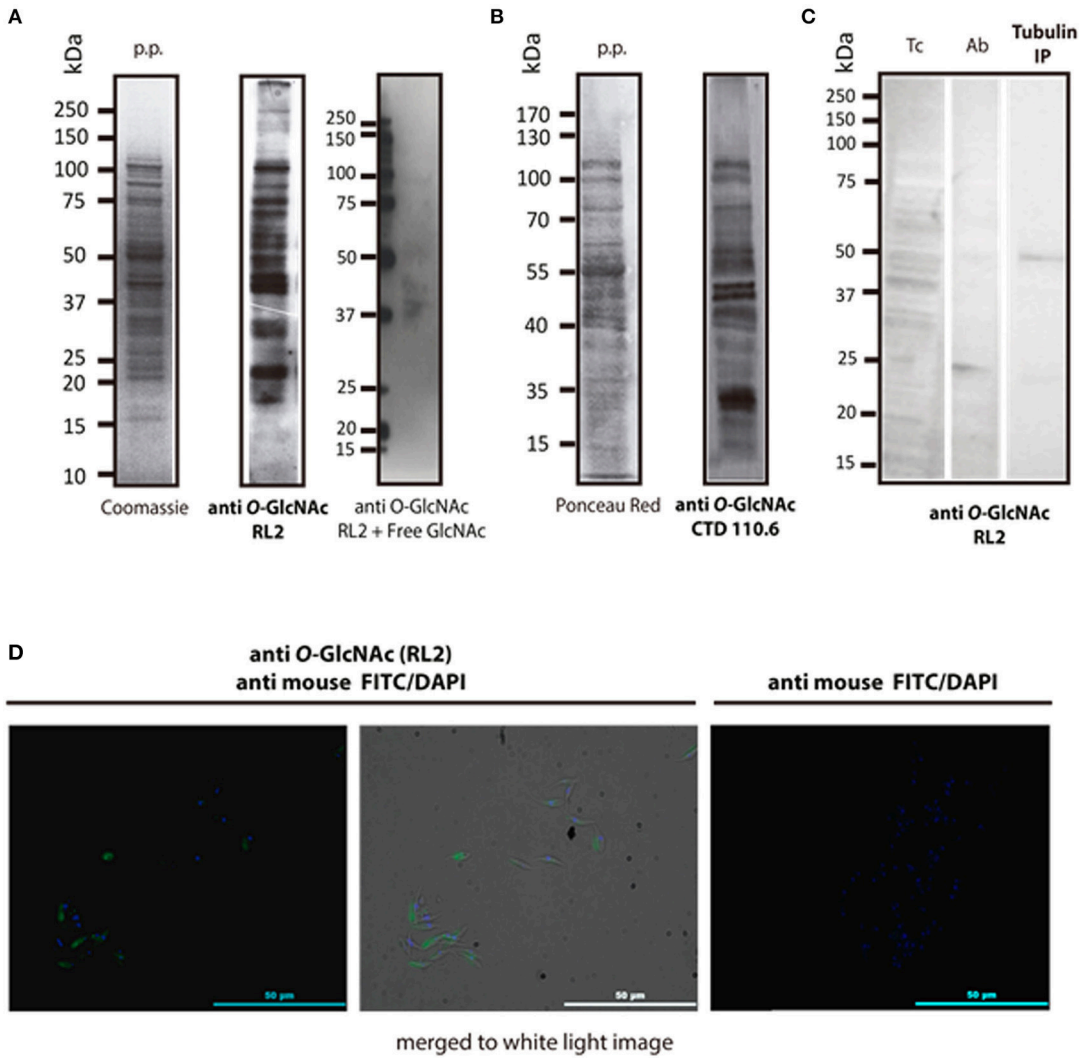

FIGURE 1 | Immune detection of *O*-GlcNAcylated proteins from *T. cruzi* epimastigotes. **(A)** RL2 antibody. Protein profile (p.p.) of epimastigotes in SDS-PAGE Coomassie blue, 20 μg, and Western blot with the RL2 antibody and Free GlcNAc control. Visualized by chemiluminescence. **(B)** CTD 110.6 antibody. Protein profile (p.p.) of epimastigotes stained with Red Ponceau, 30 μg. B2, Western blot with CTD 110.6. Visualized by chemiluminescence. **(C)** *T. cruzi* Alpha tubulin immunoprecipitation (DM1A ab) in western blot with anti *O*-GlcNAc RL-2. Tc, epimastigote lisate; Ab, antibody DM1A Tubulin IP; Immunoprecipitated Tubulin. **(D)** Immunofluorescence microscopy. Anti-*O*-GlcNAc RL-2 was used as the primary antibody and FITC-labeled anti-mouse as the secondary antibody.

galactose and copper-mediated click chemistry was used herein, followed by purification of modified proteins on an alkyne-resin (17) (**Figure 4**). On-resin trypsin proteolysis followed by LC-MS/MS allowed the identification of 1,271 putative *O*-GlcNAc proteins at 5% false discovery rate (FDR) and eliminating the proteins with the lowest intensities which could be considered as potential background as mentioned in materials and methods. These proteins belong to a broad range of biological functions and participating in various cellular pathways. Of the 10 most abundant putative *O*-GlcNAcylated proteins, three are constitutive of the cytoskeleton, three participate in oxidation reduction processes and the others include kinases, and proteins that participate in biosynthesis and stress response. The classification by function of the 100 most abundant based on Top3 quantification, are shown in **Figure 5**, and full data are available via ProteomeXchange, ID PXD010285 and **Supplementary Table 1**. Subsequent elution of on-resin *O*-GlcNAcylated peptides by β-elimination led to the identification of 6 peptides corresponding to *O*-GlcNAc modification sites at 5% FDR (**Supplementary Figure 1**).

DISCUSSION

Protein *O*-GlcNAcylation is ubiquitous in pluricellular organisms and has also been described in simple organisms, including viruses (26) and bacteria (27). Nevertheless, there are only few publications about protein *O*-GlcNAcylation in protist

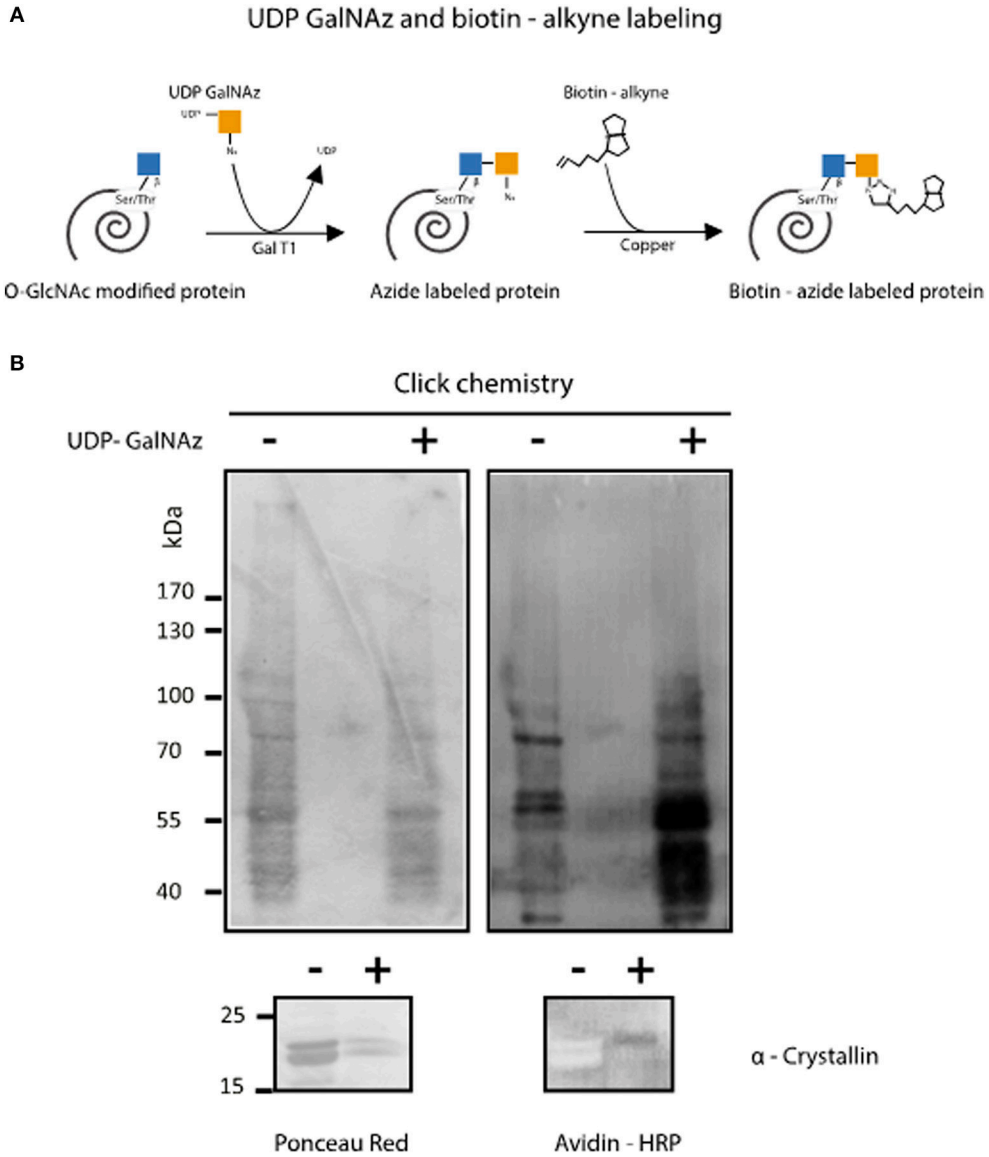

FIGURE 2 | Enzymatic detection of *T. cruzi O*-GlcNAcilayted proteins by click chemistry. **(A)** *O*-GlcNAcylated protein labeling by GalNAz and biotin alkyne using the Click iT^{TM} *O*-GlcNAc Enzymatic Labeling System and the Glycoprotein Detection Kit. **(B)** After labeling, *Trypanosoma cruzi O*-GlcNAcylated proteins were separated by SDS-PAGE, and Western blot was performed using HRP-labeled avidin. Protein load was assessed by Ponceau Red staining. α-Crystallin was used to control labeling efficiency.

organisms like *Giardia lamblia* and *Cryptosporidium parvum* (17), *Toxoplasma gondii* (18), and *Plasmodium falciparum* (19). To date, there is no report about protein *O*-GlcNAcylation in *T. cruzi* or any Kinetoplastid protist. In this work, we demonstrated the presence of *O*-GlcNAcylated proteins in *T. cruzi* epimastigotes and determined the identity of 1,271 putative *O*-GlcNAcylated proteins. Surprisingly, only 6 *O*-GlcNAc modifications sites were identified using dehydratation of Ser and Thr after beta-elimination from beads. MS-MS spectra of these peptides are given as **Supplementary Figure 1**. This low detection of modified peptides varies from our previous similar study (28). The explanation could be associated to the lower amount of proteins initially used and to the higher number of *O*-GlcNAc proteins. Each *O*-GlcNAc modified peptide is related to one of the following protein groups: clathrins, RNA helicases, DNA polymerases, trans-sialidases and two uncharacterized proteins as seen in **Supplementary Table 2**.

Several methods have been reported to detect *O*-GlcNAcylation. First, the sugar nucleotide UDP-GlcNAc is known to be a substrate for this PTM. UDP-GlcNAc is relatively abundant in *T. cruzi,* being produced by conventional HBP as

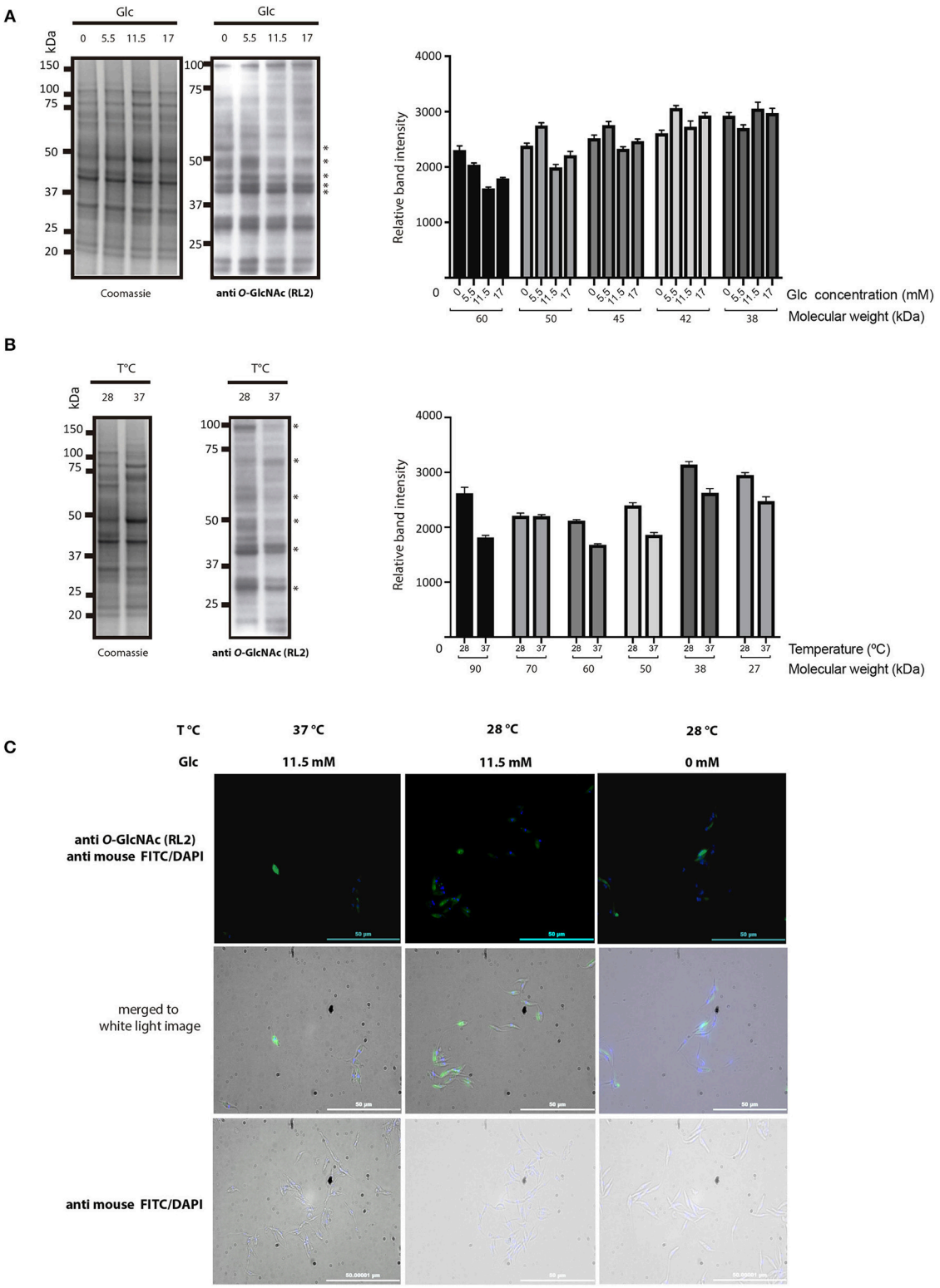

FIGURE 3 | *Trypanosoma cruzi* epimastigotes *O*-GlcNAcylation under various glucose availability and heat stress conditions. **(A)** *O*-GlcNAcylation profile under glucose availability variations. Glucose availability in culture media was 0, 5.5, 11.5, and 17 mM. Densitometry of several bands (*). **(B)** *O*-GlcNAcylation profile under heat stress at 37°C (28°C was the normal culture temperature). Densitometry of several bands (*). **(C)** Immunofluorescence microscopy. 28°C and Glc 11.5 mM were normal culture conditions. Heat stress at 37°C and low Glc availability (0 mM). Anti *O*-GlcNAc RL-2 antibody was used as the primary antibody and FITC-labeled anti mouse as the secondary antibody.

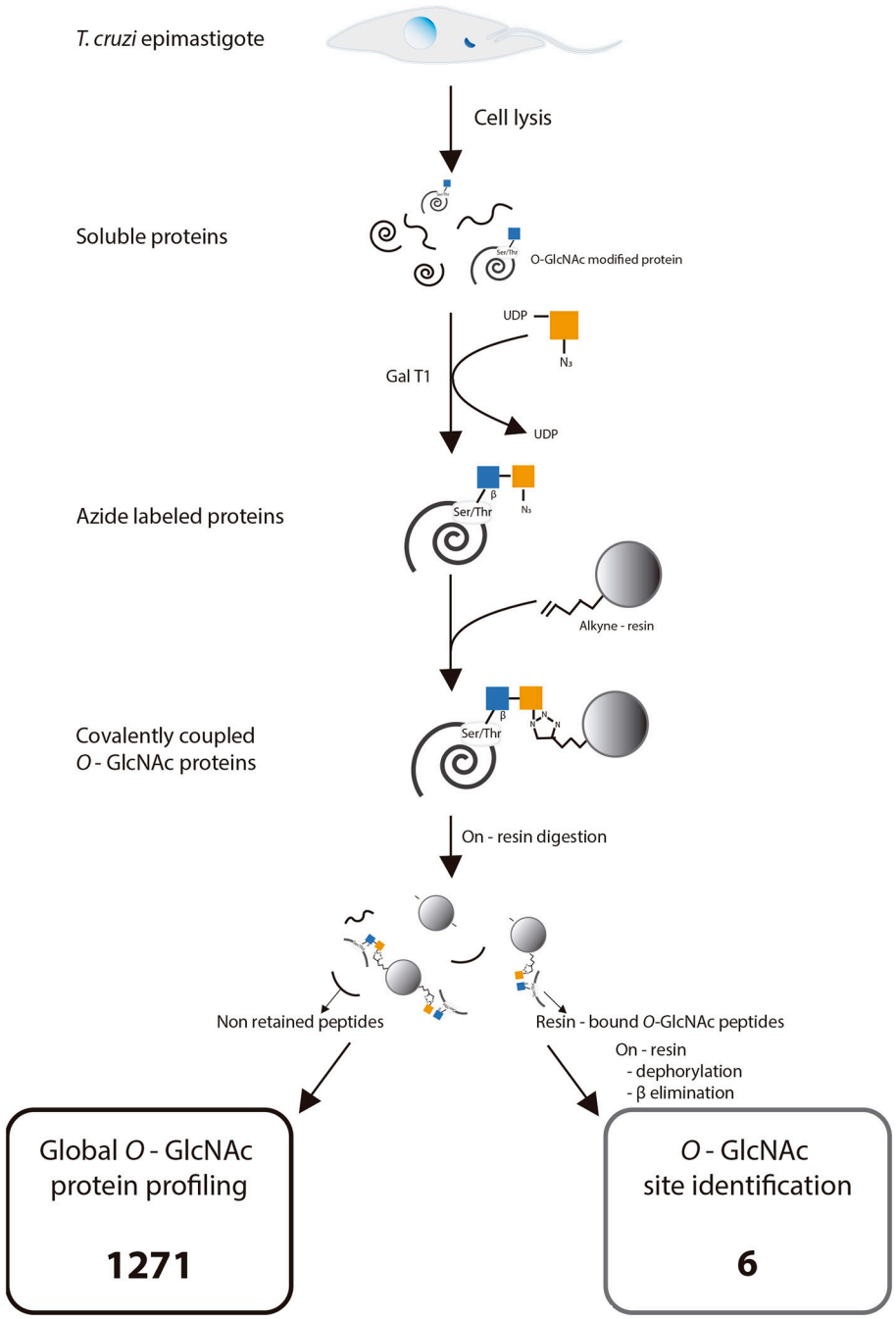

FIGURE 4 | Experimental strategy for click chemistry-based labeling, enrichment, and identification of *Trypanosoma cruzi O*-GlcNAc modified proteins. Adapted with permission from Hahne et al. (21). Copyright 2013 American Chemical Society.

- **1271** putative proteins identified by Global *O*-GlcNAcylated protein profiling.
- **6** modification sites.

Full data are available via ProteomeXchange with identifier PXD010285.

previously reported by Turnock and Ferguson (29). Second, a search for the sequences of the regulatory enzymes OGT and OGA in *T. cruzi* genome databases (for instance, by Banerje et al.) has been unfruitful, maybe due to the great number of unknown proteins in the parasite genome and the fact that it is not completely cured. Nevertheless, some organisms have been reported as producing *O*-GlcNAcylated proteins, like the protist *P. falciparum*, whose OGT and OGA enzyme variants have not been characterized yet. Bacterial species like *Listeria monocytogenes* (30) and *Streptococcus*

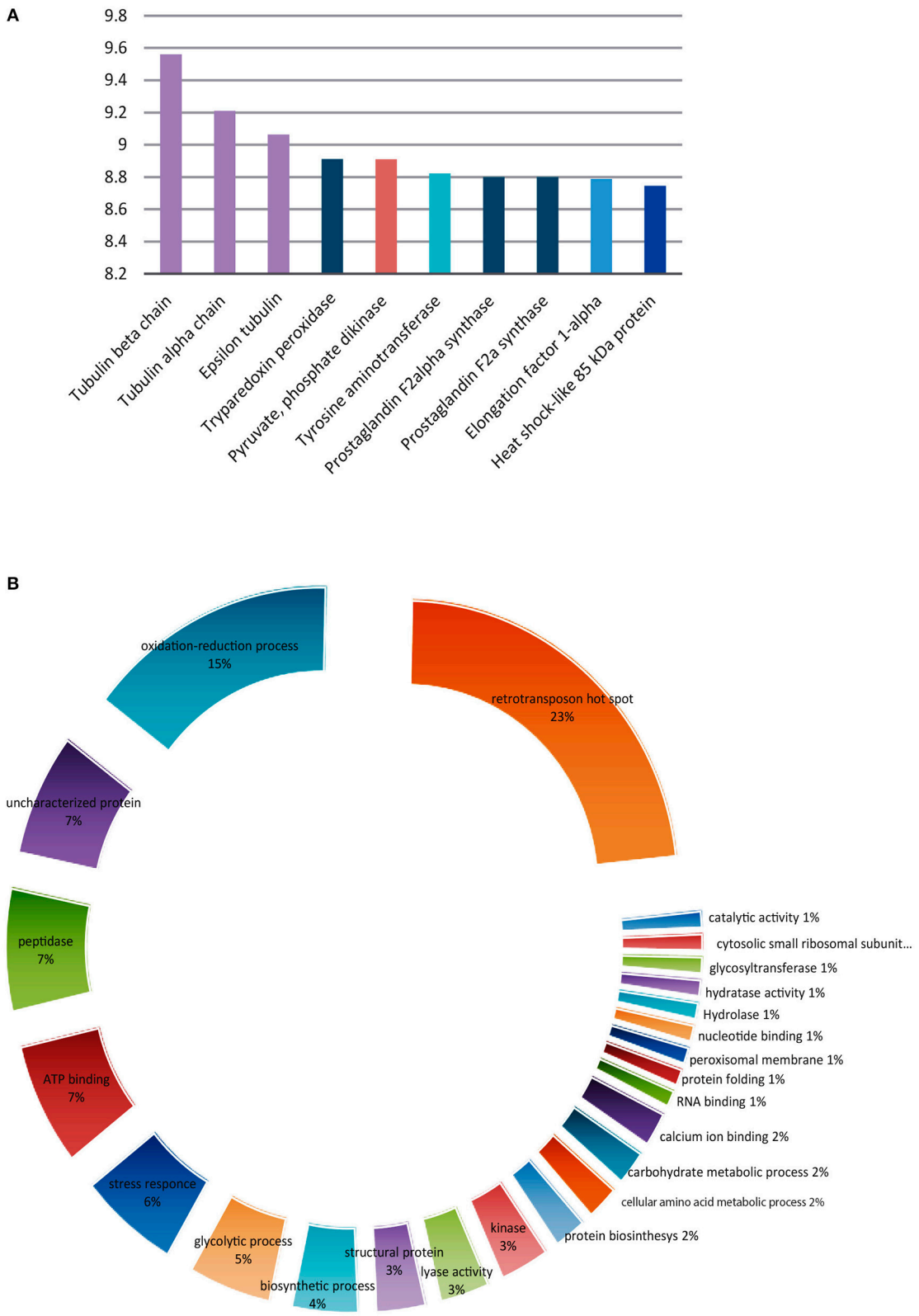

FIGURE 5 | *Trypanosoma cruzi* putative O-GlcNAcylated proteins. **(A)** The 10 most abundant using the TOP three method. **(B)** Classification according to their function of the 100 most abundant.

pneumoniae (31) code for different OGT variants, which are not homologous to the animal enzymes even when they have been proved to have critical roles in functions like motility and adhesion. All OGT-detecting methods rely on antibodies or activity measurement, even though antibody detection is only acceptable when the OGT coding gene has been fully identified.

This work is focused on detecting *O*-GlcNAcylated proteins by proteomic approaches (32). Various monoclonal antibodies that recognize *O*-GlcNAcylated proteins are available, including the RL2, CTD 110.6, 18B10.C7, 9D1.E4, and 1F5.D6 antibodies. The most widely used and more readily available antibodies to detect *O*-GlcNAcylation by Western blot are RL2 (33) and CTD 110.6 (34); these antibodies can detect a variety of modified proteins in different organisms, including protist cells (18, 19). Both antibodies were used herein to visualize *O*-GlcNAcylated protein in *T. cruzi* epimastigotes proteome; additionally, RL2 was used for fluorescence microscopy analysis. The parasite life cycle includes three development stages, and we focused our research on epimastigotes, being the only replicative extracellular stage, so we can prevent mammal cell contamination during protein extraction. As shown in **Figure 1**, the *T. cruzi* proteome is rich in *O*-GlcNAcylated proteins with a wide range of molecular weights, as previously observed for *T. gondii* and *P. falciparum*. RL2 is an IgG antibody that was raised specifically against *O*-GlcNAc moieties of nuclear pore complex (24). However, it can also detect some other *O*-GlcNAc modified proteins. CTD110.6 is an IgM antibody directed against the *O*-GlcNAcylated C-terminal domain of RNA polymerase II proteins (34). The latter has a broader reactivity than RL2, recognizing a variety of *O*-GlcNAc-modified proteins. These antibodies RL2 and CTD 110.6 did not recognize the same epitopes and therefore the observed patterns were not equal, as it has been previously reported (35). Western blot using RL2, still revealed that immunoprecipitated alpha tubulin was also *O*-GlcNAcylated, which have been reported for *P. falciparum* and *T. gondii* (19, 20). Immunofluorescence analysis with RL2 allowed us to visualize the *O*-GlcNac modification directly in the whole parasite. This first evidence of the presence of *O*-GlcNAcylated proteins in this parasite was further confirmed by a different approach. The *O*-GlcNAc modification (36) was first described by elongating *O*-GlcNAcylated residues with bovine GalT using UDP-[^{3}H]-galactose; in the last 10 years, this method has evolved to include techniques from click chemistry, which use a engineered modified GalT (GalT1 Y289L) that transfers GalNAz to *O*-GlcNAcylated residues, followed by a selective addition of biotin alkyne. This approach demonstrated a rich pattern of protein bands in *T. cruzi* lysates (**Figure 2**), confirming the presence of this PTM in *T. cruzi*.

Since *O*-GlcNAcylation is characterized by a dynamic response to medium stimuli, we exposed parasites to different amounts of glucose, a nutrient required for UDP-GlcNAc production, also considering that nutrient deprivation triggers metacyclogenesis in the hindgut of the insect host. Heat stress is another environmental condition that *T. cruzi* faces during mammal infection. *O*-GlcNAcylation patterns as observed by immunofluorescence showed no significant variations (**Figure 3C**); in contrast, the level of reaction observed in 60–42 kDa components by Western blot was higher in protein extracts from the low-glucose group (0–5.5 mM) (**Figure 3A**)and in 70-kDa band in the group under heat stress (**Figure 3B**), which could correspond to one of the previously reported parasite heat-shock protein (HSP) (7) and suggest a possible role of *O*-GlcNAcylation in the cellular homeostatic response in *T. cruzi*.

Once the presence of *O*-GlcNAcylated proteins in *T. cruzi* was established, we focused on identifying them. Thousands of *O*-GlcNAcylated proteins have been reported in mammal cells; however, only few *O*-GlcNAcylated proteins have been identified in protist organisms; HSP70 and tubulin were confirmed in *T. gondii* by immunoprecipitation (18). The same proteins were identified in *P. falciparum* by a combination of click chemistry enrichment and specific HSP70 and tubulin immune detection. In the same work, WGA- and click chemistry-enriched extracts were resolved by SDS-PAGE; the bands were excised and analyzed by mass spectrometry, identifying 13 proteins that participate in cell functions like glycolysis and cytoskeleton organization, or as chaperones (19). A similar approach allowed the detection of 357 *O*-GlcNAcylated proteins in *T. gondii,* including rhoptries, which play a role in host infection (20). Considering the work by Kupfershmid and other authors, reporting that click chemistry-based strategies improved protein identification (21, 37, 38), we combined click chemistry-based *O*-GlcNAcylated protein labeling, click chemistry enrichment on alkyn resin, and on-resin trypsin proteolysis with MS/MS peptide sequencing. However, it must be noted that there is a potential interference in the enrichment procedure with non-reducing GlcNAc residues on *O*-linked and *N*-linked glycoproteins as have been reported for ovalbumin (39); when in a similar approach only 1% of the proteins were unspecifically bound, as the summed intensity of the labeled sample were 60-fold higher than the negative control (21), in the present work an additional threshold was set based on the MS area as described in the material and methods section. This combination of methods allowed us to identify 1,271 proteins displaying a wide variety of biological functions, including nucleic acid synthesis, transcription, protein synthesis, structural constitution of cytoskeleton, mitochondrial function, stress response, ATP cycling, peptidase activity and noteworthy retro-transposon hot spot (RHS) that are kinetoplastids exclusive proteins whose functions remain unveiled (data are available via ProteomeXchange, ID PXD010285 and **Supplementary Table 1**). It is well-known that the most abundant surface glycoproteins of *T. cruzi* are the mucin-like proteins, which can be modified with multiple glycan chains attached to the peptide by α-GlcNAc-*O*-Thr linkages (40, 41). Also when it is unusual for surface glycoproteins, in some strains, an amount of non-substituted *O*-linked GlcNAc has been reported (42). Many cell surface, lysosomal, and secreted proteins like trans-sialidases, mucins and some proteases, are post-translationally modified by the addition of a β-GlcNAc to the asparagine (Asn) residues, usually followed by complex branched high mannose glycans

but it could also be found as a small chitobiose glycan ($GlcNAc_{1-2}Asn$) (43). So, the identification of extracellular proteins that are not expected to be *O*-GlcNAc modified is a matter of concern. However, only four of the 1,271 putative *O*-GlcNAcylated proteins were considered extracellular. Nevertheless, we cannot rule out the possibility that some of the identified surface or secreted proteins might also not be *O*-GlcNAc modified.

Several identified proteins were previously described as *O*-GlcNAcylated in other models, a finding that supports the universal role of *O*-GlcNAcylation in cell biology. The 10 most abundant putative modified proteins are listed in **Figure 5**. As shown, tubulin is abundantly represented among protist *O*-GlcNAcylated proteins and we found it on *T. cruzi* epimastigotes by immunoprecipitation as can be seen on **Figure 1C**; this was expected, since *T. cruzi* microtubules are cytoskeletal structures composed of two α- and one β-tubulin isoforms and are present in the flagellum and under the plasma membrane as subpellicular microtubules, and have important functions in motility, cellular morphology, intracellular transport, and cell division. Tubulin isoforms have also been studied as a target for substances with possible antichagasic activity (44) and as vaccine antigen candidates (45). Our results suggest the possibility to influence *T. cruzi* microtubule polymerization by interfering in tubulin *O*-GlcNAcylation, given the known role of *O*-GlcNAcylation in regulating microtubule formation (46).

Notably, the detection of the 6 *O*-GlcNAc peptides (**Supplementary Table 2**) gave us more possible targets to study the role of the *O*-GlcNAc modification in *T. cruzi*. Trans-sialidases are a highly studied group of proteins of *T. cruzi* that are involved in pathogenesis (47). Clathrins expression has been previously reported on *T. cruzi* and are known to mediate endocytosis at the flagellar pocket and the cytostome complex (48). Helicases and DNA polymerases are linked to replication and transcription processes and even DNA repair of oxidative lesions (49). All these proteins play important roles in *T. cruzi* stress response, nutrition and life cycle progression as have been reported for mammal cells (50). The meaning of these specific *O*-GlcNAc motifs is not possible to be predicted, nevertheless, this highlights the necessity of further research to elucidate the functions of *O*-GlcNAcylation in specific proteins and cellular processes of *T. cruzi*.

CONCLUSIONS

This is the first demonstration of the occurrence of the *O*-GlcNAc modification in *T. cruzi*. We also provide a large-scale identification of putative *O*-GlcNAcylated proteins with several cellular functions and 6 *O*-GlcNAc modification sites. Experimental evidence suggests the possible role of *O*-GlcNAcylation in the cellular homeostatic response in *T. cruzi* and opens a totally new field to study the mechanisms of parasite adaptation, survival, and invasion, which would help us to identify new drug targets.

DATA AVAILABILITY

Mass spectrometry proteomics data were deposited and can be found in the ProteomeXchange Consortium via the PRIDE (25) partner repository with the dataset identifier PXD010285.

AUTHOR CONTRIBUTIONS

ET-G, PS-S, YP-C, and EZ developed the hypotheses. ET-G performed most of the biochemical experiments and interpreted the data. MA-G and OR-D contributed performing certain experiments. LC performed the on resin digest, the mass spectrometry analysis and provided the resulting data. MB-T, MC-B, and TL provided biological material and technical support. PS-S, YP-C, and EZ initiated the project. ET-G, YP-C, TL, EZ, and PS-S analyzed the results. ET-G, PS-S, and YP-C drafted the manuscript. All authors contributed to refining the manuscript, read and approved the final version.

ACKNOWLEDGMENTS

To Karen Julissa Loaeza-Reyes, Yolanda Guevara Gomez, and Mariana De Alba Alvarado for their technical support. MA-G hold a fellowship of CONACyT from the government of Mexico. The authors thank the UNAM DGAPA-PAPIIT project IN227816 and IN216118, Red Temática de Glicociencia en Salud CONACyT, Cuerpo Académico Investigación en Salud UABJO CA-63 for their financial support. Proteomics analysis was supported by the Institut Paoli-Calmettes and the Centre de Recherche en Cancérologie de Marseille. Proteomic analyses were done using the mass spectrometry facility of Marseille Proteomics (marseille-proteomique.univ-amu.fr) supported by IBISA (Infrastructures Biologie Santé et Agronomie), Plateforme Technologique Aix-Marseille, the Cancéropôle PACA, the Provence-Alpes-Côte d'Azur Région, the Institut Paoli-Calmettes, and the Centre de Recherche en Cancérologie de Marseille. The mass spectrometry proteomics data have been deposited to the ProteomeXchange Consortium via the PRIDE partner repository with the dataset identifier PXD010285. This work fulfills one of the requirements for Elia Torres Gutiérrez to obtain a Ph.D. degree in Posgrado en Ciencias Biológicas, Universidad Nacional Autónoma de México (UNAM).

SUPPLEMENTARY MATERIAL

The Supplementary Material for this article can be found online at: https://www.frontiersin.org/articles/10.3389/fendo.2019.00199/full#supplementary-material

Supplementary Figure 1 | MS-MS spectra of the *O*-GlcNAcylated peptides.

Supplementary Table 1 | *T. cruzi* putative *O*-GlcNAcylated proteins in blue and potential background in red. Full data are available via ProteomeXchange with identifier PXD010285.

Supplementary Table 2 | *T. cruzi O*-GlcNAc peptides. Full data are available via ProteomeXchange with identifier PXD010285.

REFERENCES

1. WHO/World Health Organization. *Chagas Disease (American Trypanosomiasis) Fact Sheets*. Fact sheets. (2018). Available online at: http://www.who.int/news-room/fact-sheets/detail/chagas-disease-(american-trypanosomiasis) (accessed 2018 May, 15).
2. Rodriques Coura J, de Castro SL. A critical review on chagas disease chemotherapy. *Mem Inst Oswaldo Cruz.* (2002) 97:3–24. doi: 10.1590/S0074-02762002000100001
3. de Morais CGV, Castro Lima AK, Terra R, dos Santos RF, Da-Silva SAG, Dutra PML. The dialogue of the host-parasite relationship: *Leishmania* spp. and *Trypanosoma cruzi* Infection. *Biomed Res Int.* (2015) 2015:1–19. doi: 10.1155/2015/324915
4. Pérez-Morales D, Lanz-Mendoza H, Hurtado G, Martínez-Espinosa R, Espinoza B, Pérez-Morales D, et al. Proteomic analysis of *Trypanosoma cruzi* epimastigotes subjected to heat shock. *J Biomed Biotechnol.* (2012) 2012:902803. doi: 10.1155/2012/902803
5. Tyler KM, Engman DM. Flagellar elongation induced by glucose limitation is preadaptive for *Trypanosoma cruzi* differentiation. *Cell Motil Cytoskeleton.* (2000) 46:269–78. doi: 10.1002/1097-0169(200008)46:4<269::AID-CM4>3.0.CO;2-V
6. Jimenez V. Dealing with environmental challenges: mechanisms of adaptation in *Trypanosoma cruzi*. *Res Microbiol.* (2014) 165:155–65. doi: 10.1016/j.resmic.2014.01.006
7. Urményi TP, Silva R, Rondinelli E. The heat shock proteins of *Trypanosoma cruzi*. *Subcell Biochem.* (2014) 74:119–35. doi: 10.1007/978-94-007-7305-9_5
8. Clayton C, Shapira M. Post-transcriptional regulation of gene expression in trypanosomes and leishmanias. *Mol Biochem Parasitol.* (2007) 156:93–101. doi: 10.1016/j.molbiopara.2007.07.007
9. de Lederkremer RM, Agusti R. Glycobiology of *Trypanosoma cruzi*. *Adv Carbohydr Chem Biochem.* (2009) 62:311–66. doi: 10.1016/S0065-2318(09)00007-9
10. Souto-Padron T, Cunha e Silva NL, Souza W de. Acetylated alpha-tubulin in *Trypanosoma cruzi*: immunocytochemical localization. *Mem Inst Oswaldo Cruz.* (1993) 88:517–28. doi: 10.1590/S0074-02761993000400004
11. Picchi GFA, Zulkievicz V, Krieger MA, Zanchin NT, Goldenberg S, de Godoy LMF. Post-translational modifications of *Trypanosoma cruzi* canonical and variant histones. *J Proteome Res.* (2017) 16:1167–79. doi: 10.1021/acs.jproteome.6b00655
12. Cardoso J, Lima CDP, Leal T, Gradia DF, Fragoso SP, Goldenberg S, et al. Analysis of proteasomal proteolysis during the *in vitro* metacyclogenesis of *Trypanosoma cruzi*. *PLoS ONE*. (2011) 6:e21027.
13. Bayona JC, Nakayasu ES, Laverrière M, Aguilar C, Sobreira TJP, Choi H, et al. SUMOylation pathway in *Trypanosoma cruzi*: functional characterization and proteomic analysis of target proteins. *Mol Cell Proteomics.* (2011) 10:M110.007369.
14. Marchini FK, de Godoy LMF, Rampazzo RCP, Pavoni DP, Probst CM, Gnad F, et al. Profiling the *Trypanosoma cruzi* phosphoproteome. *PLoS ONE.* (2011) 6:e25381. doi: 10.1371/journal.pone.0025381
15. Bond MR, Hanover JA. A little sugar goes a long way: the cell biology of O-GlcNAc. *J Cell Biol*. (2015) 208:869–80. doi: 10.1083/jcb.201501101
16. Butkinaree C, Park K, Hart GW. O-linked beta-N-acetylglucosamine (O-GlcNAc): extensive crosstalk with phosphorylation to regulate signaling and transcription in response to nutrients and stress. *Biochim Biophys Acta*. (2010) 1800:96–106. doi: 10.1016/j.bbagen.2009.07.018
17. Banerjee S, Robbins PW, Samuelson J. Molecular characterization of nucleocytosolic O-GlcNAc transferases of Giardia lamblia and Cryptosporidium parvum. *Glycobiology*. (2009) 19:331–6. doi: 10.1093/glycob/cwn107
18. Perez-Cervera Y, Harichaux G, Schmidt J, Debierre-Grockiego F, Dehennaut V, Bieker U, et al. Direct evidence of O-GlcNAcylation in the apicomplexan Toxoplasma gondii: a biochemical and bioinformatic study. *Amino Acids*. (2011) 40:847–56. doi: 10.1007/s00726-010-0702-4
19. Kupferschmid M, Aquino-Gil MO, Shams-Eldin H, Schmidt J, Yamakawa N, Krzewinski F, et al. Identification of O-GlcNAcylated proteins in Plasmodium falciparum. *Malar J*. (2017) 16:485. doi: 10.1186/s12936-017-2131-2
20. Aquino-Gil MO, Kupferschmid M, Shams-Eldin H, Schmidt J, Yamakawa N, Mortuaire M, et al. Apart from rhoptries, identification of toxoplasma gondii's o-glcnacylated proteins reinforces the universality of the O-GlcNAcome. *Front Endocrinol*. (2018) 9:450. doi: 10.3389/fendo.2018.00450
21. Hahne H, Sobotzki N, Nyberg T, Helm D, Borodkin VS, van Aalten DMF, et al. Proteome Wide Purification and Identification of *O* -GlcNAc-modified proteins using click chemistry and mass spectrometry. *J Proteome Res*. (2013) 12:927–36. doi: 10.1021/pr300967y
22. Brosch M, Yu L, Hubbard T, Choudhary J. Accurate and sensitive peptide identification with mascot percolator. *J Proteome Res*. (2009) 8:3176–81. doi: 10.1021/pr800982s
23. Silva JC, Gorenstein MV, Li G-Z, Vissers JPC, Geromanos SJ. Absolute quantification of proteins by LCMS ^{E}. *Mol Cell Proteomics*. (2006) 5:144–56. doi: 10.1074/mcp.M500230-MCP200
24. Ahrné E, Molzahn L, Glatter T, Schmidt A. Critical assessment of proteome-wide label-free absolute abundance estimation strategies. *Proteomics*. (2013) 13:2567–78. doi: 10.1002/pmic.201300135
25. Vizcaíno JA, Csordas A, del-Toro N, Dianes JA, Griss J, Lavidas I, et al. 2016 update of the PRIDE database and its related tools. *Nucleic Acids Res*. (2016) 44:D447–56. doi: 10.1093/nar/gkv1145
26. Ko Y-C, Tsai W-H, Wang P-W, Wu I-L, Lin S-Y, Chen Y-L, et al. Suppressive regulation of KSHV RTA with O-GlcNAcylation. *J Biomed Sci*. (2012) 19:12. doi: 10.1186/1423-0127-19-12
27. Ostrowski A, Gundogdu M, Ferenbach AT, Lebedev AA, van Aalten DMF. Evidence for a functional O-GlcNAc system in the thermophilic bacterium Thermobaculum terrenum. *J Biol Chem*. (2015) 290:30291–305. doi: 10.1074/jbc.M115.689596
28. Deracinois B, Camoin L, Lambert M, Boyer J-B, Dupont E, Bastide B, et al. O-GlcNAcylation site mapping by (azide-alkyne) click chemistry and mass spectrometry following intensive fractionation of skeletal muscle cells proteins. *J Proteomics*. (2018) 186:83–97. doi: 10.1016/j.jprot.2018.07.005
29. Turnock DC, Ferguson MAJ. Sugar nucleotide pools of Trypanosoma brucei, *Trypanosoma cruzi*, and Leishmania major. *Eukaryot Cell*. (2007) 6:1450–63. doi: 10.1128/EC.00175-07
30. Shen A, Kamp HD, Gründling A, Higgins DE. A bifunctional O-GlcNAc transferase governs flagellar motility through anti-repression. *Genes Dev*. (2006) 20:3283–95. doi: 10.1101/gad.1492606
31. Shi W-W, Jiang Y-L, Zhu F, Yang Y-H, Shao Q-Y, Yang H-B, et al. Structure of a novel O-linked N-acetyl-D-glucosamine (O-GlcNAc) transferase, GtfA, reveals insights into the glycosylation of pneumococcal serine-rich repeat adhesins. *J Biol Chem*. (2014) 289:20898–907. doi: 10.1074/jbc.M114.581934
32. Vercoutter-Edouart A-S, Yazidi-Belkoura IE, Guinez C, Baldini S, Leturcq M, Mortuaire M, et al. Detection and identification of O-GlcNAcylated proteins by proteomic approaches. *Proteomics*. (2015) 15:1039–50. doi: 10.1002/pmic.201400326
33. Holt GD, Snow CM, Senior A, Haltiwanger RS, Gerace L, Hart GW. Nuclear pore complex glycoproteins contain cytoplasmically disposed O-linked N-acetylglucosamine. *J Cell Biol*. (1987) 104:1157–64. doi: 10.1083/jcb.104.5.1157
34. Comer FI, Vosseller K, Wells L, Accavitti MA, Hart GW. Characterization of a mouse monoclonal antibody specific for O-linked N-acetylglucosamine. *Anal Biochem*. (2001) 293:169–77. doi: 10.1006/abio.2001.5132
35. Okuda T. Western blot data using two distinct anti-O-GlcNAc monoclonal antibodies showing unique glycosylation status on cellular proteins under 2-deoxy-d-glucose treatment. *Data Br*. (2017) 10:449–53. doi: 10.1016/j.dib.2016.12.001
36. Torres CR, Hart GW. Topography and polypeptide distribution of terminal N-acetylglucosamine residues on the surfaces of intact lymphocytes. Evidence for O-linked GlcNAc. *J Biol Chem*. (1984) 259:3308–17.
37. Zaro BW, Yang Y-Y, Hang HC, Pratt MR. Chemical reporters for fluorescent detection and identification of O-GlcNAc-modified proteins reveal glycosylation of the ubiquitin ligase NEDD4-1. *Proc Natl Acad Sci USA*. (2011) 108:8146–51. doi: 10.1073/pnas.1102458108
38. Alfaro JF, Gong C-X, Monroe ME, Aldrich JT, Clauss TRW, Purvine SO, et al. Tandem mass spectrometry identifies many mouse brain O-GlcNAcylated proteins including EGF domain-specific O-GlcNAc transferase targets. *Proc Natl Acad Sci USA*. (2012) 109:7280–5. doi: 10.1073/pnas.1200425109
39. Boeggeman E, Ramakrishnan B, Kilgore C, Khidekel N, Hsieh-Wilson LC, Simpson JT, et al. Direct identification of nonreducing GlcNAc residues on

N-glycans of glycoproteins using a novel chemoenzymatic method. *Bioconjug Chem.* (2007) 18:806–14. doi: 10.1021/bc060341n
40. Previato JO, Jones C, Gonçalves LP, Wait R, Travassos LR, Mendonça-Previato L. O-glycosidically linked N-acetylglucosamine-bound oligosaccharides from glycoproteins of *Trypanosoma cruzi*. *Biochem J.* 1994) 301 (Pt 1):151–9. doi: 10.1042/bj3010151
41. Previato JO, Sola-Penna M, Agrellos OA, Jones C, Oeltmann T, Travassos LR, et al. Biosynthesis of O-N-acetylglucosamine-linked glycans in *Trypanosoma cruzi*. characterization of the novel uridine diphospho-N-acetylglucosamine:polypeptide N-acetylglucosaminyltransferase-catalyzing formation of N-acetylglucosamine alpha1–>O-threonine. *J Biol Chem.* (1998) 273:14982–8. doi: 10.1074/jbc.273.24.14982
42. Salto ML, Gallo-Rodriguez C, Lima C, de Lederkremer RM. Separation of Galfβ1→ XGlcNAc and Galpβ1→ XGlcNAc (X = 3, 4, and 6) as the alditols by high-pH anion-exchange chromatography and thin-layer chromatography: characterization of mucins from *Trypanosoma cruzi*. *Anal Biochem.* (2000) 279:79–84. doi: 10.1006/abio.1999.4466
43. Alves MJM, Kawahara R, Viner R, Colli W, Mattos EC, Thaysen-Andersen M, et al. Comprehensive glycoprofiling of the epimastigote and trypomastigote stages of *Trypanosoma cruzi*. *J Proteomics.* (2017) 151:182–92. doi: 10.1016/j.jprot.2016.05.034
44. Sueth-Santiago V, Decote-Ricardo D, Morrot A, Freire-de-Lima CG, Lima MEF. Challenges in the chemotherapy of Chagas disease: looking for possibilities related to the differences and similarities between the parasite and host. *World J Biol Chem.* (2017) 8:57–80. doi: 10.4331/wjbc.v8.i1.57
45. Montalvão F, Nascimento DO, Nunes MP, Koeller CM, Morrot A, Lery LMS, et al. Antibody repertoires identify β-tubulin as a host protective parasite antigen in mice infected with *Trypanosoma cruzi*. *Front Immunol.* (2018) 9:671. doi: 10.3389/fimmu.2018.00671
46. Ji S, Kang JG, Park SY, Lee J, Oh YJ, Cho JW. O-GlcNAcylation of tubulin inhibits its polymerization. *Amino Acids.* (2011) 40:809–18. doi: 10.1007/s00726-010-0698-9
47. Nardy AFFR, Freire-de-Lima CG, Pérez AR, Morrot A. Role of *Trypanosoma cruzi* trans-sialidase on the escape from host immune surveillance. *Front Microbiol.* (2016) 7:348. doi: 10.3389/fmicb.2016.00348
48. Kalb LC, Frederico YCA, Batista CM, Eger I, Fragoso SP, Soares MJ. Clathrin expression in *Trypanosoma cruzi*. *BMC Cell Biol.* (2014) 15:23. doi: 10.1186/1471-2121-15-23
49. Schamber-Reis BLF, Nardelli S, Régis-Silva CG, Campos PC, Cerqueira PG, Lima SA, et al. DNA polymerase beta from *Trypanosoma cruzi* is involved in kinetoplast DNA replication and repair of oxidative lesions. *Mol Biochem Parasitol.* (2012) 183:122–31. doi: 10.1016/j.molbiopara.2012.02.007
50. Liu C, Li J. O-GlcNAc: a sweetheart of the cell cycle and DNA damage response. *Front Endocrinol.* (2018) 9:415. doi: 10.3389/fendo.2018.00415

Conflict of Interest Statement: The authors declare that the research was conducted in the absence of any commercial or financial relationships that could be construed as a potential conflict of interest.

frontiers in Endocrinology

ORIGINAL RESEARCH
published: 08 May 2019
doi: 10.3389/fendo.2019.00289

O-GlcNAcylation Is Involved in the Regulation of Stem Cell Markers Expression in Colon Cancer Cells

Gabriela Fuentes-García[1], *M. Cristina Castañeda-Patlán*[1], *Anne-Sophie Vercoutter-Edouart*[2], *Tony Lefebvre*[2] *and Martha Robles-Flores*[1]*

[1] *Departamento de Bioquímica, Facultad de Medicina, Universidad Nacional Autónoma de México, Mexico City, Mexico,*
[2] *Unité de Glycobiologie Structurale et Fonctionnelle, CNRS, UMR 8576, University of Lille, Lille, France*

OPEN ACCESS

Edited by:
Yehiel Zick,
Weizmann Institute of Science, Israel

Reviewed by:
Hai-Bin Ruan,
Medical School - University of Minnesota, United States
Edgar Zenteno,
National Autonomous University of Mexico, Mexico
Mauricio Reginato,
College of Medicine, Drexel University, United States

***Correspondence:**
Martha Robles-Flores
rmartha@unam.mx

Specialty section:
This article was submitted to Molecular and Structural Endocrinology, a section of the journal Frontiers in Endocrinology

Received: *28 September 2018*
Accepted: *23 April 2019*
Published: *08 May 2019*

Citation:
Fuentes-García G, Castañeda-Patlán MC, Vercoutter-Edouart A-S, Lefebvre T and Robles-Flores M (2019) O-GlcNAcylation Is Involved in the Regulation of Stem Cell Markers Expression in Colon Cancer Cells. Front. Endocrinol. 10:289. doi: 10.3389/fendo.2019.00289

The dynamic *O*-linked-N-acetylglucosamine posttranslational modification of nucleocytoplasmic proteins has emerged as a key regulator of diverse cellular processes including several hallmarks of cancer. However, the role played by this modification in the establishment of CSC phenotype has been poorly studied so far and remains unclear. In this study we confirmed the previous reports showing that colon cancer cells exhibit higher *O*-GlcNAc basal levels than non-malignant cells, and investigated the role played by *O*-GlcNAcylation in the regulation of CSC phenotype. We found that the modification of *O*-GlcNAcylation levels by pharmacological inhibition of the *O*-GlcNAc-transferase enzyme that adds *O*-GlcNAc (OGT), but not of the enzyme that removes it (OGA), increased the expression of all stem cell markers tested in our colon malignant cell lines, and induced the appearance of a double positive (CD44+/CD133+) small stem cell-like subpopulation (which corresponded to 1–10%) that displayed very aggressive malignant phenotype such as increased clonogenicity and spheroid formation abilities in 3D culture. We reasoned that OGT inhibition would mimic in the tumor the presence of severe nutritional stress, and indeed, we demonstrated that nutritional stress reproduced in colon cancer cells the effects obtained with OGT inhibition. Thus, our data strongly suggests that stemness is regulated by HBP/*O*-GlcNAcylation nutrient sensing pathway, and that *O*-GlcNAc nutrient sensor represents an important survival mechanism in cancer cells under nutritional stressful conditions.

Keywords: colon cancer, *O*-GlcNAc, cancer stem cells, stemness, OGT, OGA

INTRODUCTION

Colorectal cancer (CRC) is one of the most prevalent cancers and is a leading cause of cancer mortality worldwide. It is well-known that tumors are formed by different cells, and that among them, the cancer stem cell (CSC) subpopulation are proposed to be responsible for tumor initiation, drug and radiation resistance, invasive growth, metastasis, and tumor relapse (1). Several colorectal CSC markers have been reported to date, including CD133, CD44, CD24, CD166, and leucine-rich repeat-containing G-protein-coupled receptor 5 (LGR5) (1, 2). In addition, the CD44 isoform containing variant exon v6 (CD44v6) has been reported to play an important role in the progression, metastasis, and prognosis of CRC (3, 4).

O-linked β-N-acetylglucosamine (*O*-GlcNAc) protein modification has emerged as a critical regulator of diverse cellular processes, but its role in stem cells (SCs) and pluripotency has been poorly investigated so far and remains unclear. In this respect, several studies have suggested that O-GlcNAcylation promotes SC maintenance, and decrease in *O*-GlcNAcylation may be required for SC differentiation (5). Surprisingly, this highly dynamic modification of proteins is regulated only by two enzymes: the *O*-GlcNAc transferase (OGT), which adds the residue and the *O*-GlcNAcase (OGA), which removes it. Increased OGT activity has been shown to contribute to maintenance of stemness and to prevent differentiation to specific tissue types (6, 7). In addition, it has also been reported that increased OGT activity affects transcriptional activity of Sox2 and Oct4 SC marker proteins to maintain genomic stability, thereby maintaining self-renewal (5, 8).

Growth and proliferation of cancer cells tightly depend on their nutritional environment, particularly on glucose availability. It is well- known that SCs originating in hypoxic niches reprogram their metabolism from oxidative phosphorylation to aerobic glycolysis to increase glycolytic activity even in the presence of oxygen (Warburg effect). Glutamine is also taken up actively in embryonic SCs (9). However, even though the contribution of the metabolic and nutrient sensing pathways to stemness maintenance is recognized, there is very little understanding of the molecular mechanisms that link stemness to the nutrient-sensing pathways (7). However, among these, the hexosamine biosynthesis pathway (HBP) is probably most relevant. This pathway, which is triggered by increased glucose uptake, is helpful in biosensing glucose and routing it through a shunt pathway to make UDP-N-Acetyl glucosamine (UDP-GlcNAc) which is utilized for *O*- GlcNAc modification of cytosolic, nuclear and mitochondrial proteins (7). In this respect, it is well-known that *O*-GlcNAcylation adjusts protein function according to the nutritional status of the cell. Remarkably, increased glucose uptake has been demonstrated that leads to increased OGT activity (7, 8), and may be instrumental in regulating self-renewal not only in embryonic and hematopoietic SCs but also in CSCs. In this study we investigated the role played by *O*-GlcNAcylation in the establishment of CSC cell phenotype. Our data indicate that stemness is regulated by HBP/*O*-GlcNAcylation nutrient sensing pathway, and that *O*-GlcNAc nutrient sensor represents an important survival mechanism in cancer cells under nutritional stressful conditions.

MATERIALS AND METHODS

Reagents and Antibodies

The following antibodies were used in the experiments: allophycocyanin (APC)-conjugated mouse anti-CD44 from BD Biosciences, phycoerythrin (PE)-conjugated mouse anti-CD133 from Miltenyi Biotec, rabbit anti-CD44, rabbit anti-CD133, and mouse anti-OGT from Abcam, Alexa 647-conjugated rabbit anti-mouse from Invitrogen; rabbit anti-β-tubulin from Cell Signaling Technology (Danvers, MA, USA); Alexa 488-conjugated goat anti-rabbit from Molecular Probes, Inc., (Eugene, OR, USA), mouse anti-*O*-GlcNAc (RL2) from Thermo Fisher Scientific; mouse anti-GAPDH from Santa Cruz Biotechnoloigy Inc (Sta. Cruz, CA, USA).

Cell Lines

Primary SW480 and its derivative metastatic SW620 colorectal cell lines, express a truncated version of APC (Adenomatous polyposis coli), have constitutively active Wnt signaling and are prototype of KRAS-driven cancer cells (KRAS G12V, APC A1457T/K1462R, FGFR3 S400R, TP53 R273H, and STK11 G58S mutations) (10). These cancer cell lines and the non-malignant 112CoN colon cell line used here were purchased from American Type Culture Collection (ATCC; Manassas, VA, USA) and were authenticated in June 2017 by Short Tandem Repeat DNA profiling performed at the Instituto Nacional de Medicina Genómica (INMEGEN) in Mexico City.

Cell Culture

112CoN cells were maintained in Dulbecco's Modified Eagle's medium (DMEM) supplemented with 10% (v/v) fetal bovine serum (FBS), antibiotics (120 mg/ml penicillin and 200 mg/ml streptomycin) and 2 mM L-glutamine. SW480 and SW620 cells were maintained in DMEM F-12 supplemented with 5% (v/v) FBS, antibiotics and 2mM glutamine. All cells were cultured in a humidified 5% (v/v) CO_2 incubator at 37°C. For starvation cells were washed twice with phosphate-buffered saline (PBS, GIBCO/Invitrogen) and placed in HBSS buffer (GIBCO/Invitrogen).

Western Blotting

Protein samples (30 μg) were separated by 10% SDS-PAGE followed by electrophoretic transfer onto nitrocellulose membranes (Bio-Rad, Hercules, CA, USA). The membranes were blocked with 5% (w/v) non-fat dry milk and incubated overnight at 4°C with the corresponding primary antibody. Detection was performed using the SuperSignal Kit (Pierce) with a horseradish peroxidase-conjugated second antibody. Actin or β-tubulin were used as control for equal loading.

Immunofluorescence and Confocal Microscopy

Cells were seeded into 8-chamber culture slides (LabTek®) at 5 × 10^4 cells/ml per chamber overnight. Then, samples were fixed with 1% (w/v) of paraformaldehyde in PBS for 10 min at room temperature (RT). Fixed cells were washed with PBS and cell permeabilization were performed with 1% (v/v) Triton X-100 in PBS for 5 min. Unspecific interaction sites were blocked with 3% (w/v) BSA/PBS. After washing, the slides were incubated with anti-*O*-GlcNAc, anti-CD133 or anti-CD44 primary antibodies (Abcam) diluted in 1% (m/v) BSA/PBS overnight at 4°C in darkness. Cells were washed with PBS, followed by incubation with secondary Alexa Fluor 647-conjugated goat anti-rabbit or Alexa 488-conjugated goat anti-mouse antibodies (Invitrogen) for 2 h at RT. Chambers were incubated with DAPI (SIGMA Aldrich) in PBS for 5 min at RT. After washing three times with PBS, the slides were mounted with Vectorshield® (Vector

Labs, CA). Cells were examined under a Nikon A1R+ STORM confocal microscopy. Pictures were analyzed with ImageJ.

Flow Cytometry

For membrane staining of CD44 and CD133, 1×10^4 cells were detached with EDTA-PBS 10 mM solution, scraped gently and collected by centrifugation at 500 g. Pellet were washed twice with PBS and samples were incubated with anti-CD44-APC coupled (BD Bioscience), anti-CD133-PE-coupled (Myltenyi), or with a mix of CD44/CD133 during 20 min at 4°C in darkness. Then, PBS were added and cells were newly centrifuged. Finally, samples were analyzed with an Attune® cytometer.

For intracellular staining of OGT and *O*-GlcNAc, cells were detached in the same way but immediately they were fixed with 1% (m/v) of paraformaldehyde in PBS for 10 min at 4°C. Fixed cells were permeabilized with absolute methanol for 20 min on ice and unspecific interaction sites were blocked with 3% (m/v) BSA in PBS. Anti O-GlcNAc (RL2) or anti-OGT antibodies were added during 30 min at 4°C in darkness. Cells were washed one time and incubated with FITC-coupled anti-mouse or FITC-coupled anti-rabbit secondary antibodies. Cell were washed one time with PBS. Finally, samples were analyzed with a FACScalibur cytometer. All data were analyzed by FlowJo X software.

Cell Sorting

As in flow cytometry, cells were detached in the same conditions. Samples were incubated with APC-conjugated anti CD44 (BD Bioscience), PE-conjugated anti-CD133 or a mix of ant-CD44/CD133 during 20 min at 4°C in darkness. Cells were washed. Samples were filtrated and collected in special cell cytometry sterile tubes. Cell sorting was performed to separate CD44+, CD133+ or CD44+/CD133+ (double positive) cells in a MoFlow Sorter. Later cells were seeded in different culture media types (DMEMF-12 with 5% (v/v) FBS, colony formation medium with ITS, or 3D culture media).

Pharmacological Inhibitions

8×10^5 cells were seeded in 6 -well culture plaques and incubated overnight. Then, for inhibition of OGT, cells were incubated 24 h in the absence (vehicle DMSO) or presence of Ac5SGlcNAc (50 μM final dilution), and for inhibition of OGA, were incubated 24 h in the absence (vehicle DMSO) or presence of Thiamet-G (1 μM final dilution). Cells were incubated at 37°C, and pictures of cell cultures for each treatment were taken at the end of incubation periods. The cells were then collected to perform flow cytometry and to make lysates for Western blotting.

Apoptosis

Apoptosis was measured using the Annexin-V-FLUOS Staining Kit (Sigma-Aldrich) as recommended by the manufacturer's instructions. Briefly, after 24 h of incubation with Ac5sGlcNAc or ThiametG, cells were gently scraped (we did no use trypsin to detach cells to avoid the unspecific exposure of Annexin V), centrifuged and washed twice in PBS. Annexin V-FITC in the staining buffer and propidium iodide were added to cell suspension and incubated for 10 min at room temperature. Cell were washed and analyzed with Attune Flow Cytometer.

Proliferation Assay

Proliferation was measured by labeling of cells with the fluorescent dye Carboxyfluorescein Diacetate Succinimidyl Ester (CFSE) to track generations of cells, since the associated fluorescence signal decreases by half with each cell division cycle. 5×10^4 cells were incubated with CFSE (1 μM) in PBS during 20 min at 37°C. Then, cells were centrifuged and seeded on 12-well tissue culture plates. Cells were incubated in the absence or presence of Ac5sGlcNAc or ThiametG 24 h, then collected, centrifuged and analyzed by flow cytometry.

Colony Formation Assay

After cell sorting, 500 cells were seeded in 6- well culture plaques with DMEM F-12 medium supplemented with insulin, transferrin and Selenite grow supplement (1X). After 2 weeks, pictures for each condition were taken and colonies on the plaque were counted.

3D Culture

After cell sorting, 500 cells were seeded in 6- well ultra-low attachment cell culture plaques with DMEM F-12 medium containing B27 (2% v/v) and EGF (20ng/ml) per duplicate. After 3 weeks, pictures for each condition were taken, and spheroids were collected to be lysed for Western blot analysis.

Statistical Analysis

The data are expressed as the mean ± standard error of the mean (SEM). Statistical data analysis was performed using Student's *t*-test or a one-way-ANOVA with Tukey's multiple comparison test. A value of $p < 0.05$ was considered statistically significant.

RESULTS

Expression Profile of Stem Cell Markers in Colon Cancer Cells Changes During Cancer Progression

Several colorectal CSC markers have been reported to date, including CD133, CD44, CD24, CD166, and Lgr-5 (1, 2). CD44 isoform containing variant exon v6 (CD44v6) has also been reported to play an important role in the progression, metastasis, and prognosis of colorectal cancer (CRC) (3, 4). Because CD133 and CD44 have been widely validated as CSC markers in a variety of solid tumors including colon cancer, we examined their expression in human colon cancer cells. We selected as a model the primary SW480 colon carcinoma cell line and its derivative metastatic SW620 cell line which express a truncated version of APC, have constitutively active Wnt signaling and are prototype of KRAS-driven colon cancer cells in comparison with the non-malignant colon cell line 112CoN (**Figure 1**). Western blot analysis performed in total cells extracts shown in **Figure 1A**, indicated that CD133 marker, which appears as a doublet, is enriched in metastatic SW620 cells, while CD44, also seen as a doublet, was found mainly expressed both in non-malignant 112CoN cells and in primary cancer SW480 cells. The CD44 isoform, CD44v6, was found expressed only in both cancer SW480 and SW620 cells. Interestingly, when we analyzed the membrane expression of these stem cell markers

by FACS (**Figures 1B,C**), we observed that neither CD133 nor CD44 are expressed in non-malignant colon cells at the cell membrane. In addition, we observed that SW480 cells only express CD44/CD44v6 but do not express CD133. Remarkably, SW620 cells, which are derived from a metastasis of the same tumor from which the SW480 cells were derived, only express CD133 and CD44v6, but do not longer express CD44. These results indicate therefore that there must have been a change in the expression profile of stem cell markers during malignant progression. Moreover, although non-malignant cells contain CD44, they do not express it at the cell membrane and in contrast, a great proportion of the total CD44 expressed at the cell membrane in SW480 cells corresponds to CD44v6, as shown in **Figure 1C**.

Colon Cancer Cell Lines Have Increased *O*-GlcNAcylation Levels Compared With Non-malignant Colon Cells and Perturbation of These Levels Increased the Expression of Stem Cell Markers

Increased *O*-GlcNAcylation levels have been reported in diverse types of cancers including colon cancer (10, 11). To determine the levels of *O*-GlcNAcylation, OGT expression, and OGA expression in colon cancer cells compared to non-malignant colon cells, we performed FACS analysis, Western blot analysis, and immunofluorescence assays. The results shown in **Figure 2A** (FACS analysis), **Figure 2B** (Western blot analysis), and **Figure 2C** (immunofluorescence assays) clearly indicated that, as previously reported, the *O*-GlcNAcylation levels are higher in colon cancer cells compared to non-malignant cells. Consistent with this, **Figures 2A,B** show how the expression of OGT, which adds *O*-GlcNAc, appears increased while that of OGA, which removes it, appears diminished in colon malignant cells, compared with the expression found in colon non-malignant cells.

We next investigated the effects produced by perturbation of *O*-GlcNAc levels on the expression of stem cell markers CD44 and CD133 by pharmacological inhibition of OGT or OGA in colon cancer cells. We first examined by Western blot the effectiveness of the OGT inhibitor Ac5SGlcNAc (50 μM) to decrease *O*-GlcNAc levels on cells and of the OGA inhibitor Thiamet-G (1 μM) to increase *O*-GlcNAc levels (**Figure 3**). As it can be observed in **Figure 3A**, as expected, when OGA was inhibited, a global elevation of protein *O*-GlcNAcylation was observed in both cancer cell lines, whereas inhibition of OGT induced a strong decrease in *O*-GlcNAc levels compared with controls in both cell lines. Pictures taken 24 h after incubation of cells with the OGT or OGA inhibitors are shown in **Figure 3B**. It is interesting to observe in this figure that in both cell lines the inhibition of OGT, but not of OGA, produced a decrease in the total number of cells seen in the pictures. Because the decreased amount of cells could be caused by a decrease in the proliferation rate or by an increase in the apoptotic cell death, we decided to analyze the impact of the inhibition of OGT or OGA on both processes in malignant cells. The results presented in **Figure 3C** indicate that the OGT inhibition negatively affected the proliferation of both SW480 and SW620 malignant cells, as reported before in other cancer cell types (10) and in colon cancer cells (12). The inhibition is visualized in the figure as a

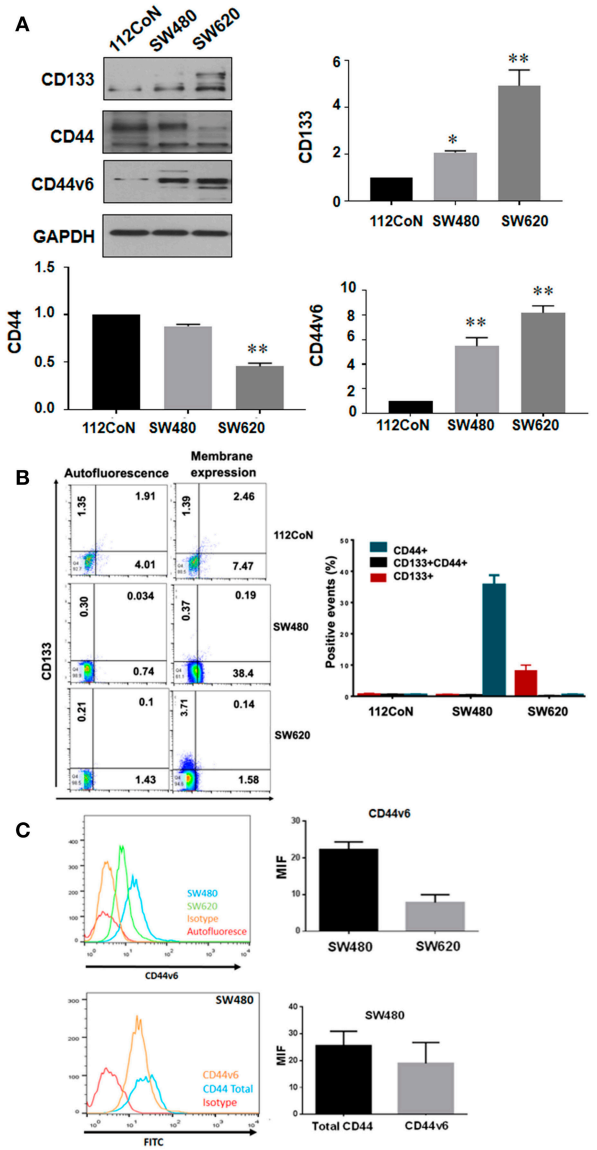

FIGURE 1 | Expression of CD133, CD44, and CD44v6 in normal and colorectal cancer cell lines. **(A)** Western blot showing the expression of CD133, CD44, and CD44v6 on total lysates of the cell lines. GAPDH were used as a load control. The results shown are representative of at least three independent experiments using different cell preparations. A densitometric analysis of the expression levels found for each marker is shown at the right and the data represent the means ± SEM from at least three independent assays $^{*}p = 0.01$; $^{**}p = 0.001$. **(B)** Membrane expression of CD133+, CD44+, and CD133+CD44+ subpopulations in 112CoN, SW480, and SW620 cell lines. Acquisition of 1 × 10^4 events. Anti-CD133 –PE-coupled and anti-CD44 –APC-coupled were used to stain proteins. MOFlow cytometer were used to acquired samples. **(C)** Membrane expression of CD44v6 in SW480 and SW620 cell lines. Acquisition of 1 × 10^4 events. CD44v6 and a secondary antibody mouse anti-CD44v6 FITC-coupled were used to stain proteins. FACScalibur cytometer were used to acquired samples.

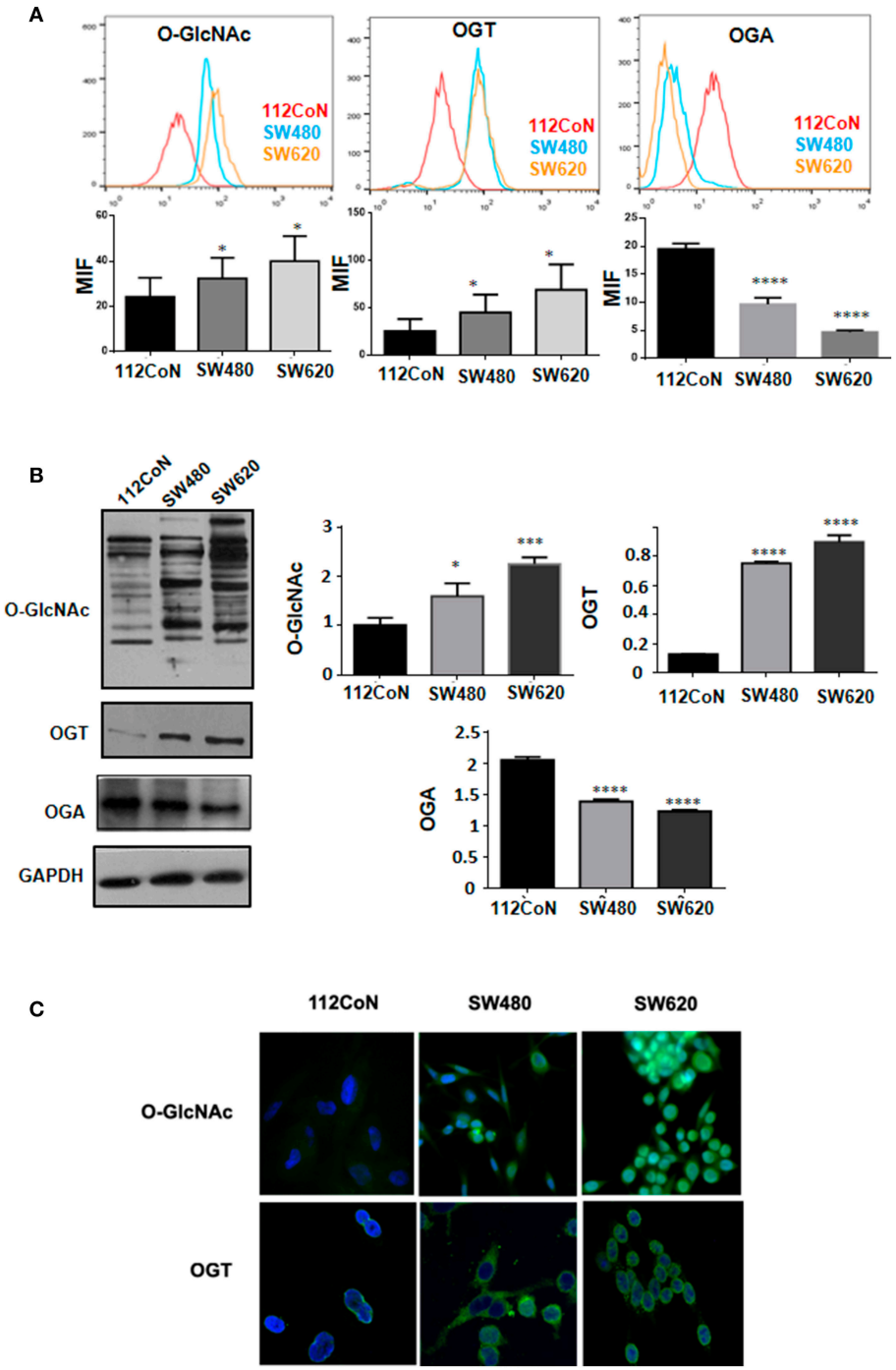

FIGURE 2 | O-GlcNAcylation levels and OGT expression are higher in colon cancer cell lines compared with normal colon cell line while OGA expression diminished in colon malignant cells compared with non-malignant ones. **(A)** Flow cytometry. The data represent the means ± SEM from at least three independent assays $*p = 0.01$; $***p = 0.001$; $****p = 0.0001$ compared with control 112CoN cells. **(B)** Western blot and **(C)** Immunofluoresce assay showing the different levels of O-GlcNAcylation and OGT expression in each cell line. Normal cells: 112CoN, cancer cells: SW480 and SW620.

retention of the fluorescent compound CFSE in cells treated with Ac5sGlcNAc because they did not proliferate, while in control or in Thiamet-G - treated cells the fluorescence signal decreased with each cell division cycle. In addition, neither the treatment of cells with the OGT inhibitor nor with the OGA inhibitor significantly affected the apoptosis rate of both SW480 or SW620 cells, as shown in **Figure 3D**.

We next investigated the effects of the modification of *O*-GlcNAc levels on the expression of cancer stem cell markers by FACS analysis. The results presented in **Figure 4A** clearly

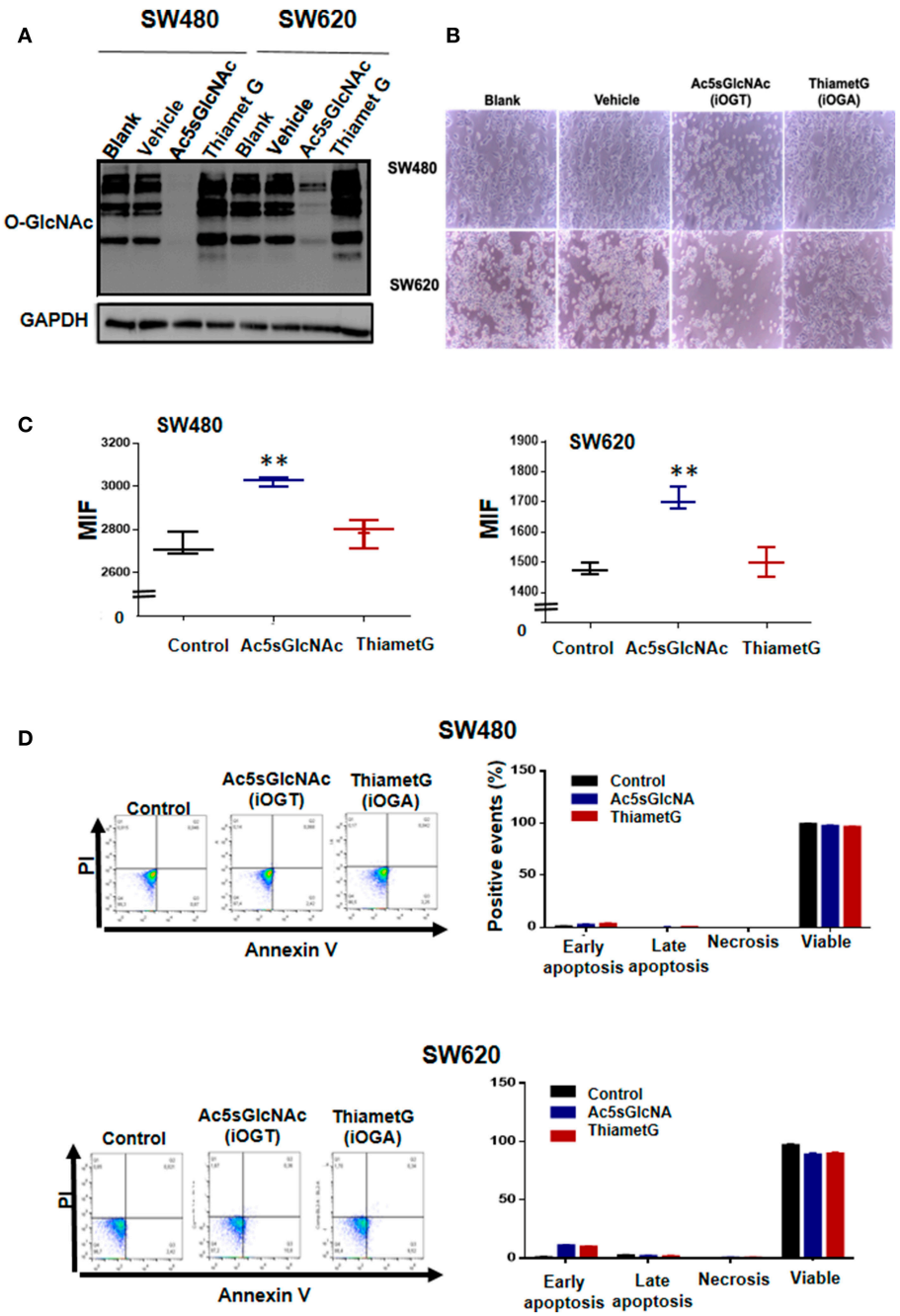

FIGURE 3 | Effects of the inhibition of OGT and OGA on the proliferation and apoptosis rates of SW480 and SW620 cells. Cells were incubated during 24 h in the absence (vehicle) or presence of 50 μM Ac5sGlcNAc to decrease the levels of O-GlcNAc, or in the absence (vehicle) or presence of 1 μM Thiamet- G to inhibit OGA and increase them **(A)** Western blotting showing the effectiveness of the inhibitors on GlcNAc cellular levels. **(B)** After 24 h, pictures of each treatment were taken with a light microscopy, augmentation 40X. **(C)** Proliferation assays were performed by flow cytometry with CellTrace CFSE. Data represent the means ± SEM from at least three independent assays $^{**}p = 0.001$ (*t*-test) compared with control 112CoN cells. **(D)** Cell death was evaluated with the Annexin V-FITC Apoptosis Detection Kit. Dotplots show early, late, necrosis or viable cells. The data represent the means ± SEM from at least three independent assays.

indicated that the inhibition of OGA did not affect the expression profile of CD44 and CD133 stem cell markers in either SW480 cells or SW620 cells compared with control untreated cells. However, and in clear contrast, the inhibition of OGT in the metastatic SW620 cell line, induced the expression of CD44 and an increase in CD133 expression. In addition, and remarkably, OGT inhibition induced the appearance of a double positive CD44+/CD133+ cell subpopulation in both primary SW480

and metastatic SW620 cancer cell lines. Thus, these results suggested that the inhibition of OGT increases the stemness in colon cancer cells. Consistent with this, when we incubated both control or treated cells with the OGT or the OGA inhibitors in sphere formation and in clonogenic activity assays, only the Ac5sGlcNAc-treated SW480 or SW620 cells formed well-defined and condensed spheres as observed in **Figure 4B**, and the clonogenic activity only increased in the OGT-inhibited cells, as it can be seen in **Figure 4C**. Moreover, the analysis of the expression of CD44 and CD133 stem cell markers by Western blotting in both SW480 and SW620 control or treated cells showed a significant increase in the CD44 and CD133 expression only in the OGT-inhibited cells compared with the OGA-inhibited and with control cells (**Figure 4D**).

Double Positive CD133/CD44 Stem Subpopulations Induced as Result of OGT Inhibition Display More Aggressive Phenotype Compared With Single Positive Subpopulations

The appearance of double positive CD133/CD44 cancer cells has been characteristically found in several highly metastatic tumors of colon, liver, pancreas, and gallbladder (13–19). Therefore, we decided to investigate if this event correlated with a change to a more aggressive malignant phenotype. To this end, we analyzed the typical cancer stem cell traits such as clonogenic and spheroid formation abilities in the double positive CD44/CD133 cell subpopulations compared with the single positive subpopulations obtained as result of OGT inhibition. As depicted in **Figure 5A**, the stem cell subpopulations found in each colon cell line after incubation with the OGT inhibitor were isolated by FACS-cell sorting and cultured for analysis of clonogenicity and of their ability to form spheroids in 3D cultures. The results presented in **Figure 5B** show that as expected, SW620 cells, which are metastatic, clearly formed more colonies than primary SW480 cells. But interestingly, when single positive stem marker subpopulation was compared with double positive CD44/CD133 subpopulation in each cell line, the double positive displayed an increased clonogenicity ability, indicative of a more aggressive malignant phenotype (**Figure 5B**). We also perfomed 3D culture in selective media to induce colonosphere formation, and as shown in **Figure 5C**, we observed that both subpopulation types in either SW480 or SW620 cells had the ability to form spheres in the selective medium. However, the double positive stem cell subpopulation in either SW480 or SW620 cells formed much bigger and condensed spheroids than single positive marker subpopulations, particularly in the metastatic cell line SW620. Finally, the evaluation of the levels of *O*-GlcNAcylation in the isolated stem cell subpopulations derived from SW480 or SW620 cells treated with OGT inhibitor (**Figure 5D**) showed that whereas SW480 double positive stem cell subpopulation displayed higher levels of *O*-GlcNAc compared with their single marker counterparts, there was no significant change in the O-GlcNAc levels found in SW620 double positive stem cells compared with single positive stem cells. It must be taken into account that after exposure of stressful conditions, and once cells adapt to the growth conditions, the O-GlcNAc levels are recuperated. However, it is interesting to note that.

Nutritional Stress Mimics OGT Inhibition Effects in Cancer Stem Cell Expression

We found that the inhibition of OGT in both primary and metastatic colon cancer cell lines induced not only an increase in stem cell markers expression but also, induced an aggressive phenotype associated with the appearance of double positive stem cell markers subpopulations. Accumulating experimental evidence has shown that microenvironmental stress signals in tumors drive phenotypic plasticity and invasion and determine therapeutic outcome. Nutritional stress, particularly glucose deprivation, would diminish UDP-GlcNAc availability and as a consequence, *O*-GlcNAc intracellular levels. Thus, we hypothesized that exposure of cells to nutritional stress would mimic the effects of OGT inhibition. To this end, growth medium from SW480 or SW620 cells was replaced with Hanks' Balanced Salt Solution (HBSS) for 4, 8, 16, or 24 h (**Figure 6**). Cells were then collected at these time points and assessed for O-GlcNAcylation levels, OGT expression levels, and stem cell markers expression by Western blot. Results presented in **Figure 6A** clearly showed that in agreement with our hypothesis, exposure of SW480 or SW620 cells to acute nutritional stress mimicked the inhibition of OGT, since the total O-GlcNAcylation levels and the OGT expression levels were both reduced in a time-dependent manner, being greatly diminished after 16 and 24 h of incubation of cells in HBSS. In addition, results presented in **Figure 6B** (CD133 expression), 6C (CD44 expression), and 6D (CD44v6 expression), show that indeed, nutritional stress induced a general increase in stem cell marker expression both in SW480 and SW620 cells compared with controls (time 0), that was significant after 8 h of starvation. It is noteworthy that SW480 cells, which under normal culture conditions do not express CD133 stem cell marker, under stressful conditions induce its expression, in addition to increase CD44/CD44v6 expression in a similar manner as when OGT is inhibited. Taken together, these results confirmed that starvation increased the expression of stem cell markers, reinforcing the notion that the activity of OGT is closely integrated with the nutritional status of the cell, and that increased *O*-GlcNAc levels appeared to be part of an endogenous nutrient stress response that is linked to cell survival.

DISCUSSION

The presence of CSC subpopulations has been identified in nearly all human malignancies. CD133, also called Prominin-1, is a pentaspan transmembrane protein which has been used as a biomarker to identify and isolate stem cells from cancer tissues, including those emerging from colorectal mucosa. The presence of CD133 positive cells have been associated with an aggressive phenotype in several tumor types including CRC. Consistent with this, it has been reported that the CD133+ subpopulation is higher in liver metastasis than in primary colorectal tumors (13). In addition, it has also been demonstrated that CD133+

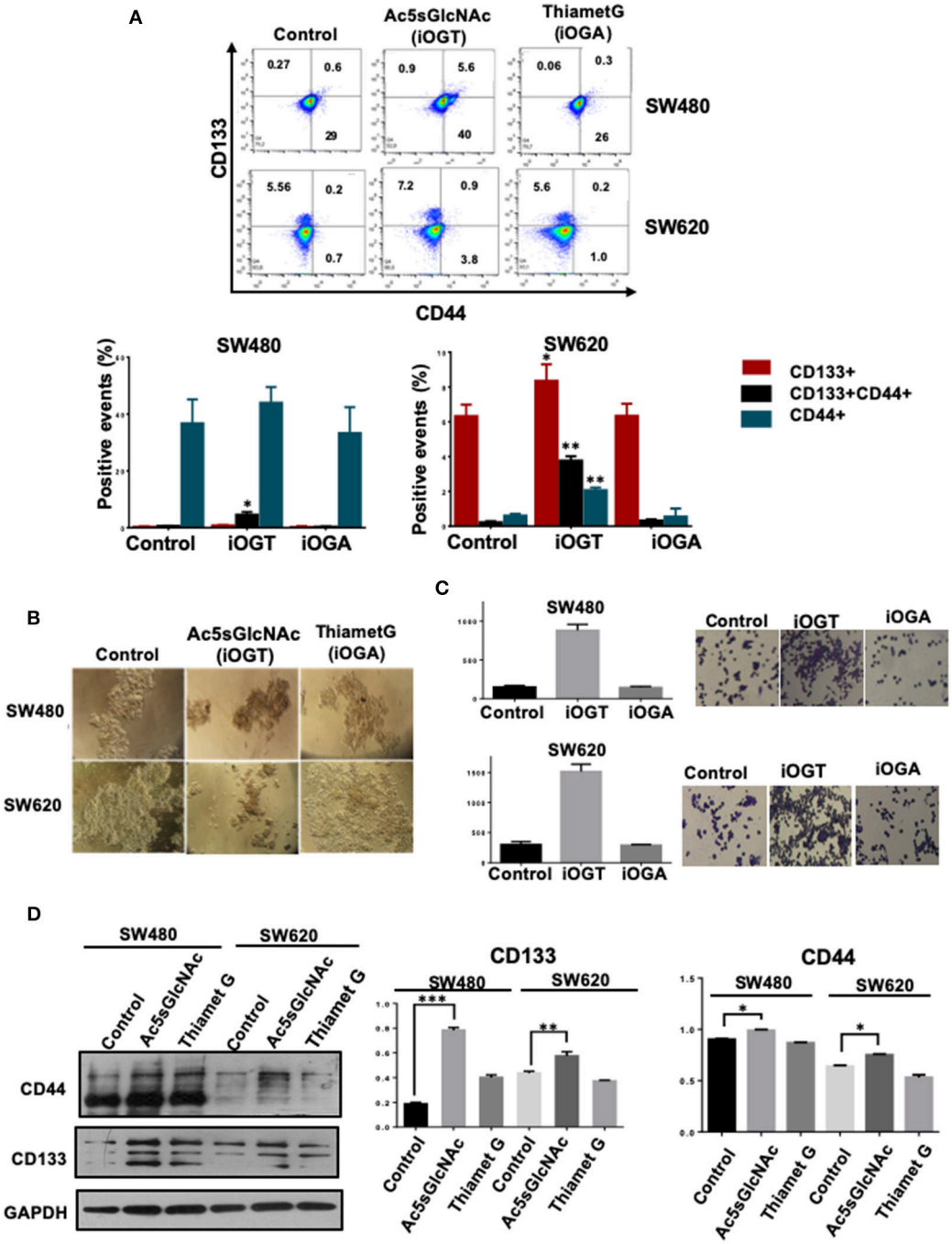

FIGURE 4 | Inhibition of OGT promoted changes in the expression of CD44+ CD133+ cancer stem cell markers. Cell were incubated 24 h in the absence (DMSO as vehicle) or presence of 50 M Ac5sGlcNAc to decrease the levels of O-GlcNAc, or in the absence (vehicle DMSO) or presence of 1 M Thiamet G to inhibit OGA and increase them. **(A)** After 24 h of inhibition, expression of CD44+ CD133+ and CD44+CD133+ subpopulations was evaluated by flow cytometry. The data represent the means ± SEM from at least three independent assays $*p = 0.01$; $**p =$ (*t*-test) compared with control. **(B)** Cells Spheroid culture. Total cell populations were cultured in ultra-low adherence six-well plates with medium supplemented with EGF and B27. After 2 weeks of incubation pictures of the spheres were taken. **(C)** Clonogenicity assay. Cells were cultured in DMEM F12 with ITS in the absence or presence of the OGT or OGA inhibitors to evaluate colony formation. Bar graphs shown represent the mean ± SEM of three independent experiments. **(D)** Western blot showing the expression of CD133 and CD44 on total cell lysates of the spheroid culture. GAPDH were used as a load control. The results shown are representative of at least three independent experiments using different cell preparations. A densitometric analysis of the expression levels found for each marker is shown at the right and the data represent the means ± SEM from at least three independent experiments. $*p = 0.01$; $**p = 0.005$; $***p = 0.001$ (*t*-test) compared with control 112CoN non-malignant cells.

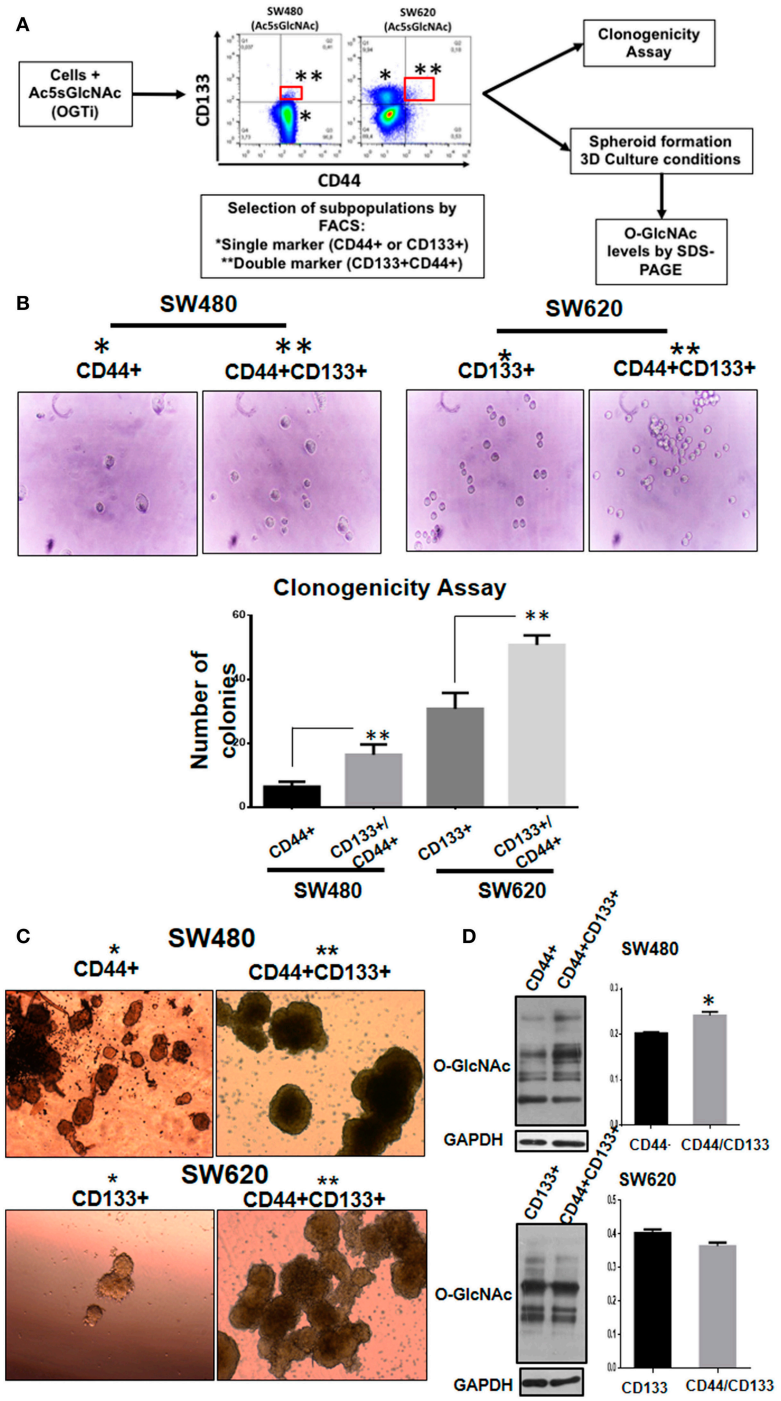

FIGURE 5 | Double positive CD133/CD44 stem subpopulations induced as result of OGT inhibition display more aggressive phenotype compared with single positive subpopulations. **(A)** Schematization of the experimental approach used. **(B)** Clonogenicity assay. Isolation by FACS of the single and double positive populations was performed. Cells co-expressing CD44 and CD133 (marked in red) were isolated and grown under different culture conditions. Cells were cultured in DMEM F12 with ITS to evaluate colony formation. Bar graphs shown represent the mean ±SEM of three independent experiments. $^{*}p = 0.01$; $^{**}p = 0.001$ (*t*-test) compared with control. **(C)** Spheroid culture. Cells were cultured in ultra- low adherence 24-well plates with medium supplemented with EGF and B27. After 3 weeks of incubation pictures of the spheres were taken. For comparison, cells expressing only one marker (CD44 for SW480 and CD133 for SW620) were cultured under the same conditions. The spheres were lysed and levels of O-GlcNAc expression were evaluated. Isolation of cells by FACS -cell sorting was performed in MOFlow cytometer. **(D)** The spheres were lysed and levels of O-GlcNAc expression were evaluated by Western blotting. GAPDH were used as a load control. The results shown are representative of at least three independent experiments using different cell preparations. A densitometric analysis of the expression levels found is shown at the right and the data represent the means ± SEM from at least three independent experiments. $^{*}p = 0.01$ (*t*-test) compared with single positive CD44+ spheroids.

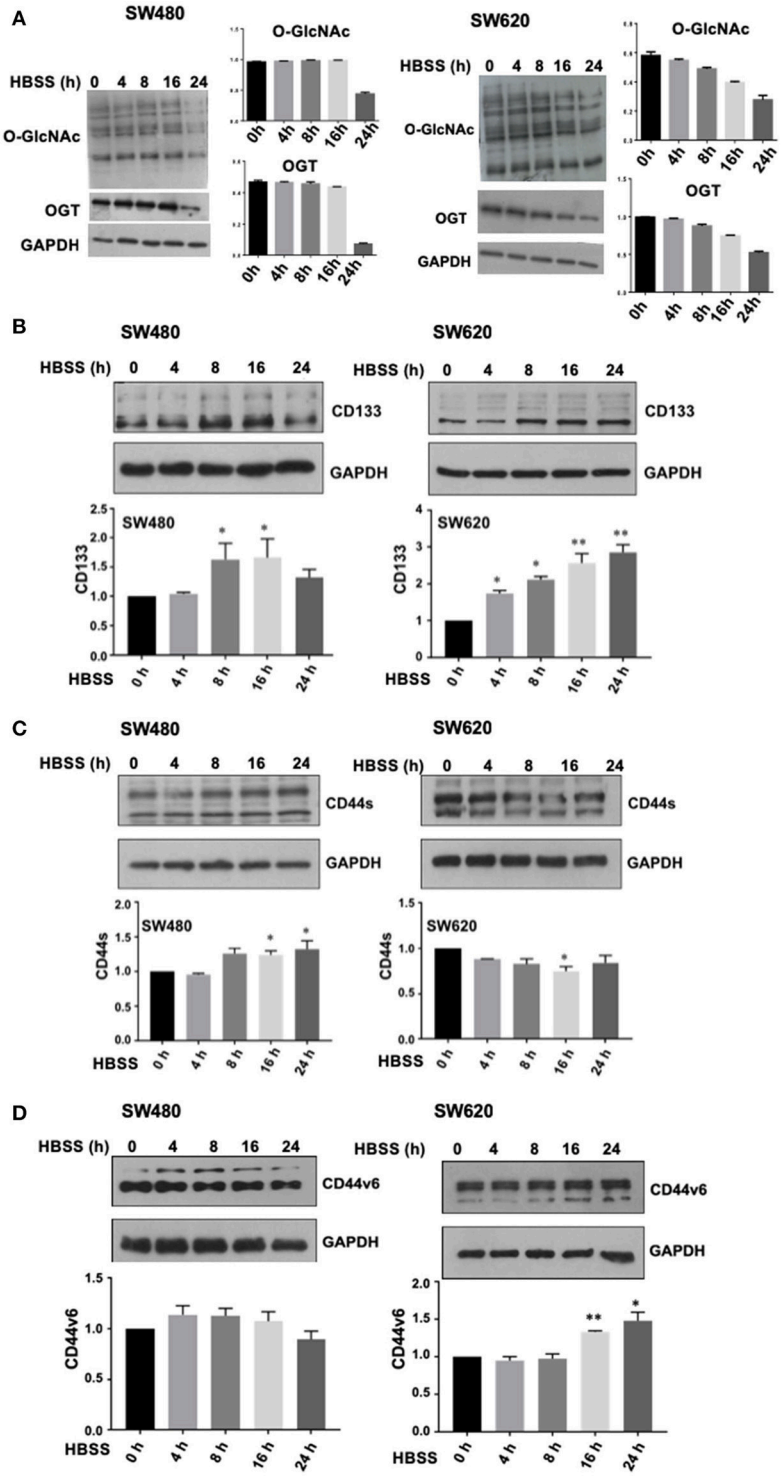

FIGURE 6 | Nutritional stress mimics OGT inhibition effects in cancer stem cells expression. Growth medium from SW480, or SW620 cells, was replaced with Hanks' Balanced Salt Solution (HBSS) for 4, 8, 16, or 24h. Cells were then collected at these time points and assessed for O-GlcNAcylation levels, OGT expression levels, and stem cell markers expression by Western blot. **(A)** O-GlcNAcylation levels and OGT expression levels diminish in a time- dependent manner during incubation of cells in HBSS. Results obtained for CD133 expression are shown in panel **(B)**, CD44 expression in panel **(C)** and CD44v6 expression levels in panel **(D)**. Results shown represent the mean ±SEM of three independent experiments. $^{*}p = 0.01$; $^{**}p = 0.001$ (*t*-test) compared with control.

cells show a high degree of chemoresistance (20, 21). It is interesting to note that in agreement with this, in our study we found that under normal culture conditions, primary SW480 colon cancer cells express the CD44 stem marker and do not express CD133, whereas their derivative metastatic SW620 cell line mainly expresses CD133.

CD44 is a transmembrane glycoprotein which has also been identified as being expressed by many tumor CSCs. It participates in a variety of biological functions such as cell adhesion, tumor cell migration, growth, differentiation, survival, or even in chemoresistance (3, 22, 23). However, CD44s is the smallest and the standard isoform codified by 10 exons, without products of variant additional exons, and the CD44 variants are isoforms expressing additional segments (v2–v10) in the extracellular domain that are generated by alternative splicing (4). Both the standard and the variants can all be recognized by an antibody directed against the standard region but importantly, the expression of CD44 variants has only been found in cancer cells and has been reported as produced during tumor progression (3, 4). Thus, different cells of a tumor can express various, and possibly different sets of CD44 isoforms. In CRC the v6-containing isoform of CD44 is the most frequently found to be associated with metastatic phenotype in the literature (24). It was also found that CD44v6 is involved in acquired drug resistance in CRC (4). According with this notion, while the glandular epithelium of the large bowel expresses the standard form of CD44 but not variant ones, in contrast, highly dysplastic colorectal adenomas, primary and metastatic CRC, express CD44v isoforms (3, 4). In agreement with this, here we found that non-malignant fetal colon 112CoN cells express CD44 but do not express CD44v6, which we found only expressed in colon malignant cells.

In this study we found that in colon cancer cells the inhibition of OGT or the exposure of cells to an acute nutritional stress mimicking the lack of OGT, induce the appearance of an aggressive CD133/CD44 double positive CSC subpopulation. In agreement with our results, these CD133+CD44+ cancer cells have been characterized in several highly metastatic tumors such as CRCs (13–16), HCCs (17), pancreatic cancers (18), and gallbladder carcinoma (19). It has also been reported that in CRC with early liver metastases, co- expression of CD133 and CD44 is significantly higher when compared to those without early liver metastases (15).

To date, the functions played by *O*-GlcNAcylation in stem cells and pluripotency has been poorly investigated and remains unclear. In this respect, Jang et al. (5) have shown that blocking *O*-GlcNAcylation inhibited ESC self-renewal and the efficiency of inducible pluripotent stem cells (iPSC) generation, whereas increasing *O*-GlcNAcylation inhibited normal ESC differentiation. Other authors have also shown that *O*-GlcNAc is required for ESC survival, and that OGT knockout mouse shows embryonic lethality (5, 25). In addition, experimental evidence has revealed that *O*-GlcNAc controls pluripotency by directly regulating transcriptional activities of core components of the pluripotency network. Numerous stem cell factors have been shown *O*-GlcNAcylated such as Oct4 (26) or Sox2 (5). Whereas, the role of Sox2 *O*-GlcNAcylation is still unclear, Oct4 interacts with OGT and is modified in order to regulate pluripotency gene networks (26).

Here we investigated the effects produced by the modification of *O*-GlcNAc levels on the expression of stem cell markers CD44 and CD133 by pharmacological inhibition of OGT or OGA, the enzymes which catalyze the addition and removal of *O*-GlcNAc, respectively. A salient feature obtained here is that we not only confirmed that *O*-GlcNAc serves as a nutrient sensor and the activity of OGT is closely integrated with the nutritional status of the cell, as previously reported in other cell systems, but also that increased *O*-GlcNAc levels appeared to be part of an endogenous stress response that is linked to cell survival. In this respect, accumulating experimental evidence has shown that *O*-GlcNAcylation acts as a nutrient sensor that associates the glucose metabolic status with cellular regulation of signal transduction, transcription, protein function and differentiation (7, 27). As mentioned before, in cancer cells, metabolism is dramatically altered compared with normal cells. They reprogram their metabolism to undergo a high rate of glycolysis and lactic acid fermentation, even under normoxic conditions [Warburg effect (28)]. One consequence of these changes is cellular addiction to glutamine, that in turn, increases the flux through the hexosamine biosynthetic pathway (HBP). Because HBP requires glucose, glutamine, fatty acids, and UTP, is thereby positioned to integrate information on the availability of nutrients (7, 10). Importantly, HBP produces the high-energy-donor UDP- GlcNAc, which is the sugar donor involved in the synthesis of other nucleotide sugars, complex glycosylation and also utilized by OGT to modify target proteins (10, 27).

Increased OGT expression has been detected in numerous cancers, including bladder cancer (29) and lung and colon cancers (30). In addition, HBP enzymes have also been reported to be over- expressed in human prostate cancer patients (10, 31). Here we confirmed that OGT is overexpressed in colon cancer cells compared with non-malignant colon cells. When we decreased *O*-GlcNAc levels as a result of OGT inhibition, we observed, as previously reported, a decrease in cell survival, but unexpectedly, we also observed that the decrease in *O*-GlcNAc levels induced the appearance of an aggressive CD44+/CD133+ small subpopulation which in turn expressed high *O*-GlcNAc levels. In this respect, we found that whereas SW620 double positive stem cells displayed lower levels of *O*-GlcNAc levels than single positive ones as expected, unexpectedly, SW480 double positive stem cell subpopulation displayed higher levels of *O*-GlcNAc compared with their single marker counterparts. But it must be taken into account that the *O*-GlcNAc levels examined in the spheroids derived from the double positive stem cells were obtained from 3-week old 3D spheroids cultures. Thus, a decrease in *O*-GlcNAc levels would be expected to happen only as result of starvation or if glucose were deprived in tumor cells, but once they adapt to the growth conditions, O-GlcNAc levels recuperate as a result of their metabolism. However, it is interesting to note that these levels are lower in the metastatic SW620 cells, compared with the primary SW480 cells from which they derived. Since a decrease in *O*-GlcNAc levels would be expected to happen if glucose were deprived, we reasoned that the exposure of cells to an acute nutritional

stress would mimic the effects produced by OGT inhibition. Indeed, our results confirmed that starvation increased the expression of stem cell markers, reinforcing the notion that the HBP pathway and OGT activity are intimately integrated with the nutritional status of the cell and contribute to regulate stemness maintenance.

In this work we also found that the increased *O*-GlcNAc levels observed in colon cancer cells appeared to be part of an endogenous nutrient stress response that is linked to cell survival. In this respect, our data are consistent with the notion that *O*-GlcNAc modification of proteins is a metabolically modulated signaling pathway that regulates cell function and plays a particularly critical role in mediating the response of cells to stress (32). Evidence of this was first reported in 2004, by Zachara et al. when *O*-GlcNAc levels were shown to increase in response to a diverse array of stress stimuli, and inhibition of this response resulted in reduced cell survival (33). Other authors have also shown that *O*-GlcNAc levels are increased in response to stress, that augmentation of *O*-GlcNAc levels conferred increased tolerance to stress (32), and that the acute augmentation of this response is cytoprotective, even in the cardiovascular system (32, 34). Therefore, our data support that *O*-GlcNAcylation modification of proteins not only functions as a nutrient status sensor which plays a critical role in stemness maintenance, but also that it is an important mediator of the response of cells to stressful conditions.

ETHICS STATEMENT

This work has been conducted following the ethical standards according to the Declaration of Helsinki and according to national and international guidelines and has been approved by the Faculty of Medicine Ethical Committee from Universidad Nacional Autónoma de México.

AUTHOR CONTRIBUTIONS

MR-F, TL, and GF-G conceived and designed the experiments. GF-G, MC-P, and A-SV-E performed the experiments. MR-F, TL, and GF-G analyzed the data. MR-F and TL contributed reagents, materials, and analysis tools. MR-F wrote the manuscript.

FUNDING

This research was supported by grants from Universidad Nacional Autónoma de México (DGAPA-UNAM IN215514 and IN225717) and from CONACYT (FOSSIS 2017-289600).

ACKNOWLEDGMENTS

We would like to thank the LABNALCIT-UNAM (CONACYT) technical support in the acquisition and analysis of flow cytometry samples, especially to MS Erick Christian Ivan Espindola Arriaga. We want also thank to Dr. Miguel Tapia Rodríguez from the Microscopy unit of IIB-UNAM and Dr. Stephan Hardivillé from the University of Lille for the kindly donation of Ac5SGlcNAc and Dr. Chan Lagadec from th Cell Plasticity and Cancer team (INSERM U808) for helping in FACS access. GF-G is a Ph.D. student in the Programa de Doctorado en Ciencias Bioquímicas, Universidad Nacional Autónoma de México (UNAM), and was granted with a Fellowship by DGAPA, UNAM, Mexico and by CONACYT.

REFERENCES

1. Taniguchi H, Moriya C, Igarashi H, Saito A, Yamamoto H, Adachi Y, et al. Cancer stem cells in human gastrointestinal cancer. *Cancer Sci.* (2016) 107:1556–62. doi: 10.1111/cas.13069
2. Kim ST, Sohn I, Do I-G, Jang J, Kim SH, Jung SH, et al. Transcriptome analysis of CD133-positive stem cells and prognostic value of survivin in colorectal cancer. *Cancer Genomics Proteomics.* (2014) 11:259–66. doi: 10.1016/S0959-8049(14)70327-2
3. Bánky B, Rásó-Barnett L, Barbai T, Tímár J, Becságh P, Rásó E. Characteristics of CD44 alternative splice pattern in the course of human colorectal adenocarcinoma progression. *Mol Cancer.* (2012) 11:83. doi: 10.1186/1476-4598-11-83
4. Lv L, Liu H-G, Dong SY, Yang F, Wang Q-X, Guo G-L, et al. Upregulation of CD44v6 contributes to acquired chemoresistance via the modulation of autophagy in colon cancer SW480 cells. *Tumor Biol.* (2015) 37:8811–24. doi: 10.1007/s13277-015-4755-6
5. Jang H, Kim TW, Yoon S, Choi SY, Kang TW, Kim SY, et al. O-GlcNAc regulates pluripotency and reprogramming by directly acting on core components of the pluripotency network. *Cell Stem Cell.* (2012) 11:62–74. doi: 10.1016/j.stem.2012.03.001
6. Ogawa M, Sawaguchi S, Kamemura K, Okajima T. Intracellular and extracellular O-linked N-acetylglucosamine in the nervous system. *Exp Neurol.* (2015) 274:166–74. doi: 10.1016/j.expneurol.2015.08.009
7. Sharma NS, Saluja AK, Banerjee S. Nutrient-sensing and self-renewal: O-GlcNAc in a new role. *J Bioenerg Biomembr.* (2017) 50:205–11. doi: 10.1007/s10863-017-9735-7
8. Jeon JH, Suh HN, Kim MO, Ryu JM, Han HJ. Glucosamine- induced OGT activation mediates glucose production through cleaved Notch1 and FoxO1, which coordinately contributed to the regulation of maintenance of self-renewal in mouse embryonic stem cells. *Stem Cells Dev.* (2014) 23:2067–79. doi: 10.1089/scd.2013.0583
9. Marsboom G, Zhang GF, Pohl-Avila N, Zhang Y, Yuan Y, Kang H, et al. Glutamine metabolism regulates the pluripotency transcription factor OCT4. *Cell Rep.* (2016) 16:323–32. doi: 10.1016/j.celrep.2016.05.089
10. Itkonen HM, Gorad SS, Duveau DY, Martin SES, Barkovskaya A, Bathen TF, et al. Inhibition of o-GlcNAc transferase activity reprograms prostate cancer cell metabolism. *Oncotarget.* (2016) 7:12464–76. doi: 10.18632/oncotarget.7039
11. Fardini Y, Dehennaut V, Lefebvre T, Issad T. O-GlcNAcylation: a new cancer hallmark? *Front Endocrinol.* (2013) 4:99. doi: 10.3389/fendo.2013.00099
12. Steenackers A, Olivier-Van Stichelen S, Baldini SF, Dehennaut V, Toillon RA, Le Bourhis W, et al. Silencing the nucleocytoplasmic O-GlcNAc transferase reduces proliferation, adhesion, and migration of cancer and fetal human colon cell lines. *Front Endocrinol.* (2016) 7:46. doi: 10.3389/fendo.2016.00046
13. Li, Z. CD133: a stem cell biomarker and beyond. *Exp Hematol Oncol.* (2013) 2:17 doi: 10.1186/2162-3619-2-17
14. Chen KL, Pan F, Jiang H, Chen JF, Pei L, Xie FW, et al. Highly enriched CD133(+)CD44(+) stem-like cells with CD133(+)CD44(high) metastatic subset in HCT116 colon cancer cells. *Clin Exp Metast.* (2011) 28:751–63. doi: 10.1007/s10585-011-9407-7
15. Huang X, Sheng Y, Guan M. Co-expression of stem cell genes CD133 and CD44 in colorectal cancers with early liver metastasis. *Surg Oncol.* (2012) 21:103–7. doi: 10.1016/j.suronc.2011.06.001

16. Bellizzi A, Sebastian S, Ceglia P, Centonze M, Divella R, Manzillo EF, et al. Co-expression of CD133 (+)/CD44(+) in human colon cancer and liver metastasis. *J Cell Physiol.* (2013) 228:408–15. doi: 10.1002/jcp.24145
17. Hou Y, Zou Q, Ge R, Shen F, Wang Y. The critical role of CD133(+)CD44 (+/high) tumor cells in hematogenous metastasis of liver cancers. *Cell Res.* (2012) 22:259–72. doi: 10.1038/cr.2011.139
18. Wang D, Zhu H, Zhu Y, Liu Y, Shen H, Yin R, et al. CD133(+)/CD44 (+)/Oct4(+)/Nestin(+) stem-like cells isolated from Panc-1 cell line may contribute to multi-resistance and metastasis of pancreatic cancer. *Acta Histochem.* (2013) 115:349–56. doi: 10.1016/j.acthis.2012.09.007
19. Shi C, Tian R, Wang M, Wang X, Jiang J, Zhang Z, et al. CD44+ CD133+ population exhibits cancer stem cell-like characteristics in human gallbladder carcinoma. *Cancer Biol Ther.* (2010) 10:1182–90. doi: 10.4161/cbt.10.11.13664
20. Zhang Q, Shi S, Yen Y, Brown J, Ta JQ, Le AD. A subpopulation of CD133 (+) cancer stem-like cells characterized in human oral squamous cell carcinoma confer resistance to chemotherapy. *Cancer Lett.* (2010) 289:151–60. doi: 10.1016/j.canlet.2009.08.010
21. Angelastro JM, Lame M. Overexpression of CD133 promotes drug resistance in C6 glioma cells. *Mol Cancer Res.* (2010) 8:1105–15. doi: 10.1158/1541-7786.MCR-09-0383
22. Tumor M, Lilly P, Bourguignon W. CD44 in cancer progression: adhesion. *Migr Growth Regul.* (2004) 35:211–31. doi: 10.1023/B:HIJO.0000032354.94213.69
23. Kuhn S, Koch M, Nübel T, Ladwein M, Antolovic D, Klingbeil P, et al. A complex of EpCAM, claudin-7, CD44 variant isoforms, and tetraspanins promotes colorectal cancer progression. *Mol Cancer Res.* (2007) 5:553–67. doi: 10.1158/1541-7786.MCR-06-0384
24. Reeder JA, Gotley DC, Walsh MD, Fawcett J, Antalis TM. Expression of antisense CD44 variant 6 inhibits colorectal tumor metastasis and tumor growth in a wound environment expression of antisense CD44 variant 6 inhibits colorectal tumor metastasis and tumor growth in a wound environment1. *Cancer Res.* (1998) 58:3719–26.
25. Shafi R, Iyer SP, Ellies LG, O'Donnell N, Marek KW, Chui D, et al. The O-GlcNAc transferase gene resides on the X chromosome and is essential for embryonic stem cell viability and mouse ontogeny. *Proc. Natl. Acad. Sci. USA.* (2000) 97:5735–9. doi: 10.1073/pnas.100471497
26. Pardo M, Lang B, Yu L, Prosser H, Bradley A, Babu MM, et al. An expanded Oct4 interaction network: implications for stem cell biology, development, and disease. *Cell Stem Cell.* (2010) 6:382–95. doi: 10.1016/j.stem.2010.03.004
27. Olivier-Van Stichelen S, Hanover JA. You are what you eat: O-linked N-acetylglucosamine in disease, development and epigenetics. *Curr Opin Clin Nutr Metab Care.* (2015) 18:339–45. doi: 10.1097/MCO.0000000000000188
28. Warburg O. On the origin of cancer cells. *Science.* (1956) 123:309–14. doi: 10.1126/science.123.3191.309
29. Rozanski W, Krzeslak A, Forma E, Brys M, Blewniewski M, Wozniak P, et al. Prediction of bladder cancer based on urinary content of MGEA5 and OGT mRNA level. *Clin Lab.* (2012) 58:579–83.
30. Mi W, Gu Y, Han C, Liu H, Fan Q, et al. O-GlcNAcylation is a novel regulator of lung and colon cancer malignancy. *Biochim Biophys Acta.* (2011) 1812:514–9. doi: 10.1016/j.bbadis.2011.01.009
31. Itkonen HM, Engedal N, Babaie E, Luhr M, Guldvik IJ, Minner S, et al. UAP1 is overexpressed in prostate cancer and is protective against inhibitors of N-linked glycosylation. *Oncogene.* (2015) 34:3744–5032. doi: 10.1038/onc.2014.307
32. Chatham JC, Marchase RB. Protein O-GlcNAcylation: a critical regulator of the cellular response to stress. *Curr Signal Transduct Ther.* (2010) 5:49–59. doi: 10.2174/157436210790226492
33. Zachara NE, O'Donnell N, Cheung WD, Mercer JJ, Marth JD, Hart GW. Dynamic O-GlcNAc modification of nucleocytoplasmic proteins in response to stress. A survival response of mammalian cells. *J Biol Chem.* (2004) 279:30133–42. doi: 10.1074/jbc.M403773200
34. Liu J, Pang Y, Chang T, Bounelis P, Chatham JC, Marchase RB. Increased hexosamine biosynthesis and protein O-GlcNAc levels associated with myocardial protection against calcium paradox and ischemia. *J. Mol. Cell Cardiol.* (2006) 40:303–12. doi: 10.1016/j.yjmcc.2005.11.003

Conflict of Interest Statement: The authors declare that the research was conducted in the absence of any commercial or financial relationships that could be construed as a potential conflict of interest.

The reviewer EZ declared a shared affiliation, with no collaboration, with several of the authors GF-G, MC-P and MR-F to the handling Editor.

frontiers in Endocrinology

ORIGINAL RESEARCH
published: 21 May 2019
doi: 10.3389/fendo.2019.00291

O-GlcNacylation Links TxNIP to Inflammasome Activation in Pancreatic β Cells

*Gaelle Filhoulaud[1,2,3], Fadila Benhamed[1,2,3], Patrick Pagesy[1,2,3], Caroline Bonner[4,5], Yann Fardini[1,2,3], Anissa Ilias[6,7], Jamileh Movassat[6,7], Anne-Françoise Burnol[1,2,3], Sandra Guilmeau[1,2,3], Julie Kerr-Conte[5], François Pattou[5,8], Tarik Issad[1,2,3] and Catherine Postic[1,2,3]**

[1] INSERM U1016, Institut Cochin, Paris, France, [2] CNRS UMR 8104, Paris, France, [3] Université Paris Descartes, Sorbonne Paris Cité, Paris, France, [4] Pasteur Institute de Lille, Lille, France, [5] INSERM U1190 - EGID, Lille, France, [6] UMR8251-CNRS, Paris, France, [7] Université Paris Diderot, Sorbonne Paris Cité, Paris, France, [8] CHU, Lille, France

OPEN ACCESS

Edited by:
Mohammed Akli Ayoub, United Arab Emirates University, United Arab Emirates

Reviewed by:
Hai-Bin Ruan, University of Minnesota, United States
Eric Reiter, Institut National de la Recherche Agronomique (INRA), France

***Correspondence:**
Catherine Postic
catherine.postic@inserm.fr

Specialty section:
This article was submitted to Molecular and Structural Endocrinology, a section of the journal Frontiers in Endocrinology

Received: *30 January 2019*
Accepted: *23 April 2019*
Published: *21 May 2019*

Citation:
Filhoulaud G, Benhamed F, Pagesy P, Bonner C, Fardini Y, Ilias A, Movassat J, Burnol A-F, Guilmeau S, Kerr-Conte J, Pattou F, Issad T and Postic C (2019) O-GlcNacylation Links TxNIP to Inflammasome Activation in Pancreatic β Cells. Front. Endocrinol. 10:291. doi: 10.3389/fendo.2019.00291

Thioredoxin interacting protein (TxNIP), which strongly responds to glucose, has emerged as a central mediator of glucotoxicity in pancreatic β cells. TxNIP is a scaffold protein interacting with target proteins to inhibit or stimulate their activity. Recent studies reported that high glucose stimulates the interaction of TxNIP with the inflammasome protein NLRP3 (NLR family, pyrin domain containing 3) to increase interleukin-1 β (IL1β) secretion by pancreatic β cells. To better understand the regulation of TxNIP by glucose in pancreatic β cells, we investigated the implication of O-linked β-N-acetylglucosamine (O-GlcNAcylation) in regulating TxNIP at the posttranslational level. O-GlcNAcylation of proteins is controlled by two enzymes: the O-GlcNAc transferase (OGT), which transfers a monosaccharide to serine/threonine residues on target proteins, and the O-GlcNAcase (OGA), which removes it. Our study shows that TxNIP is subjected to O-GlcNAcylation in response to high glucose concentrations in β cell lines. Modification of the O-GlcNAcylation pathway through manipulation of OGT or OGA expression or activity significantly modulates TxNIP O-GlcNAcylation in INS1 832/13 cells. Interestingly, expression and O-GlcNAcylation of TxNIP appeared to be increased in islets of diabetic rodents. At the mechanistic level, the induction of the O-GlcNAcylation pathway in human and rat islets promotes inflammasome activation as evidenced by enhanced cleaved IL1β. Overexpression of OGT in HEK293 or INS1 832/13 cells stimulates TxNIP and NLRP3 interaction, while reducing TxNIP O-GlcNAcylation through OGA overexpression destabilizes this interaction. Altogether, our study reveals that O-GlcNAcylation represents an important regulatory mechanism for TxNIP activity in β cells.

Keywords: O-GlcNAcylation, TXNIP (thioredoxin-interacting protein), pancreatic beta cells, hyperglycemia, inflammasome

INTRODUCTION

Chronic exposure to high glucose exerts deleterious effects on pancreatic β cell function leading to a disruption of their secretory capacities and/or a decrease in their cellular mass. The mechanisms driving β cells destruction are numerous including increased fatty acid cellular content, reactive oxygen species (ROS) production, macrophage infiltration, inflammation processes, and/or increased flux through the hexosamine biosynthetic pathway. Over the past years, Thioredoxin interacting protein (TxNIP) has emerged as a major mediator of β cell dysfunction, being one of the most up-regulated genes in response to hyperglycemia (1–3). As part of a negative-feedback loop, TxNIP inhibits glucose uptake and promotes caspase-1 cleavage, contributing to glucose-dependent β-cell death (2–6). TxNIP also regulates pro-inflammatory processes through the inflammasome activation *via* binding to NLRP3 (NOD-like receptor family pyrin domain containing 3) (7, 8). In this context, TxNIP is an important actor of pancreatic β cell biology and its tight regulation appears necessary for β cell survival.

The mechanisms driving TxNIP expression involve a crosstalk between several transcription factors. The *Txnip* promoter contains two carbohydrate response elements (ChoRE) for binding of the glucose sensitive transcription factor Carbohydrate Responsive Element Binding Protein (ChREBP) (2). While the Forkhead boxO1 transcription factor (FoxO1) was reported to up-regulate *Txnip* expression in neurons and endothelial cells, it was shown to significantly decrease its expression in pancreatic β cells. Mechanistically, FoxO1 was reported to prevent the glucose-induced *Txnip* expression by reducing the glucose-induced binding of ChREBP at the promoter, suggesting that FoxO1 competes with ChREBP for binding to the *Txnip* promoter. The TxNIP protein is also regulated at the posttranslational level through phosphorylation (9). In the current study, we addressed whether the TxNIP protein could be regulated through O-GlcNAcylation, a posttranslational modification that depends on intracellular glucose flux through the hexosamine biosynthetic pathway. O-GlcNAcylation, which is linked to glucotoxicity in many cell types, modulates protein activity and/or partner interactions (10, 11). O-GlcNAcylation requires the activity of two enzymes: the O-GlcNAc transferase (OGT), which transfers the monosaccharide to serine/threonine residues on target proteins, and the O-GlcNAcase (OGA), which hydrolyses this sugar.

Our study demonstrates that the TxNIP protein is modified by O-GlcNAcylation in both rodent and human pancreatic β cells and that this modification enhances its interaction with its binding partner NLRP3, leading in turn to inflammasome activation.

Abbreviations: ChoRE, carbohydrate response element; ChREBP, carbohydrate responsive element binding protein; FoxO1, forkhead boxO1 transcription factor; GK, Goto-Kakizaki; IGFBP1, insulin-like growth factor-binding protein 1; IL1β, interleukin 1β; NLRP3, NOD-like receptor family pyrin domain containing 3; OGA, O-GlcNAcase; O-GlcNAc, O-linked N-acetylglucosamine; OGT, O-GlcNAc transferase; qPCR, quantitative real time PCR; ROS, reactive oxygen species; TxNIP, thioredoxin-interacting protein; BRET, bioluminescence resonance energy transfer.

RESEARCH DESIGN AND METHODS

Animals

Animal experiments were performed in agreement with protocols approved by French guidelines. Eight week-old male C57BL/6J and *db/db* mice were purchased from Harlan®. Mice were adapted to the environment for 1-week prior to study and maintained in a 12-h light/dark cycle with water and regular diet (65% carbohydrate, 11% fat, and 24% protein). When specified mice were fasted for 24 h and then refed for 18 h with a high carbohydrate diet (72.2% carbohydrate, 1% fat, 26.8% protein). Ten weeks-old male Wistar rats were purchased from Harlan®. Goto-Kakizaki (GK) rats were obtained from the GK/Par colony obtained from the Movassat's laboratory (12).

Isolation of Islets of Langerhans From Rodent Models

Islets of Langerhans were obtained from 3 months old Wistar and Goto-Kakizaki (GK) rats by collagenase digestion and Ficoll gradient and then hand-picked as described previously (13). Freshly isolated islets were cultured in 6 wells plates and incubated in 5.5 or 16.7 mM glucose in the absence or presence of 100 μM PUGNAc (Sigma) for 72 h in RPMI 1640 supplemented with 10% fetal calf serum, 100 U/ml penicillin, 100 mg/ml streptomycin and 10 mM L-glutamine.

Culture and Transfection Experiments in HEK293

Human embryonic kidney cells (HEK293) were grown in 6 wells plates in 25 mM D-glucose DMEM supplemented with 10% fetal calf serum (Sigma®). The OGT and OGA plasmids were previously described (10), the TxNIP plasmid was purchased from Genecust® and pcDNA3-N-Flag-NLRP3 was a gift from Bruce Beutler (Addgene plasmid # 75127). Transfections of HEK293 cell were performed using Lipofectamine 2000 and OptiMEM, and 1 μg of plasmid/well.

Culture and Transfection Experiments in INS1 832/13 Cells

INS1 832/13 cells (kindly provided by Dr. CB Newgard, Duke University Medical Center, Durham, NC) were cultured in RMPI 1640 supplemented with 10% fetal calf serum (Life Technology®), 100 U/ml penicillin, 100 mg/ml streptomycin, 1 mM sodium pyruvate, 10 mM HEPES and β-mercaptoethanol. Cells were then washed, starved during 6 h in 2.5 mM glucose without serum and further incubated with 2.5 or 20 mM glucose during 24 h. INS1 832/13 cells were infected with shOGT, shcontrol, GFP (Genecust®) and OGA adenoviruses (a kind gift from Dr. Xao Yang) during 24 h. Cells were then washed, starved during 6 h in 2.5 mM glucose without serum and stimulated in 5 or 25 mM during 24 h.

For TxNIP reporter assays, INS1 832/13 cells were transfected with a Txnip luciferase reporter (a promoter containing the two tandem ChoRE) and a plasmid expressing β Galactosidase (0.2 μg DNA of each plasmid per well) using Lipofectamine 2000. β Galactosidase assays were performed for normalization of the ChoRE luciferase activity. The luciferase assay was conducted using the dual luciferase substrate system (E1501; Promega,

Madison, WI), and the result was normalized with the internal control *Renilla luciferase*. Each experiment was repeated at least three times.

For Bioluminescence Resonance Energy Transfer (BRET) experiments, INS1 832/13 cells were transfected with the cDNA coding for a biosensor (14, 15) based on BRET, in which the precursor pro–IL1β is fused at its terminals to RLuc8 (a variant of *Renilla* luciferase) and Venus (a variant of yellow fluorescent protein). Forty-eight hours after transfection BRET measurements were performed as described previously (16). Results are expressed in milliBRET units as defined previously (17).

Isolation, Culture, and Analysis of Human Islets

Human islets were isolated from pancreata harvested from adult brain-dead individuals in the context of the traceability requirements for our clinical islet transplantation program (clinicaltrials.gov, NCT01123187, NCT00446264, NCT01148680) as described previously (18). The experimental design was approved in agreement with French regulations, our Institutional Ethical Committee of the University of Lille and the Center Hospitalier Régional Universitaire de Lille. Islets were allowed to recover in culture after isolation for at least 18 h before cell treatments. For experiments investigating glucose dependence of TxNIP, OGT, and OGA mRNA and protein levels, human islets were cultured in glucose-free medium (Gibco, Life Technologies, Paris, France) supplemented with 10% FBS, 1% P/S, 15 mM HEPES, and 5.5 or 16.7 mM glucose with and without PUGNAc (100 μM). Pellets were harvested for RNA and protein analysis. Total RNA was extracted using the RNeasy Mini Kit (Qiagen, Courtabœuf, France) (19).

Quantitative Real-Time PCR

Total RNA was extracted using RNeasy micro Kit (Qiagen®) for rodent islets and RNeasy Kit (Promega®) for INS1 832/13 cells. cDNA was reversed transcribed. The levels of expression of each gene were normalized to cyclophylin expression (INS1832/13 and rat islets) and β-actin and cyclophylin (human islets).

Western Blotting Analysis

Proteins from rodent and human islets and cell lines were subjected to 10% SDS-PAGE and transferred to nitrocellulose membranes. Rabbit polyclonal NLRP3 (Cell signaling), OGT (Sigma), cleaved IL1β (Cell Signaling) and monoclonal TxNIP (MBL) antibodies were used. O-GlcNAc was detected using RL2 anti-OGlcNAc antibody (Abcam). HSP90 (Cell Signaling), GAPDH (Cell Signaling), and β-actin were used to normalize data as indicated on Figure legends.

Immunoprecipitation and Wheat Germ Agglutinin Purification

For TxNIP immunoprecipitation, cells were lysed on IPH buffer (20 mmol/L Tris/HCl, 150 mmol/L NaCl, 0.5% NP-40 [v/v], and protease inhibitors). Proteins were incubated with 2 μg of anti-TxNIP antibody (MBL) and placed at 4°C overnight. Bound proteins were recovered after addition of 30 μl of Sepharose-labeled protein G (Sigma) for 1 h at 4°C. Beads were gently centrifuged for 1 min and washed four times for 5 min each. Bound proteins were analyzed by Western blot with a polyclonal anti-Flag (Sigma) or NRLP3 (Cell signaling) antibodies. For wheat germ agglutinin ([WGA] a GlcNAc-binding lectin) precipitation, 1 mg of proteins was incubated with 30 μl of WGA agarose beads (Sigma). Then, proteins were eluted from the beads in a Laemmli buffer and separated by SDS-PAGE.

RESULTS

TxNIP Expression and O-GlcNAcylation Are Increased in Pancreas and Islets of Rodent Models of Type 2 Diabetes

We first evaluated TxNIP expression and O-GlcNAcylation in islets of GK rats, a diabetic but non-obese rat model with moderate hyperglycemia but severe β cell defect (20) (**Figure 1**). We confirmed that GK rats were hyperglycemic (**Figure 1A**) and showed that *txnip* mRNA expression was markedly increased (8-fold) (**Figure 1B**), while no significant modification in either *Ogt* or *Oga* expression was observed (**Figure 1C**). In control islets, TxNIP protein was barely detectable, neither in cell lysates nor on WGA eluates (**Figure 1B**). In contrast, TxNIP protein could be detected in cell lysates from GK islets. Recovery of TxNIP on WGA beads (**Figure 1C**) suggested that TxNIP was O-GlcNAcylated in rat GK islets.

We next examined TxNIP protein content and O-GlcNAcylation of TxNIP (TxNIP O-GlcNAc) in pancreas from *db/db* mice. Blood glucose measurement confirmed the marked hyperglycemia of *db/db* mice vs. C57BL/6J mice (**Figure 1D**). Although total TxNIP protein content was unchanged in pancreas from *db/db* mice, the amount of TxNIP immunoprecipitated on WGA beads was higher in *db/db* mice than in control C57BL/6J mice. Densitometric analysis of the signals revealed a 3-fold increase in the TxNIP O-GlcNAc/TxNIP ratio (**Figure 1E**). Taken together, our data suggest that TxNIP is O-GlcNAcylated in pancreas of diabetic rodents.

O-GlcNAcylation of TxNIP Depends on OGT Activity

To characterize the role of OGT in the regulation of TxNIP O-GlcNAcylation, the enzyme was silenced through a shRNA approach in INS1 832/13 cells (**Figures 2A,B**). We first verified the efficiency of the shRNA to knock down OGT expression and global protein O-GlcNAcylation in these cells. As shown in **Figure 2A**, OGT silencing under high glucose concentrations (20 mM) led to a decrease in O-GlcNAcylated proteins levels compared to shcontrol conditions. We then examined, under shOGT conditions, TxNIP O-GlcNAcylation by WGA precipitation. We observed that TxNIP recovery on WGA beads was markedly reduced compared to shcontrol conditions. However, total TxNIP protein content was also reduced when OGT was silenced (**Figure 2B**). Therefore, to evaluate TxNIP O-GlcNAcylation independently of any change

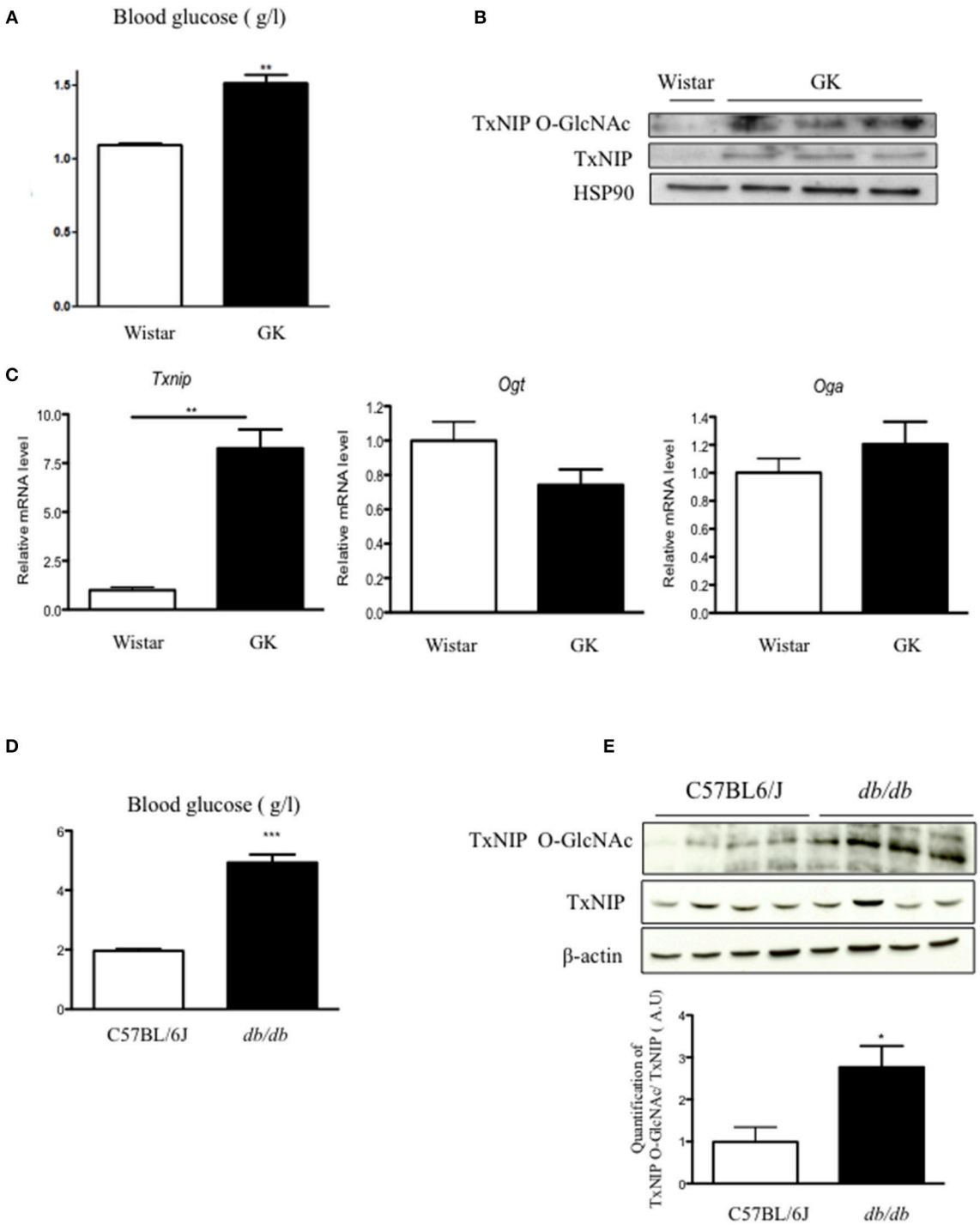

FIGURE 1 | O-GlcNAcylation of TxNIP is increased in rodent models of diabetes. **(A)** Blood glucose concentrations were measured in fed condition in wister and GK rats. **(B)** *Txnip*, *Ogt,* and *Oga* mRNA levels in islets of wistar and GK rats. Significance is based on Mann-Whitney test. $^{**}p < 0.01$. $n = 3$–5. **(C)** TxNIP O-GlcNAcylation level evaluated by WGA binding experiments. Islet lysate proteins were immunoblotted with TxNIP and HSP90 was used as a loading control. **(D)** Blood glucose concentrations were measured in C57/B6J and *db/db* mice. Significance is based on Mann-Whitney test. $^{***}p < 0.001$ **(E)** TxNIP O-GlcNAcylation was evaluated by WGA binding experiments. Whole pancreas proteins were immunoblotted with a TxNIP antibody and β-actin was used as a loading control. Quantification of the ratio of O-GlcNAcylated TxNIP corrected to total TxNIP protein is shown. Significance is based on student's *T*-test followed by Welch correction *post-hoc* test. $^{*}p < 0.05$. $n = 4$.

in TxNIP expression, we transfected HEK293 cells with a TxNIP expression plasmid together with an OGT or OGA plasmid (**Figure 2C**). TxNIP was then immunoprecipitated and its O-GlcNAcylation level was evaluated using an anti-O-GlcNAc antibody in HEK293 cells cultured under low (5 mM) or high (25 mM) glucose concentrations, or under low glucose supplemented with glucosamine (Gln, 5 mM) and PUGNAc (an inhibitor of OGA activity). We observed that TxNIP O-GlcNAcylation increased in response to 25 mM glucose and was reduced when OGA was overexpressed. Moreover, TxNIP O-GlcNAc markedly increased when OGT was overexpressed under 5 mM glucose. Altogether, these results show that TxNIP is O-GlcNAcylated in response to high glucose concentrations and that this modification depends on OGT activity.

Increased TxNIP O-GlcNAcylation Promotes Inflammasome Activation in Human and Rat Islets

To better understand the regulation of TxNIP by O-GlcNAcylation, we performed a series of experiments *ex vivo* in response to glucose with or without PUGNAc (**Figure 3**). The regulation of TxNIP by O-GlcNAcylation was examined in isolated rat islets cultured in 2.8 mM glucose, 16.7 mM glucose, or 16.7 mM glucose supplemented with PUGNAc (**Figures 3A,B**). As previously reported in other cell types (21, 22), treatment of rat islets with the OGA inhibitor PUGNAc increased *Oga* and decreased *Ogt* mRNA levels (**Figure 3A**). *Txnip* mRNA expression, protein levels and O-GlcNAcylation were significantly induced in response to elevated glucose concentrations (a 5-fold increase when comparing 2.8–16.7 mM glucose concentrations) and was further increased (a 2-fold increase) when PUGNAc was present (**Figure 3A**). Using a luciferase reporter gene under the control of *Txnip* promoter (containing the two tandem ChoRE), we confirmed transcriptional regulation by glucose in pancreatic beta cells (**Supplementary Figure 1**). Indeed, in INS1 832/13 cells, high glucose concentration (20 mM) stimulated by about 30-fold *Txnip* promoter activity compared to low glucose concentrations (5 mM). Interestingly, *Txnip* promoter activity was reduced by 50% when INS1 832/13 cells were cultivated under high glucose concentrations and infected by the OGA adenovirus (**Supplementary Figure 1**).

A marked increase in TxNIP total protein content was also observed in rat islets cultured in presence of 16.7 mM when compared to 2.8 mM glucose, and a further increase in total TxNIP protein content could be detected in presence of PUGNAc. O-GlcNAcylated forms of TxNIP were enhanced and paralleled with global O-GlcNAcylation of proteins under glucose conditions with or without PUGNAc (**Figure 3B**).

We also cultured human islets for 48 h in glucose 5.5, 16.7, or 16.7 mM supplemented with PUGNAc and analyzed for expression and O-GlcNAcylation of TxNIP (**Figures 3C,D**). We observed a 4-fold induction of *TxNIP* expression in response to elevated glucose concentrations (16.7 mM). Adding PUGNAc to high glucose concentration did not further increase *TxNIP* expression. *OGA* expression was upregulated in human islets cultured under high glucose concentrations and PUGNAc whereas no difference in *OGT* expression was observed (**Figure 3C**). In agreement with *TxNIP* mRNA expression, TxNIP protein content was increased with 16.7 mM glucose and adding PUGNAc did not modify total TxNIP protein content but increased its O-GlcNAcylated form as well as global O-GlcNAcylation levels (**Figure 3D**). Since a link between TxNIP and the inflammasome was previously evidenced (23), we measured cleaved IL1β under glucose ± PUGNAc conditions. Human islets cultured with 16.7 mM glucose exhibited a 1.6-fold increase in cleaved IL1β and supplementation of the culture medium with PUGNAc led to a further 2.9-fold increase, suggesting potentiation of inflammasome activation (**Figure 3D**). Similarly to human islets, a significant increase in cleaved IL1β was observed in response to 16.7 mM glucose and PUGNAC conditions in rat islets (**Figure 3B**).

TxNIP O-GlcNAcylation Modifies Its Scaffold Function With NLRP3

TxNIP functions as a scaffold protein and interacts with different partners to inhibit or activate their biological activities (24). Therefore, we next addressed whether O-GlcNAcylation of TxNIP could affect IL1β cleavage through its interaction with NLRP3. Experiments were performed in both HEK293 and INS1 832/13 cells (**Figure 4**). HEK293 cells were co-transfected with a TxNIP expression vector and a NLRP3 expression vector tagged with a FLAG epitope (NLRP3-FLAG). Immunoprecipitation of cell lysates with a TxNIP antibody and immunoblotting with anti-Flag antibody revealed that TxNIP co-immunoprecipitated with NLRP3 (**Figure 4A**). A 2-fold increase in the interaction between TxNIP and NLRP3 was observed under high glucose (25 mM) compared to low glucose concentrations (5 mM) (**Figures 4A,B**). OGT overexpression under low glucose concentrations induced a level of interaction similar to that obtained under high glucose conditions alone (**Figures 4A,B**). Inhibition of O-GlcNAcylation *via* OGA overexpression significantly decreased the interaction between the two partners. Finally, stimulation of O-GlcNAcylation with glucosamine (Gln) and PUGNAc led to a greater interaction between TxNIP and NLRP3 (**Figures 4A,B**).

Interaction between endogenous TxNIP and NLRP3 proteins was also evidenced in INS1 832/13 cells upon immunoprecipitation with anti-TxNIP antibody and immunobloting with anti-NLRP3 antibody (**Figure 4C**). Under high glucose concentrations (20 mM), the interaction between TxNIP and NLRP3 was increased compared to low glucose concentration (2.5 mM). Finally, we used a BRET approach in INS1 832/13 cells to address the importance of the O-GlcNAcylation modification for the activation of the inflammasome pathway. INS1 832/13 cells were transfected with a plasmid coding a BRET biosensor comprising the pro-Il1β sequence flanked by a Luciferase and an YFP (14). Cleavage of the pro-Il1β results in a decreased in BRET signal (**Figure 4D**). A significant decrease in BRET signal was observed when INS1 832/13 cells were cultured under 11 mM glucose with PUGNAc (**Figure 4D**), similar to that obtained with 25 mM glucose. Higher

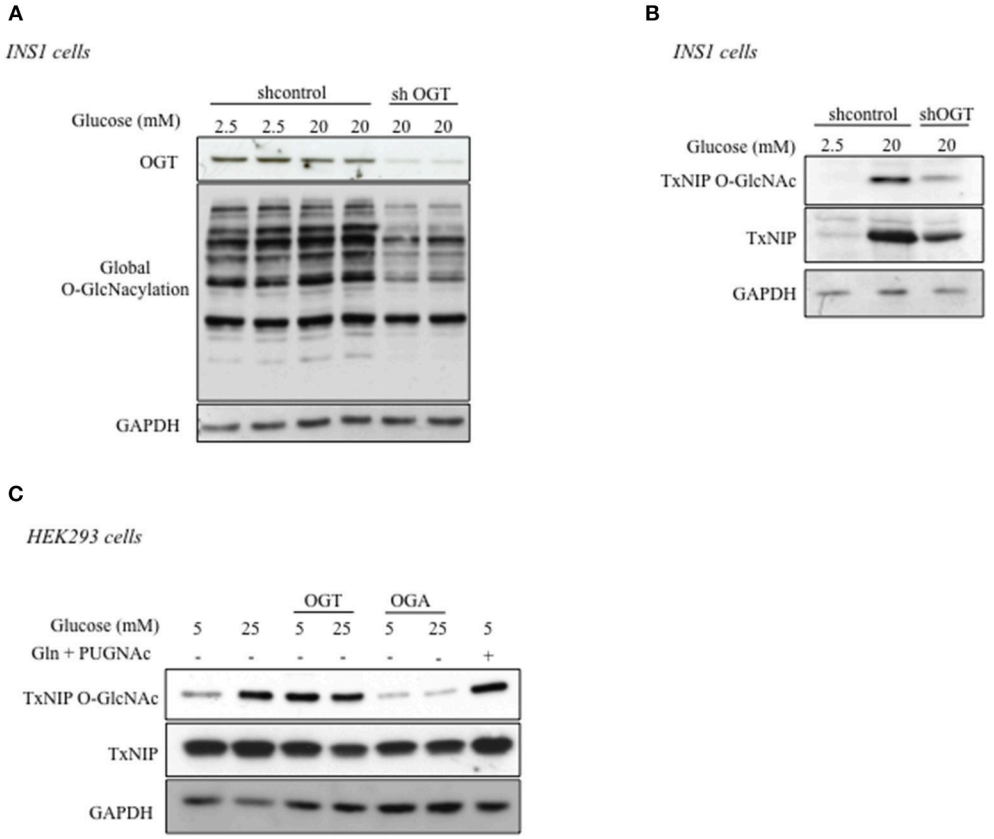

FIGURE 2 | TxNIP O-GlcNAcylation is dependent on OGT. **(A,B)** INS1 832/13 cells were infected by a shControl or shOGT adenovirus for 24 h. INS1 832/13 cells were later stimulated for 24 h under low glucose (2.5 mM) or high glucose (20 mM) concentrations. **(A)** Global O-GlcNAcylation levels and OGT protein content. GAPDH was used as a loading control. **(B)** TxNIP O-GlcNAcylation was evaluated by WGA binding experiments. Protein lysates from INS1 832/13 cells were immunoblotted with TxNIP and GAPDH was used as a loading control. **(C)** HEK293 cells were co-transfected with TxNIP, OGT, and OGA plasmids and incubated for 24 h under low (5 mM) or high glucose conditions (25 mM) supplemented or not by PUGNAc and glucosamine (Gln). O-GlcNAcylation level of TxNIP was evaluated using an anti-O-GlcNAc antibody (RL2). Immunoprecipitation (IP) of TxNIP was analyzed by immunoblotting with a Flag antibody. Representative Western blot from $n = 3$ experiments for TxNIP protein content are shown. GAPDH was used as loading control.

glucose concentrations (33 mM glucose) further decreased the BRET signal. Of note, the effect of PUGNAc on BRET signal was confirmed using Thiamet G, a more specific inhibitor of O-GlcNAcase activity (**Supplemental Figure 2**). Altogether, our results reveal that increased TxNIP O-GlcNAcylation correlates with the induction of the inflammasome pathway.

DISCUSSION

The current study demonstrates that TxNIP protein is modified by O-GlcNAcylation in pancreatic β-cells in an OGT dependent manner. We report here that this posttranslational modification, dependent on high glucose concentrations, increases the interaction of TxNIP with its partner NLRP3, correlating with enhanced cleavage of the interleukin IL1β in both rodent and human cells.

Over the past years, TxNIP has emerged as a central regulator of β-cell function. TxNIP is one of the most up-regulated gene in response to glucose in human islets and INS1 cells (2, 9, 25). We confirmed that *Txnip* promoter activity is markedly increased in response to glucose in INS1 cells, an effect previously reported to be ChREBP dependent (25). Overexpression of TxNIP in INS1 cells is associated with increased apoptosis (3, 26) while β-cell specific TxNIP inhibition protects against β cell dysfunction under high glucose concentrations by increasing β cell mass and stimulating the cellular survival pathway Akt/Bcl-xl. TxNIP is also implicated in the production of insulin by regulating miR-204 expression which in turn targets the transcription factor MafA that binds to the promoter in the *insulin* gene (27). While the regulation of TxNIP was essentially described at the transcriptional level, in particular by the transcription factors ChREBP and FoxO1 in pancreatic β cells (9), post-translational regulation of the TxNIP protein by phosphorylation was described in adipocytes and myotubes in response to insulin (28). Interestingly, in these cells, phosphorylation of TxNIP by AMPK or AKT leads to its dissociation from glucose transporters and to its degradation thereby enhancing glucose uptake (29, 30).

While experiments from Ayer's laboratory previously showed the importance of the hexosamine biosynthetic pathway for the regulation of TxNIP (31), a regulation of TxNIP protein by O-GlcNAcylation had never been described to our knowledge. In the present work, we provide several lines of evidence in

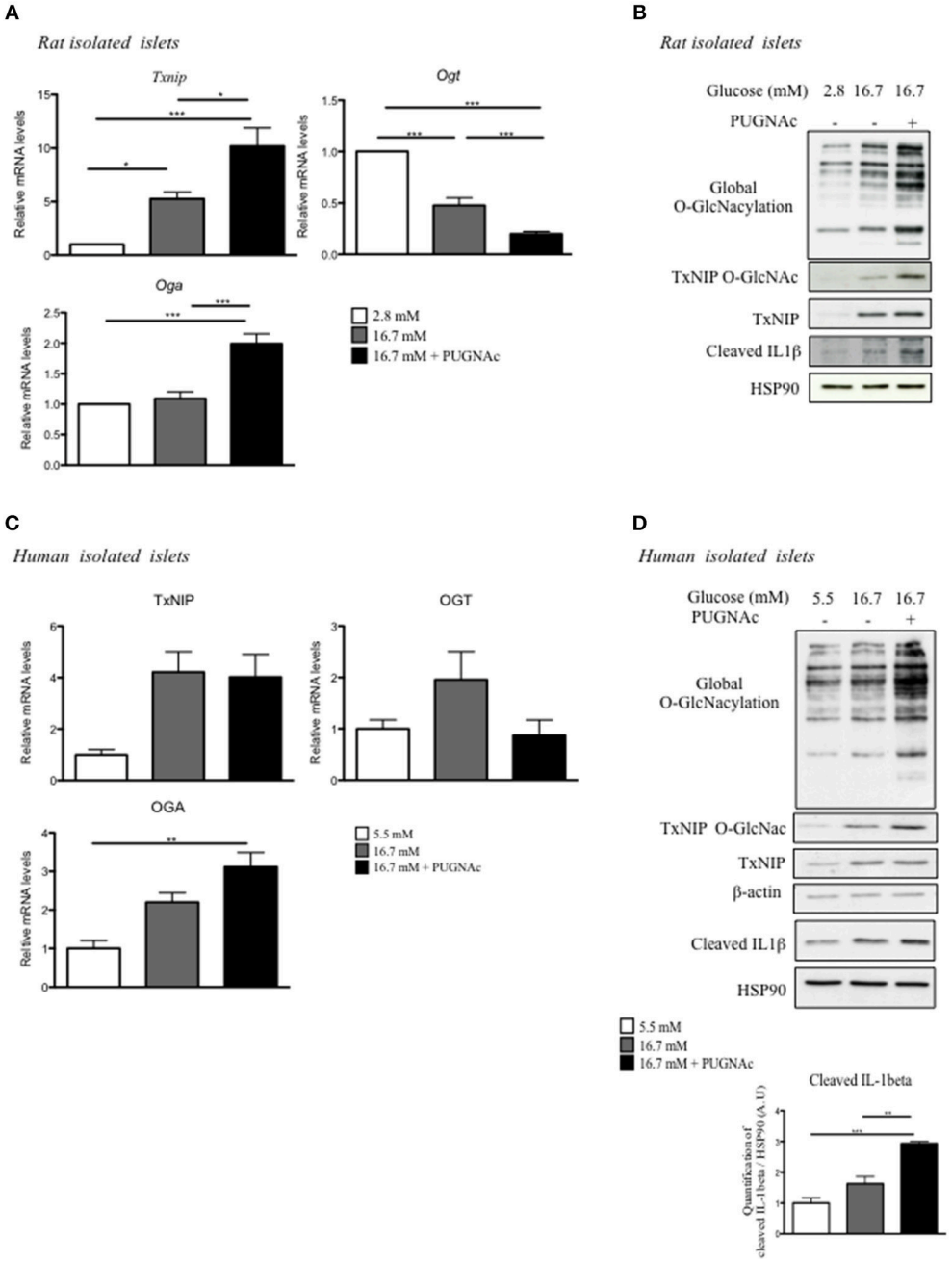

FIGURE 3 | Increasing O-GlcNAcylation in rat and human islets promotes inflammasome activation. **(A,B)** Islets isolated from Wistar rat were incubated for 72 h under low glucose (2.8 mM), high glucose (16.7 mM), or high glucose plus PUGNAc (16.7 mM + PUGNAc) **(A)** Q-PCR analysis of OGT, OGA, and TxNIP. Data are means ± SEM of eight independent experiments. Significance is based on two-way ANOVA followed by a Bonferroni *post-hoc* test $^{*}p < 0.05$, $^{**}p < 0.01$, $^{***}p < 0.001$. **(B)** Global O-GlcNAcylation levels and TxNIP protein content. TxNIP O-GlcNAcylation was evaluated by WGA binding experiments. Representative Western blot for cleaved Il1β protein content is shown. HSP90 was used as a loading control. **(C,D)** Human islets were incubated for 72 h under low glucose (5.5 mM), high glucose (16.7 mM), or high glucose plus PUGNAc (16.7 mM + PUGNAc) **(C)** QPCR analysis of TxNIP, OGT, and OGA mRNA expression. Data are means ± SEM. $n = 3$ independent experiments. Significance is based on two-way ANOVA followed by a Bonferroni *post-hoc* test $^{**}p < 0.01$. **(D)** Global O-GlcNAcylation levels, TxNIP protein content, and O-GlcNAcylation of TxNIP evaluated by WGA binding experiments. β-actin was used as a loading control. Representative Western Blot of Cleaved Il1β and HSP90 are also shown. Data are means ± SEM. $n = 3$ independent cultures. Significance is based on two-way ANOVA followed by a Bonferroni *post-hoc* test $^{**}p < 0.01$, $^{***}p < 0.001$.

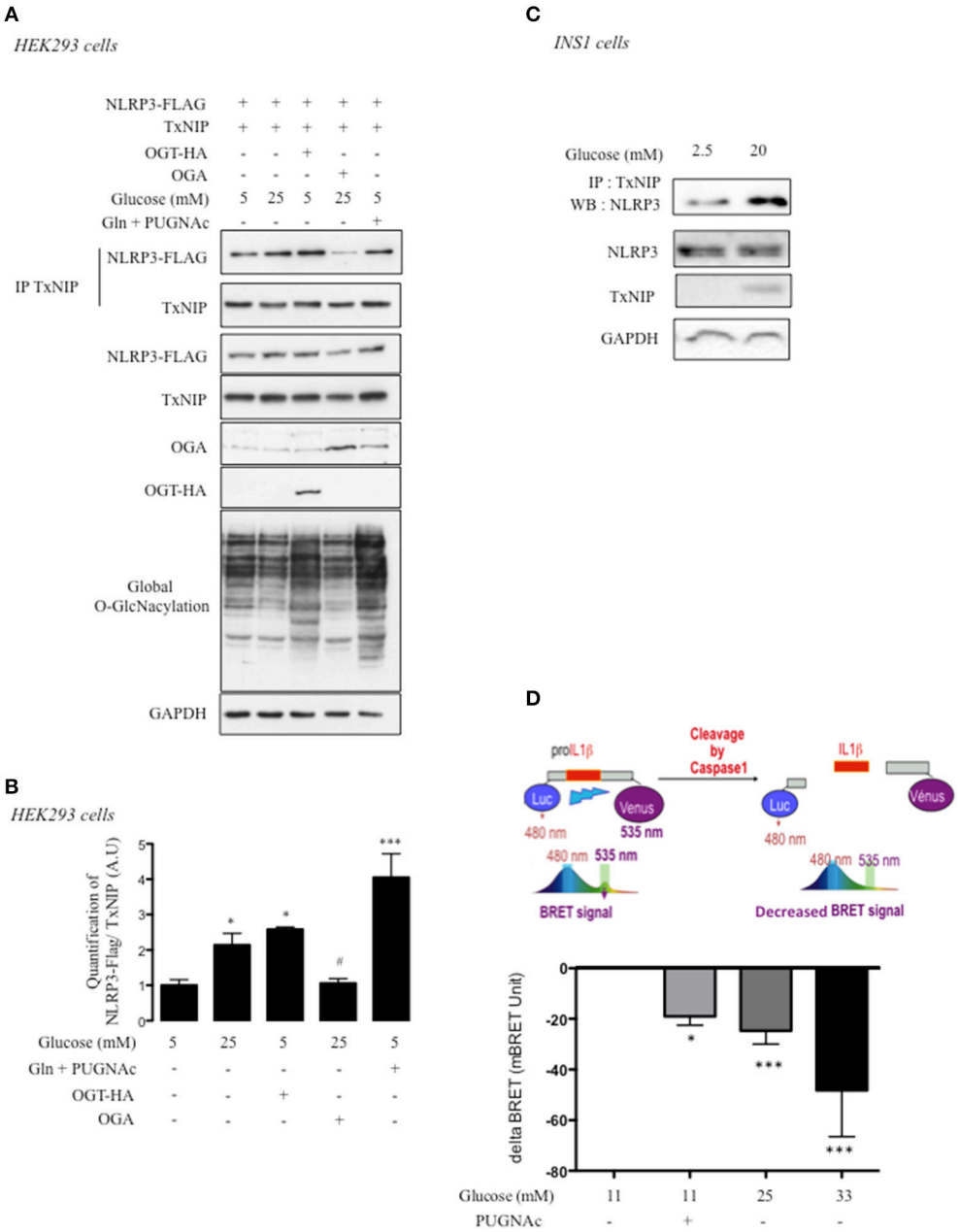

FIGURE 4 | O-GlcNAcylation promotes TxNIP interaction with NLRP3 and pro-Il1β cleavage. **(A)** HEK293 cells were co-transfected with TxNIP, NLRP3-flag, OGT, and OGA plasmids and incubated for 24 h under low glucose condition (5 mM), high glucose condition (25 mM), or low glucose condition supplemented with PUGNAc and glucosamine (Gln). Immunoprecipitation (IP) of TxNIP was analyzed by immunoblotting with a Flag antibody. Representative Western blot for NLRP3, TxNIP, OGA, and OGT protein content are shown $n = 4$–7 independent experiments. GAPDH was used as loading control. **(B)** Quantification of the interaction between TxNIP and NLRP3 normalized to total TxNIP protein. Significance is based on two-way ANOVA followed by a Bonferroni *post-hoc* test. $^{*}p < 0.05$, $^{***}p < 0.001$ when compared to 5 mM glucose; $^{\#}p < 0.05$ when compared to 25 mM glucose. **(C)** INS1 832/13 cells were stimulated for 24 h under low glucose (2.5 mM) or high glucose (20 mM) concentrations supplemented with PUGNAc. Immunoprecipitation (IP) of TxNIP was analyzed by immunoblotting with a NLRP3 antibody. Representative Western blot for NLRP3 and TxNIP protein content are shown. GAPDH was used as loading control ($n = 4$–7 independent experiments). **(D)** INS1 832/13 cells were transfected with a BRET-based biosensor that monitors pro-Il1β cleavage. The histogram shows the decreased in BRET signal measured in INS1 832/13 cells after 24 h of incubation with PUGNAc or with 25 mM or 33 mM of glucose. Significance is based on two-way ANOVA followed by a Dunnett's test for BRET experiments. $^{*}p < 0.05$, $^{***}p < 0.001$ ($n = 4$–14).

favor of TxNIP O-GlcNAcyaltion. It is important to note that although binding of a protein to WGA does not necessarily prove that this protein is O-GlcNAcylated, the experiments we performed in HEK cells in which a transfected Flag-TxNIP was immunprecipitated and probed with an anti-O-GlcNAc antibody, strongly supports the fact that the TxNIP protein is indeed modified by O-GlcNAcylation. Similar experiments with the endogenous TxNIP in pancreatic β-cells, were

problematic given that TxNIP expression was also increased upon induction of O-GlcNAcylation in beta cell, thereby limiting clear interpretation. O-GlcNAcylation, which involves the addition of a single O-GlcNAc to serine and threonine residues of proteins acts as a nutrient sensor. A couple of enzymes is involved in the regulation of the pathway: OGT, the enzyme which transfers the mono- saccharide to serine/threonine residues on target proteins, and OGA, which hydrolyses the sugar. Several studies have established that inhibition of OGA activity and subsequent increase in O-GlcNAcylation result in an enhanced OGA mRNA and protein expression (22, 32–34), probably as an adaptive mechanism to maintain O-GlcNAc homeostasis in the cell. In agreement with this notion, several lines of evidence indicated that in patients with diabetes, increased O-GlcNAcylation associated with chronic hyperglycaemia was also associated with an increased expression of OGA (35, 36). Interestingly, in a recent study (37) OGA mRNA levels in leucocytes from patients with type 2 diabetes were significantly correlated with TxNIP mRNA levels, as well as with blood markers of hyperglycaemia (HbA1C, Fructosamine). We report here that OGA mRNA levels are increased in response to enhanced O-GlcNAcylation pathway in both human and rat islets. The regulation of OGT by O-GlcNAc homeostasis is less clear. In rat islets, we observed that OGT expression is negatively regulated in response to high glucose concentrations and that this inhibition is stronger when the OGA enzyme is blocked by PUGNAc. Interestingly, OGT expression was not modified by the different treatments in human islets suggesting a species dependent regulation.

Several transcription factors are regulated by O-GlcNAcylation in pancreatic β cells (11). For example, O-GlcNAcylation of FoxO1 in INS1 cells results in a 2-fold increase in its transcriptional activity and a 3-fold increase in the expression of the insulin-like growth factor-binding protein 1 (*Igfbp1*) gene at the mRNA level, resulting in IGFBP1 protein hypersecretion by INS1 cells. In turn, increased IGFBP1 production in the culture medium blunts the Akt transduction pathway, revealing a novel mechanism by which O-GlcNAcylation inhibits Akt activity in INS1 cells through an autocrine mechanism (38). Of note, O-GlcNAcylation not only regulates transcriptional activity but has also been shown to influence protein-protein interactions (39, 40). In the current study, we revealed a novel mechanism by which O-GlcNAcylation of TxNIP favors its interaction with its partner NLRP3. NLRP3 is an inflammasome protein that once activated leads to the processing of IL1β, a cytokine involved in the pathology of type 2 diabetes (41). By performing both Western blot and BRET analysis, we demonstrated that production of IL1β by pancreatic cells could be induced by both glucose and PUGNAc. Therefore, increased TxNIP O-GlcNAcylation in pancreatic islets could play a part in diabetes pathogenesis. In the current study, two rodent models of diabetes (GK rats and *db/db* mice) suggested O-GlcNAcylation of TxNIP in pancreatic cells. Of note, TxNIP expression level was increased in isolated islets from GK rats while no difference was observed in the *db/db* mouse model. The difference could be explained by the fact that we had access to isolated islets for GK rats but not for *db/db* mice.

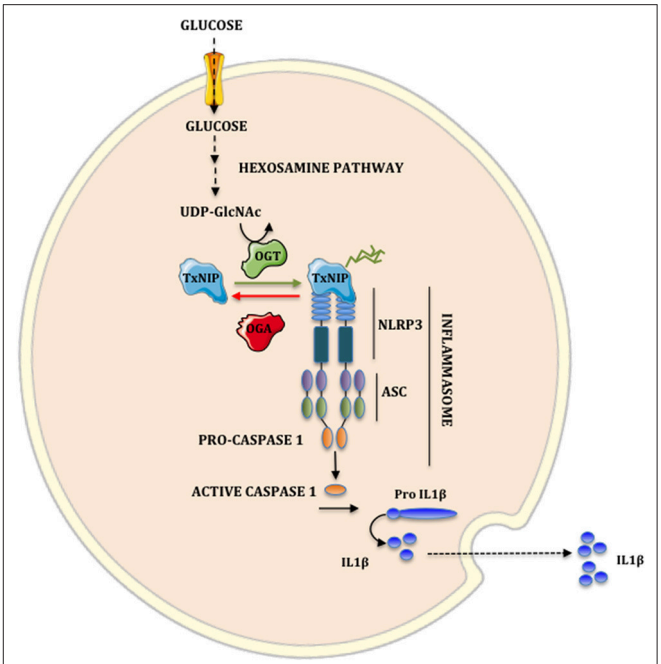

FIGURE 5 | Implication of hexosamine biosynthetic pathway on the NLRP3 inflammasome. A fraction of glucose flux is metabolized by the hexosamine biosynthetic pathway to synthesize UDP-GlcNAc. OGT uses UDP-GlcNAc to O-GlcNAcylate TxNIP. This modification increases TxNIP-NLRP3 interaction. The formation of the TxNIP-NLRP3-ASC oligomer complex activates Caspase 1. Once activated, Caspase 1 cleaves the inactive form pro-IL1β to the biologically active form IL1β.

In conclusion, our study reveals that O-GlcNAcylation represents an important regulatory mechanism for TxNIP activity in β cells by increasing its interaction with NLRP3 and the subsequent stimulation of IL1β production (**Figure 5**). Additional studies will be required to identify TxNIP O-GlcNAcylation sites, and to establish the specific contribution of TxNIP O-GlcNAcylation to pancreatic glucotoxicity in diabetes. Overall, strategies to inhibit this novel regulatory node in pancreatic β cells could be of interest to limit inflammation in the context of hyperglycemia.

ETHICS STATEMENT

Procedures were carried out according to the French guidelines for the care and use of experimental animals (validated by the Paris Descartes Ethical Committee).

AUTHOR CONTRIBUTIONS

FB and CP wrote the manuscript. GF, FB, PP, YF, and TI designed experiments, performed experiments, and analyzed the data. AI and JM prepared and provided islets from GK rats. CB, JK-C, and FP prepared and provided human islets. A-FB, SG, and TI provided critical comments on experimental design and on the manuscript.

FUNDING

This work was supported by grants from ANR (Agence Nationale de la Recherche, Grant Diab-O-Glyc), FRM (Foundation for the Medical Research, DEQ20150331744), ARD (Association de Recherche sur le Diabète), and the SFD (Société Francophone du Diabète). This project was performed in the context of the DHU Authors.

SUPPLEMENTARY MATERIAL

The Supplementary Material for this article can be found online at: https://www.frontiersin.org/articles/10.3389/fendo.2019.00291/full#supplementary-material

Supplementary Figure 1 | Transcriptional regulation of the *Txnip* promoter in response to glucose and OGA expression **(A)**. Schematic representation of the *Txnip* promoter (1081 base pairs; the two ChREBP binding sites (ChoRE) and the FoxO1 binding site (IRE) are indicated). **(B)** INS1 832/13 cells were infected by GFP or OGA adenovirus for 24 h. INS1 832/13 cells were then stimulated for 24 h under low glucose (2.5 mM) or high glucose (20 mM) concentrations. Luciferase activity of the *Txnip* promoter was measured. Figure is presented as means ± SEM from 3 to 4 independent cultures. Significance is based on two-way ANOVA followed by a Bonferroni *post-hoc* test. $^{**}p < 0.01$ when compared to GFP conditions, $^{***}p < 0.005$ when compared to 5 mM glucose condition (GFP), $^{\$\$}p < 0.01$ when compared to 20 mM glucose condition (GFP).

Supplemental Figure 2 | INS1 832/13 cells were transfected with a BRET-based biosensor that monitors pro-Il1β cleavage. The histogram shows the decreased in BRET signal measured in INS1 832/13 cells after 24 h of incubation with PUGNAc (100 μM) or with ThiametG (10 μM). Significance is based on two-way ANOVA followed by a Dunnett's test for BRET experiments. $^{**}p < 0.01$ ($n = 4$).

REFERENCES

1. Andrews Guzman M, Arredondo Olguin M, Olivares Gronhert M. Glycemic control and oxidative stress markers and their relationship with the thioredoxin interacting protein (TXNIP) gene in type 2 diabetic patients. *Nutr Hosp.* (2014) 31:1129–33. doi: 10.3305/nh.2015.31.3.7955
2. Minn AH, Hafele C, Shalev A. Thioredoxin-interacting protein is stimulated by glucose through a carbohydrate response element and induces beta-cell apoptosis. *Endocrinology.* (2005) 146:2397–405. doi: 10.1210/en.2004-1378
3. Chen J, Saxena G, Mungrue IN, Lusis AJ, Shalev A. Thioredoxin-interacting protein: a critical link between glucose toxicity and beta-cell apoptosis. *Diabetes.* (2008) 57:938–44. doi: 10.2337/db07-0715
4. Shao W, Yu Z, Fantus IG, Jin T. Cyclic AMP signaling stimulates proteasome degradation of thioredoxin interacting protein (TxNIP) in pancreatic beta-cells. *Cell Signal.* (2010) 22:1240–6. doi: 10.1016/j.cellsig.2010.04.001
5. Oslowski CM, Hara T, O'Sullivan-Murphy B, Kanekura K, Lu S, Hara M, et al. Thioredoxin-interacting protein mediates ER stress-induced beta cell death through initiation of the inflammasome. *Cell Metab.* (2012) 16:265–73. doi: 10.1016/j.cmet.2012.07.005
6. Zhou R, Tardivel A, Thorens B, Choi I, Tschopp J. Thioredoxin-interacting protein links oxidative stress to inflammasome activation. *Nat Immunol.* (2010) 11:136–40. doi: 10.1038/ni.1831
7. Liu Y, Lian K, Zhang L, Wang R, Yi F, Gao C, et al. TXNIP mediates NLRP3 inflammasome activation in cardiac microvascular endothelial cells as a novel mechanism in myocardial ischemia/reperfusion injury. *Basic Res Cardiol.* (2014) 109:415. doi: 10.1007/s00395-014-0415-z
8. Schroder K, Zhou R, Tschopp J. The NLRP3 inflammasome: a sensor for metabolic danger? *Science.* (2010) 327:296–300. doi: 10.1126/science.1184003
9. Kibbe C, Chen J, Xu G, Jing G, Shalev, A. FOXO1 competes with carbohydrate response element-binding protein (ChREBP) and inhibits thioredoxin-interacting protein (TXNIP) transcription in pancreatic beta cells. *J Biol Chem.* (2013) 288:23194–202. doi: 10.1074/jbc.M113.473082
10. Guinez C, Filhoulaud G, Rayah-Benhamed F, Marmier S, Dubuquoy C, Dentin R, et al. O-GlcNAcylation increases ChREBP protein content and transcriptional activity in the liver. *Diabetes.* (2011) 60:1399–413. doi: 10.2337/db10-0452
11. Issad T, Kuo M. O-GlcNAc modification of transcription factors, glucose sensing and glucotoxicity. *Trends Endocrinol Metab.* (2008) 19:380–9. doi: 10.1016/j.tem.2008.09.001
12. Movassat J, Saulnier C, Portha B. Beta-cell mass depletion precedes the onset of hyperglycaemia in the GK rat, a genetic model of non-insulin-dependent diabetes mellitus. *Diabete Metab.* (1995) 21:365–70.
13. Lacraz G, Figeac F, Movassat J, Kassis N, Portha B. Diabetic GK/Par rat beta-cells are spontaneously protected against H2O2-triggered apoptosis. A cAMP-dependent adaptive response. *Am J Physiol Endocrinol Metab.* (2010) 298:E17–27. doi: 10.1152/ajpendo.90871.2008
14. Compan V, Baroja-Mazo A, Bragg L, Verkhratsky A, Perroy J, Pelegrin P. A genetically encoded IL-1beta bioluminescence resonance energy transfer sensor to monitor inflammasome activity. *J Immunol.* (2012) 189:2131–7. doi: 10.4049/jimmunol.1201349
15. Compan V, Pelegrin P. Measuring IL-1beta processing by bioluminescence sensors I: using a bioluminescence resonance energy transfer biosensor. *Methods Mol Biol.* (2016) 1417:89–95. doi: 10.1007/978-1-4939-3566-6_5
16. Blanquart C, Achi J, Issad T. Characterization of IRA/IRB hybrid insulin receptors using bioluminescence resonance energy transfer. *Biochem Pharmacol.* (2008) 76:873–83. doi: 10.1016/j.bcp.2008.07.027
17. Lacasa D, Boute N, Issad T. Interaction of the insulin receptor with the receptor-like protein tyrosine phosphatases PTPalpha and PTPepsilon in living cells. *Mol Pharmacol.* (2005) 67:1206–13. doi: 10.1124/mol.104.009514
18. Kerr-Conte J, Vandewalle B, Moerman E, Lukowiak B, Gmyr V, Arnalsteen L, et al. Upgrading pretransplant human islet culture technology requires human serum combined with media renewal. *Transplantation.* (2010) 89:1154–60. doi: 10.1097/TP.0b013e3181d154ac
19. Bonner C, Kerr-Conte J, Gmyr V, Queniat G, Moerman E, Thevenet J, et al. Inhibition of the glucose transporter SGLT2 with dapagliflozin in pancreatic alpha cells triggers glucagon secretion. *Nat Med.* (2015) 21:512–7. doi: 10.1038/nm.3828
20. Portha B, Giroix MH, Tourrel-Cuzin C, Le-Stunff H, Movassat J. The GK rat: a prototype for the study of non-overweight type 2 diabetes. *Methods Mol Biol.* (2012) 933:125–59. doi: 10.1007/978-1-62703-068-7_9
21. Taylor RP, Geisler TS, Chambers JH, McClain DA. Up-regulation of O-GlcNAc transferase with glucose deprivation in HepG2 cells is mediated by decreased hexosamine pathway flux. *J Biol Chem.* (2009) 284:3425–32. doi: 10.1074/jbc.M803198200
22. Zhang Z, Tan EP, VandenHull NJ, Peterson KR, Slawson C. O-GlcNAcase Expression is Sensitive to Changes in O-GlcNAc Homeostasis. *Front Endocrinol.* (2014) 5:206. doi: 10.3389/fendo.2014.00206
23. Abderrazak A, Syrovets T, Couchie D, El Hadri K, Friguet B, Simmet T, et al. NLRP3 inflammasome: from a danger signal sensor to a regulatory node of oxidative stress and inflammatory diseases. *Redox Biol.* (2015) 4:296–307. doi: 10.1016/j.redox.2015.01.008
24. Shalev A. Minireview: thioredoxin-interacting protein: regulation and function in the pancreatic beta-cell. *Mol Endocrinol.* (2014) 28:1211–20. doi: 10.1210/me.2014-1095
25. Shalev A, Pise-Masison CA, Radonovich M, Hoffmann SC, Hirshberg B, Brady JN, et al. Oligonucleotide microarray analysis of intact human pancreatic islets: identification of glucose-responsive genes and a highly regulated TGFbeta signaling pathway. *Endocrinology.* (2002) 143:3695–8. doi: 10.1210/en.2002-220564
26. Chen J, Hui ST, Couto FM, Mungrue IN, Davis DB, Attie AD, et al. Thioredoxin-interacting protein deficiency induces Akt/Bcl-xL signaling and

pancreatic beta-cell mass and protects against diabetes. *FASEB J.* (2008) 22:3581–94. doi: 10.1096/fj.08-111690
27. Xu G, Chen J, Jing G, Shalev A. Thioredoxin-interacting protein regulates insulin transcription through microRNA-204. *Nat Med.* (2013) 19:1141–6. doi: 10.1038/nm.3287
28. Robinson KA, Brock JW, Buse MG. Posttranslational regulation of thioredoxin-interacting protein. *J Mol Endocrinol.* (2013) 50:59–71. doi: 10.1530/JME-12-0091
29. Wu N, Zheng B, Shaywitz A, Dagon Y, Tower C, Bellinger G, et al. AMPK-dependent degradation of TXNIP upon energy stress leads to enhanced glucose uptake via GLUT1. *Mol Cell.* (2013) 49:1167–75. doi: 10.1016/j.molcel.2013.01.035
30. Waldhart AN, Dykstra H, Peck AS, Boguslawski EA, Madaj ZB, Wen J, et al. Phosphorylation of TXNIP by AKT mediates acute influx of glucose in response to insulin. *Cell Rep.* (2017) 19:2005–13. doi: 10.1016/j.celrep.2017.05.041
31. Stoltzman CA, Kaadige MR, Peterson CW, Ayer DE. MondoA senses non-glucose sugars: regulation of thioredoxin-interacting protein (TXNIP) and the hexose transport curb. *J Biol Chem.* (2011) 286:38027–34. doi: 10.1074/jbc.M111.275503
32. Buren S, Gomes AL, Teijeiro A, Fawal MA, Yilmaz M, Tummala KS, et al. Regulation of OGT by URI in response to glucose confers c-MYC-dependent survival mechanisms. *Cancer Cell.* (2016) 30:290–307. doi: 10.1016/j.ccell.2016.06.023
33. Park SK, Zhou X, Pendleton KE, Hunter OV, Kohler JJ, O'Donnell KA, et al. A conserved splicing silencer dynamically regulates O-GlcNAc transferase intron retention and O-GlcNAc homeostasis. *Cell Rep.* (2017) 20:1088–99. doi: 10.1016/j.celrep.2017.07.017
34. Groussaud D, Khair M, Tollenaere AI, Waast L, Kuo MS, Mangeney M, et al. Hijacking of the O-GlcNAcZYME complex by the HTLV-1 Tax oncoprotein facilitates viral transcription. *PLoS Pathog.* (2017) 13:e1006518. doi: 10.1371/journal.ppat.1006518
35. Park K, Saudek CD, Hart GW. Increased expression of beta-N-acetylglucosaminidase in erythrocytes from individuals with pre-diabetes and diabetes. *Diabetes.* (2010) 59:1845–50. doi: 10.2337/db09-1086
36. Springhorn C, Matsha TE, Erasmus RT, Essop MF. Exploring leukocyte O-GlcNAcylation as a novel diagnostic tool for the earlier detection of type 2 diabetes mellitus. *J Clin Endocrinol Metab.* (2012) 97:4640–9. doi: 10.1210/jc.2012-2229
37. Pagesy P, Tachet C, Mostefa-Kara A, Larger E, Issad T. Increased OGA expression and activity in leukocytes from patients with diabetes: correlation with inflammation markers. *Exp Clin Endocrinol Diabetes.* (2018) 37. doi: 10.1055/a-0596-7337
38. Fardini Y, Masson E, Boudah O, Ben Jouira R, Cosson C, Pierre-Eugene C, et al. O-GlcNAcylation of FoxO1 in pancreatic beta cells promotes Akt inhibition through an IGFBP1-mediated autocrine mechanism. *FASEB J.* (2014) 28:1010–21. doi: 10.1096/fj.13-238378
39. Hart GW, Housley MP, Slawson C. Cycling of O-linked beta-N-acetylglucosamine on nucleocytoplasmic proteins. *Nature.* (2007) 446:1017–22. doi: 10.1038/nature05815
40. Yang X, Qian K. Protein O-GlcNAcylation: emerging mechanisms and functions. *Nat Rev Mol Cell Biol.* (2017) 18:452–65. doi: 10.1038/nrm.2017.22
41. Banerjee M, Saxena M. Interleukin-1 (IL-1) family of cytokines: role in type 2 diabetes. *Clin Chim Acta.* (2012) 413:1163–70. doi: 10.1016/j.cca.2012.03.021

Conflict of Interest Statement: The authors declare that the research was conducted in the absence of any commercial or financial relationships that could be construed as a potential conflict of interest.

Advantages of publishing in Frontiers

OPEN ACCESS
Articles are free to read for greatest visibility and readership

FAST PUBLICATION
Around 90 days from submission to decision

HIGH QUALITY PEER-REVIEW
Rigorous, collaborative, and constructive peer-review

TRANSPARENT PEER-REVIEW
Editors and reviewers acknowledged by name on published articles

Frontiers
Avenue du Tribunal-Fédéral 34
1005 Lausanne | Switzerland

Visit us: www.frontiersin.org
Contact us: info@frontiersin.org | +41 21 510 17 00

REPRODUCIBILITY OF RESEARCH
Support open data and methods to enhance research reproducibility

DIGITAL PUBLISHING
Articles designed for optimal readership across devices

FOLLOW US
@frontiersin

IMPACT METRICS
Advanced article metrics track visibility across digital media

EXTENSIVE PROMOTION
Marketing and promotion of impactful research

LOOP RESEARCH NETWORK
Our network increases your article's readership